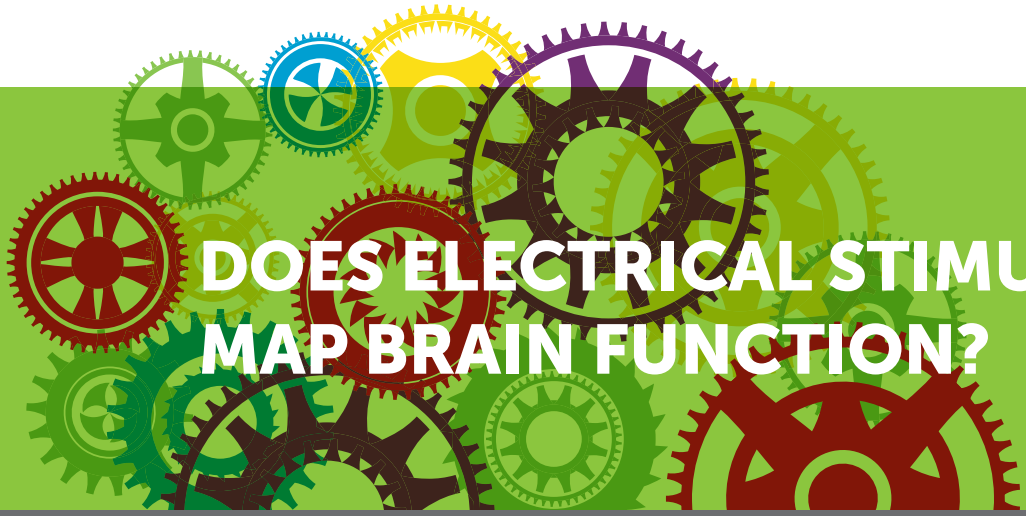

DOES ELECTRICAL STIMULATION MAP BRAIN FUNCTION?

EDITED BY: Patrick Chauvel, Nathan Earl Crone,
Jorge Alvaro Gonzalez-Martinez and Riki Matsumoto

PUBLISHED IN: Frontiers in Human Neuroscience and
Frontiers in Systems Neuroscience

frontiers Research Topics

frontiers

ISSN 1664-8714
ISBN 978-2-88974-173-1
DOI 10.3389/978-2-88974-173-1

About Frontiers

Frontiers is more than just an open-access publisher of scholarly articles: it is a pioneering approach to the world of academia, radically improving the way scholarly research is managed. The grand vision of Frontiers is a world where all people have an equal opportunity to seek, share and generate knowledge. Frontiers provides immediate and permanent online open access to all its publications, but this alone is not enough to realize our grand goals.

Frontiers Journal Series

The Frontiers Journal Series is a multi-tier and interdisciplinary set of open-access, online journals, promising a paradigm shift from the current review, selection and dissemination processes in academic publishing. All Frontiers journals are driven by researchers for researchers; therefore, they constitute a service to the scholarly community. At the same time, the Frontiers Journal Series operates on a revolutionary invention, the tiered publishing system, initially addressing specific communities of scholars, and gradually climbing up to broader public understanding, thus serving the interests of the lay society, too.

Dedication to Quality

Each Frontiers article is a landmark of the highest quality, thanks to genuinely collaborative interactions between authors and review editors, who include some of the world's best academicians. Research must be certified by peers before entering a stream of knowledge that may eventually reach the public - and shape society; therefore, Frontiers only applies the most rigorous and unbiased reviews.
Frontiers revolutionizes research publishing by freely delivering the most outstanding research, evaluated with no bias from both the academic and social point of view. By applying the most advanced information technologies, Frontiers is catapulting scholarly publishing into a new generation.

What are Frontiers Research Topics?

Frontiers Research Topics are very popular trademarks of the Frontiers Journals Series: they are collections of at least ten articles, all centered on a particular subject. With their unique mix of varied contributions from Original Research to Review Articles, Frontiers Research Topics unify the most influential researchers, the latest key findings and historical advances in a hot research area! Find out more on how to host your own Frontiers Research Topic or contribute to one as an author by contacting the Frontiers Editorial Office: frontiersin.org/about/contact

DOES ELECTRICAL STIMULATION MAP BRAIN FUNCTION?

Topic Editors:
Patrick Chauvel, University of Pittsburgh Medical Center, United States
Nathan Earl Crone, Johns Hopkins University, United States
Jorge Alvaro Gonzalez-Martinez, University of Pittsburgh, United States
Riki Matsumoto, Kobe University, Japan

Citation: Chauvel, P., Crone, N. E., Gonzalez-Martinez, J. A., Matsumoto, R., eds. (2022). Does Electrical Stimulation Map Brain Function?
Lausanne: Frontiers Media SA. doi: 10.3389/978-2-88974-173-1

Table of Contents

frontiers in Human Neuroscience

PERSPECTIVE
published: 07 August 2020
doi: 10.3389/fnhum.2020.00315

What Direct Electrostimulation of the Brain Taught Us About the Human Connectome: A Three-Level Model of Neural Disruption

Hugues Duffau[1,2]*

[1]Department of Neurosurgery, Montpellier University Medical Center, Montpellier, France, [2]Institute of Functional Genomics, INSERM U-1191, University of Montpellier, Montpellier, France

For a long time, the relevance of the information provided by direct electrostimulation (DES) for mapping brain functions was debated. Recently, major advances in intraoperative DES for guiding resection of cerebral tumors in awake patients enabled the validation of this method and its increased utilization in basic neurosciences. Indeed, in addition to the cortical stimulation used for many decades in epilepsy surgery, axonal mapping was developed thanks to DES of the white matter tracts, giving original insights into the neural connectivity. Moreover, functional results collected during intrasurgical mapping have been correlated with neuropsychological performances before and after DES-guided resection, and with perioperative neuroimaging data. Thus, it was evidenced that DES offers the unique opportunity to identify both cortical and subcortical structures *critical* for cerebral functions. Here, the first aim is to propose a three-level model of DES-generated functional disruption, able to explain the behavioral consequences elicited during awake surgery, i.e., (i) DES of an input/output unimodal (e.g., somatosensory or motor) network inducing "positive" responses (as involuntary movement); (ii) DES of a distributed specialized network inducing a within-system disruption leading to specific "negative" disorders (e.g., exclusive language deficit with no other disorders); (iii) DES generating an inter-system disruption leading to more complex behavioral disturbances (e.g., the inability to perform dual-task while each function can be performed separately). Second, in light of this model, original findings gained from DES concerning the human connectome, complementary to those provided by functional neuroimaging (FNI), are reviewed. Further longitudinal multimodal investigations are needed to explore neuroplasticity mechanisms.

Keywords: awake mapping, direct electrostimulation, human connectome, neural networks, neurophysiology, neuroplasticity

OPEN ACCESS

Edited by:
Riki Matsumoto,
Kobe University, Japan

Reviewed by:
Giovanni Pellegrino,
McGill University, Canada
Mitsutoshi Nakada,
Kanazawa University, Japan
Akihiro Shimotake,
Kyoto University, Japan

***Correspondence:**
Hugues Duffau
h-duffau@chu-montpellier.fr

Specialty section:
This article was submitted to Brain Imaging and Stimulation, a section of the journal Frontiers in Human Neuroscience

Received: *20 April 2020*
Accepted: *16 July 2020*
Published: *07 August 2020*

Citation:
Duffau H (2020) What Direct Electrostimulation of the Brain Taught Us About the Human Connectome: A Three-Level Model of Neural Disruption. Front. Hum. Neurosci. 14:315. doi: 10.3389/fnhum.2020.00315

INTRODUCTION

Since its popularization by Penfield (1954), intraoperative direct electrostimulation (DES) has regularly been used during brain resection to detect eloquent areas, especially for epilepsy surgery (Ojemann et al., 1989). Beyond the clinical benefit which consists in minimizing the risk of permanent neurological deficits, pioneering works proposed new models

of cerebral anatomo-functional organization based upon the DES findings, e.g., the sensorimotor homunculus (Penfield and Boldrey, 1937) or a mosaic distribution of language sites (Ojemann et al., 1989). However, the relevance of the information provided by DES for mapping brain functions was debated for many decades, because: (i) these data were collected in brain-damaged patients, who often experienced preoperative functional disturbances—notably in intractable epilepsy; (ii) DES is an invasive method; and (iii) mechanisms underlying DES were poorly understood, particularly with a bias related to possible cortical spreading. Therefore, because of the emergence of non-invasive functional neuroimaging (FNI) techniques, the place of DES was marginalized in fundamental neurosciences.

Recently, major advances in intraoperative DES for guiding resection of cerebral tumors in awake patients changed the way neuroscientists think of stimulation mapping. This technique is increasingly used in patients who undergo early surgery, thereby with only mild or even no preoperative functional disturbances—as in the incidental discovery of slow-growing low-grade glioma (Duffau, 2018). Thus, a normal cognitive assessment before surgery allows a more extensive neuropsychological mapping throughout the resection. Furthermore, in addition to the cortical stimulation utilized for many decades in epilepsy surgery (commonly with extra operative mapping using grids), axonal mapping was developed using DES of the white matter tracts (Duffau, 2015). By gathering findings gained from both cortical and subcortical stimulation, accuracy, reliability, and reproducibility of DES mapping were dramatically improved. Indeed, functional results collected during intrasurgical mapping have been correlated with neuropsychological performances before and after DES-guided resection. Such correlations enabled to validate DES method, by demonstrating that the introduction of new cognitive tasks during awake mapping resulted in a minimization of the persistent postsurgical deficits in the domain monitored intraoperatively, e.g., decrease of complex movement disorders by mapping the bimanual coordination during surgery (Rech et al., 2014), or decrease of mentalizing disturbances by mapping theory of mind during resection (Herbet et al., 2015a). Importantly, DES offers the unique opportunity to identify cortical and subcortical structures *critical* for cerebral functions, especially because axonal DES provides original insights into the direct functioning of neural connectivity (Duffau, 2015). These correlations between DES and cognitive scores have also permitted a better understanding of the neural foundations underpinning sensorimotor, visuospatial, language, cognitive, and emotional processing, leading to new models of dynamic anatomo-functional architecture (Herbet and Duffau, 2020).

Here, the first aim is to propose a three-level model of DES-generated functional disruption, able to explain the behavioral consequences elicited during awake surgery. Second, in light of this model, original findings gained from DES concerning the human connectome and its plastic potential are reviewed: these data evidence that DES mapping currently plays a pivotal role in basic neurosciences.

A THREE-LEVEL MODEL OF DES NEURAL DISRUPTION

DES can modify the activity of a population of neurons by changing the voltage gradient across the neuronal membrane: when the current crosses cells, it can modulate their membrane potential and trigger neuronal responses (Vincent et al., 2016). Therefore, DES is helpful to identify the functional role of each brain area stimulated, which should nonetheless be conceived only as a part of a more distributed neural network. Indeed, every structure responsive to DES is an input gate into a large-scale circuit rather than an isolated discrete eloquent structure (Mandonnet et al., 2010). Therefore, by generating a "virtual transitory dysfunction," DES detects the cortical hubs and white matter fascicles which are critical for brain function by disrupting a subnetwork for a few seconds (Duffau, 2015). Interestingly, the same functional responses are reproduced when repeated DES is applied over the same site. In surgical practice, such behavioral interferences guide the resection, by pursuing the tumor removal until functional boundaries have been reached in awake patients, allowing an increase of the extent of resection while minimizing postoperative neurological morbidity, even in areas traditionally considered as essential in a localizationist dogma (Duffau, 2014).

Besides its clinical implication, DES can also shed light on the networking organization of the brain. However, although any kind of inappropriate response induced by DES represents sufficient information for surgical purposes (since the resection is stopped as soon as neurological deficits are elicited to avoid sequelae), it is more difficult to draw robust neuroscientific conclusions about the neural architecture without an optimized understanding of mechanisms underpinning the large spectrum of transient disturbances caused by DES. To clarify this wide variety of transitory dysfunctions, a three-level model of DES-generated functional disruption is proposed, based upon two types of troubles:

- a "positive response," which is defined as the induction by DES of an unexpected neurological response in a patient at rest (as involuntary movement, tingling or phosphenes)
- a "negative trouble," which is defined as a functional disturbance (whatever its nature, that is, from complete arrest to response error) evoked by DES while the patient is performing a task, this interference within the neural network preventing him/her transitorily to achieve successfully the on-going task.

The first "basic" level corresponds to the DES of an input network, which is the first relay of information entering the brain, or to DES of an output network, which is the last relay sending information outside the brain (Ius et al., 2011). The input circuits include the thalamocortical tracts running to the primary somatosensory cortex and the optic radiations running to the primary visual cortex, whereas the output circuit is composed of the primary motor cortex and the cortico-spinal tracts. When DES is applied at their level, it generates a "positive" response, namely, paresthesias during stimulation of the primary

somatosensory system (more rarely feeling of heaviness of the limb or fading limb), phosphenes during stimulation of the primary visual system, and involuntary movement during stimulation of the primary motor system. In surgical practice, the patient should be at rest when DES is performed. Such basic responses seem to be because these networks, composed of a cortical area and its projection fibers, are mainly unimodal (Ius et al., 2011).

The second "intermediate" level consists of DES of distributed function-specific networks, composed of multiple delocalized cortical areas interconnected by associative white matter pathways. These functional systems subserve movement control, spatial cognition, language, working memory, or emotion (Duffau, 2015). DES of a specialized network induces a within-system disruption leading to specific "negative" troubles, namely, with task inhibition. Because these networks are constituted by several parallel and interactive subnetworks, DES may cause a discrete deficit related to the disruption of one subcircuit, or a more global deficit due to the disruption of the entire system. For example, concerning the language system, stimulating specifically the dorsal stream mediated by the arcuate fasciculus during a naming task elicits phonological paraphasia; stimulating specifically the ventral stream mediated by the inferior fronto-occipital fasciculus (IFOF) evokes semantic paraphasias; whereas stimulating both pathways [especially at their junction underneath the posterior temporal areas or dorsolateral prefrontal cortex (dlPFC)] causes complete anomia due to disruption of the whole network (Duffau et al., 2014). Importantly, no non-language deficit is generated simultaneously, e.g., the patient is still able to move despite transient DES-elicited language disorders. In surgical practice, the patient should be asked to perform the appropriate task according to the sub-network that the neurosurgeon wants to map depending on the tumor location. For instance, if a naming task is achieved to monitor language semantic processing into the contact of the left IFOF in a left-hander with right hemispheric lateralization of language, no semantic paraphasia will likely be induced with a high risk to damage the ventral stream because of "false negative." Nonetheless, if the patient is asked to achieve a non-verbal semantic association task, semantic disturbances will probably occur during the DES of the same neural structure allowing the preservation of the pathway devoted to multimodal semantic processes (Moritz-Gasser et al., 2013). Combining intraoperative neurophysiologically-sophisticated methods, namely, DES and electrocorticographic recording of cortico-cortical evoked potentials (Kunieda et al., 2015) and subcortical-cortical evoked potentials (Yamao et al., 2014) could be of utmost interest to better investigate the mechanisms underpinning DES neural disruption (Vincent et al., 2020).

The third "integrated" level consists of an inter-system disruption evoked by DES, that is, disturbances in the interactions between function-specific networks (e.g., between language and working memory), leading to more complex behavioral disturbances, such as the inability to perform several tasks simultaneously (multi-tasking). Neural processing cannot be conceived in a segregated account, with parallel circuits acting in isolation: complex cognitions at the service of adaptive, context-specific behaviors emerge from spatiotemporal dynamic interactions between the specialized functional systems. Such integration should transitorily be generated to succeed in cognitive demanding, functionally multi-determined behavior tasks (Herbet and Duffau, 2020). An example of complex cognitive activities is dual-tasking, in which the brain must coordinate its networks to reach the task goal. In surgical practice, the patient is regularly asked to perform a movement of the upper limb simultaneously with a picture-naming task. With no DES, a cross-system interaction between the language (semantics, phonology, and articulation), motor (movement control and execution), and executive functions (goal maintenance) networks are needed to achieve the task efficiently thanks to integrative hubs such as the dlPFC. As mentioned above (second level of DES disruption), when the language system is impaired by DES, the patient can maintain the task goal, but only the motor task is performed; while when the motor system is disturbed, the patient is still able to maintain the task goal, but only the naming task is achieved. Interestingly, the third level of DES disruption can be illustrated by the impairment of dlPFC as an entry window to a complex inter-system integration: the brain has difficulties to coordinate its networks and the patient cannot achieve dual-task anymore, he/she is only able to perform each task separately but not conjointly (**Figure 1**).

This three-level model of DES functional disruption offers several clinical and neuro-scientific advantages. From a surgical perspective, it allows the optimal selection of tasks during surgery and how to administrate them (order, sequence, combination) throughout the resection, based upon the better understanding of DES mechanisms. Indeed, beyond the symptom itself, these mechanisms of neural disruption can be deciphered into the operating theater, enabling a more accurate interpretation of the awake mapping in real-time to make the best decision to optimize the tumor removal while preserving a high level of quality of life—as defined by the patient him(her)self before surgery, according to his/her needs, job, hobbies and lifestyle (Herbet and Duffau, 2019). In other words, this model can be helpful to plan awake surgery in order not only to avoid severe permanent deteriorations as hemiplegia or aphasia but also to spare networks subserving higher-order cognitive and emotional functions, as well as their dynamic interactions, to preserve behavior and to enable a return to an active familial, social and professional life. From a fundamental perspective, this model permits a refined analysis of DES-derived responses to investigate the human connectome uniquely. Indeed, findings collected during transient network interferences induced by DES provide unprecedented direct access into the actual neural dynamics.

REUNIFYING CLINICAL DES BRAIN MAPPING AND BASIC NEUROSCIENCES

Arguments supporting that DES mapping in tumor surgery allows valid conclusions on the localization of human brain functions have already been detailed (Duffau, 2011). Furthermore, DES offers two major interests in comparison with the commonly used FNI to study the human connectome. First,

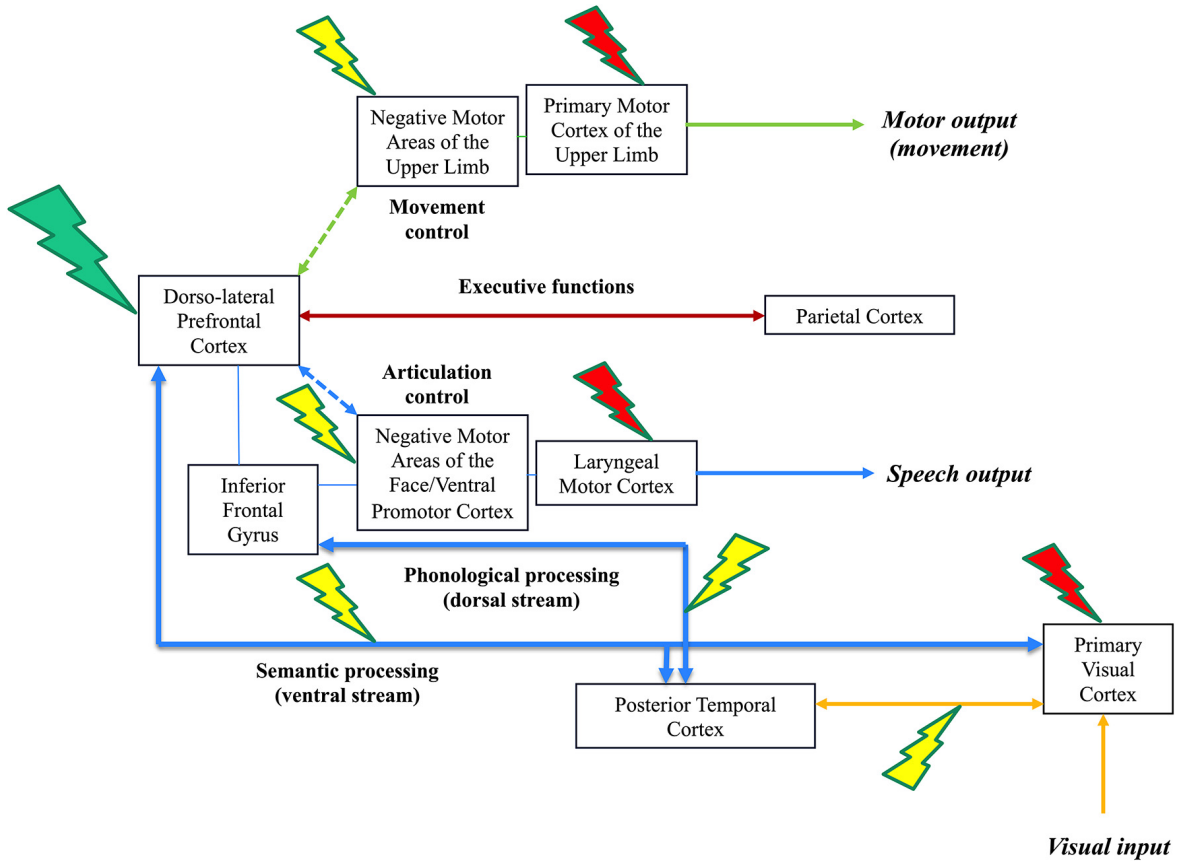

FIGURE 1 | Illustration of the three-level model of direct electrostimulation (DES) neural disruption: red lightning bolt symbolizes the first level (input/output disruption), yellow lightning bolt symbolizes the second level (within-network disruption) and green lightning bolt symbolizes the third level (inter-network disruption). This is a schematic representation of the visual system (lower, connectivity in yellow), speech and language system (lower, connectivity in blue), executive functions system (middle, connectivity in brown) and motor system (upper, connectivity in green) in the left hemisphere of an awake patient who performs a dual-task associating picture naming and movement of the right upper limb. DES of the primary visual system induces phosphenes (1st level, a red lightning bolt at the level of the optic tracts and/or primary visual cortex), while DES of the occipito-temporal connections induces visual hemiagnosia [2nd level, a yellow lightning bolt over the posterior inferior longitudinal fasciculus (ILF)]. In parallel, the patient can continue to move the right upper limb. In the speech and language system, DES of the laryngeal motor cortex elicits involuntary vocalization (1rst level, red lightning); DES of the ventral premotor cortex and frontoparietal articulatory loop (not shown) elicits speech apraxia/arrest (anarthria); while DES of the dorsal phonological route induces phonemic paraphasia and DES of the ventral semantic route induces semantic paraphasia (2nd level, red lightning). Of note, stimulating both dorsal and semantic streams may generate complete anomia. In parallel, the patient can continue to move the right upper limb. In the motor system, DES of the primary motor cortex of the upper limb and its corticospinal tracts (motor execution, output) causes an involuntary movement (1st level, red lightning); DES of the negative motor cortex (movement control) and its fibers (not shown) generates an arrest of movement (2nd level, yellow lightning). In parallel, the patient can continue to perform the picture naming task. During DES of the dorsolateral prefrontal cortex (integrative hub), the brain is not able to coordinate its networks (including the frontoparietal connections involved in the executive functions and then the goal maintenance), the patient cannot achieve dual-task anymore: the patient is only capable to perform each task separately, naming or upper limb movement, but not both simultaneously (3rd level, green lightning).

although functional MRI is an indirect reflection of the areas involved in a given brain function, without the possibility to distinguish those participating vs. those essential to this function, stimulation mapping allows the identification of the structures critical for neural functions—i.e., generating permanent behavioral consequences if damaged (Sarubbo et al., 2020). Second, whereas tractography enables a reconstruction of the anatomical trajectory of white matter tracts using biostatistics modeling, axonal DES is capable to give direct information regarding the function of the subcortical connectivity (Duffau, 2015). Consequently, in light of the three-level model of DES-neural disruption, the bridge between surgical DES mapping and fundamental neurosciences can be reinforced, by translating the findings issued from brain-damaged patients to improved knowledge of the physiology of the human central nervous system, and by proposing new models of dynamic connectivity (Herbet and Duffau, 2020).

In a first step, structural-functional correlations gained from intraoperative DES and neuropsychological assessments provided original insights into the neurobiology of function-specific network. For example, regarding movement and visual function, DES of the output primary motor cortex and pyramidal tracts evokes involuntary motor responses, and DES of the optic tracts or primary visual cortex provokes basic positive

responses (e.g., phosphenes) or more complex visual illusion (e.g., metamorphopsia), respectively (1st level; Ius et al., 2011). At a higher level, DES of the so-called "negative motor areas" and its subcortical pathways (such as the frontostriatal tract) generates arrest of ongoing movement, possibly with interruption of complex bimanual coordination due to a disruption of the network devoted to movement control (2nd level; Rech et al., 2019). Similarly, DES of the posterior inferior longitudinal fasciculus (ILF) that connects the visual cortex and fusiform gyrus may generate visual hemiagnosia during a picture-naming task because of disturbances of the object recognition abilities (2nd level; Fernández Coello et al., 2013). At the most integrated level, DES of plurimodal hubs, such as dlPFC implicated in executive functions, may prevent to perform movement and visual picture naming task simultaneously (3rd level, inter-system disruption; Herbet and Duffau, 2020).

Concerning speech and language, DES of the laryngeal motor cortex and its projection fibers induces uncontrolled vocalization (1st level; Dichter et al., 2018); within-system DES of the ventral premotor cortex and articulatory loop generates anarthria or DES of the basal temporal areas and anterior ILF causes lexical access deficit (2nd level; Herbet et al., 2016b); while DES of the prefrontal cortex and superior longitudinal fasciculus (SLF) may elicit control disturbances in switching from one language to another one in multilingual patients—due to disruption between executive system and each subnetwork sustaining each language (3rd level; Moritz-Gasser and Duffau, 2009). Here, the goal is not to exhaustively review the neural foundations of every functional system that have previously been pooled in original probabilistic atlases of essential cortico-subcortical structures, based upon DES-driven responses in awake patients (Tate et al., 2014; Sarubbo et al., 2020). Rather, the main purpose is to highlight the multilevel organization of segregated and interactive networks revealed by DES. Indeed, taken as a whole, these original data have recently led to the proposal of a meta-networking theory of brain functions, relying on transitory changes of relationship within and across neural circuits, resulting in a perpetual succession of new equilibrium states reflecting moment-to-moment environmental demands—as well as to more long-lasting modifications of network properties, including use-dependent neuroplasticity (Herbet and Duffau, 2020).

A step forward, in this meta-networking view of brain processing, potentiating neuroplastic dynamics can sustain not only the human propensity to learn complex abilities and to be creative but also the brain capacity to compensate for neural loss after cerebral insult. An atlas of neuroplasticity has been elaborated based on neurological recovery (or not) following brain tumors surgery (Herbet et al., 2016a). Interestingly, a parallel can be made between this atlas, which identified structures with low, intermediate, and high potential of functional compensation, and the 3-level model of intraoperative DES neural disruption. Indeed, input and output neural networks that generate "positive" responses when stimulated correspond to the main foundations of the "minimal common brain," namely, the structures where compensatory mechanisms are the most limited (Ius et al., 2011). In the event of injury, the risk of a severe and irrevocable deficit, such as hemiplegia or hemianopia, is very high. Interestingly, the interindividual variability of these structures is very low (Duffau, 2017). Concerning the structures where DES causes a specific disturbance due to a within-specialized network disruption (second level), the potential of recovery is higher, especially for cortical areas. Although a lesion of associative pathways (e.g., surgical injury of long-distance white matter bundles) has a high risk to generate a permanent disconnection syndrome, such as conduction aphasia if the left arcuate fasciculus is damaged, hemineglect if the right SLF is damaged, or semantic disorders if the IFOF is damaged (Herbet et al., 2015c), a focal cortical lesion might be (at least partly) compensated by the rest of the distributed network. Recovery is nonetheless possible if the highly integrative cortical hubs, such as the dlPDF, and their subcortical connectivity have been preserved, resulting in more subtle deficits, regardless the domain—e.g., difficulties in complex bimanual movement (Rech et al., 2014); increase of reaction time for lexical access; slight impairment of working memory (du Boisgueheneuc et al., 2006); or mild impairment of mentalistic processes such as subjective empathy (Herbet et al., 2015b). These mechanisms of cerebral reallocation are possible in a connectomal account of neural distribution, explaining recovery following resection of tumors within regions deemed inoperable in a rigid localizationist framework, as Broca's area or Wernicke's area (Duffau, 2014). Of note, the interindividual anatomo-functional variability of these structures is high (Duffau, 2017). Finally, regarding the third level, disruption of the integrative process between conation, cognition and emotion may lead to more complex behavioral changes, impacting, for example, the personality (at the extreme with a risk to generate various neurological or psychiatric diseases, possibly due to the decompensation of borderline traits) or creativity (Herbet and Duffau, 2020). Therefore, beyond the simplistic standard neurological examination, even an extensive neurocognitive evaluation performed according to the current guidelines could not be sensitive enough to objectively reveal such an unbalance in the metanetwork. More sophisticated behavioral tasks should be developed to assess more subtly brain-damaged patients with neuropsychological performances wrongly considered as "normal."

LIMITATIONS

This study may have some limitations.

First, DES is an invasive technique, then available in the limited clinical situation. However, to prevent any deleterious effects, DES consist of stimulating the surface of the exposed brain, conversely to electro-microstimulation (EMS) used in animals, which activates neurons by applying a current through microelectrodes implanted in the parenchyma. This is the reason why EMS became the preferred method for modulating neural activity and demonstrating functional properties in animal experiments (Histed et al., 2013). Therefore, in humans, a combination of DES with non-invasive stimulation mapping method as transcranial magnetic stimulation (TMS) may be of great interest. Nonetheless, in a recent study which compared navigated repetitive TMS with intraoperative DES in brain tumor patients, TMS had only 81.6% sensitivity, 59.6% specificity, 78.5%

positive predictive value and 64.1% negative predictive value for preoperative language mapping (Motomura et al., 2020), confirming that DES remains the gold standard.

Second, it is unclear how the extent of the whole-brain network is inhibited by local block for axon using DES. Nevertheless, if the repetitive stimulation is <200 Hz, γ-aminobutyric acid-related inhibition seems to prevent the propagation of electrostimulation beyond the first synapse (Logothetis et al., 2010): thus, DES may inform us about its effect on a network's functional status when only a part of this network is stimulated.

Third, data gained from DES come from the pathological model, with a possibility that reorganization has already occurred in the brain network of tumor patients, especially with low-grade glioma. However, gathering many patients' data into the database can compensate these potential confounding factors: therefore, DES findings in glioma patients have been shown to represent a valid model for exploring normal brain functions (Herbet and Duffau, 2020). Indeed, in a recent functional atlas of critical neural circuits based upon 1,821 DES responses in 256 glioma patients, the overall distribution of the functional responses was topographically congruent with the current literature using FNI (Sarubbo et al., 2020), including large meta-analysis involving healthy human subject (Zhang et al., 2010; Thiebaut de Schotten et al., 2011). Of note, to make full use of the original findings provided by DES, very detailed knowledge of cortical and subcortical anatomy is needed for the precise stimulation mapping (Vincent et al., 2016).

CONCLUSIONS AND PERSPECTIVES

DES is a reliable tool to map brain functions, complementary to FNI, since providing unique data regarding the indispensability of cerebral structures, especially concerning the neural connectivity. These original findings can be translated from brain-damaged patients to the modeling of the physiological functioning of nervous system processes. The next step is to combine intraoperative neurophysiology, i.e., DES and electrocorticographic recording of cortico-cortical and axonal-cortical evoked potentials (to refine the understanding of DES neural disruption; Vincent et al., 2020), with pre- and post-operative optimized cognitive and behavioral assessments as well as with longitudinal structural and FNI, to decipher the pathophysiological mechanisms underlying neuroplasticity. Preliminary serial multimodal studies evidenced morphometric (Almairac et al., 2018) and functional reorganization of the human connectome, notably with contralesional homotopic compensation (Vassal et al., 2017), and with changes of the connectivity between the cortex, the deep gray nuclei and the cerebellum (Boyer et al., 2016). Beyond brain mapping, perspectives could be to actively modulate such dynamic intra-system and inter-system integration using non-invasive neural electrostimulation, particularly by using TMS.

AUTHOR CONTRIBUTIONS

HD conceived the idea and wrote the manuscript.

REFERENCES

Almairac, F., Duffau, H., and Herbet, G. (2018). Contralesional macrostructural plasticity of the insular cortex in patients with glioma: a VBM study. *Neurology* 91, e1902–e1908. doi: 10.1212/wnl.0000000000006517

Boyer, A., Deverdun, J., Duffau, H., Le Bars, E., Molino, F., Menjot de Champfleur, N., et al. (2016). Longitudinal changes in cerebellar and thalamic spontaneous neuronal activity after wide-awake surgery of brain tumors: a resting-state fMRI study. *Cerebellum* 15, 451–465. doi: 10.1007/s12311-015-0709-1

Dichter, B. K., Breshears, J. D., Leonard, M. K., and Chang, E. F. (2018). The control of vocal pitch in human laryngeal motor cortex. *Cell* 174, 21.e9–31.e9. doi: 10.1016/j.cell.2018.05.016

du Boisgueheneuc, F., Levy, R., Volle, E., Seassau, M., Duffau, H., Kinkingnehun, S., et al. (2006). Functions of the left superior frontal gyrus in humans: a lesion study. *Brain* 129, 3315–3328. doi: 10.1093/brain/awl244

Duffau, H. (2011). Do brain tumours allow valid conclusions on the localisation of human brain functions? *Cortex* 47, 1016–1017. doi: 10.1016/j.cortex.2010.11.010

Duffau, H. (2014). The huge plastic potential of adult brain and the role of connectomics: new insights provided by serial mappings in glioma surgery. *Cortex* 58, 325–337. doi: 10.1016/j.cortex.2013.08.005

Duffau, H. (2015). Stimulation mapping of white matter tracts to study brain functional connectivity. *Nat. Rev. Neurol.* 11, 255–265. doi: 10.1038/nrneurol.2015.51

Duffau, H. (2017). A two-level model of interindividual anatomo-functional variability of the brain and its implications for neurosurgery. *Cortex* 86, 303–313. doi: 10.1016/j.cortex.2015.12.009

Duffau, H. (2018). Diffuse low-grade glioma, oncological outcome and quality of life: a surgical perspective. *Curr. Opin. Oncol.* 30, 383–389. doi: 10.1097/cco.0000000000000483

Duffau, H., Moritz-Gasser, S., and Mandonnet, E. (2014). A re-examination of neural basis of language processing: proposal of a dynamic hodotopical model from data provided by brain stimulation mapping during picture naming. *Brain Lang.* 131, 1–10. doi: 10.1016/j.bandl.2013.05.011

Fernández Coello, A., Duvaux, S., De Benedictis, A., Matsuda, R., and Duffau, H. (2013). Involvement of the right inferior longitudinal fascicle in visual hemiagnosia: a brain stimulation mapping study. *J. Neurosurg.* 118, 202–205. doi: 10.3171/2012.10.jns12527

Herbet, G., and Duffau, H. (2020). Revisiting the functional anatomy of the human brain: toward a meta-networking theory of cerebral functions. *Physiol. Rev.* 100, 1181–1228. doi: 10.1152/physrev.00033.2019

Herbet, G., and Duffau, H. (2019). "Awake craniotomy and bedside cognitive mapping in neurosurgery," in *Neurosurgical Neuropsychology*, eds C. M. Pearson, E. Ecklund-Johnson and S. D. Gale (Academic Press), 113–138. doi: 10.1016/B978-0-12-809961-2.00008-4

Herbet, G., Lafargue, G., Moritz-Gasser, S., Bonnetblanc, F., and Duffau, H. (2015a). Interfering with the neural activity of mirror-related frontal areas impairs mentalistic inferences. *Brain Struct. Funct.* 220, 2159–2169. doi: 10.1007/s00429-014-0777-x

Herbet, G., Lafargue, G., Moritz-Gasser, S., Menjot de Champfleur, N., Costi, E., Bonnetblanc, F., et al. (2015b). A disconnection account of subjective empathy impairments in diffuse low-grade glioma patients. *Neuropsychologia* 70, 165–176. doi: 10.1016/j.neuropsychologia.2015.02.015

Herbet, G., Latorre, J. G., and Duffau, H. (2015c). The role of cerebral disconnection in cognitive recovery after brain damage. *Neurology* 84, 1390–1391. doi: 10.1212/wnl.0000000000001453

Herbet, G., Maheu, M., Costi, E., Lafargue, G., and Duffau, H. (2016a). Mapping neuroplastic potential in brain-damaged patients. *Brain* 139, 829–844. doi: 10.1093/brain/awv394

Herbet, G., Moritz-Gasser, S., Boiseau, M., Duvaux, S., Cochereau, J., and Duffau, H. (2016b). Converging evidence for a cortico-subcortical network mediating lexical retrieval. *Brain* 139, 3007–3021. doi: 10.1093/brain/aww220

Histed, M. H., Ni, A. M., and Maunsell, J. H. R. (2013). Insights into cortical mechanisms of behavior from microstimulation experiments. *Prog. Neurobiol.* 103, 115–130. doi: 10.1016/j.pneurobio.2012.01.006

Ius, T., Angelini, E., Thiebaut de Schotten, M., Mandonnet, E., and Duffau, H. (2011). Evidence for potentials and limitations of brain plasticity using an atlas of functional resectability of WHO grade II gliomas: towards a "minimal common brain". *NeuroImage* 56, 992–1000. doi: 10.1016/j.neuroimage.2011.03.022

Kunieda, T., Yamao, Y., Kikuchi, T., and Matsumoto, R. (2015). New approach for exploring cerebral functional connectivity: review of cortico-cortical evoked potential. *Neurol. Med. Chir.* 55, 374–382. doi: 10.2176/nmc.ra.2014-0388

Logothetis, N. K., Augath, M., Murayama, Y., Rauch, A., Sultan, F., Goense, J., et al. (2010). The effects of electrical microstimulation on cortical signal propagation. *Nat. Neurosci.* 13, 1283–1291. doi: 10.1038/nn.2631

Mandonnet, E., Winkler, P. A., and Duffau, H. (2010). Direct electrical stimulation as an input gate into brain functional networks: principles, advantages and limitations. *Acta Neurochir.* 152, 185–193. doi: 10.1007/s00701-009-0469-0

Moritz-Gasser, S., and Duffau, H. (2009). Cognitive processes and neural basis of language switching: proposal of a new model. *Neuroreport* 20, 1577–1580. doi: 10.1097/wnr.0b013e328333907e

Moritz-Gasser, S., Herbet, G., and Duffau, H. (2013). Mapping the connectivity underlying multimodal (verbal and non-verbal) semantic processing: a brain electrostimulation study. *Neuropsychologia* 51, 1814–1822. doi: 10.1016/j.neuropsychologia.2013.06.007

Motomura, K., Takeuchi, H., Nojima, I., Aoki, K., Chalise, L., Iijima, K., et al. (2020). Navigated repetitive transcranial magnetic stimulation as preoperative assessment in patients with brain tumors. *Sci. Rep.* 10:9044. doi: 10.1038/s41598-020-65944-8

Ojemann, G., Ojemann, J., Lettich, E., and Berger, M. (1989). Cortical language localization in left, dominant hemisphere. An electrical stimulation mapping investigation in 117 patients. *J. Neurosurg.* 71, 316–326. doi: 10.3171/jns.1989.71.3.0316

Penfield, W. (1954). Mechanisms of voluntary movement. *Brain* 77, 1–17. doi: 10.1093/brain/77.1.1

Penfield, W., and Boldrey, E. (1937). Somatic motor and sensory representation in the cerebral cortex of man as studied by electrical stimulation. *Brain* 60, 389–443. doi: 10.1093/brain/60.4.389

Rech, F., Herbet, G., Gaudeau, Y., Mézières, S., Moureau, J. M., Moritz-Gasser, S., et al. (2019). A probabilistic map of negative motor areas of the upper limb and face: a brain stimulation study. *Brain* 142, 952–965. doi: 10.1093/brain/awz021

Rech, F., Herbet, G., Moritz-Gasser, S., and Duffau, H. (2014). Disruption of bimanual movement by unilateral subcortical electrostimulation. *Hum. Brain Mapp.* 35, 3439–3445. doi: 10.1002/hbm.22413

Sarubbo, S., Tate, M., De Benedictis, A., Merler, S., Moritz-Gasser, S., Herbet, G., et al. (2020). Mapping critical cortical hubs and white matter pathways by direct electrical stimulation: an original functional atlas of the human brain. *NeuroImage* 205:116237. doi: 10.1016/j.neuroimage.2019.116237

Tate, M. C., Herbet, G., Moritz-Gasser, S., Tate, J. E., and Duffau, H. (2014). Probabilistic map of critical functional regions of the human cerebral cortex: broca's area revisited. *Brain* 137, 2773–2782. doi: 10.1093/brain/awu168

Thiebaut de Schotten, M., Ffytche, D. H., Bizzi, A., Dell'Acqua, F., Allin, M., Walshe, M., et al. (2011). Atlasing location, asymmetry, and inter-subject variability of white matter tracts in the human brain with MR diffusion tractography. *NeuroImage* 54, 49–59. doi: 10.1016/j.neuroimage.2010.07.055

Vassal, M., Charroud, C., Deverdun, J., Le Bars, E., Molino, F., Bonnetblanc, F., et al. (2017). Recovery of functional connectivity of the sensorimotor network after surgery for diffuse low-grade gliomas involving the supplementary motor area. *J. Neurosurg.* 126, 1181–1190. doi: 10.3171/2016.4.jns152484

Vincent, M. A., Bonnetblanc, F., Mandonnet, E., Boyer, A., Duffau, H., and Guiraud, D. (2020). Measuring the electrophysiological effects of direct electrical stimulation after awake brain surgery. *J. Neural. Eng.* 17:016047. doi: 10.1088/1741-2552/ab5cdd

Vincent, M. A., Rossel, O., Hayashibe, M., Herbet, G., Duffau, H., Guiraud, D., et al. (2016). The difference between electrical microstimulation and direct electrical stimulation—towards new opportunities for innovative functional brain mapping? *Rev. Neurosci.* 27, 231–258. doi: 10.1515/revneuro-2015-0029

Yamao, Y., Matsumoto, R., Kunieda, T., Arakawa, Y., Kobayashi, K., Usami, K., et al. (2014). Intraoperative dorsal language network mapping by using single-pulse electrical stimulation. *Hum. Brain Mapp.* 35, 4345–4361. doi: 10.1002/hbm.22479

Zhang, Y., Zhang, J., Oishi, K., Faria, A. V., Jiang, H., Li, K., et al. (2010). Atlas-guided tract reconstruction for automated and comprehensive examination of the white matter anatomy. *NeuroImage* 52, 1289–1301. doi: 10.1016/j.neuroimage.2010.05.049

Conflict of Interest: The author declares that the research was conducted in the absence of any commercial or financial relationships that could be construed as a potential conflict of interest.

frontiers in Human Neuroscience

REVIEW
published: 07 December 2020
doi: 10.3389/fnhum.2020.611291

Electrical Stimulation Mapping of Brain Function: A Comparison of Subdural Electrodes and Stereo-EEG

Krista M. Grande[1], *Sarah K. Z. Ihnen*[1] *and Ravindra Arya*[1,2]*

[1]Division of Neurology, Comprehensive Epilepsy Center, Cincinnati Children's Hospital Medical Center, Cincinnati, OH, United States, [2]Department of Pediatrics, University of Cincinnati College of Medicine, Cincinnati, OH, United States

Despite technological and interpretative advances, the non-invasive modalities used for pre-surgical evaluation of patients with drug-resistant epilepsy (DRE), fail to generate a concordant anatomo-electroclinical hypothesis for the location of the seizure onset zone in many patients. This requires chronic monitoring with intracranial electroencephalography (EEG), which facilitates better localization of the seizure onset zone, and allows evaluation of the functional significance of cortical regions-of-interest by electrical stimulation mapping (ESM). There are two principal modalities for intracranial EEG, namely subdural electrodes and stereotactic depth electrodes (stereo-EEG). Although ESM is considered the gold standard for functional mapping with subdural electrodes, there have been concerns about its utility with stereo-EEG. This is mainly because subdural electrodes allow contiguous sampling of the dorsolateral convexity of cerebral hemispheres, and permit delineation of the extent of eloquent functional areas on the cortical surface. Stereo-EEG, while having relatively sparse sampling on the cortical surface, offers the ability to access the depth of sulci, mesial and basal surfaces of cerebral hemispheres, and deep structures such as the insula, which are largely inaccessible to subdural electrodes. As stereo-EEG is increasingly the preferred modality for intracranial monitoring, we find it opportune to summarize the literature for ESM with stereo-EEG in this narrative review. Emerging evidence shows that ESM for defining functional neuroanatomy is feasible with stereo-EEG, but probably requires a different approach for interpretation and clinical decision making compared to ESM with subdural electrodes. We have also compared ESM with stereo-EEG and subdural electrodes, for current thresholds required to evoke desired functional responses vs. unwanted after-discharges. In this regard, there is preliminary evidence that ESM with stereo-EEG may be safer than ESM with subdural grids. Finally, we have highlighted important unanswered clinical and scientific questions for ESM with stereo-EEG in the hope to encourage future research and collaborative efforts.

Keywords: functional brain mapping, electrical cortical stimulation, intracranial EEG, epilepsy surgery, drug-resistant epilepsy (DRE)

OPEN ACCESS

Edited by:
Riki Matsumoto,
Kobe University, Japan

Reviewed by:
Kiyohide Usami,
Kyoto University, Japan
Cristian Donos,
University of Bucharest, Romania
Rei Enatsu,
Sapporo Medical University, Japan

***Correspondence:**
Ravindra Arya
ravindra.arya@cchmc.org

***Specialty section**:*
This article was submitted to Brain Imaging and Stimulation, a section of the journal Frontiers in Human Neuroscience

Received: *28 September 2020*
Accepted: *16 November 2020*
Published: *07 December 2020*

Citation:
Grande KM, Ihnen SKZ and Arya R (2020) Electrical Stimulation Mapping of Brain Function: A Comparison of Subdural Electrodes and Stereo-EEG. Front. Hum. Neurosci. 14:611291. doi: 10.3389/fnhum.2020.611291

INTRODUCTION

A behavioral response to direct electrical stimulation of the human brain was first reported in 1874 from Cincinnati when Bartholow stimulated visible brain tissue in a 30-years-old woman whose parietal bone was eroded by a scalp epithelioma (Bartholow, 1874). He most likely stimulated the left supplementary sensorimotor area, and observed: "...arm was thrown out, the fingers extended, and the leg was projected forward. The muscles of the neck were thrown into action, and the head was strongly defected to the right". Subsequent pioneering work of Penfield, Ojemann, and others, generated novel information about functional neuroanatomy and established electrical stimulation mapping (ESM) as the gold-standard for pre-surgical localization of eloquent cortical areas (Penfield and Boldrey, 1937; Penfield and Jasper, 1954; Whitaker and Ojemann, 1977; Ojemann and Mateer, 1979; Jayakar et al., 2014). Although early ESM studies allowed some neuroanatomic generalizations based on convergence with lesion data, significant inter-individual variability in the location and extent of eloquent cortical regions was also realized (Ojemann, 1979; Ojemann et al., 2003). This variability in functional anatomy is even more relevant in pediatric patients and those with developmental neuropathology, which may be associated with structural distortion and/or altered plasticity of the functional neuronal networks (Duchowny et al., 1996). Therefore, ESM is necessary for accurate pre-surgical localization of functional areas on an individual basis.

Functional ESM is especially important for patients with drug-resistant epilepsy (DRE) who are being evaluated for neurosurgical treatment. The overarching goal of epilepsy surgery is to ensure long-term seizure freedom and avoid or minimize postoperative neurological deficits. Thus, in preparation for epilepsy surgery, a multi-modal approach is used to develop a patient-specific hypothesis for the location of the seizure onset zone and determine the functional significance of adjacent cortical regions, initially by using several non-invasive tests. However, these non-invasive modalities may not always converge on a single location of the seizure-onset zone and have a limited spatial resolution for defining functional neuroanatomy. Therefore, chronic intracranial electroencephalography (EEG) is required in several DRE patients and offers superior sensitivity for localization of seizure-onset zone mainly because of a higher signal-to-noise ratio compared to scalp EEG (Jayakar et al., 2016). Intracranial EEG also allows the ability to perform ESM by applying small amounts of electrical currents to the same recording arrays and observing behavioral responses. This facilitates the characterization of the functional anatomy of the cortical regions-of-interest, using the principle discovered by Bartholow that electrical brain stimulation may elicit consistent and observable behavioral responses (**Table 1**).

There are two principal modalities for intracranial EEG including subdural electrodes (SDE) and stereo-EEG (SEEG). Although SEEG was developed in the 1960s by Bancaud, Talairach, and others, it has made a resurgence in the last decade in the United States (**Figure 1**), probably due to advances in neuroimaging and robotics resulting in safer and more precise electrode implantation. A recent Medicare/Medicaid study showed over 1.5 times increase in the use of SEEG as the preferred intracranial modality from 2000 to 2016 (Abou-Al-Shaar et al., 2018). SEEG has been shown to be safer than SDE, with the overall incidence of surgical complications being 0.9–1.7% with SEEG compared to 1.5–4.8% with SDE in large meta-analyses (Arya et al., 2013; Mullin et al., 2016). Also, there is emerging evidence for equivalent seizure outcomes after epilepsy surgery planned with SEEG or SDE (Young et al., 2018; Tandon et al., 2019).

However, compared to SDE which allows contiguous sampling from the dorsolateral convexity of the cerebral hemispheres, SEEG lacks cortical surface contiguity but allows sampling from deeper cortices, such as insula or depth of sulci, and medial and basal surfaces of cerebral hemispheres, which have minimal or no access with SDE (**Figure 2**). Given the increasing use of SEEG and concerns about the ability to perform functional mapping due to relatively sparse sampling on the cerebral cortical surface, there is a need to consolidate available information on ESM with SEEG to compare and contrast with SDE ESM (Isnard et al., 2018). Furthermore, although ESM has been performed both intra- and extra-operatively, challenges with awake craniotomy particularly for language testing which requires patient cooperation, severely limit the use of intra-operative ESM in pediatric practice. Therefore, this narrative review will attempt to summarize the evidence for extra-operative ESM with SEEG, compare ESM with SEEG and SDE with a focus on pediatric epilepsy surgery, and will highlight knowledge gaps and potential avenues for future research.

PROCEDURE

ESM consists of passing small currents through surgically implanted intracranial electrodes and recording behavioral and electrographic responses. Extra-operative ESM is a time and resource-intensive procedure, requiring one or more sessions of several hours each, sometimes spread over multiple days.

Pre-medication

Some providers choose to administer an anti-seizure medication before ESM to decrease the risks of after-discharges (AD's) and iatrogenic seizures. However, there is no consensus on this practice, with scant data on its safety and effectiveness. A retrospective pediatric study found that the incidence of ESM-induced seizures was 23% in 40 patients pre-medicated with fosphenytoin, compared to 43% in 82 non-pre-medicated patients (Arya et al., 2018). However, the current threshold for eliciting language responses in the temporal lobe was increased. We could not find any similar study on pre-medication before SEEG ESM, perhaps because eliciting a habitual seizure is sometimes the desired endpoint of SEEG ESM (see later). At our center, we do not routinely pre-medicate patients before SEEG ESM, but have a rescue medication available during the procedure.

TABLE 1 | Selected landmarks in the history of electrical stimulation mapping of brain function with intracranial electroencephalography (EEG).

Year(s)	Investigator	Significance
1809	Luigi Rolando	Used a voltaic pile and bimetallic electrodes to stimulate the cortex of live animals to consistently produce limb movement.
1848	Gustav Fritsch and Eduard Hitzig	Applied electricity to the exposed cerebral cortex of awake dogs to demonstrate the function of the motor strip.
1874	Roberts Bartholow	Applied electrical stimulation to the human cortex and observed a unique pattern of movements.
1876	David Ferrier	Stimulated the cortex of dogs and monkeys and created a map of functions across the cortex.
1888	Victor Horsely	First to use electrocortical stimulation intraoperatively for localization of the seizure onset zone.
1909	Harvey Cushing	Performed the first awake craniotomy.
1937	Wilder Penfield and Edwin Boldrey	Described the cortical sensorimotor homunculi.
1950s	Wilder Penfield and Herbert Jasper	Pioneered electrocorticography recording with electrical stimulation mapping as part of the "Montreal Procedure" for surgical treatment of epilepsy.
1950s	Robert Hayne and Russell Meyers	Published the first report on stereotactically implanted EEG electrodes in humans with epilepsy.
1950s	Jean Talairachand Jean Bancaud	Developed SEEG and conceptualized the "epileptogenic zone".
1980s	George Ojemann	Showed importance of individual functional mapping for predicting post-operative function.

SEEG, stereotactic electroencephalography. This list is not exhaustive.

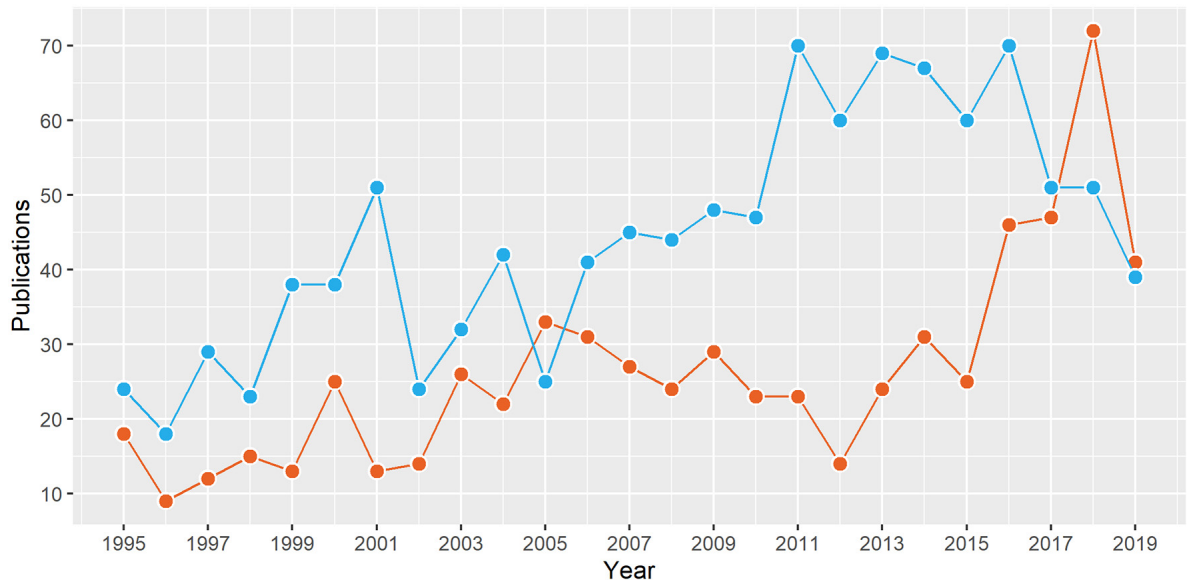

FIGURE 1 | The number of publications from North America on stereotactic electroencephalography (SEEG; red) and subdural electrodes (blue) in the last 25 years. Data from structured PubMed queries ("Electroencephalography"[Mesh]) and "Stereotaxic Techniques"[Mesh] ("Electroencephalography"[Mesh] and "subdural").

Stimulation Settings

Despite being the gold-standard for pre-surgical localization of cortical functions, ESM remains insufficiently standardized, with heterogeneity in stimulation protocols among different centers (Hamberger et al., 2014). For extra-operative ESM, reasonable settings include pulse widths of 0.2–0.3 ms (range 0.1–1 ms), frequencies of 50 or 60 Hz (1–100 Hz), train durations of 3–5 s (2–10 s), and current amplitudes of 1–20 mA. In terms of current strength, a common practice is to start at 0.5–2 mA and increase by 0.5–1 mA, until a functional response, evolving AD's, or a seizure is observed, or until the instrument limit is reached. Because of differences in the response properties of various brain regions and different patients, which cannot necessarily be predicted based on clinical factors (Corley et al., 2017), stimulation at each target site should begin at a low current intensity and be optimized. The train duration is dependent on the task. Shorter durations are commonly used for motor mapping, while longer durations are preferred for language mapping to allow sufficient time for the patient to undergo multiple trials of the language task.

The choice of pulse frequency often depends on the need to avoid interaction with the frequency of the electrical mains and

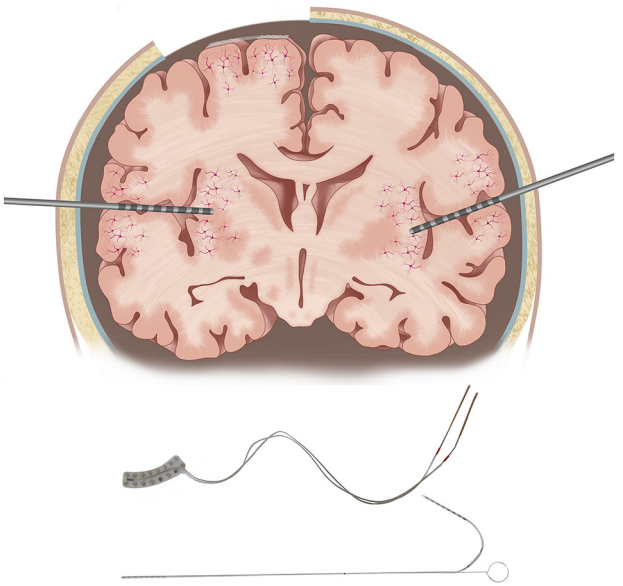

FIGURE 2 | Some important differences between subdural electrodes (SDE) and SEEG electrodes. SDE requires a craniotomy for implantation, while SEEG electrodes are implanted through burr holes. SDE cover the crowns of gyri nearly perpendicular to the dendrites of pyramidal cells, while SEEG electrodes pass at various angles concerning pyramidal cells, through both gray and white matter. Illustrations of an SDE grid and an SEEG electrode are provided in the lower panel.

is either 50 Hz (in the US) or 60 Hz (in Europe). However, there is some evidence that stimulation of SDE at lower frequencies may result in reduced incidence of AD's (Zangaladze et al., 2008). In pediatric patients, higher current densities attained using higher current strengths and/or wider pulse widths may be necessary to obtain responses, particularly in children with malformations of cortical development (Chitoku et al., 2001; Sala et al., 2002). Higher functional thresholds in younger children may also be partly explained by a relatively greater proportion of small unmyelinated fibers (Jayakar et al., 1992). Protocols that alternate increases in current intensity with increases in pulse width, called *dual-increment paradigms*, may increase the likelihood of achieving sufficient stimulation, and therefore improve the sensitivity of ESM in the pediatric population (Jayakar et al., 1992).

Intracranial electrodes, whether SDE or SEEG, can be stimulated in a bipolar or unipolar manner. Bipolar stimulation entails the application of recurrent trains of alternating polarity to pairs of often contiguous electrode contacts, whereas unipolar stimulation involves testing a single electrode contact in comparison to a distant reference electrode. Given other settings being constant, the brain volume being electrically stimulated with bipolar stimulation is a function of the distance between the two contacts. Therefore, higher local current densities can be achieved for a given current strength with bipolar stimulation compared to unipolar stimulation (Nathan et al., 1993). We always stimulate in a bipolar fashion.

With SEEG, the stimulation settings are fairly similar to those used with SDE, with two important differences. First,

TABLE 2 | Suggested protocol for electrical stimulation mapping with stereo-EEG based on practice at the Cincinnati Children's Hospital.

Setting	High-frequency stimulation	Low-frequency stimulation
Pulse frequency	50 Hz	1 Hz
Pulse duration	200–300 μs	≤500 μs
Train duration	5 s for language mapping 2–3 s for motor mapping	≤30 s
Current strength	1–8 mA	1–8 mA
Suggested use	Functional mapping	Seizure induction

This table was modified and reproduced with permission from Arya et al. (2019).

although the maximum current used with SDE ESM has varied from 10 to 20 mA, it has been lower (3–8 mA) with SEEG ESM (Trebuchon and Chauvel, 2016; Britton, 2018; Arya et al., 2019, 2020; Cuisenier et al., 2020). The use of lower maximum current with SEEG ESM is based on calculations extrapolated from the estimates of safe current strengths for SDE ESM, and the desire to maintain similar charge density with SEEG and SDE ESM (Shannon, 1992; Britton, 2018). It is estimated that 8 mA stimulation with a 200 μs pulse will result in charge densities of 12.7 $\mu C/cm^2$ with SDE compared to 31.8 $\mu C/cm^2$ with SEEG electrodes (Britton, 2018). However, the maximum current strength for SEEG ESM remains arbitrary, and not based on rigorous clinical or biophysical evidence. Secondly, it is common in SEEG practice to perform low frequency (1 Hz) stimulation with wider pulse durations (0.5 ms) and train duration (up to 30 s; Cossu et al., 2006; Trebuchon and Chauvel, 2016; Britton, 2018). There is a difference of opinion in the literature if low-frequency stimulation with SEEG should be performed to elicit functional responses or to reproduce habitual seizures (Cossu et al., 2006; Cuisenier et al., 2020). In our experience, low-frequency stimulation can only rarely elicit consistent functional responses. However, we found that 1 Hz stimulation was able to reproduce habitual seizures or auras in 4/6 patients. On the other hand, although 50 Hz stimulation resulted in seizures in 5/15 patients, habitual semiology was observed in only 2/5 patients (Arya et al., 2019, 2020). Therefore, at our center, we prefer 50 Hz stimulation for functional mapping, and 1 Hz stimulation to attempt to reproduce habitual seizures (**Table 2**).

Clinical Suggestions

Before starting ESM, it is desirable to plan the sequence of stimulation of different electrodes based on the localization of the seizure-onset zone, and presumptive locations of functional areas (either anatomical or obtained from non-invasive modalities). The guiding principle is that electrode(s) lying in the seizure-onset zone should be stimulated last, and only if it is considered essential to stimulate within the ictal core. With SEEG, we always stimulate from deep to superficial contacts, on individual electrodes. This is probably safer due to the lower risk of seizures on white matter stimulation and obviates the concern that deeper contacts may be refractory after stimulation of the superficial contacts in the cortex, because of preferential orthodromic conduction of the stimulation impulse (Trebuchon and Chauvel, 2016). The issue of bipolar stimulation of electrode contacts

which may be close to each other in 3D, but lie on different SEEG electrodes, is currently unresolved in the literature.

Even with SEEG, it is preferable to stimulate outwards from the presumptive functional areas. For example, it is preferable to first stimulate the electrode(s) lying in the pre-central gyrus when trying to map the primary motor cortex and then move peripherally towards other electrodes to define the boundaries. This is less intuitive with SEEG compared to SDE. For language ESM, we prefer to stimulate the presumptive frontal language sites first, and then the posterior language regions in temporal and parietal lobes, based on some evidence for directional connectivity from temporal to frontal language regions in the perisylvian language network (Matsumoto et al., 2004).

BIOPHYSICS AND NEUROPHYSIOLOGY OF ESM

The pathway from electrical stimulation of the brain tissue up to the observed behavioral response perhaps has two components. The first stage includes conduction of the stimulation current through the brain tissue and the second stage includes the interaction of this propagated current with different cellular elements to perturb their steady-state. This perturbation in the cellular microenvironment likely results in the observed behavioral response. Both of these stages are extremely complex, and our understanding of the involved processes and variables is currently inadequate to evolve a comprehensive biophysical model for ESM. The core assumption of ESM is that an electric current applied to a small, targeted region of cortex will critically alter local network physiology, resulting in an observable and preferably reproducible response, both within and between patients. In general, an applied current is believed to produce a complex summation effect that depends on multiple factors including, but not limited to, stimulation parameters, electrode type, brain region, lesion type, and patient's age. Let us consider some of these variables in the following paragraphs.

Intracranial electrodes are usually made from a platinum-iridium alloy or stainless steel, the former being compatible with 1.5T magnetic resonance imaging (MRI) scanners, and in some cases, even with 3T scanners. SDE consists of 3–5 mm metal discs, having 1–2 mm exposed surfaces, embedded in flexible, biocompatible sheets of polyurethane or Silastic, with 5–10 mm center-to-center distance. In comparison, SEEG electrode contacts are cylinders with 0.8–1.2 mm diameter, 1–3 mm length, and 5–10 mm inter-contact distance. While SDE rest on the cortical surface above pia, SEEG electrodes are implanted at an angle to the cortex along a carefully planned trajectory. Thus, it is possible with SEEG ESM that one contact of the stimulated pair may lie in gray matter and another in the white matter. Therefore, the geometry of current spread during SEEG ESM will have to incorporate differences in electrical properties of gray and white matter (Kombos and Suss, 2009; Koessler et al., 2017).

The electric charge delivered by the current pulse is the product of current strength and pulse width. Charge density, in turn, is the electric charge divided by the surface area of the target. For the typical diameter of an SDE disc of 2.5 mm, the contact area is 4.9 mm^2. Further, for a typical diameter of 0.8 mm and length of 2 mm, the contact area of an SEEG cylinder is 5 mm^2. Hence, while the contact surfaces of SDE and SEEG electrodes are numerically similar, the charge density at identical settings may be different. In homogeneous media, charge density decreases as the square of the distance from the dipole source. However, as discussed above, SEEG may be susceptible to heterogeneity in electrical properties of the surrounding tissues, especially at the gray-white matter junction. Additionally, in the case of SDE, up to 87% of the current may be shunted by the cerebrospinal fluid, thereby decreasing the effectively delivered current (Nathan et al., 1993). This perhaps justifies using lower current strengths for SEEG ESM compared to SDE ESM.

Another consideration about the spread of applied current is whether it is limited to regional volume conduction or does it propagate through axonal connections. Data suggest that both types of spread may exist. In both monkeys and humans, clinically relevant electrical stimulation has been shown to produce consistent local signal changes on optical imaging, dependent on current intensity and duration, with rapid drop-off as a function of the distance from the electrode tip (Haglund et al., 1992, 1993). In primate models with a recording of functional MRI blood-oxygen-level-dependent response paired to electrical micro-stimulation, the distant trans-synaptic spread of induced current after stimulation of V1 and frontal eye field has been demonstrated (Tolias et al., 2005). In clinical studies, the occurrence of AD's remote from the site of stimulation, and recording of cortico-cortical evoked potentials (CCEPs) provide evidence for preferential propagation of brain electrical activity (not necessarily the applied current) along functional pathways interconnecting multiple brain regions (Matsumoto et al., 2004, 2012; Afif et al., 2010; Oya et al., 2017; Malîia et al., 2018; Oane et al., 2020). When functional responses are seen during stimulations associated with distant CCEPs, the localization of the evoked function to the stimulated cortex vs. the remote site with the CCEP remains a dilemma (Afif et al., 2010; Malîia et al., 2018; Oane et al., 2020). However, there is some evidence for functional responses evoked by activation of remote regions, with the stimulation site perhaps serving as an input into the larger functional network (David et al., 2010). Differences in ESM-induced power modulations in high-frequency (70–150 Hz) SEEG spectra at remote sites, during ESM trials with/without speech/language responses provide support for network effects of local stimulation, and supplement the CCEPs data (Perrone-Bertolotti et al., 2020). Therefore, the functional consequences of transient local current delivery to brain tissue during ESM may be relatively widespread. This is particularly relevant with SEEG because it allows direct stimulation of white matter containing axonal pathways (Sarubbo et al., 2020).

The functional consequences of electrical stimulation of a brain area can include physiologic excitation (functional activation), pathologic excitation (AD's and seizures), and inhibition (negative function). This has some regional specificity, for example, a majority of stimulations in the primary

motor cortex result in activation-type behavior, while those in perisylvian language cortices are primarily inhibitory and are revealed when the patient is actively engaged in a linguistic task. There is evidence that stimulation at the same site can evoke both positive and negative responses (Borchers et al., 2012). The larger repertoire of positive responses reported in the literature may reflect the relative ease of eliciting positive responses rather than negative (inhibitory) responses because negative responses can be detected only when the relevant function is engaged during testing. While it is known that axon initial segments and nodes of Ranvier, rather than cell bodies, are the likely sites of direct neuronal activation because of high concentrations of sodium channels resulting in higher electrical excitability (Rattay, 1999); it remains undetermined if regional differences in cell types or neurotransmitter milieu are responsible for variation in the functional responses. How the interaction of the propagated current with cellular elements translates into the diversity of responses, remains unknown at present.

SAFETY CONSIDERATIONS WITH ESM

In this section, we discuss some of the risks associated with ESM. The risks involved in pre-requisite implantation of SDE or SEEG electrodes are beyond the scope of this article and have been reviewed elsewhere (Arya et al., 2013; Mullin et al., 2016).

ESM-Induced Seizures

The most consequential adverse event during ESM is the occurrence of an unwanted seizure. ESM-induced seizures are frightening for the patient and the family and may interrupt functional mapping for several hours. In a study including 122 children undergoing SDE ESM (maximum current 15 mA), seizures were triggered in 35% of patients, with secondary generalization in 12% of seizures (Aungaroon et al., 2017). Urgent administration of an anti-seizure medication was needed in 37% of these seizures. This study also showed that current thresholds for the occurrence of seizures and AD's were significantly associated across the age span and for different lobes of the brain, leading the authors to caution against the continuation of ESM when frequent or evolving AD's are observed. This finding is consistent with an earlier observation that AD's may be followed by seizures even in the cortex which does not produce spontaneous seizures (Blume et al., 2004). To compare, the incidence of iatrogenic seizures has varied from 13% to 30% in patients undergoing high-frequency SEEG ESM (Arya et al., 2019, 2020).

Whether ESM-induced seizures can be used to localize the onset of habitual seizures is currently unclear (Kovac et al., 2016). It is common to attempt to reproduce the habitual semiology with SEEG ESM. In a study including 103 SEEG patients, better seizure outcomes were associated with the inclusion of a higher proportion of sites with ESM-induced seizures in the resection (63% vs. 33% electrodes; Oderiz et al., 2019). At our center, we attempt stimulation of habitual seizures, only in patients who have not had a spontaneous seizure usually by the second week of monitoring.

After-Discharges

AD's are rhythmic runs of spikes and/or sharp waves that are seen after the electrical stimulation has ceased. The incidence of AD's has been well documented for ESM with SDE. In a study of 29 patients, aged 6–39 years, 12% of stimulations elicited AD's (Blume et al., 2004). Importantly, 65% of AD's involved more than just stimulated electrodes. In another study of 20 adults, 14% of stimulations were associated with AD's including even those outside the irritative zone (Gollwitzer et al., 2018). In the large pediatric study referred to above, AD's were seen in 77% of patients (Aungaroon et al., 2017). However, the incidence of AD's with SEEG ESM has been sparsely reported. Our experience suggests it is probably similar to that with SDE ESM and occurs with 32%–43% of stimulations (Arya et al., 2019, 2020).

Whether stimulation settings used for ESM impact the incidence of AD's remains unclear. One SDE ESM study showed that the occurrence of AD's at a given site may be related to prior stimulation at the same site (Lee et al., 2010). This study found that repeat stimulation of the same SDE pair produced AD's in 19% of trials compared to 5% of trials when a different electrode pair was stimulated. If a trial showed AD's, the incidence of AD's on repeat stimulation of the same electrode pair was 46%, compared to 13% if the previous stimulation at the same site was not associated with AD's. The probability of occurrence of AD's increased with stimulus duration and decreased with inter-trial interval, leading the authors to suggest waiting for 1 min before repeating stimulation particularly at a site showing AD's. However, this may further prolong the already lengthy procedure of ESM. In a case report, higher frequency (100 Hz vs. 50 Hz) and longer pulse width (1 ms vs. 0.2 ms) were more likely to cause AD's (Motamedi et al., 2007). At present, no consistent patient-specific variables that determine the incidence of AD's have been reported (Aungaroon et al., 2017; Corley et al., 2017).

There is further heterogeneity among studies regarding determinants of threshold currents that produce AD's. At a group level, a decrease in AD thresholds with age has been documented (see later; Chitoku et al., 2003; Zea Vera et al., 2017), which has been attributed to a higher prevalence of cortical malformations in children (Chitoku et al., 2003), shorter duration of epilepsy (Guojun et al., 2014), and a higher proportion of unmyelinated axons having higher rheobase compared to myelinated axons (Jayakar et al., 1992). However, in addition to inter-person variability, AD thresholds have been shown to vary according to brain region and from day-to-day in the same region (Corley et al., 2017). In a series of 21 patients with SDE, AD thresholds varied from 2 to 15 mA over the tested cortex even between adjacent electrodes (Lesser et al., 1984a), however, in another series of 11 patients, aged 14–47 years, no significant inter-lobar differences in AD thresholds were reported (Suzuki et al., 2018).

The occurrence of AD's can compromise the safety and neurophysiologic validity of ESM. Whether an associated functional response is attributable to stimulation or AD's becomes difficult to distinguish. Particularly, in the case of AD's remote from the site of stimulation, localization of any observed

behavioral response to the stimulated cortical site vs. the region showing AD's, remains unclear.

Relationship Between AD and Functional Thresholds

An important consideration in designing an optimal ESM strategy is to compare threshold currents required for producing desired functional responses and those resulting in unwanted AD's. This is particularly relevant in younger children, where functional response thresholds may be higher than older children and adults (Chitoku et al., 2001, 2003). An SDE ESM study including 20 children found AD thresholds to be lower than functional thresholds in children aged 5-years and younger (Jayakar and Lesser, 2008). This was substantiated by a larger (n = 122) SDE study that showed language response thresholds to be above AD thresholds throughout the included age range (1–26 years), while motor response thresholds were higher than AD thresholds below 8-years of age (Zea Vera et al., 2017). Therefore, at the group level, the current strengths required to produce functional responses incur a significant risk of producing AD's. Given the association between the occurrence of AD's and ESM-induced seizures, as well as their current thresholds, this poses a significant risk with SDE ESM.

The preliminary experience with SEEG ESM suggests a different age-relationship between functional and AD thresholds (**Figure 3**). In 10 patients undergoing language ESM with SEEG, speech/language response thresholds were below AD thresholds throughout the age range (5–21 years; Arya et al., 2019). Similarly, in 15 patients aged 6–21 years, sensorimotor thresholds remained below the AD thresholds (Arya et al., 2020). Therefore, ESM with SEEG may be safer than that with SDE, regarding the risks of ESM-induced AD's and seizures, because of lower functional thresholds.

Pain and Tissue Injury

Another potential concern with ESM includes pain on inadvertent stimulation of dura mater including its feeding vasculature, large venous sinuses, or proximal parts of large arteries (Fontaine et al., 2018). The exact incidence of this adverse event with extra-operative ESM is unknown, but is probably low, based on the clinical experience. Because the proportion of electrode contacts with the dura is lower with SEEG, it is expected, but not proven, that nociceptive experiences will be rarer with SEEG compared to SDE.

The application of extrinsic currents during ESM has also raised concerns for tissue injury. Animal studies with prolonged continuous stimulation, sometimes lasting for days, have shown cortical damage, with proposed mechanisms of heat produced by hydrolysis, accumulation of negative charges at the cathode, and generation of metal ions at the anode (Jayakar and Lesser, 2008). However, ESM in humans consists of brief intermittent stimulation with pulses of alternating polarity (biphasic). Therefore, these risks are probably irrelevant in clinical practice. A histological examination of 11 SDE sites in three patients, 1 day after ESM with 50 Hz, 0.3 ms, biphasic pulses at 12.5–15 mA, having estimated charge density of 52–57 $\mu C/cm^2$, did not show any abnormalities attributable to ESM (Gordon et al., 1990). Corresponding data with SEEG ESM is not available at present.

FUNCTIONAL RESPONSES

There is a wealth of information about experiential and behavioral phenomena associated with intra-operative stimulation and extra-operative ESM with SDE, which has been exhaustively reviewed (Selimbeyoglu and Parvizi, 2010). A systematic review of functional responses seen with SEEG ESM is beyond the scope of this article. Here, we have focused on contrasting the responses seen during SEEG ESM with those seen during SDE ESM. We also limited the discussion to actual responses observed during SEEG ESM and not the semiology components seen during seizure propagation.

Speech and Language

With SDE ESM, naming errors have been described during stimulation of left inferior frontal gyrus (IFG), left posterior superior temporal gyrus (STG), left anterior middle temporal gyrus (MTG), and bilateral premotor cortex and post-central gyrus (Ojemann and Mateer, 1979; Lesser et al., 1984b, 1994; Lüers et al., 1986; Krauss et al., 1996; Schwartz et al., 1999; Bhatnagar et al., 2000; Corina et al., 2010; Selimbeyoglu and Parvizi, 2010; Suarez et al., 2010). Specific errors of syntactic morphology, word order, and paraphasic errors have been reported with stimulation of left IFG, posterior STG, and anterior MTG, additionally with difficulties in auditory comprehension on stimulation of left posterior STG. Complete anomia has been reported during stimulation at the left IFG, inferior temporal gyrus, and temporoparietal junction.

Similarly, difficulties in naming were seen on stimulation of SEEG electrode contacts located in bilateral STG, transverse temporal gyri, post-central gyrus, and angular gyrus; and left IFG (triangular and opercular parts), MTG, and amygdala (Arya et al., 2019). Interestingly, similar naming deficits were seen on stimulation of white mater SEEG contacts in bilateral temporal and left frontal lobes. Paraphasic errors had an anatomic distribution similar to those seen with SDE ESM but were strictly lateralized to the left cerebral hemisphere. This illustrates an important advantage of ESM with SEEG, which is the ability to study the contribution of deeper structures, such as transverse temporal gyri, essentially inaccessible to SDE, in networks underlying linguistic or other cognitive abilities (see later also).

An important consideration in evaluating ESM speech/language responses is the lack of standardization of task paradigms. In a survey that included 56 epilepsy centers from different countries, a lack of uniformity in what is considered adequate for pre-surgical language mapping was reported (Hamberger et al., 2014). Only half of the epilepsy centers reported testing four main components of language (speech production, comprehension, naming, and reading). Additionally, while over 90% of respondents agreed that non-responses, anomia, and paraphasic errors constituted significant language interruption, the consensus was lacking for the functional significance of hesitations and perseverations. Other areas of discrepancy included interpretation of AD's and

brain regions that should be queried during language ESM. Furthermore, there is evidence for task-specific topography of speech/language function, at least with SDE ESM (Hamberger, 2007). Hence, there is a need to standardize task selection for language ESM, particularly for children and those with limited ability for sustained participation.

Sensorimotor

SDE ESM was crucial in mapping the somatotopic representation of body parts in the primary sensorimotor cortex located in the pre-and post-central gyri (Penfield and Boldrey, 1937). Additionally, turning of head and eyes, reaching/grasping, and tonic or other postural manifestations in extremities (predominantly contralateral) have been described on stimulation of supplementary sensorimotor area (SSMA) and pre-SSMA (Lim et al., 1994; Kanno et al., 2018). Dysarthria, sometimes severe enough to cause complete speech arrest, is documented on stimulation of bilateral inferior precentral gyrus and left pars opercularis of IFG. Interference with smooth eye movements and generation of saccades is known to be associated with stimulation of frontal eye fields in superior frontal gyri and is rarely seen also on stimulation of right superior parietal lobule (Selimbeyoglu and Parvizi, 2010).

The topography of sensorimotor responses seen with SEEG ESM is largely consistent with that seen with SDE ESM but offers some additional insights. We have reported conjugate gaze deviation on stimulation of superior occipital gyrus and middle cingulate region, suggesting a more elaborate system for control of extra-ocular movements (Arya et al., 2020). We also noted highly specific motor responses such as the extension of the distal inter-phalangeal joint of a single digit, or pronation of proximal radio-ulnar joint, on stimulation of specific sites within pre-central gyrus, which were consistent across patients. This suggests that the cortical representation of certain muscles, most likely intrinsic muscles of the hand, is finer than hitherto realized.

Another possibility with SEEG ESM is to map "negative" motor areas characterized by the arrest of voluntary movements on stimulation. Intra-operative stimulation of white matter underneath the dorsal premotor cortex and SSMA in 18 patients, was found to be associated with cessation of limb movements, interference with bimanual coordination, or speech (Rech et al., 2016). Removal of sites participating in this negative motor network in five patients resulted in post-operative akinesia and mutism, with persistent deficits in fine motor control and bimanual coordination at 3 months, compared to complete recovery in eight patients with preservation of negative motor sites (Rech et al., 2017). Because SEEG allows extra-operative stimulation of white matter, it offers an opportunity to map negative motor sites. However, the continued performance of voluntary movements for such mapping may not be feasible in children and patients with intellectual or motor impairment.

Somatosensory responses were seen with SEEG ESM also have similar localization to those reported with SDE ESM. However, a couple of unique observations are worth mentioning. First, we noted that a majority of somatosensory responses lateralized to the right hemisphere, even for ipsilateral responses (Arya et al., 2020). This was in contrast to the conventional view that well-localized somatic sensations are primarily represented in the contralateral sensorimotor cortex. Some perfusion and lesion studies support our observations and have reported a preeminent role of the right parietal lobe in processing bilateral tactile and thermal stimuli (Peyron et al., 1999; Coghill et al., 2001). Second, we observed that circumscribed tingling, vibrating, or shaking sensations almost always localized to post-central gyrus or underlying parietal white matter, thermal sensations localized to superior parietal lobule, while non-specific sensations had a variable localization. Therefore, we speculated that perhaps the human brain has localization specific to sensory modalities in addition to somatotopic representation. However, these observations require verification by future SEEG ESM studies.

Mapping the Insula and Cingulate Gyrus

SEEG ESM offers direct access to study functional roles of the insula and cingulate gyrus, which have not been sufficiently mapped with SDE (**Figure 2**).

Insular stimulations have shown a wide spectrum of responses including special sensory (olfactory, gustatory, and auditory), noxious (suffocation, burning, stinging, and "electric shock"), somatosensory (warmth, paresthesia in various parts of the body), viscerosensory (nausea, epigastric sensation), and vestibular (vertigo; Selimbeyoglu and Parvizi, 2010). Also, psychic or emotional responses (sensation of unreality or out of this world, fear, and anxiety), autonomic phenomena (heart rate changes), and motor responses (automatisms and dysarthria) have been described with insular stimulation, attesting to its integrative role in multiple functional networks (Ostrowsky et al., 2000; Afif et al., 2010; Mazzola et al., 2014, 2019). There is probably some regional specialization within the insula with the posterior insula serving sensory (particularly nociceptive) and vestibular functions, while the anterior insula serving visceral and emotional functions.

There has been limited access to cingulate gyrus for functional mapping with SDE, given the challenges of inserting midline inter-hemispheric strips. However, a wide repertoire of responses on SEEG ESM of the cingulate cortex has been described, which is briefly summarized here. Stimulation of anterior cingulate cortex (anterior to vertical posterior commissure line) has resulted in sensory (epigastric, whole body swaying or rocking sensations), motor (various body parts), anticipatory (intention or urge to move), emotional (laughter, anxiety), speech (arrest), and autonomic (blushing, mydriasis, change in heart rate or respiration, increase in skin conductive response) responses (Talairach et al., 1973; Mangina and Beuzeron-Mangina, 1996; Kahane et al., 2003; Sperli et al., 2006; Mulak et al., 2008). Specifically, motor responses similar to those seen on SSMA stimulation (tonic posturing, reaching, grasping, and eye or head deviation) has resulted in recognition of a cingulate motor area (Chassagnon et al., 2008; Basha et al., 2013; Arya et al., 2020). Stimulation of the posterior cingulate cortex has been associated with similar motor responses and speech arrest, but has additionally shown contralateral upper extremity sensory changes and occasionally visual changes.

Diagnostic Validity of Localization With SEEG ESM

The diagnostic performance of SEEG ESM for anatomic localization of functional responses has been rigorously evaluated only sparsely. A large adult study (n = 209), reported somatic motor responses in 138 (66%) and somatosensory responses in 32 (15%) patients respectively with SEEG ESM (Cossu et al., 2005a). Similarly, sensorimotor responses were reported in 21/35 (60%) of children as well (Cossu et al., 2005b). However, there remains a need to validate the localization of these responses against a reference standard. Ideally, ESM should be evaluated by risk reduction achieved in long-term post-operative neurological or neuropsychological deficits, which requires longitudinal data collection in a large sample.

Therefore, we validated SEEG ESM using a meta-analytic functional MRI framework as reference neuroanatomy, albeit in small samples. Although our comparisons between SEEG ESM performed in individual patients and functional MRI meta-analysis performed in a large heterogeneous dataset are methodologically imperfect, they offer preliminary data for such diagnostic validation. In 10 pediatric patients, we found SEEG ESM (50 Hz, 1–8 mA) to result in speech/language inhibition at 87/304 (29%) electrode contacts. SEEG ESM was a good classifier of anatomic language sites with high specificity (0.87) but limited sensitivity (0.57; Arya et al., 2019). In addition to other methodological differences, this relatively low sensitivity may reflect the wider range of language tasks used to generate the fMRI dataset compared to the single task used for SEEG ESM in our patients. Another recent study including 27 adults (50 Hz, 0.2–3 mA), reported language interference at 85/1914 (4.4%) sites, also with a topography confirming the canonical neuroanatomy (Cuisenier et al., 2020). For sensorimotor mapping, in 15 children, SEEG ESM was noted to localize anatomic sensorimotor parcels with high accuracy (0.80) and high specificity (0.86; Arya et al., 2020).

ESM AND POST-OPERATIVE OUTCOMES

The core purpose of pre-surgical ESM is to establish the functional significance of the seizure-onset zone and establish its anatomical relationship with eloquent cortical areas. This is supposed to help eliminate or minimize post-operative deficits by avoiding eloquent cortical regions during neurosurgery. In case of overlap between seizure-onset zone and eloquent cortex, pre-surgical ESM can help facilitate an informed choice, anticipate potential deficits, and plan for rehabilitation and accommodations.

That epilepsy surgery can affect postoperative motor and cognitive function is well established (Sherman et al., 2011). While epilepsy surgery can improve executive function and memory in some patients, probably by removing the pathological effects of seizures and epileptiform discharges, more frequently it is associated with a decline in verbal memory, naming, attention, and other domains (Lendt et al., 1999; de Koning et al., 2009; Ives-Deliperi and Butler, 2012). The neuropsychological outcomes after epilepsy surgery are driven by multiple factors, including but not limited to the age at onset of seizures, age at the time of surgery, anti-seizure medications, presence and nature of an epileptogenic lesion, location of the seizure-onset zone, its relationship with the eloquent cortices, neurosurgical planning, and most importantly, post-operative seizure outcomes (Skirrow et al., 2011; Puka et al., 2017; Sakpichaisakul et al., 2020). Whether pre-surgical ESM reduces the risk of adverse postoperative outcomes, over and above what may be expected from demographic and clinical information, remains a vexing question. Designing randomized studies to address this question is precluded by ethical principles.

However, the groundwork laid by studies on brain tumor surgery offers some insights. In 40 patients undergoing awake craniotomy for removal of dominant temporal lobe gliomas, the distance of resection margin from the nearest language site was the most important determinant of post-operative language outcomes (Haglund et al., 1994). Authors observed that if this distance was more than 1 cm, significantly fewer permanent language deficits occurred, and proposed it as a safety margin. Another study of 55 patients undergoing resection of tumors located within and adjacent to corticospinal tracts, used tractography-based navigation with real-time guidance from intra-operative ultrasound, and cortical and subcortical motor evoked potentials (Nossek et al., 2011). This study found 87% of their patients recovered without deficits when motor mapping nodes were respected.

The literature on language outcomes after epilepsy surgery, mostly derived from adults undergoing awake craniotomy with intra-operative language ESM, is more heterogeneous. Significantly worse post-operative language function after dominant anterior temporal lobectomy (ATL) was reported in 13/15 patients in one study (Hermann and Wyler, 1988), while no significant deterioration in neuropsychological scores were reported in 18 patients after dominant ATL in another study (Davies et al., 1994). Recently, in 89 patients aged 6–24 years, comprehensive standardized pre- and 1-year post-operative neuropsychological data were examined to evaluate the impact of pre-surgical ESM with SDE (Sakpichaisakul et al., 2020). The multi-domain neuropsychological data were collapsed into three principal component scores representing general cognition, memory, and naming. A significant impact of ESM was seen on all three component scores, in mathematical models adjusted for other clinical variables, with an improvement of 7.5 z-scores in the general cognition score in patients who underwent pre-surgical ESM, vs. a worsening of 8.5 z-scores in those who did not. Only 30% of patients who underwent language ESM experienced a postoperative decrease in general cognition score, compared to 68% of those who did not. Whereas the above study used only a visual naming task for language ESM that is often considered the gold-standard (Hamberger, 2007; Sakpichaisakul et al., 2020), others have emphasized the need for including multiple languages tasks (Wellmer et al., 2009). In a study where language ESM was performed extra-operatively in 12 patients, and intra-operatively in seven patients, all undergoing dominant temporal lobe surgery, all visual naming sites were preserved (Hamberger et al., 2005). However, 6/7 patients with the removal of auditory naming sites experienced a post-operative decline,

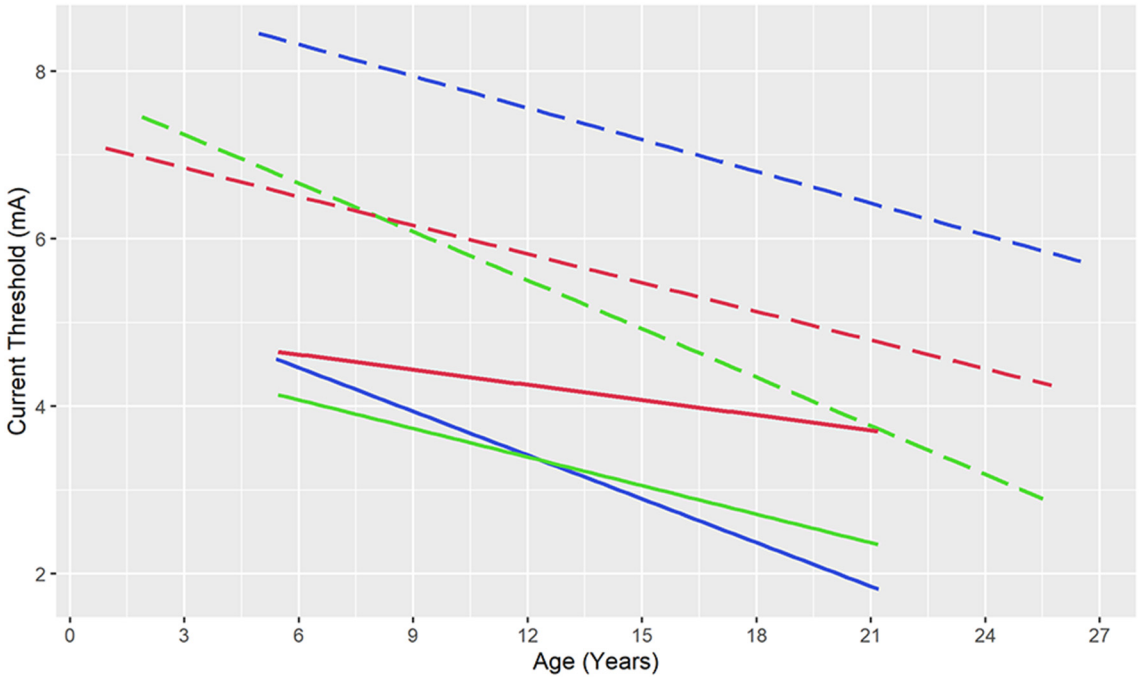

FIGURE 3 | Current thresholds for speech and language responses (blue), motor responses (green), and after-discharges (red) during electrical stimulation mapping with stereotactic electroencephalography (solid lines) and subdural electrodes (dashed lines). Note that after-discharge thresholds are lower than language thresholds (throughout the included age range) and motor thresholds (up to 8-years of age) raising concerns for the safety of subdural electrical stimulation, while functional thresholds remain below after-discharge thresholds for stereotactic electrodes. Ordinary least squares regression lines based on data from Zea Vera et al. (2017) and Arya et al. (2019, 2020).

compared to only 3/12 patients where auditory naming sites were also preserved.

As far as chronic intracranial monitoring of DRE patients is concerned, the above studies are limited to SDE. A large-scale validation of SEEG ESM against post-operative language and neuropsychological outcomes remains an important unmet clinical need. It is also desirable to compare neuropsychological outcomes in cohorts of epilepsy surgery patients evaluated with SEEG vs. SDE, to identify subgroups where one intracranial modality may be preferable over another for ESM.

CONCLUSIONS AND AVENUES FOR FUTURE RESEARCH

This narrative review attests that SEEG is rapidly becoming the preferred modality for pre-surgical intracranial monitoring given its relative safety compared to SDE and avoidance of craniotomy (**Figure 1**). Evidence from early studies suggests that seizure outcomes after epilepsy surgery guided respectively by SEEG and SDE are comparable (Young et al., 2018; Tandon et al., 2019). ESM for sensorimotor and speech/language areas is feasible with SEEG, based on the emerging group-level evidence for agreement with reference neuroanatomy (Arya et al., 2019, 2020; Cuisenier et al., 2020). Based on our experience, we suggest 50 Hz ESM for mapping brain function, at pulse widths and train durations similar to those used with SDE ESM, however, using current intensities up to 8 mA (Trebuchon and Chauvel, 2016; Britton, 2018; Arya et al., 2019, 2020). We believe that future studies will further refine this suggested protocol (**Table 2**). Given that the functional thresholds are lower than AD thresholds for SEEG ESM, compared to the inverse relationship for SDE ESM (**Figure 3**), it appears that SEEG ESM may be safer compared to SDE ESM, particularly in young children.

However, SEEG ESM requires a different clinical approach for interpretation compared to SDE ESM. While SDE affords surface contiguity and the ability to potentially map the extent of functional areas on the cortical surfaces, SEEG offers the ability to sample from areas typically inaccessible to SDE, including depth of sulci, medial and basal surfaces of cerebral hemispheres, and insula (**Figure 2**). At our center, after ascertaining the functional significance of electrode contact(s) lying within a particular gyrus using SEEG ESM, we plan surgical resections based on the anatomy of the sulci delimiting that gyrus. SEEG ESM also has the potential to expand our understanding of human functional neuroanatomy. Early studies already show two specific advantages. First, the potential to obtain a more granular map of functional representations, with highly specific sensory or motor responses (Arya et al., 2020). Secondly, the ability to study the functional significance of structures is typically not sampled by SDE (Mazzola et al., 2019; Taussig et al., 2020). SEEG also allows simultaneous bilateral sampling which permits delineating contributions of both cerebral hemispheres in task-related networks, particularly with high-gamma

modulation (Forseth et al., 2018; Cuisenier et al., 2020). Translating the methodology of high-gamma modulation mapping from SDE to SEEG is another open research area (Ervin et al., 2020).

Although early studies with SEEG ESM appear encouraging, several clinical and scientific questions remain unanswered. First, there is a need to better understand the physics of current propagation in the brain tissue after bipolar stimulation of SEEG contacts, which may sometimes lie respectively in white matter and gray matter (Koessler et al., 2017). Such biophysical models will then, hopefully, inform the neurophysiology of interaction of these current injections with different cellular elements in the brain tissue to effect electrochemical changes in proximate and distant neuronal assemblies, and ultimately explain the behavioral and experiential phenomena observed with ESM. These biophysical models will also help refine the stimulation protocols by optimizing the local charge density and establishing safety limits for the delivered energy. This is important, because clinical experimentation with different stimulation settings, is largely precluded by ethical principles.

We have mentioned that bipolar stimulation, at least with SDE, may result in the localized current spread. There is some evidence, based on studies of intraoperative motor evoked potentials, that bipolar stimulation may specifically limit current spread perpendicular to the cortical surface (Kombos and Suss, 2009). Therefore, it has been hypothesized that monopolar stimulation may be preferable for excitation of the pyramidal tract. It is likely, but currently unproven, that orthogonally implanted SEEG electrodes may achieve mapping of subcortical tracts at relatively low current settings with bipolar stimulation. Another procedure-related concern is the role of pre-medication before SEEG ESM, including the effect of different medications on cortical excitability and functional thresholds.

To better learn from clinical data, it will be important to develop relatively homogeneous protocols for SEEG ESM. An important consideration will be to develop a modular approach towards the selection of different language and cognitive tasks, particularly for pediatric ESM. Also, it may be desirable to routinely evaluate for interference with voluntary movements during ESM, to map for "negative" motor areas, which may require higher current strengths and sustained patient participation (Kanno et al., 2018). Studies with SDE have shown that neuropsychological deficits do occur after epilepsy surgeries guided by language ESM, particularly in higher-order cognitive domains which may underlie linguistic development and ability, but may not be crucial for cued naming, thus demonstrating the need for multi-paradigm ESM to evaluate different domains (Wellmer et al., 2009; Sakpichaisakul et al., 2020). Although assessment of positive motor responses and patient-reported sensory responses is fairly straightforward, the sensitivity of sensorimotor ESM may be further refined by the use of surface electromyography to detect visually obscure muscle contractions, and by evaluation for negative motor responses by white matter stimulation (Rech et al., 2016, 2017). This is particularly important for SEEG ESM because relatively subtle motor responses are sometimes limited to a single small muscle (Arya et al., 2020). Therefore, it will be worthwhile to develop consensus protocols for SEEG ESM to harmonize data acquisition and enable clinically useful inferences from large samples.

Finally, the most important unmet clinical need is to quantify the risk reduction in adverse post-operative outcomes achieved by pre-surgical SEEG ESM. The purpose of ESM is to help improve the safety of neurosurgical decisions, by offering a safe operative corridor between the seizure-onset zone and eloquent cortical regions. ESM can also help anticipate and prepare for post-operative deficits if there is an overlap between the seizure-onset zone and eloquent functional regions. With SDE, although earlier studies were somewhat discordant (Lendt et al., 1999; de Koning et al., 2009; Skirrow et al., 2011; Puka et al., 2017), a recent large study has demonstrated the relationship between ESM and neuropsychological outcomes (Sakpichaisakul et al., 2020). A multi-center study with sufficient sample size, using valid and comprehensive age-appropriate assessments, both pre-and post-operatively, to establish the predictive value of SEEG ESM for neurological outcomes is imminently needed.

AUTHOR CONTRIBUTIONS

All authors participated in literature review, data extraction, and data interpretation. KG and SI drafted the manuscript that was critically reviewed and modified by RA. All authors contributed to the article and approved the submitted version.

FUNDING

Publication expenses were funded by the Procter Foundation and the Division of Neurology, Cincinnati Children's Hospital Medical Center. RA receives research support from NIH (NINDS) R01 NS115929, Procter Foundation, and Maxon Foundation.

REFERENCES

Abou-Al-Shaar, H., Brock, A. A., Kundu, B., Englot, D. J., and Rolston, J. D. (2018). Increased nationwide use of stereoencephalography for intracranial epilepsy electroencephalography recordings. *J. Clin. Neurosci.* 53, 132–134. doi: 10.1016/j.jocn.2018.04.064

Afif, A., Minotti, L., Kahane, P., and Hoffmann, D. (2010). Anatomofunctional organization of the insular cortex: a study using intracerebral electrical stimulation in epileptic patients. *Epilepsia* 51, 2305–2315. doi: 10.1111/j.1528-1167.2010.02755.x

Arya, R., Aungaroon, G., Zea Vera, A., Horn, P. S., Byars, A. W., Greiner, H. M., et al. (2018). Fosphenytoin pre-medication for pediatric extra-operative electrical stimulation brain mapping. *Epilepsy Res.* 140, 171–176. doi: 10.1016/j.eplepsyres.2018.01.017

Arya, R., Ervin, B., Dudley, J., Buroker, J., Rozhkov, L., Scholle, C., et al. (2019). Electrical stimulation mapping of language with stereo-EEG. *Epilepsy Behav.* 99:106395. doi: 10.1016/j.yebeh.2019.06.038

Arya, R., Ervin, B., Holloway, T., Dudley, J., Horn, P. S., Buroker, J., et al. (2020). Electrical stimulation sensorimotor mapping with stereo-EEG. *Clin. Neurophysiol.* 131, 1691–1701. doi: 10.1016/j.clinph.2020.04.159

Arya, R., Mangano, F. T., Horn, P. S., Holland, K. D., Rose, D. F., and Glauser, T. A. (2013). Adverse events related to extraoperative invasive EEG monitoring with subdural grid electrodes: a systematic review and meta-analysis. *Epilepsia* 54, 828–839. doi: 10.1111/epi.12073

Aungaroon, G., Zea Vera, A., Horn, P. S., Byars, A. W., Greiner, H. M., Tenney, J. R., et al. (2017). After-discharges and seizures during pediatric extra-operative electrical cortical stimulation functional brain mapping: incidence, thresholds and determinants. *Clin. Neurophysiol.* 128, 2078–2086. doi: 10.1016/j.clinph.2017.06.259

Bartholow, R. (1874). Experiments on the functions of the human brain. *Br. Med. J.* 1:727.

Basha, M. M., Vaca, G. F.-B., and Lüders, H. O. (2013). Mapping of cingulate motor function by cortical stimulation. *Epileptic Disord.* 15, 333–337. doi: 10.1684/epd.2013.0595

Bhatnagar, S. C., Mandybur, G. T., Buckingham, H. W., and Andy, O. J. (2000). Language representation in the human brain: evidence from cortical mapping. *Brain Lang.* 74, 238–259. doi: 10.1006/brln.2000.2339

Blume, W. T., Jones, D. C., and Pathak, P. (2004). Properties of after-discharges from cortical electrical stimulation in focal epilepsies. *Clin. Neurophysiol.* 115, 982–989. doi: 10.1016/j.clinph.2003.11.023

Borchers, S., Himmelbach, M., Logothetis, N., and Karnath, H.-O. (2012). Direct electrical stimulation of human cortex—the gold standard for mapping brain functions? *Nat. Rev. Neurosci.* 13, 63–70. doi: 10.1038/nrn3140

Britton, J. W. (2018). Electrical stimulation mapping with stereo-EEG electrodes. *J. Clin. Neurophysiol.* 35, 110–114. doi: 10.1097/WNP.0000000000000443

Chassagnon, S., Minotti, L., Kremer, S., Hoffmann, D., and Kahane, P. (2008). Somatosensory, motor and reaching/grasping responses to direct electrical stimulation of the human cingulate motor areas. *J. Neurosurg.* 109, 593–604. doi: 10.3171/JNS/2008/109/10/0593

Chitoku, S., Otsubo, H., Harada, Y., Jay, V., Rutka, J. T., Weiss, S. K., et al. (2001). Extraoperative cortical stimulation of motor function in children. *Pediatr. Neurol.* 24, 344–350. doi: 10.1016/s0887-8994(01)00264-8

Chitoku, S., Otsubo, H., Harada, Y., Jay, V., Rutka, J. T., Weiss, S. K., et al. (2003). Characteristics of prolonged afterdischarges in children with malformations of cortical development. *J. Child Neurol.* 18, 247–253. doi: 10.1177/08830738030180041101

Coghill, R. C., Gilron, I., and Iadarola, M. J. (2001). Hemispheric lateralization of somatosensory processing. *J. Neurophysiol.* 85, 2602–2612. doi: 10.1152/jn.2001.85.6.2602

Corina, D. P., Loudermilk, B. C., Detwiler, L., Martin, R. F., Brinkley, J. F., and Ojemann, G. (2010). Analysis of naming errors during cortical stimulation mapping: implications for models of language representation. *Brain Lang.* 115, 101–112. doi: 10.1016/j.bandl.2010.04.001

Corley, J. A., Nazari, P., Rossi, V. J., Kim, N. C., Fogg, L. F., Hoeppner, T. J., et al. (2017). Cortical stimulation parameters for functional mapping. *Seizure* 45, 36–41. doi: 10.1016/j.seizure.2016.11.015

Cossu, M., Cardinale, F., Castana, L., Citterio, A., Francione, S., Tassi, L., et al. (2005a). Stereoelectroencephalography in the presurgical evaluation of focal epilepsy: a retrospective analysis of 215 procedures. *Neurosurgery* 57, 706–718. doi: 10.1227/01.NEU.0000176656.33523.1e

Cossu, M., Cardinale, F., Colombo, N., Mai, R., Nobili, L., Sartori, I., et al. (2005b). Stereoelectroencephalography in the presurgical evaluation of children with drug-resistant focal epilepsy. *J. Neurosurg.* 103, 333–343. doi: 10.3171/ped.2005.103.4.0333

Cossu, M., Cardinale, F., Castana, L., Nobili, L., Sartori, I., and Lo Russo, G. (2006). Stereo-EEG in children. *Childs Nerv. Syst.* 22, 766–778. doi: 10.1007/s00381-006-0127-2

Cuisenier, P., Testud, B., Minotti, L., El Bouzaidi Tiali, S., Martineau, L., Job, A. S., et al. (2020). Relationship between direct cortical stimulation and induced high-frequency activity for language mapping during SEEG recording. *J. Neurosurg.* 2020, 1–11. doi: 10.3171/2020.2.JNS192751

David, O., Bastin, J., Chabardès, S., Minotti, L., and Kahane, P. (2010). Studying network mechanisms using intracranial stimulation in epileptic patients. *Front. Syst. Neurosci.* 4:148. doi: 10.3389/fnsys.2010.00148

Davies, K. G., Maxwell, R. E., Jennum, P., Dhuna, A., Beniak, T. E., Destafney, E., et al. (1994). Language function following subdural grid-directed temporal lobectomy. *Acta Neurol. Scand.* 90, 201–206. doi: 10.1111/j.1600-0404.1994.tb02706.x

de Koning, T., Versnel, H., Jennekens-Schinkel, A., van Schooneveld, M. M., Dejonckere, P. H., van Rijen, P. C., et al. (2009). Language development before and after temporal surgery in children with intractable epilepsy. *Epilepsia* 50, 2408–2419. doi: 10.1111/j.1528-1167.2009.02264.x

Duchowny, M., Jayakar, P., Harvey, A. S., Resnick, T., Alvarez, L., Dean, P., et al. (1996). Language cortex representation: effects of developmental versus acquired pathology. *Ann. Neurol.* 40, 31–38. doi: 10.1002/ana.410400108

Ervin, B., Buroker, J., Rozhkov, L., Holloway, T., Horn, P. S., Scholle, C., et al. (2020). High-gamma modulation language mapping with stereo-EEG: a novel analytic approach and diagnostic validation. *Clin. Neurophysiol.* 131, 2851–2860. doi: 10.1016/j.clinph.2020.09.023

Fontaine, D., Almairac, F., Santucci, S., Fernandez, C., Dallel, R., Pallud, J., et al. (2018). Dural and pial pain-sensitive structures in humans: new inputs from awake craniotomies. *Brain* 141, 1040–1048. doi: 10.1093/brain/awy005

Forseth, K. J., Kadipasaoglu, C. M., Conner, C. R., Hickok, G., Knight, R. T., and Tandon, N. (2018). A lexical semantic hub for heteromodal naming in middle fusiform gyrus. *Brain* 141, 2112–2126. doi: 10.1093/brain/awy120

Gollwitzer, S., Hopfengärtner, R., Rössler, K., Müller, T., Olmes, D. G., Lang, J., et al. (2018). Afterdischarges elicited by cortical electric stimulation in humans: when do they occur and what do they mean? *Epilepsy Behav.* 87, 173–179. doi: 10.1016/j.yebeh.2018.09.007

Gordon, B., Lesser, R. P., Rance, N. E., Hart, J. Jr., Webber, R., Uematsu, S., et al. (1990). Parameters for direct cortical electrical stimulation in the human: histopathologic confirmation. *Electroencephalogr. Clin. Neurophysiol.* 75, 371–377. doi: 10.1016/0013-4694(90)90082-u

Guojun, Z., Duanyu, N., Fu, P., Lixin, C., Tao, Y., Wei, D., et al. (2014). The threshold of cortical electrical stimulation for mapping sensory and motor functional areas. *J. Clin. Neurosci.* 21, 263–267. doi: 10.1016/j.jocn.2013.04.015

Haglund, M. M., Berger, M. S., Shamseldin, M., Lettich, E., and Ojemann, G. A. (1994). Cortical localization of temporal lobe language sites in patients with gliomas. *Neurosurgery* 34, 567–576. doi: 10.1227/00006123-199404000-00001

Haglund, M. M., Ojemann, G. A., and Blasdel, G. G. (1993). Optical imaging of bipolar cortical stimulation. *J. Neurosurg.* 78, 785–793. doi: 10.3171/jns.1993.78.5.0785

Haglund, M. M., Ojemann, G. A., and Hochman, D. W. (1992). Optical imaging of epileptiform and functional activity in human cerebral cortex. *Nature* 358, 668–671. doi: 10.1038/358668a0

Hamberger, M. J., Seidel, W. T., McKhann, G. M. II, Perrine, K., and Goodman, R. R. (2005). Brain stimulation reveals critical auditory naming cortex. *Brain* 128, 2742–2749. doi: 10.1093/brain/awh621

Hamberger, M. J., Williams, A. C., and Schevon, C. A. (2014). Extraoperative neurostimulation mapping: results from an international survey of epilepsy surgery programs. *Epilepsia* 55, 933–939. doi: 10.1111/epi.12644

Hamberger, M. J. (2007). Cortical language mapping in epilepsy: a critical review. *Neuropsychol. Rev.* 17, 477–489. doi: 10.1007/s11065-007-9046-6

Hermann, B. P., and Wyler, A. R. (1988). Effects of anterior temporal lobectomy on language function: a controlled study. *Ann. Neurol.* 23, 585–588. doi: 10.1002/ana.410230610

Isnard, J., Taussig, D., Bartolomei, F., Bourdillon, P., Catenoix, H., Chassoux, F., et al. (2018). French guidelines on stereoelectroencephalography (SEEG). *Neurophysiol. Clin.* 48, 5–13. doi: 10.1016/j.neucli.2017.11.005

Ives-Deliperi, V. L., and Butler, J. T. (2012). Naming outcomes of anterior temporal lobectomy in epilepsy patients: a systematic review of the literature. *Epilepsy Behav.* 24, 194–198. doi: 10.1016/j.yebeh.2012.04.115

Jayakar, P., Alvarez, L. A., Duchowny, M. S., and Resnick, T. J. (1992). A safe and effective paradigm to functionally map the cortex in childhood. *J. Clin. Neurophysiol.* 9, 288–293. doi: 10.1097/00004691-199204010-00009

Jayakar, P., Gaillard, W. D., Tripathi, M., Libenson, M. H., Mathern, G. W., Cross, J. H., et al. (2014). Diagnostic test utilization in evaluation for resective epilepsy surgery in children. *Epilepsia* 55, 507–518. doi: 10.1111/epi.12544

Jayakar, P., Gotman, J., Harvey, A. S., Palmini, A., Tassi, L., Schomer, D., et al. (2016). Diagnostic utility of invasive EEG for epilepsy surgery: indications, modalities and techniques. *Epilepsia* 57, 1735–1747. doi: 10.1111/epi.13515

Jayakar, P., and Lesser, R. P. (2008). "Extraoperative functional mapping," in *Epilepsy: A Comprehensive Textbook 2*, 2nd Edn., J. J. Engel and T. A. Pedley (Philadelphia, PA: Lippincott Williams and Wilkins), 1851–1858.

Kahane, P., Hoffmann, D., Minotti, L., and Berthoz, A. (2003). Reappraisal of the human vestibular cortex by cortical electrical stimulation study. *Ann. Neurol.* 54, 615–624. doi: 10.1002/ana.10726

Kanno, A., Enatsu, R., Ookawa, S., Ochi, S., and Mikuni, N. (2018). Location and threshold of electrical cortical stimulation for functional brain mapping. *World Neurosurg.* 119, e125–e130. doi: 10.1016/j.wneu.2018.07.059

Koessler, L., Colnat-Coulbois, S., Cecchin, T., Hofmanis, J., Dmochowski, J. P., Norcia, A. M., et al. (2017). *In vivo* measurements of human brain tissue conductivity using focal electrical current injection through intracerebral multicontact electrodes. *Hum. Brain Mapp.* 38, 974–986. doi: 10.1002/hbm.23431

Kombos, T., and Suss, O. (2009). Neurophysiological basis of direct cortical stimulation and applied neuroanatomy of the motor cortex: a review. *Neurosurg. Focus* 27:E3. doi: 10.3171/2009.8.FOCUS09141

Kovac, S., Kahane, P., and Diehl, B. (2016). Seizures induced by direct electrical cortical stimulation—mechanisms and clinical considerations. *Clin. Neurophysiol.* 127, 31–39. doi: 10.1016/j.clinph.2014.12.009

Krauss, G. L., Fisher, R., Plate, C., Hart, J., Uematsu, S., Gordon, B., et al. (1996). Cognitive effects of resecting basal temporal language areas. *Epilepsia* 37, 476–483. doi: 10.1111/j.1528-1157.1996.tb00594.x

Lee, H. W., Webber, W., Crone, N., Miglioretti, D. L., and Lesser, R. P. (2010). When is electrical cortical stimulation more likely to produce afterdischarges? *Clin. Neurophysiol.* 121, 14–20. doi: 10.1016/j.clinph.2009.10.001

Lendt, M., Helmstaedter, C., and Elger, C. E. (1999). Pre- and postoperative neuropsychological profiles in children and adolescents with temporal lobe epilepsy. *Epilepsia* 40, 1543–1550. doi: 10.1111/j.1528-1157.1999.tb02038.x

Lesser, R., Gordon, B., and Uematsu, S. (1994). Electrical stimulation and language. *J. Clin. Neurophysiol.* 11, 191–204. doi: 10.1097/00004691-199403000-00004

Lesser, R. P., Lüders, H., Klem, G., Dinner, D. S., Morris, H. H., and Hahn, J. (1984a). Cortical afterdischarge and functional response thresholds: results of extraoperative testing. *Epilepsia* 25, 615–621. doi: 10.1111/j.1528-1157.1984.tb03471.x

Lesser, R. P., Lueders, H., Dinner, D. S., Hahn, J., and Cohen, L. (1984b). The location of speech and writing functions in the frontal language area. Results of extraoperative cortical stimulation. *Brain* 107, 275–291. doi: 10.1093/brain/107.1.275

Lim, S. H., Dinner, D. S., Pillay, P. K., Lüders, H., Morris, H. H., Klem, G., et al. (1994). Functional anatomy of the human supplementary sensorimotor area: results of extraoperative electrical stimulation. *Electroencephalogr. Clin. Neurophysiol.* 91, 179–193. doi: 10.1016/0013-4694(94)90068-x

Lüers, H., Lesser, R. P., Hahn, J., Dinner, D. S., Morris, H., Resor, S., et al. (1986). Basal temporal language area demonstrated by electrical stimulation. *Neurology* 36, 505–510. doi: 10.1212/wnl.36.4.505

Malìia, M. D., Donos, C., Barborica, A., Popa, I., Ciurea, J., Cinatti, S., et al. (2018). Functional mapping and effective connectivity of the human operculum. *Cortex* 109, 303–321. doi: 10.1016/j.cortex.2018.08.024

Mangina, C. A., and Beuzeron-Mangina, J. H. (1996). Direct electrical stimulation of specific human brain structures and bilateral electrodermal activity. *Int. J. Psychophysiol.* 22, 1–8. doi: 10.1016/0167-8760(96)00022-0

Matsumoto, R., Nair, D. R., Ikeda, A., Fumuro, T., Lapresto, E., Mikuni, N., et al. (2012). Parieto-frontal network in humans studied by cortico-cortical evoked potential. *Hum. Brain Mapp.* 33, 2856–2872. doi: 10.1002/hbm.21407

Matsumoto, R., Nair, D. R., LaPresto, E., Najm, I., Bingaman, W., Shibasaki, H., et al. (2004). Functional connectivity in the human language system: a cortico-cortical evoked potential study. *Brain* 127, 2316–2330. doi: 10.1093/brain/awh246

Mazzola, L., Lopez, C., Faillenot, I., Chouchou, F., Mauguiere, F., and Isnard, J. (2014). Vestibular responses to direct stimulation of the human insular cortex. *Ann. Neurol.* 76, 609–619. doi: 10.1002/ana.24252

Mazzola, L., Mauguiere, F., and Isnard, J. (2019). Functional mapping of the human insula: data from electrical stimulations. *Rev. Neurol.* 175, 150–156. doi: 10.1016/j.neurol.2018.12.003

Motamedi, G. K., Okunola, O., Kalhorn, C. G., Mostofi, N., Mizuno-Matsumoto, Y., Cho, Y. W., et al. (2007). Afterdischarges during cortical stimulation at different frequencies and intensities. *Epilepsy Res.* 77, 65–69. doi: 10.1016/j.eplepsyres.2007.08.001

Mulak, A., Kahane, P., Hoffmann, D., Minotti, L., and Bonaz, B. (2008). Brain mapping of digestive sensations elicited by cortical electrical stimulations. *Neurogastroenterol. Motil.* 20, 588–596. doi: 10.1111/j.1365-2982.2007.01066.x

Mullin, J. P., Shriver, M., Alomar, S., Najm, I., Bulacio, J., Chauvel, P., et al. (2016). Is SEEG safe? A systematic review and meta-analysis of stereo-electroencephalography-related complications. *Epilepsia* 57, 386–401. doi: 10.1111/epi.13298

Nathan, S. S., Sinha, S. R., Gordon, B., Lesser, R. P., and Thakor, N. V. (1993). Determination of current density distributions generated by electrical stimulation of the human cerebral cortex. *Electroencephalogr. Clin. Neurophysiol.* 86, 183–192. doi: 10.1016/0013-4694(93)90006-h

Nossek, E., Korn, A., Shahar, T., Kanner, A. A., Yaffe, H., Marcovici, D., et al. (2011). Intraoperative mapping and monitoring of the corticospinal tracts with neurophysiological assessment and 3-dimensional ultrasonography-based navigation. *J. Neurosurg.* 114, 738–746. doi: 10.3171/2010.8.JNS10639

Oane, I., Barborica, A., Chetan, F., Donos, C., Maliia, M. D., Arbune, A. A., et al. (2020). Cingulate cortex function and multi-modal connectivity mapped using intracranial stimulation. *NeuroImage* 220:117059. doi: 10.1016/j.neuroimage.2020.117059

Oderiz, C. C., von Ellenrieder, N., Dubeau, F., Eisenberg, A., Gotman, J., Hall, J., et al. (2019). Association of cortical stimulation-induced seizure with surgical outcome in patients with focal drug-resistant epilepsy. *JAMA Neurol.* 76, 1070–1078. doi: 10.1001/jamaneurol.2019.1464

Ojemann, G., and Mateer, C. (1979). Human language cortex: localization of memory, syntax and sequential motor-phoneme identification systems. *Science* 205, 1401–1403. doi: 10.1126/science.472757

Ojemann, G. A. (1979). Individual variability in cortical localization of language. *J. Neurosurg.* 50, 164–169. doi: 10.3171/jns.1979.50.2.0164

Ojemann, S. G., Berger, M. S., Lettich, E., and Ojemann, G. A. (2003). Localization of language function in children: results of electrical stimulation mapping. *J. Neurosurg.* 98, 465–470. doi: 10.3171/jns.2003.98.3.0465

Ostrowsky, K., Isnard, J., Ryvlin, P., Guenot, M., Fischer, C., and Mauguiere, F. (2000). Functional mapping of the insular cortex: clinical implication in temporal lobe epilepsy. *Epilepsia* 41, 681–686. doi: 10.1111/j.1528-1157.2000.tb00228.x

Oya, H., Howard, M. A., Magnotta, V. A., Kruger, A., Griffiths, T. D., Lemieux, L., et al. (2017). Mapping effective connectivity in the human brain with concurrent intracranial electrical stimulation and BOLD-fMRI. *J. Neurosci. Methods* 277, 101–112. doi: 10.1016/j.jneumeth.2016.12.014

Penfield, W., and Boldrey, E. (1937). Somatic motor and sensory representation in the cerebral cortex of man as studied by electrical stimulation. *Brain* 60, 389–443. doi: 10.1093/brain/60.4.389

Penfield, W., and Jasper, H. (1954). *Epilepsy and the Functional Anatomy of the Human Brain.* (Boston: Little, Brown & Co), 363–365

Perrone-Bertolotti, M., Alexandre, S., Jobb, A. S., De Palma, L., Baciu, M., Mairesse, M. P., et al. (2020). Probabilistic mapping of language networks from high frequency activity induced by direct electrical stimulation. *Hum. Brain Mapp.* 41, 4113–4126. doi: 10.1002/hbm.25112

Peyron, R., Garcia-Larrea, L., Gregoire, M. C., Costes, N., Convers, P., Lavenne, F., et al. (1999). Haemodynamic brain responses to acute pain in humans: sensory and attentional networks. *Brain* 122, 1765–1780. doi: 10.1093/brain/122.9.1765

Puka, K., Tavares, T. P., and Smith, M. L. (2017). Development of intelligence 4 to 11 years after pediatric epilepsy surgery. *J. Neuropsychol.* 11, 161–173. doi: 10.1111/jnp.12081

Rattay, F. (1999). The basic mechanism for the electrical stimulation of the nervous system. *Neuroscience* 89, 335–346. doi: 10.1016/s0306-4522(98)00330-3

Rech, F., Duffau, H., Pinelli, C., Masson, A., Roublot, P., Billy-Jacques, A., et al. (2017). Intraoperative identification of the negative motor network during awake surgery to prevent deficit following brain resection in premotor regions. *Neurochirurgie* 63, 235–242. doi: 10.1016/j.neuchi.2016.08.006

Rech, F., Herbet, G., Moritz-Gasser, S., and Duffau, H. (2016). Somatotopic organization of the white matter tracts underpinning motor control in humans: an electrical stimulation study. *Brain Struct. Funct.* 221, 3743–3753. doi: 10.1007/s00429-015-1129-1

Sakpichaisakul, K., Byars, A. W., Horn, P. S., Aungaroon, G., Greiner, H. M., Mangano, F. T., et al. (2020). Neuropsychological outcomes after pediatric epilepsy surgery: role of electrical stimulation language mapping. *Seizure* 80, 183–191. doi: 10.1016/j.seizure.2020.06.029

Sala, F., Kržan, M. J., and Deletis, V. (2002). Intraoperative neurophysiological monitoring in pediatric neurosurgery: why, when, how? *Childs Nerv. Syst.* 18, 264–287. doi: 10.1007/s00381-002-0582-3

Sarubbo, S., Tate, M., De Benedictis, A., Merler, S., Moritz-Gasser, S., Herbet, G., et al. (2020). Mapping critical cortical hubs and white matter pathways by direct electrical stimulation: an original functional atlas of the human brain. *NeuroImage* 205:116237. doi: 10.1016/j.neuroimage.2019.116237

Schwartz, T. H., Devinsky, O., Doyle, W., and Perrine, K. (1999). Function-specific high-probability "nodes" identified in posterior language cortex. *Epilepsia* 40, 575–583. doi: 10.1111/j.1528-1157.1999.tb05559.x

Selimbeyoglu, A., and Parvizi, J. (2010). Electrical stimulation of the human brain: perceptual and behavioral phenomena reported in the old and new literature. *Front. Hum. Neurosci.* 4:46. doi: 10.3389/fnhum.2010.00046

Shannon, R. V. (1992). A model of safe levels for electrical-stimulation. *IEEE Trans. Biomed. Eng.* 39, 424–426. doi: 10.1109/10.126616

Sherman, E. M., Wiebe, S., Fay-McClymont, T. B., Tellez-Zenteno, J., Metcalfe, A., Hernandez-Ronquillo, L., et al. (2011). Neuropsychological outcomes after epilepsy surgery: systematic review and pooled estimates. *Epilepsia* 52, 857–869. doi: 10.1111/j.1528-1167.2011.03022.x

Skirrow, C., Cross, J. H., Cormack, F., Harkness, W., Vargha-Khadem, F., and Baldeweg, T. (2011). Long-term intellectual outcome after temporal lobe surgery in childhood. *Neurology* 76, 1330–1337. doi: 10.1212/WNL.0b013e31821527f0

Sperli, F., Spinelli, L., Pollo, C., and Seeck, M. (2006). Contralateral smile and laughter, but no mirth, induced by electrical stimulation of the cingulate cortex. *Epilepsia* 47, 440–443. doi: 10.1111/j.1528-1167.2006.00442.x

Suarez, R. O., Golby, A., Whalen, S., Sato, S., Theodore, W. H., Kufta, C. V., et al. (2010). Contributions to singing ability by the posterior portion of the superior temporal gyrus of the non-language-dominant hemisphere: first evidence from subdural cortical stimulation, wada testing and fMRI. *Cortex* 46, 343–353. doi: 10.1016/j.cortex.2009.04.010

Suzuki, H., Enatsu, R., Kanno, A., Suzuki, Y., Yokoyama, R., Ookawa, S., et al. (2018). Threshold and distribution of afterdischarges with electrical cortical stimulation. *J. Clin. Neurosci.* 55, 71–75. doi: 10.1016/j.jocn.2018.06.039

Talairach, J., Bancaud, J., Geier, S., Bordas-Ferrer, M., Bonis, A., Szikla, G., et al. (1973). The cingulate gyrus and human behaviour. *Electroencephalogr. Clin. Neurophysiol.* 34, 45–52. doi: 10.1016/0013-4694(73)90149-1

Tandon, N., Tong, B. A., Friedman, E. R., Johnson, J. A., Von Allmen, G., Thomas, M. S., et al. (2019). Analysis of morbidity and outcomes associated with use of subdural grids vs. stereoelectroencephalography in patients with intractable epilepsy. *JAMA Neurol.* 76, 672–681. doi: 10.1001/jamaneurol.2019.0098

Taussig, D., Chipaux, M., Fohlen, M., Dorison, N., Bekaert, O., Ferrand-Sorbets, S., et al. (2020). Invasive evaluation in children (SEEG vs. subdural grids). *Seizure* 77, 43–51. doi: 10.1016/j.seizure.2018.11.008

Tolias, A. S., Sultan, F., Augath, M., Oeltermann, A., Tehovnik, E. J., Schiller, P. H., et al. (2005). Mapping cortical activity elicited with electrical microstimulation using FMRI in the macaque. *Neuron* 48, 901–911. doi: 10.1016/j.neuron.2005.11.034

Trebuchon, A., and Chauvel, P. (2016). Electrical stimulation for seizure induction and functional mapping in stereoelectroencephalography. *J. Clin. Neurophysiol.* 33, 511–521. doi: 10.1097/WNP.0000000000000313

Wellmer, J., Weber, C., Mende, M., von der Groeben, F., Urbach, H., Clusmann, H., et al. (2009). Multitask electrical stimulation for cortical language mapping: hints for necessity and economic mode of application. *Epilepsia* 50, 2267–2275. doi: 10.1111/j.1528-1167.2009.02192.x

Whitaker, H. A., and Ojemann, G. A. (1977). Graded localization of naming from electrical stimulation mapping of left cerebral cortex. *Nature* 270, 50–51. doi: 10.1038/270050a0

Young, J. J., Coulehan, K., Fields, M. C., Yoo, J. Y., Marcuse, L. V., Jette, N., et al. (2018). Language mapping using electrocorticography versus stereoelectroencephalography: a case series. *Epilepsy Behav.* 84, 148–151. doi: 10.1016/j.yebeh.2018.04.032

Zangaladze, A., Sharan, A., Evans, J., Wyeth, D. H., Wyeth, E. G., Tracy, J. I., et al. (2008). The effectiveness of low-frequency stimulation for mapping cortical function. *Epilepsia* 49, 481–487. doi: 10.1111/j.1528-1167.2007.01307.x

Zea Vera, A., Aungaroon, G., Horn, P. S., Byars, A. W., Greiner, H. M., Tenney, J. R., et al. (2017). Language and motor function thresholds during pediatric extra-operative electrical cortical stimulation brain mapping. *Clin. Neurophysiol.* 128, 2087–2093. doi: 10.1016/j.clinph.2017.07.006

Conflict of Interest: The authors declare that the research was conducted in the absence of any commercial or financial relationships that could be construed as a potential conflict of interest.

frontiers in Human Neuroscience

ORIGINAL RESEARCH
published: 16 December 2020
doi: 10.3389/fnhum.2020.584136

Anodal Transcranial Direct Current Stimulation of Anterior Cingulate Cortex Modulates Subcortical Brain Regions Resulting in Cognitive Enhancement

Ahsan Khan[1], *Xin Wang*[1], *Chun Hang Eden Ti*[1], *Chun-Yu Tse*[2] *and Kai-Yu Tong*[1,3]*

[1] *Biomedical Engineering Department, The Chinese University of Hong Kong, Hong Kong, China,* [2] *Department of Social and Behavioural Science, City University of Hong Kong, Hong Kong, China,* [3] *Hong Kong Brain and Mind Institute, The Chinese University of Hong Kong, Hong Kong, China*

Transcranial direct current stimulation (tDCS) has been widely utilized in research settings and modulates brain activity. The application of anodal tDCS on the prefrontal cortex has indicated improvement in cognitive functioning. The cingulate cortex, situated in the medial aspect of the prefrontal cortex, has been identified as a core region performing cognitive functions. Most of the previous studies investigating the impact of stimulation on the prefrontal cortex stimulated the dorsolateral prefrontal cortex (DLPFC), however, the impact of stimulation on cingulate has not been explored. The current study investigates the effect of stimulation on the resting-state functional connectivity of the anterior cingulate cortex with other regions of the brain and changes in behavioral results in a color-word Stroop task, which has repeatedly elicited activation in different regions of the cingulate. Twenty subjects were randomly assigned to the experimental and sham group, and their medial prefrontal area was stimulated using MRI compatible tDCS. Resting-state functional magnetic resonance imaging (rs-fMRI) and cognitive Stroop task were monitored before, during, and after the stimulation. Neuroimaging results indicated a significant decrease in resting-state functional connectivity in the experimental group during and after stimulation as compared to before stimulation in two clusters including right insular cortex, right central operculum cortex, right frontal operculum cortex and right planum polare with the left anterior cingulate cortex (L-ACC) selected as the seed. The behavioral results indicated a significant decrease in reaction time (RT) following stimulation in the experimental group compared to the sham group. Moreover, the change in functional connectivity in subcortical regions with L-ACC as the seed and change in RT was positively correlated. The results demonstrated that ACC has a close functional relationship with the subcortical regions, and stimulation of ACC can modulate these connections, which subsequently improves behavioral performance, thus, providing another potential target of stimulation for cognitive enhancement.

Clinical Trial Registration: ClinicalTrials.gov Identifier: NCT04318522.

Keywords: transcranial direct current stimulation (tDCS), stroop task, anterior cingulate cortex (ACC), functional magnetic resonance imaging (fMRI), functional connectivity

OPEN ACCESS

Edited by:
Jorge Alvaro Gonzalez-Martinez, University of Pittsburgh, United States

Reviewed by:
Chunhong Liu, Capital Medical University, China
Amanda Elton, University of North Carolina at Chapel Hill, United States

***Correspondence:**
Kai-Yu Tong
kytong@cuhk.edu.hk

Specialty section:
This article was submitted to Brain Imaging and Stimulation, a section of the journal Frontiers in Human Neuroscience

Received: *16 July 2020*
Accepted: *24 November 2020*
Published: *16 December 2020*

Citation:
Khan A, Wang X, Ti CHE, Tse C-Y and Tong K-Y (2020) Anodal Transcranial Direct Current Stimulation of Anterior Cingulate Cortex Modulates Subcortical Brain Regions Resulting in Cognitive Enhancement. Front. Hum. Neurosci. 14:584136. doi: 10.3389/fnhum.2020.584136

1. INTRODUCTION

The process of cognitive control is one of the mysteries in cognitive neuroscience, and several studies have been performed to understand how millions of neurons in the prefrontal cortex interact with each other to exhibit a goal-directed behavior (Shackman et al., 2011; Gratton et al., 2018; Wu et al., 2019). Recent evidence suggests that we can manipulate the brain activity through external stimulation and transcranial direct current stimulation (tDCS), a non-invasive brain stimulation method, has emerged as a prime tool for manipulating brain activity (Nitsche et al., 2008). The last decade has seen a sharp increase in the use of stimulation methodologies not just in understanding cognition but also in treating Parkinson's disease (Biagioni et al., 2018), motor rehabilitation following stroke (Bao et al., 2020), chronic pain (O'Connell et al., 2018), and other anxiety disorders (Kuo et al., 2014). Stimulation at the target region provides a causal inference on how the directly induced neural alterations influence behavioral changes, establishing a better understanding of the brain-behavior relationship. In this study, we utilized tDCS to understand the impact of stimulation on the prefrontal region of the brain and investigate if it can interfere with the cognitive control in the human brain.

Previous prefrontal tDCS studies mainly targeting the lateral prefrontal cortex (LPFC) region have reported that stimulation can influence a wide range of cognitive functions ranging from low-level attentional processes to higher-order decision making and working memory functions (Boonstra et al., 2016; Westphal et al., 2019) with some conflicting results (Berryhill et al., 2014; Tremblay et al., 2014). However, the impact of tDCS on the cingulate cortex is not clearly understood. Activation of different regions of cingulate during cognitive control processes (Dum and Strick, 1993; Medford and Critchley, 2010; Rolls, 2019) and a central location of cingulate gives a notion that the stimulation of this region could also provide a better insight into cognitive control processes and possibly enhance cognitive functioning of the human brain.

The cingulate cortex is a complex structure having anatomical connections with various brain regions and has reported involvement in cognitive control functions (Dum and Strick, 1993; Medford and Critchley, 2010; Rolls, 2019). Traditionally, cingulate has been subdivided into three subregions: the anterior cingulate cortex (ACC), the midcingulate cortex (MCC), and the posterior cingulate cortex (PCC) (Tzourio-Mazoyer et al., 2002). ACC has reported activations in certain executive functions, including attention allocation, perception, anticipation, decision making, and impulse control (Paus, 2001). The role of MCC is controversial; however, it has elicited activation in goal-directed behaviors (Tolomeo et al., 2016). PCC, a key component in the default mode network (DMN), has shown heterogeneous connections with widespread brain regions. It plays an active role in cognitive control (Leech et al., 2012) and has shown changes with learning, memory, and task engagement (Pearson et al., 2011).

Stroop Task is one of the most widely used paradigms to study cognitive control and is termed as the "gold standard" of attentional measures (MacLeod, 1992). The most basic color-word version of stroop task involves goal-directed selective attention (West and Alain, 2000), inhibition (Bélanger et al., 2010), conflict detection and conflict resolution (Coderre et al., 2011) along with other cognitive control processes depending on the paradigm. Several brain regions have reported activation during the stroop task including dorsolateral prefrontal cortex (DLPFC) (Vanderhasselt et al., 2009) and different regions of cingulate cortex (Carter and Van Veen, 2007; Badzakova-Trajkov et al., 2009). Specifically, the ACC has been reported to mediate conflict adaptation when conflicting information is simultaneously presented (Kim et al., 2014). As it occurs in incongruent trials of the Stroop task when the color of the word is different than the word itself, and the participant has to resolve the conflict and respond to the color of the word, which takes longer processing time than congruent trials where the word and the color are same (Carter and Van Veen, 2007; Kim et al., 2014).

This study's objective was to understand the impact of tDCS on the ACC and executive functions using the Stroop task. First, functional magnetic resonance imaging (fMRI) was used to explore if stimulation of anterior region of cingulate with a small direct current can affect the resting-state functional connectivity of ACC with other brain regions during the stimulation and immediately after the stimulation. Second, we examined if stimulation can enhance performance in cognitive stroop task and if changes in stroop task have a carryover effect in resting-state connectivity in other cingulate regions including MCC and PCC. Third, we investigated if there is an association between stimulation induced resting-state fMRI changes in ACC with behavioral changes. We hypothesized that stimulation would modulate the ACC connectivity with other brain regions and facilitate conflict adaptation, thus resulting in an improvement in performance in incongruent trials of the stroop task.

2. MATERIALS AND METHODS

The current study adopted a single-blinded, placebo-controlled, randomized parallel-group design. Volunteers were screened for inclusion and exclusion criteria (see below) before enrollment in the study. They were instructed about the task on the day of the experiment, and written consent was taken from all the participants. Subjects were randomly assigned to the experimental and sham groups with ten subjects in each group. At pre-stimulation, resting-state fMRI was collected for 5 min before the participants performed a color-word version of the Stroop task, which lasted for 8 min. Following pre-stimulation measurements, tDCS was performed. During the 15-min stimulation, a 5-min resting-state fMRI was acquired at the beginning of the stimulation, followed by a Stroop task. Following stimulation, resting-state fMRI was collected, and the Stroop task was performed. For the sham group, the stimulation ramped up to 2 mA for 30 s and then ramped down in the next 30 s to 0 mA. No stimulation followed this for the next 15 min. The study design is shown in **Figure 1A**.

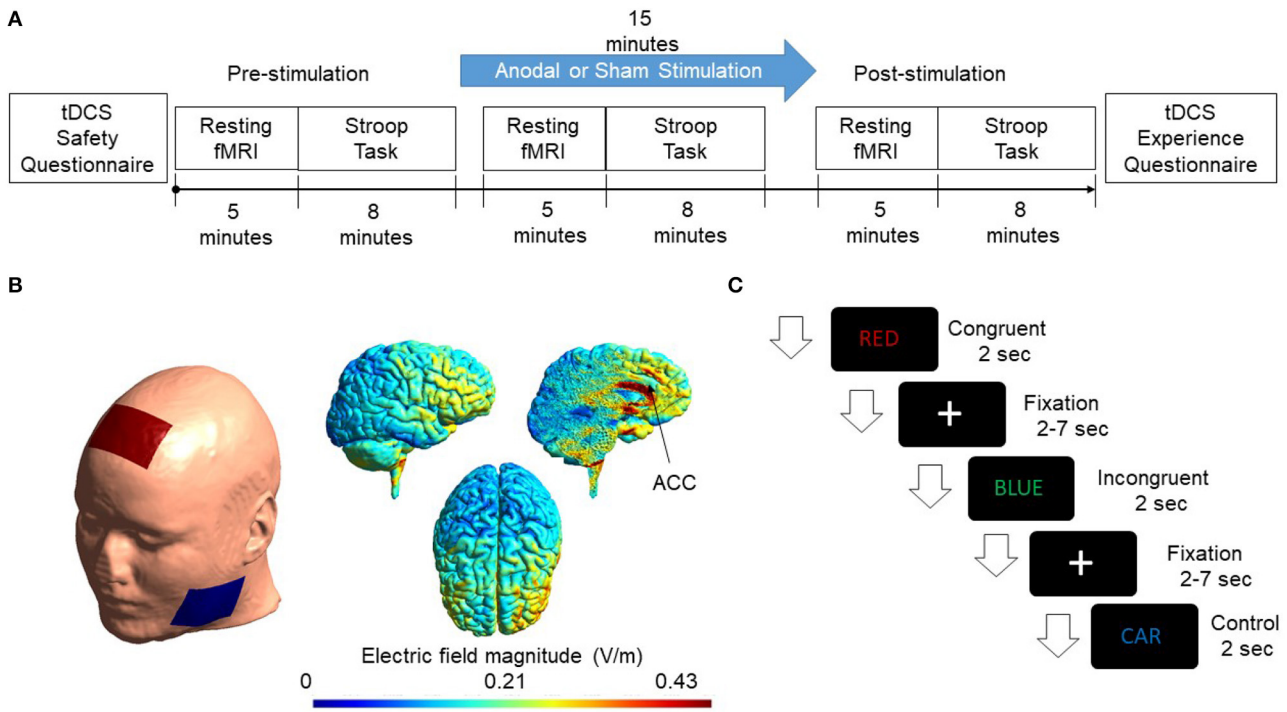

FIGURE 1 | (A) Flow chart of the experimental design is shown. Subjects were randomly assigned to the Experimental & Sham group. The cingulate cortex was stimulated for 15 min with a current intensity of 2 mA. Resting-state fMRI and Stroop task were administered pre, during, and post-stimulation. **(B)** A FEM model was used to simulate the electric field distribution adopted in this study. Electrodes were modeled as rubber electrodes with a sponge soaked in saline solution. Anode was placed at Fz according to the International 10/20 system. The cathode was placed at the cheek to minimize the effect of cathodal stimulation. The applied current was 2mA. Simulated electric field distribution in sagittal, axial, and the sliced sagittal view is shown. **(C)** The figure shows the presentation of events. Congruent, incongruent, and control trials appeared randomly on the screen. Each event occurred for 2 s while a fixation cross appeared after each trial with a jitter of 2–7 s.

2.1. Subjects

Twenty healthy subjects (15 males and five females) were recruited for this study with a mean age of 23.61 $\pm$ 2.77 years. However, only 18 subjects (13 males and five females) were able to finish the experiment, of which 10 were in the experimental group and eight in the sham stimulation group. Two subjects were not comfortable with the fMRI procedures and not able to finish the study. The inclusion criteria were: Right handedness and Age $\geq$ 18, normal or corrected-to-normal vision. All the participants were undergraduate or post-graduate students at The Chinese University of Hong Kong. The exclusion criteria were: a history of any neurological disease, any psychological or psychiatric disease, significant visual or auditory impairment, tDCS, or fMRI contraindications including implanted metallic or electronic devices, seizures, or convulsions, and pregnancy. The study was conducted in accordance with the Helsinki declaration ethical standards and approved by the Joint Chinese University of Hong Kong New Territories East Cluster Clinical Research Ethics Committee.

2.2. Transcranial Direct Current Stimulation

2.2.1. Stimulation Parameters

A direct current of 2 mA was administered for 15 min using conventional transcranial direct current stimulator (tDCS) (DC-Stimulator, Neuroconn GmbH, Ilmenau, Germany). Two conductive sponges act as cathode and anode with current flowing from one sponge to the other. The anode was placed at Fz location based on the 10–20 system as done in previous studies (To et al., 2018) while cathode was placed at the cheek. Conductive saline solution was applied on the sponge electrode to keep the impedance below 15 kΩ.

tDCS is bipolar, i.e., both cathode and anode impact the brain in opposite directions. Anodal stimulation increases the activation of brain activity while cathodal results in a decrease in brain activity (Stagg and Nitsche, 2011). Most of the studies reported an increase in brain excitability as a result of anodal stimulation. Thus, we utilized anodal stimulation in the present study. While performing anodal stimulation, we want to minimize the impact of cathodal stimulation. One possible methodology is to place anode over the target region in one hemisphere and cathode over the same region in the other hemisphere (Kadosh et al., 2010). However, this placement results in activation of one hemisphere and deactivation of the other, and any changes in behavioral outcome could result from either of them, which makes it difficult to conclude any specific function of the target brain area. Another possible placement methodology is to place the anode over the target area and cathode on one of the cheeks (Tseng et al., 2012) to minimize the impact of the cathode

as much as possible. The field produced by cathodal stimulation only affects facial muscles and gums, which provide the least resistance path to the current, thus reducing the cathode's impact on the brain. Scalp-cheek placement methodology was used in the study.

Furthermore, the human skull offers resistance to the current flow, and a considerable amount of current is shunted by the skull. Approximately, 75% of the current is attenuated by the scalp tissues and the skull (Vöröslakos et al., 2018). The duration of the current also plays an essential rule in determining the impact of stimulation. A meta-analysis examining the impact of stimulation reported that stimulation duration of more than 10 min and a current density of more than 0.029 mA/cm^2 could have a significant impact on behavioral results (Hill et al., 2016). Thus, we chose 2mA current with a duration of 15 min.

2.2.2. Simulation of the Electric Field Generated by tDCS

A Finite element model (FEM) was generated to simulate the electric field and current density distribution induced from tDCS using SIMNIBS 3.0.1 (Thielscher et al., 2015). FEM head mesh was first generated using T1 structural MRI data provided by the software. The head mesh was segmented as a six-compartment model with segmented scalp, skull, gray matter, white matter, cerebrospinal fluid (CSF), and eyes. Simulations were then initialized by placing modeled electrode montage on the surface of the scalp. Electrodes were configured as 5 × 7 cm rubber electrodes and placed in a customized location to mimic the actual stimulation montage. Electric field and current density distributions were calculated using volume normalized anisotropic conductivities (Güllmar et al., 2010). The diffusion tensor data provided by the software was normalized to have the same trace and rescaled in accordance with the reference isotropic conductivity of respective tissues (Opitz et al., 2015). Simulated results are shown in **Figure 1B**.

2.3. Color-Word Stroop Task

Stroop task is considered a gold standard for studying executive functions of the human brain. In the standard color-word version of the Stroop task, a word is presented in different colors. The color could be the word itself, for example, the word "RED" written in red color (congruent trials), or it could be different from the word, for example, the word "BLUE" written in green color (incongruent trials) (Zysset et al., 2001) or it could be a neutral trial in different colors in which the word used is not a color, for example, the word "CAR" written in blue color (control trials). For congruent and incongruent trials, there were four color words, and each of them was paired with each of the four colors. For the control trials, ten neutral words, which were not the name of a color or with a dominant color, were paired with the four colors to produce the neutral/control word stimuli. The experiment was presented using E-prime 3.0 (Schneider et al., 2013). Subjects were asked to respond to the color of the word and were given time to memorize the combination prior to the experiment. Two two-button panels were used inside the scanner numbering from 1 to 4. Subjects were asked to press 1 for blue, 2 for red, 3 for green, and 4 for yellow. One hundred twenty words were presented randomly with 40 words for each condition, i.e., congruent, incongruent, and control. Each of the word events lasted for 2 s with a fixation cross (2–7 s) between trials and an equal probability of occurring. The design of the stimuli presentation is shown in **Figure 1C**.

2.4. Functional Magnetic Resonance Imaging

Functional magnetic resonance imaging (fMRI) has been frequently utilized to understand the functioning of the human brain and the impact of non-invasive stimulation. Functional connectivity analysis is one of the principal methodologies to evaluate the connectivity between two or more brain regions based on their simultaneous engagement in oscillatory activity (Van Den Heuvel and Pol, 2010).

2.4.1. Data Acquisition

Subjects were scanned using a 3T Philips MR scanner with an 8-channel head coil. High resolution T1-weighted anatomical images (TR/TE = 7.47/3.45 ms, flip angle = 8°, 308 slices, voxel size = 0.6 × 1.042 ×1.042 mm^3) using a T1-TFE sequence (ultrafast spoiled gradient echo pulse sequence) and BOLD fMRI images (TR/TE = 2,000/30 ms, flip angle = 70°, 37 slices/volume, voxel size = 2.8 × 2.8 ×3.5 mm^3) using a gradient-echo-EPI sequence (gradient-echo echo-planar-imaging sequence) were acquired. fMRI run lasting for 5 min was acquired both before and after the stimulation. During the 15-min stimulation, a 5-min resting-state fMRI run was acquired at the beginning of the stimulation. The subjects were asked to rest while focusing on the white crosshair displayed on the screen and keep still.

2.4.2. Pre-processing

The preprocessing was performed with the default pipeline using the CONN toolbox (Whitfield-Gabrieli and Nieto-Castanon, 2012). Preprocessing steps included slice timing correction, outlier identification from the global signal and framewise displacement, motion correction, and co-registration of the anatomical image to the mean functional volume. All the functional images were then normalized to standard MNI space and resampled to 2 mm. Spatial smoothing was performed with an 8 mm isotropic FWHM Gaussian kernel to increase the signal-to-noise ratio. The resulting images were further processed in additional steps, including band-pass filtering (0.01–0.1 Hz) and regression of motion parameters, signals from white matter, and cerebrospinal fluid.

2.4.3. Functional Connectivity Analysis

Six regions of interest (ROIs) in the cingulate cortex were selected from the AAL template (Tzourio-Mazoyer et al., 2002; Rolls et al., 2015), including the bilateral anterior cingulate cortex (L-ACC and R-ACC), middle cingulate cortex (L-MCC and R-MCC) and posterior cingulate cortex (L-PCC and R-PCC). The purpose of including bilateral seeds was to investigate if stimulation modulates the interhemispheric connectivity between cingulate seeds. Furthermore, some previous studies have reported significant connectivity differences between left and right cingulate regions (Margulies et al., 2007; Yan et al.,

2009). Functional connectivity was calculated between the mean time series of each pair of the ROIs. Besides, for each ROI, a seed-based analysis was performed to explore the functional connectivity between the ROI and the whole brain voxels. Pearson correlation coefficient was used for all the connectivity analysis following by the Fisher r-to-z transformation. The locations of the ROIs generated using BrainNet Viewer (Xia et al., 2013) are shown in **Figure 2**.

3. STATISTICAL ANALYSIS

3.1. Behavioral Data

Statistical analyses were conducted with the SPSS 19 statistical software package. (IBM SPSS Statistics, NY, US). At pre-stimulation, a two-sample *t*-test was performed to check for any differences between the groups. For the change in RT in the Stroop task, a repeated measures ANOVA (stim × time × condition) was applied with group (experimental vs. sham) as the between-subjects variable and time (pre vs. during vs. post) and condition (congruent vs. incongruent vs.control) as within-subjects variables. To further study the conditional effects, separate ANOVAs were performed for individual conditions. If a significant ANOVA difference was observed, then *post-hoc* analyses were performed using *t*-tests. For accuracy, ANOVA was performed with group (experimental vs. sham) as between-subject variable and time (pre vs. during vs. post) as a within-subject variable. Bonferroni correction was used for multiple comparison correction. Effect sizes for *t*-tests and ANOVAs were estimated using Cohen's d and partial eta square, respectively (Lakens, 2013).

3.2. Neuroimaging Data

CONN 2nd level analysis module was used to perform statistical analysis on the group level data. At pre-stimulation, ROI-voxel and ROI-ROI group differences (experimental vs. sham) were assessed using a two sample *t*-test. To investigate stimulation-induced ROI-voxel and ROI-ROI changes, a 2 × 3 ANOVA was performed for each ROI with the group (experimental vs. sham) as between-subject variable and time (pre vs. during vs. post) as a within-subject variable. If a significant effect was observed for any of the ROI, then one-way ANOVA was performed for each group with three time-periods (pre vs. during vs. post). For ROI-voxel analysis, if significant clusters were identified, then the whole cluster was used as a mask for *post-hoc* analysis, and one way-ANOVA was performed for each group with three time periods (pre vs. during vs. post). For multiple comparison correction, random field theory parametric statistics were utilized. First, a statistical parametric map was estimated with a voxel threshold of $p < 0.001$, and a series of non-overlapping clusters were identified using the 18-connectivity criterion on neighboring voxels. Then, false discovery rate (FDR) corrections (Chumbley et al., 2010) with a cluster threshold of $p < 0.05$ were applied. Further, Bonferroni correction was applied on two anterior cingulate seeds and four mid and posterior cingulate seeds.

3.3. Brain-Behavior Correlations

To further understand the relationship between resting-state fMRI changes and behavioral changes, Spearman's correlation analysis was performed between significant changes in RT and significant changes in functional connectivity for the experimental group. Bonferroni correction was used for multiple comparison correction.

4. RESULTS

4.1. Demographic and Descriptive Information

A comparison between the ages of the participants in the experimental and sham group did not show any significant difference (t = 0.148, p = 0.884). Subjects in the experimental group reported mild to moderate itchiness on the skin and scalp following stimulation. No other tDCS related experiences were reported by any of the subjects.

4.2. Behavioral Results

ANOVA results at the pre-stimulation revealed a significant effect between conditions ($F = 5.892, p = 0.007, \eta_p^2 = 0.269$). Further analysis showed that the subjects were slower for incongruent trials (Mean = 882.781 ± 148.411 s) as compared to congruent (Mean = 757.475 ± 106.851 s) and control trials (Mean =796.062 ± 122.045 s). Comparison between the RT of experimental and sham group at pre-stimulation did not show any significant difference for the congruent ($t = 0.163, p = 0.873$), incongruent ($t = 1.397, p = 0.182$) and control ($t = 1.543, p = 0.142$) trials.

Repeated measures ANOVA results with stimulation group (experimental vs. sham) as between-subject variable and time (pre. vs. during. vs. post) and condition (congruent vs. incongruent vs. control) as within-subject variable showed a significant difference for Time ($F = 8.312, p = 0.001, \eta_p^2 = 0.342$), Condition ($F = 66.204, p < 0.001, \eta_p^2 = 0.805$), Time × Group ($F = 5.494, p = 0.009, \eta_p^2 = 0.256$), and Group × Condition ($5.659, p = 0.008, \eta_p^2 = 0.261$). However, no significant Time × Group × Condition interaction was observed ($F = 0.457, p = 0.767, \eta_p^2 = 0.028$). Further ANOVA was performed for experimental and sham group separately with time (pre vs. during vs. post) as a within-subject variable. A significant effect was observed ($F = 11.176, p < 0.001, \eta_p^2 = 0.554$) for the experimental group but no significant difference ($F = 0.543, p = 0.593, \eta_p^2 = 0.072$) was observed for the sham group. Paired *t*-test were conducted in experimental group between time periods (pre vs. during, pre vs. post, and during vs. post). A significant decrease in RT was observed during stimulation ($t = 4.363, p = 0.002, d = 0.745$), and post-stimulation ($t = 4.850, p = 0.001, d = 1.253$) as compared to pre-stimulation. The change in RT in the experimental and sham group are shown in **Figure 3A**. Furthermore, no significant effect was observed for accuracy ($F = 1.214, p = 0.310, \eta_p^2 = 0.044$) with group (experimental vs. sham) as a between-subject variable and time (pre vs. during vs. post) as a within-subject variable. At pre-stimulation experimental group showed an accuracy of ($Mean = 93.446 \pm 2.907\%$) and sham group showed an accuracy

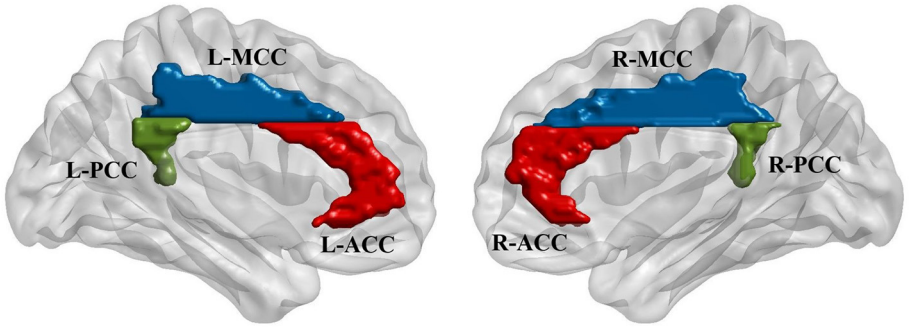

FIGURE 2 | Regions of interest (ROIs) were defined based on automatic anatomic labeling (AAL) atlas. Six cingulate ROIs were defined in both hemispheres including bilateral anterior cingulate cortex (L-ACC & R-ACC), bilateral midcingulate cortex (L-MCC & R-MCC), and bilateral posterior cingulate cortex (L-PCC & R-PCC) as shown in the left and right figures, respectively.

of ($Mean = 93.49 \pm 3.07\%$). The accuracy changes are shown in **Figure 3B**.

ANOVA results for individual conditions showed a significant group × time effect for congruent trials ($F = 3.603, p = 0.039$, $\eta_p^2 = 0.184$), marginally significant for incongruent trials ($F = 3.278, p = 0.051$, $\eta_p^2 = 0.170$) and strongly significant for control trials ($F = 6.284, p = 0.005$, $\eta_p^2 = 0.282$). For *post-hoc* analysis, we conducted paired *t*-test in the experimental and sham group for congruent, incongruent, and control trials between time periods (pre vs. post, pre vs. during, and during vs. post). For congruent trials in the experimental group, a significant decrease in RT was observed during stimulation ($t = 4.711, p = 0.001$, $d = 0.888$) and post-stimulation ($t = 3.749, p = 0.005$, $d = 1.176$) as compared to pre-stimulation. For incongruent trials in the experimental group, a significant decrease was observed during stimulation ($t = 2.949, p = 0.016$, $d = 0.552$) and post-stimulation ($t = 3.681, p = 0.005$, $d = 0.930$) as compared to pre-stimulation. For control trials in the experimental group, a significant decrease was observed during stimulation ($t = 3.335, p = 0.009$, $d = 0.757$), and post-stimulation ($t = 6.406, p < 0.001$, $d = 1.5451$) as compared to pre-stimulation and a significant decrease in post-stimulation ($t = 2.695, p = 0.025$, $d = 0.520$) as compared to during stimulation. Changes in RT in the experimental and sham group for individual conditions are shown in **Figure 3C**. No significant effect was observed for individual conditions in the sham group.

4.3. Functional Connectivity Analysis

4.3.1. ROI to Voxels

At pre-stimulation, no significant difference was observed between the experimental and sham groups. The ANOVA results with group (experimental vs. sham) as between-subject variable and time (pre vs. during vs. post) as a within-subject variable showed a significant difference in connectivity for two clusters including R anterior insular cortex, Right Planum Polare ($F = 16.69$, p-corrected = 0.010685, $\eta_p^2 = 0.481$) and R Central Opercular Cortex, R Frontal Operculum Cortex ($F = 16.69$,-corrected = 0.011217, $\eta_p^2 = 0.481$) with L-ACC as the seed as shown in **Table 1**. Axial, sagittal, and coronal views are shown in **Figures 4A,B** at the center of cluster 1 and cluster 2, respectively. Further, one-way ANOVA was performed for experimental and sham groups separately with time (pre vs. during. vs. post) as a within subject variable. For the experimental group, we observed a significant difference ($F = 10.407, p = 0.001$, $\eta_p^2 = 0.536$) between time periods (pre vs. during vs. post). For the sham group, we also observed a significant difference ($F = 6.571, p = 0.010$, $\eta_p^2 = 0.484$) between time periods (pre vs. during vs. post). For *post-hoc* analysis we performed paired *t*-tests which showed a significant decrease in connectivity during stimulation ($t = 4.566, p = 0.001$, $d = 1.253$), and post-stimulation ($t = 2.490, p = 0.034$, $d = 0.789$) as compared to pre-stimulation in the experimental group and a significant increase in connectivity during stimulation ($t = 3.771, p = 0.007$, $d = 1.388$) as compared to pre-stimulation in the sham group. No significance was observed for post-stimulation ($t = 1.697, p = 0.133$, $d = 0.630$) as compared to pre-stimulation in the sham group.

4.3.2. ROI-ROI

ANOVA results did not show any significance for ROI—ROI functional connectivity between any of the defined seeds.

4.4. Brain-Behavior Relationship

To investigate the relation between neuroimaging results and behavioral results, we performed a Spearman's rho correlation between the change in RT for all the conditions and the change in functional connectivity for L-ACC with significant clusters. Two 5mm ROIs were defined at the center of cluster 1 [+40 +04 +12] and cluster 2 [+40 −02 −10] in MNI space. The connectivity changes during stimulation for cluster 1 and cluster 2 are shown in **Figures 4C,D**, respectively. Similarly, post-stimulation connectivity variations for cluster 1 and cluster 2 are shown in **Figures 4E,F**, respectively. A correlation analysis was performed on the experimental group to assess stimulation related brain-behavior relationships. A significant positive correlation ($r = 0.818$, p-corrected = 0.008) was observed between decrease in RT (Pre—During) for incongruent trials and decrease in connectivity (pre—during) for cluster 1 as shown in **Figure 5A** and a positive correlation ($r = 0.758$, p-corrected = 0.022) between

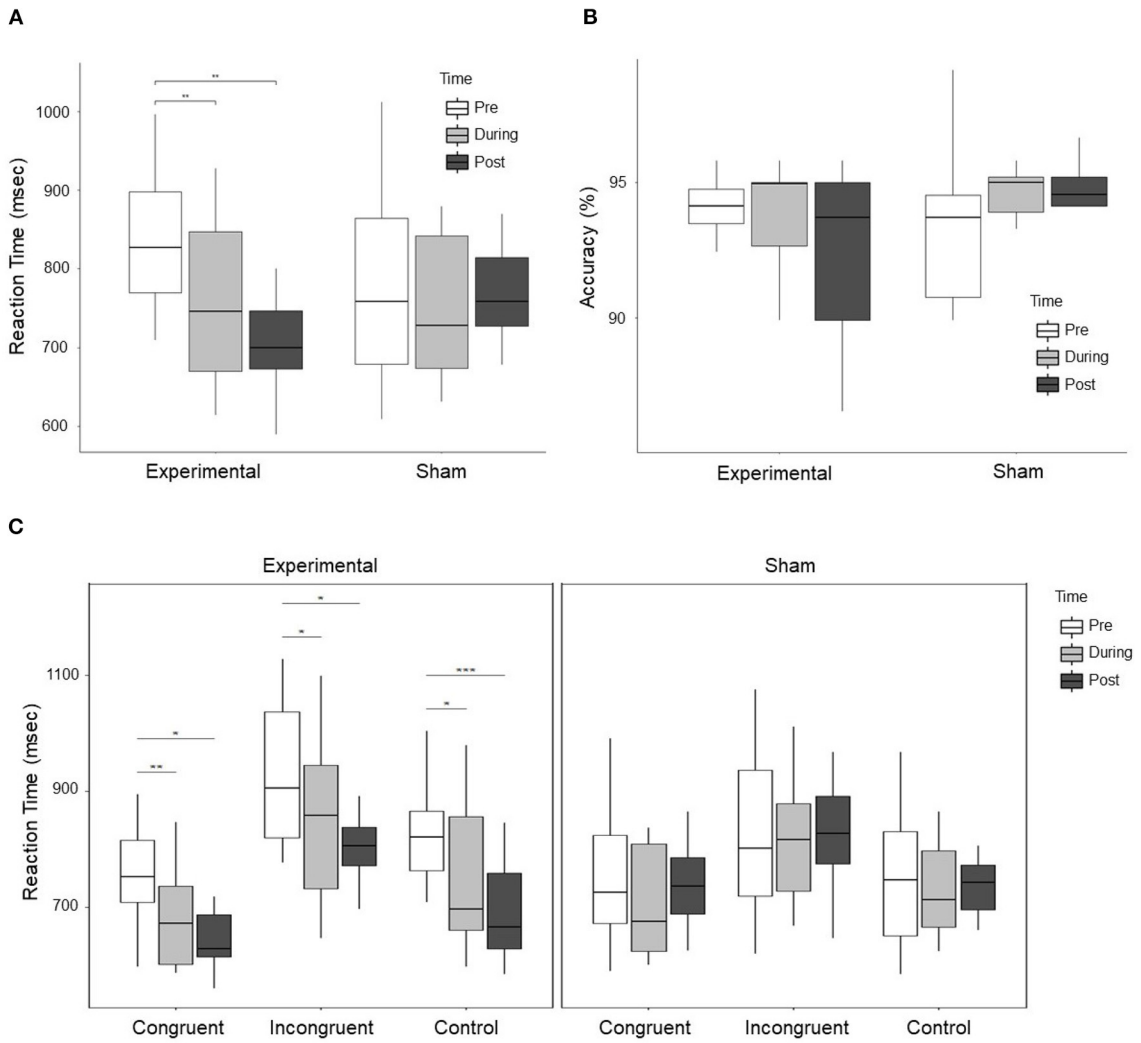

FIGURE 3 | (A) Shows the RT of subjects in the experimental and sham group for three time periods, i.e., pre, during, and post-stimulation. A significant Time × Group effect between experimental and sham group was observed. Further exploration indicated a significant decrease in RT in the experimental group during stimulation as compared to pre-stimulation, and post-stimulation as compared to pre-stimulation. **(B)** Shows the accuracy of subjects response to cognitive stroop task. No significant effect was observed for the change in accuracy, however, the trend shows that the accuracy reduced in the experimental group and improved in the sham group. **(C)** Shows the change in RT in the experimental and sham group for each condition, i.e., congruent, incongruent, and control trials. The left figure displays the change in RT for all the conditions in the experimental group, while the right figure shows the change in RT for all the conditions in the sham group. In the experimental group, a significant decrease in RT for congruent, incongruent, and control trials was observed during stimulation and post-stimulation as compared to pre-stimulation. For control trials, a significant decrease in RT was observed post-stimulation as compared to during stimulation. In the figure * represents $p < 0.05$, ** represents $p < 0.01$, and *** represents $p < 0.001$.

decrease in RT (pre—post) for incongruent trials and decrease in connectivity (pre—during) for cluster 1 as shown in **Figure 5B**.

5. DISCUSSION

Distinct neural mechanisms have been reported to mediate various aspects of cognitive control (Gratton et al., 2018). However, these mechanisms are not clearly understood due to the involvement of various brain regions in cognitive processing. Brain stimulation offers a possible approach to understand these mechanisms by modulating specific regions with small electric currents and observe changes in the brain signals and behavioral outcome. Here in this study, we aimed to stimulate the cingulate cortex using tDCS to observe the changes in the resting-state brain activity and the subsequent changes in the performance during a cognitive Stroop task.

5.1. Behavioral Results

In the behavioral results, we observed a significantly faster RT in the experimental group as compared to the sham group. This improvement in RT was observed during and after the stimulation for congruent, incongruent, and control trials in the

experimental group with no significant change in accuracy. Such behavioral gains have been observed in other stimulation related studies targeting different regions of the frontal cortex (Martin et al., 2014; Gbadeyan et al., 2016).

However, the results contradict a recent study that involved stimulation of ACC using high-definition tDCS (HD-tDCS) (To et al., 2018). They reported decreased RT in the incongruent trials of cognitive Stroop task after anodal stimulation, while no effect was observed for congruent and control trials. This can be related to the fact that HD-tDCS is more focal than conventional tDCS, and specific brain regions can be targeted using HD-tDCS (Villamar et al., 2013). However, conventional tDCS impacts broad areas in cortical and subcortical regions resulting in a more general improvement in all the trials irrespective of the trial type. Furthermore, an information theory account of cognitive control suggests that the role of ACC is not just conflict detection, as suggested by several other studies (Kerns et al., 2004; Carter and Van Veen, 2007); rather, it has a more general role in cognitive control (Fan, 2014). According to this theory, ACC, Anterior Insular cortex (AIC), and other brain areas are information processing entities that process information, and conflict is a special case of this information processing. Thus, stimulation of ACC could result in a general improvement in behavioral performance, as indicated in the current study.

TABLE 1 | The table shows 2 × 3 ANOVA results with group (experimental vs. sham) as a between-subject variable and time (pre vs. during vs. post) as a within subject variable with L-ACC selected as the seed.

Clusters	Cluster (x, y, z)	Cluster size	*p*-FDR	Regions
Cluster 1	[+40 +04 +12]	145 voxels	0.010685	R Ant Insular Cortex
				R Planum Polare
Cluster 2	[+40 −02 −10]	170 voxels	0.011217	R Central Opercular Cortex
				R Pos Insular Cortex
				R Frontal Operculum Cortex

p-*FDR* = p-*value after false discovery rate correction, R = right, Pos = posterior, Ant = anterior.*

5.2. Neuroimaging Results

Studies have reported that the functional organization of various networks exist in the brain even when the participant is not subjected to any external attentional demands, i.e., during

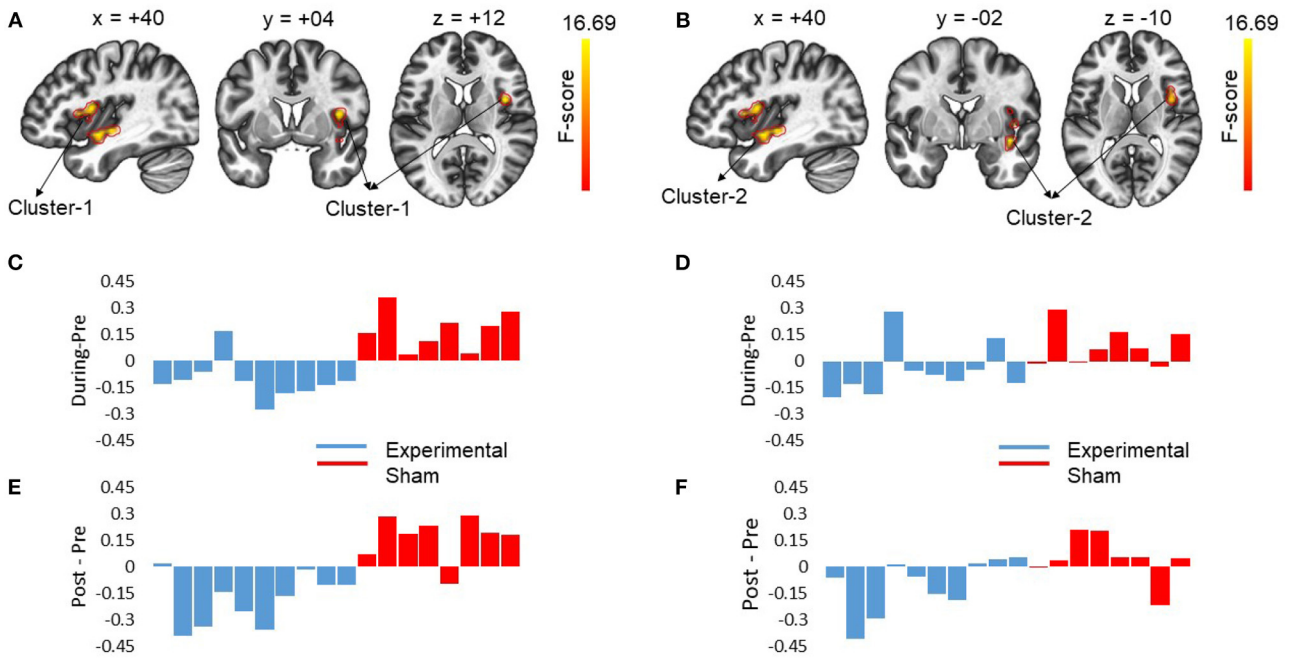

FIGURE 4 | The figures show the changes in functional connectivity for cluster 1 [+40 +04 +12] and cluster 2 [40 −02 −10] with L-ACC selected as the seed. The results are obtained by calculating ANOVA difference between groups (experimental vs. sham) as between-subject variable and time (pre vs. during vs. post) as a within-subject variable. **(A)** Sagittal, coronal and axial slices of brain from left to right with significant changes in connectivity between L-ACC and cluster 1 covering right anterior insular cortex (R-AIC) and right planum Polare are shown. The center of cluster 1 [+40 +04 +12] was chosen as the target slice. **(B)** shows the sagittal, coronal, and axial slices of brain from left to right with significant changes in connectivity between L-ACC and cluster 2 covering right central opercular cortex, right posterior insular cortex, and right frontal opercular cortex. The center of cluster 2 [+40 −02 −10] was chosen as the target slice. **(C)** Displays the difference between during stimulation connectivity and pre-stimulation connectivity for cluster 1. **(D)** Depicts the difference between during stimulation connectivity and pre-stimulation connectivity for cluster 2. **(E)** Shows the difference between post-stimulation connectivity and pre-stimulation connectivity for cluster 1. **(F)** Shows the difference between post-stimulation connectivity and pre-stimulation connectivity for cluster 2. The results indicate that stimulation resulted in a decrease in connectivity in the experimental group which lasted beyond stimulation period. However, for the sham group an opposite effect was observed. Moreover, the impact of stimulation showed inter-subject variability.

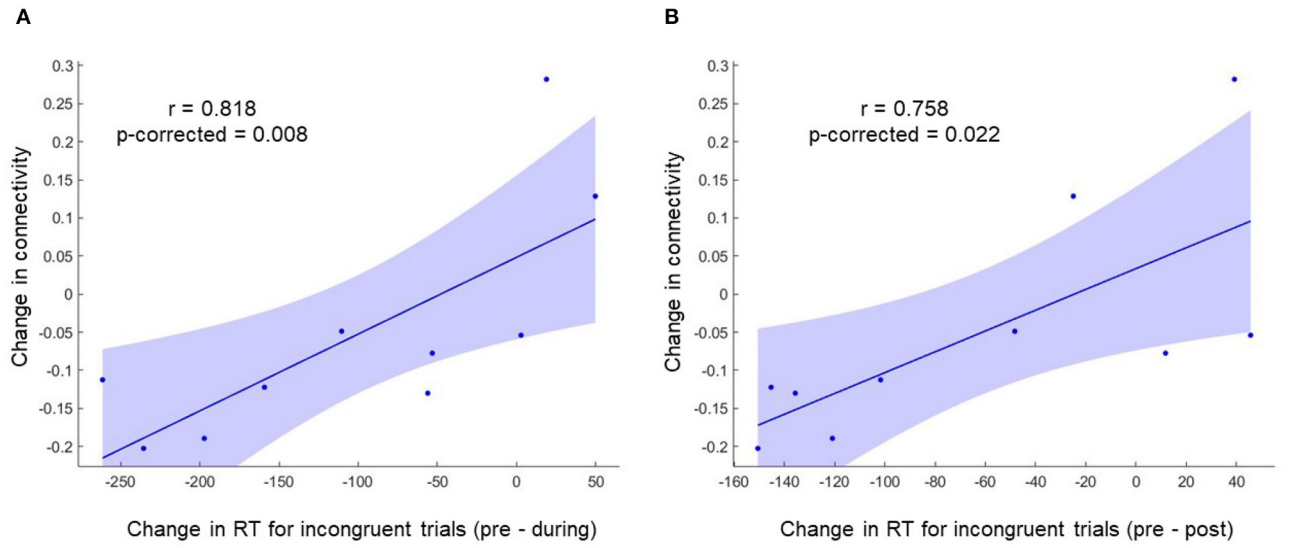

FIGURE 5 | A significant positive correlation was observed between change in RT for incongruent trials and change in functional connectivity for cluster 1. **(A)** Shows the correlation between change in RT (During—Pre) for incongruent trials and change in functional connectivity for cluster 1 (During—Pre). **(B)** Shows the correlation between change in RT (Post—Pre) for incongruent trials and change in functional connectivity for cluster 1 (During—Pre).

rest (Fox et al., 2006). Our study investigated stimulation-induced resting-state connectivity changes in different regions of cingulate. A significant decrease in the functional connectivity between the L-ACC and R-Insula, along with other subcortical regions, was observed as a result of stimulation in the experimental group. Further analysis revealed two clusters of change, one including the anterior insular cortex (AIC) and one including posterior insular cortex (PIC). The insular cortex has been reported to play a critical role in attentional processes and cognitive control (Seeley et al., 2007; Menon and Uddin, 2010). Moreover, the ACC and the AIC are two significant parts of the cognitive control network and have shown a close functional relationship across emotional processing, memory, cognition, sensation, and other behavioral contexts (Medford and Critchley, 2010; Menon and Uddin, 2010). Furthermore, Right AIC has been implicated to play a critical role in switching between two other major networks the default mode network (DMN) and the executive control network (ECN) during cognitive information processing and has been termed as the bottleneck of cognitive control (Wu et al., 2019).

Similar results have been reported by another study targeting DLPFC, which resulted in a change in the activation in the ACC and a decrease in connectivity between ACC and the whole brain along with subcortical regions (Weber et al., 2014). However, in the mentioned study, stimulation was performed outside the scanner, and they did not observe changes in brain connectivity during the stimulation. Moreover, they used a bilateral electrode montage in which anode was placed above the right DLPFC and cathode over its left counterpart, which makes it difficult to properly interpret the results (Reinhart et al., 2017). A recent study on normal aging indicated that older adults have a stronger connection between ACC and AIC as compared with younger adults, which was attributed to cognitive decline in elderly subjects (Cao et al., 2014). Furthermore, meditation studies have reported that the meditation modulates the activity between left ACC and insula thus creating interhemispheric frontal asymmetry (Tang et al., 2015). The frontal asymmetry has been reported to be an index for positive mood (Tang et al., 2015) which may enhance cognitive performance. These studies suggest that altered resting-state connectivity between L-ACC and insular regions, as shown in the present study might indicate enhanced cognitive functioning.

Moreover, an increase in the connectivity for the sham group following a Stroop task indicates a relaxation phenomenon in relevant brain regions after engaging in a cognitively demanding task. This increase in connectivity following a task has been previously observed in prefrontal regions following a language task (Waites et al., 2005), prefrontal regions in visual cognitive tasks utilizing different faces and complex scenes (Stevens et al., 2010), and bilateral motor regions following a button press task (Tung et al., 2013). However, we could not observe such carryover effect neither in experimental or sham group in other cingulate regions including MCC and PCC which have reported activations during stroop task.

Moreover, we observed inter-individual variability in stimulation induced connectivity changes. This variability in the impact of tDCS has been reported at an individual level in several other studies (Dedoncker et al., 2016; Lefebvre and Liew, 2017). One major reason causing such variations is the difference in individual anatomy, which suggests that the same stimulation protocol applied to different subjects can result in varying electric field strength around the target due to different scalp and skull thickness and white matter anisotropy for each individual (Laakso et al., 2019; Mikkonen et al., 2020). Simulation of electric

fields could potentially help to reduce the heterogeneity of the results by determining the optimal stimulation protocols for each individual before comparing the effect of stimulation. Furthermore, in our study, the ROIs were selected based on the AAL template (Tzourio-Mazoyer et al., 2002; Rolls et al., 2015), which parcellates the cingulate into fairly large anterior, mid, and posterior cingulate regions. A recent study proposed a cingulate parcellation scheme at the subregional level, which showed consistency of functional connectivity with anatomical subregions (Jin et al., 2018). Future stimulation-related studies may focus on small cingulate subregions, thus enhancing our understanding of stimulation's impact on cingulate subregional levels. Moreover, utilization of network neuroscience approach (Bassett and Sporns, 2017) in different brain networks, i.e., neurons, circuits, systems, whole brain, behavior, and across various spatial and temporal scales could pave the way for a better understanding of the impact of tDCS on the human brain.

5.3. Brain-Behavior Relationship

A correlation analysis was performed between change in RT and change in connectivity between L-ACC and ROIs defined at the center of two clusters. A positive correlation was observed between change in functional connectivity (during stimulation—pre-stimulation) and change in RT for incongruent trials during and post-stimulation as compared to pre stimulation, which suggests that the impact of stimulation on the brain during-stimulation can indicate subsequent improvement in behavioral tasks after stimulation. Previous studies have also reported that the changes in brain activity as a result of stimulation correspond to the changes in behavioral results. For example, anodal stimulation of the medial-frontal region increased learning rates in simple stimulus-response mapping tasks while cathodal stimulation resulted in a decrease in learning (Reinhart and Woodman, 2014). Furthermore, anodal stimulation over the parietal cortex improved acuity and amplitude of event-related potentials (ERPs), while cathodal stimulation resulted in a decrease of both (Reinhart et al., 2016). Here, we demonstrated that tDCS targeted at the ACC could induce neurological changes at resting-state, which further correlated with the changes in the reaction time for incongruent trails. However, such correlations were not observed for congruent and control trials which indicate that stimulation may have impacted relevant brain regions in prefrontal cortex other than ACC resulting in an improvement in these trials which can be further explored in future studies.

5.4. Conclusion

We conclude that a 15 min direct current stimulation of 2 mA can penetrate deeper brain structures like cingulate and alters its activity, which results in the reduction of the resting-state functional connectivity of ACC with subcortical regions during stimulation and after stimulation. This decrease in connectivity indicates an enhancement in cognitive functioning, which results in an improvement in performance during the stroop task. Thus, ACC could be another potential target of stimulation to enhance cognitive functioning.

DATA AVAILABILITY STATEMENT

The raw data supporting the conclusions of this article will be made available by the authors, without undue reservation.

ETHICS STATEMENT

The studies involving human participants were reviewed and approved by Joint Chinese University of Hong Kong New Territories East Cluster Clinical Research Ethics Committee. The patients/participants provided their written informed consent to participate in this study.

AUTHOR CONTRIBUTIONS

AK conducted the experiments and analyzed the data with support from XW. CT planned and carried out the simulations. K-YT and C-YT supervised the project. All authors provided critical feedback in analyzing the data and drafting the manuscript.

FUNDING

This study was supported by the Hong Kong Research Grant Council (GRF No: 14207617), Hong Kong SAR, China.

REFERENCES

Badzakova-Trajkov, G., Barnett, K. J., Waldie, K. E., and Kirk, I. J. (2009). An ERP investigation of the stroop task: the role of the cingulate in attentional allocation and conflict resolution. *Brain Res.* 1253, 139–148. doi: 10.1016/j.brainres.2008.11.069

Bao, S., Khan, A., Song, R., and Tong, R. K. (2020). Rewiring the lesioned brain: electrical stimulation for post-stroke motor restoration. *J. Stroke* 22:47. doi: 10.5853/jos.2019.03027

Bassett, D. S., and Sporns, O. (2017). Network neuroscience. *Nat. Neurosci.* 20:353. doi: 10.1038/nn.4502

Bélanger, S., Belleville, S., and Gauthier, S. (2010). Inhibition impairments in alzheimer's disease, mild cognitive impairment and healthy aging: effect of congruency proportion in a stroop task. *Neuropsychologia* 48, 581–590. doi: 10.1016/j.neuropsychologia.2009.10.021

Berryhill, M. E., Peterson, D. J., Jones, K. T., and Stephens, J. A. (2014). Hits and misses: leveraging tDCS to advance cognitive research. *Front. Psychol.* 5:800. doi: 10.3389/fpsyg.2014.00800

Biagioni, M. C., Sharma, K., Migdadi, H. A., and Cucca, A. (2018). "Non-invasive neuromodulation therapies for Parkinson's disease," in *Parkinson's Disease-Understanding Pathophysiology and Developing Therapeutic Strategies*, ed S. C. Yenisetti (IntechOpen), 51–76. doi: 10.5772/intechopen.75052

Boonstra, T. W., Nikolin, S., Meisener, A.-C., Martin, D. M., and Loo, C. K. (2016). Change in mean frequency of resting-state electroencephalography after transcranial direct current stimulation. *Front. Hum. Neurosci.* 10:270. doi: 10.3389/fnhum.2016.00270

Cao, W., Luo, C., Zhu, B., Zhang, D., Dong, L., Gong, J., et al. (2014). Resting-state functional connectivity in anterior cingulate cortex in normal aging. *Front. Aging Neurosci.* 6:280. doi: 10.3389/fnagi.2014.00280

Carter, C. S., and Van Veen, V. (2007). Anterior cingulate cortex and conflict detection: an update of theory and data. *Cogn. Affect. Behav. Neurosci.* 7, 367–379. doi: 10.3758/CABN.7.4.367

Chumbley, J., Worsley, K., Flandin, G., and Friston, K. (2010). Topological FDR for neuroimaging. *Neuroimage* 49, 3057–3064. doi: 10.1016/j.neuroimage.2009.10.090

Coderre, E., Conklin, K., and van Heuven, W. J. (2011). Electrophysiological measures of conflict detection and resolution in the stroop task. *Brain Res.* 1413, 51–59. doi: 10.1016/j.brainres.2011.07.017

Dedoncker, J., Brunoni, A. R., Baeken, C., and Vanderhasselt, M.-A. (2016). A systematic review and meta-analysis of the effects of transcranial direct current stimulation (tDCS) over the dorsolateral prefrontal cortex in healthy and neuropsychiatric samples: influence of stimulation parameters. *Brain Stimul.* 9, 501–517. doi: 10.1016/j.brs.2016.04.006

Dum, R. P., and Strick, P. L. (1993). "Cingulate motor areas," in *Neurobiology of Cingulate Cortex and Limbic Thalamus*, eds B. A. Vogt and M. Gabriel (Springer), 415–441. doi: 10.1007/978-1-4899-6704-6_15

Fan, J. (2014). An information theory account of cognitive control. *Front. Hum. Neurosci.* 8:680. doi: 10.3389/fnhum.2014.00680

Fox, M. D., Corbetta, M., Snyder, A. Z., Vincent, J. L., and Raichle, M. E. (2006). Spontaneous neuronal activity distinguishes human dorsal and ventral attention systems. *Proc. Natl. Acad. Sci. U.S.A.* 103, 10046–10051. doi: 10.1073/pnas.0604187103

Gbadeyan, O., McMahon, K., Steinhauser, M., and Meinzer, M. (2016). Stimulation of dorsolateral prefrontal cortex enhances adaptive cognitive control: a high-definition transcranial direct current stimulation study. *J. Neurosci.* 36, 12530–12536. doi: 10.1523/JNEUROSCI.2450-16.2016

Gratton, G., Cooper, P., Fabiani, M., Carter, C. S., and Karayanidis, F. (2018). Dynamics of cognitive control: theoretical bases, paradigms, and a view for the future. *Psychophysiology* 55:e13016. doi: 10.1111/psyp.13016

Güllmar, D., Haueisen, J., and Reichenbach, J. R. (2010). Influence of anisotropic electrical conductivity in white matter tissue on the EEG/MEG forward and inverse solution. A high-resolution whole head simulation study. *Neuroimage* 51, 145–163. doi: 10.1016/j.neuroimage.2010.02.014

Hill, A. T., Fitzgerald, P. B., and Hoy, K. E. (2016). Effects of anodal transcranial direct current stimulation on working memory: a systematic review and meta-analysis of findings from healthy and neuropsychiatric populations. *Brain Stimul.* 9, 197–208. doi: 10.1016/j.brs.2015.10.006

Jin, F., Zheng, P., Liu, H., Guo, H., and Sun, Z. (2018). Functional and anatomical connectivity-based parcellation of human cingulate cortex. *Brain Behav.* 8:e01070. doi: 10.1002/brb3.1070

Kadosh, R. C., Soskic, S., Iuculano, T., Kanai, R., and Walsh, V. (2010). Modulating neuronal activity produces specific and long-lasting changes in numerical competence. *Curr. Biol.* 20, 2016–2020. doi: 10.1016/j.cub.2010.10.007

Kerns, J. G., Cohen, J. D., MacDonald, A. W., Cho, R. Y., Stenger, V. A., and Carter, C. S. (2004). Anterior cingulate conflict monitoring and adjustments in control. *Science* 303, 1023–1026. doi: 10.1126/science.1089910

Kim, C., Johnson, N. F., and Gold, B. T. (2014). Conflict adaptation in prefrontal cortex: now you see it, now you don't. *Cortex* 50, 76–85. doi: 10.1016/j.cortex.2013.08.011

Kuo, M.-F., Paulus, W., and Nitsche, M. A. (2014). Therapeutic effects of non-invasive brain stimulation with direct currents (tDCS) in neuropsychiatric diseases. *Neuroimage* 85, 948–960. doi: 10.1016/j.neuroimage.2013.05.117

Laakso, I., Mikkonen, M., Koyama, S., Hirata, A., and Tanaka, S. (2019). Can electric fields explain inter-individual variability in transcranial direct current stimulation of the motor cortex? *Sci. Rep.* 9:626. doi: 10.1038/s41598-018-37226-x

Lakens, D. (2013). Calculating and reporting effect sizes to facilitate cumulative science: a practical primer for *t*-tests and ANOVAs. *Front. Psychol.* 4:863. doi: 10.3389/fpsyg.2013.00863

Leech, R., Braga, R., and Sharp, D. J. (2012). Echoes of the brain within the posterior cingulate cortex. *J. Neurosci.* 32, 215–222. doi: 10.1523/JNEUROSCI.3689-11.2012

Lefebvre, S., and Liew, S.-L. (2017). Anatomical parameters of tdcs to modulate the motor system after stroke: a review. *Front. Neurol.* 8:29. doi: 10.3389/fneur.2017.00029

MacLeod, C. M. (1992). The stroop task: the "gold standard" of attentional measures. *J. Exp. Psychol. Gen.* 121:12. doi: 10.1037/0096-3445.121.1.12

Margulies, D. S., Kelly, A. C., Uddin, L. Q., Biswal, B. B., Castellanos, F. X., and Milham, M. P. (2007). Mapping the functional connectivity of anterior cingulate cortex. *Neuroimage* 37, 579–588. doi: 10.1016/j.neuroimage.2007.05.019

Martin, D. M., Liu, R., Alonzo, A., Green, M., and Loo, C. K. (2014). Use of transcranial direct current stimulation (tDCS) to enhance cognitive training: effect of timing of stimulation. *Exp. Brain Res.* 232, 3345–3351. doi: 10.1007/s00221-014-4022-x

Medford, N., and Critchley, H. D. (2010). Conjoint activity of anterior insular and anterior cingulate cortex: awareness and response. *Brain Struct. Funct.* 214, 535–549. doi: 10.1007/s00429-010-0265-x

Menon, V., and Uddin, L. Q. (2010). Saliency, switching, attention and control: a network model of insula function. *Brain Struct. Funct.* 214, 655–667. doi: 10.1007/s00429-010-0262-0

Mikkonen, M., Laakso, I., Tanaka, S., and Hirata, A. (2020). Cost of focality in tDCS: interindividual variability in electric fields. *Brain Stimul.* 13, 117–124. doi: 10.1016/j.brs.2019.09.017

Nitsche, M. A., Cohen, L. G., Wassermann, E. M., Priori, A., Lang, N., Antal, A., et al. (2008). Transcranial direct current stimulation: state of the art 2008. *Brain Stimul.* 1, 206–223. doi: 10.1016/j.brs.2008.06.004

O'Connell, N. E., Marston, L., Spencer, S., DeSouza, L. H., and Wand, B. M. (2018). Non-invasive brain stimulation techniques for chronic pain. *Cochrane Database Syst. Rev.* 3:CD008208. doi: 10.1002/14651858.CD008208.pub5

Opitz, A., Paulus, W., Will, S., Antunes, A., and Thielscher, A. (2015). Determinants of the electric field during transcranial direct current stimulation. *Neuroimage* 109, 140–150. doi: 10.1016/j.neuroimage.2015.01.033

Paus, T. (2001). Primate anterior cingulate cortex: where motor control, drive and cognition interface. *Nat. Rev. Neurosci.* 2, 417–424. doi: 10.1038/35077500

Pearson, J. M., Heilbronner, S. R., Barack, D. L., Hayden, B. Y., and Platt, M. L. (2011). Posterior cingulate cortex: adapting behavior to a changing world. *Trends Cogn. Sci.* 15, 143–151. doi: 10.1016/j.tics.2011.02.002

Reinhart, R. M., Cosman, J. D., Fukuda, K., and Woodman, G. F. (2017). Using transcranial direct-current stimulation (tDCS) to understand cognitive processing. *Attent. Percept. Psychophys.* 79, 3–23. doi: 10.3758/s13414-016-1224-2

Reinhart, R. M., and Woodman, G. F. (2014). Causal control of medial-frontal cortex governs electrophysiological and behavioral indices of performance monitoring and learning. *J. Neurosci.* 34, 4214–4227. doi: 10.1523/JNEUROSCI.5421-13.2014

Reinhart, R. M., Xiao, W., McClenahan, L. J., and Woodman, G. F. (2016). Electrical stimulation of visual cortex can immediately improve spatial vision. *Curr. Biol.* 26, 1867–1872. doi: 10.1016/j.cub.2016.05.019

Rolls, E. T. (2019). The cingulate cortex and limbic systems for emotion, action, and memory. *Brain Struct. Funct.* 166, 23–37. doi: 10.1007/s00429-019-01945-2

Rolls, E. T., Joliot, M., and Tzourio-Mazoyer, N. (2015). Implementation of a new parcellation of the orbitofrontal cortex in the automated anatomical labeling atlas. *Neuroimage* 122, 1–5. doi: 10.1016/j.neuroimage.2015.07.075

Schneider, W., Eschman, A., and Zuccolotto, A. (2013). *E-prime 3.0 Getting Started Guide*. Pittsburgh: Psychology Software Tools, Inc.

Seeley, W. W., Menon, V., Schatzberg, A. F., Keller, J., Glover, G. H., Kenna, H., et al. (2007). Dissociable intrinsic connectivity networks for salience processing and executive control. *J. Neurosci.* 27, 2349–2356. doi: 10.1523/JNEUROSCI.5587-06.2007

Shackman, A. J., Salomons, T. V., Slagter, H. A., Fox, A. S., Winter, J. J., and Davidson, R. J. (2011). The integration of negative affect, pain and cognitive control in the cingulate cortex. *Nat. Rev. Neurosci.* 12, 154–167. doi: 10.1038/nrn2994

Stagg, C. J., and Nitsche, M. A. (2011). Physiological basis of transcranial direct current stimulation. *Neuroscientist* 17, 37–53. doi: 10.1177/1073858410386614

Stevens, W. D., Buckner, R. L., and Schacter, D. L. (2010). Correlated low-frequency bold fluctuations in the resting human brain are modulated by recent experience in category-preferential visual regions. *Cereb. Cortex* 20, 1997–2006. doi: 10.1093/cercor/bhp270

Tang, Y.-Y., Lu, Q., Feng, H., Tang, R., and Posner, M. I. (2015). Short-term meditation increases blood flow in anterior cingulate cortex and insula. *Front. Psychol.* 6:212. doi: 10.3389/fpsyg.2015.00212

Thielscher, A., Antunes, A., and Saturnino, G. B. (2015). "Field modeling for transcranial magnetic stimulation: a useful tool to understand the physiological effects of TMS?" in *2015 37th Annual International Conference of the IEEE Engineering in Medicine and Biology Society (EMBC)* (Milan: IEEE), 222–225. doi: 10.1109/EMBC.2015.7318340

To, W. T., Eroh, J., Hart, J., and Vanneste, S. (2018). Exploring the effects of anodal and cathodal high definition transcranial direct current stimulation targeting the dorsal anterior cingulate cortex. *Sci. Rep.* 8:4454. doi: 10.1038/s41598-018-22730-x

Tolomeo, S., Christmas, D., Jentzsch, I., Johnston, B., Sprengelmeyer, R., Matthews, K., et al. (2016). A causal role for the anterior mid-cingulate cortex in negative affect and cognitive control. *Brain* 139, 1844–1854. doi: 10.1093/brain/aww069

Tremblay, S., Lepage, J.-F., Latulipe-Loiselle, A., Fregni, F., Pascual-Leone, A., and Théoret, H. (2014). The uncertain outcome of prefrontal tdcs. *Brain Stimul.* 7, 773–783. doi: 10.1016/j.brs.2014.10.003

Tseng, P., Hsu, T.-Y., Chang, C.-F., Tzeng, O. J., Hung, D. L., Muggleton, N. G., et al. (2012). Unleashing potential: transcranial direct current stimulation over the right posterior parietal cortex improves change detection in low-performing individuals. *J. Neurosci.* 32, 10554–10561. doi: 10.1523/JNEUROSCI.0362-12.2012

Tung, K.-C., Uh, J., Mao, D., Xu, F., Xiao, G., and Lu, H. (2013). Alterations in resting functional connectivity due to recent motor task. *Neuroimage* 78, 316–324. doi: 10.1016/j.neuroimage.2013.04.006

Tzourio-Mazoyer, N., Landeau, B., Papathanassiou, D., Crivello, F., Etard, O., Delcroix, N., et al. (2002). Automated anatomical labeling of activations in SPM using a macroscopic anatomical parcellation of the MNI MRI single-subject brain. *Neuroimage* 15, 273–289. doi: 10.1006/nimg.2001.0978

Van Den Heuvel, M. P., and Pol, H. E. H. (2010). Exploring the brain network: a review on resting-state fmri functional connectivity. *Eur. Neuropsychopharmacol.* 20, 519–534. doi: 10.1016/j.euroneuro.2010.03.008

Vanderhasselt, M.-A., De Raedt, R., and Baeken, C. (2009). Dorsolateral prefrontal cortex and stroop performance: tackling the lateralization. *Psychon. Bull. Rev.* 16, 609–612. doi: 10.3758/PBR.16.3.609

Villamar, M. F., Volz, M. S., Bikson, M., Datta, A., DaSilva, A. F., and Fregni, F. (2013). Technique and considerations in the use of 4 × 1 ring high-definition transcranial direct current stimulation (HD-tDCS). *J. Vis. Exp.* e50309. doi: 10.3791/50309

Vöröslakos, M., Takeuchi, Y., Brinyiczki, K., Zombori, T., Oliva, A., Fernández-Ruiz, A., et al. (2018). Direct effects of transcranial electric stimulation on brain circuits in rats and humans. *Nat. Commun.* 9:483. doi: 10.1038/s41467-018-02928-3

Waites, A. B., Stanislavsky, A., Abbott, D. F., and Jackson, G. D. (2005). Effect of prior cognitive state on resting state networks measured with functional connectivity. *Hum. Brain Mapp.* 24, 59–68. doi: 10.1002/hbm.20069

Weber, M. J., Messing, S. B., Rao, H., Detre, J. A., and Thompson-Schill, S. L. (2014). Prefrontal transcranial direct current stimulation alters activation and connectivity in cortical and subcortical reward systems: a tDCS-fmri study. *Hum. Brain Mapp.* 35, 3673–3686. doi: 10.1002/hbm.22429

West, R., and Alain, C. (2000). Effects of task context and fluctuations of attention on neural activity supporting performance of the stroop task. *Brain Res.* 873, 102–111. doi: 10.1016/S0006-8993(00)02530-0

Westphal, A. J., Chow, T. E., Ngoy, C., Zuo, X., Liao, V., Storozuk, L. A., et al. (2019). Anodal transcranial direct current stimulation to the left rostrolateral prefrontal cortex selectively improves source memory retrieval. *J. Cogn. Neurosci.* 31, 1380–1391. doi: 10.1162/jocn_a_01421

Whitfield-Gabrieli, S., and Nieto-Castanon, A. (2012). Conn: a functional connectivity toolbox for correlated and anticorrelated brain networks. *Brain Connect.* 2, 125–141. doi: 10.1089/brain.2012.0073

Wu, T., Wang, X., Wu, Q., Spagna, A., Yang, J., Yuan, C., et al. (2019). Anterior insular cortex is a bottleneck of cognitive control. *Neuroimage* 195, 490–504. doi: 10.1016/j.neuroimage.2019.02.042

Xia, M., Wang, J., and He, Y. (2013). Brainnet viewer: a network visualization tool for human brain connectomics. *PLoS ONE* 8:e68910. doi: 10.1371/journal.pone.0068910

Yan, H., Zuo, X.-N., Wang, D., Wang, J., Zhu, C., Milham, M. P., et al. (2009). Hemispheric asymmetry in cognitive division of anterior cingulate cortex: a resting-state functional connectivity study. *Neuroimage* 47, 1579–1589. doi: 10.1016/j.neuroimage.2009.05.080

Zysset, S., Müller, K., Lohmann, G., and von Cramon, D. Y. (2001). Color-word matching stroop task: separating interference and response conflict. *Neuroimage* 13, 29–36. doi: 10.1006/nimg.2000.0665

Conflict of Interest: The authors declare that the research was conducted in the absence of any commercial or financial relationships that could be construed as a potential conflict of interest.

frontiers in Human Neuroscience

ORIGINAL RESEARCH
published: 21 December 2020
doi: 10.3389/fnhum.2020.555054

Combining Gamma With Alpha and Beta Power Modulation for Enhanced Cortical Mapping in Patients With Focal Epilepsy

Mario E. Archila-Meléndez[1,2,3,4], Giancarlo Valente[1,2,5], Erik D. Gommer[2,6], João M. Correia[1,7,8], Sanne ten Oever[1,2,5], Judith C. Peters[1,5,9], Joel Reithler[1,5,9], Marc P. H. Hendriks[10,11,12], William Cornejo Ochoa[13], Olaf E. M. G. Schijns[10,11,14], Jim T. A. Dings[10,11], Danny M. W. Hilkman[6,10], Rob P. W. Rouhl[2,10,14,15], Bernadette M. Jansma[1,2,5], Vivianne H. J. M. van Kranen-Mastenbroek[2,6,10,15] and Mark J. Roberts[1,2]*

[1] Department of Cognitive Neuroscience, Faculty of Psychology and Neuroscience, Maastricht University, Maastricht, Netherlands, [2] Center for Integrative Neuroscience (CIN), Maastricht University, Maastricht, Netherlands, [3] Neuroscientific MR-Physics Research Group, Department of Diagnostic and Interventional Neuroradiology, Klinikum rechts der Isar, School of Medicine, Technische Universität München, Munich, Germany, [4] Technical University of Munich Neuroimaging Center (TUM-NIC), Klinikum rechts der Isar, School of Medicine, Technische Universität München, Munich, Germany, [5] Maastricht Brain Imaging Center (M-BIC), Maastricht University, Maastricht, Netherlands, [6] Department of Clinical Neurophysiology, Maastricht University Medical Center, Maastricht University, Maastricht, Netherlands, [7] Basque Center on Cognition, Brain and Language (BCBL), Donostia-San Sebastian, Spain, [8] Centre for Biomedical Research (CBMR)/Department of Psychology, Universidade do Algarve, Faro, Portugal, [9] Department of Vision & Cognition, Netherlands Institute for Neuroscience, An Institute of the Royal Netherlands Academy of Arts and Sciences (KNAW), Amsterdam, Netherlands, [10] Academic Center for Epileptology, Kempenhaeghe/Maastricht University Medical Center, Maastricht, Netherlands, [11] Department of Neurosurgery, Maastricht University Medical Center Maastricht, Maastricht University, Maastricht, Netherlands, [12] Donders Institute for Brain, Cognition and Behaviour, Radboud University, Nijmegen, Netherlands, [13] Grupo Pediaciencias, Facultad de Medicina, Universidad de Antioquia, Medellín, Antioquia, Colombia, [14] School for Mental Health and Neuroscience (MHeNS), Maastricht University, Maastricht, Netherlands, [15] Department of Neurology, Maastricht University Medical Center, Maastricht, Netherlands*

OPEN ACCESS

Edited by:
Nathan Earl Crone, Johns Hopkins University, United States

Reviewed by:
Abbas Babajani-Feremi, University of Tennessee Health Science Center (UTHSC), United States
Milena Korostenskaja, Florida Hospital for Children, United States
Mario Tombini, Campus Bio-Medico University, Italy

***Correspondence:**
Mario E. Archila-Meléndez
mario.archila@tum.de

Specialty section:
This article was submitted to Brain Imaging and Stimulation, a section of the journal Frontiers in Human Neuroscience

Received: *23 April 2020*
Accepted: *17 November 2020*
Published: *21 December 2020*

Citation:
Archila-Meléndez ME, Valente G, Gommer ED, Correia JM, ten Oever S, Peters JC, Reithler J, Hendriks MPH, Cornejo Ochoa W, Schijns OEMG, Dings JTA, Hilkman DMW, Rouhl RPW, Jansma BM, van Kranen-Mastenbroek VHJM and Roberts MJ (2020) Combining Gamma With Alpha and Beta Power Modulation for Enhanced Cortical Mapping in Patients With Focal Epilepsy. Front. Hum. Neurosci. 14:555054. doi: 10.3389/fnhum.2020.555054

About one third of patients with epilepsy have seizures refractory to the medical treatment. Electrical stimulation mapping (ESM) is the gold standard for the identification of "eloquent" areas prior to resection of epileptogenic tissue. However, it is time-consuming and may cause undesired side effects. Broadband gamma activity (55–200 Hz) recorded with extraoperative electrocorticography (ECoG) during cognitive tasks may be an alternative to ESM but until now has not proven of definitive clinical value. Considering their role in cognition, the alpha (8–12 Hz) and beta (15–25 Hz) bands could further improve the identification of eloquent cortex. We compared gamma, alpha and beta activity, and their combinations for the identification of eloquent cortical areas defined by ESM. Ten patients with intractable focal epilepsy (age: 35.9 ± 9.1 years, range: 22–48, 8 females, 9 right handed) participated in a delayed-match-to-sample task, where syllable sounds were compared to visually presented letters. We used a generalized linear model (GLM) approach to find the optimal weighting of each band for predicting ESM-defined categories and estimated the diagnostic ability by calculating the area under the receiver operating characteristic (ROC) curve. Gamma activity increased more in eloquent than in non-eloquent areas, whereas alpha and beta power decreased more in eloquent areas. Diagnostic ability of each band was close to 0.7 for all bands but depended on multiple factors including the time period of the cognitive

task, the location of the electrodes and the patient's degree of attention to the stimulus. We show that diagnostic ability can be increased by 3–5% by combining gamma and alpha and by 7.5–11% when gamma and beta were combined. We then show how ECoG power modulation from cognitive testing can be used to map the probability of eloquence in individual patients and how this probability map can be used in clinical settings to optimize ESM planning. We conclude that the combination of gamma and beta power modulation during cognitive testing can contribute to the identification of eloquent areas prior to ESM in patients with refractory focal epilepsy.

Keywords: electrical stimulation mapping, broadband gamma frequency, alpha frequency band, beta frequency band, drug-resistant epilepsy, epilepsy surgery, electrocorticography-based functional mapping, frequency-based cortical mapping

HIGHLIGHTS

- Gamma, alpha and beta band activity have significant diagnostic ability to identify electrical stimulation mapping (ESM)-defined eloquent cortical areas.
- We present a novel method to combine gamma and lower frequency activity for enhanced identification.
- We quantify how identification is dependent on analysis time window, cortical function, and patient's attentional engagement.
- We show how ECoG responses can be used to make a probabilistic map, useful for the improvement of patient-specific planning of ESM.

INTRODUCTION

Invasive cortical mapping for the precise characterization of "eloquent" cortical areas is necessary to minimize neurological or cognitive complications following resection of pathological tissue. In the current gold standard "electrical cortical stimulation mapping" (ESM, Penfield and Boldrey, 1937; Hamberger, 2007), electrical stimulation of subdural electrode-pairs that disrupts function (e.g., speech production) or produces neurological symptoms (e.g., paraesthesia) indicates that the stimulated cortex is "eloquent" and should be preserved during resection. Despite its usefulness (Ojemann et al., 1989), ESM can elicit after-discharges, seizures (Lesser et al., 1984; Lee et al., 2010), or pain (Lesser et al., 1985). Furthermore, it requires the patient's continuous compliance, rendering it challenging to use in some patients (Arya et al., 2015). ESM is also time consuming, requiring individual testing of each implanted electrode-contact, restricting the number of electrodes that can be tested and precluding the use of high density arrays (Bouchard et al., 2013; Mesgarani et al., 2014; Muller et al., 2016) thereby limiting the spatial resolution of ESM (Hermiz et al., 2018). These and other factors motivate the search for alternative ways to identify eloquent cortex (Crone et al., 2006, 1998a,b; Brunner et al., 2009; Lachaux et al., 2007; Vansteensel et al., 2010).

Abbreviations: DMTS, Delayed match-to-sample; ESM, Electrical Stimulation Mapping; ROC, Receiver Operating Characteristic curve; AUROC, Area Under the Receiver Operating Characteristic curve; GLM, Generalized Linear Model.

Activation of neuronal networks leads to a change in the spectral power of electrical field potentials of local neuronal populations (Buzsaki, 2004; Fries et al., 2007; Buzsáki et al., 2012). For example, an enhancement of gamma band power (>30 Hz) during visual (Gray et al., 1989) and auditory (Brosch et al., 2002) processing, motor preparation (Pfurtscheller et al., 1993; Vansteensel et al., 2013), and sensorimotor integration (Murthy and Fetz, 1992). Gamma power varies with high temporal and spatial resolution, such that increasing gamma power is specific to active neuronal populations (Crone et al., 1998a, 2006; Aoki et al., 1999, p. 199; Sinai et al., 2005; Leuthardt et al., 2007; Miller et al., 2007; Nagasawa et al., 2010; Wu et al., 2010; Buzsáki et al., 2012; Arya et al., 2018; Hamilton et al., 2018). Consequently, gamma modulation has been proposed as an alternative for ESM (Crone et al., 1998a, 2006; Aoki et al., 1999; Lachaux et al., 2003; Sinai et al., 2005; Leuthardt et al., 2007; Miller et al., 2007; Brunner et al., 2009; Wu et al., 2010; Vansteensel et al., 2013; Wang et al., 2016; Arya et al., 2017) whereby a task-dependent increase in gamma power indicates eloquent cortex. However, results are mixed and gamma band-based mapping typically has insufficient accuracy in replicating ESM results, with some studies (Wu et al., 2010) reporting high sensitivity but low specificity, while others report the opposite (Bauer et al., 2013). In a recent review Arya et al. concluded that mapping based on gamma was not sufficient, and also highlighted the heterogeneity in the diagnostic threshold and the cognitive task employed (Arya et al., 2018). Thus, there is scope for improvement both in the implementation and interpretation of ECoG response based mapping.

Activation of neuronal networks is typically accompanied by a reduction in power in the alpha (8–12 Hz) and beta (15–25 Hz) frequency bands. Recent empirical evidence demonstrates that alpha and beta power is related to active inhibition processes (Jensen and Mazaheri, 2010) and can be highly spatially specific to activated populations (de Pesters et al., 2016; Muller et al., 2016). Thus, power modulation in lower frequency bands represents a plausible source of additional information for cortical mapping. Moreover, given that different frequency bands have different functions (Scheeringa and Fries, 2017) and are not directly correlated to each other (Bonaiuto et al., 2018), additional information may come from the combination of bands. A limited number of studies have investigated the use of lower frequency bands for cortical mapping (Crone et al., 1998b;

Sinai et al., 2005; Leuthardt et al., 2007; Wu et al., 2010; Hermes et al., 2012; Bauer et al., 2013; Vansteensel et al., 2013). The results from these studies have been variable in terms of the reported diagnostic ability of the low frequency bands. Some studies have also investigated the combination of frequency bands (Leuthardt et al., 2007; Wu et al., 2010). These studies showed that accepting electrodes with a high response in either the gamma band, the beta band, or in both, as potentially eloquent yielded better results than using either band alone, especially in the language cortex. Likewise, machine- and deep- learning approaches (Prakash et al., 2017; RaviPrakash et al., 2020) have shown that using the entire frequency spectrum, rather than only the gamma band, yields better mapping results, although it was not made clear which part of the spectrum offered the most additional information. In addition, while there is considerable heterogeneity in the task employed between studies, few studies have directly compared different tasks in the same group of patients. Thus, little is known about how the cognitive engagement of the patient, i.e., the task performed during cortical mapping, impacts the quality of ECoG based mapping.

We hypothesized that alpha and beta band power modulation, either on their own or in combination with the gamma power modulation, could enhance the accuracy of the identification of eloquent cortex compared with the use of gamma alone. To investigate this, we registered (recorded) ECoG signals from subdural electrodes in 10 patients with drug-resistant focal epilepsy who underwent ESM. Patients performed a delayed match-to-sample (DMTS) task or listened to the same stimuli without an active task. We show that beta power generally had equal diagnostic ability to gamma, while alpha power was less effective. Withdrawing attention from the stimuli reduced the diagnostic ability. The combination of gamma and beta frequency bands, using a Generalized Linear Model (GLM) was consistently better than either band individually.

MATERIALS AND METHODS

Participants

We included 10 patients (age: 35.9 ± 9.1 years, range: 22–48, 8 females, 9 right handed, native Dutch speakers with normal cognitive ability, with normal or corrected to normal vision, and normal hearing) with drug-resistant focal epilepsy, who underwent continuous, extraoperative ECoG with subdural electrodes and ESM as part of pre-surgical evaluation for resective epilepsy surgery. The electrode implantation scheme was strictly chosen according to the clinical criteria (see **Supplementary Material** section "1.1 Electrode implantation procedure") for a complete implantation description of all patients. All patients scheduled for epilepsy surgery were invited to join the study during preoperative consultation. No financial incentive for joining the study was given. Those who volunteered as participants for the study signed an informed consent form and performed the DMTS task similar to that used in Archila-Meléndez et al. (2018) (see **Supplementary Material** section "1.4 Delayed Match-to-Sample Task"). The used audiovisual stimuli and the delayed match-to-sample (DMTS) task performed by the patients were designed to test hypotheses about the processing of acoustic properties of speech in the language network under conditions of varying selective attention, yet we reasoned that, considering the multimodal nature of the task which engaged language listening, reading, working memory and a motor response, the ECoG data collected during the performance of the DMST task might be also useful to test our current hypothesis. The task was performed during the first 5 days after surgical implantation, when clinical condition (alertness, pain level, no recent seizure activity) allowed and when the patient was willing to participate. One patient performed poorly in the DMTS task (**Table 1**), however her data was included in our analyses. The study complies with the Declaration of Helsinki for research studies in humans and was approved by the Medical Ethical Committee of the Maastricht University Medical Center, Maastricht, The Netherlands.

Electrical-Cortical Stimulation Mapping (ESM)

ESM was performed using bipolar stimulation between electrode pairs sequentially, selecting neighboring electrode pairs of the subdural grid and/or strips. The procedure for ESM differs between centers, with consequences for the reproducibility of comparisons between ESM and ECoG response-based mapping approaches (Mooij et al., 2018). Therefore, we provide a detailed description of our ESM procedure in **Supplementary Material**. No patients included in the study experienced immediate evident impairments following resection surgery.

Data Pre-processing, Time-Frequency Analysis and Filtering

Data were analyzed in MATLAB (R2017b version 9.3.0.713579; The Mathworks Inc.; Natick, MA, United States) using the FieldTrip toolbox (Oostenveld et al., 2011) and custom scripts. Data were first cut into epochs from 1 s before the sound onset until 1 s after the behavioral response with a maximum data length of 8 s. We then applied a discrete time filter at 50, 100, and 150 Hz to remove line noise and down-sampled the data from 2048 to 500 Hz. Data were re-referenced to the average signal recorded in all electrodes, after excluding electrodes with high noise.

Time-frequency representations (TFR) were calculated in 2 Hz steps from 6 to 250 Hz using Hanning tapers (7 cycles) and 10 ms step size, 6 Hz being the lowest frequency that could be reliably measured in the trial structure composing our DMTS task. Power was expressed as the normalized change, where the change was defined as the difference between post-stimulus time window and pre-stimulus "baseline" period -700 to -100 ms before sound onset. To better represent the spectral response around each trial event, TFRs were aligned and cut around the onset of each event. Thus, we represent −0.5 to 1 s around the onset of the sound, −0.2 to 0.7 s around onset of the letters and −0.3 to 0.7 s around the onset of the behavioral response. For frequency specific analysis, data were filtered at alpha (8–12 Hz), beta (15–25 Hz) and broad gamma band (55–200 Hz) using a 4th order Infinite impulse response (IIR) Butterworth two-pass filter. Power was calculated per trial as the absolute values of the

TABLE 1 | Demographic information and clinical summary of the patients included in the study.

Patient	Age (y)	Sex	Electrode implantation scheme	Seizure frequency	Cognitive status	Education	Wada	fMRI	Handedness	% correct trials	Total number of trials
1	42	F	Grid temporal L	Daily	Average*	Medium professional	Not performed	Not performed	Right	90	1,126
2	39	M	Grid temporal L	Weekly	Low average*	Lower vocational	Not performed	Left dominance	Right	87.1	644
3	22	F	Grid temporal L	Daily	High average	Higher professional	Not performed	Right dominance	Right	98.5	810
4	28	F	Grid frontal L	Twice per week	Average	Higher professional	Not performed	Left dominance	Right	89.3	486
5	33	F	Strips ventro-latero-temporal L and R	Daily	Average*	Lower vocational	Not performed	Not performed	Right	93.3	972
6	38	M	Grid temporal R	Weekly to daily	Low averge	Higher professional	Right dominance	Not performed	Left	96.6	1,134
7	23	F	Grid temporal and perieto-frontal L	Weekly	Average	Higher professional	Not performed	Left dominance	Right	99	810
8	39	F	Grid parieto-Occipital R	Daily	No data	Medium professional	Not performed	Not performed	Right	96.9	773
9	48	F	Grid temporal and perieto-frontal L	Twice per month	Average	Lower vocational	Not performed	Not performed	Right	53.8	236
10	47	F	Grid parieto-temporo-occipital + ventro-temporal strips R	Twice per month	Average	Medium professional	Not performed	Not performed	Right	98.3	810

**Deterioration from previous evaluation. L: left, R: right.*

Hilbert transform and the resulting time courses were expressed as normalized power change. For non-time resolved analysis, average power was first calculated per trial and then across trials.

Generalized Linear Model (GLM) Fitting and Validation

We aim at testing if a linear combination of different frequency bands results in a better diagnostic ability, as compared to single frequency bands. We used a GLM with binomial likelihood and logit link function (McCullagh and Nelder, 1998), where for each electrode the dependent variable (y) was the ESM category (i.e., eloquent and non-eloquent) and the predictors were the ECoG power change in each frequency band. The estimated model was used to determine the optimal weighting of power change per frequency band as regression coefficients to predict the ESM response. The process was performed in k-fold cross-validation, in k-1 partitions. The resulting model was used to predict the ESM category in a remaining k-partition. The process was then repeated 20 times with random partitions and compared with the ground truth ESM and the results were averaged (see details in **Supplementary Material**).

Area Under the Receiver Operating Characteristic Curve Analysis and Bootstrap Procedure for Statistical Testing

We aimed to calculate the diagnostic ability of the three frequency bands, and of their combination. We calculated the area under the curve (AU) from the receiver operating characteristic (ROC) curve (Green and Swets, 2000). This procedure calculates the ratio of sensitivity to specificity for all potential discrimination thresholds. The resulting AUROC represents the maximum performance (i.e., correct discrimination) of an "ideal observer" using the optimal threshold. To facilitate the comparison of AUROC with changes in power spectrum for alpha and beta frequencies, we display significant AUROC values below 0.5 where power in eloquent channels is suppressed more strongly than power in non-eloquent channels (see **Supplementary Material** section "1.6 Area Under the Receiver Operating Characteristic Curve Analysis"). Foe statistical testing we implemented a bootstrap procedure with replacement for statistical testing in which we constructed a distribution of AUROC values for each model (i.e., frequency bands and their combination; see **Supplementary Material** section "1.7 Bootstrap Procedure for Statistical Testing Receiver Operating Characteristic Between Models").

Function-Specific and Attention-Dependent Analyses

We were interested in studying whether different functional areas might exhibit characteristic power spectra, however we were limited by the low numbers of electrodes representing some ESM categories. We therefore grouped electrodes into two broad categories, which we call "input," being mostly involved in processing cortical inputs (i.e., sensory processing) and "*output*" as being mostly concerned with cortical *outputs*

(motor function). This categorization is based on the concept that one of the nervous system's fundamental functions is the processing of sensory input to guide behavioral (motor) *output*. Those electrodes labeled as *auditory, visual, sensory, language-Wernicke,* and *language-temporobasal* were grouped into the "*input*" category as being more functionally involved in processing incoming sensory events. Those labeled as *motor*, *mixed-sensorimotor,* and *language-Broca* were grouped into the "*output*" category as being more involved in generating behavioral responses. Two neighboring electrodes in one patient labeled as *emotion* were excluded from the function-specific analysis as they did not seem to fit in either category.

Anatomical Segmentation and Intracranial Electrode Localization

Presurgical T1-weighted MRI were segmented using FreeSurfer (version 6.0)[1] (Dale et al., 1999; Fischl et al., 1999a). Briefly, this procedure includes removal of non-brain tissue using a hybrid watershed/surface deformation method, automated Talairach transformation, intensity normalization, tessellation of the gray/white matter boundary, automated topology correction, and surface deformation following intensity gradients. After the process was finished, quality control was performed by visually inspecting each subject's brain and the overlay of the tissue boundaries. Remaining errors were manually corrected using ITK-SNAP software (version 3.4.0[2]; Yushkevich et al., 2006). After segmentation, the postsurgical CT scan was coregistered to the presurgical T1-weighted MRI using rigid affine transformations via FSL's FLIRT algorithm (Jenkinson and Smith, 2001). To localize the intracranial electrodes, we used the MATLAB toolbox iELVis following the procedure described by Groppe et al. (2017). Briefly, the locations of the electrodes in the postsurgical CT scan were manually identified using intensity thresholding in BioimageSuite[3]. To correct for post-implantation brain shift, electrodes were projected to the nearest point on the dural surface reconstructed from the presurgical MRI (Dykstra et al., 2012). Finally, for visualization purposes, electrodes of all patients were projected to the brain average surface of FreeSurfer (Fischl et al., 1999b, see **Figure 1A** using iELVis; Groppe et al., 2017).

Probabilistic Map of Eloquence

We considered how our analysis could be clinically useful without providing a diagnostic test. A probabilistic map, that shows the likelihood of eloquence for each electrode and that does not require the ESM labels but only the ECoG signal during the DMST task (and thus could be obtained before the ESM), could be used to optimize the planning of the sequence of electrode pairs for ESM testing. We took GLM-calculated probabilities for each patient separately using only data from the remaining patients to calculate the GLM beta weights. This procedure represents a special case of our standard analysis in which data was separated into training and test datasets: In the standard analysis the separation was done randomly, thus data from all patients could be included for training and the same could be done for testing; in the current analysis the data separation was performed according to the patient identity. In this way we show how a probabilistic map of eloquence during ESM can be generated for an individual patient without reference to the ESM results of that patient. This procedure allows, in a new patient, the creation of a probabilistic map of eloquence using only data from the DMTS task that is acquired before the ESM, enabling the incorporation of the probabilistic map in the planning of the ESM.

[1]http://surfer.nmr.mgh.harvard.edu/

[2]www.itksnap.org

[3]http://www.bioimagesuite.org

RESULTS

Relationship Between Electrical Cortical Stimulation and Frequency Modulation

As a descriptive analysis, we selected all electrodes from all ESM categories as defined by the electrophysiologist (see **Supplementary Material**) and projected them into a common brain space (**Figure 1A**). We registered in total 129 eloquent and 443 non-eloquent electrodes (**Table 2**). Eloquent electrodes were located bilaterally over the temporal neocortex (superior and middle temporal gyri), over the inferior frontal gyrus, and over the pre- and post-central gyri.

We represented the change in power spectral density, relative to the baseline period (−0.7 to −0.1 s from sound onset) across time (time-frequency representation, TFR) of the ECoG signal during each epoch of the DMTS task (**Figure 1B**). ESM categories exhibited characteristic response patterns during the task. For example, electrodes labeled as "*auditory*" exhibited increased gamma activity and decreased alpha/beta power after sound onset. Likewise, electrodes labeled as "*visual*" exhibited increased gamma and decreased alpha/beta after letter onset. Electrodes labeled as "*motor*" exhibited an increase gamma activity and a decrease in alpha/beta around the button press. Interestingly, "*language temporobasal*" and "*language Broca*" electrodes were active after sound onset and letter presentation possibly pointing toward covert rehearsal of the sound and silent reading of the letters. For further analysis, we grouped all electrodes labeled as eloquent for comparison with all electrodes that were tested using ESM but labeled as non-eloquent.

Receiver Operating Characteristic (ROC) Curve Analysis

We compared the power spectrum of eloquent and non-eloquent electrodes' ECoG during the DMTS task. Power was generally increased relative to baseline for frequencies above 50 Hz, and generally decreased for frequencies below 30 Hz (**Figure 2A**). This effect was larger in eloquent- (red) than non-eloquent electrodes (blue). To test the diagnostic ability of this difference we calculated AUROC (**Figure 2B**) and applied a permutation test for statistical assessment. AUROC was significant (darker line, $P < 0.05$, two-sided test, uncorrected for multiple comparisons) for frequencies between 50 and 180 Hz and

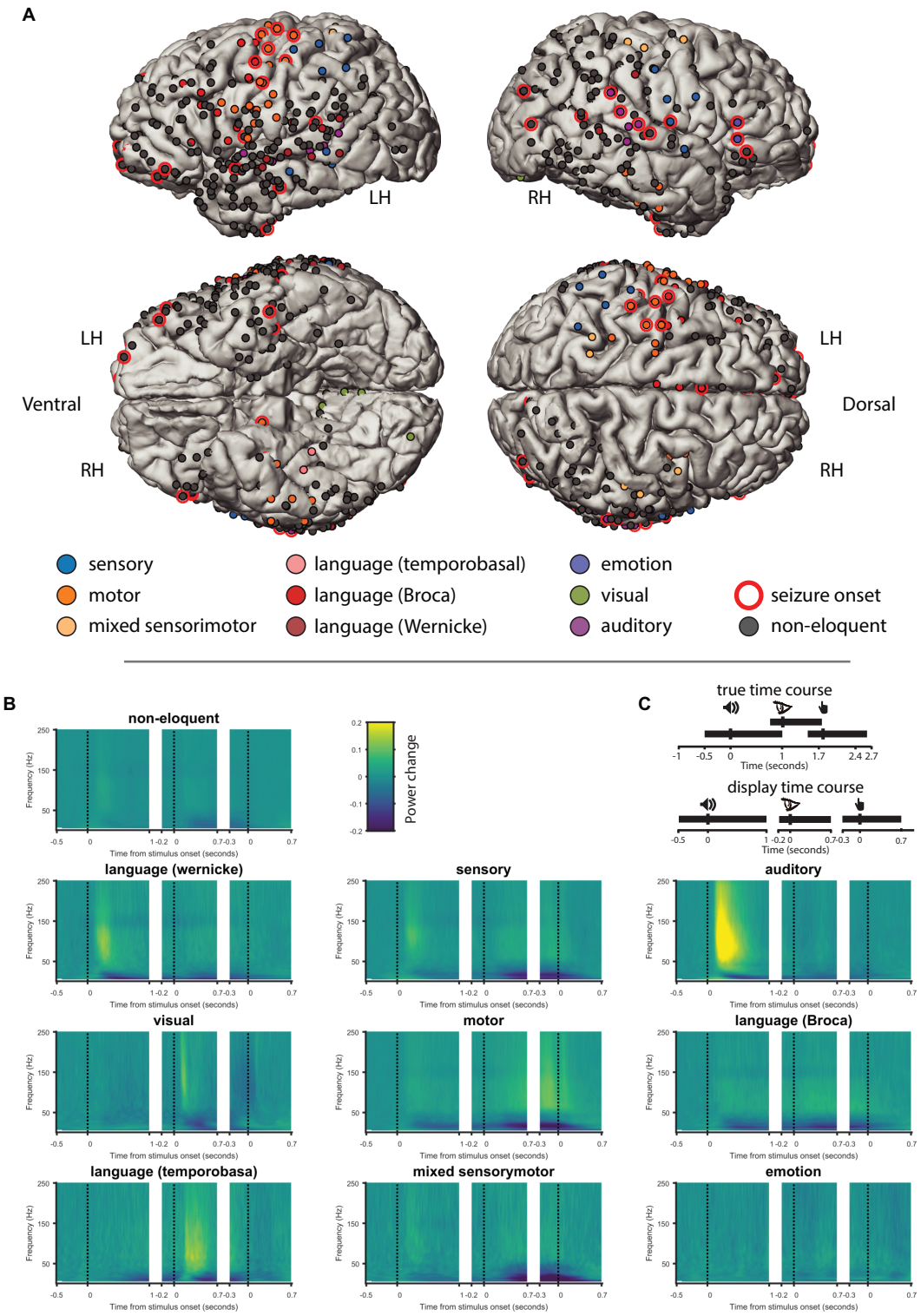

FIGURE 1 | ESM categories and ECoG responses. **(A)** Electrodes tested during electrical-cortical stimulation mapping (ESM) in 10 patients projected in the common space, color coded according to the ESM category. LH, left hemisphere; RH, right hemisphere; Ventral, ventral (caudal) view of left and right hemispheres; Dorsal, dorsal (cranial) view of left and right hemispheres. **(B)** Time frequency representations (TFR) of time periods of the delayed match-to-sample task from all tested electrodes grouped by the ESM category. The TFRs represent the three different trial events (i.e., sound onset, letter onset, and button-press), which are illustrated by the three vertical dotted lines in each TFR). **(C)** Illustration of the time course in the task (upper cartoon, events are represented at their average time after sound onset) and the "exaggerated" time between the events used for display time (lower cartoon).

TABLE 2 | Electrode details.

Patient	Total stimulated	Total non-eloquent	Total eloquent	Seizure onset	Sensory	Motor	Mixed sensorimotor	Language (Wernicke)	Language (Broca)	Language (temporobasal)	Auditory	Visual	Emotion
1	39	35	4	5	2	0	0	1	1	0	0	0	0
2	39	39	0	2	0	0	0	0	0	0	0	0	0
3	40	29	11	0	4	0	0	1	0	0	6	0	0
4	74	59	15	12	0	8	0	0	7	0	0	0	0
5	29	29	0	0	0	0	0	0	0	0	0	0	0
6	40	26	14	8	4	2	0	1	0	2	3	0	2
7	79	43	36	7	5	14	2	7	7	0	1	0	0
8	74	63	11	3	1	0	3	1	0	0	2	4	0
9	80	57	23	1	2	14	3	3	1	0	0	0	0
10	78	63	15	3	4	8	0	0	0	0	0	3	0
Total	572	443	129	41	22	46	8	14	16	2	12	7	2

Number of electrodes in each ESM functional category, electrically stimulated and seizure onset per patient.

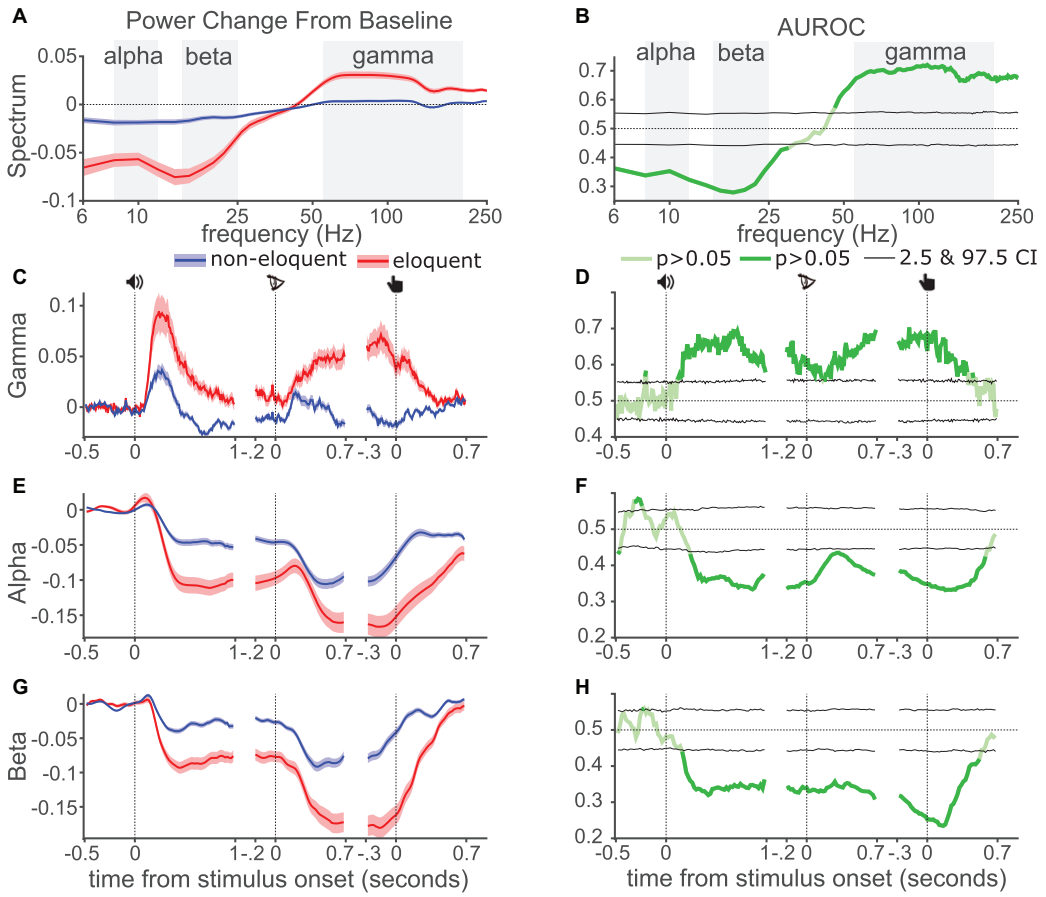

FIGURE 2 | AUROC analysis. **(A)** Normalized change in ECoG signal power spectral density from baseline from eloquent (red) and non-eloquent electrodes (blue). Shading shows standard error, center line shows mean. **(B)** AUROC values across frequencies, pale green, non-significant, dark green significant. Black lines show 2.5 and 97.5 percentiles from permutation distribution. Dotted line shows chance performance. Background shading indicates filter boundaries for each band. **(C)** Gamma power modulation during each task event (icons indicate sound onset, letter onset, and button-press). **(D)** AUROC values across time for gamma. **(E,F)** Alpha power and AUROC values, as in **(C,D)**. **(G,H)** Beta power and AUROC values, as in **(C,D)**.

for frequencies between 6 and 30 Hz, indicating significant diagnostic ability, with a performance of 65–70% for an ideal observer.

To represent the time courses of gamma-, alpha- and beta bands over the trial we filtered the ECoG signal in each band (gray background shading, **Figures 2A,B**) and calculated the

absolute value of the Hilbert transform, which was subsequently represented as the normalized change against the pre-sound baseline. We found stronger gamma increase in eloquent than non-eloquent electrodes (**Figure 2C**) during the three task epochs. The AUROC values across time (**Figure 2D**) were larger than 0.5 and significant for all three events.

Alpha power (**Figure 2E**) decreased in all three events (**Figure 2E**) especially in eloquent electrodes. The AUROC values were significantly below 0.5 for all three events (**Figure 2F**) indicating that power for eloquent electrodes was lower than non-eloquent electrodes according to the definition of our AUROC calculation (see **Supplementary Material** section "1.6 Area Under the Receiver Operating Characteristic Curve Analysis"). A similar pattern was observed for beta power (**Figures 2G,H**), however, the decrease in power was especially prominent around the button-press. AUROC values were generally lower for beta than for alpha band, indicating greater diagnostic ability for beta, especially around the button-press.

Next, we combined the responses from different bands using a GLM including 10-fold cross-validation (methods) and calculated AUROC values across time using the GLM response (**Figure 3A**). For smoothing, and to reduce processing time, we used a sliding time window of 100 ms with 50 ms step size. The GLM based AUROC values for gamma-only closely matched standard AUROC values (**Figure 3A**, green line). For alpha-only (red) and beta-only (blue) the GLM based AUROC values also closely matched the standard AUROC, except that values were above 0.5 rather than below due to the fitting procedure. Interestingly, time courses for the three individual band models peaked at different times in the trial. The gamma-only model performed best after the sound onset while the beta-only model performed best around the button-press. The alpha-only model performed generally worse than the other models, but interestingly outperformed the gamma-only model around the letter onset and late after the button-press. The combined model AUROC values (**Figure 3A**–dashed lines) tended to be either higher than, or equal to, whichever individual curve was highest at any given time point. This was especially true for the beta&gamma model (blue dashed lines), although the alpha&gamma (red dashed) model also tended to outperform the gamma-only model. Interestingly the three-band model (black dashed) did not outperform the beta&gamma model indicating that including alpha brought no additional information.

To statistically test the AUROC results of each model against chance performance and against each other, we first reduced the dimensionality of the data by calculating average power for each electrode, collapsing over the time dimension. Using this data we conducted a bootstrap analysis in which we constructed a

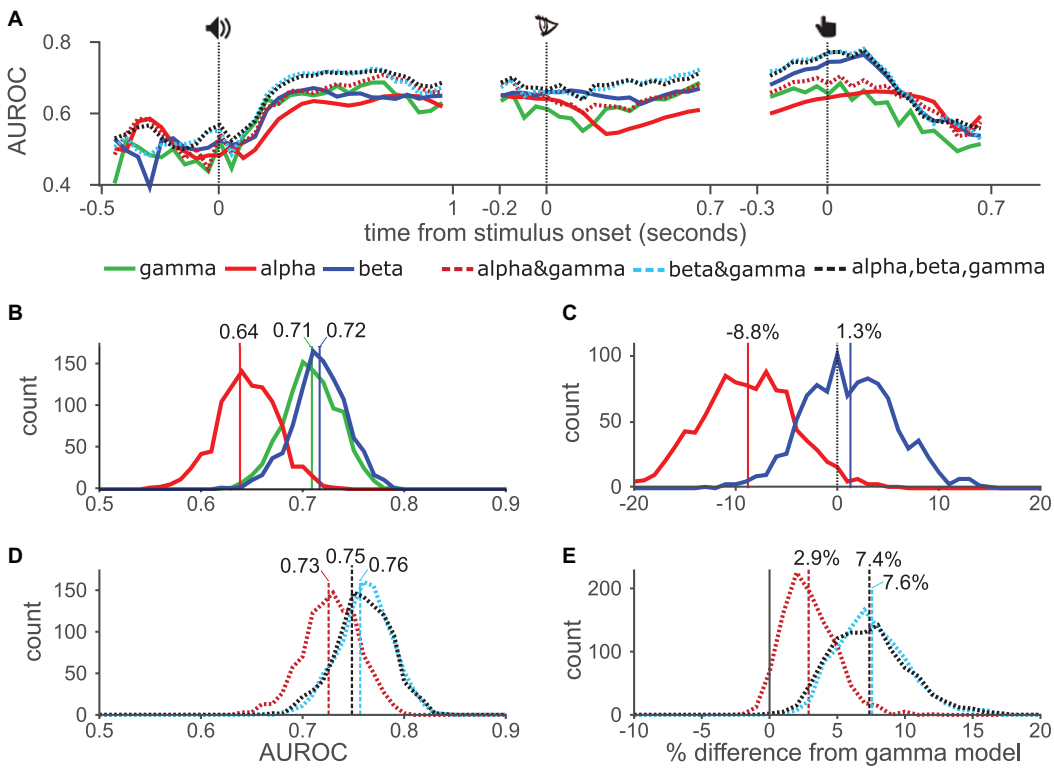

FIGURE 3 | Temporal AUROC and model comparison. **(A)** AUROC values using GLM approach for gamma, alpha, and beta (solid lines), and their combinations (dashed lines). **(B)** Distribution of the AUROC values from 1000 bootstrap samples for single models. Vertical lines show AUROC values without resampling. **(C)** Pairwise comparison from bootstrap distribution of alpha (red) and beta (blue) AUROC values against gamma. Vertical lines show mean percentage change from gamma-only model. **(D,E)** Distribution of AUROC values for combination models, as in **(B)**. **(E)** Pairwise comparisons of combination models with gamma-only model.

distribution of 1000 AUROC values for each model by creating multiple datasets of the same size as the original, while randomly drawing electrodes with replacement. For each dataset, and the original, we computed the AUROC for each model using 10-fold cross-validation. Histograms in **Figure 3B** show the distribution of AUROC values of the single band models, vertical lines show the AUROC values from the original dataset. All three models performed better than chance, with 100% of the resampled datasets returning AUROC values greater than 0.5. Of the three models the alpha-only model (red) performed the worst, with an AUROC of 0.64 in the original dataset, the gamma-only (green) and beta-only (blue) performed similarly. The gamma-only approach has previously been used most widely, therefore, to test the usefulness of alpha- and beta bands we made pairwise comparisons of those models against the gamma-only model (**Figure 3C**), i.e., using the same selection of randomly chosen channels for each model. The alpha-only model was worse than the gamma-only model in 98% of datasets, which we consider to show a significant difference. The mean performance reduction was 8.8% (vertical red line). While the beta-only model offered a slightly increase performance (1.3%), which was not significant. We next compared the performance of the combination models (**Figure 3D**). These generally outperformed the individual-band models although the alpha&gamma (red dashed) model performed the worst. The beta&gamma (blue dashed) and three-band (black dashed) model performed equally. In pairwise comparisons with the gamma-only model, all three models offered enhanced performance although this just failed to meet the threshold of significance for the alpha&gamma model (94% of datasets improved). The beta&gamma and three-band models both performed significantly better than the gamma-only model (in 100% of datasets) offering respectively 7.6 and 7.4% average improvement. Their distributions overlapped indicating again, that there was no advantage to including the alpha band to the beta&gamma model.

Taken together these results show that the alpha-only model generally performed worse than the other single-band models, whereas the beta-only and gamma-only models performed about equally. Combining alpha with gamma provided some improvement, whereas combining beta and gamma provided a larger improvement.

AUROC Performance Depends on Functional Category

Alpha-, beta- and gamma bands have been ascribed different functional roles, with gamma associated with feedforward processes and alpha associated with feedback (Scheeringa and Fries, 2017). The beta-band has been associated with motor activity, whereby beta power drops in preparation for motor output. Thus, these bands may have relatively different importance in different cortical areas, depending on the area's place in the cortical hierarchy (Felleman and Van Essen, 1991). Specifically, we can anticipate that input areas, early in the hierarchy, may have a high dependence on gamma, while output areas, late in the hierarchy may be more dependent on alpha and beta. Importantly, this implies for our current question that, in patients with many output electrodes, alpha or beta may be more informative, or their combination with gamma may give greater improvement.

To test this hypothesis we divided all eloquent electrodes into two broad categories which we defined as output and input and repeated our analysis (**Figure 4**) for each group. Notice that this grouping was intended as a procedural means to split the data into denominated groups. With the possible exception of primary areas, all cortical areas have roles in both processing incoming stimuli and generating responses, thus the distinction between output and input areas is only an approximation.

Descriptively, gamma power increased in the first task epoch for all electrodes (**Figure 4A**). Input electrodes (red) showed the highest power followed by output electrodes (green). Non-eloquent electrodes (blue) showed the weakest response. After letter onset, gamma power increased for all electrodes. While power in input electrodes peaked soon after letter onset, power in output electrodes continued to increase, peaking shortly before the button-press. Non-eloquent electrodes showed low power after a weak response to letter onset and button-press. Alpha power (**Figure 4B**) was suppressed in all channels with greater suppression for eloquent than non-eloquent channels. Interestingly, alpha power suppression in both output and input channels was approximately equal for the majority of the time course. Only at the end of the trial did output channels show somewhat greater suppression. By contrast, beta band (**Figure 4C**) suppression was considerably stronger in output channels than input channels at all-time points, especially after the button press. With our stated caveat about the distinction between output and input areas, these data supported our grouping, as " *input*" electrodes seemed most involved during stimulus processing and " output" electrodes seemed most involved near the behavioral response.

We calculated AUROC values for the three bands separately and for the three combination models using the time-averaged responses and tested significance of the difference using the bootstrap method. In *input* (**Figure 4D**) electrodes the distribution of gamma (green) AUROC values was higher than the alpha-only (red) or beta-only (blue) models, however the distributions heavily overlapped and this difference was not significant in pairwise comparisons (**Figure 4E**). In *output* electrodes (**Figure 4F**) the beta-only model outperformed both gamma-only and alpha-only models. Pairwise comparisons (**Figure 4G**) showed that this difference corresponded to a 6.1% increase but did not pass significance (93% of datasets showed an increase). The alpha-only model performed significantly worse than the gamma-only model, corresponding to a 11% drop.

Analysis of the combination models showed that in *input* channels all three models offered approximately equal performance (**Figure 4H**), which was somewhat, but not significantly, better than the individual band models (**Figure 4I**). Among *output* channels the combination models offered better performance (**Figure 4J**) and a greater improvement over the gamma-only model (**Figure 4K**): The alpha-gamma model mean improvement was 3% but failed to reach significance, while the beta-gamma and three-band models both showed an improvement in 100% of dataset with a mean improvement of

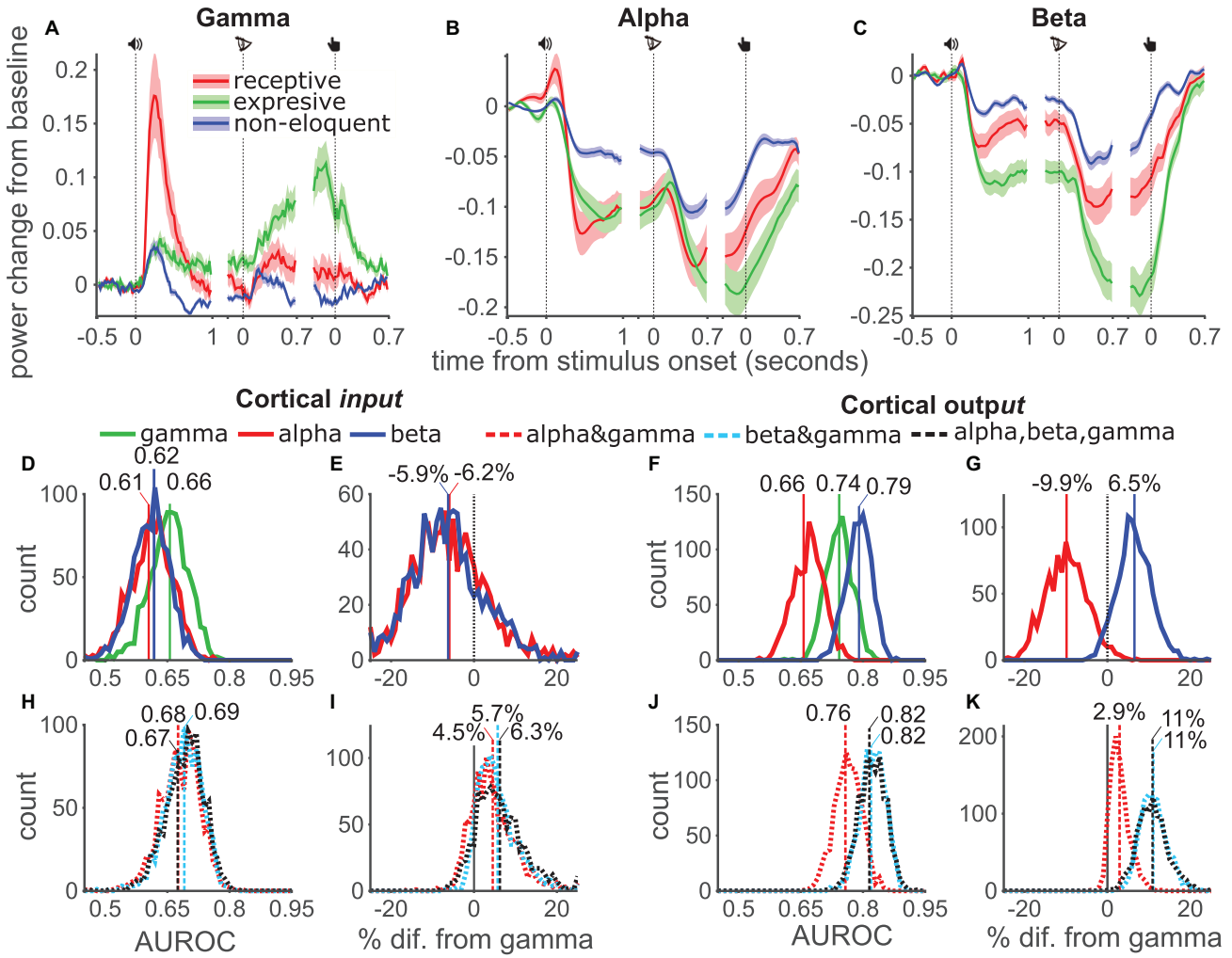

FIGURE 4 | AUROC analysis per functional category. **(A–C)** Gamma, Alpha and Beta power modulation and SE (shades) for three subtypes of electrodes (input, output and non-eloquent) during the three events of the task. **(D)** Distribution of the AUROC values from 1000 bootstrap samples for single models and input channels. **(E)** Pairwise comparison from bootstrap distribution of alpha (red) and beta (blue) AUROC values against gamma for input channels. **(F,G)** Same as **(D,E)** for output channels. **(H–K)**, same as **(D–G)** using combined models.

11%. These results were in line with our expectation that *output* electrodes, being higher in the cortical hierarchy, would be most sensitive to low frequency power modulations. Taken together these results suggest that eloquent areas may be best mapped using gamma or beta-band power depending on the distribution of electrodes in an individual patient. However, irrespective of the ESM functional category, the combination of beta and gamma bands was reliably the best measure for the identification of eloquent electrodes.

Influence of Attention on AUROC Values

Most patients performed well in the task, however, one patient performed poorly and withdrew early from the experiment. This experience prompted us to question how well ECoG mapping would perform in a less demanding task, which might be particularly relevant when applying ECoG mapping in pediatric populations, patients with low general cognitive ability (Ruiz-Rizzo et al., 2018, 2019) or patients who are otherwise unable or unwilling to engage in demanding cognitive testing (Haupt et al., 2020; Ruiz-Rizzo et al., 2020). Our cognitive experiment included a passive condition in which the same auditory stimuli were presented without any explicit task. We repeated our analysis using the ECoG response, from eloquent (red, **Figure 5**) and non-eloquent electrodes (blue), during the sound presentation in the active (solid lines) and passive tasks (dashed lines, **Figure 5**). Gamma band (**Figure 5A**) responses were weaker in the passive task compared to active task for both eloquent and non-eloquent electrodes. Alpha and beta band suppression (**Figures 5B,C**) was weaker in the passive task compared to the active task, especially late in the response.

As before, we calculated AUROC values of the GLM models and tested significance using the time-averaged responses, however, here we used only the period from sound onset to 900 ms which could be compared for both tasks. In the active

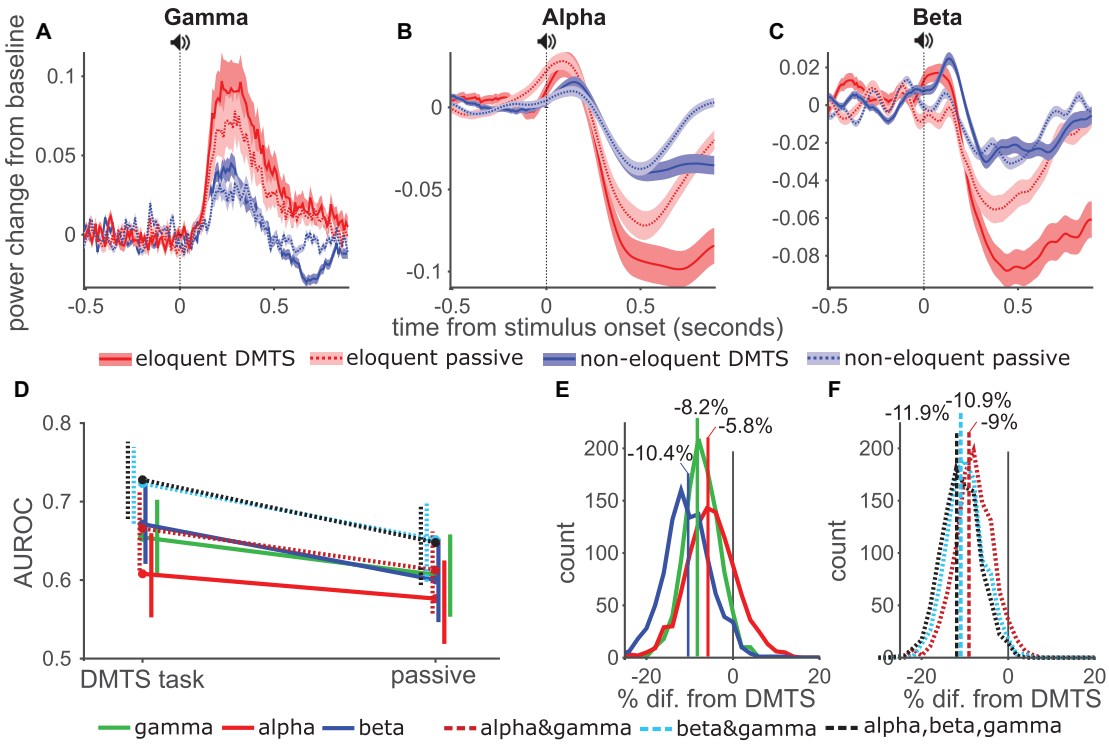

FIGURE 5 | Influence of attention on AUROC values. **(A–C)** Gamma, Alpha and Beta power across time for eloquent (red) and non-eloquent (blue) electrodes during the active (DMTS, solid lines, darker shading-SE) and the passive (dashed lines, lighter shading-SE) tasks. **(D)** Effect of attention on diagnostic ability per model. Vertical lines show 5 and 95 percentiles from 1000 bootstrap samples, horizontal offset to aid visibility. **(E)** Pairwise comparison between active and passive tasks per single band models. Negative values imply a better performance in the active task. **(F)** Same as **(E)** but using combination models.

task AUROC values were unsurprisingly lower than in previous analysis (**Figure 4H**) where we had used the response during the entire trial. However, when comparing the performance of the three bands and the combination, the pattern matched our previous findings. Comparing the two tasks (**Figure 5D**) showed that withdrawing attention in the passive task lowered performance of all models. In pairwise comparisons between the two tasks we found that performance of the models dropped by as much as 11.9% in the three-band models (**Figure 5F**). The drop was significant ($p < 0.05$) for all models except the alpha-only model ($p = 0.19$).

These data showed that an active task which engages attention is required for optimal mapping using ECoG, with important implications for studies which attempt to classify eloquent cortex without explicit cognitive tasks (Vansteensel et al., 2013). Nevertheless, the GLM approach combining gamma and beta band activity offered a significant improvement over single-band models.

Probabilistic Map of Likely Eloquence

We aimed to use the GLM fitting to calculate a map showing the probability that each electrode would be eloquent given the ECoG power modulation during the DMTS task. Such a map could be used to optimally plan the sequence of ESM mapping. For this analysis we used data from the full trial and full dataset (i.e., data presented in **Figure 3**) and the beta&gamma model. As in the main analysis we estimated GLM weights on a training dataset and applied those weights to a test dataset. However unlike in the main analysis, here the training dataset comprised all electrodes from nine patients, and the testing dataset comprised all electrodes from the remaining tenth patient. Thus, this analysis could be performed for a new patient using data available before the ESM. After calculating the prediction of all electrodes in the dataset the AUROC for this procedure was 0.73, as compared to 0.76 using the K-fold approach, in line with the results from the standard analysis.

The GLM response corresponds to a prediction of the binomial probability that an electrode is eloquent or not. To visualize the relationship between GLM prediction and the empirical probability of eloquence we binned electrodes into 10 equally spaced bins (with 50% overlap) according to the GLM response. **Figure 6A** shows the number of electrodes per bin (black line, rightward Y axis) and the proportion of those electrodes with a positive ESM response (blue line and colored dots, leftward *Y*-axis). The proportion of eloquent channels across the whole population is shown by horizontal line. We then showed how the GLM could be used to map five representative patients. The probability of eloquence was represented by color-coding the electrode locations, with darker-red colors indicating higher probability of eloquence (see dot colors in **Figure 6A**). For comparison, electrodes that were eventually labeled as eloquent by the ESM were marked with

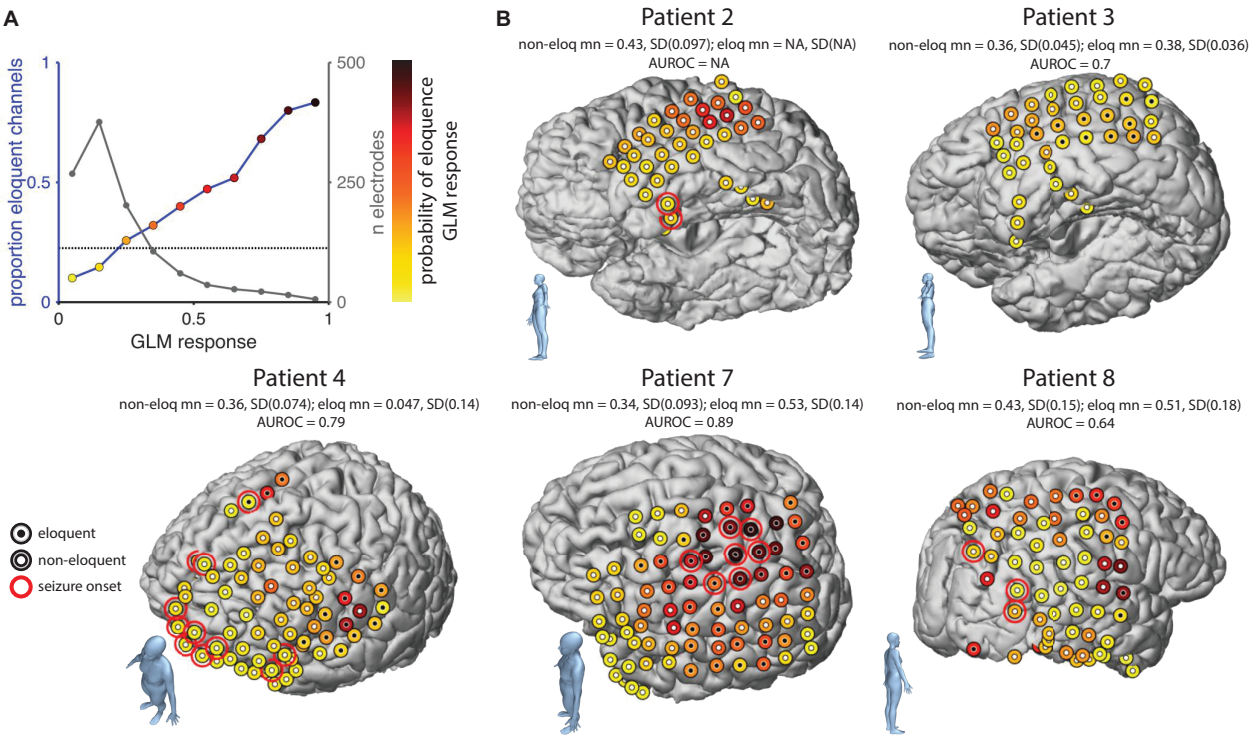

FIGURE 6 | Probabilistic maps of eloquence. **(A)** Relationship between GLM response (i.e., prediction of the binomial probability that an electrode is eloquent) and probability of eloquence (leftward axis) and numbers of electrodes (rightward axis). Dot colors indicate color-scale used in other panels. **(B)** Electrode locations projected onto the individual patient MRI in five patients. Dot color indicates GLM response, dot centers indicate ESM results, white: non-eloquent, black: eloquent. Red rings; seizure onset zones. Bodies in the lower left of each panel indicate the brain orientation. Values above each brain show the quantification of the performance of the GLM. This is given in terms of the mean and standard deviation GLM response of ESM positive (eloquent) and negative (non-eloquent) electrodes, and an AUROC value where patients have both positive and negative electrodes. Non-eloq, non-eloquent; mn, mean; SD, standard deviation; eloq, eloquent; AUROC, area under the receiver operating characteristic curve.

a central black dot while electrodes eventually labeled as non-eloquent were marked with a central white dot. For completeness, seizure onset sites were labeled with a red ring. Patient 4 and 8 appear to have a good match between ESM and ECoG prediction, in that darkest colored dots also have black centers. Eloquent areas were far from seizure onset zones, allowing a safe resection. Patient 7 also had a good match between ESM and the ECoG prediction, however, the overlap between eloquent areas and seizure onset precluded a safe resection. Patient 3 showed a good match between ESM and ECoG, however, notice that the estimated probabilities were generally low in this patient such that ESM-positive electrodes were found at a level of ECoG response that would be negative in other patients. This observation indicates that a fixed diagnostic threshold applied to all patients may not be the ideal approach. Patient 2 showed the reverse pattern. In this patient, no eloquent electrodes were found with ESM despite quite high ECoG responses. In this patient the seizure onset zone was located at the temporal pole, while ESM results do not contra-indicate a full resection of the temporal lobe, the ECoG response suggests active cortex above the 5th row of the grid. Taken together, results from the probabilistic map suggest that such a map might be useful as an additional source of information when planning a resection for the removal of epileptogenic tissue, while preserving regions with high ECoG responses.

DISCUSSION

We found that activity in the alpha, beta and gamma bands could be used to identify eloquent cortex at above chance level, and with rates in line with previous reports (Arya et al., 2018). In line with our hypothesis, combining frequency bands via a generalized linear model (GLM) enhanced the information given by each band alone, thereby increasing the performance in predicting ESM results. Combining beta and gamma was found to be more useful than combining alpha with gamma. Time-resolved analysis showed that the different frequency bands alternated as the "better" measure throughout the trial. Likewise segregating the signal from the eloquent electrodes into cortical *input* and cortical *output* groups showed that the relative performance of alpha, beta and gamma depended on the cortical area, whereby gamma gave better results in *input* areas and beta band gave better results in *output* areas, in line with previous results by Wu et al. (2010). These analyses reveal that the identification of ESM positive electrodes with a specific frequency band (i.e., alpha,

beta or gamma) or any frequency combination are not mutually exclusive options. Moreover, our analysis suggests that whether alpha, beta or gamma power are the "better" measure, will depend on several factors, including the patient's implantation scheme, the task performed, and the selected analysis window. Thus, depending on the implantation scheme, some patients might have additional benefits in the identification of ESM positive electrodes by including beta power modulation. Our GLM approach cuts through this complexity because, regardless of which band provided the better diagnostic ability, the combined approach allowed a performance at least as good as the best individual frequency band and typically offered a significant improvement.

Previous studies have investigated whether ECoG recording could be used as an alternative to ESM by setting a significant response as a diagnostic criterion for identifying eloquent cortex. Here we investigated the diagnostic ability without implementing a diagnostic test. After demonstrating that ECoG responses can reliably predict the probability of a positive ESM response, we showed how a probabilistic map could be constructed that could be used to guide ESM. Guided ESM may reduce the time and effort required of both the patient and clinical team to stimulate all possible neighboring pairs of electrodes. The time-consuming aspect of ESM becomes especially problematic as the number of electrodes increases, for example when using high-density grids. These are becoming more widely used as they increase the spatial resolution of the mapping procedure, thereby increasing surgical precision and decreasing the risk of postsurgical neurological deficits (Escabí et al., 2014). However, cortical mapping using ESM in a high-density grid is time consuming and becomes impractical. In contrast, identifying eloquent cortex using the frequency modulation responses during a cognitive task processes all channels simultaneously. Thus, this approach has the potential to significantly improve the general time efficiency of the mapping procedure. Because ESM can cause seizures, after-discharges (Blume et al., 2004; Aungaroon et al., 2017) and, in some cases, pain (e.g., in the proximity of parieto-opercular cortex; Mazzola et al., 2012), frequency modulation mapping also reduces the chance of stimulation side-effects. Our procedure to create a probabilistic map could be used to guide ESM mapping in a high-density grid such that boundaries between eloquent and non-eloquent cortex could be identified with ECoG and confirmed with ESM.

Although the DMTS task was not designed for cortical mapping, we found that these data were able to be used to identify the eloquent electrodes with performance similar to that reported in previous studies. This aspect points to the wide cortical network that is recruited even when performing a relatively simple task. The used DMTS task involved auditory processing of the syllable, maintenance of the auditory stimulus in short term memory, visual perception of the written cue, comparison of the auditory and visual stimuli for a match-to-sample decision, a motor response, and error monitoring post-response. It hence engages multiple different relevant stages of cognition. Nevertheless, we do not argue that the DMTS task used here is the optimal task. An optimal task would presumably include a wider range of motor actions (our task included only the index and middle finger of the right hand), a wider range of visual stimuli (to activate e.g., face-, place-, and motion-sensitive areas), and a language production section—and has to be feasible in the limited time the patient is available. Our main finding is a proof of concept that the inclusion of low frequency bands, especially the beta band, improves the identification of eloquent electrodes. We would expect that a similar analysis in a dataset acquired during the performance of a structured cognitive task explicitly designed to activate eloquent cortex would result in better performance of ECoG mapping.

The possibility also exists, however, that including low frequency power was only useful in the context of a non-optimal task. It may be that, in an optimal task all eloquent cortices may be sufficiently activated, such that they can be readily identified using the gamma band alone. Our finding that the beta band was more useful in identifying *output* areas than *input* areas argues against this possibility, since the task was arguably better tuned for identifying input areas than *output* areas (e.g., auditory cortex was adequately activated, while IFG (Broca's area) was only weakly involved during covert rehearsal and reading). Ultimately, additional data or re-analysis of data collected by other groups will be required to clarify this aspect.

In order to better understand the validity of cortical mapping with ECoG, it is relevant to evaluate whether false positives identified by ECoG mapping are in fact false positives or perhaps may be ESM false negatives. The true test of whether an area is eloquent or not is the effect of surgical resection of that area on the neuropsychological function. Currently, ESM is the best predictor of the effect of resection (Arya et al., 2018), however to control for the possibility of false negatives in ESM, it will be important to evaluate the cognitive performance of a large cohort of patients after surgical resection. A large, multi-center effort will likely be required to identify false positive and negative electrodes after both ECoG and ESM mapping. These data were not available in our study.

In our analysis we used the power of gamma, alpha and beta bands as indicators for the eloquence of cortex beneath subdural electrodes. However, with the cross-validation procedure implemented in our analysis it is possible to include a multitude of indicators. Other factors that might further improve mapping could include power, adding modulations from other frequency bands such as theta or delta (Daume et al., 2017; Grooms et al., 2017), power modulations recorded during additional tests, and responses measured in other modalities (e.g., functional mapping using fMRI; Picht et al., 2013; Trimmel et al., 2019, 2020—or transcranial magnetic stimulation). Prior predictions about the likelihood of eloquence at a particular cortical area may also be of interest and help to increase mapping accuracy.

Given the relatively small number of patients included in the present study and the task used, which was developed to study language processing rather than cortical mapping, the method described is a proof of concept not ready to be used as a diagnostic clinical test. In order to further develop our findings into a reliable diagnostic test it will be important to replicate our analysis in a larger patient population, e.g., multi-center clinical trial, in which we would be willing to contribute. It is also important to compare the results with the presence of neurological or cognitive impairments after neurosurgical resection. The optimized ECoG test should clearly outperform ESM in predicting presence

of neurological or cognitive impairments after neurosurgical resection. However, inspection of the probabilistic maps seems to argue against this scenario since the maps suggest that between-patient variability in the overall level of ECoG responsiveness is too large to instigate a universal diagnostic criterion. Thus it is more likely that any future ECoG test will be of use in addition to, or as a screening before, ESM.

CONCLUSION

Using advanced signal analysis in combination to functional and attentional specific analysis we have shown that including alpha and especially beta power modulations from a DMTS task can improve the diagnostic ability in the identification of eloquent cortical areas over the use of gamma-band power alone. We provided a method to construct probabilistic maps of eloquence based on cortical activity during a DMTS task that can be used as a clinical tool to optimize the planning of electrical cortical stimulation mapping. We conclude that cortical mapping with power modulation is a useful clinical tool to identify potentially eloquent cortical areas (ESM positive) but does not replace the need for electrical cortical stimulation mapping. Further studies using tasks specifically designed for eloquent cortical function identification, the use of tailored individual frequency bands, and comparison of different models with post-resection outcomes will elucidate whether this approach could replace or enhance ESM in clinical settings.

DATA AVAILABILITY STATEMENT

According to patient's clinical data privacy conditions, deidentified copies of the raw data supporting the conclusions presented in this study can be provided upon reasonable request. Please contact the corresponding author via email with any inquiries about the data. Custom scripts were written for data reading and visualization and are available upon request.

ETHICS STATEMENT

The studies involving human participants were reviewed and approved by the Medical Ethical Committee of the Maastricht University Medical Center, Maastricht, Netherlands. The patients/participants provided their written informed consent to participate in this study.

AUTHOR CONTRIBUTIONS

MEA-M: conceptualization, data curation, resources, software, formal analysis, validation, investigation, visualization, methodology, writing—original draft, and writing—review and editing. GV: software, formal analysis, validation, methodology, writing—original draft, and writing—review and editing. EG: data curation, resources, software, and writing—review and editing. JC: resources, software, and writing—review and editing. SO, JP, and JR: data curation and writing—review and editing. RR: data curation, resources, and writing—review and editing. OS and JD: resources and writing—review and editing. MH, WC, DH, and BJ: writing—review and editing. VK-M: conceptualization, data curation, formal analysis, validation, investigation, resources, writing—original draft, and writing—review and editing. MR: conceptualization, data curation, software, formal analysis, validation, visualization, methodology, writing—original draft, and writing—review and editing. All authors contributed to the article and approved the submitted version.

FUNDING

This work was supported by grants from the Colombian Administrative Department of Science, Technology and Innovation, COLCIENCIAS Colombia (scholarship call 568 to MEA-M).

ACKNOWLEDGMENTS

We would like to show our sincere gratitude to the patients and their families for their cooperation during the study. The authors greatly appreciate the experts who have dedicated considerable effort from their own time to substantially improve the present manuscript. As proposed by The 450 Movement (https://osf.io/tvdcg/), peer review is an essential endeavor in the scientific process and should be recognized beyond the "ACKNOWLEDGMENTS" section. Consequently, the authors would like to express their gratitude to the editor Prof. Nathan E. Crone, M.D. and reviewers Prof. Abbas Babajani-Feremi, Ph.D., Prof. Milena Korostenskaja, Ph.D., and Prof. Mario Tombini, M.D., for their generous contribution. This manuscript has been released as a pre-print at biorxiv.org (Archila-Meléndez et al., 2019).

SUPPLEMENTARY MATERIAL

The Supplementary Material for this article can be found online at: https://www.frontiersin.org/articles/10.3389/fnhum.2020.555054/full#supplementary-material

REFERENCES

Aoki, F., Fetz, E. E., Shupe, L., Lettich, E., and Ojemann, G. A. (1999). Increased gamma-range activity in human sensorimotor cortex during performance of visuomotor tasks. *Clin. Neurophysiol.* 110, 524–537. doi: 10.1016/s1388-2457(98)00064-9

Archila-Meléndez, M. E., Valente, G., Correia, J. M., Rouhl, R., van Kranen-Mastenbroek, V. H., and Jansma, B. M. (2018). Sensorimotor representation

of speech perception. Cross-decoding of place of articulation features during selective attention to syllables in 7T fMRI. *eNeuro* 5:ENEURO.0252-17.2018. doi: 10.1523/ENEURO.0252-17.2018

Archila-Meléndez, M. E., Valente, G., Gommer, E., Rouhl, R. P. W., Schijns, O. E. M. G., Dings, J. T. A., et al. (2019). A novel approach for combining task-dependent gamma with alpha and beta power modulation for enhanced identification of eloquent cortical areas using ECoG in patients with medical-refractory epileps. *Neuroscience* doi: 10.1101/677195

Arya, R., Horn, P. S., and Crone, N. E. (2018). ECoG high-gamma modulation versus electrical stimulation for presurgical language mapping. *Epilepsy Behav.* 79, 26–33. doi: 10.1016/j.yebeh.2017.10.044

Arya, R., Wilson, J. A., Fujiwara, H., Rozhkov, L., Leach, J. L., Byars, A. W., et al. (2017). Presurgical language localization with visual naming associated ECoG high- gamma modulation in pediatric drug-resistant epilepsy. *Epilepsia* 58, 663–673. doi: 10.1111/epi.13708

Arya, R., Wilson, J. A., Vannest, J., Byars, A. W., Greiner, H. M., Buroker, J., et al. (2015). Electrocorticographic language mapping in children by high-gamma synchronization during spontaneous conversation: comparison with conventional electrical cortical stimulation. *Epilepsy Res.* 110, 78–87. doi: 10.1016/j.eplepsyres.2014.11.013

Aungaroon, G., Zea Vera, A., Horn, P. S., Byars, A. W., Greiner, H. M., Tenney, J. R., et al. (2017). After-discharges and seizures during pediatric extra-operative electrical cortical stimulation functional brain mapping: incidence, thresholds, and determinants. *Clin. Neurophysiol.* 128, 2078–2086. doi: 10.1016/j.clinph.2017.06.259

Bauer, P. R., Vansteensel, M. J., Bleichner, M. G., Hermes, D., Ferrier, C. H., Aarnoutse, E. J., et al. (2013). Mismatch between electrocortical stimulation and electrocorticography frequency mapping of language. *Brain Stimul.* 6, 524–531. doi: 10.1016/j.brs.2013.01.001

Blume, W. T., Jones, D. C., and Pathak, P. (2004). Properties of after-discharges from cortical electrical stimulation in focal epilepsies. *Clin. Neurophysiol.* 115, 982–989. doi: 10.1016/j.clinph.2003.11.023

Bonaiuto, J. J., Meyer, S. S., Little, S., Rossiter, H., Callaghan, M. F., Dick, F., et al. (2018). Lamina-specific cortical dynamics in human visual and sensorimotor cortices. *eLife* 7:e33977. doi: 10.7554/eLife.33977

Bouchard, K. E., Mesgarani, N., Johnson, K., and Chang, E. F. (2013). Functional organization of human sensorimotor cortex for speech articulation. *Nature* 495, 327–332. doi: 10.1038/nature11911

Brosch, M., Budinger, E., and Scheich, H. (2002). Stimulus-related gamma oscillations in primate auditory cortex. *J. Neurophysiol.* 87, 2715–2725. doi: 10.1152/jn.2002.87.6.2715

Brunner, P., Ritaccio, A. L., Lynch, T. M., Emrich, J. F., Wilson, J. A., Williams, J. C., et al. (2009). A practical procedure for real-time functional mapping of eloquent cortex using electrocorticographic signals in humans. *Epilepsy Behav.* 15, 278–286. doi: 10.1016/j.yebeh.2009.04.001

Buzsaki, G. (2004). Neuronal oscillations in cortical networks. *Science* 304, 1926–1929. doi: 10.1126/science.1099745

Buzsáki, G., Anastassiou, C. A., and Koch, C. (2012). The origin of extracellular fields and currents — EEG, ECoG, LFP and spikes. *Nat. Rev. Neurosci.* 13, 407–420. doi: 10.1038/nrn3241

Crone, N. E., Miglioretti, D. L., Gordon, B., and Lesser, R. P. (1998a). Functional mapping of human sensorimotor cortex with electrocorticographic spectral analysis. II. Event-related synchronization in the gamma band. *Brain* 121(Pt 12), 2301–2315. doi: 10.1093/brain/121.12.2301

Crone, N. E., Miglioretti, D. L., Gordon, B., Sieracki, J. M., Wilson, M. T., Uematsu, S., et al. (1998b). Functional mapping of human sensorimotor cortex with electrocorticographic spectral analysis. I. Alpha and beta event-related desynchronization. *Brain* 121(Pt 12), 2271–2299. doi: 10.1093/brain/121.12.2271

Crone, N. E., Sinai, A., and Korzeniewska, A. (2006). High-frequency gamma oscillations and human brain mapping with electrocorticography. *Prog. Brain Res.* 159, 275–295. doi: 10.1016/S0079-6123(06)59019-3

Dale, A. M., Fischl, B., and Sereno, M. I. (1999). Cortical surface-based analysis. I. Segmentation and surface reconstruction. *NeuroImage* 9, 179–194. doi: 10.1006/nimg.1998.0395

Daume, J., Graetz, S., Gruber, T., Engel, A. K., and Friese, U. (2017). Cognitive control during audiovisual working memory engages frontotemporal theta-band interactions. *Sci. Rep.* 7:12585. doi: 10.1038/s41598-017-12511-3

de Pesters, A., Coon, W. G., Brunner, P., Gunduz, A., Ritaccio, A. L., Brunet, N. M., et al. (2016). Alpha power indexes task-related networks on large and small scales: a multimodal ECoG study in humans and a non-human primate. *NeuroImage* 134, 122–131. doi: 10.1016/j.neuroimage.2016.03.074

Dykstra, A. R., Chan, A. M., Quinn, B. T., Zepeda, R., Keller, C. J., Cormier, J., et al. (2012). Individualized localization and cortical surface-based registration of intracranial electrodes. *NeuroImage* 59, 3563–3570. doi: 10.1016/j.neuroimage.2011.11.046

Escabí, M. A., Read, H. L., Viventi, J., Kim, D.-H., Higgins, N. C., Storace, D. A., et al. (2014). A high-density, high-channel count, multiplexed μECoG array for auditory-cortex recordings. *J. Neurophysiol.* 112, 1566–1583. doi: 10.1152/jn.00179.2013

Felleman, D. J., and Van Essen, D. C. (1991). Distributed hierarchical processing in the primate cerebral cortex. *Cereb. Cortex* 1, 1–47. doi: 10.1093/cercor/1.1.1

Fischl, B., Sereno, M. I., and Dale, A. M. (1999a). Cortical surface-based analysis. II: inflation, flattening, and a surface-based coordinate system. *Neuroimage* 9, 195–207. doi: 10.1006/nimg.1998.0396

Fischl, B., Sereno, M. I., Tootell, R. B., and Dale, A. M. (1999b). High-resolution intersubject averaging and a coordinate system for the cortical surface. *Hum. Brain Mapp.* 8, 272–284. doi: 10.1002/(sici)1097-0193(1999)8:4<272::aid-hbm10>3.0.co;2-4

Fries, P., Nikolić, D., and Singer, W. (2007). The gamma cycle. *Trends Neurosci.* 30, 309–316. doi: 10.1016/j.tins.2007.05.005

Gray, C. M., König, P., Engel, A. K., and Singer, W. (1989). Oscillatory responses in cat visual cortex exhibit inter-columnar synchronization which reflects global stimulus properties. *Nature* 338, 334–337. doi: 10.1038/338334a0

Green, D. M., and Swets, J. A. (2000). *Signal Detection Theory and Psychophysics, Repr*. Los Altos Hills, CA: Peninsula Publ.

Grooms, J. K., Thompson, G. J., Pan, W.-J., Billings, J., Schumacher, E. H., Epstein, C. M., et al. (2017). Infraslow electroencephalographic and dynamic resting state network activity. *Brain Connect.* 7, 265–280. doi: 10.1089/brain.2017.0492

Groppe, D. M., Bickel, S., Dykstra, A. R., Wang, X., Mégevand, P., Mercier, M. R., et al. (2017). iELVis: an open source MATLAB toolbox for localizing and visualizing human intracranial electrode data. *J. Neurosci. Methods* 281, 40–48. doi: 10.1016/j.jneumeth.2017.01.022

Hamberger, M. J. (2007). Cortical language mapping in epilepsy: a critical review. *Neuropsychol. Rev.* 17, 477–489. doi: 10.1007/s11065-007-9046-6

Hamilton, L. S., Edwards, E., and Chang, E. F. (2018). A spatial map of onset and sustained responses to speech in the human superior temporal gyrus. *Curr. Biol.* 28, 1860–1871. doi: 10.1016/j.cub.2018.04.033

Haupt, M., Ruiz-Rizzo, A. L., Sorg, C., and Finke, K. (2020). Right-lateralized fronto-parietal network and phasic alertness in healthy aging. *Sci. Rep.* 10, 1–10. doi: 10.1038/s41598-020-61844-z

Hermes, D., Miller, K. J., Vansteensel, M. J., Aarnoutse, E. J., Leijten, F. S. S., and Ramsey, N. F. (2012). Neurophysiologic correlates of fMRI in human motor cortex. *Hum. Brain Mapp.* 33, 1689–1699. doi: 10.1002/hbm.21314

Hermiz, J., Rogers, N., Kaestner, E., Ganji, M., Cleary, D. R., Carter, B. S., et al. (2018). Sub-millimeter ECoG pitch in human enables higher fidelity cognitive neural state estimation. *Neuroimage* 176, 454–464. doi: 10.1016/j.neuroimage.2018.04.027

Jenkinson, M., and Smith, S. (2001). A global optimisation method for robust affine registration of brain images. *Med. Image Anal.* 5, 143–156. doi: 10.1016/s1361-8415(01)00036-6

Jensen, O., and Mazaheri, A. (2010). Shaping functional architecture by oscillatory alpha activity: gating by inhibition. *Front. Hum. Neurosci.* 4:186. doi: 10.3389/fnhum.2010.00186

Lachaux, J.-P., Jerbi, K., Bertrand, O., Minotti, L., Hoffmann, D., Schoendorff, B., et al. (2007). A blueprint for real-time functional mapping via human intracranial recordings. *PLoS One* 2:e1094. doi: 10.1371/journal.pone.0001094

Lachaux, J. P., Rudrauf, D., and Kahane, P. (2003). Intracranial EEG and human brain mapping. *J. Physiol. Paris* 97, 613–628. doi: 10.1016/j.jphysparis.2004.01.018

Lee, H. W., Webber, W. R. S., Crone, N., Miglioretti, D. L., and Lesser, R. P. (2010). When is electrical cortical stimulation more likely to produce afterdischarges? *Clin. Neurophysiol.* 121, 14–20. doi: 10.1016/j.clinph.2009.10.001

Lesser, R. P., Lüders, H., Klem, G., Dinner, D. S., Morris, H. H., and Hahn, J. (1984). Cortical afterdischarge and functional response thresholds: results of extraoperative testing. *Epilepsia* 25, 615–621. doi: 10.1111/j.1528-1157.1984.tb03471.x

Lesser, R. P., Lüders, H., Klem, G., Dinner, D. S., Morris, H. H., and Hahn, J. (1985). Ipsilateral trigeminal sensory responses to cortical stimulation by subdural electrodes. *Neurology* 35, 1760–1763. doi: 10.1212/wnl.35.12.1760

Leuthardt, E. C., Miller, K., Anderson, N. R., Schalk, G., Dowling, J., and Miller, J. (2007). Electrocorticographic frequency alteration mapping: a clinical technique for mapping the motor cortex. *Neurosurgery* 60, 260–270. doi: 10.1227/01.NEU.0000255413.70807.6E discussion 270-271,

Mazzola, L., Isnard, J., Peyron, R., and Mauguière, F. (2012). Stimulation of the human cortex and the experience of pain: wilder Penfield's observations revisited. *Brain* 135, 631–640. doi: 10.1093/brain/awr265

McCullagh, P., and Nelder, J. A. (1998). *Generalized linear Models, Monographs on Statistics and Applied Probability*, 2nd Edn. Boca Raton, FL: Chapman & Hall/CRC.

Mesgarani, N., Cheung, C., Johnson, K., and Chang, E. F. (2014). Phonetic feature encoding in human superior temporal gyrus. *Science* 343, 1006–1010. doi: 10.1126/science.1245994

Miller, K. J., Leuthardt, E. C., Schalk, G., Rao, R. P. N., Anderson, N. R., Moran, D. W., et al. (2007). Spectral changes in cortical surface potentials during motor movement. *J. Neurosci.* 27, 2424–2432. doi: 10.1523/JNEUROSCI.3886-06.2007

Mooij, A. H., Sterkman, L. C. M., Zijlmans, M., and Huiskamp, G. J. M. (2018). Electrocorticographic high gamma language mapping: mind the pitfalls of comparison with electrocortical stimulation. *Epilepsy Behav.* 82, 196–199. doi: 10.1016/j.yebeh.2018.02.001

Muller, L., Hamilton, L. S., Edwards, E., Bouchard, K. E., and Chang, E. F. (2016). Spatial resolution dependence on spectral frequency in human speech cortex electrocorticography. *J Neural Eng.* 13:056013. doi: 10.1088/1741-2560/13/5/056013

Murthy, V. N., and Fetz, E. E. (1992). Coherent 25- to 35-Hz oscillations in the sensorimotor cortex of awake behaving monkeys. *Proc. Natl. Acad. Sci. U.S.A.* 89, 5670–5674. doi: 10.1073/pnas.89.12.5670

Nagasawa, T., Rothermel, R., Juhász, C., Fukuda, M., Nishida, M., Akiyama, T., et al. (2010). Cortical gamma-oscillations modulated by auditory-motor tasks-intracranial recording in patients with epilepsy. *Hum. Brain Mapp.* 31, 1627–1642. doi: 10.1002/hbm.20963

Ojemann, G., Ojemann, J., Lettich, E., and Berger, M. (1989). Cortical language localization in left, dominant hemisphere. *J. Neurosurg.* 71, 316–326. doi: 10.3171/jns.1989.71.3.0316

Oostenveld, R., Fries, P., Maris, E., and Schoffelen, J. M. (2011). FieldTrip: open source software for advanced analysis of MEG, EEG, and invasive electrophysiological data. *Comput. Intell. Neurosci.* 2011:156869. doi: 10.1155/2011/156869

Penfield, W., and Boldrey, E. (1937). Somatic motor and sensory representation in man. *Brain* 60, 389–443. doi: 10.1093/brain/60.4.389

Pfurtscheller, G., Neuper, C., and Kalcher, J. (1993). 40-Hz oscillations during motor behavior in man. *Neurosci. Lett.* 164, 179–182. doi: 10.1016/0304-3940(93)90886-p

Picht, T., Krieg, S. M., Sollmann, N., Rösler, J., Niraula, B., Neuvonen, T., et al. (2013). A comparison of language mapping by preoperative navigated transcranial magnetic stimulation and direct cortical stimulation during awake surgery. *Neurosurgery* 72, 808–819. doi: 10.1227/NEU.0b013e3182889e01

Prakash, H. R., Korostenskaja, M., Lee, K., Baumgartner, J., Castillo, E., Bagci, U., et al. (2017). "Automatic response assessment in regions of language cortex in epilepsy patients using ECoG-based functional mapping and machine learning in,"*2017 IEEE International Conference on Systems, Man, and Cybernetics (SMC) Presented at the 2017 IEEE International Conference on Systems, Man and Cybernetics (SMC)*, Banff, AB: IEEE, 519–524. doi: 10.1109/SMC.2017.8122658

RaviPrakash, H., Korostenskaja, M., Castillo, E. M., Lee, K. H., Salinas, C. M., Baumgartner, J., et al. (2020). Deep Learning provides exceptional accuracy to ECoG-based functional language mapping for epilepsy surgery. *Front. Neurosci.* 14:409. doi: 10.3389/fnins.2020.00409

Ruiz-Rizzo, A. L., Neitzel, J., Müller, H. J., Sorg, C., and Finke, K. (2018). Distinctive correspondence between separable visual attention functions and intrinsic brain networks. *Front. Hum. Neurosci.* 12:89. doi: 10.3389/fnhum.2018.00089

Ruiz-Rizzo, A. L., Sorg, C., Napiórkowski, N., Neitzel, J., Menegaux, A., Müller, H. J., et al. (2019). Decreased cingulo-opercular network functional connectivity mediates the impact of aging on visual processing speed. *Neurobiol. Aging* 73, 50–60. doi: 10.1016/j.neurobiolaging.2018.09.014

Ruiz-Rizzo, A. L., Beissner, F., Finke, K., Müller, H. J., Zimmer, C., Pasquini, L., et al. (2020). Human subsystems of medial temporal lobes extend locally to amygdala nuclei and globally to an allostatic-interoceptive system. *NeuroImage* 207:116404. doi: 10.1016/j.neuroimage.2019.116404

Scheeringa, R., and Fries, P. (2017). Cortical layers, rhythms and BOLD signals. *Neuroimage* 197, 689–698. doi: 10.1016/j.neuroimage.2017.11.002

Sinai, A., Bowers, C. W., Crainiceanu, C. M., Boatman, D., Gordon, B., Lesser, R. P., et al. (2005). Electrocorticographic high gamma activity versus electrical cortical stimulation mapping of naming. *Brain* 128, 1556–1570. doi: 10.1093/brain/awh491

Trimmel, K., Graan, L. A., Gonzálvez, G. G., Haag, A., Caciagli, L., Vos, S. B., et al. (2019). Naming fMRI predicts the effect of temporal lobe resection on language decline. *Ann. Clin. Transl. Neurol.* 6, 2186–2196. doi: 10.1002/acn3.50911

Trimmel, K., Caciagli, L., Xiao, F., van Graan, L. A., Koepp, M. J., Thompson, P. J., and Duncan, J. S. (2020). Impaired naming performance in temporal lobe epilepsy: language fMRI responses are modulated by disease characteristics. *J. Neurol.* 1–14. doi: 10.1007/s00415-020-10116-x

Vansteensel, M. J., Bleichner, M. G., Dintzner, L. T., Aarnoutse, E. J., Leijten, F. S. S., Hermes, D., et al. (2013). Task-free electrocorticography frequency mapping of the motor cortex. *Clin. Neurophysiol.* 124, 1169–1174. doi: 10.1016/j.clinph.2012.08.048

Vansteensel, M. J., Hermes, D., Aarnoutse, E. J., Bleichner, M. G., Schalk, G., van Rijen, P. C., et al. (2010). Brain-computer interfacing based on cognitive control. *Ann. Neurol.* 67, 809–816. doi: 10.1002/ana.21985

Wang, Y., Fifer, M. S., Flinker, A., Korzeniewska, A., Cervenka, M. C., Anderson, W. S., et al. (2016). Spatial-temporal functional mapping of language at the bedside with electrocorticography. *Neurology* 86, 1181–1189. doi: 10.1212/WNL.0000000000002525

Wu, M., Wisneski, K., Schalk, G., Sharma, M., Roland, J., Breshears, J., et al. (2010). Electrocorticographic frequency alteration mapping for extraoperative localization of speech cortex. *Neurosurgery* 66, E407–E409. doi: 10.1227/01.NEU.0000345352.13696.6F

Yushkevich, P. A., Piven, J., Hazlett, H. C., Smith, R. G., Ho, S., Gee, J. C., et al. (2006). User-guided 3D active contour segmentation of anatomical structures: significantly improved efficiency and reliability. *NeuroImage* 31, 1116–1128. doi: 10.1016/j.neuroimage.2006.01.015

Conflict of Interest: The authors declare that the research was conducted in the absence of any commercial or financial relationships that could be construed as a potential conflict of interest.

frontiers in Human Neuroscience

SYSTEMATIC REVIEW
published: 22 January 2021
doi: 10.3389/fnhum.2020.617061

Electrical Stimulation-Induced Seizures and Breathing Dysfunction: A Systematic Review of New Insights Into the Epileptogenic and Symptomatogenic Zones

Manuela Ochoa-Urrea[1]*, *Mojtaba Dayyani*[1], *Behnam Sadeghirad*[2], *Nitin Tandon*[1], *Nuria Lacuey*[1] *and Samden D. Lhatoo*[1]

[1] Department of Neurology, University of Texas Health Sciences Center at Houston, Houston, TX, United States,
[2] Department of Health Research Methods, Evidence, and Impact, McMaster University, Hamilton, ON, Canada

OPEN ACCESS

Edited by:
Patrick Chauvel,
University of Pittsburgh Medical Center, United States

Reviewed by:
Stephan Schuele,
Northwestern University, United States
Sacit Karamürsel,
Koç University, Turkey

***Correspondence:**
Manuela Ochoa-Urrea
Manuela.ochoaurrea@uth.tmc.edu

Specialty section:
This article was submitted to Brain Imaging and Stimulation, a section of the journal Frontiers in Human Neuroscience

Received: 13 October 2020
Accepted: 18 December 2020
Published: 22 January 2021

Citation:
Ochoa-Urrea M, Dayyani M, Sadeghirad B, Tandon N, Lacuey N and Lhatoo SD (2021) Electrical Stimulation-Induced Seizures and Breathing Dysfunction: A Systematic Review of New Insights Into the Epileptogenic and Symptomatogenic Zones. Front. Hum. Neurosci. 14:617061. doi: 10.3389/fnhum.2020.617061

Objective: Electrical stimulation (ES) potentially delineates epileptogenic cortex through induction of typical seizures. Although frequently employed, its value for epilepsy surgery remains controversial. Similarly, ES is used to identify symptomatogenic zones, but with greater success and a long-standing evidence base. Recent work points to new seizure symptoms such as ictal central apnea (ICA) that may enhance presurgical hypotheses. The aims of this review are 2-fold: to determine the value of ES-induced seizures (ESIS) in epilepsy surgery and to analyze current evidence on ICA as a new surrogate of symptomatogenic cortex.

Methods: Three databases were searched for ESIS. Investigators independently selected studies according to pre-specified criteria. Studies reporting postoperative outcome in patients with ESIS were included in a meta-analysis. For ES-induced apnea, a thorough search was performed and reference list searching was employed.

Results: Of 6,314 articles identified for ESIS, 25 were considered eligible to be reviewed in full text. Fourteen studies were included in the qualitative synthesis (1,069 patients); six studies were included in the meta-analysis (530 patients). The meta-analysis showed that favorable outcome is associated with ESIS prior to surgery (OR: 2.02; 95% CI: 1.332–3.08). In addition, the overall estimation of the occurrence of favorable outcome among cases with ESIS is 68.13% (95% CI: 56.62–78.7). On the other hand, recent studies have shown that stimulation of exclusively mesial temporal lobe structures elicits central apnea and represents symptomatogenic anatomic substrates of ICA. This is in variance with traditional teaching that mesial temporal ES is non-symptomatogenic.

Conclusions: ES is a tool highly likely to aid in the delineation of the epileptogenic zone, since ESIS is associated with favorable postoperative outcomes (Engel I). There is an urgent need for prospective evaluation of this technique, including effective stimulation parameters and surgical outcomes, that will provide knowledge base for practice. In

addition, ES-induced apnea studies suggest that ICA, especially when it is the first or only clinical sign, is an important semiological feature in localizing the symptomatogenic zone to mesial temporal lobe structures, which must be considered in SEEG explorations where this is planned, and in surgical resection strategies.

Keywords: electrical stimulation-induced seizures, refractory epilepsy, seizure onset zone, epilepsy surgery, outcome, ictal central apnea (ICA), electrical stimulation (ES)

INTRODUCTION

Electrical stimulation (ES) using invasive electrodes is primarily intended to map eloquent areas of sampled brain in order to formulate resection strategies. In addition, ES can be used to identify seizure onset and symptomatogenic zones (Trébuchon and Chauvel, 2016; Jobst et al., 2020). The seizure onset zone is the "area of cortex from which clinical seizures are generated" (Rosenow and Lüders, 2001). The symptomatogenic zone is the "area of the cortex which when activated by an epileptiform discharge, produces ictal symptoms" (Rosenow and Lüders, 2001). The epileptogenic zone is the area indispensable for the generation of seizures, and may be inferred by defining the symptomatogenic zone, the seizure onset zone, and other areas (Rosenow and Lüders, 2001).

Identification of the seizure onset zone can be challenging in some intracranial EEG studies, and ES can be carried out to reproduce typical seizures, thus lending additional support to identifying putative seizure onset electrodes. However, epilepsy centers differ in their attitudes and approaches to ES (Kovac et al., 2016). There is limited evidence of an association between ES induced seizures (ESIS) and surgical outcomes (Kovac et al., 2016). In addition, stimulation methodology varies between centers, making practice heterogeneous (So and Alwaki, 2018). However, there is some evidence that ESIS have the potential to reliably identify seizure onset zones and help guide successful epilepsy surgery (Munari et al., 1993; Cuello Oderiz et al., 2019; Spilioti et al., 2020; Trebuchon et al., 2021).

Similarly, ES is used to reproduce seizure symptoms, thus identifying symptomatogenic zones (Borchers et al., 2012; Landazuri and Minotti, 2019). Much of this practice is based on long-standing, well-established literature on motor, motor association, sensory, visual, auditory, special sensory, and language cortices (Landazuri and Minotti, 2019). Recent evidence suggests that with appropriate multimodal monioring, semiological signs of breathing disturbances such as ictal central apnea (ICA), reproducible with ES, may enhance presurgical hypotheses for implantation or resection (Lacuey et al., 2017, 2019a).

This review is divided into two parts: (1) a systematic review of literature to determine the state of the art and value of ESIS in epilepsy surgery outcomes, and (2) a review of evidence regarding ICA as a surrogate of symptomatogenic cortex.

METHODS

ES to Localize the Seizure Onset Zone

Three study authors with expertise in the subject (MOU, NL, and SDL) designed search strategy, terms, and translation in each database. Our main research question was defined as "does removal of seizure onset zone, identified by ESIS, predict favorable surgical outcome in patients with refractory epilepsy?" In addition, we gathered information regarding definitions and stimulation techniques implemented around the world. MEDLINE (via Ovid), EMBASE, and Scopus were searched as of April 1, 2020, without language or date restrictions. The search strategy included the terms "electrical stimulation," "brain stimulation," "cortical stimulation," "epileptogenic zone," "ictal onset zone," "seizure onset zone," and "symptomatogenic zone" (available in **Supplementary Material**). The search strategy was first developed for MEDLINE and then tailored for each database taking into account differences in vocabulary and syntax rules. Additionally, we incorporated reference list searching (snowballing) into our search strategy. References were exported and managed with Mendeley and duplicates were eliminated. Finally, we adhered to the PRISMA guidelines and checklist to report our findings (Liberati et al., 2009; Moher et al., 2009).

We included randomized/non-randomized controlled trials, cohort studies, and case series reporting use of ESIS in humans, in which methodology of stimulation was described. We included articles in English, Spanish, and French. Unpublished data, studies that did not contain primary data (i.e., review articles), and studies on patients with no diagnosis of epilepsy were excluded. The Rayyan website (Ouzzani et al., 2016) was used for screening of titles and abstracts by three authors (MOU, NL, and SDL), who independently selected studies according to criteria mentioned above. The third reviewer resolved discrepancies in selection between two reviewers. We only included those studies that reported postoperative outcome in patients who had received ES to induce seizures into the meta-analysis.

Demographics, stimulation characteristics, rate of induced seizures, outcomes, adverse events, and key conclusions data were collected. Two reviewers (MOU and MD) assessed risk of bias independently and in duplicate using the Cochrane risk of bias instrument (Higgins et al., 2011) with specific adjustments for methodologic evaluation of case series (Murad et al., 2018). The adjusted tool addresses the four following potential sources of bias: selection, ascertainment (exposure and outcome), causality (alternative causes and follow-up), and reporting (**Figures 1A,B**) (Murad et al., 2018). Any disagreements between reviewers in data extraction or risk of bias assessments were resolved by discussion or involvement of a third reviewer (SDL) as an arbitrator. Using STATA (Version 16.1, College Station, TX), we calculated pooled estimation of rates for favorable outcomes among studies (Engel I). In addition, a conventional meta-analysis with random effect model was used to calculate odds of having favorable outcome following the ES.

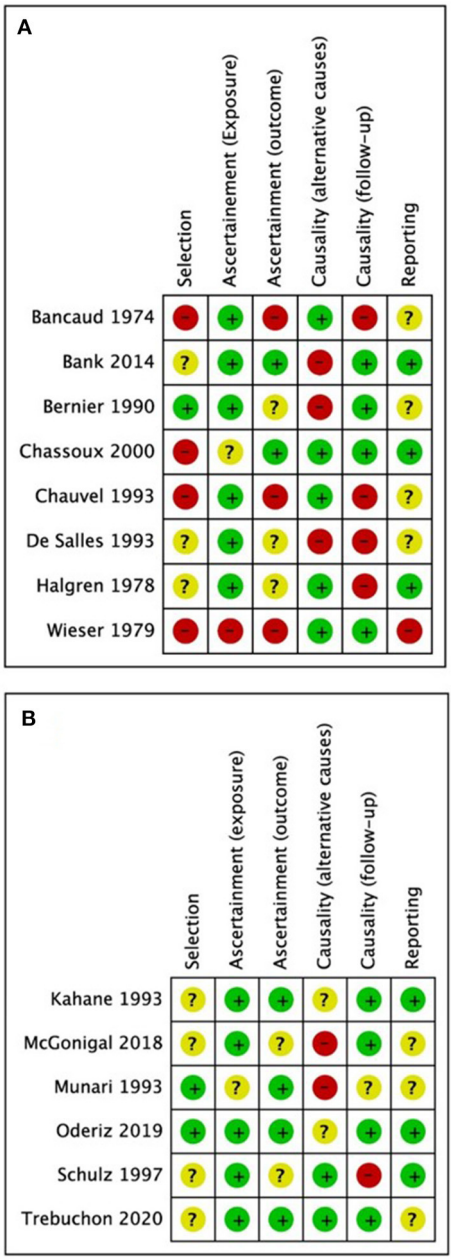

FIGURE 1 | Quality assessment results from **(A)** studies excluded from the meta-analysis; **(B)** studies included in the meta-analysis. Green = low risk of bias, yellow = undetermined risk of bias, red = high risk of bias.

ES for Induction of Central Apnea Semiology

Three study authors with expertise in the subject (MOU, NL, and SDL), designed search strategy and terms to include in a non-systematic literature review. We intended to gather all available information regarding ES and ICA with the goal of summarizing this information. To achieve this we searched MEDLINE (via Ovid) using search terms such as "electrical stimulation," "cortical stimulation," "apnea," and "epilepsy" (for a full description of the search strategy used, please refer to **Supplementary Material**). This search strategy yielded 140 results. Additionally, we incorporated reference list searching (snowballing) into our search, yielding 157 results. References were exported and managed with Mendeley. An expert in the field of breathing and ES (NL) selected studies that were included in our review. A total of 19 studies were selected that included information regarding apnea as part of the ictal semiology and studies that included ES-induced apnea.

RESULTS

ES to Localize the Seizure Onset Zone

A total of 6,314 articles were identified through database searches and snowballing (**Figure 2**). After eliminating duplicates (2,817 duplicates), 3,497 articles were screened using title and abstract. Of these, we excluded 3,472, and 25 were considered eligible for review in full text. Eleven articles were further excluded because they did not meet inclusion criteria, yielding 14 studies included in a qualitative synthesis, comprising 1,069 participants (see **Supplementary Table 1** for details of each study). One of the studies retrieved was in abstract form (Trebuchon et al., 2021). Since it was of scientific interest, we contacted the author who provided a full-text article in press. It fulfilled the remaining inclusion criteria, and we decided to include it despite its unpublished status.

The majority of studies were retrospective case series, from France (Bancaud et al., 1974; Wieser et al., 1979; Chauvel et al., 1993; Kahane et al., 1993; Munari et al., 1993; Chassoux et al., 2000; McGonigal et al., 2018), in collaboration with Canada (Cuello Oderiz et al., 2019) and Italy (Trebuchon et al., 2021), and from USA (Halgren et al., 1978; DeSalles et al., 1994; Schulz et al., 1997; Bank et al., 2014) and Canada (Bernier et al., 1990). All were SEEG series, except for three that used subdural grids or strips (DeSalles et al., 1994; Schulz et al., 1997; Bank et al., 2014). For the studies that reported the putative epileptic focus, the most frequent epilepsy type was temporal (56.5%), followed by frontal (25%) and multilobar (11%).

Definition of ESIS

We found variability in author definitions of ESIS but broad agreement that it should resemble a spontaneous seizure or aura, described as habitual by the patient or witness (Halgren et al., 1978; Bernier et al., 1990; Kahane et al., 1993; Munari et al., 1993; Cuello Oderiz et al., 2019; Trebuchon et al., 2021). Munari et al. defined it as a clinical manifestation, either subjective or objective, resembling those previously described by patient and/or witnesses or as seen during seizure recordings (Munari et al., 1993). Bernier et al. added the electrophysiological aspect, defining it as first signs of a seizure resembling the patient's habitual symptoms in the context of a simultaneous after discharge localized to the stimulation contacts only (Bernier et al., 1990). Similarly, for other authors, electrographic changes with spatial and temporal evolution had to accompany clinical changes (Bank et al., 2014; Cuello Oderiz et al., 2019). In contrast,

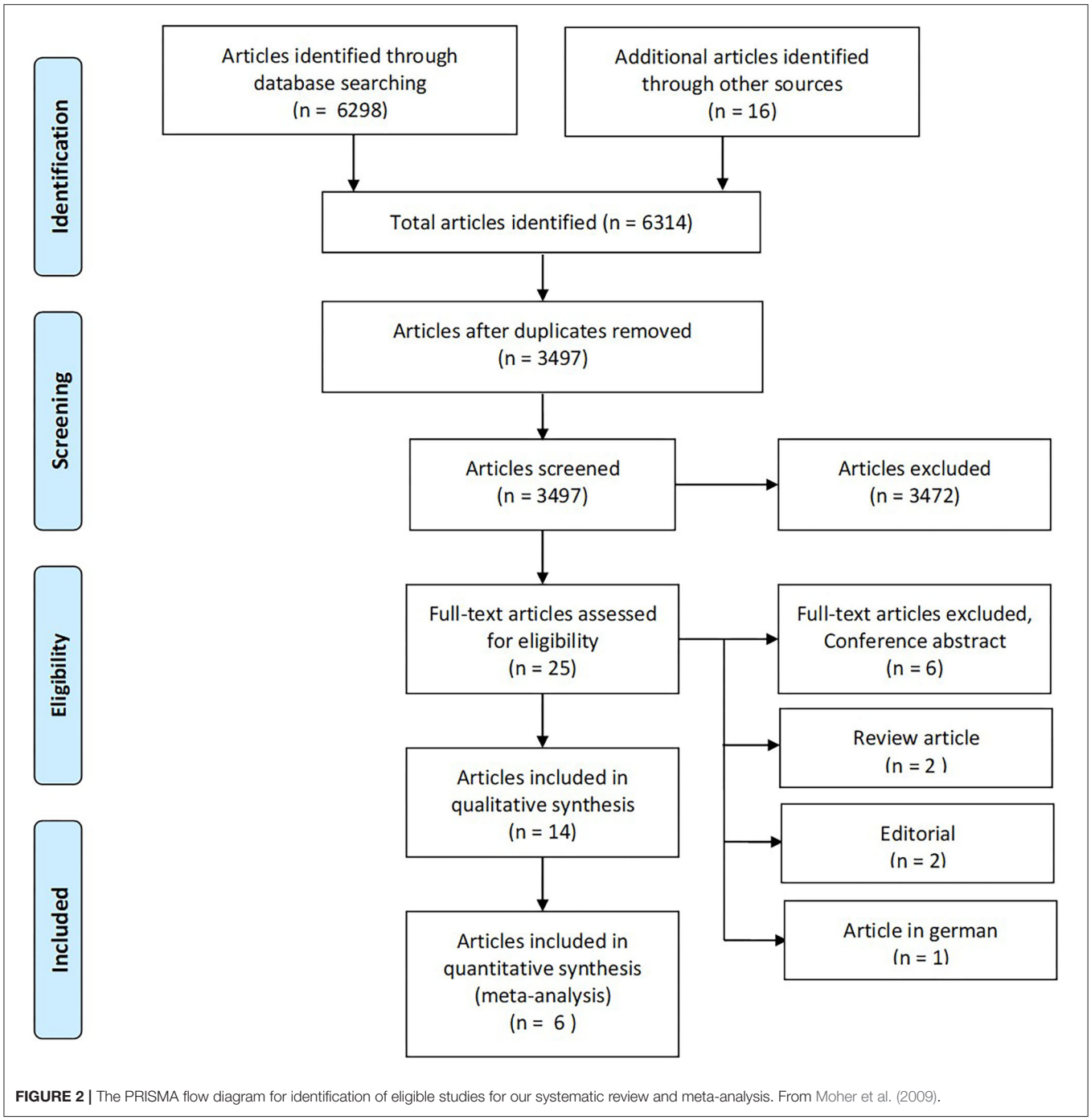

FIGURE 2 | The PRISMA flow diagram for identification of eligible studies for our systematic review and meta-analysis. From Moher et al. (2009).

some specified absence of ES-induced afterdischarges as a main characteristic of stimulation-induced aura (Schulz et al., 1997).

Stimulation Parameters and Responses

Both low-frequency (<5 Hz) and high-frequency (>5 Hz) stimulation approaches were used. High-frequency stimulation was used in all included studies at 50 Hz, with one exception where stimulation frequency was not specified (Wieser et al., 1979). One study also used 10- and 20-Hz stimulation (Bank et al., 2014). Pulsewidth varied from 0.1 to 3 ms (**Supplementary Table 1**). High-frequency stimulation was usually 50-Hz pulses using 0.2–1 ms pulse width. When low-frequency stimulation at 1 Hz was used, the train duration lasted from 20 to 40 s (Kahane et al., 1993; Munari et al., 1993; Cuello Oderiz et al., 2019). On the other hand, high-frequency stimulation was carried out from 3 to 10 s (Bancaud et al., 1974; Bernier et al., 1990; Chauvel et al., 1993; Kahane et al., 1993; Munari et al., 1993; Schulz et al., 1997; Bank

et al., 2014; McGonigal et al., 2018; Cuello Oderiz et al., 2019). Current intensity varied between studies. A titrated approach was used starting with low intensities of 0.25–0.5 mA, increasing progressively to a maximum of 15 mA, with lower intensities used in temporal lobes (Cuello Oderiz et al., 2019).

ESIS were elicited on average in 69.4% ± 23.6 (range 27.7–100) of patients (Halgren et al., 1978; Bernier et al., 1990; Chauvel et al., 1993; Munari et al., 1993; DeSalles et al., 1994; Schulz et al., 1997; Bank et al., 2014; McGonigal et al., 2018; Cuello Oderiz et al., 2019; Trebuchon et al., 2021). These rates varied depending on type of stimulation. Cuello Oderiz et al. found high-frequency stimulation (50 Hz) to be more effective in inducing seizures (54.9 vs. 18.2%) (Cuello Oderiz et al., 2019). Similarly, Kahane et al. reported 37.5% seizures with high frequency vs. 9.7% with low frequency (Kahane et al., 1993). ES-induced adverse effects were more frequent with high frequency (5.9 vs. 3.5%) compared to low frequency (Munari et al., 1993). Adverse effect rates up to 10% rate were found with high-frequency settings in one study (Kahane et al., 1993). Difficulty with mouth opening and restricted cephalic symptoms were adverse effects of ES (Munari et al., 1993; DeSalles et al., 1994). In addition, atypical electroclinical seizures, although rare, were reported to be more frequent with 50-Hz stimulation in one study (7.8 vs. 1.5%) (Cuello Oderiz et al., 2019). Rate and type of adverse effects were not described in some studies (Bancaud et al., 1974; Wieser et al., 1979; Bernier et al., 1990; Chauvel et al., 1993; Schulz et al., 1997).

Meta-Analysis: Epilepsy Surgery Outcome

We included in our meta-analysis studies that reported outcomes after epilepsy surgery. Only six studies fulfilled criteria (Kahane et al., 1993; Munari et al., 1993; Schulz et al., 1997; McGonigal et al., 2018; Cuello Oderiz et al., 2019; Trebuchon et al., 2021). The sample sizes of individual studies included ranged from 10 to 346. In total, included studies consisted of 530 subjects with intractable epilepsy who received ES, of which a total of 508 underwent epilepsy surgery with reported outcomes. Among those who underwent surgery, 376 cases had ESIS, and 132 did not have ESIS (**Figure 3**).

Based on the six studies included, our meta-analysis revealed that overall estimation of the occurrence of favorable outcome (Engel class I) among cases who had ESIS is 68.13% [95% confidence interval (CI): 56.62–78.7] (**Figure 4**). After excluding the study with the highest event rate of a favorable outcome (Trebuchon et al., 2021), the overall estimated rate did not change.

Four studies investigated epilepsy surgery outcome in patients with ESIS (Munari et al., 1993; Schulz et al., 1997; Cuello Oderiz et al., 2019; Trebuchon et al., 2021). Schulz et al. analyzed if ES-induced auras, without afterdischarges or seizures, could delineate a resectable epileptogenic zone (Schulz et al., 1997). Complete resection of the ESIS demarcated area did not correlate with favorable postoperative outcomes (Schulz et al., 1997). In contrast, Cuello Oderiz et al. found ESIS to portend favorable surgical outcomes (Cuello Oderiz et al., 2019). In the favorable outcome group, the percentage of ESIS was greater and the number of resected electrode contacts where stimulation induced seizures was higher, compared to the poor outcome group. They concluded that ESIS could be an indicator of the epileptogenic zone. In line with these findings, Trebuchon et al. indicated, in a multivariate analysis of 346 patients, that ESIS with low-frequency parameters was independently associated with positive seizure outcome after surgery (Trebuchon et al., 2021). In addition, Munari et al. reported that patients in whom low-frequency stimulation was effective in inducing seizures and who underwent epilepsy surgery had a favorable outcome (Engel I) with a mean follow-up of 15.4 months (Munari et al., 1993).

Of these four studies, three reported detailed outcomes based on favorable (Engel I) and unfavorable (Engel II–IV) results among those with/without ESIS (Munari et al., 1993; Cuello Oderiz et al., 2019; Trebuchon et al., 2021). Thus, we conducted another conventional meta-analysis with these studies to assess a possible association between favorable outcomes and ESIS. Results showed that favorable outcome is associated with presence of ESIS with an odds ratio (OR) of 2.02 (95% CI: 1.33–3.08) compared to its absence (**Figure 5**).

ES for Induction of Central Apnea Semiology

Whereas ES is widely used for identification of functional cortex, ES can also be used to reproduce seizure signs and symptoms (Rasmussen and Penfield, 1947; Penfield and Perot, 1963; Borchers et al., 2012; Landazuri and Minotti, 2019). Identification of cortical areas involved in symptom production is important to understand the epileptogenic zone and seizure propagation networks. ICA has been recently identified as a semiological sign in temporal lobe epilepsies (Lacuey et al., 2019a), which is elicitable and may be of value in seizure analysis for presurgical assessments.

Historical Perspective

Previous evidence in animals suggests that respiratory arrest can be induced by ES of temporal pole, uncus, insula, rostral cingulate, and posterior orbitofrontal cortex (Bailey and Sweet, 1940; Smith, 1945; Kaada et al., 1949; Hoffman and Rasmussen, 1953). These studies found ES to predominantly affect the inspiratory phase (Smith, 1945; Delgado and Livingston, 1948; Kaada et al., 1949). Breathing arrest continued during the stimulation period, with resumption of normal breathing pattern once stimulation ceased. Simultaneous with apnea, other responses were variably recorded such as blood pressure and heart rate changes, decrease in gastric tone, and vocalization (Bailey and Sweet, 1940; Smith, 1945; Hoffman and Rasmussen, 1953). These studies were done under the effect of general anesthesia (Kaada et al., 1949).

Similar breathing responses were found in humans. In 1899, Hughlings Jackson described what he called uncinated fits, seizures whose semiology included respiratory arrest (Jackson, 1899). On stimulation of posterolateral orbital cortex and rostral cingulate in patients with psychiatric conditions undergoing intracranial procedures such as frontal lobotomies, scientists noted complete cessation or decrease in breathing lasting the stimulation period (Chapman et al., 1949; Pool and Ransohoff, 1949). Later, Penfield's group found better demarcation of

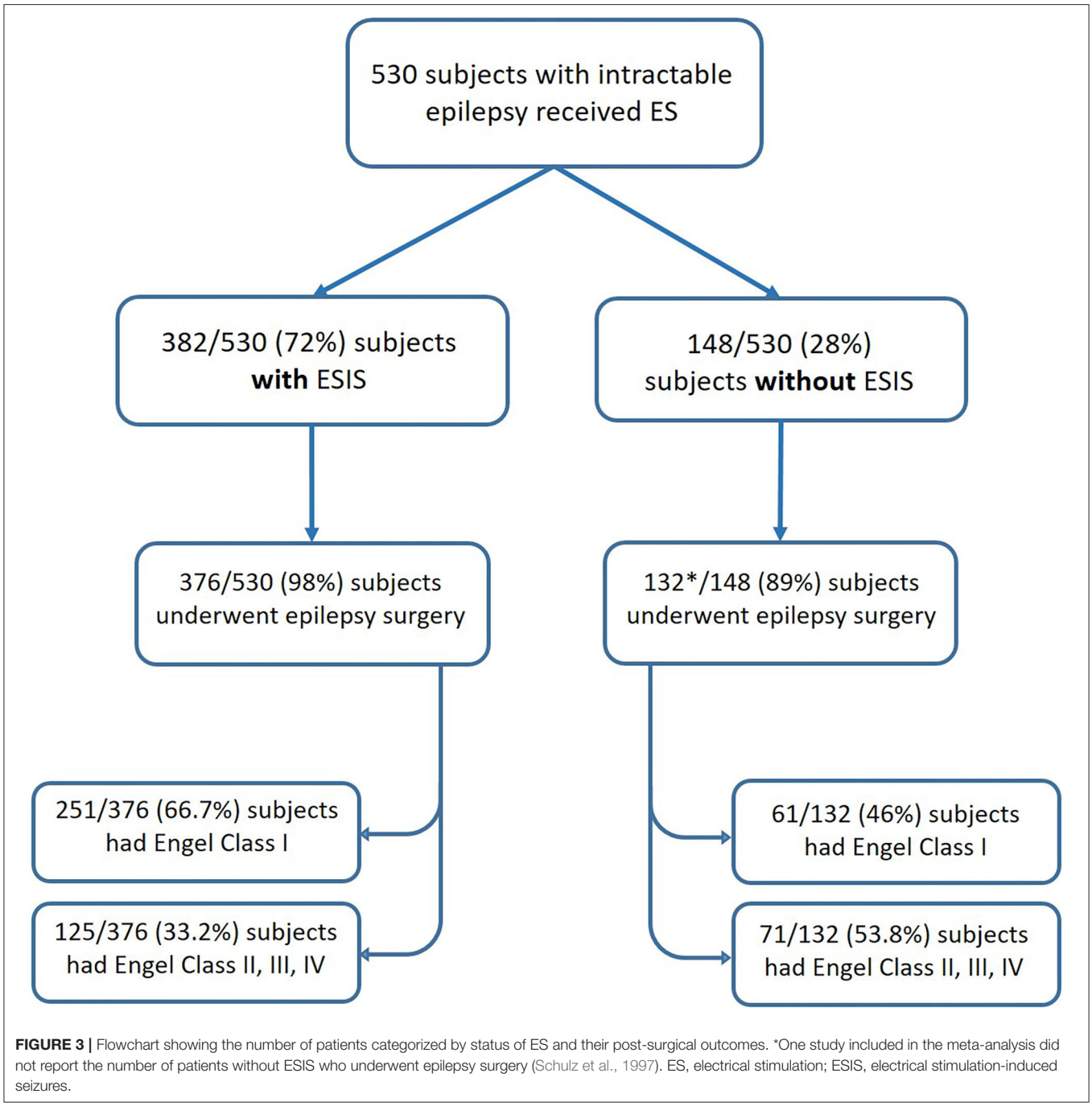

FIGURE 3 | Flowchart showing the number of patients categorized by status of ES and their post-surgical outcomes. *One study included in the meta-analysis did not report the number of patients without ESIS who underwent epilepsy surgery (Schulz et al., 1997). ES, electrical stimulation; ESIS, electrical stimulation-induced seizures.

regions, which, when stimulated in the conscious patient with local anesthesia, elicited arrest of breathing in the same regions as in monkeys (Kaada and Jasper, 1952). Specifically, this study found respiratory arrest with stimulation of the anterior hippocampal gyrus, temporal pole (medial and ventral), anterior insula, and anterior cingulate gyrus. Similarly to previous studies, respiratory arrest occurred with the chest assuming an expiratory position and was occasionally interrupted by a deep breath (Kaada and Jasper, 1952). Nelson and Ray reproduced these findings in one patient by stimulating the amygdala (Nelson and Ray, 1968). One caveat of these studies was likely imprecise localization of cortical areas stimulated, given the technical limitations of the period.

The Present of ES-Induced Central Apnea

In the last decade, the use of intracranial EEG studies with simultaneous multimodal polygraphy in the Epilepsy Monitoring Unit (EMU) has allowed for the investigation of important ictal and peri-ictal signs such as hypoxemia, central and obstructive apnea, laryngospasm, and hypercarbia (Kennedy and Seyal,

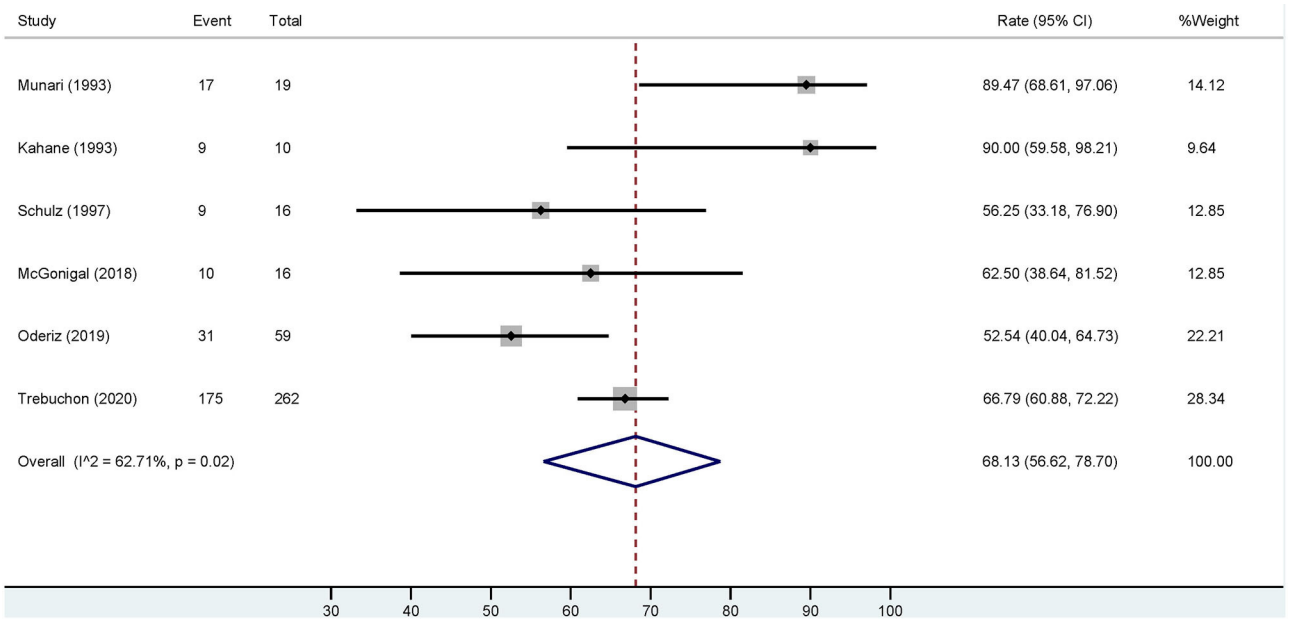

FIGURE 4 | Forest plot depicting the pooled estimate of favorable outcomes after epilepsy surgery in patients with ESIS. "Event" indicates the number of patients who had a favorable outcome and "Total" indicates the number of patients who had ESIS. Rates of favorable outcome for each study are seen to the right of the figure with their respective weights. The red dashed line indicates the pooled estimated favorable outcome value. The blue diamond indicates the pooled confidence interval. Each study is represented by a black line that indicates the confidence interval, a square that represents the weight of each study, and a dot indicating the rate of favorable outcome. The studies are heterogeneous as demonstrated by an I^2 value of 62.7%.

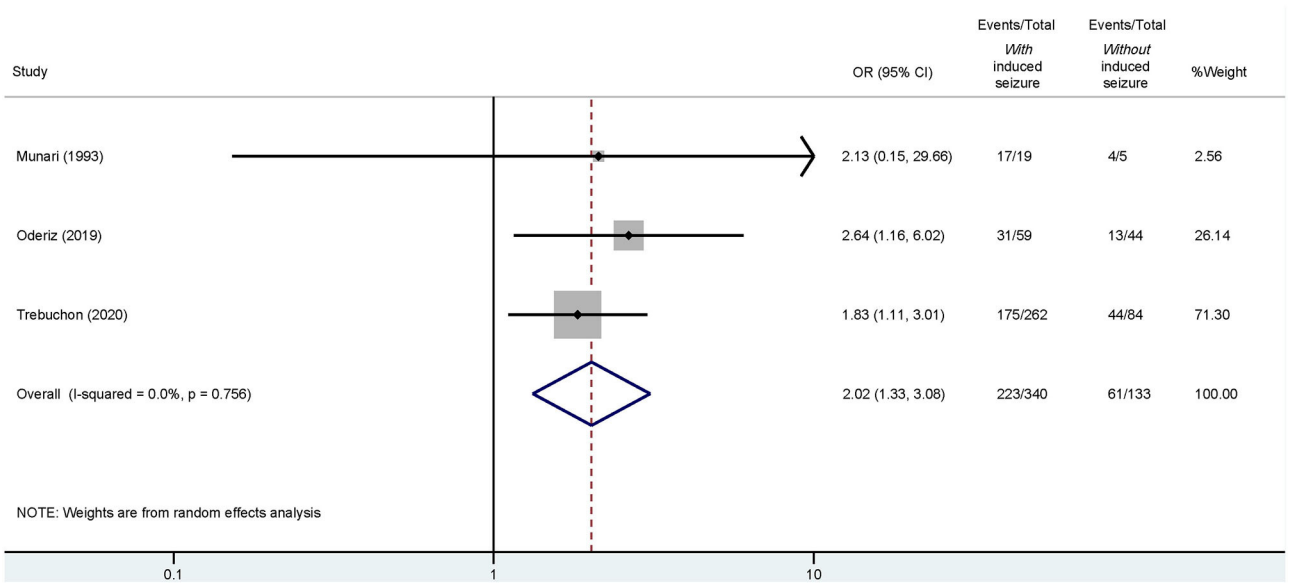

FIGURE 5 | Forest plot elucidating the association between ESIS and favorable outcome after epilepsy surgery. "Events/Total" reflects the number of patients with favorable outcome who underwent epilepsy surgery with or without ESIS over the total of patients with or without ESIS. Overall odds ratio (OR) is indicated by the red dashed line. The diamond indicates the pooled confidence interval. The black lines represent the confidence intervals of each study with the square depicting the weight of each study and the dot pointing at the OR of each study.

2015; Esmaeili et al., 2018; Lacuey et al., 2018a,b,c, 2019a; Murugesan et al., 2019; Vilella et al., 2019a,b; Allen et al., 2020). Pulse-oximetry, respiratory inductance plethysmography, nasal/oral thermistors and pressure transducers, capnography, and transcutaneous CO_2 sensors are available and provide valuable information for better understanding of breathing (Dlouhy et al., 2015). However, their use is not widespread and mainly used by SUDEP researchers.

Using ES of intracranial electrodes in patients admitted to EMU as a prelude to epilepsy surgery, several brain areas have been identified as regions where ES induces central apnea: amygdala, hippocampal head and body, anterior parahippocampal, and antero-mesial fusiform gyri (Dlouhy et al., 2015; Lacuey et al., 2017, 2019b; Nobis et al., 2018). These regions represent symptomatogenic anatomical substrates of ICA (Lacuey et al., 2019a). Contrary to studies in animals and historical stimulations in humans, with recent, anatomically precise SEEG guided stimulations, no breathing responses have been elicited from lateral temporal or orbitofrontal neocortex (Lacuey et al., 2017). As in animals, ICA occurs with the thorax adopting a resting position, allowing expiration to occur but not inspiration (Lacuey et al., 2019b). Apnea has been elicited in both hemispheres in all studies (Dlouhy et al., 2015; Lacuey et al., 2017, 2019b; Nobis et al., 2018). A minority of patients exhibit hypopnea during stimulation (Nobis et al., 2018). Interestingly, patients reported no symptoms during stimulation (apnea agnosia) and breathing cessation could be overridden if the patient was asked to voluntarily breathe (Lacuey et al., 2017; Nobis et al., 2018). Apneic responses also occurred during sleep (Nobis et al., 2018). At times, apnea lasted less than the stimulation period. In others, it continued after stimulation had stopped. Duration of apnea correlated with duration of stimulation (Lacuey et al., 2019b).

Parameters used for ES of breathing changes are similar to those used for cortical mapping (1, 5, 20, and 50 Hz frequencies; 0.2 pulse width; 2 to 40 s train duration; current intensity up to 10 mA; and 20 V) (Dlouhy et al., 2015; Lacuey et al., 2017, 2019b; Nobis et al., 2018). To monitor for breathing, researchers have simultaneously used inductance plethysmography to record chest and abdomen excursions, nasal thermistors to measure nasal airflow, capnographs for end tidal CO_2, or digital transcutaneous CO_2 sensors and electrocardiogram, along with EEG. One study also monitored beat-to-beat arterial blood pressure during stimulation sessions using continuous noninvasive arterial pressure monitoring (Lacuey et al., 2019b). The higher the stimulus current and the longer the stimulation, the greater the duration of ICA (Lacuey et al., 2019b). Frequency of stimulation affects apnea latency with low frequencies (1 Hz) provoking delayed apnea (apnea began 1–2 breaths after stimulation onset) and high frequency (50 Hz) inducing immediate breathing arrest (Lacuey et al., 2019b).

Of note, the definition of ICA has varied between studies. These include one (Vilella et al., 2019a) or two involuntary missed breaths (Lacuey et al., 2017), and an abrupt drop in peak signal excursion by >90% of pre-event baseline, cessation of breathing lasting for at least 6 or ≥10 s (Lacuey et al., 2018c, 2019a,b), or respiratory arrest for the duration of the ES (Nobis et al., 2018).

ICA as a Semiological Phenomenon

Studies indicate that ICA is a semiological phenomenon, hypothesized to arise from seizure activity in symptomatogenic brain regions, including mesial temporal structures (Lacuey et al., 2017; Vilella et al., 2019a). Recent investigations have shown that ictal activity that spreads to the amygdala elicits ICA (Nobis et al., 2020; Rhone et al., 2020). This finding supports previous observations that report that ICA preceded surface electroencephalographic onset of temporal lobe seizures, representing the first sign in 69% and occasionally the only clinical seizure manifestation (in 16% of the seizures) (Nadkarni et al., 2012; Lacuey et al., 2019a). ICA is associated with significant oxygen desaturation, especially if prolonged, and with longer EEG recovery duration (time from EEG seizure end to continuous slow generalized EEG activity) (Lacuey et al., 2018c, 2019a; Vilella et al., 2019a). ICA occurs in 36.5–44% of focal onset seizures, with a higher incidence (68.7%) in mesial temporal lobe compared to extratemporal epilepsy (OR: 10.1, 95% CI: 5.5–18.5; $p = 0.001$) (Bateman et al., 2008; Lacuey et al., 2018c, 2019a; Vilella et al., 2019a). It is exclusive to focal epilepsy (Lacuey et al., 2018c). As such, ICA as an isolated sign may indicate a mesial temporal lobe epilepsy and potentially be used as a localizing sign in presurgical epilepsy evaluation (Lacuey et al., 2018c, 2019a).

DISCUSSION

ESIS: The Seizure Onset Zone

The present systematic review of literature addresses ESIS as a technique to identify the seizure onset zone and improve outcome in epilepsy surgery. Our meta-analysis demonstrated that ESIS is associated to a greater likelihood of favorable surgical outcomes and can be used to adequately determine the seizure onset zone. We found that the definition of ESIS is heterogeneous and that ES parameters vary from study to study.

In our meta-analysis, patients with ESIS were twice as likely to have favorable outcome compared to those without ESIS. Contrary to previous studies showing discrepancies in apparent benefit in postsurgical outcomes (Kovac et al., 2016), our meta-analysis shows that ESIS are associated with favorable outcome (Engel I) after epilepsy surgery. Our meta-analysis, based on heterogeneous studies with a reasonably low/intermediate risk of bias, allows us to conclude that it may be a valuable aid to epilepsy surgery resection planning. We confirmed this even after excluding the study with the highest event rate of a favorable outcome.

Literature indicates that ES for seizure induction is a technique predominantly practiced in Europe, and less used in North America despite it being a technique employed for more than five decades. The difference in practice between countries may be explained by history and traditions. Europe has been greatly influenced by Bancaud and Tailarach's work in which induction of seizures was part of routine invasive study and helped define the epileptogenic zone (Kovac et al., 2016). On the other hand, North America follows Penfield's influence who emphasized in using ES in the operating room for eliciting afterdischarges and seizures to identify the seizure focus (Jasper, 1954). Although Penfield advocated for the use of ESIS, this practice did not become widespread in countries like the United States.

Strikingly, definition of a reliable ESIS varies greatly between studies. All authors agree in that ESIS must reproduce symptoms and signs of habitual seizures that the patient or a witness has described. Some authors take into account the electroclinical correlation of the events (Bernier et al., 1990; Bank et al., 2014; Cuello Oderiz et al., 2019); some only mention a clinical

definition (Kahane et al., 1993; Munari et al., 1993; Schulz et al., 1997; Trebuchon et al., 2021). This variability affects reproducibility and homogeneity of investigational conclusions. In addition, definitions using exclusively clinical features could potentially erroneously localize symptomatogenic zones instead of seizure onset zone (Velez-Ruiz, 2019). For these reasons, we concluded that a unified definition of reliable ESIS should be stated and used in future research. Having a unified definition will decrease difficulties that arise when comparing studies, allow for better reproducibility of results, and increase external validity of present and future research. In this regard, Cuello Oderiz et al.'s definition is comprehensive and applicable where a typical ESIS is "a seizure with clinical semiology resembling spontaneous seizure or aura and required to have electrographic changes with clear spatial and temporal evolution" (Cuello Oderiz et al., 2019). Additionally, if spontaneous seizures have been previously captured during invasive evaluation, electrographic similarity between spontaneous and induced seizures is essential.

Both low- and high-frequency ES have been employed in the studies reviewed. Induction of ESIS occurs in 51.6–75.3% of stimulated patients (Schulz et al., 1997; Cuello Oderiz et al., 2019; Trebuchon et al., 2021). Although high-frequency stimulation appears more effective in inducing seizures, it is also associated with greater frequency of adverse effects and false positives (Munari et al., 1993). False positives should be recognized as clinical events that are not acknowledged by the patient as typical, nor they have been observed spontaneously before in that patient, and they are not related to the anatomical site of ES (Munari et al., 1993). ES should be performed with the patient fully medicated so as to avoid induction of atypical seizures (Engel and Crandall, 1983; Cuello Oderiz et al., 2019). For these reasons, and since 50-Hz stimulation artifact obscures electrographic seizure onset, in our center, stimulation is started at 1 Hz and, if no seizures are elicited after increasing current intensity progressively, frequency parameters are progressively increased to 5, 20, and 50 Hz sequentially. Of note, the mesial temporal lobe is sensitive to low-frequency stimulation, and high-frequency stimulation is prone to inducing unwanted generalized convulsive seizures (Munari et al., 1993).

Comparison between ESIS and spontaneous seizures regarding epilepsy surgery and its outcome has been undertaken (Cuello Oderiz et al., 2019) and suggests that ESIS may potentially replace spontaneous seizures during presurgical invasive evaluation (Cuello Oderiz et al., 2019). Further attempts have been made to determine comparability of ESIS to spontaneous seizures. Spilioti et al. reported their experience with induced seizures during ES when mapping eloquent cortex (Spilioti et al., 2020). They elicited seizures in 23.4% of patients, of whom 55.9% where typical (similar to spontaneous seizures) and 41% were atypical. In 73.7% of the patients, the contacts involved in ESIS were fully concordant with the contacts involved in spontaneous seizures registered *a priori* (Spilioti et al., 2020). This suggests that ESIS may be a surrogate for spontaneous seizures during intracranial EEG. This approach may reduce the time needed for invasive EEG and may spare the need for decreasing anti-seizure medication since ES is performed under the effect of the patient's habitual treatment. However, the concordance between ESIS and spontaneous seizures needs further research. Of the studies included in the systematic review, none addressed this subject in a systematic manner.

Since the majority of studies assessed in this systematic review are retrospective, there is an urgent need for prospective randomized control trials that further elucidate the value of ESIS, making further comparisons with spontaneous seizures and providing additional information regarding effective, adverse event-free stimulation parameters.

ESIS Signs and Symptoms: Central Apnea and the Symptomatogenic Zone

Mesial temporal structures have not routinely stimulated for functional mapping since traditionally teaching holds these structures to be "silent" to ES (Spilioti et al., 2020). However, we find recent evidence to suggest that with appropriate multi-modal monitoring, these structures are highly symptomatogenic in both spontaneous seizures and ES, thus opening up a whole new aspect to epilepsy surgery assessments. From ES studies in animals and humans, we know that mesial temporal structures have a modulatory effect on breathing (Bailey and Sweet, 1940; Kaada et al., 1949; Kaada and Jasper, 1952; Dlouhy et al., 2015; Nobis et al., 2018; Lacuey et al., 2019b; Rhone et al., 2020). The mechanism underlying ICA is due to seizure discharge induced impairment of involuntary, suprapontine (amygdalohippocampal) breathing control through disruption of brainstem-driven inspiration (Lacuey et al., 2018c). Of the several limbic and paralimbic structures identified, amygdala influences appear most consistent. Connections of the amygdala, especially its mesial and basal regions, with brainstem respiratory nuclei allow for better understanding of breathing disruption during seizures that involve this structure, but also links amygdala and temporal mesial structures to SUDEP pathophysiology (Manolis et al., 2019). Apnea agnosia is an intriguing aspect and may reflect seizure-induced inhibitory influences that prevent chemosensitivity-driven apnea awareness. It also explains why apnea has gone unrecognized in epilepsy semiological analysis for so long. With increasing use of multimodal cardio-respiratory polygraphy, this is likely to change.

From the studies analyzed, we find that ES-induced ICA/hypopnea is an understudied but a potentially valuable localizing sign for epilepsy surgery implantation and/or resection. Central apnea is a likely result of seizure activity (ICA) and may be reproduced by ES of the mesial temporal structures, especially amygdala. One of the pillars of successful epilepsy surgery and resection hypotheses includes detailed understanding of the symptomatogenic zone with which to plan a surgery. Our review of the recent literature allows us to conclude that ES-induced ICA is a relevant sign when localizing the symptomatogenic zone for epilepsy surgery. In seizure semiology chronology, ICA appearance may be the first and at times only semiological phenomenon. This potentially allows delineation of the patient's symptomatogenic and ictal onset zones and, consequently, the putative epileptogenic zone (Lacuey et al., 2019a). Any planned SEEG exploration then must include

the brain areas known to generate ICA, including amygdala, hippocampus, anterior parahippocampal, and antero-mesial fusiform gyri. Therefore, since ICA is a reliable sign of mesial temporal lobe seizures, efforts to record breathing disturbances in the epilepsy monitoring unit should be made, with systematic monitoring using respiratory belts. Where ICA is a later semiological component in the patient's seizure chronology, implantation of the same substrate structures may still throw light on seizure spread and spread pathways.

Limitations

Our study has several limitations. Firstly, the number of studies in literature that have addressed ESIS is limited. We found only 14 studies, of variable quality, and of those, less than half could be included in the meta-analysis. In addition, studies are heterogeneous and definitions, stimulation parameters, and outcomes vary from study to study. We did not find any randomized controlled study from which to draw high-quality information. The studies pooled in the meta-analysis were of intermediate quality, and this allowed us to draw some conclusions that have been presented.

CONCLUSIONS

ESIS constitute a reliable technique to delineate the epileptogenic zone and provide distinct and complementary information to guide epilepsy surgery. Prospective research addressing ESIS is urgently needed, with special emphasis on efficacy and safety using the definition proposed in this review. This will provide the necessary evidence base, protocols, and guidelines for usage of this important aspect of patient assessment. ES of brain structures (amygdala, hippocampal head and body, anterior parahippocampal, and antero-mesial fusiform gyri) reliably demonstrated to produce central apnea suggests that these brain regions likely generate ICA. Therefore, when ICA is a seizure semiology component, these areas should be included in the surgical hypothesis, and SEEG exploration strategy if this is planned. ICA is particularly valuable if it is the first or only semiological sign, but because of apnea agnosia, this sign can only be identified if appropriate respiratory monitoring is employed in the EMU.

DATA AVAILABILITY STATEMENT

The original contributions presented in the study are included in the article/**Supplementary Material**, further inquiries can be directed to the corresponding author.

AUTHOR CONTRIBUTIONS

SL conceived the presented idea. MO-U, NL, and SL completed the systematic review. MD and BS performed the meta-analysis and did the figures. MO-U wrote the manuscript with support from NL, SL, and NT. All authors contributed to the article and approved the submitted version.

ACKNOWLEDGMENTS

We thank Travis F. Holder, librarian, for his help in the search of the literature.

SUPPLEMENTARY MATERIAL

The Supplementary Material for this article can be found online at: https://www.frontiersin.org/articles/10.3389/fnhum.2020.617061/full#supplementary-material

REFERENCES

Allen, L. A., Harper, R. M., Vos, S. B., Scott, C. A., Lacuey, N., Vilella, L., et al. (2020). Peri-ictal hypoxia is related to extent of regional brain volume loss accompanying generalized tonic-clonic seizures. *Epilepsia* 61, 1570–1580. doi: 10.1111/epi.16615

Bailey, P., and Sweet, W. H. (1940). Effects on respiration, blood pressure and gastric motility of stimulation of orbital surface of frontal lobe. *J. Neurophysiol.* 3, 276–281. doi: 10.1152/jn.1940.3.3.276

Bancaud, J., Talairach, J., and Morel, P. (1974). "Generalized" epileptic seizures elicited by electrical stimulation of the frontal lobe in man. *Electroencephalogr. Clin. Neurophysiol.* 37, 275–282. doi: 10.1016/0013-4694(74)90031-5

Bank, A. M., Schevon, C. A., and Hamberger, M. J. (2014). Characteristics and clinical impact of stimulation-evoked seizures during extraoperative cortical mapping. *Epilepsy Behav.* 34, 6–8. doi: 10.1016/j.yebeh.2014.03.004

Bateman, L. M., Li, C.-S., and Seyal, M. (2008). Ictal hypoxemia in localization-related epilepsy: analysis of incidence, severity and risk factors. *Brain* 131, 3239–3245. doi: 10.1093/brain/awn277

Bernier, G. P., Richer, F., Giard, N., Bouvier, G., Mercier, M., Turmel, A., et al. (1990). Electrical stimulation of the human brain in epilepsy. *Epilepsia* 31, 513–520. doi: 10.1111/j.1528-1157.1990.tb06099.x

Borchers, S., Himmelbach, M., Logothetis, N., and Karnath, H. O. (2012). Direct electrical stimulation of human cortex-the gold standard for mapping brain functions? *Nat. Rev. Neurosci.* 13, 63–70. doi: 10.1038/nrn3140

Chapman, W. P., Livingston, R. B., and Livingston, K. E. (1949). Frontal lobotomy and electrical stimulation of the orbital surface of frontal lobes. *Arch. Neurol. Psychiatry* 62:701. doi: 10.1001/archneurpsyc.1949.02310180002001

Chassoux, F., Devaux, B., Landre, E., Turak, B., Nataf, F., Varlet, P., et al. (2000). Stereoelectroencephalography in focal cortical dysplasia: a 3D approach to delineating the dysplastic cortex. *Brain* 123, 1733–1751. doi: 10.1093/brain/123.8.1733

Chauvel, P., Landre, E., Trottier, S., Vignel, J. P., Biraben, A., Devaux, B., et al. (1993). Electrical stimulation with intracerebral electrodes to evoke seizures. *Adv. Neurol.* 63, 115–121.

Cuello Oderiz, C., Von Ellenrieder, N., Dubeau, F., Eisenberg, A., Gotman, J., Hall, J., et al. (2019). Association of cortical stimulation-induced seizure with surgical outcome in patients with focal drug-resistant epilepsy. *JAMA Neurol.* 76, 1070–1078. doi: 10.1001/jamaneurol.2019.1464

Delgado, J. M. R., and Livingston, R. B. (1948). Some respiratory, vascular and thermal responses to stimulation of orbital surface of frontal lobe. *J. Neurophysiol.* 11, 39–55. doi: 10.1152/jn.1948.11.1.39

DeSalles, A., Swartz, B. E., Lee, T. T., and Delgado-Escueta, A. V. (1994). Subdural recording and electrical stimulation for cortical mapping and induction of usual seizures. *Proc. og XIth Meet. World Soc. Stereotact. Funct. Neurosurg.* 62, 226–231. doi: 10.1159/000098624

Dlouhy, B. J., Gehlbach, B. K., Kreple, C. J., Kawasaki, H., Oya, H., Buzza, C., et al. (2015). Breathing inhibited when seizures spread to the amygdala and upon amygdala stimulation. *J. Neurosci.* 35, 10281–10289. doi: 10.1523/JNEUROSCI.0888-15.2015

Engel, J., and Crandall, P. H. (1983). Falsely localizing ictal onsets with depth EEG telemetry during anticonvulsant withdrawal. *Epilepsia* 24, 344–355. doi: 10.1111/j.1528-1157.1983.tb04898.x

Esmaeili, B., Kaffashi, F., Theeranaew, W., Dabir, A., Lhatoo, S. D., and Loparo, K. A. (2018). Post-ictal modulation of baroreflex sensitivity in patients with intractable epilepsy. *Front. Neurol.* 9:793. doi: 10.3389/fneur.2018.00793

Halgren, E., Walter, R. D., Cherlow, D. G., and Crandall, P. H. (1978). Mental phenomena evoked by electrical stimulation of the human hippocampal formation and amygdala. *Brain* 101, 83–117. doi: 10.1093/brain/101.1.83

Higgins, J. P. T., Altman, D. G., Gotzsche, P. C., Juni, P., Moher, D., Oxman, A. D., et al. (2011). The Cochrane Collaboration's tool for assessing risk of bias in randomised trials. *BMJ* 343:d5928. doi: 10.1136/bmj.d5928

Hoffman, B. L., and Rasmussen, T. (1953). Stimulation studies of insular cortex of macaca mulatta. *J. Neurophysiol.* 16, 343–351. doi: 10.1152/jn.1953.16.4.343

Jackson, J. H. (1899). On asphyxia in slight epileptic paroxysms. *Lancet* 1, 79–80. doi: 10.1016/S0140-6736(01)79095-2

Jasper, H. (1954). "Electrocorticography," in *Epilepsy and the Functional Anatomy of the Human Brain*, eds W. Penfield, and H. Jasper (Boston, MA: American Academy of Neurology), 692–738.

Jobst, B. C., Bartolomei, F., Diehl, B., Frauscher, B., Kahane, P., Minotti, L., et al. (2020). Intracranial EEG in the 21st Century. *Epilepsy Curr.* 20, 180–188. doi: 10.1177/1535759720934852

Kaada, B., and Jasper, H. (1952). Respiratory responses to stimulation of the temporal pole, insula, and hippocampal and limbic gyri in man. *Arch. Neurol. Psychiatry* 68, 609–619. doi: 10.1001/archneurpsyc.1952.02320230035004

Kaada, B. R., Pribram, K. H., and Epstein, J. A. (1949). Respiratory and vascular responses in monkeys from temporal pole, insula, orbital surface and cingulate gyrus: a preliminary report. *J. Neurophysiol.* 12, 347–356. doi: 10.1152/jn.1949.12.5.347

Kahane, P., Tassi, L., Francione, S., Hoffmann, D., Lo Russo, G., and Munari, C. (1993). Manifestations électrocliniques induites par la stimulation électrique intracérébrale par ≪chocs dans les épilepsies temporales. *Neurophysiol. Clin./Clin. Neurophysiol.* 23, 305–326. doi: 10.1016/S0987-7053(05)80123-6

Kennedy, J. D., and Seyal, M. (2015). Respiratory pathophysiology with seizures and implications for sudden unexpected death in epilepsy. *J. Clin. Neurophysiol.* 32, 10–13. doi: 10.1097/WNP.0000000000000142

Kovac, S., Kahane, P., and Diehl, B. (2016). Seizures induced by direct electrical cortical stimulation - mechanisms and clinical considerations. *Clin. Neurophysiol.* 127, 31–39. doi: 10.1016/j.clinph.2014.12.009

Lacuey, N., Hampson, J. P., Harper, R. M., Miller, J. P., and Lhatoo, S. (2019b). Limbic and paralimbic structures driving ictal central apnea. *Neurology* 92, e655–e669. doi: 10.1212/WNL.0000000000006920

Lacuey, N., Hampson, J. P., Theeranaew, W., Zonjy, B., Vithala, A., Hupp, N. J., et al. (2018b). Cortical structures associated with human blood pressure control. *JAMA Neurol.* 75, 194–202. doi: 10.1001/jamaneurol.2017.3344

Lacuey, N., Hupp, N. J., Hampson, J., and Lhatoo, S. (2019a). Ictal Central Apnea (ICA) may be a useful semiological sign in invasive epilepsy surgery evaluations. *Epilepsy Res.* 156:106164. doi: 10.1016/j.eplepsyres.2019.106164

Lacuey, N., Vilella, L., Hampson, J. P., Sahadevan, J., and Lhatoo, S. D. (2018a). Ictal laryngospasm monitored by video-EEG and polygraphy: a potential SUDEP mechanism. *Epileptic Disord.* 20, 146–150. doi: 10.1684/epd.2018.0964

Lacuey, N., Zonjy, B., Hampson, J. P., Rani, M. R. S., Zaremba, A., Sainju, R. K., et al. (2018c). The incidence and significance of periictal apnea in epileptic seizures. *Epilepsia* 59, 573–582. doi: 10.1111/epi.14006

Lacuey, N., Zonjy, B., Londono, L., and Lhatoo, S. D. (2017). Amygdala and hippocampus are symptomatogenic zones for central apneic seizures. *Neurology* 88, 701–705. doi: 10.1212/WNL.0000000000003613

Landazuri, P., and Minotti, L. (2019). "Electrical stimulation for mapping of the epileptogenic zone," in *Invasive Studies of the Human Epileptic Brain Principles and Practice*, eds S. D. Lhatoo, P. Kahane, and H. O. Luders (Oxford: Oxford University Press), 161–172. doi: 10.1093/med/9780198714668.003.0013

Liberati, A., Altman, D. G., Tetzlaff, J., Mulrow, C., Gotzsche, P. C., Ioannidis, J. P. A., et al. (2009). The PRISMA statement for reporting systematic reviews and meta-analyses of studies that evaluate healthcare interventions: explanation and elaboration. *BMJ* 339:b2700. doi: 10.1136/bmj.b2700

Manolis, T. A., Manolis, A. A., Melita, H., and Manolis, A. S. (2019). Sudden unexpected death in epilepsy: the neuro-cardio-respiratory connection. *Seizure* 64, 65–73. doi: 10.1016/j.seizure.2018.12.007

McGonigal, A., Lagarde, S., Trébuchon-Dafonseca, A., Roehri, N., and Bartolomei, F. (2018). Early onset motor semiology in seizures triggered by cortical stimulation during SEEG. *Epilepsy Behav.* 88, 262–267. doi: 10.1016/j.yebeh.2018.09.017

Moher, D., Liberati, A., Tetzlaff, J., and Altman, D. G. (2009). Preferred reporting items for systematic reviews and meta-analyses: the PRISMA statement. *BMJ* 339:b2535. doi: 10.1136/bmj.b2535

Munari, C., Kahane, P., Tassi, L., Francione, S., Hoffmann, D., Lo Russo, G., et al. (1993). Intracerebral low frequency electrical stimulation: a new tool for the definition of the "epileptogenic area"? *Acta Neurochirurgica* 58, 181–185. doi: 10.1007/978-3-7091-9297-9_42

Murad, M. H., Sultan, S., Haffar, S., and Bazerbachi, F. (2018). Methodological quality and synthesis of case series and case reports. *Evid. Based Med.* 23, 60–63. doi: 10.1136/bmjebm-2017-110853

Murugesan, A., Rani, M. R. S., Vilella, L., Lacuey, N., Hampson, J. P., Faingold, C. L., et al. (2019). Postictal serotonin levels are associated with peri-ictal apnea. *Neurology* 93, e1485–e1494. doi: 10.1212/WNL.0000000000008244

Nadkarni, M. A., Friedman, D., and Devinsky, O. (2012). Central apnea at complex partial seizure onset. *Seizure* 21, 555–558. doi: 10.1016/j.seizure.2012.04.001

Nelson, D. A., and Ray, C. D. (1968). Respiratory arrest from seizure discharges in limbic system. *Arch. Neurol.* 19:199. doi: 10.1001/archneur.1968.00480020085008

Nobis, W. P., González Otárula, K. A., Templer, J. W., Gerard, E. E., VanHaerents, S., Lane, G., et al. (2020). The effect of seizure spread to the amygdala on respiration and onset of ictal central apnea. *J. Neurosurg.* 132, 1313–1323. doi: 10.3171/2019.1.JNS183157

Nobis, W. P., Schuele, S., Templer, J. W., Zhou, G., Lane, G., Rosenow, J. M., et al. (2018). Amygdala-stimulation-induced apnea is attention and nasal-breathing dependent. *Ann. Neurol.* 83, 460–471. doi: 10.1002/ana.25178

Ouzzani, M., Hammady, H., Fedorowicz, Z., and Elmagarmid, A. (2016). Rayyan—a web and mobile app for systematic reviews. *Syst. Rev.* 5:210. doi: 10.1186/s13643-016-0384-4

Penfield, W., and Perot, P. (1963). The brain's record of auditory and visual experience. *Brain* 86, 595–696. doi: 10.1093/brain/86.4.595

Pool, J. L., and Ransohoff, J. (1949). Autonomic effects on stimulating rostral portion of cingulate gyri in man. *J. Neurophysiol.* 12, 385–392. doi: 10.1152/jn.1949.12.6.385

Rasmussen, T., and Penfield, W. (1947). The human sensorimotor cortex as studied by electrical stimulation. *Fed. Proc.* 6:184.

Rhone, A. E., Kovach, C. K., Harmata, G. I. S., Sullivan, A. W., Tranel, D., Ciliberto, M. A., et al. (2020). A human amygdala site that inhibits respiration and elicits apnea in pediatric epilepsy. *JCI Insight* 5:134852. doi: 10.1172/jci.insight.134852

Rosenow, F., and Lüders, H. (2001). Presurgical evaluation of epilepsy. *Brain* 124, 1683–1700. doi: 10.1093/brain/124.9.1683

Schulz, R., Lüders, H. O., Tuxhorn, I., Ebner, A., Holthausen, H., Hoppe, M., et al. (1997). Localization of epileptic auras induced on stimulation by subdural electrodes. *Epilepsia* 38, 1321–1329. doi: 10.1111/j.1528-1157.1997.tb00070.x

Smith, W. K. (1945). The functional significance od the rostral cingular cortex as revealed by its responses to electrical excitation. *J. Neurophysiol.* 8, 241–255. doi: 10.1152/jn.1945.8.4.241

So, E. L., and Alwaki, A. (2018). A guide for cortical electrical stimulation mapping. *J. Clin. Neurophysiol.* 35, 98–105. doi: 10.1097/WNP.0000000000000435

Spilioti, M., Winston, J. S., Centeno, M., Scott, C., Chowdhury, F., and Diehl, B. (2020). The nature, frequency and value of stimulation induced seizures during extraoperative cortical stimulation for functional mapping. *Seizure* 81, 71–75. doi: 10.1016/j.seizure.2020.07.027

Trébuchon, A., and Chauvel, P. (2016). Electrical stimulation for seizure induction and functional mapping in stereoelectroencephalography. *J. Clin. Neurophysiol.* 33, 511–521. doi: 10.1097/WNP.0000000000000313

Trebuchon, A., Racila, R., Cardinale, F., Lagarde, S., McGonigal, A., Lo Russo, G., et al. (2021). Electrical stimulation for seizure induction during SEEG exploration: a useful predictor of postoperative seizure recurrence? *J. Neurol. Neurosurg. Psychiatry*. 92, 22–26. doi: 10.1136/jnnp-2019-322469

Velez-Ruiz, N. (2019). Is spontaneity overrated? the value of cortical stimulation–induced seizures. *Epilepsy Curr.* 19, 376–378. doi: 10.1177/1535759719878201

Vilella, L., Lacuey, N., Hampson, J. P., Rani, M. R. S., Loparo, K., Sainju, R. K., et al. (2019a). Incidence, recurrence, and risk factors for peri-ictal central apnea and sudden unexpected death in epilepsy. *Front. Neurol.* 10:166. doi: 10.3389/fneur.2019.00166

Vilella, L., Lacuey, N., Hampson, J. P., Rani, M. R. S., Sainju, R. K., Friedman, D., et al. (2019b). Postconvulsive central apnea as a biomarker for sudden unexpected death in epilepsy (SUDEP). *Neurology* 92, E171–E182. doi: 10.1212/WNL.0000000000006785

Wieser, H. G., Bancaud, J., Talairach, J., Bonis, A., and Szikla, G. (1979). Comparative value of spontaneous and chemically and electrically induced seizures in establishing the lateralization of temporal lobe seizures. *Epilepsia* 20, 47–59. doi: 10.1111/j.1528-1157.1979.tb04775.x

Conflict of Interest: The authors declare that the research was conducted in the absence of any commercial or financial relationships that could be construed as a potential conflict of interest.

frontiers in Human Neuroscience

BRIEF RESEARCH REPORT
published: 22 January 2021
doi: 10.3389/fnhum.2020.609188

Attention, Not Performance, Correlates With Afterdischarge Termination During Cortical Stimulation

Ronald P. Lesser[1,2]*, *W. R. S. Webber*[1], *Diana L. Miglioretti*[3,4], *Yuko Mizuno-Matsumoto*[5], *Ayumi Muramatsu*[5] *and Yusuke Yamamoto*[5]

[1] Departments of Neurology, Johns Hopkins University School of Medicine, Baltimore, MD, United States, [2] Neurological Surgery, Johns Hopkins University School of Medicine, Baltimore, MD, United States, [3] Department of Public Health Sciences, School of Medicine, University of California, Davis, Davis, CA, United States, [4] Kaiser Permanente Washington Health Research Institute, Seattle, WA, United States, [5] Graduate School of Applied Informatics, University of Hyogo, Kobe, Japan

OPEN ACCESS

Edited by:
Riki Matsumoto,
Kobe University, Japan

Reviewed by:
Eishi Asano,
Children's Hospital of Michigan, United States
Arun Singh,
University of South Dakota, United States
Katsuya Kobayashi,
Kyoto University, Japan

***Correspondence:**
Ronald P. Lesser
rl@jhmi.edu

Specialty section:
This article was submitted to Brain Imaging and Stimulation, a section of the journal Frontiers in Human Neuroscience

Received: 22 September 2020
Accepted: 16 November 2020
Published: 22 January 2021

Citation:
Lesser RP, Webber WRS, Miglioretti DL, Mizuno-Matsumoto Y, Muramatsu A and Yamamoto Y (2021) Attention, Not Performance, Correlates With Afterdischarge Termination During Cortical Stimulation. Front. Hum. Neurosci. 14:609188. doi: 10.3389/fnhum.2020.609188

Cortical stimulation has been used for brain mapping for over a century, and a standard assumption is that stimulation interferes with task execution due to local effects at the stimulation site. Stimulation can however produce afterdischarges which interfere with functional localization and can lead to unwanted seizures. We previously showed that (a) cognitive effort can terminate these afterdischarges, (b) when termination thus occurs, there are electrocorticography changes throughout the cortex, not just at sites with afterdischarges or sites thought functionally important for the cognitive task used, and (c) thresholds for afterdischarges and functional responses can change among stimulation trials. We here show that afterdischarge termination can occur prior to overt performance of the cognitive tasks used to terminate them. These findings, taken together, demonstrate that task-related brain changes are not limited to one or a group of functional regions or a specific network, and not limited to the time directly surrounding overt task execution. Discrete locations, networks and times importantly underpin clinical behaviors. However, brain activity that is diffuse in location and extended in time also affect task execution and can affect brain mapping. This may in part reflect fluctuating levels of attention, engagement, or motivation during testing.

Keywords: cortical stimulation, brain mapping, afterdischarges, attention, cognition

INTRODUCTION

Electrical stimulation has been a standard method for mapping brain areas important for motor, sensory, language, and other functions. This is done by delivering trains of electrical pulses to the brain over a period of several seconds. During that time, the patient and testing personnel determine if there are spontaneous changes in sensation, movement, or behavior, or if there is an altered or arrested activity while the patient performs a task (Lesser et al., 1994). However, stimulation can produce afterdischarges (ADs), epileptiform activity occurring after stimulation. These can interfere with mapping and can produce unwanted seizures.

When clinical stimulation produces ADs, additional briefer stimulation pulses can, at times, terminate the epileptiform activity, but this is only successful about half the time (Lesser et al., 1999). When ADs continue, cognitive effort can at times terminate the ADs, with this accompanied by both local (Muldoon et al., 2018) and diffuse (Lesser et al., 2019) electrophysiologic changes in the EEG. Unanswered is what aspect of the cognitive task might better correlate with success in aborting ADs.

Assessing responses to a mental task has at least two components. One is the presentation of the task by testing personnel. Another is the overt task performance by the patient or subject. In this report, we show that afterdischarge termination due to a cognitive task correlates better with presentation than with performance.

MATERIALS AND METHODS

We present results from 15 patients who had electrodes implanted for assistance in localizing the regions of onset of their medically intractable seizures. These were primarily subdural electrodes placed on the cortical surface, although some depth electrodes were used to help in recording below the cortical surface, primarily in the region of lesions noted on neuroimaging. Electrode placement, brain stimulation, the cognitive testing used to localize brain functions, and the cognitive activation used in attempts to terminate ADs all were determined by clinical needs alone. Our institutional review board approved our analysis of the recordings and testing.

Details regarding the patients and the testing have been reported previously (Lesser et al., 2019). The following is a summary.

Patients were 12–53 years old at the time of testing, seven males and eight females. Their seizures were not precipitated by mental activation. Testing occurred in the patient's hospital room with the patient supine and with the head of the bed elevated. Patients lay quietly while stimulation parameters at a given site were adjusted (see below and **Supplementary Video**).

Electrocorticography (ECoG) was recorded from a total of 1,276 platinum electrodes, with 56–109 per patient. Subdural electrodes were discs with 2.3-mm diameter exposed to the cortical surface, and with 10-mm distance between electrode centers. Depth electrodes were 1.1 mm in diameter, with 0.081 cm^2 surface area, and with 5- or 10-mm spacing (Ad-Tech Medical Instruments Corporation, Oak Creek, Wisconsin 53154, USA.) Electrode positions were verified by direct observation in the operating room, by co-registration of pre-implant 1–1.8 mm coronal slice volumetric MRI studies with post-implant 1-mm axial slice CT scans, and by brain surface renderings based on the co-registered imaging.

Continuous electrocorticography (ECoG) was obtained using Stellate Harmonie Systems (Natus Medical Incorporated, Pleasanton, CA 94566, USA) that could record at 1,000 samples per second per channel, for up to 128 channels. The amplifiers were Schwarzer EEG Amplifiers Model 210033 (Natus Europe GmbH, Robert-Koch-Str. 1, Planegg, Germany). High- and low-pass filters were set to 0.0016 and 300 Hz, respectively. Other details of the recording system are in our previous report (Lesser et al., 2019).

Clinical stimulation for functional localization was always between electrode pairs, using 50 Hz, 0.3 ms duration biphasic square wave pulse pairs, delivered in trains lasting 2–5 s, beginning at 1 mA and gradually increasing to as high as 15 mA, depending on patient or ECoG responses (Lesser et al., 1984, 1994). Patients were observed for motor changes during stimulation and asked if any sensory or cognitive changes occurred. When stimulation intensity was felt optimized, motor, sensory, language, and other testing would occur. ECoG was continuously observed by testing personnel during stimulation testing. Although the patients were in the hospital and had undergone brain surgery for electrode placement, the testing itself was done in a relaxed manner (see **Supplementary Video**). Patients were not limited with respect to body movement or lack of movement and there were no constraints regarding how quickly they needed to respond to the task, although they tried to answer as quickly as possible.

When ADs occurred, the testing team would observe the ECoG to see if the ADs stopped spontaneously. If ADs continued, the testing team used brief pulse stimulation (BPS) or a cognitive task, in these cases an arithmetic or spelling task (AST), in attempts to stop the ADs. Instructions regarding the tasks, and the tasks themselves, were presented auditorily. Clinical decisions alone determined whether to attempt AD termination with either BPS or AST. The testing personnel had no specific instructions regarding which to use, or regarding what specific task to use with AST. Patients were likely aware that ADs were occurring because of the reactions of the testing personnel but there were no other warnings that an AST would be presented. Task choices were left to the testing personnel. The tester might use an arithmetic task such as "what is 59 + 8," "what is 37 + 12," or "what is 35 – 18?" The patient might also be asked to recite the alphabet backward or to spell a word backward, i.e., "spell horse backward." **Figure 1** diagrams the overall protocol used. The **Supplementary Figures 1–3**, and the **Supplementary Video** show clinical examples.

In the previous paper, we found that in 50 of the 116 trials, ADs stopped after a cognitive task was presented. For this report, we studied these 50 trials. We compared (a) the time between initiation of the cognitive task (the Question) and AD termination and (b) the time between initiation of the patient's response (the Answer) and AD termination. We determined the percentage of trials during which AD termination occurred prior to the Answer, calculating the Clopper–Pearson exact binomial confidence interval for the percent.

RESULTS

We measured the time differences between when the question or answer was initiated and when the ADs stopped. As would be expected, given the protocol, ADs always ended after a question was asked. However, ADs often stopped before the answer was given (**Figure 2**). This occurred for 16/50 trials (32%, 95% CI =

Abbreviations: AD, afterdischarge; ADs, afterdischarges; AST, arithmetic or spelling task; ECoG, electrocorticography; fMRI, functional magnetic resonance imaging.

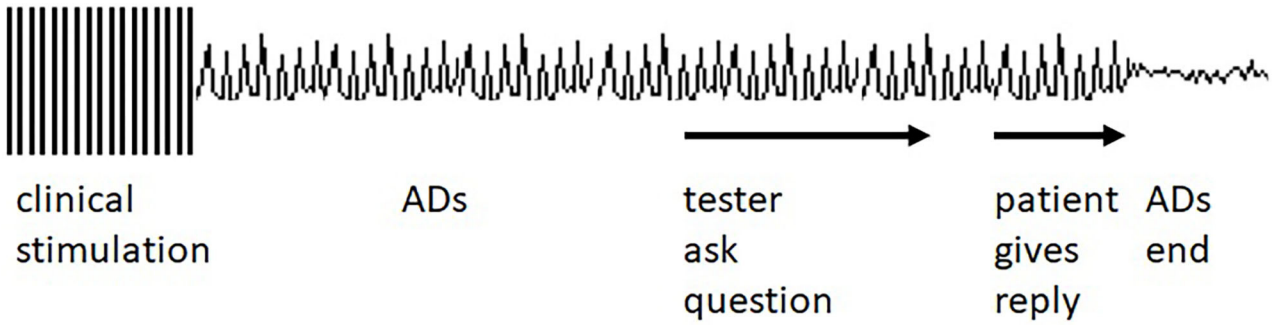

FIGURE 1 | Idealized diagram of the testing setting. Clinical stimulation occurs, and ADs occur as a result. The tester asks the patient a question which the patient answers. The answer is followed by the afterdischarge (AD) ending. See **Supplementary Figures 1–3**, **Supplementary Video** for clinical examples. However, ADs often end before the answer is given, as described in the Results section.

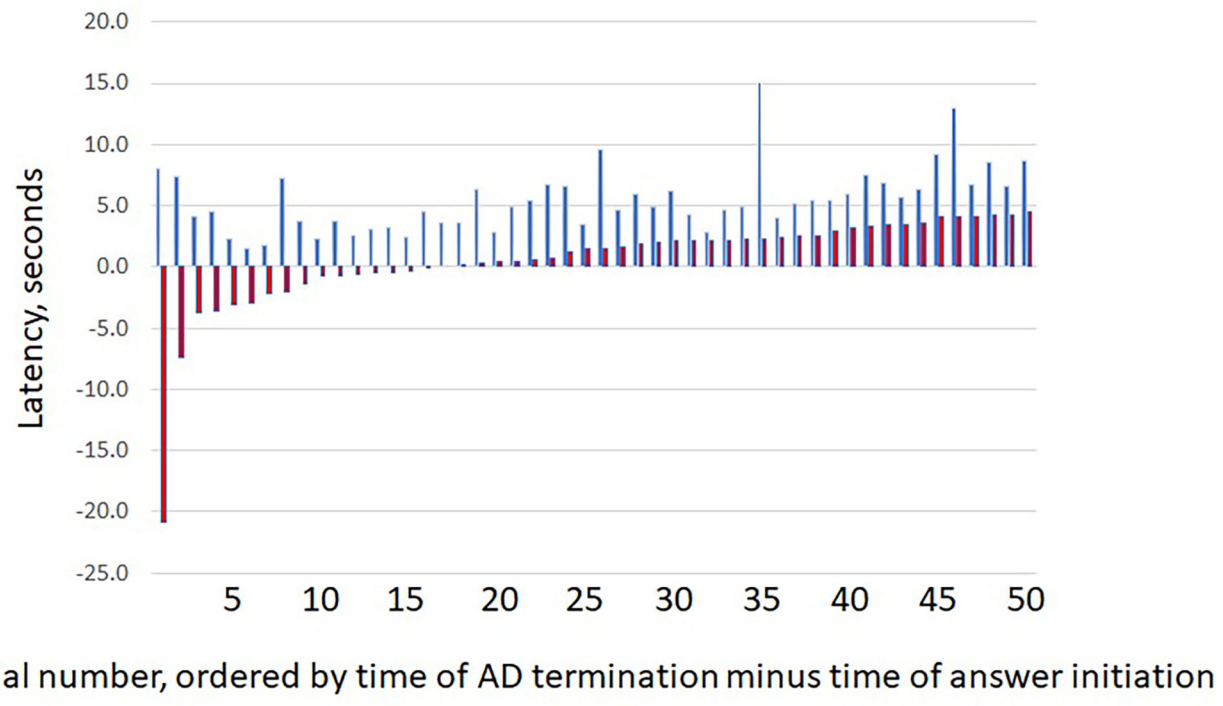

FIGURE 2 | Question and answer latencies. The figure shows the latency between (blue bars) question start and afterdischarge termination (Q) vs. (red bars) answer start and afterdischarge termination (A). For each pair, the first bar (blue) indicates the value for Q and the second bar (red) the value for (A). As would be expected, ADs always end after the question was asked. However, ADs often ended before an answer was given, as shown by the negative latencies for the first red bars. X axis shows results for the 50 trials, with pairs sorted by increasing latency for (A). Y values are in seconds.

19.5%, 46.7%). Regardless of when answers began, there was no clear temporal relationship between times of answer onset and of AD termination.

In our previous paper (Lesser et al., 2019), we reported functional magnetic resonance imaging (fMRI) results on six patients and nine controls, using ASTs similar to those used during stimulation testing. In summary, the tasks activated multiple regions, including regions thought important for mental effort. They, however, were not necessarily sites where stimulation had resulted in ADs, and the ADs were not necessarily in regions important for the ASTs (also see **Supplementary Material**).

Therefore, our results, overall, indicate that AD termination due to an AST can occur prior to overt performance of the task and can occur regardless of the location of the ADs.

DISCUSSION

It is well-known that motor activities are accompanied by electrophysiological changes such as the bereitschaftspotential, the premotor potential, and neuronal firing in both human (Shibasaki et al., 1980a,b; Thomas et al., 2019) and non-human

(Dorris et al., 2000; Boussaoud, 2001) studies. Similar changes accompany the performance of cognitive tasks (Haller et al., 2018). These potentials begin before, and continue after, the task is performed and appears to be temporally related to the timing of task performance. If AD terminations either occurred just before the onset of an answer, perhaps similar to the timing of a premotor potential, or occurred with a clear temporal linkage to the answer, this would favor the possibility that termination was related to task performance. However, in our patients, we found that AD termination often occurred before the patient performed the task and without a tight temporal relationship to task performance. This favors the conclusion that AD termination was due to the task situation, but not to the answer itself. Auditory modalities were used both for the questions and answers with these patients. Future studies might compare auditory versus visual tasks, but we think it unlikely that task modality itself was responsible for our findings: The widespread ECoG coherence that we previously have reported with ASTs (Lesser et al., 2019) was not restricted to regions important for modulating either audition or the AST modalities used. Thresholds for afterdischarges and for clinical changes in response to brain stimulation are in any case variable (Lesser et al., 1984, 2008; Pouratian et al., 2004).

Protocols for testing brain activity are often constrained by defined stimulus onset and response times. In contrast, with these patients, the AST was given in a more relaxed, perhaps more naturalistic, setting. The patients likely knew to respond quickly but had no constraints other than this. It is possible that these differences explain why AD termination could precede task performance. We suggest that AST termination was associated with internal processes regulating awareness and that were themselves widespread, not stimulus locked, not modality or task specific, and not characterized by a distinct temporal structure (Engel and Singer, 2001). Our findings suggest an extension of this idea and emphasize that in studying brain activity related to performance of a task, one must look beyond overt task performance: the overall level of attention to, engagement regarding, and motivation for completing the task also should be considered (Baddeley, 2003). Those factors are less likely to be precisely related to the time of task performance and more likely to reflect the overall conditions under which the activity is occurring. All of us vary in our level of attention, engagement, and motivation from moment to moment in our daily lives, whether we are researchers, subjects, or patients.

DATA AVAILABILITY STATEMENT

The raw data supporting the conclusions of this article will be made available by the authors, without undue reservation.

ETHICS STATEMENT

The studies involving human participants were reviewed and approved by the Johns Hopkins Medicine Institutional Review Board. Note that the subject of this report was considered exempt as it reported retrospective review of clinical investigations. Where applicable for the previous fMRI studies referenced in this report, written consents to participate in fMRI investigations were obtained.

AUTHOR CONTRIBUTIONS

RL conceived the AST paradigms for the clinical evaluations. Members of the YM–M Lab suggested analysis of question and answer times. RL and WW extracted the question, answer, and AD termination times from the data set and analyzed the results. DM performed statistical analyses of the results. RL wrote the paper, together with WW and DM. All co-authors reviewed the manuscript.

FUNDING

Portions of this study were supported by the Dr. Charles R. Fields Epilepsy and Neuroscience fund and by gifts from patients and their families. This research did not receive any specific grant from funding agencies in the public, commercial, or not-for-profit sectors.

ACKNOWLEDGMENTS

Rebecca Fisher, Karen George, Viktar Kanasevich, and Noelle Stewart performed clinical stimulation testing. We would like to thank the members of the Mizuno–Matsumoto's Lab in the University of Hyogo for their helping analysis.

SUPPLEMENTARY MATERIAL

The Supplementary Material for this article can be found online at: https://www.frontiersin.org/articles/10.3389/fnhum.2020.609188/full#supplementary-material

Supplementary Video | Testing results on patient S1. Movie is from Lesser et al. (2019). It is included with permission and published by Elsevier B. V. and is © International Federation of Clinical Neurophysiology 2019.

Supplementary Figures 1–3 | Explanation of testing paradigm in three patients. Figures are from Lesser et al. (2019). They are included with permission and published by Elsevier B. V. and is © International Federation of Clinical Neurophysiology 2019.

REFERENCES

Baddeley, A. (2003). Working memory: looking back and looking forward. *Nat.Rev.Neurosci.* 4, 829–839. doi: 10.1038/nrn1201

Boussaoud, D. (2001). Attention versus intention in the primate premotor cortex. *Neuroimage* 14(1 Pt 2), S40–S45. doi: 10.1006/nimg.2001.0816

Dorris, M. C., Paré, M., and Munoz, D. P. (2000). Immediate neural plasticity shapes motor performance. *J. Neurosci.* 20:Rc52. doi: 10.1523/JNEUROSCI.20-01-j0005.2000

Engel, A. K., and Singer, W. (2001). Temporal binding and the neural correlates of sensory awareness. *Trends Cogn Sci.* 5, 16–25. doi: 10.1016/S1364-6613(00)01568-0

Haller, M., Case, J., Crone, N. E., Chang, E. F., King-Stephens, D., Laxer, K. D., et al. (2018). Persistent neuronal activity in human prefrontal cortex links perception and action. *Nat. Hum. Behav.* 2, 80–91. doi: 10.1038/s41562-017-0267-2

Lesser, R., Gordon, B., and Uematsu, S. (1994). Electrical stimulation and language. *J. Clin. Neurophysiol.* 11, 191–204. doi: 10.1097/00004691-199403000-00004

Lesser, R., Lüders, H., Klem, G., Dinner, D., Morris, H., and Hahn, J. (1984). Cortical afterdischarge and functional response thresholds: results of extraoperative testing. *Epilepsia* 25, 615–621. doi: 10.1111/j.1528-1157.1984.tb03471.x

Lesser, R. P., Kim, S. H., Beyderman, L., Miglioretti, D. L., Webber, W. R. S., Bare, M., et al. (1999). Brief bursts of pulse stimulation terminate afterdischarges caused by cortical stimulation. *Neurology* 53, 2073–2081. doi: 10.1212/WNL.53.9.2073

Lesser, R. P., Lee, H. W., Webber, W. R., Prince, B., Crone, N. E., and Miglioretti, D. L. (2008). Short-term variations in response distribution to cortical stimulation. *Brain* 131, 1528–1539. doi: 10.1093/brain/awn044

Lesser, R. P., Webber, W. R. S., Miglioretti, D. L., Pillai, J. J., Agarwal, S., Mori, S., et al. (2019). Cognitive effort decreases beta, alpha, and theta coherence and ends afterdischarges in human brain. *Clin. Neurophysiol.* 130, 2169–2181. doi: 10.1016/j.clinph.2019.07.007

Muldoon, S. F., Costantini, J., Webber, W. R. S., Lesser, R., and Bassett, D. S. (2018). Locally stable brain states predict suppression of epileptic activity by enhanced cognitive effort. *Neuroimage Clin.* 18, 599–607. doi: 10.1016/j.nicl.2018.02.027

Pouratian, N., Cannestra, A. F., Bookheimer, S. Y., Martin, N. A., and Toga, A. W. (2004). Variability of intraoperative electrocortical stimulation mapping parameters across and within individuals. *J. Neurosurg.* 101, 458–466. doi: 10.3171/jns.2004.101.3.0458

Shibasaki, H., Barrett, G., Halliday, E., and Halliday, A. M. (1980a). Components of the movement-related cortical potential and their scalp topography. *Electroencephalogr. Clin. Neurophysiol.* 49, 213–226. doi: 10.1016/0013-4694(80)90216-3

Shibasaki, H., Barrett, G., Halliday, E., and Halliday, A. M. (1980b). Cortical potentials following voluntary and pasive finger movements. *Electroencephalogr. Clin. Neurophysiol.* 50, 201–213. doi: 10.1016/0013-4694(80)90147-9

Thomas, T. M., Candrea, D. N., Fifer, M. S., McMullen, D. P., Anderson, W. S., Thakor, N. V., et al. (2019). Decoding native cortical representations for flexion and extension at upper limb joints using electrocorticography. *IEEE Trans. Neural. Syst. Rehabil. Eng.* 27, 293–303. doi: 10.1109/tnsre.2019.2891362

Conflict of Interest: RL or his wife has stock in the following companies which sell health care products: 3M, Abbott Labs, Abbvie, Apple, Avanos, Celgene, Express Scripts, Johnson and Johnson, Merck & Company, Pfizer. These have been disclosed to and approved by the Johns Hopkins University in accordance with its conflict of interest policies.

The remaining authors declare that the research was conducted in the absence of any commercial or financial relationships that could be construed as a potential conflict of interest.

frontiers in Human Neuroscience

ORIGINAL RESEARCH
published: 16 February 2021
doi: 10.3389/fnhum.2021.612890

Preserving Right Pre-motor and Posterior Prefrontal Cortices Contribute to Maintaining Overall Basic Emotion

*Riho Nakajima[1], Masashi Kinoshita[2], Hirokazu Okita[3], Zhanwen Liu[4] and Mitsutoshi Nakada[2]**

[1]Department of Occupational Therapy, Faculty of Health Science, Institute of Medical, Pharmaceutical and Health Sciences, Kanazawa University, Kanazawa, Japan, [2]Department of Neurosurgery, Faculty of Medicine, Institute of Medical, Pharmaceutical and Health Sciences, Kanazawa University, Kanazawa, Japan, [3]Department of Physical Medicine and Rehabilitation, Kanazawa University Hospital, Kanazawa, Japan, [4]Department of Neurosurgery, Graduate School of Medical Science, Kanazawa University, Kanazawa, Japan

Basic emotions such as happiness, sadness, and anger are universal, regardless of the human species, and are governed by specific brain regions. A recent report revealed that mentalizing, which is the ability to estimate other individuals' emotional states *via* facial expressions, can be preserved with the help of awake surgery. However, it is still questionable whether we can maintain the ability to understand others' emotions by preserving the positive mapping sites of intraoperative assessment. Here, we demonstrated the cortical regions related to basic emotions *via* awake surgery for patients with frontal glioma and investigated the usefulness of functional mapping in preserving basic emotion. Of the 56 consecutive patients with right cerebral hemispheric glioma who underwent awake surgery at our hospital, intraoperative assessment of basic emotion could be successfully performed in 22 patients with frontal glioma and were included in our study. During surgery, positive responses were found in 18 points in 12 patients (54.5%). Of these, 15 points from 11 patients were found at the cortical level, mainly the premotor and posterior part of the prefrontal cortices. Then, we focused on cortical 15 positive mappings with 40 stimulations and investigated the types of emotions that showed errors by every stimulation. There was no specific rule for the region-emotional type, which was beyond our expectations. In the postoperative acute phase, the test score of basic emotion declined in nine patients, and of these, it decreased under the cut-off value (Z-score ≤ -1.65) in three patients. Although the total score declined significantly just after surgery ($p = 0.022$), it recovered within 3 months postoperatively. Our study revealed that through direct electrical stimulation (DES), the premotor and posterior parts of the prefrontal cortices are related to various kinds of basic emotion, but not a single one. When the region with a positive mapping site is preserved during operation, basic emotion function might be maintained although it declines transiently after surgery.

Keywords: basic emotion, awake surgery, intraoperative monitoring, glioma, right frontal lobe

OPEN ACCESS

Edited by:
Riki Matsumoto,
Kobe University, Japan

Reviewed by:
Jun Muto,
Fujita Health University, Japan
Yoshiki Arakawa,
Kyoto University, Japan

***Correspondence:**
Mitsutoshi Nakada
mnakada@med.kanazawa-u.ac.jp

***Specialty section**:*
This article was submitted to Brain Imaging and Stimulation, a section of the journal Frontiers in Human Neuroscience

Received: *01 October 2020*
Accepted: *25 January 2021*
Published: *16 February 2021*

Citation:
Nakajima R, Kinoshita M, Okita H, Liu Z and Nakada M (2021) Preserving Right Pre-motor and Posterior Prefrontal Cortices Contribute to Maintaining Overall Basic Emotion. Front. Hum. Neurosci. 15:612890. doi: 10.3389/fnhum.2021.612890

INTRODUCTION

Expression of emotion and meanings of facial expressions differ according to country or area. Basic emotion (e.g., anger, disgust, fear, happiness, sadness, and surprise) is a culturally universal expression and is governed by specific brain regions (Tracy and Randles, 2011). Happiness relates to the ventral prefrontal cortex, cingulate cortex, and ventral striatum, and sadness is governed by the medial prefrontal cortex, including the anterior cingulate cortex and middle frontal gyrus (MFG), while fear mainly involves the amygdala and insula (Vytal and Hamann, 2010; Celeghin et al., 2017; Gu et al., 2019). To support this knowledge, specific emotions are damaged by focal brain damage. For instance, it has been proven in humans and animals that the sense of fear is impaired by damage to the amygdala (Adolphs et al., 1994; Calder et al., 2001; Celeghin et al., 2017), and disgust might be affected by damage to the insula and basal ganglia (Calder et al., 2000, 2001; Suzuki et al., 2006). In contrast, it has also been argued that basic emotion is not necessarily governed by a specific brain region. That is, certain brain lesions relate not only to specific emotional states but also to several kinds of neurological/neuropsychological functions (Saarimäki et al., 2016; Celeghin et al., 2017). Specifically, the amygdala and medial-prefrontal cortex play a role in various emotions and are considered to be the key brain regions for basic emotion (Phan et al., 2002; Saarimäki et al., 2016; Huang et al., 2020). As for the laterality of basic emotion in healthy people, the bilateral cerebral hemispheres are involved (Vytal and Hamann, 2010; Saarimäki et al., 2016; Gu et al., 2019). However, it is considered that the laterality of emotional function is in the right cerebral hemisphere since emotional perception is damaged more severely in right lesions than in left lesions (Kucharska-Pietura et al., 2003; Yuvaraj et al., 2013; Suslow et al., 2016; Gainotti, 2019).

Previously, attempts to monitor emotional function during awake surgery for right cerebral hemispheric gliomas have been reported. Among them, Giussani et al. (2010) first reported intraoperative monitoring of emotional perception. They assessed six types of basic emotions, namely anger, happiness, fear, surprise, disgust, and sadness, in 18 patients with right cerebral hemispheric glioma. Positive mapping sites were found at five points in five cases, and they were superior to the middle temporal gyrus to the supramarginal gyrus. Later, Herbet et al. (2015) reported intraoperative monitoring of face-based mentalizing using the Reading the mind in the eyes (RME) test (Baron-Cohen et al., 2001). The research group demonstrated that the responsible region was found in the inferior frontal gyrus (IFG). Next, to verify previous data, the same research group investigated 27 patients with low-grade glioma and found positive mapping sites in the posterior IFG, dorsolateral prefrontal cortex, and posterior superior temporal gyrus at the cortical level (Yordanova et al., 2017). Their findings corresponded to those of previous neuroimaging studies (Adams et al., 2010; Celeghin et al., 2017).

Considering the above-mentioned background, the following two hypotheses arise: (1) Does direct electrical stimulation (DES) identify the region responsible for a single basic emotion? (2) Can we preserve the ability to estimate another individual's emotional state by preserving positive mapping sites with focal DES? Here, we demonstrated the cortical regions related to basic emotions *via* awake surgery for patients with frontal glioma and investigated the usefulness of functional mapping for preserving basic emotion. Consequently, the premotor and posterior parts of the prefrontal cortices relate to various kinds of basic emotion, but not a single emotion. When the region is preserved with the help of awake brain mapping, it might recover within 3 months postoperatively, although it declines immediately after surgery. To the best of our knowledge, our study using DES is the first to demonstrate that the right premotor and posterior prefrontal cortices are related to various types of basic emotion.

MATERIALS AND METHODS

Participants

Of the 139 patients who underwent awake surgery at our hospital between August 2013 and December 2019, 56 patients had lesions were localized on the right side. Patients in whom preoperative magnetic resonance imaging (MRI) demonstrated that lesions were found in the temporal, occipital, and parietal lobes were excluded. Finally, 36 patients with right frontal glioma were matched to our inclusion criteria (**Figure 1**). We decided to perform awake surgery for all patients, considering age, infiltration region, and preoperative functional condition. Of these, 22 patients underwent intraoperative assessment of basic emotion successfully (mean age: 42.8 years). Patient details are shown in **Table 1**. Written informed consent was obtained from all patients. This study was performed according to the guidelines of the Internal Review Board of Kanazawa University and was approved by the Medical Ethics Committee of Kanazawa University (approval numbers 1797 and 2593).

Awake Surgery

Awake surgery was performed using the "asleep-awake-asleep" technique, where the cortical and subcortical brain mapping was performed using DES (Duffau et al., 2002). A bipolar electrode with 5-mm-spaced tips delivering a biphasic current (pulse frequency of 60 Hz, pulse duration of 0.2 ms, amplitude between 1.5 and 6 mA, Nihon Kohden Neuromaster) was used in all cases. Patients were selected for functional monitoring during awake surgery, including visuospatial cognition, working memory, social cognition, basic emotion, and so on. In our patient group, 22 patients underwent monitoring for basic emotion. Although some reports have revealed the usefulness of functional mapping for emotional function (Herbet et al., 2015; Yordanova et al., 2017), intraoperative assessment for the neuropsychological function is still a new challenge in glioma surgery. Importantly, to achieve the best onco-functional balance for all glioma patients, we considered resection of the central part of the tumor, i.e., the enhanced lesion, and then performed intraoperative assessments on the extended resection.

To assess basic emotion intraoperatively, we used photographs of modified Japanese facial expressions of basic emotion series provided by Matsumoto and Ekman (1988). In the basic emotional test, a face of the eye region with two possible

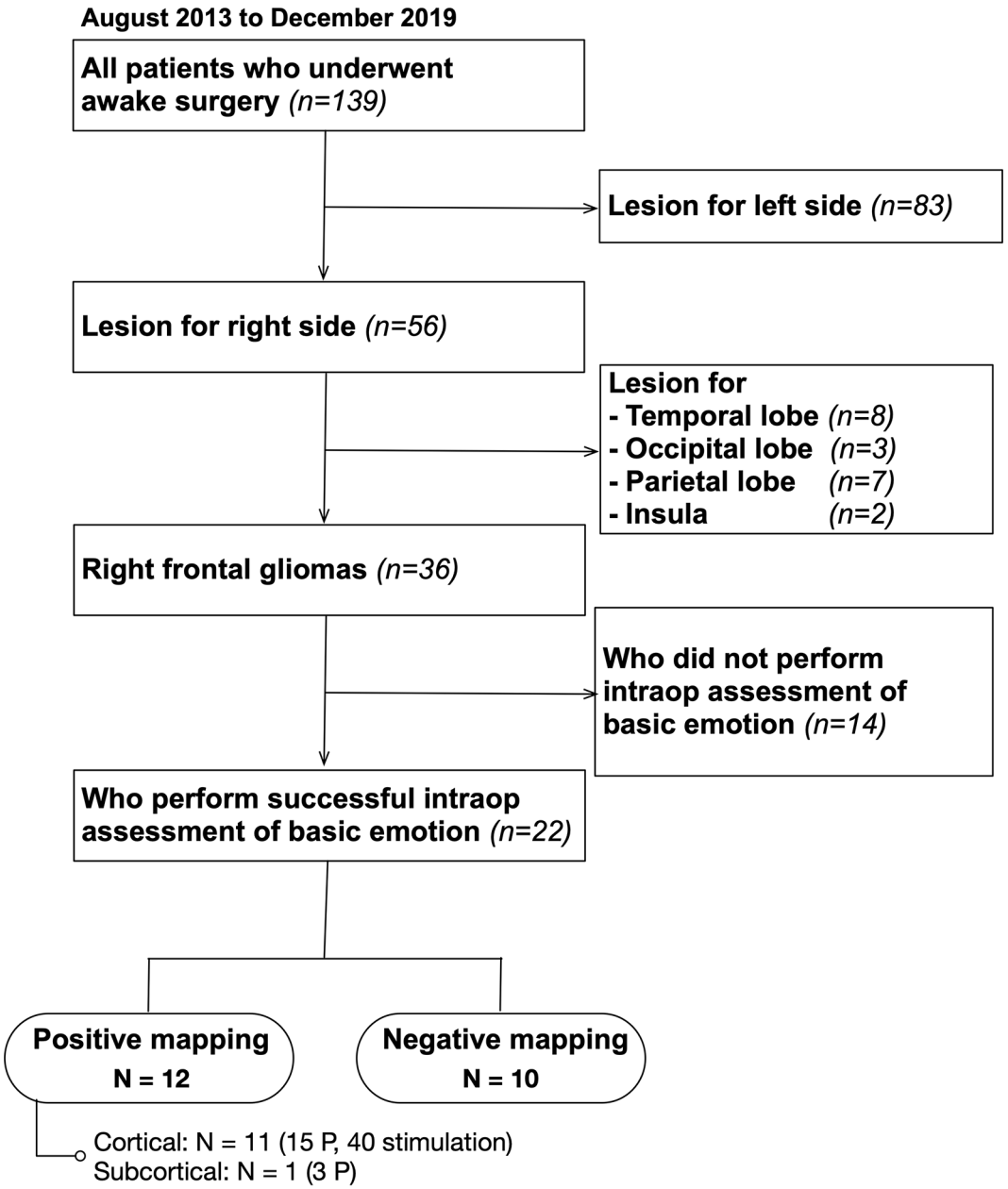

FIGURE 1 | Inclusion criteria. A total of 139 patients who underwent awake surgery in our institution were included; 36 of them matched our inclusion criteria. Of these, 22 patients underwent intraoperative monitoring of basic emotion successfully and were studied. P, point.

choices was presented on a computer monitor (**Supplementary Figure 1**). Patients were asked to select the most suitable emotional state for expressing the eyes from two choices within 2 s. Incorrect or delayed responses (≥3 s) were determined as positive responses. When positive responses were elicited in at least two out of three stimuli, the region was determined as a "positive response" and was preserved. Then, we overlaid each positive mapping site on each standardized MR image and studied the characteristics of incorrect responses during stimulation to positive mapping regions.

Functional Assessment

All patients underwent assessment of basic emotion over time until 3 months postoperatively. As for the assessment of basic emotion, we used the expression recognition test for adults, which is most widely used in Japan (Komatsu et al., 2012). It consists of 32 photographs of basic emotions, including happiness, sadness, anger, and surprise. For each of them, a photograph with five possible choices is presented, and patients are asked to select the most reasonable mental state from the choices. Of note, since there are racial

TABLE 1 | Demographic and clinical characteristic of participants.

Factors	Value
Age	42.8 ± 15.6 (14–72)
Sex; male/female	10/12
Handedness; Right/left	20/2
WHO grade	I 2, II 7, III 9, IV 4
Histology	
Dysembryoplastic neuroepithelial tumor	2
Diffuse astrocytoma	2
Oligodendroglioma	4
Ependymoma	1
Anaplastic astrocytoma	2
Anaplastic oligodendroglioma	7
Glioblastoma	4
IDH-1; mutant/wild type/ND	18/3/1
1p19q; codeletion/intact/ND	10/10/2
Preop MMSE score	28.3 ± 2.0

MMSE, mini-mental state examination; ND, not detected.

differences, assessment mainly prepared for Europeans and North Americans, such as the RME test, is not suitable for Asians (Baron-Cohen et al., 2001).

Magnetic Resonance Imaging and Lesion Mapping

Structural MRI was performed during a 3-month postoperative period as the standard care. The images were acquired using a conventional high-resolution three-dimensional (3D) T1-weighted 3.0 T MRI scanner (Signa^{TM} Excite HDx 3.0T; GE Healthcare, Little Chalfont, UK). Each MR image was reconstructed on the Montreal Neurological Institute (MNI) template using SPM12 software[1], which runs in MATLAB[2]. We composed the resection cavities manually using the MRIcron software[3]. Each step was performed initially by RN and then systematically checked by a neurosurgeon (MK).

Spatial Topography of Stimulations

The spatial topography of the stimulation points for emotion recognition was plotted in the following steps. First, the positive mapping sites were plotted on the corresponding original 3DT1-images for each patient using iPlan Stereotaxy 3.0 software (BrainLab), according to operative reports and intraoperative video records. The exact locations of the DES points were determined by considering their spatial relationships to various anatomical landmarks (the gyri, sulci, vessel, and midline), as previously described (Tate et al., 2014; Nakajima et al., 2020). Next, each positive mapping site of emotion recognition on the original MR images was transferred to normalized T1-images. Then, the spatial location of the positive mappings was overlaid on the 3D MNI template using the MRIcroGL software[4]. Finally, the anatomical location of positive mapping sites on the 3D MNI template was checked again in comparison to the original operative records. Each step was first undertaken by the RN and then systematically checked by a neurosurgeon (MK). For all positive mapping sites, we counted the times of stimulation for the same point (maximum, three) *via* intraoperative video recording. We then examined the types of emotions that were errors for each DES point. Besides, stimulated sites with negative responses were also determined using intraoperative multi-screen video record as the same procedure of positive mapping sites above mentioned. They were all overlapped on the 3D MNI template.

Statistical Analysis

First, all row scores of the expression recognition test and other neuropsychological assessments were converted to *Z*-scores using the mean and standard deviations of the age-matched controls. To compare the accuracy of basic emotion recognition over time, the Steel–Dwass analysis was used. The non-parametric test was used in the current study because our patients' data did not follow a normal distribution. All statistical analyses were performed using statistical analysis software (JMP, version 14.3.0; SAS Institute, Incorporation).

RESULTS

Anatomical Data

The overlap map of resection cavities that perform an intraoperative assessment of basic emotion (n = 22) demonstrated that the greatest overlap was in the posterior deep white matter of the medial frontal lobe (**Figure 2**).

Intraoperative Findings

Positive responses were found in 18 points in 12 cases (54.5%). Of these, 15 positive mappings from 11 patients were found at the cortical level, mainly the premotor and posterior part of the prefrontal cortices; with 3, 5, and 7 points for the superior frontal gyrus (SFG), MFG, and IFG, respectively (**Figure 3Aa**). Stimulated regions with negative responses of these patients are shown in **Figure 3Ab**. Then, we focused on patients whose positive mappings for basic emotion were identified during surgery in the following analysis. To note that three positive mapping sites from one patient of subcortical level, which were in the deep part of the MFG and IFG, were not investigated further in this study.

We found 56 total stimulations of positive mappings at the cortical level. Incorrect responses per total number of stimulations were 10 out of 14, 11 out of 15, and 19 out of 27 times, in the SFG, MFG, and IFG, respectively (**Figure 3B**). Details of patients' incorrect responses were summarized in **Supplementary Table 1**. We investigated the relationship between the spatial location of incorrect responses and the emotional type and found that incorrect responses for happiness (red circle) were found only in the IFG, and errors for neutral faces (green circles) were found only in the SFG and MFG, but not in the IFG (**Figures 3B**, **4**). In contrast, errors for sadness were found in the MFG and IFG, but not in the SFG. Also, incorrect responses were found in almost all kinds of emotions in each gyrus, and it had no other specific rule for region-emotional type.

[1]http://www.fil.ion.ucl.ac.uk/spm/software/spm12/
[2]http://www.mathworks.com/products/matlab/
[3]http://www.mccauslandcenter.sc.edu/mricro/mricron/
[4]http://www.cabiatl.com/mricrogl/

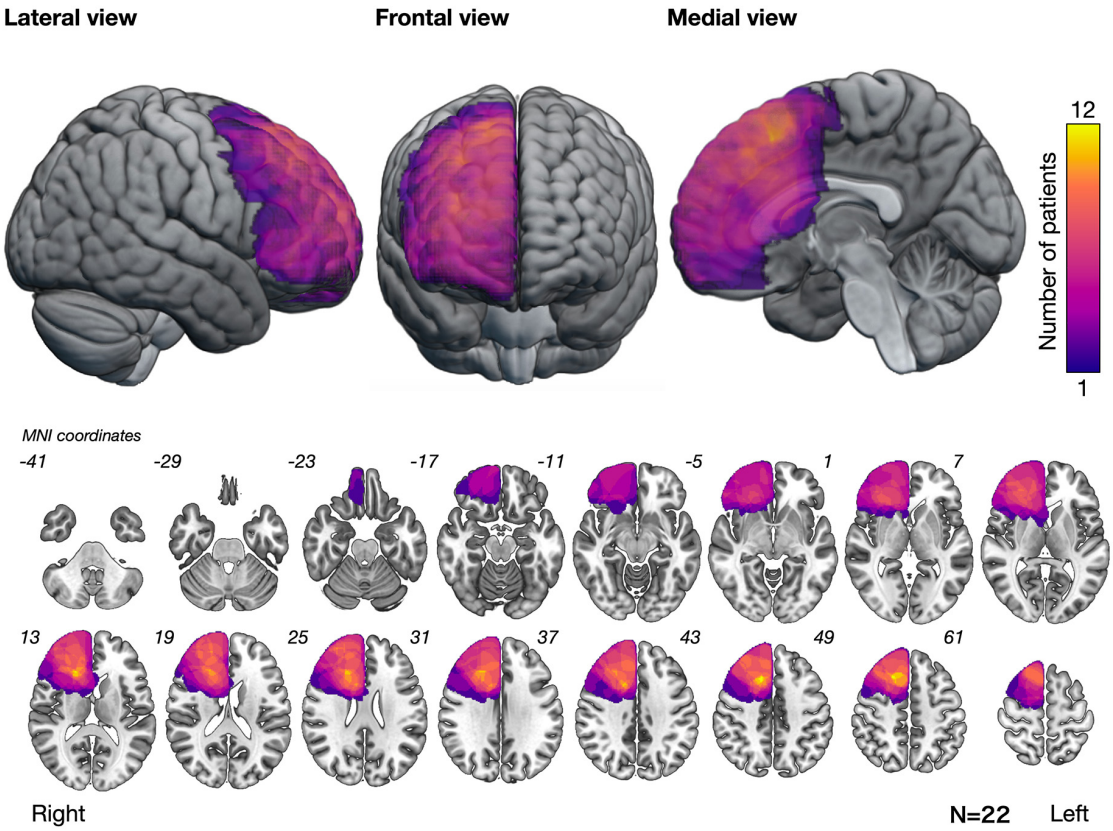

FIGURE 2 | Overlap map of resection cavities showing that the posteromedial prefrontal cortex and its deep part had the greatest overlap. Numbers at the upper left of the slice images indicate the coordinates of the Montreal Neurological Institute (MNI) template.

After surgery, the basic emotion test score declined in nine patients compared with the preoperative score, and of these, it declined under the cut-off value ($Z \leq -1.65$) in three patients (**Figure 5A**, details are shown in **Supplementary Table 2**). Although the total score declined significantly just after surgery (preoperative, 0.21 ± 0.61; postoperative 1 week, -0.98 ± 1.15; $p = 0.022$), it recovered to the same preoperative level within 3 months postoperatively (-0.28 ± 0.78; **Figure 5B**). In our patient group, there was no postoperative significant decline of neuropsychological function such as attention or executive function which may influence the accuracy of basic emotion (**Supplementary Figure 2**).

Illustrative Cases

Two illustrative cases are shown in **Figure 6**. The patient in case 1 was a 62-year-old man, whose tumor (glioblastoma, IDH-mutant) extended in the posterior pre-motor to the prefrontal area. Preoperatively, the results of neuropsychological examination revealed that attention and executive functions declined, while basic emotion was normal ($Z = -0.41$). During surgery, incorrect responses for disgust, fear, anger, and sadness were found at the posterior part of the MFG. Because incorrect responses were reproducible, the point was determined as positive mapping and it was considered to be the limit of resection. Postoperative examinations revealed that the extent of resection was 100%, and his test score for basic emotion declined under the cut-off value ($Z = -1.79$) but recovered within 3 months postoperatively. The patient in case 2 was a 39-year-old woman, whose tumor (anaplastic astrocytoma, IDH-wild type) infiltrated in the pre-motor to the prefrontal areas, and decided to undergo a second surgery. Preoperatively, a neuropsychological examination was performed, and her brain function was almost intact, except for a slight decline in working memory. She underwent awake surgery with the monitoring of basic emotion. Incorrect responses for fear, contempt, and disgust induced by DES were found at the posterior part of the IFG. Since the point was considered to be positive mapping, it was determined as the limit of resection. Postoperative MR images revealed that extended resection was performed. Postoperatively, her emotional function did not decline.

DISCUSSION

The primary aim of the current study was to reveal the cortical brain region related to basic emotion, and the secondary aim was to investigate the usefulness of functional mapping during awake surgery for preserving basic emotion. Consequently, the

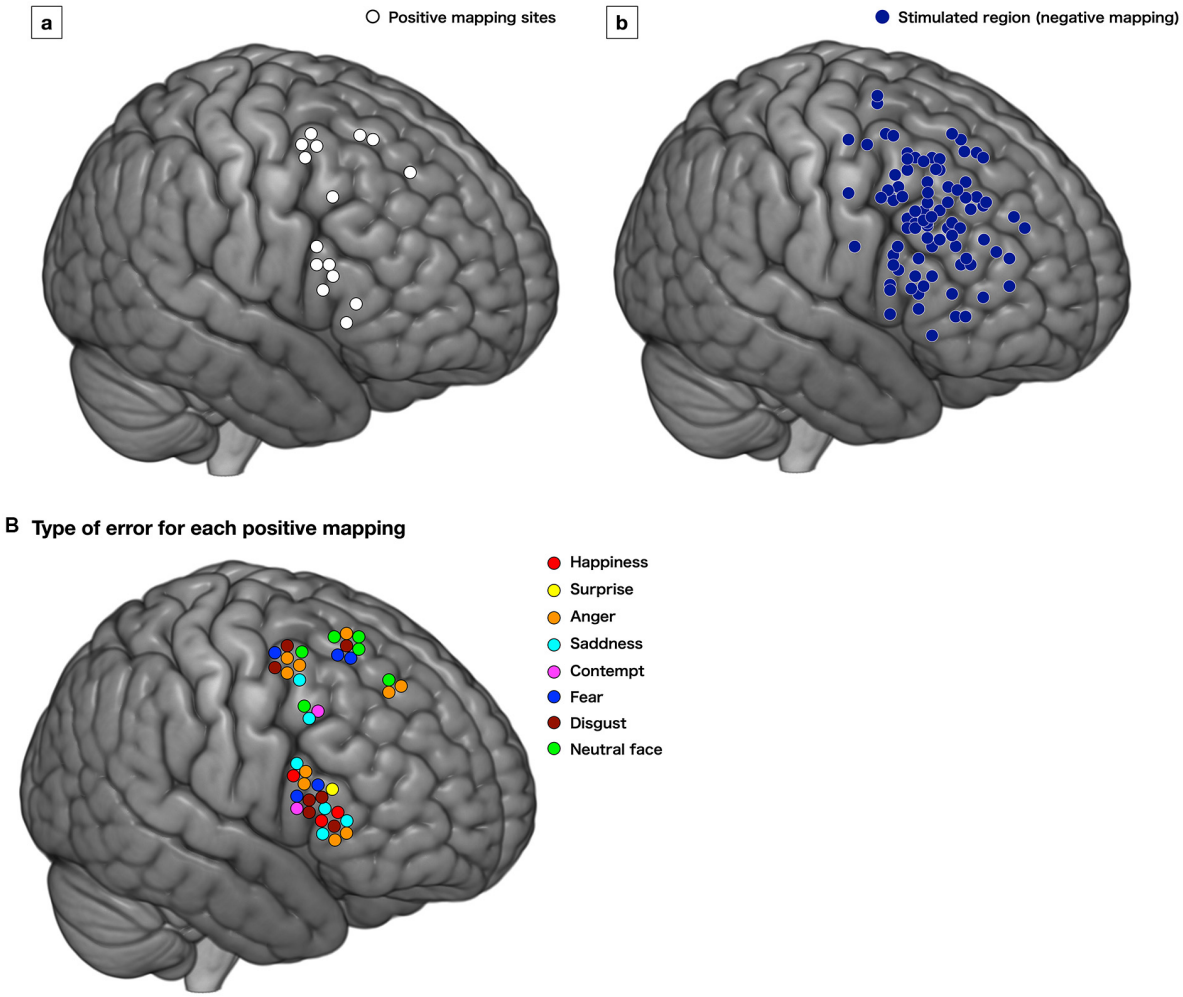

FIGURE 3 | Distribution of the positive mapping sites **(Aa**, white circle) and regions with negative responses **(Ab**, dark blue circle) at the cortical level. Each positive mapping site is stimulated two or three times, and when the error or delayed responses are observed at least twice, the region is considered as "positive." The lower image **(B)** shows the type of errors for each positive mapping. The type of emotion for which the incorrect responses were elicited is shown. Red, happiness; yellow, surprise; orange, anger; cyan, sadness; pink, contempt; blue, fear; brown, disgust; light green, neutral face.

premotor and posterior parts of the prefrontal cortices are related to various kinds of basic emotion, but no frontal region is related to a single emotion. When monitoring of basic emotion is conducted during surgery and the identified localization is preserved successfully, even though the accuracy of basic emotion might be decreased temporally, it might recover. Our study is the first to demonstrate that the right premotor and posterior prefrontal cortices are related to all kinds of basic emotion, rather than a single type.

Brain Region Relating to Basic Emotion

Through DES during awake surgery, we found that the premotor and posterior prefrontal cortices are related to various kinds of basic emotion, but we did not detect differences depending on emotional types. Previously, several studies have revealed the involvement of the premotor and prefrontal cortices in basic emotion. Indeed, the prefrontal cortex is known to be related to several kinds of emotions, such as happiness, sadness, anger, disgust, and fear (Vytal and Hamann, 2010; Dal Monte et al., 2013; Celeghin et al., 2017; Zhao et al., 2017; Gu et al., 2019). Specifically, an fMRI study demonstrated that the MFG was the common region for various kinds of facial recognition of basic emotion (Diano et al., 2017). Also, another study found that the gray matter volume of the IFG was positively related to the score of facial expression recognition for overall basic emotion (Uono et al., 2017). The mirror neuron system is also known to relate to face-based emotion recognition (Herbet et al., 2014; Perry et al., 2017). A mirror neuron is a neuron that acts selectively when observing another's action, and it senses automatically another's emotional state from facial

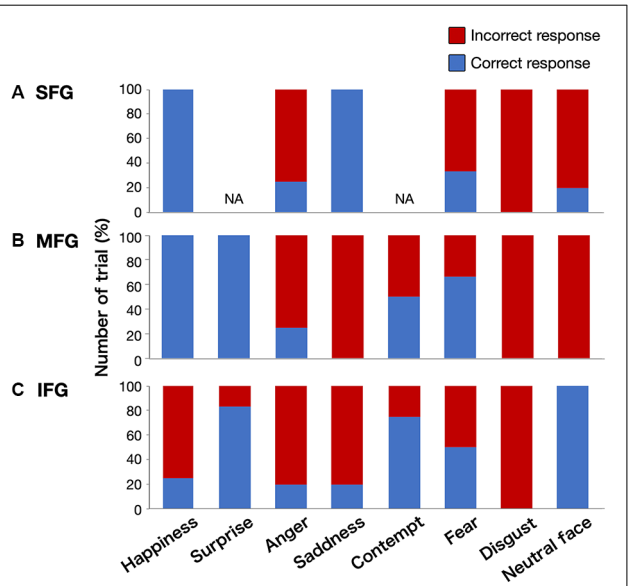

FIGURE 4 | Graphs showing the percentage of correct/incorrect responses for all stimulations by emotional type. Upper column **(A)**, superior frontal gyrus (SFG); middle column **(B)**, middle frontal gyrus (MFG); lower column **(C)**, inferior frontal gyrus (IFG); NA, not applicable.

expression or bodily action (Moor et al., 2012). Mirror neuron exists mainly in the premotor cortex, inferior parietal lobe, posterior superior temporal sulcus, anterior cingulate cortex, amygdala, and anterior insula (Rizzolatti et al., 1996; Lacoboni and Dapretto, 2006; Cattaneo and Rizzolatti, 2009). Among them, the premotor cortex, as well as insula considered as a core neural system for emotional processing (Jeon and Lee, 2018). Collectively, the frontal lobe is considered a key region for basic emotion (Saarimäki et al., 2016). That is, these results also indicated that the specific frontal region is not related to a single emotion (Kucharska-Pietura et al., 2003; Vytal and Hamann, 2010). Moreover, the prefrontal cortex, especially the ventral prefrontal cortex is structurally and functionally connected with the amygdala which is a center of various emotions (Li et al., 2013; Morawetz et al., 2017). The prefrontal-amygdala connectivity relates to emotion in healthy people (Clewett et al., 2014; Fernandes et al., 2019; Ibrahim et al., 2019). These findings suggest that premotor and prefrontal cortices play a role in basic emotion.

Looking in detail, the scores of sadness and disgust tend to be worse than other emotions. It is probably because of cultural differences between Caucasian-Americans and native Japanese for recognition of negative emotion (Harada et al., 2020). The Japanese are weak in expression recognition for negative emotion including sadness and disgust compared with Americans (Shioiri et al., 1999).

The positive mapping sites obtained in the current study mostly corresponded to previously reported results of intraoperative assessment of face-based mentalizing (Herbet et al., 2015; Yordanova et al., 2017). Interestingly, our study used basic emotion as an intraoperative task, while the study reported by Herbet et al. (2015) and Yordanova et al. (2017) used the RME-test, requiring patients to discriminate a more complex mental state of the face than a basic emotion. Several neuroimaging studies have reported the involvement of the right premotor and prefrontal cortices to the RME-test by several neuroimaging studies (Castelli et al., 2010; Herbet et al., 2014; Domínguez et al., 2019). This means that the premotor and posterior part of the prefrontal cortices relates to general face-based emotional perception, rather than a specific type of emotion. Taken together, assessment for all types of the emotional state rather than specific emotion might be appropriate for intraoperative monitoring at the right premotor and prefrontal regions. In contrast, a previous report revealed that the DES for the anterior insula induced response of a particular emotional type, such as anger and sadness (Motomura et al., 2019). We can take into consideration to use specific emotional type as an intraoperative assessment for the regions which induce unique emotional deficit by the DES.

The Usefulness of DES for Preserving Basic Emotion

In the current study, basic emotion could be maintained by preserving regions with positive mappings during surgery, even though it declined immediately after surgery. This finding corresponds to that of previous studies that performed intraoperative awake mapping of emotional function (Giussani et al., 2010; Papagno et al., 2016). Additionally, the postoperative course is similar to that of several kinds of neuropsychological/neurological function assessed during awake surgery (De Witt Hamer et al., 2012; Nakajima et al., 2019).

Ideally, it is necessary to compare functional outcomes between the with- and without-intraoperative evaluation groups to determine the usefulness of awake mapping of basic emotion. However, this method is impossible because of the following reasons. First, setting a control group that does not undergo intraoperative mapping is difficult from an ethical point of view. Since, we know the advantages of intraoperative monitoring in awake conditions for several neuropsychological functions, they are still challenging (Giussani et al., 2010; Herbet et al., 2015; Papagno et al., 2016; Yordanova et al., 2017). Also, although there were no significant differences in the mean score of basic emotion between the evaluation group and non-evaluation group before surgery (**Supplementary Table 3**), the score of the latter declined slightly in 6 out of 14 patients (42.9%) preoperatively ($Z \leq -1.65$, data not shown). Therefore, we decided not to use intraoperative assessment for some patients. Hence, we could not simply compare functional outcomes between the evaluation and non-evaluation groups.

Recently, the emotional function has gradually gained more attention in brain tumor surgery (Pertz et al., 2020). For instance, a report suggested that there is a high possibility of social cognition including the emotional function of patients with brain tumors being damaged preoperatively (Goebel et al., 2018). However, even now, the postoperative decline in emotional function in the right cerebral hemispheric glioma tends to be considered to recover

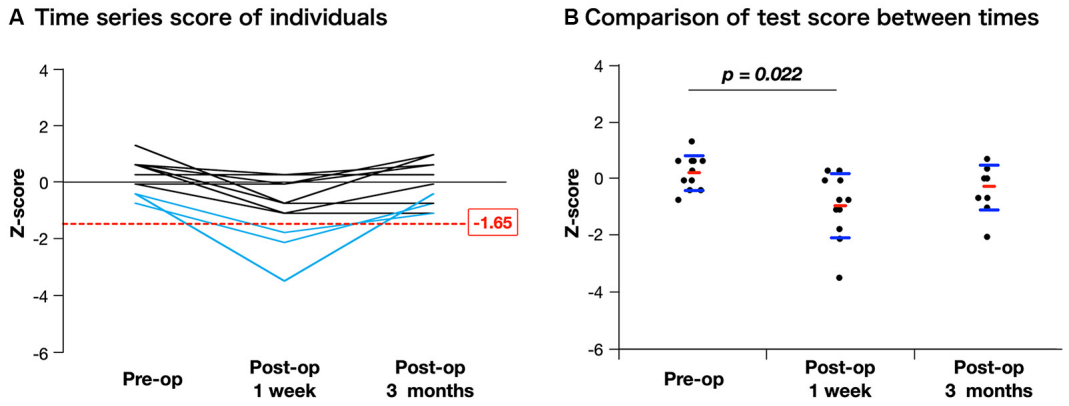

FIGURE 5 | Time course of assessment for basic emotion in patients whose positive mappings were identified during awake surgery. The figure of time series of individuals **(A)** indicates that three patients declined under cut-off value ($Z \leq -1.65$) just after surgery, but they recovered completely. When scores are compared among time series using Steel-Dwass analysis **(B)**, though the mean value declined significantly just after surgery, there is no decline at 3 months postoperatively compared with the preoperative score.

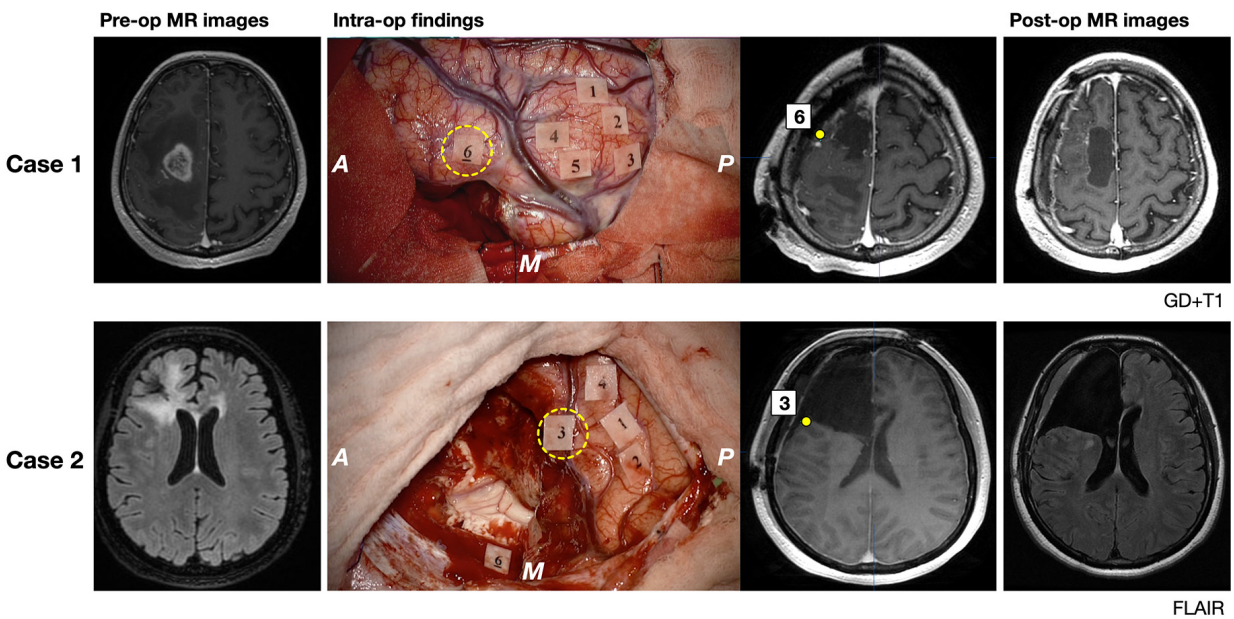

FIGURE 6 | Pre- and postoperative magnetic resonance (MR) images (gadolinium-enhanced T1 image for Case 1 and FLAIR image for Case 2) and intraoperative findings of illustrative two cases are shown. MR images and number tags with the yellow circle of the middle column show the exact location of positive mappings of basic emotion identified using iPlan Stereotaxy 3.0 software (BrainLab). A: anterior; P: posterior; M: medial side; yellow broken circle, tags of incorrect responses for basic emotion. Tags and symptoms elicited by electrical stimulation are shown. Case 1: Tag 1–5, involuntary movement; Tag 6, emotion recognition; Case 2: Tag 1 and 2, dysarthria; Tag 3, emotion recognition; Tag 4, negative motor response; Tag 6, Stroop test.

completely in a relatively short period following surgery (Campanella et al., 2015; Mattavelli et al., 2019; Pertz et al., 2020).

In contrast, there is an important study attracting clinicians' attention, although the number of cases is insufficient (Herbet et al., 2013). The authors investigated the postoperative course of emotion recognition in 10 patients with low-grade glioma divided into two groups according to resected lesion; those with the resected right dorsomedial prefrontal cortex and those with resected right IFG. As a result, although postoperative emotion recognition deficits in the former group were temporary, those in the latter group did not recover beyond 3 months postoperatively. Another study revealed that overall emotion recognition accuracy at a chronic phase in patients with the resected prefrontal cortex, especially the orbitofrontal cortex and medial prefrontal cortex, was significantly declined in comparison to the control group

(Jenkins et al., 2014). These previous findings suggest that damage to a specific region of the frontal lobe may lead to an irreversible deficit in emotion recognition. Because the basic emotion of our patient group was maintained, in patients whose localization of basic emotion could be identified during surgery, intraoperative monitoring of basic emotion should be considered in glioma surgery for the right frontal lobe.

Limitations

There are several limitations to the current study. First, as mentioned in the preceding section, we cannot validate the usefulness of intraoperative monitoring of basic emotion compared to the control group. Although several previous reports have revealed the utility of intraoperative monitoring for right cerebral hemispheric function including emotional function, assessment of right frontal lobe function is still a challenge (Thiebaut de Schotten et al., 2005; Herbet et al., 2015, 2016; Kinoshita et al., 2016; Nakajima et al., 2018). The usefulness of intraoperative monitoring of neuropsychological function should be considered from various aspects, such as the extent of resection, progression-free survival, overall survival, functional outcome, and postoperative social lives of patients. Another limitation is the small number of cases. However, the number of cases in previous studies on intraoperative monitoring of basic emotion was also not many; there were 5 of 18 patients with right cerebral hemispheric gliomas in Giussani et al. (2010), 13 patients with left insula glioma in Papagno et al. (2016), and 11 patients with right insula glioma who complete the intraoperative task in Motomura et al. (2019). Our study investigated the usefulness of intraoperative monitoring for basic emotion with a similar or marginally higher number of patients than the previous reports, with a focus on the right frontal lobe. Our patient's group includes both low-grade and high-grade gliomas, although they are not biologically the same. However, several recent studies that investigated functional localization *via* awake brain mapping include both tumor types and obtain meaningful results (Gras-Combe et al., 2012; Saito et al., 2016; Nakajima et al., 2018; Puglisi et al., 2018; Rolland et al., 2018; Nakada et al., 2020). Additionally, we could not study the white matter tract, since we found only a few positive mapping sites at the subcortical level in our patient group. Third, the current study is a retrospective study of intraoperative monitoring in a clinical setting. Hence, the cortical area that can be assessed is limited to the surrounding brain tumor within the operative field. Moreover, it is unclear whether the same results can be obtained in the normal brain since slow-growing gliomas might lead to reorganization with the functional shift from original localization at the cortical level (Duffau, 2014). Although cortical reorganization for language and motor function in gliomas has been reported (Saito et al., 2016; Southwell et al., 2016; Nakajima et al., 2020), brain plasticity regarding higher brain function, such as basic emotion, is poorly understood. In support of our results, some previous reports revealed that the premotor and posterior parts of the prefrontal cortices are related to basic emotion in the normal brain (Diano et al., 2017; Uono et al., 2017). These reports showed a relatively smaller area for emotion recognition than our results. Our results might show a broader region than the original functional localization, since our data may include the region with a functional shift.

Finally, to date, the concept for basic emotion itself and localization for each emotional type is a matter of debate without consensus (Eugène et al., 2003; Touroutoglou et al., 2015; Hutto et al., 2018; Keltner et al., 2019). Further study will be required with a large number of cases to reveal which emotional states should be used in certain brain regions for intraoperative mapping, and its method for suitable assessment.

CONCLUSION

The premotor and posterior parts of the prefrontal cortices are related to the different types of basic emotion. When the region with a positive mapping site is preserved, it might recover within 3 months postoperatively even though it declines immediately after surgery. Our findings will be useful in the field of neuroscience as well as for clinicians who are engaging in the treatment of brain damage, such as neurosurgery/neurology and rehabilitation.

DATA AVAILABILITY STATEMENT

The original contributions presented in the study are included in the article/**Supplementary Material**, further inquiries can be directed to the corresponding author.

ETHICS STATEMENT

This study was performed according to the guidelines of the Internal Review Board of Kanazawa University and was approved by the Medical Ethics Committee of Kanazawa University (approval numbers 1797 and 2593). The patients/participants provided their written informed consent to participate in this study. Written informed consent was obtained from the individual(s) for the publication of any potentially identifiable images or data included in this article.

AUTHOR CONTRIBUTIONS

MN and RN: conception and design, drafting article. RN, MK, and HO: acquisition of data. RN, MK, and ZL: analysis and interpretation of data. MN: study supervision. All authors contributed to the article and approved the submitted version.

FUNDING

This work was supported by Japan Society for the Promotion of Science (JSPS) KAKENHI Grant Numbers 18H03126, 18K19606, 19K22801, 20K21649, and 20KK0206.

SUPPLEMENTARY MATERIAL

The Supplementary Material for this article can be found online at: https://www.frontiersin.org/articles/10.3389/fnhum.2021.612890/full#supplementary-material.

SUPPLEMENTARY FIGURE 1 | Schema of intraoperative assessment for basic emotion.

SUPPLEMENTARY FIGURE 2 | These images show results of neuropsychological assessments which may influence the accuracy of emotion recognition; **(A)** Mini-mental state examination for general cognitive function; **(B)** letter cancellation test (%-correct) for selective attention; **(C)** letter cancellation test (time required) for processing speed; **(D)** Stroop test for attentional control or executive function. There were no significant differences through the course using Steel-Dwass analysis.

SUPPLEMENTARY TABLE 1 | Details of patients' incorrect responses.

SUPPLEMENTARY TABLE 2 | Details of time series score of individuals.

SUPPLEMENTARY TABLE 3 | Demographic and clinical factor for each group.

REFERENCES

Adams, R. B. Jr., Rule, N. O., Franklin, R. G. Jr., Wang, E., Stevenson, M. T., Yoshikawa, S., et al. (2010). Cross-cultural reading the mind in the eyes: an fMRI investigation. *J. Cogn. Neurosci.* 22, 97–108. doi: 10.1162/jocn.2009.21187

Adolphs, R., Tranel, D., Damasio, H., and Damasio, A. (1994). Impaired recognition of emotion in facial expressions following bilateral damage to the human amygdala. *Nature* 372, 669–672. doi: 10.1038/372669a0

Baron-Cohen, S., Wheelwright, S., Hill, J., Raste, Y., and Plumb, I. (2001). The "Reading the Mind in the Eyes" Test revised version: a study with normal adults and adults with Asperger syndrome or high-functioning autism. *J. Child Psychol. Psychiatry* 42, 241–251. doi: 10.1111/1469-7610.00715

Calder, A. J., Keane, J., Manes, F., Antoun, N., and Young, A. W. (2000). Impaired recognition and experience of disgust following brain injury. *Nat. Neurosci.* 3, 1077–1078. doi: 10.1038/80586

Calder, A. J., Lawrence, A. D., and Young, A. W. (2001). Neuropsychology of fear and loathing. *Nat. Rev. Neurosci.* 2, 352–363. doi: 10.1038/35072584

Campanella, F., Fabbro, F., Ius, T., Shallice, T., and Skrap, M. (2015). Acute effects of surgery on emotion and personality of brain tumor patients: surgery impact, histological aspects, and recovery. *Neuro Oncol.* 17, 1121–1131. doi: 10.1093/neuonc/nov065

Castelli, I., Baglio, F., Blasi, V., Alberoni, M., Falini, A., Liverta-Sempio, O., et al. (2010). Effects of aging on mindreading ability through the eyes: an fMRI study. *Neuropsychologia* 48, 2586–2594. doi: 10.1016/j.neuropsychologia.2010.05.005

Cattaneo, L., and Rizzolatti, G. (2009). The mirror neuron system. *Arch. Neurol.* 66, 557–560. doi: 10.1001/archneurol.2009.41

Celeghin, A., Diano, M., Bagnis, A., Viola, M., and Tamietto, M. (2017). Basic emotions in human neuroscience: neuroimaging and beyond. *Front. Psychol.* 8:1432. doi: 10.3389/fpsyg.2017.01432

Clewett, D., Bachman, S., and Mather, M. (2014). Age-related reduced prefrontal-amygdala structural connectivity is associated with lower trait anxiety. *Neuropsychology* 28, 631–642. doi: 10.1037/neu0000060

Dal Monte, O., Krueger, F., Solomon, J. M., Schintu, S., Knutson, K. M., Strenziok, M., et al. (2013). A voxel-based lesion study on facial emotion recognition after penetrating brain injury. *Soc. Cogn. Affect. Neurosci.* 8, 632–639. doi: 10.1093/scan/nss041

De Witt Hamer, P. C., Robles, S. G., Zwinderman, A. H., Duffau, H., and Berger, M. S. (2012). Impact of intraoperative stimulation brain mapping on glioma surgery outcome: a meta-analysis. *J. Clin. Oncol.* 30, 2559–2565. doi: 10.1200/JCO.2011.38.4818

Diano, M., Tamietto, M., Celeghin, A., Weiskrantz, L., Tatu, M. K., Bagnis, A., et al. (2017). Dynamic changes in amygdala psychophysiological connectivity reveal distinct neural networks for facial expressions of basic emotions. *Sci. Rep.* 7:45260. doi: 10.1038/srep45260

Domínguez, D. J., Nott, Z., Horne, K., Prangley, T., Adams, A. G., Henry, J. D., et al. (2019). Structural and functional brain correlates of theory of mind impairment post-stroke. *Cortex* 121, 427–442. doi: 10.1016/j.cortex.2019.09.017

Duffau, H. (2014). Diffuse low-grade gliomas and neuroplasticity. *Diagn. Intervent. Imaging* 95, 945–955. doi: 10.1016/j.diii.2014.08.001

Duffau, H., Capelle, L., Sichez, N., Denvil, D., Lopes, M., Sichez, J. P., et al. (2002). Intraoperative mapping of the subcortical language pathways using direct stimulations. An anatomo-functional study. *Brain* 125, 199–214. doi: 10.1093/brain/awf016

Eugène, F., Lévesque, J., Mensour, B., Leroux, J. M., Beaudoin, G., Bourgouin, P., et al. (2003). The impact of individual differences on the neural circuitry underlying sadness. *NeuroImage* 19, 354–364. doi: 10.1016/s1053-8119(03)00121-6

Fernandes, H. M., Cabral, J., van Hartevelt, T. J., Lord, L. D., Gleesborg, C., Moller, A., et al. (2019). Disrupted brain structural connectivity in pediatric bipolar disorder with psychosis. *Sci. Rep.* 9:13638. doi: 10.1038/s41598-019-50093-4

Gainotti, G. (2019). A historical review of investigations on laterality of emotions in the human brain. *J. Hist. Neurosci.* 28, 23–41. doi: 10.1080/0964704X.2018.1524683

Giussani, C., Pirillo, D., and Roux, F. E. (2010). Mirror of the soul: a cortical stimulation study on recognition of facial emotions. *J. Neurosurg.* 112, 520–527. doi: 10.3171/2009.5.JNS081522

Goebel, S., Mehdorn, H. M., and Wiesner, C. D. (2018). Social cognition in patients with intracranial tumors: do we forget something in the routine neuropsychological examination? *J. Neurooncol.* 140, 687–696. doi: 10.1007/s11060-018-3000-8

Gras-Combe, G., Moritz-Gasser, S., Herbet, G., and Duffau, H. (2012). Intraoperative subcortical electrical mapping of optic radiations in awake surgery for glioma involving visual pathways. *J. Neurosurg.* 117, 466–473. doi: 10.3171/2012.6.JNS111981

Gu, S., Wang, F., Cao, C., Wu, E., Tang, Y. Y., and Huang, J. H. (2019). An integrative way for studying neural basis of basic emotions with fMRI. *Front. Neurosci.* 13:628. doi: 10.3389/fnins.2019.00628

Harada, T., Mano, Y., Komeda, H., Hechtman, L. A., Pornpattananangkul, N., Parrish, T. B., et al. (2020). Cultural influences on neural systems of intergroup emotion perception: an fMRI study. *Neuropsychologia* 137:107254. doi: 10.1016/j.neuropsychologia.2019.107254

Herbet, G., Lafargue, G., Bonnetblanc, F., Moritz-Gasser, S., and Duffau, H. (2013). Is the right frontal cortex really crucial in the mentalizing network? A longitudinal study in patients with a slow-growing lesion. *Cortex* 49, 2711–2727. doi: 10.1016/j.cortex.2013.08.003

Herbet, G., Lafargue, G., Bonnetblanc, F., Moritz-Gasser, S., Menjot de Champfleur, N., and Duffau, H. (2014). Inferring a dual-stream model of mentalizing from associative white matter fibres disconnection. *Brain* 137, 944–959. doi: 10.1093/brain/awt370

Herbet, G., Lafargue, G., Moritz-Gasser, S., Bonnetblanc, F., and Duffau, H. (2015). Interfering with the neural activity of mirror-related frontal areas impairs mentalistic inferences. *Brain Struct. Funct.* 220, 2159–2169. doi: 10.1007/s00429-014-0777-x

Herbet, G., Moritz-Gasser, S., and Duffau, H. (2016). Direct evidence for the contributive role of the right inferior fronto-occipital fasciculus in non-verbal semantic cognition. *Brain Struct. Funct.* 222, 1597–1610. doi: 10.1007/s00429-016-1294-x

Huang, Y.-A., Dupont, P., Van de Vliet, L., Jastorff, J., Peeters, R., Theys, T., et al. (2020). Network level characteristics in the emotion recognition network after unilateral temporal lobe surgery. *Eur. J. Neurosci.* 52, 3470–3484. doi: 10.1111/ejn.14849

Hutto, D. D., Robertson, I., and Kirchhoff, M. D. (2018). A new, better BET: rescuing and revising basic emotion theory. *Front. Psychol.* 9:1217. doi: 10.3389/fpsyg.2018.01217

Ibrahim, K., Eilbott, J. A., Ventola, P., He, G., Pelphrey, K. A., McCarthy, G., et al. (2019). Reduced amygdala-prefrontal functional connectivity in children with autism spectrum disorder and co-occurring disruptive behavior. *Biol. Psychiatry Cogn. Neurosci. Neuroimaging* 4, 1031–1041. doi: 10.1016/j.bpsc.2019.01.009

Jenkins, L. M., Andrewes, D. G., Nicholas, C. L., Drummond, K. J., Moffat, B. A., Phal, P., et al. (2014). Social cognition in patients following surgery to the prefrontal cortex. *Psychiatry Res.* 224, 192–203. doi: 10.1016/j.pscychresns.2014.08.007

Jeon, H., and Lee, S.-H. (2018). From neurons to social beings: short review of the mirror neuron system research and its socio-psychological and psychiatric implications. *Clin. Psychopharmacol. Neurosci.* 16, 18–31. doi: 10.9758/cpn.2018.16.1.18

Keltner, D., Sauter, D., Tracy, J., and Cowen, A. (2019). Emotional expression: advances in basic emotion theory. *J. Nonverbal Behav.* 43, 133–160. doi: 10.1007/s10919-019-00293-3

Kinoshita, M., Nakajima, R., Shinohara, H., Miyashita, K., Tanaka, S., Okita, H., et al. (2016). Chronic spatial working memory deficit associated with the superior longitudinal fasciculus: a study using voxel-based lesion-symptom mapping and intraoperative direct stimulation in right prefrontal glioma surgery. *J. Neurosurg.* 125, 1024–1032. doi: 10.3171/2015.10.JNS1591

Komatsu, S., Nakamura, T., and Hakoda, Y. (2012). *Exprexxion Recognition Test for Adults*. Hukuoka: Toyo Physical.

Kucharska-Pietura, K., Phillips, M. L., Gernand, W., and David, A. S. (2003). Perception of emotions from faces and voices following unilateral brain damage. *Neuropsychologia* 41, 1082–1090. doi: 10.1016/s0028-3932(02)00294-4

Lacoboni, M., and Dapretto, M. (2006). The mirror neuron system and the consequences of its dysfunction. *Nat. Rev. Neurosci.* 7, 942–951. doi: 10.1038/nrn2024

Li, Z., Santhanam, P., Coles, C. D., Ellen Lynch, M., Hamann, S., Peltier, S., et al. (2013). Prenatal cocaine exposure alters functional activation in the ventral prefrontal cortex and its structural connectivity with the amygdala. *Psychiatry Res.* 213, 47–55. doi: 10.1016/j.pscychresns.2012.12.005

Matsumoto, D., and Ekman, P. (1988). *Japanese and Caucasian Facial Expressions of Emotion (JACFEE) and Neutral Faces (JACNeuF)*. San Francisco, CA: San Francisco State University.

Mattavelli, G., Pisoni, A., Casarotti, A., Comi, A., Sera, G., Riva, M., et al. (2019). Consequences of brain tumour resection on emotion recognition. *J. Neuropsychol.* 13, 1–21. doi: 10.1111/jnp.12130

Moor, B. G., Macks, Z. A., Guroglu, B., Rombouts, S. A., Molen, M. W., and Crone, E. A. (2012). Neurodevelopmental changes of reading the mind in the eyes. *Soc. Cogn. Affect. Neurosci.* 7, 44–52. doi: 10.1093/scan/nsr020

Morawetz, C., Bode, S., Baudewig, J., and Heekeren, H. R. (2017). Effective amygdala-prefrontal connectivity predicts individual differences in successful emotion regulation. *Soc. Cogn. Affect. Neurosci.* 12, 569–585. doi: 10.1093/scan/nsw169

Motomura, K., Terasawa, Y., Natsume, A., Iijima, K., Chalise, L., Sugiura, J., et al. (2019). Anterior insular cortex stimulation and its effects on emotion recognition. *Brain Struct. Funct.* 224, 2167–2181. doi: 10.1007/s00429-019-01895-9

Nakada, M., Nakajima, R., Okita, H., Nakade, Y., Yuno, T., Tanaka, S., et al. (2020). Awake surgery for right frontal lobe glioma can preserve visuospatial cognition and spatial working memory. *J. Neurooncol.* doi: 10.1007/s11060-020-03656-9 [Epub ahead of print].

Nakajima, R., Kinoshita, M., and Nakada, M. (2020). Motor functional reorganization is triggered by tumor infiltration into the primary motor area and repeated surgery. *Front. Hum. Neurosci.* 14:327. doi: 10.3389/fnhum.2020.00327

Nakajima, R., Kinoshita, M., Okita, H., Yahata, T., Matsui, M., and Nakada, M. (2018). Neural networks mediating high-level mentalizing in patients with right cerebral hemispheric gliomas. *Front. Behav. Neurosci.* 12:33. doi: 10.3389/fnbeh.2018.00033

Nakajima, R., Kinoshita, M., Okita, H., Yahata, T., and Nakada, M. (2019). Glioma surgery under awake condition can lead to good independence and functional outcome excluding deep sensation and visuospatial cognition. *Neurooncol. Pract.* 6, 354–363. doi: 10.1093/nop/npy054

Papagno, C., Pisoni, A., Mattavelli, G., Casarotti, A., Comi, A., Fumagalli, F., et al. (2016). Specific disgust processing in the left insula: new evidence from direct electrical stimulation. *Neuropsychologia* 84, 29–35. doi: 10.1016/j.neuropsychologia.2016.01.036

Perry, A., Saunders, S. N., Stiso, J., Dewar, C., Lubell, J., Meling, T. R., et al. (2017). Effects of prefrontal cortex damage on emotion understanding: EEG and behavioural evidence. *Brain* 140, 1086–1099. doi: 10.1093/brain/awx031

Pertz, M., Okoniewski, A., Schlegel, U., and Thoma, P. (2020). Impairment of sociocognitive functions in patients with brain tumours. *Neurosci. Biobehav. Rev.* 108, 370–392. doi: 10.1016/j.neubiorev.2019.11.018

Phan, K. L., Wager, T., Taylor, S. F., and Liberzon, I. (2002). Functional neuroanatomy of emotion: a meta-analysis of emotion activation studies in PET and fMRI. *NeuroImage* 16, 331–348. doi: 10.1006/nimg.2002.1087

Puglisi, G., Sciortino, T., Rossi, M., Leonetti, A., Fornia, L., Conti Nibali, M., et al. (2018). Preserving executive functions in nondominant frontal lobe glioma surgery: an intraoperative tool. *J. Neurosurg.* 131, 474–480. doi: 10.3171/2018.4.JNS18393

Rizzolatti, G., Fadiga, L., Gallese, V., and Fogassi, L. (1996). Premotor cortex and the recognition of motor actions. *Cogn. Brain Res.* 3, 131–141. doi: 10.1016/0926-6410(95)00038-0

Rolland, A., Herbet, G., and Duffau, H. (2018). Awake surgery for gliomas within the right inferior parietal lobule: new insights into the functional connectivity gained from stimulation mapping and surgical implications. *World Neurosurg.* 112, e393–e406. doi: 10.1016/j.wneu.2018.01.053

Saarimäki, H., Gotsopoulos, A., Jääskeläinen, I. P., Lampinen, J., Vuilleumier, P., Hari, R., et al. (2016). Discrete neural signatures of basic emotions. *Cereb. Cortex* 26, 2563–2573. doi: 10.1093/cercor/bhv086

Saito, T., Muragaki, Y., Maruyama, T., Tamura, M., Nitta, M., Tsuzuki, S., et al. (2016). Difficulty in identification of the frontal language area in patients with dominant frontal gliomas that involve the pars triangularis. *J. Neurosurg.* 125, 803–811. doi: 10.3171/2015.8.JNS151204

Shioiri, T., Someya, T., Helmeste, D., and Tang, S. W. (1999). Misinterpretation of facial expression: a cross-cultural study. *Psychiatry Clin. Neurosci.* 53, 45–50. doi: 10.1046/j.1440-1819.1999.00469.x

Southwell, D. G., Hervey-Jumper, S. L., Perry, D. W., and Berger, M. S. (2016). Intraoperative mapping during repeat awake craniotomy reveals the functional plasticity of adult cortex. *J. Neurosurg.* 124, 1460–1469. doi: 10.3171/2015.5.JNS142833

Suslow, T., Kugel, H., Rufer, M., Redlich, R., Dohm, K., Grotegerd, D., et al. (2016). Alexithymia is associated with attenuated automatic brain response to facial emotion in clinical depression. *Prog. Neuropsychopharmacol. Biol. Psychiatry* 65, 194–200. doi: 10.1016/j.pnpbp.2015.10.006

Suzuki, A., Hoshino, T., Shigemasu, K., and Kawamura, M. (2006). Disgust-specific impairment of facial expression recognition in Parkinson's disease. *Brain* 129, 707–717. doi: 10.1093/brain/awl011

Tate, M. C., Herbet, G., Moritz-Gasser, S., Tate, J. E., and Duffau, H. (2014). Probabilistic map of critical functional regions of the human cerebral cortex: broca's area revisited. *Brain* 137, 2773–2782. doi: 10.1093/brain/awu168

Thiebaut de Schotten, M., Urbanski, M., Duffau, H., Volle, E., Levy, R., Dubois, B., et al. (2005). Direct evidence for a parietal-frontal pathway subserving spatial awareness in humans. *Science* 309, 2226–2228. doi: 10.1126/science.1116251

Touroutoglou, A., Lindquist, K. A., Dickerson, B. C., and Barrett, L. F. (2015). Intrinsic connectivity in the human brain does not reveal networks for 'basic' emotions. *Soc. Cogn. Affect. Neurosci.* 10, 1257–1265. doi: 10.1093/scan/nsv013

Tracy, J. L., and Randles, D. (2011). Four models of basic emotions: a review of ekman and cordaro, izard, levenson and panksepp and watt. *Emot. Rev.* 3, 397–405. doi: 10.1177/1754073911410747

Uono, S., Sato, W., Kochiyama, T., Sawada, R., Kubota, Y., Yoshimura, S., et al. (2017). Neural substrates of the ability to recognize facial expressions: a voxel-based morphometry study. *Soc. Cogn. Affect. Neurosci.* 12, 487–495. doi: 10.1093/scan/nsw142

Vytal, K., and Hamann, S. (2010). Neuroimaging support for discrete neural correlates of basic emotions: a voxel-based meta-

analysis. *J. Cogn. Neurosci.* 22, 2864–2885. doi: 10.1162/jocn.2009.21366

Yordanova, Y. N., Duffau, H., and Herbet, G. (2017). Neural pathways subserving face-based mentalizing. *Brain Struct. Funct.* 222, 3087–3105. doi: 10.1007/s00429-017-1388-0

Yuvaraj, R., Murugappan, M., Norlinah, M. I., Sundaraj, K., and Khairiyah, M. (2013). Review of emotion recognition in stroke patients. *Dement. Geriatr. Cogn. Disord.* 36, 179–196. doi: 10.1159/000353440

Zhao, K., Zhao, J., Zhang, M., Cui, Q., and Fu, X. (2017). Neural responses to rapid facial expressions of fear and surprise. *Front. Psychol.* 8:761. doi: 10.3389/fpsyg.2017.00761

Conflict of Interest: The authors declare that the research was conducted in the absence of any commercial or financial relationships that could be construed as a potential conflict of interest.

frontiers in Human Neuroscience

REVIEW
published: 18 February 2021
doi: 10.3389/fnhum.2021.635453

Intraoperative Brain Mapping by Cortico-Cortical Evoked Potential

Yukihiro Yamao[1]*, *Riki Matsumoto*[2], *Takayuki Kikuchi*[2], *Kazumichi Yoshida*[1], *Takeharu Kunieda*[3] and *Susumu Miyamoto*[1]

[1] Department of Neurosurgery, Kyoto University Graduate School of Medicine, Kyoto, Japan, [2] Division of Neurology, Kobe University Graduate School of Medicine, Kobe, Japan, [3] Department of Neurosurgery, Ehime University Graduate School of Medicine, Toon, Japan

To preserve postoperative brain function, it is important for neurosurgeons to fully understand the brain's structure, vasculature, and function. Intraoperative high-frequency electrical stimulation during awake craniotomy is the gold standard for mapping the function of the cortices and white matter; however, this method can only map the "focal" functions and cannot monitor large-scale cortical networks in real-time. Recently, an *in vivo* electrophysiological method using cortico-cortical evoked potentials (CCEPs) induced by single-pulse electrical cortical stimulation has been developed in an extraoperative setting. By using the CCEP connectivity pattern intraoperatively, mapping and real-time monitoring of the dorsal language pathway is available. This intraoperative CCEP method also allows for mapping of the frontal aslant tract, another language pathway, and detection of connectivity between the primary and supplementary motor areas in the frontal lobe network. Intraoperative CCEP mapping has also demonstrated connectivity between the frontal and temporal lobes, likely *via* the ventral language pathway. Establishing intraoperative electrophysiological monitoring is clinically useful for preserving brain function, even under general anesthesia. This CCEP technique demonstrates potential clinical applications for mapping and monitoring large-scale cortical networks.

Keywords: cortico-cortical evoked potential, intraoperative monitoring, large-scale cortical network, brain function, awake craniotomy, electrical stimulation, brain mapping

OPEN ACCESS

Edited by:
Shozo Tobimatsu,
Kyushu University, Japan

Reviewed by:
Eishi Asano,
Children's Hospital of Michigan, United States
Masaki Iwasaki,
National Center of Neurology and Psychiatry, Japan
Stephan Schuele,
Northwestern University, United States

***Correspondence:**
Yukihiro Yamao
yyamao@kuhp.kyoto-u.ac.jp

Specialty section:
This article was submitted to Brain Imaging and Stimulation, a section of the journal Frontiers in Human Neuroscience

Received: *30 November 2020*
Accepted: *21 January 2021*
Published: *18 February 2021*

Citation:
Yamao Y, Matsumoto R, Kikuchi T, Yoshida K, Kunieda T and Miyamoto S (2021) Intraoperative Brain Mapping by Cortico-Cortical Evoked Potential. Front. Hum. Neurosci. 15:635453. doi: 10.3389/fnhum.2021.635453

INTRODUCTION

To preserve brain function postoperatively, it is necessary to identify and have a thorough understanding of the neural connectivity between cortical eloquent areas. This is important to help neurosurgeons in maximally preserving brain function when surgically treating brain lesions.

Intraoperative high-frequency direct electrical stimulation (DES) is a popular method to detect eloquent areas during brain resection. During awake craniotomy, DES introduces a biphasic constant-current stimulation (50–60 Hz) whilst optimizing intraoperative tasks (e.g., motor or language tasks) (Berger et al., 1989; Silbergeld et al., 1992). DES can map the eloquent cortices related to language or higher cognitive functions. The "eloquent" white matter pathways (e.g., association fibers related to language or motor functions) have been extensively identified (Duffau et al., 2005); however, the mechanisms through which DES works are poorly understood, particularly in terms of cortical spreading. Moreover, DES can only map stimulus site regions during awake craniotomy and can cause seizures. Therefore, additional methods are required to detect brain function intraoperatively.

Other methods have recently been developed to probe *in vivo* brain connectivity, including anatomical and functional connectivity. Anatomical connectivity can be described by magnetic resonance imaging (MRI)-based diffusion tractography. Diffusion tractography allows the visualization of *in vivo* large white matter pathways (Catani et al., 2002; Mori and Van Zijl, 2002). This non-invasive technique is widely used for preoperative and intraoperative evaluations, aimed at tracing white matter pathways, which are related to eloquent brain functions; however, these fibers are solely identified by the reflection of anisotropic diffusion of their water molecules through tractography, suggesting that these tracts may not necessarily have the associated function. Combination of tractography with electrophysiological methods such as DES complement each other and help to elucidate brain function.

As an electrophysiological method of probing functional brain connectivity, we review the efficacy of cortico-cortical evoked potentials (CCEPs) in mapping functional brain networks and evaluate its clinical utility in preserving brain function intraoperatively.

CCEP METHOD

Procedure

The CCEP technique was originally introduced as an extra-operative procedure preceding epilepsy surgery (Matsumoto et al., 2004, 2007). To prevent possible seizure induction, CCEP methods are performed after antiepileptic medications are administered. Single-pulse (1 Hz) electrical stimulation (ES) is applied to the cortex, and CCEPs are recorded from functionally connected cortices. The ES comprises a constant-current pulse (square-wave pulse width of 0.1–1 ms) at a fixed frequency of 1 Hz (0.2, 0.5, or 2 Hz), delivered in a bipolar fashion through a pair of adjacent electrodes placed on the cortices. In our intraoperative setting, the intensity is set at 10–15 mA (monophasic square wave pulse, alternating polarity, 0.3 ms duration). An electrocorticogram is recorded at a 1,000–5,000 Hz sampling rate, with the low-frequency filter set at 0.08–1 Hz. The reference electrodes of all subdural electrodes are placed on the skin over the mastoid process of the side contralateral to the implanted electrodes. CCEPs are obtained by averaging the electrocorticogram with a time window from −100 to 500 ms, time-locked to the stimulus. In each session, to confirm the reproducibility of each response, two or three trials of 20–30 stimulations are averaged independently.

CCEP generally comprises an early sharp negative potential (N1: peak latency 10–50 ms) and a consecutive slow negative potential (N2: peak latency 50–300 ms) (Matsumoto et al., 2004; Yamao et al., 2014). An N1 response can occasionally be recorded as a positive potential probably because it represents the positive end of the dipolar activity in the recorded sulcus (Matsumoto et al., 2004; Terada et al., 2008).

General Mechanism of CCEP

The mechanism underlying CCEPs remains unclear. Two mechanisms of impulse propagation have been suggested: (1) cortico-cortical propagation is directly conveyed through white matter fibers; and (2) cortico-subcortico-cortical propagation is indirectly conducted *via* subcortical structures, such as thalamus. A previous CCEP study investigating the parieto-frontal connectivity revealed a linear correlation between the N1 peak latencies and distance from the stimulus to the CCEP response sites (Matsumoto et al., 2012). This supports a direct cortico-cortical pathway rather than an indirect cortico-subcortico-cortical circuit, since the longer the surface distance is, the longer the actual white matter pathway (i.e., conducting time) connecting the two cortical sites is. This hypothesis has been further supported by an intraoperative study that demonstrated CCEP connectivity can be recorded between the anterior (AL) and posterior language areas (PL) (Yamao et al., 2014). Additionally, subcortico-cortical evoked potentials were also recorded from both the AL and PL by single-pulse ES to the arcuate fasciculus (AF) at the floor of the resection cavity. Comparisons between subcortico-cortical evoked potential and CCEP latencies revealed that the first volley from the stimulation, namely the N1 onset, was directly conveyed through the white matter pathway (i.e., the AF; **Figure 1**). The N1 onset response (approximate latency $\leq$10 ms) may represent the fastest monosynaptic impulse conveying the middle or deep cortical layers by the projection of cortico-cortical fibers (Terada et al., 2012). The N2 response may be generated from the surrounding cortex *via* either a local cortico-cortical projection or a cortico-subcortico-cortical reverberating circuit (Matsumoto et al., 2004, 2017).

INTRAOPERATIVE PROBING OF FUNCTIONAL NETWORKS BY CCEPS

Extraoperatively, CCEPs are clinically used to probe functional networks and seizure propagation to identify epileptogenicity *via* subdural or depth electrodes (Matsumoto et al., 2004, 2007, 2017; Koubeissi et al., 2012; Enatsu et al., 2013b, 2015; Matsuzaki et al., 2013; Keller et al., 2014; Mitsuhashi et al., 2020, 2021). CCEP recording is highly practical for various reasons, including that patients are not required to perform any specific task during stimulation and can simply lie on a bed. Moreover, cortico-cortical connectivity can be probed from one stimulus site within 1 min, and seizure induction is extremely rare (0.39% reported in a recent CCEP study) (Kobayashi et al., 2021). Because of the marked practicality and feasibility, CCEP monitoring is now also used in intraoperative settings to probe and monitor functional brain networks, such as those involved in language and motor functions (Kikuchi et al., 2012; Saito et al., 2014; Yamao et al., 2014, 2017b; Enatsu et al., 2016; Tamura et al., 2016; Ookawa et al., 2017; Kanno et al., 2018; Suzuki et al., 2019; Yoshimoto et al., 2019; Nakae et al., 2020; Shibata et al., 2020; Vincent

Abbreviations: AF, arcuate fasciculus; AL, anterior language area; CCEP, cortico-cortical evoked potential; DES, direct electrical stimulation; ES, electrical stimulation; FAT, frontal aslant tract; IFG, inferior frontal gyrus; IFOF, inferior fronto-occipital fasciculus; MEP, motor evoked potential; MRI, magnetic resonance imaging; PL, posterior language area; SEP, somatosensory evoked potential; SMA, supplementary motor area; UF, uncinate fasciculus.

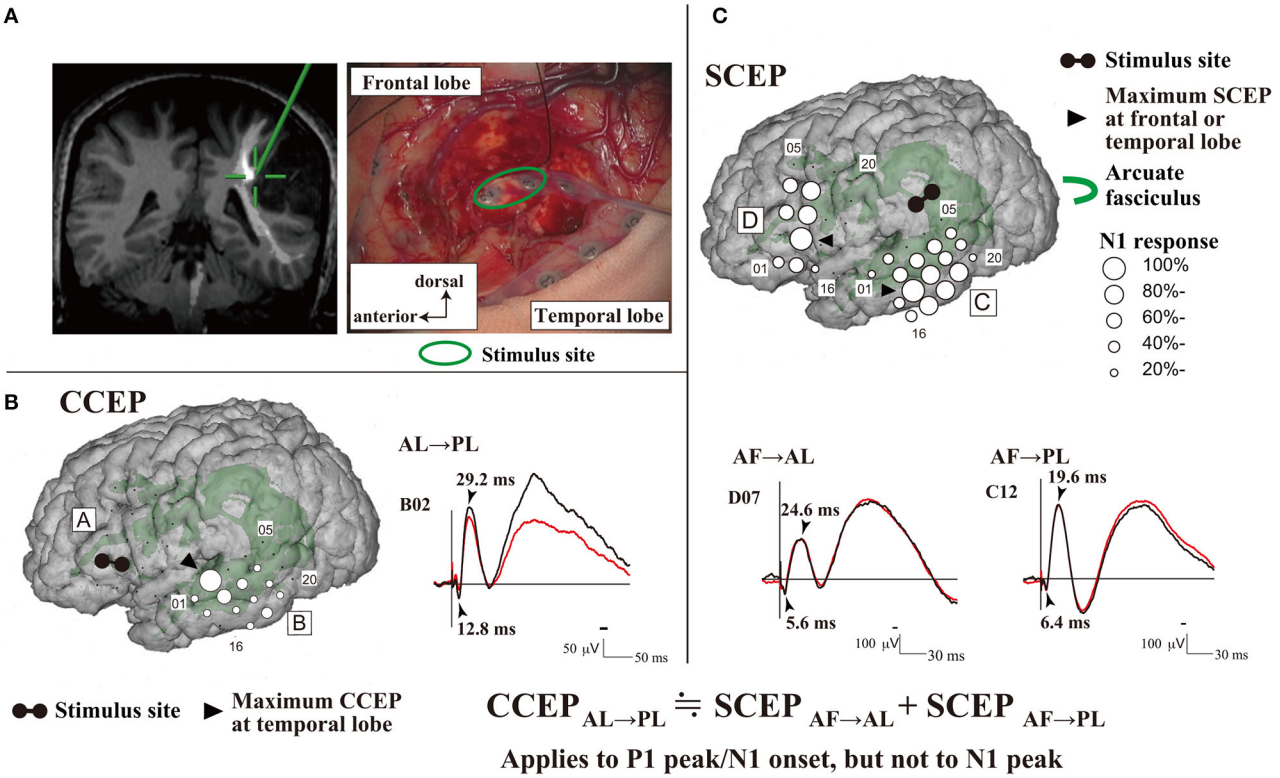

FIGURE 1 | Intraoperative CCEPs and SCEPs. **(A)** The schema of stimulus site (electrode pair, green circle) at the floor of the tumor resection cavity is shown. The stimulus site (green cross) was closely attached to the AF. **(B)** Single-pulse electrical stimulation of the AL produced CCEPs in the temporal lobe. The diameter of the circle at each electrode represents the percentile to the largest amplitude (N1) at the maximum CCEP response site. **(C)** Single-pulse electrical stimulation was applied to the stimulus site (AF), and SCEPs were recorded both from the anterior language area ($SCEP_{AF\rightarrow AL}$, D plate) and posterior language area ($SCEP_{AF\rightarrow PL}$, C plate) at and around the terminations of the AF tract. The diameter of the circle at each electrode represents the percentile to the largest amplitude (N1) at the each maximum $SCEP_{AF\rightarrow AL}$ or $SCEP_{AF\rightarrow PL}$ response site, respectively. Notably, at the maximum response sites, the summation of P1 peak/N1 onset latencies of SCEPs ($SCEP_{AF\rightarrow AL}$ + $SCEP_{AF\rightarrow PL}$, 12.0 ms) was close to the P1 peak/N1 onset latency of $CCEP_{AL\rightarrow PL}$ (12.8 ms). AF, arcuate fasciculus; AL, anterior language area; CCEP, cortico-cortical evoked potential; PL, posterior language area; SCEP, subcortico-cortical evoked potential. Adapted with permission from Yamao et al. (2014).

et al., 2020). CCEP monitoring is also able to detect connection or disconnection of an epileptogenic network during epilepsy surgery (Inoue et al., 2018; Kamada et al., 2018, 2020) (**Table 1**).

Language Function

A dual-stream model for language processing has been recently proposed (Hickok and Poeppel, 2004). The dorsal pathway carries auditory–motor integration by mapping acoustic speech sounds to the articulatory representations, while the ventral pathway serves as a sound-to-meaning interface. Recent tractography and DES studies have demonstrated that the dorsal and ventral pathways primarily involve the AF or superior longitudinal fasciculus, and the uncinate (UF), inferior longitudinal, or inferior fronto-occipital fasciculus (IFOF), respectively (Catani et al., 2005; Duffau et al., 2005).

Intraoperative online sequential recording of motor evoked potentials (MEPs) and somatosensory evoked potentials (SEPs) can map the motor cortices and output pathway (cortico-spinal tract), and the sensory cortices and ascending pathway, respectively, under general anesthesia (Macdonald et al., 2013, 2019). Contrastingly, no intraoperative electrophysiological methods have been established for real-time monitoring of language function under general anesthesia. We recently applied intraoperative CCEPs for intraoperative monitoring of the dorsal language white matter pathway (the AF) mainly in awake patients (Yamao et al., 2014, 2017b), in the following sequence (**Figure 1**):

(1) Subdural electrodes were covered on the ventrolateral frontal and lateral temporoparietal cortices, which were localized based on anatomical criteria or by using preoperative neuroimaging studies (i.e., language-tasked functional MRI and/or diffusion tractography).

(2) Single-pulse ES was applied to the ventrolateral frontal cortices. Based on the CCEP distribution (the largest CCEP connectivity) in the lateral temporoparietal cortices, we determined the stimulus site (the putative AL) and recording site (the putative PL).

(3) To evaluate the integrity of the dorsal language pathway, online sequential $CCEP_{AL\rightarrow PL}$ (stimulating the AL and recording CCEPs from the PL) monitoring was performed under general

TABLE 1 | Intraoperative CCEP and SCEP studies.

TARGET FIBERS	
Language network	
Dorsal pathway	Saito et al., 2014; Yamao et al., 2014, 2017b; Enatsu et al., 2016; Tamura et al., 2016; Kanno et al., 2018; Suzuki et al., 2019; Vincent et al., 2020
Ventral pathway	Nakae et al., 2020
Frontal aslant tract	Ookawa et al., 2017
Motor network	
Pyramidal tract	Enatsu et al., 2016
Short U fibers	Kikuchi et al., 2012; Shibata et al., 2020; Vincent et al., 2020
Epileptogenic network	Inoue et al., 2018; Kamada et al., 2018

CCEP, cortico-cortical evoked potential; SCEP, subcortico-cortical evoked potential.

anesthesia, and in the awake condition by measuring the N1 amplitude at the largest CCEP response site.

(4) When available, DES was also applied only to the AL to confirm the language function, due to the time limitation in the intraoperative setting. To identify the reciprocal connection between the AL and PL, single-pulse ES was also applied to the electrode in the lateral temporoparietal area, and $CCEP_{PL\rightarrow AL}$ was recorded.

The anatomical AL is localized, and projection from the PL to AL is more convergent. Thus, the connection between the two areas appears to be bidirectional, and $CCEP_{AL\rightarrow PL}$ responses are observed to have a larger distribution than $CCEP_{PL\rightarrow AL}$ responses (Matsumoto et al., 2004). Contrarily, the PL areas have a wide distribution, and their functional shifts can affect the surrounding cortices (Enatsu et al., 2013a). Thus, the $CCEP_{AL\rightarrow PL}$ was performed to monitor the dorsal language pathway, and the frontal stimulus site was confirmed as the core AL by using DES in all available cases (Yamao et al., 2017b). By combining 50 Hz and 1 Hz cortical and subcortical ES, we demonstrated that CCEP connectivity could map the AL and PL, even intraoperatively, and that the eloquent subcortical fiber (AF) provided a direct electrophysiological connection to the cortices (AL and PL). Moreover, we found that intraoperative dorsal language network monitoring may be feasible even under general anesthesia or even without full preoperative neuroimaging. $CCEP_{PL\rightarrow AL}$ responses were successfully recorded from the frontal stimulus site of $CCEP_{AL\rightarrow PL}$ in all available cases (Yamao et al., 2017b). Intraoperative dorsal language pathway monitoring by $CCEP_{PL\rightarrow AL}$ was available for tumors in certain locations (Saito et al., 2014; Yamao et al., 2017b).

CCEP has the potential for clinical applications in intraoperative mapping and monitoring of the language network. Based on a small cohort, patients with a 50% N1 decrease only suffer transient language dysfunction; however, one patient with a 51.5% N1 decrease suffered postoperative language dysfunction until their final follow-up, which is likely due to damage to the AF (Yamao et al., 2017b) (**Figure 2**). Although further case accumulation is warranted, this suggests the cut-off value for preserving the dorsal language pathway might be a 50% decrease in the CCEP N1 amplitude, as MEPs and SEPs (Macdonald, 2006; Macdonald et al., 2019; Saito et al., 2019). CCEP amplitudes are increased in the awake condition compared to the general anesthesia condition (Suzuki et al., 2019). Moreover, CCEP distribution, including the maximum CCEP response site, does not change (Yamao et al., 2017a). Even during vascular surgery under general anesthesia, CCEP monitoring is feasible, and it is sensitive to ischemic change, compared to MEPs or SEPs (Yoshimoto et al., 2019). Thus, the CCEP method enables intraoperative monitoring to preserve the dorsal language pathway, even under general anesthesia.

The ventral language pathway has been reported to involve the UF, inferior longitudinal fasciculus, or IFOF (Duffau et al., 2005); however, in previous dissection and tractography studies (Catani et al., 2002; Martino et al., 2011), the cortical terminations of these three fibers did not reach the lateral temporal aspects (i.e., the PL). DES of the UF does not disturb object naming, and thus, resection of the UF is considered acceptable (Duffau et al., 2009). Therefore, the fibers involved in the ventral pathway remain unidentified. In a recent intraoperative CCEP study (Nakae et al., 2020), the pars opercularis of the inferior frontal gyrus (IFG) is connected to the posterior temporal cortices and supramarginal gyrus, whereas the pars orbitalis is connected to the anterior lateral temporal cortices and angular gyrus. The different connectivity of each IFG subdivision to the temporal lobe can result in an anterior–posterior gradient connectivity map (**Figures 3A,B**). The connection between the pars orbitalis of the IFG and anterior lateral temporal lobe implies the existence of a temporal branch of the IFOF, which is referred to as the IFOF-t (**Figure 3C**). The clinical implications of this branch remain unclear, and therefore, further ES studies investigating it are necessary.

Recently, a new language-related white matter fiber pathway has been described in the frontal lobe (Catani et al., 2012). This pathway, the frontal aslant tract (FAT), runs between the supplementary motor area (SMA) and the pars opercularis of the IFG (Catani et al., 2012; Vergani et al., 2014). A DES study revealed that the FAT is associated with verbal fluency as part of the negative motor network (Kinoshita et al., 2015). Therefore, its preservation is also required to prevent postoperative language dysfunction. In another recent study (Ookawa et al., 2017), intraoperative CCEPs were found to describe a cortico-cortical network between the IFG and superior frontal gyrus *via* the FAT, in a reciprocal manner. Thus, the CCEP method also allows for intraoperative monitoring of the FAT.

The dynamics of synchronous or oscillatory patterns of neuronal activity recorded on electrocorticogram have been recently proposed as potential neurophysiological factors of cortical processes (Salinas and Sejnowski, 2001). Notably, high gamma activity, ranging between 60 and 140 Hz, is considered to reflect localized cortical processing, such as language function (Crone et al., 2001). "Passive mapping" by combining high gamma activity and CCEP has been proposed (Tamura et al., 2016). First, real-time high gamma activity mapping of the PL is performed by listening to linguistic sounds. Second, 1 Hz ES is delivered to the identified PL to detect CCEPs in the frontal

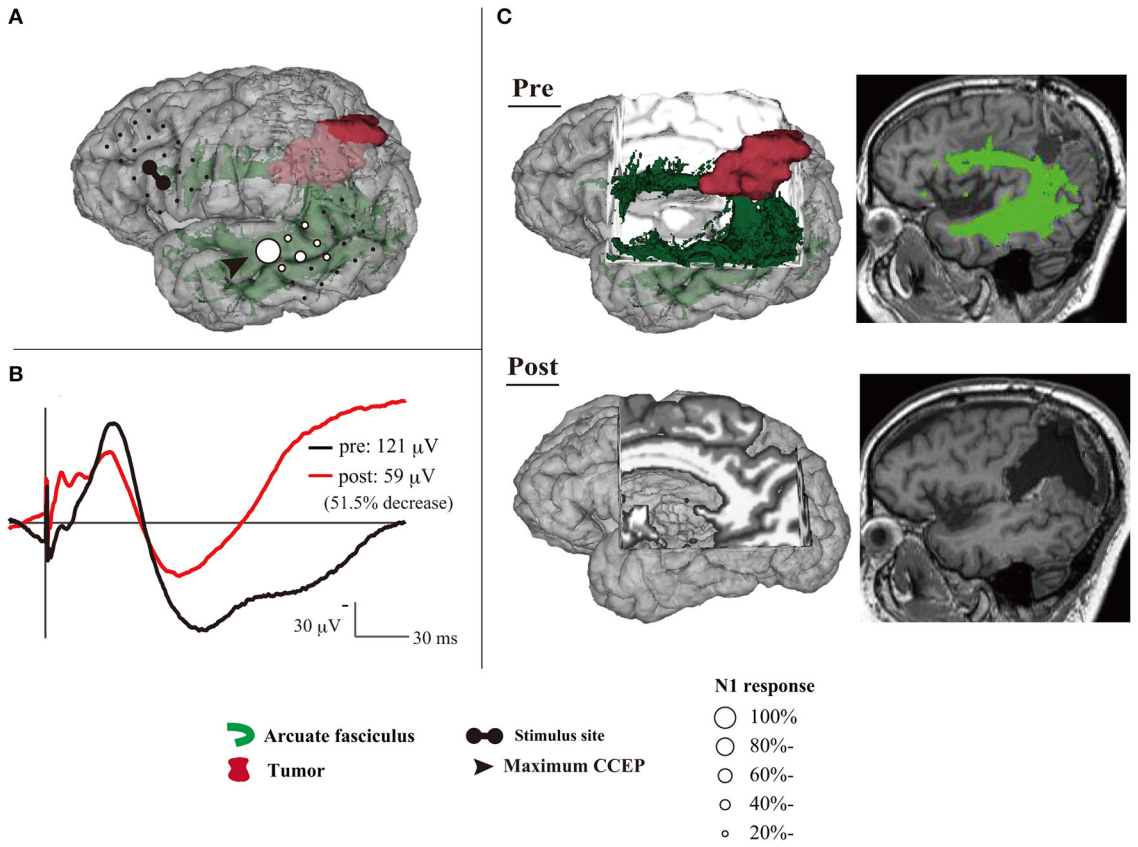

FIGURE 2 | An illustrative case with > 50% decrease of $CCEP_{AL \rightarrow PL}$ N1 amplitude during tumor removal. **(A)** Three-dimensional MRI shows CCEP distribution under general anesthesia, using a circle map. **(B)** The change of N1 waveforms at the maximum $CCEP_{AL \rightarrow PL}$ response site are described. The black line shows the N1 waveform before the tumor removal, and the red line represents the N1 after tumor removal. The N1 amplitude decreased by 51.5% during the tumor removal. **(C)** Two- and three-dimensional MRI reveals that the postoperative AF tract became untraceable. The patient developed further phonemic paraphasia and impairment of repetition after surgery; these symptoms continued until the final follow-up. AF, arcuate fasciculus; CCEP, cortico-cortical evoked potential; MRI, magnetic resonance imaging. Adapted with permission from Yamao et al. (2017b).

lobe (i.e., the AL). Then, the functioning of the AL and PL are confirmed by DES. The sensitivity and specificity of this passive mapping method are reported to be 93.8 and 89%, respectively. This passive mapping technique allows for neurosurgeons to create a new method of brain mapping using CCEPs.

Although additional studies are needed to establish intraoperative monitoring methods, CCEP is an efficient intraoperative method for mapping and preserving language function.

Motor Function

The SMA is an eloquent brain region that controls complex motor functions, such as planning, initiation, learning, and language function, particularly in the dominant hemisphere (Vergani et al., 2014). Surgical resection of the SMA causes contralateral akinesia, mutism or speech disturbances, and difficulties with alternating hand movements, which is referred to as SMA syndrome (Laplane et al., 1977). These symptoms tend to resolve in several weeks, but are occasionally permanent (Krainik et al., 2001). The severity of the symptoms is related to the extent of SMA resection (Fontaine et al., 2002). Therefore, intraoperative mapping and preservation of the SMA are necessary for preserving postoperative motor function, or to minimize the severity of symptoms, analogous to preserving the primary motor area (M1).

The SMA is divided into two functional subdivisions: the pre-SMA and SMA proper. The pre-SMA is related to higher-order aspects of motor control when performing motor tasks, whereas the SMA proper is activated during pure motor function (Picard and Strick, 1996). A previous dissection and tractography study (Vergani et al., 2014) demonstrates that the SMA-proper is connected to the precentral gyrus *via* short U-fibers connecting neighboring gyri. In an extra-operative setting, cortico-cortical functional connections between the lateral motor cortex (including the M1) and the medial motor cortex (including the SMA) are detected using CCEPs (Matsumoto et al., 2007). Additionally, studies have investigated the electrophysiological mapping of the SMA in intra- or extra-operative settings (Usui et al., 2008; Kikuchi et al., 2012).

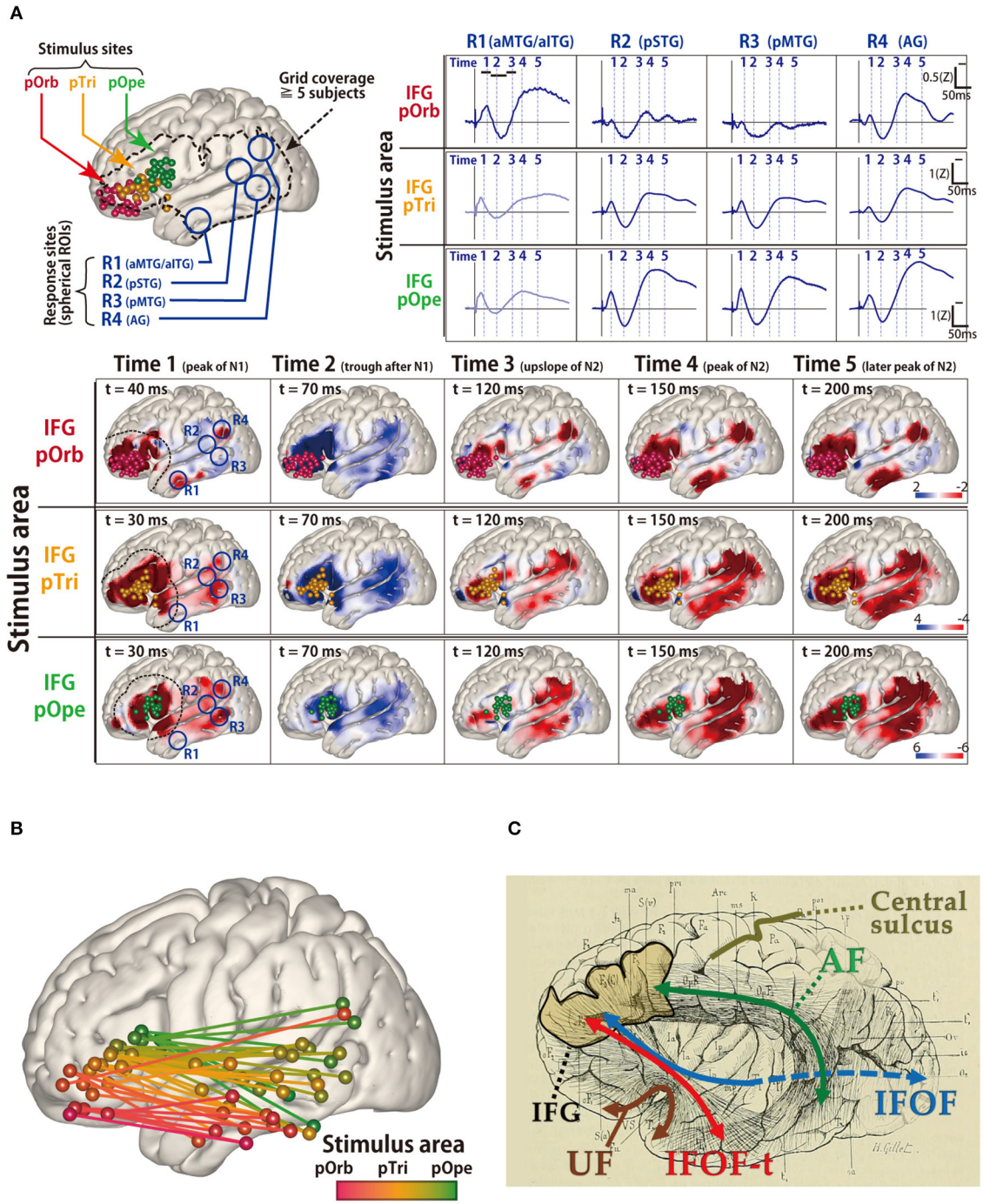

FIGURE 3 | Probing of the perisylvian language pathway by intraoperative cortico-cortical evoked potential (CCEP). **(A)** The CCEP response map at the temporal lobe in 14 patients. (Upper left) MRI shows all stimulus sites in the inferior frontal gyrus (IFG), which are transferred to Montreal Neurosciences Institute space with spheres (red, pOrb; yellow, pTri; green, pOpe). The dotted line represents a recording area. (Upper right) The representative waveforms of the response sites in the four ROIs. The four ROIs were located as follows: R1, anterior parts of the MTG/ITG; R2, posterior part of the STG; R3, posterior part of the MTG; and R4, the AG. (Lower) The table shows the averaged response maps in the time sequence stratified by IFG subdivision. The five time points were set (Time 1; the peak of N1, Time 2; the trough after N1, Time 3; the upslope of N2, Time 4; the peak of N2, and Time 5; the peak of the latest N2). Electrical stimulation of the pOpe elicited CCEP responses widely in the temporoparietal area, while electrical stimulation of the pOrb responses in the anterior part of the MTG and IFG, and AG. By electrical stimulation of the pTri, a mixture of the patterns for the two stimulus areas is elicited. (Upper right) The representative waveforms of the response sites in the four ROIs. The four ROIs were located as follows: R1, the aMTG/aITG; R2, the pSTG; R3, the pMTG; and R4, the AG. **(B)** The schema of the connectivity between the IFG and lateral aspect of temporal lobe detected by CCEP. The gradation from red to green colors shows the transfer from the anterior to the posterior stimulation site at the IFG. **(C)** The schema of the white matter pathways in the vicinity of the IFG, overlaid on the reprinted schema of dissection from the classical textbook "Anatomie des centers

(Continued)

FIGURE 3 | nerveux" (Dejerine and Dejerine-Klumpke, 1895). A fan-shaped fiber is shown which connects the frontal lobe to the anterior part of the temporal lobe through the temporal stem, which is newly referred to as the temporal branch of the IFOF (IFOF-t). AG, angular gyrus; CCEP, cortico-cortical evoked potential; IFOF, inferior fronto-occipital fasciculus; ITG, inferior temporal gyrus; MRI, magnetic resonance imaging; MTG, middle temporal gyrus; pOpe, pars opecularis; pOrb, pars orbitalis; pTri, pars triangularis; ROI, region of interest; STG, superior temporal gyrus. Adapted with permission from Nakae et al. (2020).

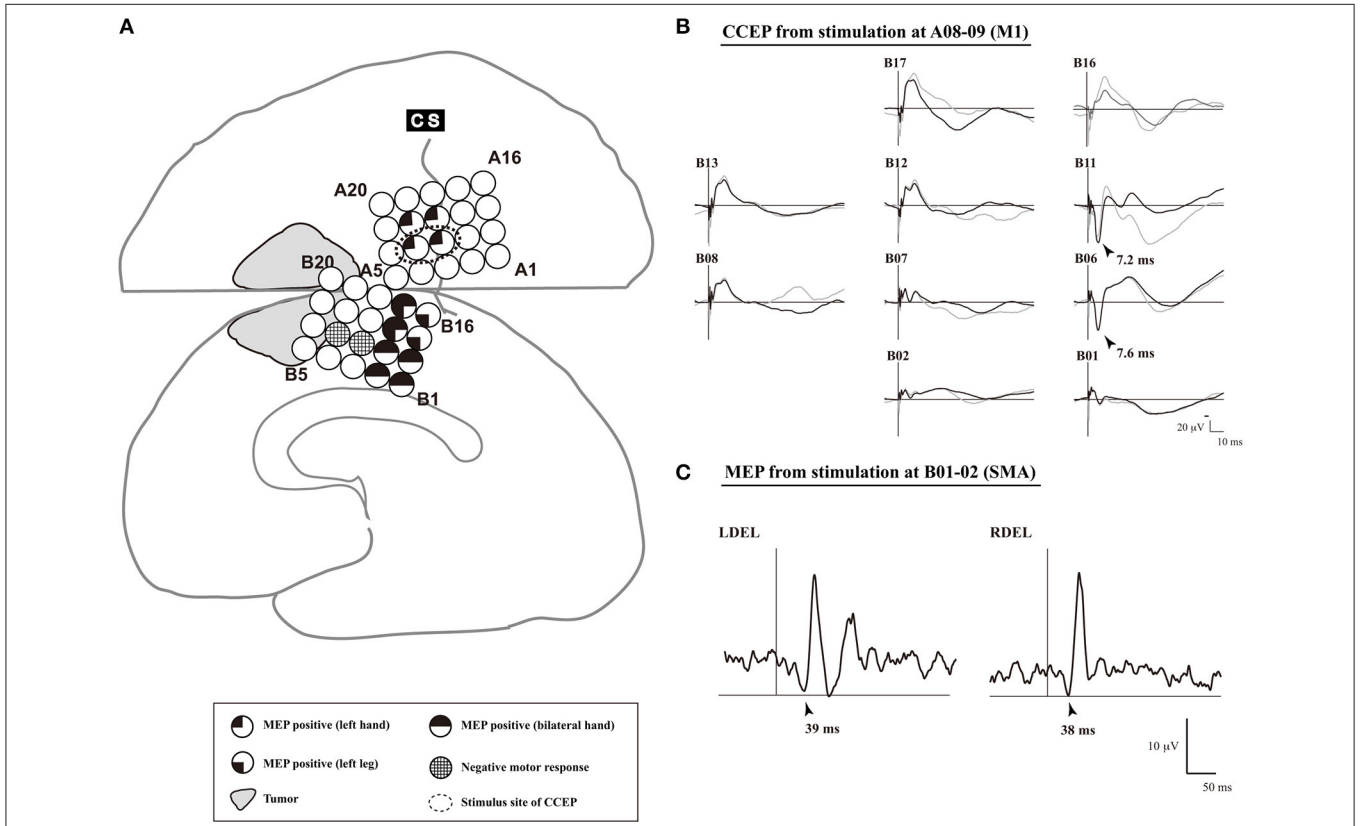

FIGURE 4 | An illustrative case of SMA mapping. **(A)** The schema of cortical mapping by MEPs. Subdural grid electrodes are placed on the right lateral frontoparietal and medial frontal cortices. Single pulse electrical stimulation reveals positive motor functions based on MEPs. In electrodes B08–09, a negative motor response is elicited by 5-train electrical stimulation. **(B)** CCEP waveforms (Plate B). Single-pulse electrical stimulation was applied to a pair of electrodes A08–09 (Plate A), which was defined as the primary motor area of the left hand. Two trials are plotted in superimposition. A large CCEP response was recorded in electrodes B06, B11-13, and B17. The functional brain region associated with those electrodes was confirmed as the SMA by MEP. **(C)** MEP waveforms (electrodes B06–07). MEP was elicited from the bilateral deltoid muscles, and the site of electrodes B06-07 was defined as the SMA. CCEP, cortico-cortical evoked potential; CS, central sulcus; DEL, deltoid muscle; L, left; MEP, motor evoked potential; R, right; SMA, supplementary motor area. Adapted with permission from Shibata et al. (2020) and Yamao et al. (2015).

These studies found that a single-pulse or trains of five high-frequency ES of the SMA proper elicits MEPs with a longer latency than does a similar stimulation of the M1. Mapping using implanted subdural electrodes in an extra-operative setting requires two-stage surgery. Therefore, to reduce the burden on patients, intraoperative mapping of the SMA proper by means of CCEP connectivity in the following sequence was recently proposed (Yamao et al., 2015; Shibata et al., 2020) (**Figure 4**):

(1) Under general anesthesia, subdural electrodes are placed on the lateral frontoparietal and medial frontal cortices to cover the anatomical M1 and SMA.

(2) After recording the SEP obtained with median nerve stimulation, we apply a 5-train ES (with a pulse width of 0.2–0.3 ms at a frequency of 500 Hz, in a bipolar fashion) to the candidate electrodes through a pair of adjacent electrodes, and record the MEP of the contralateral extensor carpi radialis or first dorsal interosseous to detect the M1.

(3) Single-pulse ES is applied to the detected M1, and CCEPs are recorded from the medial frontal cortices, to probe the cortico-cortical connections between the M1 and the SMA proper. The SMA proper is defined by distinguished CCEP N1 responses in the medial frontal area. A 5-train ES is delivered to the estimated SMA proper, to confirm the SMA proper by recording MEPs from the upper and lower extremities.

In a previous study, patients with preservation of the identified SMA proper did not display any new neurological deficits during or after surgery (Shibata et al., 2020). Thus, intraoperative CCEP monitoring can be clinically useful for mapping the SMA proper and preserving permanent motor deficits due to disturbance of the SMA proper. Further case accumulation is necessary to establish methods that can be used even under general anesthesia.

LIMITATIONS

Intraoperative CCEP has some limitations. First, the data were obtained from patients with tumors or epilepsy. Their backgrounds, with regard to drugs, including antiepileptic drugs, location and pathology of the tumors, the grid coverage areas, and stimulus intensities varied across studies, and could have affected the CCEP results. Second, the subdural electrodes used have limitations in terms of spatial resolution and exploration of the cortical sulci (Ookawa et al., 2017). In addition, CCEP data were available only within the coverage area (i.e., the electrode placement area). Due to the lack of information outside this limited area, there may be functional connections other than those detected by CCEP. Third, the mechanisms of CCEP are not yet fully understood. Thus, there is no consensus in measuring N1 or N2 responses to monitor brain function intraoperatively. The integrity of the language pathway was monitored using the maximum N1 amplitude in our previous studies (Yamao et al., 2014, 2017b), while N2 was adapted to monitor the language pathway in another intraoperative study (Saito et al., 2014). Additionally, because of a limited number of cases, a genuine cut-off value for application in intraoperative monitoring for preserving brain function is unclear. Fourth, the anesthetic effects on CCEP responses remains unclear. Intraoperative CCEPs were recorded in the awake surgery by intravenous propofol infusion. The depth of general anesthesia is usually monitored by the bispectral index, and in previous studies (Yamao et al., 2017a; Suzuki et al., 2019), even under deep anesthesia within a bispectral index monitor range of 40 ± 5, CCEPs were available. In previous cases (Jones et al., 2014; Yamao et al., 2017b), CCEPs could also be recorded under general anesthesia by using other intravenous anesthetics (ketamine or etomidate) or volatile anesthetics (sevoflurane or isoflurane). Although CCEPs are feasible under deep anesthesia, future systematic studies are required to clarify the stimulation protocol and anesthetic effects on the CCEPs. Fifth, we do not discuss which tracts from the CCEP connectivity are reflected in the CCEP responses. DES to the white matter pathway is required to detect the tracts beneath the sulci of the cortex or the lesion. Because DES may not be feasible in all cases due to clinical limitations, the combination of 50 Hz with 1 Hz subcortical electrical stimulation may help clarify the function of the CCEP connectivity.

CONCLUSIONS

Many institutions, including our own, have recently reported the use of CCEPs for intraoperative mapping to preserve brain function, such as language and motor function. Although alternative preoperative neuroimaging studies, i.e., functional MRI or diffusion tractography, are still required, intraoperative CCEPs may allow efficient mapping and monitoring of functional networks. This single-pulse ES method may represent a new intraoperative monitoring technique to preserve language or motor function under general anesthesia only, analogous to MEPs or SEPs. We hope that further studies will establish intraoperative CCEP methods under general anesthesia.

AUTHOR CONTRIBUTIONS

YY: data collection, literature review, and manuscript writing. RM, TKi, and TKu: data collection and manuscript review. KY and SM: supervision. All authors contributed to the article and approved the submitted version.

FUNDING

This work was partly supported by JSPS KAKENHI Grant Number 19K18424 (YY), 18K19514, 18H02709, and 20H05471 (RM).

ACKNOWLEDGMENTS

We would like to thank Editage (www.editage.com) for English language editing.

REFERENCES

Berger, M. S., Kincaid, J., Ojemann, G. A., and Lettich, E. (1989). Brain mapping techniques to maximize resection, safety, and seizure control in children with brain tumors. *Neurosurgery* 25, 786–792. doi: 10.1227/00006123-198911000-00015

Catani, M., Dell'acqua, F., Vergani, F., Malik, F., Hodge, H., Roy, P., et al. (2012). Short frontal lobe connections of the human brain. *Cortex* 48, 273–291. doi: 10.1016/j.cortex.2011.12.001

Catani, M., Howard, R. J., Pajevic, S., and Jones, D. K. (2002). Virtual *in vivo* interactive dissection of white matter fasciculi in the human brain. *NeuroImage* 17, 77–94. doi: 10.1006/nimg.2002.1136

Catani, M., Jones, D. K., and Ffytche, D. H. (2005). Perisylvian language networks of the human brain. *Ann. Neurol.* 57, 8–16. doi: 10.1002/ana.20319

Crone, N. E., Hao, L., Hart, J. Jr., Boatman, D., Lesser, R. P., Irizarry, R., et al. (2001). Electrocorticographic gamma activity during word production in spoken and sign language. *Neurology* 57, 2045–2053. doi: 10.1212/WNL.57.11.2045

Dejerine, J., and Dejerine-Klumpke, A. (1895) *Anatomie des centres nerveux: Méthodes générales d'étude-embryologie-histogénèse et histologie*. Rueff: Anatomie du Cerveau.

Duffau, H., Gatignol, P., Mandonnet, E., Peruzzi, P., Tzourio-Mazoyer, N., and Capelle, L. (2005). New insights into the anatomo-functional connectivity of the semantic system: a study using cortico-subcortical electrostimulations. *Brain* 128, 797–810. doi: 10.1093/brain/awh423

Duffau, H., Gatignol, P., Moritz-Gasser, S., and Mandonnet, E. (2009). Is the left uncinate fasciculus essential for language? A cerebral stimulation study. *J. Neurol.* 256, 382–389. doi: 10.1007/s00415-009-0053-9

Enatsu, R., Gonzalez-Martinez, J., Bulacio, J., Kubota, Y., Mosher, J., Burgess, R. C., et al. (2015). Connections of the limbic network: a corticocortical evoked potentials study. *Cortex* 62, 20–33. doi: 10.1016/j.cortex.2014.06.018

Enatsu, R., Kanno, A., Ohtaki, S., Akiyama, Y., Ochi, S., and Mikuni, N. (2016). Intraoperative subcortical fiber mapping with subcortico-cortical evoked potentials. *World Neurosurg.* 86, 478–483. doi: 10.1016/j.wneu.2015.10.043

Enatsu, R., Kubota, Y., Kakisaka, Y., Bulacio, J., Piao, Z., O'connor, T., et al. (2013a). Reorganization of posterior language area in temporal lobe epilepsy: a cortico-cortical evoked potential study. *Epilepsy Res* 103, 73–82. doi: 10.1016/j.eplepsyres.2012.07.008

Enatsu, R., Matsumoto, R., Piao, Z., O'connor, T., Horning, K., Burgess, R. C., et al. (2013b). Cortical negative motor network in comparison with sensorimotor network: a cortico-cortical evoked potential study. *Cortex* 49, 2080–2096. doi: 10.1016/j.cortex.2012.08.026

Fontaine, D., Capelle, L., and Duffau, H. (2002). Somatotopy of the supplementary motor area: evidence from correlation of the extent of surgical resection with the clinical patterns of deficit. *Neurosurgery* 50, 297–303; discussion: 303–295. doi: 10.1227/00006123-200202000-00011

Hickok, G., and Poeppel, D. (2004). Dorsal and ventral streams: a framework for understanding aspects of the functional anatomy of language. *Cognition* 92, 67–99. doi: 10.1016/j.cognition.2003.10.011

Inoue, T., Kawawaki, H., Fukuoka, M., Kim, K., Nukui, M., Kuki, I., et al. (2018). Intraoperative cortico-cortical evoked potentials show disconnection of the motor cortex from the epileptogenic network during subtotal hemispherotomy. *Clin. Neurophysiol.* 129, 455–457. doi: 10.1016/j.clinph.2017.11.026

Jones, S. E., Zhang, M., Avitsian, R., Bhattacharyya, P., Bulacio, J., Cendes, F., et al. (2014). Functional magnetic resonance imaging networks induced by intracranial stimulation may help defining the epileptogenic zone. *Brain Connect* 4, 286–298. doi: 10.1089/brain.2014.0225

Kamada, K., Kapeller, C., Takeuchi, F., Gruenwald, J., and Guger, C. (2020). Tailor-made surgery based on functional networks for intractable epilepsy. *Front. Neurol.* 11:73. doi: 10.3389/fneur.2020.00073

Kamada, K., Ogawa, H., Kapeller, C., Prueckl, R., Hiroshima, S., Tamura, Y., et al. (2018). Disconnection of the pathological connectome for multifocal epilepsy surgery. *J. Neurosurg.* 129, 1182–1194. doi: 10.3171/2017.6.JNS17452

Kanno, A., Enatsu, R., Ookawa, S., Noshiro, S., Ohtaki, S., Suzuki, K., et al. (2018). Interhemispheric asymmetry of network connecting between frontal and temporoparietal cortices: a corticocortical-evoked potential study. *World Neurosurg.* 120, e628–e636. doi: 10.1016/j.wneu.2018.08.137

Keller, C. J., Honey, C. J., Entz, L., Bickel, S., Groppe, D. M., Toth, E., et al. (2014). Corticocortical evoked potentials reveal projectors and integrators in human brain networks. *J. Neurosci.* 34, 9152–9163. doi: 10.1523/JNEUROSCI.4289-13.2014

Kikuchi, T., Matsumoto, R., Mikuni, N., Yokoyama, Y., Matsumoto, A., Ikeda, A., et al. (2012). Asymmetric bilateral effect of the supplementary motor area proper in the human motor system. *Clin. Neurophysiol.* 123, 324–334. doi: 10.1016/j.clinph.2011.06.011

Kinoshita, M., De Champfleur, N. M., Deverdun, J., Moritz-Gasser, S., Herbet, G., and Duffau, H. (2015). Role of fronto-striatal tract and frontal aslant tract in movement and speech: an axonal mapping study. *Brain Struct. Funct.* 220, 3399–3412. doi: 10.1007/s00429-014-0863-0

Kobayashi, K., Matsumoto, R., Usami, K., Matsuhashi, M., Shimotake, A., Kikuchi, T., et al. (2021). Cortico-cortical evoked potential by single-pulse electrical stimulation is a generally safe procedure. *Clin. Neurophysiol.* (in press). doi: 10.1016/j.clinph.2020.12.022

Koubeissi, M. Z., Lesser, R. P., Sinai, A., Gaillard, W. D., Franaszczuk, P. J., and Crone, N. E. (2012). Connectivity between perisylvian and bilateral basal temporal cortices. *Cereb. Cortex* 22, 918–925. doi: 10.1093/cercor/bhr163

Krainik, A., Lehéricy, S., Duffau, H., Vlaicu, M., Poupon, F., Capelle, L., et al. (2001). Role of the supplementary motor area in motor deficit following medial frontal lobe surgery. *Neurology* 57, 871–878. doi: 10.1212/WNL.57.5.871

Laplane, D., Talairach, J., Meininger, V., Bancaud, J., and Orgogozo, J. M. (1977). Clinical consequences of corticectomies involving the supplementary motor area in man. *J. Neurol. Sci.* 34, 301–314. doi: 10.1016/0022-510X(77)90148-4

Macdonald, D. B. (2006). Intraoperative motor evoked potential monitoring: overview and update. *J. Clin. Monit. Comput* 20, 347–377. doi: 10.1007/s10877-006-9033-0

Macdonald, D. B., Dong, C., Quatrale, R., Sala, F., Skinner, S., Soto, F., et al. (2019). Recommendations of the International Society of Intraoperative Neurophysiology for intraoperative somatosensory evoked potentials. *Clin. Neurophysiol.* 130, 161–179. doi: 10.1016/j.clinph.2018.10.008

Macdonald, D. B., Skinner, S., Shils, J., and Yingling, C. (2013). Intraoperative motor evoked potential monitoring - a position statement by the American Society of Neurophysiological Monitoring. *Clin. Neurophysiol.* 124, 2291–2316. doi: 10.1016/j.clinph.2013.07.025

Martino, J., De Witt Hamer, P. C., Vergani, F., Brogna, C., De Lucas, E. M., Vazquez-Barquero, A., et al. (2011). Cortex-sparing fiber dissection: an improved method for the study of white matter anatomy in the human brain. *J. Anat.* 219, 531–541. doi: 10.1111/j.1469-7580.2011.01414.x

Matsumoto, R., Kunieda, T., and Nair, D. (2017). Single pulse electrical stimulation to probe functional and pathological connectivity in epilepsy. *Seizure* 44, 27–36. doi: 10.1016/j.seizure.2016.11.003

Matsumoto, R., Nair, D. R., Ikeda, A., Fumuro, T., Lapresto, E., Mikuni, N., et al. (2012). Parieto-frontal network in humans studied by cortico-cortical evoked potential. *Hum. Brain Mapp.* 33, 2856–2872. doi: 10.1002/hbm.21407

Matsumoto, R., Nair, D. R., Lapresto, E., Bingaman, W., Shibasaki, H., and Lüders, H. O. (2007). Functional connectivity in human cortical motor system: a cortico-cortical evoked potential study. *Brain* 130, 181–197. doi: 10.1093/brain/awl257

Matsumoto, R., Nair, D. R., Lapresto, E., Najm, I., Bingaman, W., Shibasaki, H., et al. (2004). Functional connectivity in the human language system: a cortico-cortical evoked potential study. *Brain* 127, 2316–2330. doi: 10.1093/brain/awh246

Matsuzaki, N., Juhász, C., and Asano, E. (2013). Cortico-cortical evoked potentials and stimulation-elicited gamma activity preferentially propagate from lower- to higher-order visual areas. *Clin. Neurophysiol.* 124, 1290–1296. doi: 10.1016/j.clinph.2013.02.007

Mitsuhashi, T., Sonoda, M., Iwaki, H., Luat, A. F., Sood, S., and Asano, E. (2020). Effects of depth electrode montage and single-pulse electrical stimulation sites on neuronal responses and effective connectivity. *Clin. Neurophysiol.* 131, 2781–2792. doi: 10.1016/j.clinph.2020.09.010

Mitsuhashi, T., Sonoda, M., Jeong, J., Silversterin, B., Iwaki, H., Luat, A., et al. (2021). Four-dimensional tractography animates propagations of neural activation via distinct interhemispheric pathways. *Clin. Neurophysiol.* 132, 520–529. doi: 10.1016/j.clinph.2020.11.030

Mori, S., and Van Zijl, P. C. (2002). Fiber tracking: principles and strategies - a technical review. *NMR Biomed.* 15, 468–480. doi: 10.1002/nbm.781

Nakae, T., Matsumoto, R., Kunieda, T., Arakawa, Y., Kobayashi, K., Shimotake, A., et al. (2020). Connectivity gradient in the human left inferior frontal gyrus: intraoperative cortico-cortical evoked potential study. *Cereb. Cortex* 30, 4633–4650. doi: 10.1093/cercor/bhaa065

Ookawa, S., Enatsu, R., Kanno, A., Ochi, S., Akiyama, Y., Kobayashi, T., et al. (2017). Frontal fibers connecting the superior frontal gyrus to broca area: a corticocortical evoked potential study. *World Neurosurg.* 107, 239–248. doi: 10.1016/j.wneu.2017.07.166

Picard, N., and Strick, P. L. (1996). Motor areas of the medial wall: a review of their location and functional activation. *Cereb. Cortex* 6, 342–353. doi: 10.1093/cercor/6.3.342

Saito, T., Muragaki, Y., Tamura, M., Maruyama, T., Nitta, M., Tsuzuki, S., et al. (2019). Awake craniotomy with transcortical motor evoked potential monitoring for resection of gliomas in the precentral gyrus: utility for predicting motor function. *J. Neurosurg.* 15, 1–11. doi: 10.3171/2018.11.JNS182609

Saito, T., Tamura, M., Muragaki, Y., Maruyama, T., Kubota, Y., Fukuchi, S., et al. (2014). Intraoperative cortico-cortical evoked potentials for the evaluation of language function during brain tumor resection: initial experience with 13 cases. *J. Neurosurg.* 121, 827–838. doi: 10.3171/2014.4.JNS131195

Salinas, E., and Sejnowski, T. J. (2001). Correlated neuronal activity and the flow of neural information. *Nat. Rev. Neurosci.* 2, 539–550. doi: 10.1038/35086012

Shibata, S., Yamao, Y., Kunieda, T., Inano, R., Nakae, T., Nishida, S., et al. (2020). Intraoperative electrophysiologic mapping of medial frontal motor areas and functional outcomes. *World Neurosurg.* 4, 30404–30406. doi: 10.1016/j.wneu.2020.02.129

Silbergeld, D. L., Mueller, W. M., Colley, P. S., Ojemann, G. A., and Lettich, E. (1992). Use of propofol (Diprivan) for awake craniotomies: technical note. *Surg. Neurol.* 38, 271–272. doi: 10.1016/0090-3019(92)90038-O

Suzuki, Y., Enatsu, R., Kanno, A., Yokoyama, R., Suzuki, H., Tachibana, S., et al. (2019). The influence of anesthesia on corticocortical evoked potential monitoring network between frontal and temporoparietal cortices. *World Neurosurg.* 123, e685–e692. doi: 10.1016/j.wneu.2018.11.253

Tamura, Y., Ogawa, H., Kapeller, C., Prueckl, R., Takeuchi, F., Anei, R., et al. (2016). Passive language mapping combining real-time oscillation analysis with cortico-cortical evoked potentials for awake craniotomy. *J. Neurosurg.* 125, 1580–1588. doi: 10.3171/2015.4.JNS15193

Terada, K., Umeoka, S., Usui, N., Baba, K., Usui, K., Fujitani, S., et al. (2012). Uneven interhemispheric connections between left and right primary sensori-motor areas. *Hum. Brain Mapp.* 33, 14–26. doi: 10.1002/hbm.21189

Terada, K., Usui, N., Umeoka, S., Baba, K., Mihara, T., Matsuda, K., et al. (2008). Interhemispheric connection of motor areas in humans. *J. Clin. Neurophysiol.* 25, 351–356. doi: 10.1097/WNP.0b013e31818f4fec

Usui, N., Terada, K., Baba, K., Matsuda, K., Tottori, T., Umeoka, S., et al. (2008). Extraoperative functional mapping of motor areas in epileptic patients by high-frequency cortical stimulation. *J. Neurosurg* 109, 605–614. doi: 10.3171/JNS/2008/109/10/0605

Vergani, F., Lacerda, L., Martino, J., Attems, J., Morris, C., Mitchell, P., et al. (2014). White matter connections of the supplementary motor area in humans. *J. Neurol. Neurosurg. Psychiatry*. 85, 1377–1385. doi: 10.1136/jnnp-2013-307492

Vincent, M. A., Bonnetblanc, F., Mandonnet, E., Boyer, A., Duffau, H., and Guiraud, D. (2020). Measuring the electrophysiological effects of direct electrical stimulation after awake brain surgery. *J. Neural. Eng.* 17:016047. doi: 10.1088/1741-2552/ab5cdd

Yamao, Y., Matsumoto, R., Kunieda, T., Arakawa, Y., Kikuchi, T., Shibata, S., et al. (2015). A possible variant of negative motor seizure arising from the supplementary negative motor area. *Clin. Neurol. Neurosurg.* 134, 126–129. doi: 10.1016/j.clineuro.2015.04.024

Yamao, Y., Matsumoto, R., Kunieda, T., Arakawa, Y., Kobayashi, K., Usami, K., et al. (2014). Intraoperative dorsal language network mapping by using single-pulse electrical stimulation. *Hum. Brain Mapp.* 35, 4345–4361. doi: 10.1002/hbm.22479

Yamao, Y., Matsumoto, R., Kunieda, T., Arakawa, Y., Nakae, T., Kikuchi, T., et al. (2017a). "Anesthetic effect on cortico-cortical evoked potentials during intraoperative dorsal language pathway monitoring," in *The 40th Annual Meeting of the Japan Neuroscience Society* (Makuhari).

Yamao, Y., Suzuki, K., Kunieda, T., Matsumoto, R., Arakawa, Y., Nakae, T., et al. (2017b). Clinical impact of intraoperative CCEP monitoring in evaluating the dorsal language white matter pathway. *Hum. Brain Mapp.* 38, 1977–1991. doi: 10.1002/hbm.23498

Yoshimoto, T., Maruichi, K., Itoh, Y., Takamiya, S., and Kaneko, T. (2019). Monitoring corticocortical evoked potentials during intracranial vascular surgery. *World Neurosurg.* 122, e947–e954. doi: 10.1016/j.wneu.2018.10.179

Conflict of Interest: The authors declare that the research was conducted in the absence of any commercial or financial relationships that could be construed as a potential conflict of interest.

frontiers in Human Neuroscience

REVIEW
published: 02 March 2021
doi: 10.3389/fnhum.2021.612891

Intraoperative Cognitive Mapping Tasks for Direct Electrical Stimulation in Clinical and Neuroscientific Contexts

Linghao Bu[1,2,3,4,5], *Junfeng Lu*[1,2,3,4,5]*, *Jie Zhang*[1,2,3,4,5] *and Jinsong Wu*[1,2,3,4,5]

[1] Department of Neurosurgery, Huashan Hospital, Shanghai Medical College, Fudan University, Shanghai, China, [2] Brain Function Laboratory, Neurosurgical Institute of Fudan University, Shanghai, China, [3] Zhangjiang Lab, Institute of Brain-Intelligence Technology, Shanghai, China, [4] Shanghai Key Laboratory of Brain Function and Restoration and Neural Regeneration, Shanghai, China, [5] Shanghai Clinical Medical Center of Neurosurgery, Shanghai, China

Direct electrical stimulation (DES) has been widely applied in both guidance of lesion resection and scientific research; however, the design and selection of intraoperative cognitive mapping tasks have not been updated in a very long time. We introduce updated mapping tasks for language and non-language functions and provide recommendations for optimal design and selection of intraoperative mapping tasks. In addition, with DES becoming more critical in current neuroscientific research, a task design that has not been widely used in DES yet (subtraction and conjunction paradigms) was introduced for more delicate mapping of brain functions especially for research purposes. We also illustrate the importance of designing a common task series for DES and other non-invasive mapping techniques. This review gives practical updated guidelines for advanced application of DES in clinical and neuroscientific research.

Keywords: direct electrical stimulation, cognitive function, awake surgery, neuroscience, neurophysiology

OPEN ACCESS

Edited by:
Riki Matsumoto,
Kobe University, Japan

Reviewed by:
Tracy L. Luks,
University of California, San Francisco, United States
Liankun Ren,
Capital Medical University, China

***Correspondence:**
Junfeng Lu
junfeng_lu@fudan.edu.cn

Specialty section:
This article was submitted to Brain Imaging and Stimulation, a section of the journal Frontiers in Human Neuroscience

Received: *01 October 2020*
Accepted: *25 January 2021*
Published: *02 March 2021*

Citation:
Bu L, Lu J, Zhang J and Wu J (2021) Intraoperative Cognitive Mapping Tasks for Direct Electrical Stimulation in Clinical and Neuroscientific Contexts. Front. Hum. Neurosci. 15:612891. doi: 10.3389/fnhum.2021.612891

INTRODUCTION

The persevering efforts of Penfield (Penfield and Boldrey, 1937; Penfield, 1958), Ojemann (Ojemann et al., 1989), Duffau (Tate et al., 2014; Rech et al., 2019), Berger (Sanai et al., 2008), and other neurosurgeons (Roux et al., 2003, 2004; Démonet et al., 2011; Wu et al., 2011) in awake surgery coupled with direct electrical stimulation (DES) led to the wide application of DES in identifying the "eloquent area" before lesion resection due to its high effectiveness and reliability. Accumulating evidence lent support to the importance of this technique, which aided in achieving more extensive resection with lower permanent neurological deficits (Sacko et al., 2011; De Witt Hamer et al., 2012; Gerritsen et al., 2019). Apart from clinical application, DES also provides a tremendous opportunity for neurosurgeons to step into neuroscientific research. Unlike traditional lesion studies, DES disturbs temporarily and reversibly the neural activity in a limited brain area or neural network. This method largely avoids the influence of functional reorganization after focal brain damage and provides a causal link between neural substrates and cognitive functions (Desmurget et al., 2013; Vaidya et al., 2019). Following in the footsteps of Penfield's famous cortical homunculus research, other higher-order cognitive functions have been investigated using DES in the past decades pushing forward the frontiers of neuroscience (Sanai et al., 2008; Tate et al., 2014; Rech et al., 2019).

With the increasing popularity of DES in both clinical and scientific research, multiple teams have developed their own intraoperative cognitive mapping tasks, and the brain functions they mapped extend from sensorimotor to language and even non-language functions (Duffau, 2010). However, the details of task design and selection were rarely reported, leading to potential heterogeneity between institutions in mapping results and the efficacy of electrical stimulation. Therefore, a practical and standardized protocol for intraoperative task design and selection is needed in awake surgery. Moreover, with the frontier of neuroscience expanding, traditional tasks no longer fulfill the needs of current research; thus, the design of more complicated mapping tasks has become an important issue.

In this paper, we first summarize the electrical stimulation parameters (current intensity, stimulation duration, stimulation onset) used in DES. Next, we introduce popular tasks for the mapping of cognitive function and further propose a protocol for task selection to guide lesion resection. In addition, recent neuroscientific findings based on DES were reviewed, and an optimal way to design a delicate mapping task series for research purposes was demonstrated. With the increasing popularity of multimodal fusion in both clinical and scientific research, the importance of common task series for different mapping techniques was proposed.

ELECTRICAL STIMULATION PARAMETERS

Current intensity is one of the most important parameters that affects the sensitivity and specificity of DES. During cortical mapping, a bipolar electrode is used to deliver 1 ms (0.5 ms for anodal phase and another 0.5 ms for cathodal phase) biphasic square waves at 60 Hz, which facilitates the excitement of neural cells parallel to the bipolar axis. There are two main mapping strategies with distinct current intensities. Some researchers adopt a "negative mapping strategy" in which the amplitude for each cortical site is increased from 2 mA to a predetermined threshold (usually 6 mA) or until an after discharge is evoked (Sanai et al., 2008; Sarubbo et al., 2013). During cognitive mapping, the current intensity was 0.5–1 mA lower than the intensity determined in motor mapping (Sanai et al., 2008; Sarubbo et al., 2013; Hervey-Jumper et al., 2015). After brain mapping, tumor resection was guided by the "negative sites" that referred to the cortical areas without stimulation-induced motor or language function. Therefore, a minimal cortical exposure was allowed in this strategy. Another mapping strategy, which was used in our institute, focused more on the identification of positive cortical sites. The stimulation also began with the localization of primary sensory or motor area, but the current intensity increased gradually until the detection of sensory or motor changes. This intensity was then used for the cognitive mapping. Even though a larger cortical exposure was needed, more positive sites could be identified with this strategy, which made it more popular in current neuroscientific researches (Duffau et al., 2004; Khan et al., 2014; Tate et al., 2014; Sarubbo et al., 2020). Since the frequency was slightly different among institutes, the charge density/phase is a reliable parameter to describe the current intensity (Gordon et al., 1990). This parameter was widely used in animal studies (Agnew et al., 1983; Agnew and McCreery, 1987) or extraoperative stimulation (Elisevich et al., 2006; Cogan et al., 2016); however, it was rarely used in studies about awake surgery. Gordon et al. (1990) investigated the histological change within the proximity of electrode in the human brain, but the charge density/phase was lower than that commonly applied during intraoperative DES and the influence of electrical stimulation remained unknown. Therefore, further studies are needed to settle the safe threshold of charge density/phase.

Although numerous studies have used DES to reveal the functions of white matter tracts, rarely has a study provided detailed analysis of the current threshold of subcortical mapping (Bello et al., 2007; Duffau et al., 2008; Zemmoura et al., 2015; Puglisi et al., 2019). Most stated that the same intensity for cortical mapping was also used for subcortical mapping (Bello et al., 2007; Fujii et al., 2015; Puglisi et al., 2019). Even though the underlying neurophysiological mechanisms remains unknown and no clinical research is available to verify the efficacy, this strategy is now the only practical way to set current intensity for subcortical mapping and therefore is also the strategy adopted by our institute.

Another stimulation parameter needed to consider is the time course. Normally, the stimulation lasts 1 s for language and other non-language mapping and is applied slightly earlier than stimulus onset. More recently, Morshed et al. (2020) proposed that prolonged stimulation duration resulted in higher sensitivity of DES. With the identification of time course of human cognitive activities, other studies have also attempted to change the temporal relation between electrical stimulation and stimulus to interfere a specific physiological stage (Nakai et al., 2019; Morshed et al., 2020). Further studies are needed on these new mapping protocols.

INTRAOPERATIVE TASKS IN CLINICAL CONTEXT

Language Tasks

Currently, a majority of the DES carried out clinically are performed to locate language areas in the dominant hemisphere. A set of common language mapping tasks (counting, picture naming, reading) has been used since the era of Penfield (Penfield and Boldrey, 1937; Penfield, 1958), with the detailed design and selection of these tasks varying between institutes and countries.

Number Counting

Counting is an automatic speech task that is widely used in language assessment especially in patients who cannot complete complex cognitive tasks (Bookheimer et al., 2000). During language mapping, number counting is carried out first to identify cortical and subcortical structures related to speech output (Fernandez Coello et al., 2013; Mandonnet et al., 2017). The patients are asked to count from 1 to 50, and an interruption without movement (i.e., speech arrest) can be induced when

stimulating the ventral premotor cortex (Sanai et al., 2008; Tate et al., 2014; Wu et al., 2015; Sarubbo et al., 2020), inferior frontal gyrus (Sanai et al., 2008; Wu et al., 2015), or area 55b (Rech et al., 2019), as well as white matter fibers including frontal aslant tract (Kinoshita et al., 2015) and arcuate fasciculus (Duffau, 2015; Sarubbo et al., 2020). Dysarthria is another disruption that is elicited during counting. Dysarthria-related sites are distributed within the lateral precentral and postcentral gyrus over the underlying white matter tracts (e.g., superior longitudinal fasciculus-III) (Tate et al., 2014; Duffau, 2015; Sarubbo et al., 2020) that participate in the articulatory network.

Picture Naming

Picture naming is one of the most widely used tasks in language mapping. Most institutions follow the protocol that was first used byPenfield and Boldrey (1937) and Penfield (1958), and further described in detail by Ojemann and Mateer (1979). In this task, pictures of common objects are presented to patients one by one, and each is shown for 4 s. Patients need to name the object with a carrier phrase "This is a . . ." as soon as possible.

One major advantage of the picture naming task is that it is a "multifunctional" task that can evaluate multiple brain functions including visual recognition, conceptual formation, lexical retrieval, and the final speech output (Gleichgerrcht et al., 2015). Errors can be induced by the disruption of any single stage in naming processing. The most common language interference found in this task is anomia, which is defined as the DES-induced phenomenon in which the patient is able to speak out the carrier phrase but unable to name the object (Sanai et al., 2008) or name with incorrect words. Other errors [e.g., perseveration (Duffau et al., 2005, 2008; Gil Robles et al., 2005; Khan et al., 2014; Mandonnet et al., 2019b), hesitation (Hamberger et al., 2005), and tip-of-the-tongue (Hamberger et al., 2005)] are also reported in the literature. In addition, since speech output can also be assessed by this task, some researchers map speech arrest during picture naming instead of counting (Petrovich Brennan et al., 2007). DES-induced speech arrest can be distinguished from anomia through the inability of saying the carrier phase. **Figure 1** shows an illustrative case of direct electrical mapping with picture naming task.

Although task protocol and the definition of DES-induced errors are relatively consistent, stimulating materials vary among different institutes, and only a few studies report the source of the pictures they used. Compared to image sets found randomly from the Internet, usage of batteries and image sets with normative data available is more recommended. Duffau et al. (2005); Mandonnet et al. (2017, 2019b), and Rech et al. (2019) select pictures from DO 80, which comprises of 80 black-and-white pictures with variables such as frequency, familiarity, and age of acquisition controlled. Some teams advocate the application of the Boston Naming test, which contains 60 line drawings with decreasing frequency. However, both our experience and previous literature (Chen et al., 2014) has revealed that this test contains several objects with relatively low frequency in Chinese (e.g., igloo, harp), which causes a higher probability of false positive. Therefore, cultural adjustment is needed in intraoperative task design. In our institute, the Snodgrass and Vanderwart picture set (Snodgrass and Vanderwart, 1980) is adopted, since the test contains 260 easily recognizable drawings of common objects from different categories and, more importantly, has norms for Mandarin Chinese available (Liu et al., 2011). For teams from other countries, the International Picture-Naming Project (IPNP) provides norms in seven different languages (American English, German, Mexican Spanish, Italian, Bulgarian, Hungarian, and Chinese) for a corpus of 520 drawings including those from the Snodgrass and Vanderwart picture set. Thus, this picture set showed a distinct advantage in language mapping.

In addition, another important point is the selection of drawings. If the difficulty of a naming task is too high, some intraoperative naming errors may not be directly caused by electrical stimulation and further lead to false positive readings. Thus, Little and Friedman (2004) proposed that patients should be trained preoperatively, and pictures that could not be named by most patients should be removed from the intraoperative task. However, no quantitative parameters like frequency, age of acquisition, and familiarity are used in their selection criteria, which deteriorates its practical value for other institutes. Previous psycholinguistic research have demonstrated that familiarity and age of acquisition are two major predictors for naming latencies (Weekes et al., 2007; Liu et al., 2011); thus, we recommend that only pictures with high concept familiarity and low age of acquisition should be included into intraoperative tasks to ensure the reliability of language mapping. Further studies are still needed to determine the cutoff of these parameters in our new selection criteria.

Other Language Mapping Tasks

Besides these two major tasks (counting and picture naming), there are several other language mapping tasks reported in the literature. Several studies demonstrated that stimulating the posterior temporal lobe (Sanai et al., 2008) and inferior parietal lobule (Roux et al., 2004; Sanai et al., 2008; Wu et al., 2015) could induce alexia in word reading task. Tasks such as repetition (Fernandez Coello et al., 2013; Mandonnet et al., 2017; Sarubbo et al., 2020) and writing (Roux et al., 2003; Morrison et al., 2016) are also performed according to the tumor location (e.g., applying repetition task to identify arcuate fasciculus; Moritz-Gasser and Duffau, 2013). Moreover, for multilingual patients, a sentence translation task could be used to protect their function of switching between multiple languages.

In a recent review, Rofes and Miceli (2014) emphasized the importance of tasks with verbs and sentences in language mapping because the daily language activity poses far more demands on the cognitive network than simple automatic speech and picture naming tasks applied in awake surgery. More sophisticated tasks (e.g., auditory naming, sentence comprehension, completion, and reading) could be designed and added into language mapping procedure. These tasks could engage speech output, as well as conceptual formation and lexical retrieval in picture naming tasks, and in addition, higher level language processing such as syntax could also be tackled. Although these tasks are currently rarely applied in clinical

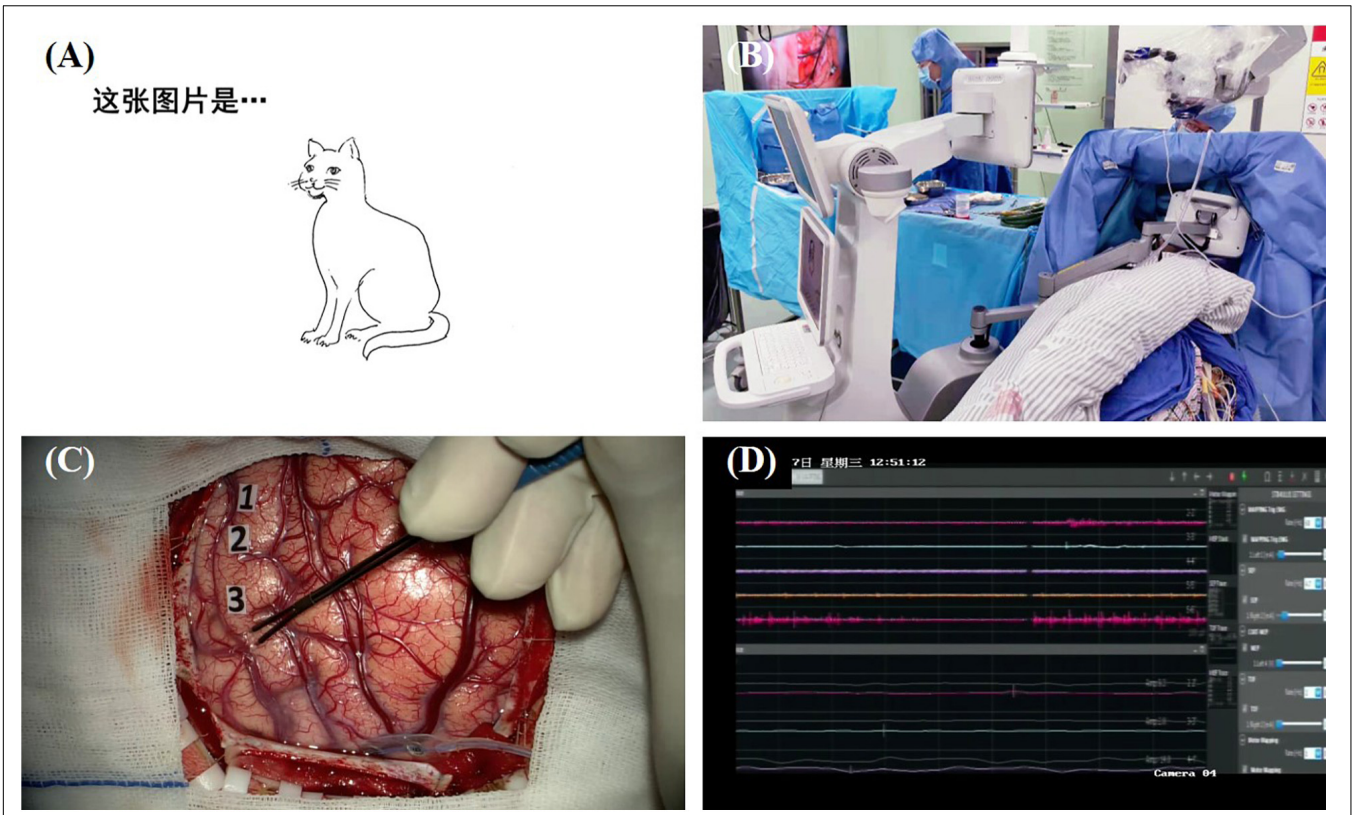

FIGURE 1 | Illustration of direct electrical mapping with picture naming task. **(A)** A series of black-and-white line drawing of a common object is used as stimulating materials; **(B)** a specially designed machine is used to present the stimulus with a moveable screen [*more details about this machine on our forthcoming article (Hameed et al., 2021)*]; **(C)** neurosurgeon applies electrical stimulations with a bipolar electrode and uses sterile tags to mark the positive sites; **(D)** electrophysiological monitoring is used to record after-discharge activity.

setting due to their complexity, these tasks shed light on the sophisticated human language activity.

Non-language Tasks

Despite the increasing application of DES by neurosurgeons in the past few decades (Sanai et al., 2008; De Witt Hamer et al., 2012; Tate et al., 2014; Rech et al., 2019), a majority of cases enrolled are those with lesions within or near the language areas in dominant hemisphere, and only language tasks are applied routinely during surgery. Recently, studies have started focusing on other non-language functions that also have a strong relation with postoperative quality of life (Duffau et al., 2004; Duffau, 2010; Gras-Combe et al., 2012; Fox et al., 2020).

Vision

Visual processing is another important neurological ability used for perceiving the surrounding environment. Previous studies based on non-invasive methods such as functional MRI (fMRI), lesion studies, and electroencephalography have proposed a dual stream network of visual processing. Like language deficits, disruptions in this network may lead to failure of sensory awareness of visual stimulus and interfere with daily activities. In order to protect such a critical function, tasks are added to detect the structures related to visual processing.

Permanent visual field deficit due to disruption of optic radiation is a common postoperative complication of patients with lesions in temporal or occipital lobe. Despite the application of multimodal neuroimaging in visual protection, direct mapping of optic radiation was not achieved by these non-invasive methods. Duffau et al. (2004) first reported that electrical stimulation of optic radiations induced visual disorder during picture naming task in a patient with lesions invading the temporal lobe and the temporo-occipital junction. An intraoperative visual task was later introduced in Gras-Combe et al. (2012). In this task, patients are asked to name the two pictures located diagonally on the screen with their eyes fixed on the center. They reported that all the 14 patients experienced visual symptoms during awake surgery; thus, optic radiations were identified and protected with only one patient having permanent postoperative hemianopia. Recently, an integrated method of visual pathway tracking using both diffusion tensor imaging and DES was reported, indicating the potential advantages of multimodal brain mapping (Mazerand et al., 2017).

Another deficit in visual processing is spatial neglect. Unlike visual field deficit, spatial neglect is an attentional deficit in which the patient has an intact visual field but ignores part of the visual

space. Even though this phenomenon has gained the attention of neurologists and there are extensive number of assessments available, few studies report on a method to protect visuospatial function during neurosurgery. The main reason for this is that visuospatial function is related to non-dominant hemisphere whose cognitive role has long been ignored. Some pioneers have proposed the line bisection task, which could be used to map visuospatial function. In this task, patients are asked to mark the midpoint of a line with a pen or finger. Some researchers have successfully identified that spatial neglect in line bisection task could be induced when electrically stimulating the inferior parietal lobule and the posterior temporal lobe (Thiebaut de Schotten et al., 2005; Démonet et al., 2011; Velasquez et al., 2018), which is consistent with fMRI results. Démonet et al. (2011) reported that no postoperative spatial neglect was found in all 20 cases whose positive sites of line bisection errors were spared, indicating the clinical value of line bisection task. Other neuropsychological tests including clock test and judgment of line orientation for visuospatial function could also be used in awake surgery. Compared to the line bisection task, these tasks are easier to complete during surgery since no hand movement is needed. However, these new tasks have not been widely applied yet, and further investigation is needed to illustrate the reliability of these tasks in DES for minimizing the postoperative spatial neglect.

Other Higher Cognitive Functions

Compared to visual field and visuospatial function, other higher cognitive functions (e.g., calculation, working memory, music) have received lesser attention during surgery. However, these functions are also closely related to patients' quality of life. For example, arithmetic processing is an indispensable brain function for a mass of daily activities, and recently, a few teams have begun using calculation task to prevent permeant acalculia (Duffau et al., 2002; Della Puppa et al., 2013; Della Puppa et al., 2015; Matsuda et al., 2019). Another important issue in mapping higher cognitive functions is that patients have differing demands of their postoperative functions based on their jobs and lifestyles. We have previously reported on a music student with glioma in Broca's area (Zhang et al., 2013). In order to protect her musical ability, two music tasks including humming a popular Chinese song and reading a piece of musical note were performed after routine language mapping. During surgery, two music interference sites were identified and spared. Postoperative evaluation showed that her music function had surprisingly improved slightly relative to the preoperative level.

In addition to the cognitive functions mentioned above, studies have also attempted to locate domain-general cognitive networks involved in emotion and working memory. Thus, more complex tasks like emotion (Gordon et al., 1996; Fox et al., 2020), Stroop test (Wager et al., 2013; Puglisi et al., 2019), and N-back test (Motomura et al., 2018, 2019) were introduced into awake surgery. Fox et al. (2020) showed that stimulation in the limbic system could elicit different emotion responses (e.g., joy, nervousness). For the N-back task, errors could be elicited when stimulating the dorsolateral prefrontal cortex (Motomura et al., 2018, 2019). It is important to note that in most studies (Démonet et al., 2011; Fox et al., 2020), these higher cognitive function tasks are performed solely for scientific purpose instead of function preservation, and the identified neural substrates were resected even though positive sites existed. Therefore, further studies, especially those with large cohorts, are needed to settle their practicability in clinical contexts.

Optimal Selection of Intraoperative Tasks

Varying cognitive mapping tasks available for different cognitive domains are accumulating with the increasing application of DES. However, the maximum duration that patients can stay conscious and complete mapping tasks is about 1 h based on our and others experience (Mandonnet et al., 2019a), which means that tasks used in surgery is tightly limited. Under these circumstances, tasks that integrate multiple cognitive domains are recommended more since several cerebral functions can be evaluated simultaneously.

During tasks selection, the first thing to take into account is the patient's basic information, including job, hobbies, lifestyles, and, more importantly, their preoperative cognitive function. Thus, a set of detailed neuropsychological assessments should be performed to set a baseline for each patient. In our institute, every patient is assessed pre- and postoperatively using a series of comprehensive batteries, including a questionnaire for personal information, the Edinburgh Handedness Inventory for handedness, the Mini-Mental State Examination for potential cognitive impairments, as well as the Boston Naming Test and the Aphasia Battery of Chinese for language function. Calculation and visuospatial function are also evaluated in the Aphasia Battery of Chinese. Based on the assessment results of different cognitive functions, tasks are chosen based on the preoperatively intact or mildly compromised functions deserving more attention.

Characteristics of a tumor, especially its location, is another important factor in task selection. **Figure 2** illustrates the tasks recommended for lesions in different regions. In addition, the role of white matter tracts in cognitive function has been confirmed by multiple studies and Fernandez Coello et al. (2013) proposed that plasticity of white matter tracts made them more crucial in brain function protection. In neurosurgery, these tracts mark the boundary of lesion resection; thus, applying subcortical electrical stimulation to identify these fiber tracts is as important as cortical mapping. Based on the available neuroscientific research results, we present our proposed intraoperative tasks for tumors invading different white mater tracts in **Figure 3**.

Table 1 summarizes common language and non-language tasks that we recommend for clinical practice. Information including hemisphere, lesion location, task design, and responses are also given.

DES AND INTRAOPERATIVE TASKS IN NEUROSCIENTIFIC RESEARCH

In addition to its application as a clinical tool, DES is currently a popular method in neuroscientific research due

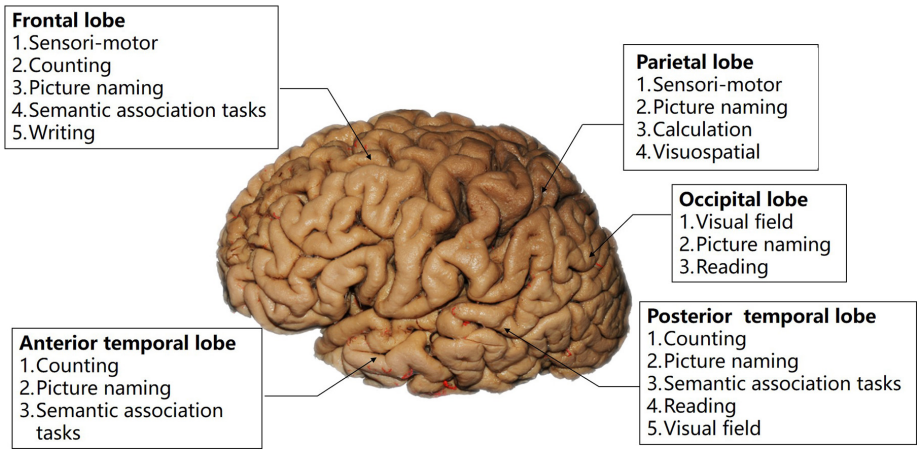

FIGURE 2 | Illustration of the relation between intraoperative tasks and cortical regions.

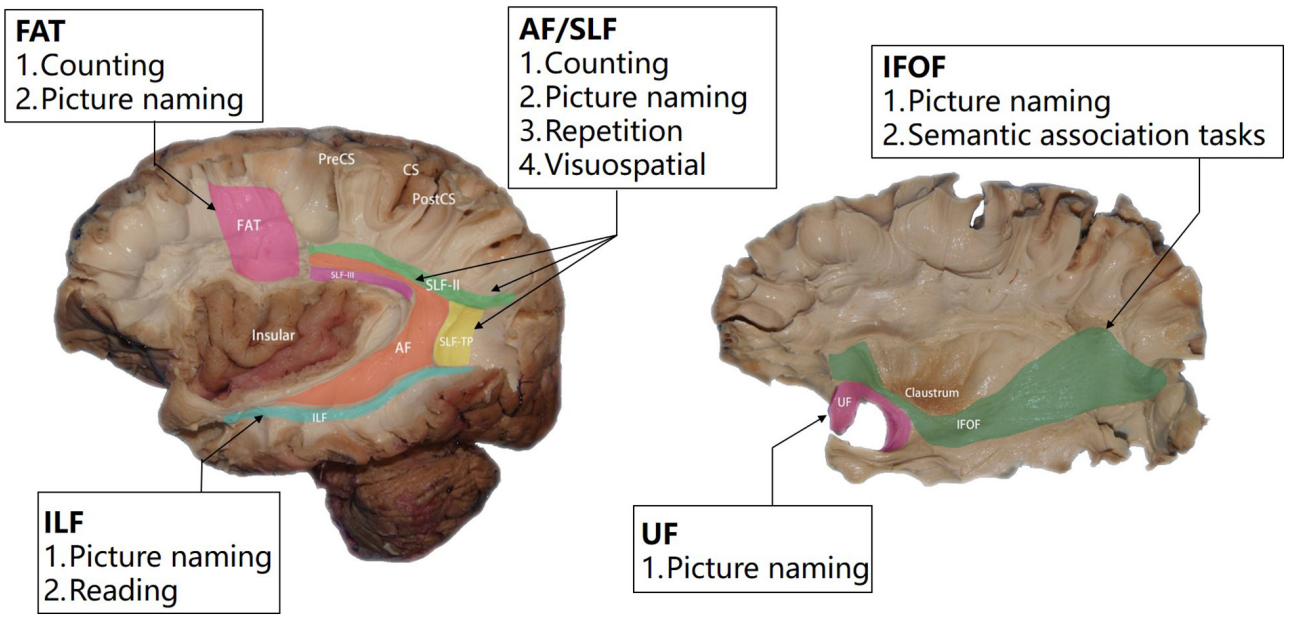

FIGURE 3 | Illustration of the relation between intraoperative tasks and major white matter tracts.

to its ability to probe the causal relation between brain functions and structures.

As mentioned above, DES is mostly performed to identify language areas; therefore, most significant results have been obtained in neurolinguistic research. In the past 20 years, tasks such as counting, picture naming, and reading have been used by different teams to construct the probabilistic maps of language areas. A preliminary consensus had been achieved that key regions for language processing include the pars triangularis, pars opercularis, and ventral precentral gyrus in frontal lobe, as well as the posterior part of temporal lobe (Sanai et al., 2008; Wu et al., 2015; Sarubbo et al., 2020). Language-related white matter tracts were also revealed for the first time using subcortical stimulation, demonstrating the structural connectivity between key language areas. Furthermore, Duffau (2015) proposed a language processing model, which illustrates the anatomical basis of dual stream model of Hickok and Poeppel (Hickok and Poeppel, 2007; Hickok, 2012).

While the general framework of language processing has been constructed, there are still controversies on the exact role that a certain brain region play. Therefore, current neurolinguistic studies focus more on a specific stage in language processing rather than the whole stream. However, traditional tasks, like picture naming, engage plenty of processing stages, and the interruption of each stage could cause dysfunctions. In most

TABLE 1 | Summary of recommended language and non-language tasks.

Cognitive functions		Tasks	Tumor location			Task design		Responses
			Hemis-phere	Cortical regions	WM tracts	Stimulus	Carrier phrase	
Language	Standard	Number counting	L	Perisylvian region	FAT, AF	NA	NA	Speech arrest, dysarthria
		Picture naming	L	Perisylvian region	SLF, AF, IFOF, UF, ILF	Line drawings from *Snodgrass and Vanderwart picture set*	This is a . . .	Speech arrest, dysarthria, anomia, phonological/semantic paraphasia
	Optional	Reading	L	PTL, IPL	IFOF, ILF	Words/Sentences	This word/sentence is . . .	Alexia
		Repetition	L	IPL	AF, SLF	Words/Sentences	NA	Repetition deficit
Non-language		Vision	L, R	TPOJ	Optic radiations	Two line drawings located diagonally on the screen	These two pictures are . . .	Blurred vision, phosphenes, visual field deficit
		Line bisection	R	IPL	SLF	A horizontal line	NA	Spatial neglect
		Calculation	L, R	IPL	SLF	1-digit addition with 1 operand	NA	Hesitation, no answer, incorrect answer

PTL, posterior temporal lobe; IPL, inferior parietal lobule; TPOJ, temporo-parieto-occipital junction; FAT, frontal aslant tract; AF, arcuate fasciculus; SLF, superior longitudinal fasciculus; IFOF, inferior frontal occipital fasciculus; ILF, inferior longitudinal fasciculus; UF, uncinate fasciculus.

studies, despite the generation of spatial map of anomia, it is nearly impossible to identify which stage in language processing was blocked in stimulation-induced anomia. Thus, the functional role of each structure is illustrated by evidence from other modality [e.g., fMRI, electrocorticography (ECoG), lesion studies] rather than direct evidence from DES. To address this issue, some researchers adopted the cognitive subtraction and conjunction paradigms in fMRI studies. These two paradigms usually contain a series of tasks, so, as their names suggest, the subtraction paradigm aims to locate the different processing stage between tasks and the conjunction paradigm is designed to locate the shared one (Price and Friston, 1997). Forseth et al. (2018) combined these two paradigms and compared the disruption of positive sites for a series of tasks including picture naming, naming to definition, sentence repetition, and sensorimotor effects. For the first time, a solid evidence derived from DES was provided to support the role of middle fusiform gyrus as the lexical semantic hub. Another study from Lee and his colleagues also applied the same paradigm and successfully demonstrated that the morphological characteristic in syntax is attributed to a small region within the posterior part of superior temporal gyrus (Lee et al., 2018). Even though the application of this task design strategy is still in its initial stage, an increasing amount of literature using this strategy could be expected since there are abundant task series available for adaptation in previous fMRI studies.

COMMON TASKS FOR DES AND OTHER MODALITIES

Despite its irreplaceable role as the sole reliable method to identify the eloquent neural substrates during surgery, DES, as an invasive mapping method, cannot be applied pre- and postoperatively. Except for the rare studies based on repeated brain mapping in cases with glioma recurrence (Krieg et al., 2014; Southwell et al., 2016), findings on brain plasticity are mainly derived from non-invasive techniques including fMRI, transcranial magnetic stimulation (TMS), and positron emission tomography (PET). Several case reports have tried to investigate the perioperative reorganization of cognitive networks with both DES and other techniques (Krieg et al., 2014; Spena et al., 2015). However, the task variation between techniques in studies affects the reliability of the findings. Therefore, a common task series that could be applied for different modalities is needed for the direct comparison of eloquent structures pre-, intra-, and postoperatively. In our institute, a set of language tasks, including counting, reading, and picture naming, is used in task-fMRI, DES, as well TMS for perioperative language mapping. More tasks for other cognitive domains could also be added into this common task series in our future work. This common task series can be used to not only investigate brain plasticity but also compare the reliability of DES and other non-invasive techniques in brain mapping.

CONCLUSION AND PERSPECTIVE

In spite of the increasing number of institutes applying DES in the clinical context, the design and selection of mapping tasks vary among institutions. In this review, we proposed a practical method for the optimization of existing mapping tasks and personalized selection of tasks based on patients' situation. Such a universal principle in task design and selection may provide guidance for other teams and further eliminate the heterogeneity caused by tasks difference between institutions. Additionally, to

match the advances in neuroscientific research, direction of task design (i.e., subtraction and conjunction paradigms) for the next era of DES studies is discussed, and the importance of combing DES and other techniques is also illustrated.

AUTHOR CONTRIBUTIONS

JW and LB were responsible for the execution, data collection, and manuscript writing. JZ and JL involved in data collection. JW supervised the study and reviewed the manuscript. All authors contributed to the article and approved the submitted version.

FUNDING

This study was funded by the National Natural Science Foundation of China (project no. 81701289), the Shanghai Rising-Star Program (project no. 19QA1401700), the Shanghai Shenkang Hospital Development Center (SHDC12018114), the Shanghai Municipal Science and Technology Major Project (no. 2018SHZDZX01), and ZJLab.

REFERENCES

Agnew, W. F., and McCreery, D. B. (1987). Considerations for safety in the use of extracranial stimulation for motor evoked potentials. *Neurosurgery* 20, 143–147. doi: 10.1097/00006123-198701000-00030

Agnew, W. F., Yuen, T. G., and McCreery, D. B. (1983). Morphologic changes after prolonged electrical stimulation of the cat's cortex at defined charge densities. *Exp. Neurol.* 79, 397–411. doi: 10.1016/0014-4886(83)90221-2

Bello, L., Gallucci, M., Fava, M., Carrabba, G., Giussani, C., Acerbi, F., et al. (2007). Intraoperative subcortical language tract mapping guides surgical removal of gliomas involving speech areas. *Neurosurgery* 60, 67–80; discussion 80-62. doi: 10.1227/01.NEU.0000249206.58601.DE

Bookheimer, S. Y., Zeffiro, T. A., Blaxton, T. A., Gaillard, P. W., and Theodore, W. H. (2000). Activation of language cortex with automatic speech tasks. *Neurology* 55, 1151–1157. doi: 10.1212/wnl.55.8.1151

Chen, T. B., Lin, C. Y., Lin, K. N., Yeh, Y. C., Chen, W. T., Wang, K. S., et al. (2014). Culture qualitatively but not quantitatively influences performance in the Boston naming test in a chinese-speaking population. *Dement. Geriatr. Cogn. Dis. Extra* 4, 86–94. doi: 10.1159/000360695

Cogan, S. F., Ludwig, K. A., Welle, C. G., and Takmakov, P. (2016). Tissue damage thresholds during therapeutic electrical stimulation. *J. Neural. Eng.* 13:021001. doi: 10.1088/1741-2560/13/2/021001

De Witt Hamer, P. C., Robles, S. G., Zwinderman, A. H., Duffau, H., and Berger, M. S. (2012). Impact of intraoperative stimulation brain mapping on glioma surgery outcome: a meta-analysis. *J. Clin. Oncol.* 30, 2559–2565. doi: 10.1200/JCO.2011.38.4818

Della Puppa, A., De Pellegrin, S., d'Avella, E., Gioffre, G., Munari, M., Saladini, M., et al. (2013). Right parietal cortex and calculation processing: intraoperative functional mapping of multiplication and addition in patients affected by a brain tumor. *J. Neurosurg.* 119, 1107–1111. doi: 10.3171/2013.6.JNS122445

Della Puppa, A., De Pellegrin, S., Lazzarini, A., Gioffre, G., Rustemi, O., Cagnin, A., et al. (2015). Subcortical mapping of calculation processing in the right parietal lobe. *J. Neurosurg.* 122, 1038–1041. doi: 10.3171/2014.10.JNS14261

Démonet, J.-F., Lotterie, J.-A., Draper, L., Brauge, D., Boukhatem, L., Lauwers-Cances, V., et al. (2011). Electrostimulation mapping of spatial neglect. *Neurosurgery* 69, 1218–1231. doi: 10.1227/NEU.0b013e31822aefd2

Desmurget, M., Song, Z., Mottolese, C., and Sirigu, A. (2013). Re-establishing the merits of electrical brain stimulation. *Trends Cogn. Sci.* 17, 442–449. doi: 10.1016/j.tics.2013.07.002

Duffau, H. (2010). Awake surgery for nonlanguage mapping. *Neurosurgery* 66, 523–528; discussion 528-529. doi: 10.1227/01.NEU.0000364996.97762.73

Duffau, H. (2015). Stimulation mapping of white matter tracts to study brain functional connectivity. *Nat. Rev. Neurol.* 11, 255–265. doi: 10.1038/nrneurol.2015.51

Duffau, H., Denvil, D., Lopes, M., Gasparini, F., Cohen, L., Capelle, L., et al. (2002). Intraoperative mapping of the cortical areas involved in multiplication and subtraction: an electrostimulation study in a patient with a left parietal glioma. *J. Neurol. Neurosurg. Psychiatry* 73, 733–738. doi: 10.1136/jnnp.73.6.733

Duffau, H., Gatignol, P., Mandonnet, E., Peruzzi, P., Tzourio-Mazoyer, N., and Capelle, L. (2005). New insights into the anatomo-functional connectivity of the semantic system: a study using cortico-subcortical electrostimulations. *Brain* 128(Pt 4), 797–810. doi: 10.1093/brain/awh423

Duffau, H., Peggy Gatignol, S. T., Mandonnet, E., Capelle, L., and Taillandier, L. (2008). Intraoperative subcortical stimulation mapping of language pathways in a consecutive series of 115 patients with Grade II glioma in the left dominant hemisphere. *J. Neurosurg.* 109, 461–471. doi: 10.3171/JNS/2008/109/9/0461

Duffau, H., Velut, S., Mitchell, M. C., Gatignol, P., and Capelle, L. (2004). Intra-operative mapping of the subcortical visual pathways using direct electrical stimulations. *Acta Neurochir. (Wien)* 146, 265–269; discussion 269-270. doi: 10.1007/s00701-003-0199-7

Elisevich, K., Jenrow, K., Schuh, L., and Smith, B. (2006). Long-term electrical stimulation-induced inhibition of partial epilepsy. Case report. *J. Neurosurg.* 105, 894–897. doi: 10.3171/jns.2006.105.6.894

Fernandez Coello, A., Moritz-Gasser, S., Martino, J., Martinoni, M., Matsuda, R., and Duffau, H. (2013). Selection of intraoperative tasks for awake mapping based on relationships between tumor location and functional networks. *J. Neurosurg.* 119, 1380–1394. doi: 10.3171/2013.6.JNS122470

Forseth, K. J., Kadipasaoglu, C. M., Conner, C. R., Hickok, G., Knight, R. T., and Tandon, N. (2018). A lexical semantic hub for heteromodal naming in middle fusiform gyrus. *Brain* 141, 2112–2126. doi: 10.1093/brain/awy120

Fox, K. C. R., Shi, L., Baek, S., Raccah, O., Foster, B. L., Saha, S., et al. (2020). Intrinsic network architecture predicts the effects elicited by intracranial electrical stimulation of the human brain. *Nat. Hum. Behav.* 4, 1039–1052. doi: 10.1038/s41562-020-0910-1

Fujii, M., Maesawa, S., Motomura, K., Futamura, M., Hayashi, Y., Koba, I., et al. (2015). Intraoperative subcortical mapping of a language-associated deep frontal tract connecting the superior frontal gyrus to Broca's area in the dominant hemisphere of patients with glioma. *J. Neurosurg.* 122, 1390–1396. doi: 10.3171/2014.10.JNS14945

Gerritsen, J. K. W., Vietor, C. L., Rizopoulos, D., Schouten, J. W., Klimek, M., Dirven, C. M. F., et al. (2019). Awake craniotomy versus craniotomy under general anesthesia without surgery adjuncts for supratentorial glioblastoma in eloquent areas: a retrospective matched case-control study. *Acta Neurochir.* 161, 307–315.

Gil Robles, S., Gatignol, P., Capelle, L., Mitchell, M. C., and Duffau, H. (2005). The role of dominant striatum in language: a study using intraoperative electrical stimulations. *J. Neurol. Neurosurg. Psychiatry* 76, 940–946. doi: 10.1136/jnnp.2004.045948

Gleichgerrcht, E., Fridriksson, J., and Bonilha, L. (2015). Neuroanatomical foundations of naming impairments across different neurologic conditions. *Neurology* 85, 284–292. doi: 10.1212/WNL.0000000000001765

Gordon, B., Hart, J., Lesser, R. P., and Arroyo, S. (1996). "Chapter 37 Mapping cerebral sites for emotion and emotional expression with direct cortical electrical stimulation and seizure discharges," in *The Emotional Motor System*, eds G. Holstege, R. Bandler, and C. B. Saper (Amsterdam: Elsevier), 617–622.

Gordon, B., Lesser, R. P., Rance, N. E., Hart, J. Jr., Webber, R., Uematsu, S., et al. (1990). Parameters for direct cortical electrical stimulation in the human: histopathologic confirmation. *Electroencephalogr. Clin. Neurophysiol.* 75, 371–377. doi: 10.1016/0013-4694(90)90082-u

Gras-Combe, G., Moritz-Gasser, S., Herbet, G., and Duffau, H. (2012). Intraoperative subcortical electrical mapping of optic radiations in awake surgery for glioma involving visual pathways. *J. Neurosurg.* 117, 466–473. doi: 10.3171/2012.6.JNS111981

Hamberger, M. J., Seidel, W. T., McKhann, G. M. II, Perrine, K., and Goodman, R. R. (2005). Brain stimulation reveals critical auditory naming cortex. *Brain* 128(Pt 11), 2742–2749. doi: 10.1093/brain/awh621

Hameed, N. U. F., Zhao, Z., Zhang, J., Bu, L., Zhou, Y., Jin, L., et al. (2021). A novel intraoperative brain mapping integrated task-presentation platform. *Oper. Neurosurg*. doi: 10.1093/ons/opaa476

Hervey-Jumper, S. L., Li, J., Lau, D., Molinaro, A. M., Perry, D. W., Meng, L., et al. (2015). Awake craniotomy to maximize glioma resection: methods and technical nuances over a 27-year period. *J. Neurosurg.* 123, 325–339. doi: 10.3171/2014.10.JNS141520

Hickok, G. (2012). Computational neuroanatomy of speech production. *Nat. Rev. Neurosci.* 13, 135–145. doi: 10.1038/nrn3158

Hickok, G., and Poeppel, D. (2007). The cortical organization of speech processing. *Nat. Rev. Neurosci.* 8, 393–402. doi: 10.1038/nrn2113

Khan, O. H., Herbet, G., Moritz-Gasser, S., and Duffau, H. (2014). The role of left inferior fronto-occipital fascicle in verbal perseveration: a brain electrostimulation mapping study. *Brain Topogr.* 27, 403–411. doi: 10.1007/s10548-013-0343-5

Kinoshita, M., de Champfleur, N. M., Deverdun, J., Moritz-Gasser, S., Herbet, G., and Duffau, H. (2015). Role of fronto-striatal tract and frontal aslant tract in movement and speech: an axonal mapping study. *Brain Struct. Funct.* 220, 3399–3412. doi: 10.1007/s00429-014-0863-0

Krieg, S. M., Sollmann, N., Hauck, T., Ille, S., Meyer, B., and Ringel, F. (2014). Repeated mapping of cortical language sites by preoperative navigated transcranial magnetic stimulation compared to repeated intraoperative DCS mapping in awake craniotomy. *BMC Neurosci.* 15:20. doi: 10.1186/1471-2202-15-20

Lee, D. K., Fedorenko, E., Simon, M. V., Curry, W. T., Nahed, B. V., Cahill, D. P., et al. (2018). Neural encoding and production of functional morphemes in the posterior temporal lobe. *Nat. Commun.* 9:1877. doi: 10.1038/s41467-018-04235-3

Little, K. M., and Friedman, A. H. (2004). Awake craniotomy for malignant glioma resection. *Int. Congress Series* 1259, 409–414. doi: 10.1016/s0531-5131(03)01727-8

Liu, Y., Hao, M., Li, P., and Shu, H. (2011). Timed picture naming norms for Mandarin Chinese. *PLoS One* 6:e16505. doi: 10.1371/journal.pone.0016505

Mandonnet, E., Herbet, G., and Duffau, H. (2019a). Letter: introducing new tasks for intraoperative mapping in awake glioma surgery: clearing the line between patient care and scientific research. *Neurosurgery* 86, E256–E257. doi: 10.1093/neuros/nyz447

Mandonnet, E., Herbet, G., Moritz-Gasser, S., Poisson, I., Rheault, F., and Duffau, H. (2019b). Electrically induced verbal perseveration: a striatal deafferentation model. *Neurology* 92, e613–e621. doi: 10.1212/WNL.0000000000006880

Mandonnet, E., Sarubbo, S., and Duffau, H. (2017). Proposal of an optimized strategy for intraoperative testing of speech and language during awake mapping. *Neurosurg. Rev.* 40, 29–35. doi: 10.1007/s10143-016-0723-x

Matsuda, R., Tamura, K., Nishimura, F., Nakagawa, I., and Motoyama, Y. (2019). Subcortical calculation mapping during parietal glioma surgery in the dominant hemisphere: a case report. *World Neurosurg.* 121, 205–210. doi: 10.1016/j.wneu.2018.10.046

Mazerand, E., Le Renard, M., Hue, S., Lemee, J. M., Klinger, E., and Menei, P. (2017). Intraoperative subcortical electrical mapping of the optic tract in awake surgery using a virtual reality headset. *World Neurosurg.* 97, 424–430. doi: 10.1016/j.wneu.2016.10.031

Moritz-Gasser, S., and Duffau, H. (2013). The anatomo-functional connectivity of word repetition: insights provided by awake brain tumor surgery. *Front. Hum. Neurosci.* 7:405. doi: 10.3389/fnhum.2013.00405

Morrison, M. A., Tam, F., Garavaglia, M. M., Golestanirad, L., Hare, G. M., Cusimano, M. D., et al. (2016). A novel tablet computer platform for advanced language mapping during awake craniotomy procedures. *J. Neurosurg.* 124, 938–944. doi: 10.3171/2015.4.JNS15312

Morshed, R. A., Young, J. S., Lee, A. T., Berger, M. S., and Hervey-Jumper, S. L. (2020). Clinical pearls and methods for intraoperative awake language mapping. *Neurosurgery* [Epub ahead of print], nyaa440. doi: 10.1093/neuros/nyaa440

Motomura, K., Chalise, L., Ohka, F., Aoki, K., Tanahashi, K., Hirano, M., et al. (2018). Supratotal resection of diffuse frontal lower grade gliomas with awake brain mapping, preserving motor, language, and neurocognitive functions. *World Neurosurg.* 119, 30–39. doi: 10.1016/j.wneu.2018.07.193

Motomura, K., Chalise, L., Ohka, F., Aoki, K., Tanahashi, K., Hirano, M., et al. (2019). Neurocognitive and functional outcomes in patients with diffuse frontal lower-grade gliomas undergoing intraoperative awake brain mapping. *J. Neurosurg.* 132, 1683–1691. doi: 10.3171/2019.3.JNS19211

Nakai, Y., Sugiura, A., Brown, E. C., Sonoda, M., Jeong, J. W., Rothermel, R., et al. (2019). Four-dimensional functional cortical maps of visual and auditory language: intracranial recording. *Epilepsia* 60, 255–267. doi: 10.1111/epi.14648

Ojemann, G., and Mateer, C. (1979). Human language cortex: localization of memory, syntax, and sequential motor-phoneme identification systems. *Science* 205, 1401–1403. doi: 10.1126/science.472757

Ojemann, G., Ojemann, J., Lettich, E., and Berger, M. (1989). Cortical language localization in left, dominant hemisphere. An electrical stimulation mapping investigation in 117 patients. *J. Neurosurg.* 71, 316–326. doi: 10.3171/jns.1989.71.3.0316

Penfield, W. (1958). Some mechanisms of consciousness discovered during electrical stimulation of the brain. *Proc. Natl. Acad. Sci. U.S.A.* 44, 51–66. doi: 10.1073/pnas.44.2.51

Penfield, W., and Boldrey, E. (1937). Somatic motor and sensory representation in the cerebral cortex of man as studied by electrical stimulation. *Brain* 60, 389–443. doi: 10.1093/brain/60.4.389

Petrovich Brennan, N. M., Whalen, S., de Morales Branco, D., O'Shea, J. P., Norton, I. H., and Golby, A. J. (2007). Object naming is a more sensitive measure of speech localization than number counting: converging evidence from direct cortical stimulation and fMRI. *Neuroimage* 37(Suppl. 1), S100–S108. doi: 10.1016/j.neuroimage.2007.04.052

Price, C. J., and Friston, K. J. (1997). Cognitive conjunction: a new approach to brain activation experiments. *Neuroimage* 5(4 Pt 1), 261–270. doi: 10.1006/nimg.1997.0269

Puglisi, G., Howells, H., Sciortino, T., Leonetti, A., Rossi, M., Conti Nibali, M., et al. (2019). Frontal pathways in cognitive control: direct evidence from intraoperative stimulation and diffusion tractography. *Brain* 142, 2451–2465. doi: 10.1093/brain/awz178

Rech, F., Herbet, G., Gaudeau, Y., Mezieres, S., Moureau, J. M., Moritz-Gasser, S., et al. (2019). A probabilistic map of negative motor areas of the upper limb and face: a brain stimulation study. *Brain* 142, 952–965. doi: 10.1093/brain/awz021

Rofes, A., and Miceli, G. (2014). Language mapping with verbs and sentences in awake surgery: a review. *Neuropsychol. Rev.* 24, 185–199. doi: 10.1007/s11065-014-9258-5

Roux, F. E., Boetto, S., Sacko, O., Chollet, F., and Tremoulet, M. (2003). Writing, calculating, and finger recognition in the region of the angular gyrus: a cortical stimulation study of Gerstmann syndrome. *J. Neurosurg.* 99, 716–727. doi: 10.3171/jns.2003.99.4.0716

Roux, F. E., Lubrano, V., Lauwers-Cances, V., Tremoulet, M., Mascott, C. R., and Demonet, J. F. (2004). Intra-operative mapping of cortical areas involved in reading in mono- and bilingual patients. *Brain* 127(Pt 8), 1796–1810. doi: 10.1093/brain/awh204

Sacko, O., Lauwers-Cances, V., Brauge, D., Sesay, M., Brenner, A., and Roux, F. E. (2011). Awake craniotomy vs surgery under general anesthesia for resection of supratentorial lesions. *Neurosurgery* 68, 1192–1198.

Sanai, N., Mirzadeh, Z., and Berger, M. S. (2008). Functional outcome after language mapping for glioma resection. *N. Engl. J. Med.* 358, 18–27. doi: 10.1056/NEJMoa067819

Sarubbo, S., De Benedictis, A., Maldonado, I. L., Basso, G., and Duffau, H. (2013). Frontal terminations for the inferior fronto-occipital fascicle: anatomical dissection, DTI study and functional considerations on a multi-component bundle. *Brain Struct. Funct.* 218, 21–37. doi: 10.1007/s00429-011-0372-3

Sarubbo, S., Tate, M., De Benedictis, A., Merler, S., Moritz-Gasser, S., Herbet, G., et al. (2020). Mapping critical cortical hubs and white matter pathways by direct electrical stimulation: an original functional atlas of the human brain. *Neuroimage* 205:116237. doi: 10.1016/j.neuroimage.2019.116237

Snodgrass, J. G., and Vanderwart, M. (1980). A standardized set of 260 pictures: norms for name agreement, image agreement, familiarity, and visual complexity. *J. Exp. Psychol. Hum. Learn.* 6, 174–215. doi: 10.1037//0278-7393.6.2.174

Southwell, D. G., Hervey-Jumper, S. L., Perry, D. W., and Berger, M. S. (2016). Intraoperative mapping during repeat awake craniotomy reveals the functional plasticity of adult cortex. *J. Neurosurg.* 124, 1460–1469. doi: 10.3171/2015.5.Jns142833

Spena, G., Costi, E., Panciani, P. P., Roca, E., Migliorati, K., and Fontanella, M. M. (2015). Acute functional reactivation of the language network during awake intraoperative brain mapping. *Neurocase* 21, 403–407. doi: 10.1080/13554794.2014.910306

Tate, M. C., Herbet, G., Moritz-Gasser, S., Tate, J. E., and Duffau, H. (2014). Probabilistic map of critical functional regions of the human cerebral cortex: broca's area revisited. *Brain* 137(Pt 10), 2773–2782. doi: 10.1093/brain/awu168

Thiebaut de Schotten, M., Urbanski, M., Duffau, H., Volle, E., Levy, R., Dubois, B., et al. (2005). Direct evidence for a parietal-frontal pathway subserving spatial awareness in humans. *Science* 309, 2226–2228. doi: 10.1126/science.1116251

Vaidya, A. R., Pujara, M. S., Petrides, M., Murray, E. A., and Fellows, L. K. (2019). Lesion studies in contemporary neuroscience. *Trends Cogn. Sci.* 23, 653–671. doi: 10.1016/j.tics.2019.05.009

Velasquez, C., Gomez, E., and Martino, J. (2018). Mapping visuospatial and self-motion perception functions in the left parietal lobe. *Neurosurg. Focus* 45(VideoSuppl. 2), V8. doi: 10.3171/2018.10.FocusVid.18286

Wager, M., Du Boisgueheneuc, F., Pluchon, C., Bouyer, C., Stal, V., Bataille, B., et al. (2013). Intraoperative monitoring of an aspect of executive functions: administration of the Stroop test in 9 adult patients during awake surgery for resection of frontal glioma. *Neurosurgery* 72(2 Suppl. Operative), ons169–ons180; discussion ons180-161. doi: 10.1227/NEU.0b013e31827bf1d6

Weekes, B. S., Shu, H., Hao, M., Liu, Y., and Tan, L. H. (2007). Predictors of timed picture naming in Chinese. *Behav. Res. Methods* 39, 335–342. doi: 10.3758/bf03193165

Wu, J., Lu, J., Zhang, H., Zhang, J., Yao, C., Zhuang, D., et al. (2015). Direct evidence from intraoperative electrocortical stimulation indicates shared and distinct speech production center between Chinese and English languages. *Hum. Brain Mapp.* 36, 4972–4985. doi: 10.1002/hbm.22991

Wu, J. S., Zhang, J., Zhuang, D. X., Yao, C. J., Qiu, T. M., Lu, J. F., et al. (2011). Current status of cerebral glioma surgery in China. *Chin. Med. J. (Engl.)* 124, 2569–2577. doi: 10.3760/cma.j.issn.0366-6999.2011.17.002

Zemmoura, I., Herbet, G., Moritz-Gasser, S., and Duffau, H. (2015). New insights into the neural network mediating reading processes provided by cortico-subcortical electrical mapping. *Hum. Brain Mapp.* 36, 2215–2230. doi: 10.1002/hbm.22766

Zhang, J., Lu, J. F., Wu, J. S., Yao, C. J., Zhuang, D. X., Qiu, T. M., et al. (2013). A unique case of Chinese language and music dissociation with tumor located in Broca's area: multimodal mapping for tumor resection and functional preservation. *Clin. Neurol. Neurosurg.* 115, 2230–2233. doi: 10.1016/j.clineuro.2013.07.011

Conflict of Interest: The authors declare that the research was conducted in the absence of any commercial or financial relationships that could be construed as a potential conflict of interest.

frontiers in Human Neuroscience

REVIEW
published: 10 March 2021
doi: 10.3389/fnhum.2021.619521

Language Mapping Using Stereo Electroencephalography: A Review and Expert Opinion

*Olivier Aron[1,2], Jacques Jonas[1,2], Sophie Colnat-Coulbois[3] and Louis Maillard[1,2]**

[1] Department of Neurology, Nancy University Hospital Center, Nancy, France, [2] CRAN, Université de Lorraine, CNRS, Nancy, France, [3] Department of Neurosurgery, Nancy University Hospital Center, Nancy, France

Stereo-electroencephalography (sEEG) is a method that uses stereotactically implanted depth electrodes for extra-operative mapping of epileptogenic and functional networks. sEEG derived functional mapping is achieved using electrical cortical stimulations (ECS) that are currently the gold standard for delineating eloquent cortex. As this stands true especially for primary cortices (e.g., visual, sensitive, motor, etc.), ECS applied to higher order brain areas determine more subtle behavioral responses. While anterior and posterior language areas in the dorsal language stream seem to share characteristics with primary cortices, basal temporal language area (BTLA) in the ventral temporal cortex (VTC) behaves as a highly associative cortex. After a short introduction and considerations about methodological aspects of ECS using sEEG, we review the sEEG language mapping literature in this perspective. We first establish the validity of this technique to map *indispensable* language cortices in the dorsal language stream. Second, we highlight the contrast between the growing empirical ECS experience and the lack of understanding regarding the fundamental mechanisms underlying ECS behavioral effects, especially concerning the dispensable language cortex in the VTC. Evidences for considering network architecture as determinant for ECS behavioral response complexities are discussed. Further, we address the importance of designing new research in network organization of language as this could enhance ECS ability to map interindividual variability, pathology driven reorganization, and ultimately identify network resilience markers in order to better predict post-operative language deficit. Finally, based on a whole body of available studies, we believe there is strong evidence to consider sEEG as a valid, safe and reliable method for defining eloquent language cortices although there have been no proper comparisons between surgical resections with or without extra-operative or intra-operative language mapping.

Keywords: language, stereo-electroencephalography, basal temporal language area, functional mapping, cortical electrical stimulation, naming, epilepsy

Abbreviations: AD, After Discharges; ALA, Anterior Language Area; BTLA, Basal temporal language area; ECoG, Electrocorticography; ECS, Electrical Cortical Stimulations; ESM, Electrical Stimulation Mapping; HFA, High Frequency Activity; PLA, Posterior Language Area; sEEG, stereo-Electroencephalography; VTC, Ventral Temporal Cortex.

OPEN ACCESS

Edited by:
Jorge Alvaro Gonzalez-Martinez, University of Pittsburgh, United States

Reviewed by:
Eishi Asano, Children's Hospital of Michigan, United States
Shalini Narayana, University of Tennessee Health Science Center (UTHSC), United States

***Correspondence:**
Louis Maillard
l.maillard@chru-nancy.fr

Specialty section:
This article was submitted to Speech and Language, a section of the journal Frontiers in Human Neuroscience

Received: *21 October 2020*
Accepted: *11 February 2021*
Published: *10 March 2021*

Citation:
Aron O, Jonas J, Colnat-Coulbois S and Maillard L (2021) Language Mapping Using Stereo Electroencephalography: A Review and Expert Opinion. Front. Hum. Neurosci. 15:619521. doi: 10.3389/fnhum.2021.619521

INTRODUCTION

Cognitive mapping of the cerebral cortex using electrical cortical stimulation (ESC) is a safe, readily available technique that has largely contributed to current practice in functional neurosurgery. However, it has remained one of the most complex endeavor for functional neurosurgery, especially epilepsy surgery. There is indeed an important gap between the growing empirical experience and the lack of fundamental evidences regarding the mechanisms underlying behavioral effects of electrical cortical stimulation (Borchers et al., 2012). Moreover, its ability to reliably map brain function and predict post-operative outcome is debated when it comes to cortical regions beyond primary cortices.

We chose to review language mapping with sEEG in a way that parallels this debate. We will first address methodological aspects of ECS using sEEG. In the next two sections, we will review and discuss separately the findings of ECS in what Penfield called *indispensable* and *dispensable* eloquent cortices (Penfield, 1954). In *indispensable* language eloquent cortices discussed in the second section, we will mainly address the issue of reliability of ECS for mapping brain areas considering individual variability or pathology driven reorganization. In the last section, focusing on the *dispensable* language eloquent cortices in the ventro-temporal cortex, we will mainly address the pertinence of ECS for mapping language considered as a complex function within distributed dynamic systems organized in spatially segregated modules.

METHODOLOGICAL ASPECTS OF ELECTRICAL CORTICAL STIMULATION USING sEEG

Historical Considerations of ECS

The technique of applying direct electrical stimulation to the human brain has been intimately linked to the development of functional neurosurgery and also to concepts regarding cerebral organization and function. The first ECS of the mammalian cortex performed by Fritsch and Hitzig (1870) provided experimental evidences for a functional segregation of the brain as opposed to the first half of the nineteenth century conception of the brain functioning as a "single unit" (Flourens, 1824). The use of alternating current for ECS in animals by Ferrier (1873) definitely provided reproducible experimental evidence of brain stimulation effects, heralding the functional localization era.

Macewen and Horsley were the first to integrate ECS in their neurosurgical practice in order to map brain functions. They performed in 1886 intraoperative cortical stimulations in a patient presenting seizures starting from the face with no obvious underlying brain lesion and used their ECS localization findings to plan the resection, setting the theoretical and empirical base for functional epilepsy surgery relying on anatomo-clinical correlations (Horsley, 1887; Horsley and Schafer, 1888). These conceptual and technical advances strongly supported Jackson clinical observations on epilepsy and his concept of focal seizures as resulting from a "discharging lesion of the brain" that starts locally and is able to "spread" to the adjacent cortex (Jackson, 1863). Nevertheless, it took almost half a century until Krause and also Foerster, thanks to the progress in anesthesiology, described the epileptogenic or "excitable" cortex and proposed a wider cerebral functional mapping by correlating behavioral effect of ECS with post-operative deficits (Foerster, 1931, 1936). Further progress and the dawn of modern epilepsy came with the discovery of EEG (Berger, 1929), technique that was rapidly integrated by Foerster who also reported the first series of intraoperative cortical EEG recordings (Foerster and Altenburger, 1935). Wilder Penfield, a student of Foerster, who used intraoperative ECS and electrocorticography (ECoG), compiled the most comprehensive and influential studies of brain functional mapping, setting the frame for nowadays methodology for extra and intraoperative cortical stimulations (Penfield and Rasmussen, 1950). He also was the first to report and extensively use ECoG to extra-operatively record and map the human cortex as modern technological advances allowed transition from the "peg" epidural electrodes (Penfield, 1954). Further reports on the safety and efficacy of ECoG have led to its increasing worldwide use that is still on-going (Ojemann, 1983; Wyler et al., 1984; Schaffler et al., 1994; Hermann et al., 1999; Tandon et al., 2019).

Stereo-electroencephalography developed by Talairach and Bancaud emerged as a completely new technique and method with a new philosophy in the mid-1960s in France (Talairach et al., 1962). It allowed extra operative recordings of interictal and more importantly, ictal discharges. Bancaud and Talairach proposed the new concept of epileptogenic zone derived from these recordings and also from electrical cortical stimulation. Since then, ECS during sEEG have been used to both elicit habitual seizures and map brain functions.

The main advantages of sEEG are the ability to target deep structures, and sulci. The targets are chosen according to prior individualized anatomo-electro-clinical hypothesis established on non-invasive work-up (Chauvel and McGonigal, 2014). It further allows bilateral implantation and has low complication rates (Mullin et al., 2016). This method relies on a 3D representation of the epileptogenic zone (EZ) (Kahane et al., 2006), later conceptualized as an epileptogenic network (Bartolomei et al., 2017). The relevance of sEEG for language mapping using ECS has been questioned by some users of ECS with subdural grids (Young et al., 2018). These authors have argued that in contrast to sEEG, subdural grids or strips of circular electrodes placed at the surface of the brain, offered a wider and denser spatial coverage of the cortical surface in a given anatomical area. It is important to keep in mind that sEEG has never aimed at providing a uniform and dense spatial coverage of the brain convexity since it relies on an intra-cortical sampling of distributed regions of interest carefully selected on anatomo-electro-clinical correlations as part of the presumed epileptogenic and propagation networks. The resulting individualized strategy of electrodes implantation not only allows delineating the epileptogenic network but also mapping eloquent cortex (Li et al., 2020). There have been in the past decade a growing interest in sEEG because it allows accessing deep structures such as insula or hippocampus (Salado et al., 2018) and

has a lower complication rates than subdural grids (Tandon et al., 2019; George et al., 2020).

Technical Consideration of Electrical Stimulation Mapping (ESM)

Electrical stimulation mapping can be performed using probe electrodes intra-operatively or extra-operatively using subdural grids and sEEG. Intraoperative setting offers more flexibility in choosing stimulation sites (although limited by the bone window) but is limited by poor testing conditions (short time and limited patient cooperation). Extra operative setting provides fixed pre-established electrode location but better patient cooperation and more extended time or repeated sessions. ECoG uses grids or strips of circular electrodes placed at the surface of the brain with a diameter of 2.4 mm and distanced of 10 mm. sEEG uses deep electrodes inserted in the brain of 0.8–0.86 mm diameter with contacts (5–18 depending of the electrode length) of 2–2.29 mm and distanced of 1.5–10 mm (DIXIT®, ADTech®).

French guidelines on stereo electroencephalography recommend applying ECS between two contiguous contacts of the same electrode using bipolar and biphasic square wave current (Isnard et al., 2018). Two types of stimulations protocols have been recommended:

(1) High frequency, 50 Hz, phase duration of 0.5–1 ms, intensity of 0.5–5 mA and stimulation duration of 3–8 s best suited for functional mapping outside the primary cortices.
(2) Low frequency, 1 Hz, phase duration of 0.5–3 ms, intensity of 0.5–4 mA and stimulation duration of 20–60 s best suited for functional mapping of the primary cortices because of the risk of triggering generalized tonic-clonic seizures.

For language mapping, considering the *intensity of stimulation*, a French team used the above parameters with intensities varying from 0.5 to 2.5 mA (phase duration: 1000 μs) with effects increasing with stimulation intensity. To prevent false negative stimulation the authors concluded that intensities up to at least 1.5 mA were required (Trébuchon and Chauvel, 2016). Other sEEG studies reported comparable parameters (Bédos Ulvin et al., 2017; Arya et al., 2019) applied ECS with intensities up to 8 mA (phase duration: 300 μs) or until the occurrence of behavioral effects, after discharge (AD) or seizure. Higher intensities, up to 10 mA were reported for ECS in anterior language area (ALA) but were also coupled with narrower phase width of 0.3 ms (Alonso et al., 2016). Compared to subdural grids, sEEG stimulation parameters were found to be slightly different. Globally a larger pulse duration is used in sEEG (0.5–1 ms for high frequency ECS protocol and 0.5–3 ms for low frequency ECS protocol) compared to grids (0.30 ms) while stimulation intensity is generally lower in sEEG (1–5 mA) than in grids (1–10 mA). However, density charge remains comparable (see section below) (Donos et al., 2016).

Considering the *frequency of stimulation*, the low frequency protocol tends to lack sensitivity for language mapping (Cuisenier et al., 2020).

Considering delivered *density charge,* this parameter takes into consideration safety issues to avoid possible tissue injury. For both the subdural grids and sEEG electrodes a charge density less than 50 $\mu C/cm^2$ is considered safe. Usual ECS protocols deliver a charge density much lower than this threshold that would require intensities around 8 mA for continuous stimulation up to 50 Hz to be reached (Ritaccio et al., 2018). It is interesting to note that the magnitude of the responses to single-pulse electrical stimulation depends of the charge per phase parameter as amplitude or phase duration can vary in both ways simultaneously (Donos et al., 2016).

Procedural Considerations for Electrical Stimulation Mapping of Language

The general principles of ESM imply a behavioral (positive or negative) response defining the eloquent cortex corresponding anatomically to the stimulated sites. Electrical stimulation is thought to disrupt a particular function at a particular site (Hamberger, 2007). For language, using proper neuropsychological tasks during stimulation is of paramount importance because high order cortex is generally "silent" if not simultaneously tested. Failing to do so results in false negative conclusions and erroneous mapping (Trébuchon et al., 2020). Language ESM studies have converged toward the segregation of three main functional regions coined anterior language area, posterior language area and basal temporal language area (Schaffler et al., 1996; Trébuchon and Chauvel, 2016).

Considering functional organization of language, *basic tasks* such as automatic speech (counting, reciting the alphabet) have been used during ECS. The drawback of those basic language tasks is their low sensitivity as they fail to unveil about 2/3 of language sites detected with more oriented tasks (Schwartz et al., 1999). Most of the epilepsy centers use in their clinical practice *higher level tasks* such as visual naming, auditory description naming, reading, comprehension or verb generation. For a comprehensive review see Hamberger (2007). The advantage of these tasks is, beside their sensitivity, the ability to disentangle different specific language processes and to better address functional specificity of language sites. Of particular interest is visual naming because it is easy to use, disturbed in most forms of aphasia and therefore considered sensitive for language ESM (Ojemann, 1983; Corina et al., 2010). Emerging evidences emphasize auditory confrontation naming especially in mapping basal temporal and lateral temporal language regions (Hamberger et al., 2003).

There is currently no consensus on a unified clinical language testing protocol. It is generally admitted that multiple language tasks specifically oriented to the targeted language site should be used (Wellmer et al., 2009). Specifically for sEEG ESM, most of the centers use visual naming and consider this task relevant for all language areas (Trébuchon and Chauvel, 2016; Arya et al., 2019) specifically analyzed the effect of task according to stimulated regions. Results indicate that naming and reading are the most sensitive tasks for the majority of studied regions. Naming seems more sensitive for the ALA (generally assigned to the posterior part of the inferior frontal gyrus corresponding cyto-architectonically to Broadman areas BA44 and BA45 – as discussed in the following sections), middle and posterior

VTC and lateral temporal cortex. Automatic speech was the least sensitive task although one team successfully managed to find ALA in all patients using a speech arrest task (Alonso et al., 2016). Visual naming coupled with a control semantic matching task was used in Bédos Ulvin et al. (2017) for the basal temporal language area (BTLA – located generally from 2 to 9 cm from the temporal pole in the VTC and whose ECS evoke language disturbances – as discussed in the following sections). These authors reported a clear-cut dissociation between these two tasks with a preserved performance at the control semantic matching task at the sites whose stimulation evoked anomia or paraphasia. They also reported right and left positive sites (whose ECS determine naming impairment) across patients but strictly unilateral at the individual level, suggesting that the BTLA was strongly lateralized, and could be a marker of hemispheric dominance. *Passive Mapping* based on intracranial recordings during linguistic tasks have also been widely used to map human language regions (Martin et al., 2019). Complex and specific linguistic tasks are designed in cognitive research protocols using sEEG (Lochy et al., 2018) in order to consider multiple steps underlying reading processes or multiple modalities, e.g., auditory, visual as well as other complex cerebral function as memory (Llorens et al., 2011; Cuisenier et al., 2020). Intracranial studies have been used to map the auditory and visual language networks at the whole-brain level (e.g., Nakai et al., 2017). Particularly, the auditory naming task was suggested to recruit the left frontal region more extensively than picture naming (Nakai et al., 2019).

Seizures (Bank et al., 2014) or sustained electrical after discharges (AD) evoked during ESM (or appearing a few seconds after) can be observed. AD presence is proportional to the charge density of the stimulation (Donos et al., 2016) and its functional signification has remained elusive (Blume et al., 2004). It appears that both intra and inter patient high variability exists across different brain region regarding the threshold for AD but none of the analyzed patient characteristics predicted its occurrence (Corley et al., 2017). Interestingly, the behavioral threshold was below the AD threshold in gray matter but not white matter in a recent sEEG study (Arya et al., 2019). Findings might also depend on the orientation and location of stimulated sites. In this matter, sEEG differs dramatically from subdural grids as sEEG contacts are intra-cortical and have a variable orientation in relation to cortical layers as opposed to subdural grids where contacts are parallel to the cortical surface. Using pre-medication with phenytoin before ECS language mapping was found to decrease the cortical excitability threshold and ECS induced seizure but not affecting the temporal language threshold (Arya et al., 2018). This pharmacological approach is generally not used in adults. Overall, it is believed that language disturbance in the presence of AD results from a wider effect of stimulation. In this line, assessing AD threshold is useful because it would allow inferring a more local and specific effect of ECS when language disturbance is obtained below this threshold. In the absence of language disturbance, it is recommended to increase intensity of ECS up to the AD threshold in order to maximize sensitivity (Trébuchon and Chauvel, 2016).

Electrical stimulation mapping using SEEG is considered to be safe in children as demonstrated by Taussig et al. (2014) and by an Italian team in very young children (Cossu et al., 2012). Specific elements as the early impact of epilepsy on language and myelination should be considered. Developmental lesion and early onset seizures are thought to not displace language cortex from prenatally determined sites but acquired lesions before the age of 5 may relocate language areas to the opposite hemisphere (Duchowny et al., 1996). Stimulation parameters should be adapted as a subdural electrodes study showed that with age, current thresholds decrease and the probability for AD or seizure occurrence increases (Aungaroon et al., 2017). Similar results were found using sEEG. In contrast to subdural electrodes, mean behavioral thresholds were below mean AD thresholds. This may be explained by the more focal stimulation in SEEG, limited to cortical layer (Arya et al., 2019). In one subdural grids study, phenytoin was used in order to decrease the incidence of iatrogenic seizures in children (Arya et al., 2018). "Ecologic" language tasks (language production as counting, reading a book aloud or spontaneously generating speech) were used by a team while performing language mapping with sEEG. Speech arrest were found on eight out of 184 depth electrode contacts in three patients using stimulation intensities between 2 and 5 mA while 6 mA (phase duration of 0.3 ms) was the maximum stimulation for the negative contacts (de Ribaupierre et al., 2012).

MAPPING INDISPENSABLE ELOQUENT LANGUAGE CORTEX USING sEEG

Electrical cortical stimulation was the first technique to provide experimental proof for the concept of functional brain localization (Fritsch and Hitzig, 1870). Reproducible behavioral responses during ECS under strict methodological conditions allow delineating the eloquent cortex for a specific function. Observing strong correlations with postoperative outcome after resections of such eloquent areas, Penfield further differentiated indispensable eloquent cortex (whose resection would be associated with permanent and significant deficit) from dispensable eloquent cortex (whose resection would lead mostly to minimal and/or reversible functional deficit) (Penfield, 1954). In this section we will address the following question: are ECS induced deficits able to predict a severe and permanent postoperative deficit? This correlation was clearly established in the primary motor cortex (Laplane et al., 1977) where the ECS induced deficit closely correlated with the post-operative deficit, respecting the somatotopy of the central sulcus. But does it hold true for language mapping and where?

Anterior language area is generally assigned to the posterior part of the inferior frontal gyrus corresponding cyto-architectonically to Broadman areas BA44 and BA45, with some authors suggesting a larger representation including areas 47 and 46 (Ardila et al., 2016) as represented in **Figure 1A**. Anterior eloquent language cortex (corresponding to the ECS definition) was extensively studied in 117 patients by Ojemann using intra-operative ECS (Ojemann et al., 1989) and found to be usually organized in patches limited to one or two

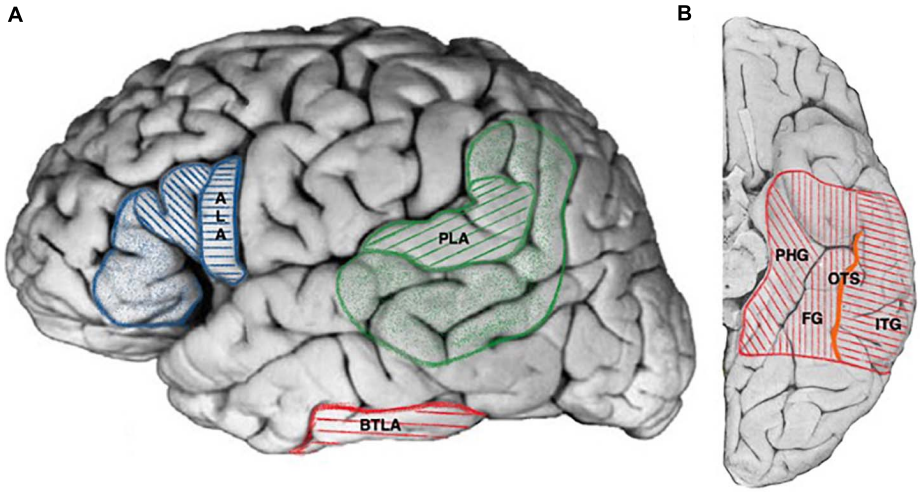

FIGURE 1 | Cortical projections of human language areas. Hatched areas for projections common to all publications, colored areas for extended and debated limits (see text for details). **(A)** Lateral view, ALA, anterior language area (blue, hatched areas: pars opercularis, pars triangularis of the frontal operculum; colored areas: pars orbitalis of the frontal operculum), PLA, posterior language area (green hatched areas: posterior part of the superior temporal gyrus, angular gyrus, colored areas: posterior part of the middle temporal gyrus including the inferior temporal sulcus, supra-marginal gyrus, part of the angular gyrus), BTLA, basal temporal language area (red). **(B)** Ventral view, BTLA (red hatched area). PHG, parahippocampal gyrus; FG, fusiform gyrus; ITG, inferior temporal gyrus; OTS, occipito-temporal sulcus (orange).

centimeters-square with clear cut borders most of the times in the close anterior vicinity of the ventral premotor cortex. Although intra-operative setting allowed the neurosurgeon to "freely" apply bipolar ECS to exposed sites, ECS did not allow localizing eloquent frontal cortex in 21% of patients. In another extensive study using extra-operative ECoG in 45 patients (Schaffler et al., 1996), the authors found anterior eloquent language cortex within the same cortical region but with less inter-individual variation. The authors failed to find anterior eloquent cortex in 30% of the patients. Discrepancies could be explained by the technical differences between extra-operative (fixed electrodes) and intra-operative settings. Despite the facts that ECS were able to map discrete location of the anterior eloquent language cortex that were predictable based on cortical anatomy (Quiñones-Hinojosa et al., 2003), for other authors, the discrete and variable localizations between individuals reflected the lack of reliability of anatomical landmarks alone to localize ALA (Ojemann et al., 1989; Pouratian and Bookheimer, 2010). Indeed, anatomical landmarks can vary largely across normal individuals (Ebeling et al., 1989) and brain pathology can further alter the ability to anatomically localize specific language regions (Skirboll et al., 1996), stressing the importance of an individual assessment of the ALA by ECS.

Posterior language area (PLA) resides in the posterior part of the superior and middle temporal gyrus, angular gyrus, and supramarginal gyrus (Penfield and Rasmussen, 1950; Ojemann, 1991; Ardila et al., 2016) as represented in **Figure 1A**. It was extensively studied with intra-operative (Ojemann, 1991) and extra-operative ECS (Schaffler et al., 1996). Both studies found discrete and limited regions whose stimulation interfered with language as in the case of anterior eloquent language cortex. Ojemann (1979) emphasized that "The Wernicke language area of the classical model is clearly an artifact of combining the locations of these essential areas in different patients, for rarely if ever are essential language areas covering the entire classical Wernicke area found in an individual patient." In the same perspective other authors found language sites at an average on three adjacent cortical electrodes although with a range or 1–7 (1.9 for ALA) (Schaffler et al., 1996).

Few studies have correlated the ECS functional mapping findings (eloquent language cortex) with post-operative language outcome in order to infer indispensable language cortex. However, in an elegantly designed study on low grade glioma awake surgery, Ius et al. (2011) proposed the concept of "minimal common brain." Using intra-operative ECS functional mapping, they observed that the anterior language area can be largely and safely resected provided that a small portion of cortex located anterior to the left ventral premotor cortex and contiguous to subcortical language tracts was spared. The same observation holds true for the angular gyrus and posterior part of the superior temporal gyrus for the indispensable eloquent posterior language area. It is generally admitted that a resection limit of 1 cm from a language site determined by ECS must be observed in order to not produce permanent and important deficit (Ojemann, 1979). Moreover, authors reported total resection of the classical anterior language cortex in glioma surgery if no language impairment were demonstrated with intra-operatory ECS mapping (Benzagmout et al., 2007). Considering the ECS ability to predict indispensable eloquent language cortex (ALA or PLA), to our knowledge, no study reported ECS functional language false negative responses with permanent massive language deficit observed after correct ECS mapping. Finally, authors have confirmed the resectability of sites with inconsistent language

TABLE 1 | Reviewed studies reporting language mapping using electrical cortical stimulations applied with depth electrodes (sEEG).

Study	Nb. of subj.	Mean age at sEEG	Stimulation parameters	Main findings of the study
Abdallah et al., 2021	29	37	50 Hz, 5–10 s, 0.5–2 mA, 0.5 ms	BTLA resection identified by sEEG ECS predicts early naming decline in temporal lobe epilepsy
Cuisenier et al., 2020	42	NR	50 Hz, 5 s, 0.2–3 mA, 1–3 ms	ECS appears more appropriate for temporal lobe language mapping than induced HFA during sEEG
Ervin et al., 2020	21	4.8–21.2	50 Hz, NR, 1–8 mA, NR	High-gamma modulation language mapping with sEEG can accurately localized neuroanatomic and ECS delineated language sites
Perrone-Bertolotti et al., 2020	29	NR (adult)	50 Hz, 5 s, 1–3 mA, 1–3 ms	High frequency activity induced during ECS maps functional language networks during sEEG
Arya et al., 2019	10	5.4–21.2	50 Hz, 5 s, 1–8 mA, 0.3 ms	Language mapping with sEEG is a valid technique compared to a fMRI standard reference.
Young et al., 2018	10	NR (Adults)	50 Hz, NR, 2–10 mA, 0.5 ms	Language mapping using sEEG may be considered as a clinically useful alternative to language mapping with ECoG
Măîîa et al., 2018	31	33	50 Hz, 5 s, 1–3 mA, 1 ms	Description of the effective connectivity of the human operculum using cortico-cortical evoked potential for functional mapping
Bédos Ulvin et al., 2017	23	33	50 Hz, 5–10 s, 0.5–2 mA, 0.5 ms	ECS language mapping in the VTC showed bilateral with left more than right naming impairments especially in the occipito-temporal sulcus
Alonso et al., 2016	4	NR, (Pediatric)	50 Hz, 5 s, 1–10 mA, 0.3 ms	sEEG is a feasible method to lateralize speech dominance making Wada test unnecessary in bilateral electrode implantations
Trébuchon and Chauvel, 2016	68	NR	50 Hz, 3–5 s, 0.2–2.5 mA, 1 ms	ECS during sEEG is a reliable method for Seizure Induction and Functional Mapping in epilepsy
Balestrini et al., 2015	172	25.6	50 Hz, 5 s, NR, 1 ms	Overview of neurophysiology of parietal region assessed using ECS during sEEG
Taussig et al., 2014	65	39/127 m	NR	sEEG in children is a safe and useful method with surgical outcome in younger children at least as good as in older children.
Cossu et al., 2012	15	34 m	NR	sEEG has a prominent role in the presurgical evaluation of focal epilepsies in children also in the first years of life
de Ribaupierre et al., 2012	8	11.2	50 Hz, 3–5 s, 1–10 mA, 0.3 ms	Prior fMRI was found useful for the planning of ECS language mapping in children in order to increase its sensitivity
Afif et al., 2010	25	29.3	50 Hz, 5 s, 0.2–3 mA, 1 ms	The middle short gyrus of insula was found to be involved in speech production using ECS during sEEG
Fonseca et al., 2009	1	25	NR, NR, 0.5–2.5 mA, NR	Using ECS of the VTC during sEEG BTLA was found to be a multimodal region involved in lexico-semantic processing

Age at sEEG in years (if not otherwise specified) or months (m). Stimulation parameters (all biphasic) stated in order: frequency, total length, intensity, phase length. NR, not reported.

disturbances evoked by ECS functional mapping (Ojemann, 1979; Gil Robles et al., 2008).

Stereo-electroencephalography is routinely used in epilepsy surgery to map eloquent cortex (Isnard et al., 2018). However, few sEEG studies specifically reported mapping eloquent language cortex (see **Table 1** for details). In a recent study, Trébuchon and Chauvel (2016) reported findings from ECS for functional language mapping in 68 patients and found task specific positive sites in the classical ALA (naming difficulties followed by reading difficulties but less automatic speech impairments) and PLA (naming difficulties and reading aloud difficulties with less repetition impairment). However, no correlation was performed with post-operative outcome according to the resection status of these eloquent sites. Perrone-Bertolotti et al. (2020) similarly reported in 29 patients bilateral, left predominant, widespread positive language sites in the frontal, temporal and parietal lobes using a naming task. No correlation was performed with post-operative outcome. Cuisenier in a recent study found language functional sites using sEEG in both hemispheres with at least three patients having bilateral representation of language in fMRI. Regarding the left hemisphere, more than half language sites were found in the temporal lobe, a fifth in the frontal lobe and 5% in the parietal lobe. No correlation was done with the expected anatomical boundary of classical language areas (Cuisenier et al., 2020). Mălîia et al. (2018) reported on the opercular functional responses after ECS mapping using sEEG. Bilateral positive language sites (whose stimulation resulted in speech arrest) were found in the frontal operculum with a larger volume distribution of about 1.1 cm^3 in the left hemisphere. Expressive type of aphasia was reported in 90% of the responses while a mixed type of aphasia was reported in the remaining cases using a naming task. Same authors found language functional responses in the posterior part of the temporal operculum only in the left hemisphere in 11% of the stimulated contacts. The resulting deficit was expressive aphasia in two thirds of cases. They found only one site whose ECS elicited expressive language deficit in the parietal operculum. After a comprehensive parietal lobe exploration using more than a thousand ECS delivered at low frequency via sEEG electrodes, Balestrini obtained only two speech arrests in the dominant inferior parietal lobule (Balestrini et al., 2015). In a previous sEEG study, using bilateral symmetric implantation in four patients, Alonso et al. correctly lateralized ALA using ECS. They obtained speech arrest after strictly unilateral posterior inferior frontal gyrus ECS during a naming task thus validating the ability of the ECS language mapping to correctly lateralize language (Alonso et al., 2016). Young et al. (2018) compared ECS language mapping with sEEG and subdural grids in two different groups of patients and found similar results. Authors concluded that sEEG was safe, slightly better tolerated and provided similar information for ECS language mapping as ECoG. Arya et al. (2019) prospectively compared sEEG ECS language mapping to a reference standard of meta-analytic fMRI in 10 patients. ECS language positive sites did not perfectly match with the ALA and PLA as identified by fMRI at the group level. It is important to observe that the two populations were different. This study suggested that findings derived from ECS may diverge from findings derived from fMRI. There are very few reported cases of false positive sites identified by ECS: (Gil Robles et al., 2008) reported a single case of sEEG ECS positive language site in the posterior part of the superior temporal gyrus in a case of ganglioglioma epilepsy that was not reproduced with intra-operative ECS and could be completely resected without post-operative deficit. It is important to note that in this single case, language disturbance evoked by ECS in this site was "inconsistent" according to the authors.

An alternative language mapping approach with intracranial recordings consist of using High Frequency Activity (HFA) evoked by language task such as visual or auditory naming. An early ECoG study showed that auditory-language-related gamma-increase could provide additional information useful to localize the indispensable language areas (Kojima et al., 2013). In the same perspective a recent sEEG study compared ECS and induced HFA for language mapping. Authors observed that the induced HFA methods as compared to the reference methods of ECS had a high specificity but a very low sensitivity (8.9%). When considering whole brain recordings sites, induced HFA had a high negative predictive value but this did not hold true when focusing on the anatomical regions of interest classically involved in language which led the authors to state that ECS was more appropriate for extensive temporal mapping than induced HFA (Cuisenier et al., 2020). Similar results were obtained by Ervin et al. (2020) using sEEG by comparing ECS and high gamma induced activity during a visual naming task.

Considering the assessment of the anterior and the posterior eloquent language cortex in epilepsy surgery, we believe that sEEG is a safe and useful technique for functional mapping. Depending on the proximity of the presumed epileptogenic zone and in order to assess eloquent cortex involvement, specific electrodes trajectories may be necessary, taking into account both electro-clinical hypothesis regarding the presumed EZ and also the presumed cortical locations of indispensable brain language areas (see discussion above), especially the pars opercularis in the inferior frontal gyrus for the ALA and the posterior part of the superior temporal gyrus and the angular gyrus for the PLA. As mentioned in the previous section, an important aspect is to carefully set the stimulation parameters in order to avoid false negatives. Delivering a proper stimulation intensity is of paramount importance as well as AD monitoring throughout the stimulation. Likewise, using multiple appropriate language tasks such as visual naming, reading, completed with auditory confrontation naming and a more specific semantic task (such as semantic matching for example) is crucial in our opinion.

In line with other authors (Gil Robles et al., 2008; Arya et al., 2019), our opinion is that sEEG has a good negative predictive value in mapping anterior and posterior eloquent language cortex provided that relevant electrode trajectories, relevant stimulation parameters and tasks have been used. However, when eloquent sites are found inconsistent with sEEG ECS, surgery can still be considered if the EZ is well delineated and chances of seizure freedom are high. In these cases, we would recommend using awake surgery with intra-operative ECS mapping. In those cases, if awake surgery is not possible, using subdural grids may be an alternative as this technique offers the opportunity to more densely and extensively cover the cortical surface surrounding the

anterior and posterior language areas to determine their borders (Britton, 2018). When complete resection is not an option, a partial resection up to the eloquent cortex may still be useful and has to be considered according to some authors (Devinsky et al., 2003; Jayakar et al., 2018).

Electrical cortical stimulations language mapping is a well-studied, relatively simple to interpret and cost-efficient technique to map anterior and posterior language areas. It stands actually as the gold standard to individually delineate indispensable eloquent language cortex (ALA and PLA) and take into account individual variability and functional reorganization.

MAPPING DISPENSABLE ELOQUENT LANGUAGE CORTEX USING sEEG

As discussed in the previous section, most published reports on language mapping using ECS have been related to the mapping of the classical anterior and posterior language areas. However, behavioral language impairments have been obtained outside the ALA or PLA especially in the ventral temporal cortex.

The so-called basal temporal language area (BTLA) was first described by Lüders et al. (1986) who reported transient anomia resulting from the subdural grids stimulation of the left fusiform gyrus (FG). Subsequent studies using subdural electrodes extended the spectrum of ECS induced language disturbances in the VTC to comprehension and reading tasks (Krauss et al., 1996), and the anatomical localization of the BTLA to the left inferior temporal gyrus and the left parahippocampal gyrus from 1 to 9 cm from the temporal tip (Burnstine et al., 1990; Schaffler et al., 1994, 1996) as represented in the **Figure 1B**. More recently, Bédos Ulvin et al. (2017), assessed the lateralization and boundaries of the BTLA taking advantage of the sEEG to explore deep structures and especially sulci with depth electrodes stereotactically implanted in the right and left VTC. The authors first reproduced earlier findings from ECoG regarding the involvement of the dominant fusiform, inferior temporal and parahippocampal gyri in the BTLA and further extended its location to the lateral occipito-temporal sulcus. It further showed a clear left predominance of BTLA sites and that in cases with bilateral implantation, the BTLA was strictly lateralized, presumably in the dominant hemisphere.

Basal temporal language area could be a good example of *eloquent but dispensable* cortex. Although anomia is considered to be the most frequent cognitive deficit after left temporal resection (Sherman et al., 2011), post-operative language deficits after BTLA resection have been discordant across studies (Abdallah et al., 2021). Krauss et al. (1996) found that patients with BTLA resection performed worse on early (6–12 months) post-operative confrontation naming task whereas (Lüders et al., 1991) found no lasting language deficit. In a recent study Abdallah et al. (2021) evaluated early (within 1 year) and late (at 2 years) naming outcome according to the resection status of the BTLA. Authors found that almost 60% of patients with resection including BTLA positive sites had an early clinically significant decline in visual naming. In contrast, sparing BTLA prevented patients from postoperative naming decline (9%) provided that a sufficient spatial sampling had been performed with an anterior and a posterior basal temporal depth electrodes. This study emphasized also the fact that early naming decline observed after dominant temporal corticectomy did not depend on the posterior limits of temporal neocortical resection but was related to the great inter-individual variability of the BTLA anterior limit. Indeed, all resected BTLA positive sites were located within the 30 mm from the temporal tip (in average, 24.5 mm) and were thus included within the usual limits of the so-called standard left anterior temporal lobectomy. These results strongly suggest that resection of BTLA increases the risk of post resection early naming decline and thus plead for an important structural (and local) role of this area. However, the fact that not all patients with BTLA resection had post-operative anomia and that when present early post-operative anomia recovered at least partially at longer follow-up (2 years) interrogates the role of this structure within the entire language network.

The location of the BTLA in the contiguity of the ventral visual stream involved in visual categorization (Cauchoix et al., 2016) and of the anterior parts of the temporal lobe involved in semantic processing (Lambon Ralph, 2013) suggests a highly functional convergence zone (Fonseca et al., 2009). Shimotake et al. (2015) using subdural electrodes, considered the anterior FG – ITG as a semantic hub after observing impairments in semantic tasks during cortical stimulation. Indeed, Forseth et al. (2018) showed that ECS in the left fusiform gyrus interfered with both visual and auditory naming and proposed a lexico-semantic role for this region. Recent reports emphasized the importance of long distance connections in language models (Hagoort, 2017). Enatsu et al. (2017) showed that the BTLA was structurally connected to the temporal pole, medial temporal structures, and lateral temporal and occipital structures through the inferior longitudinal fasciculus. Using low frequency ECS in order to compute cortico-cortical evoked potentials, Araki et al. (2015) found bidirectional connections between the BTLA and the posterior language area. These structural and functional evidences suggest that the BLTA could be strongly structurally and functionally connected to both the ventral and the dorsal streams of the perisylvian language network (Duffau et al., 2014). In a recent study (Perrone-Bertolotti et al., 2020) assessed large-scale language network correlated with ECS induced naming errors by quantifying ECS induced HFA changes outside the stimulated cortical region. The authors found long distance HFA modification contemporary to ECS naming impairments suggesting distant effect of ECS. However, using HFA induced by naming, Cuisenier et al. (2020) found that HFA predicted electrically induced language disturbances with high specificity but very low sensitivity. These observations strongly suggest that ECS positive sites of the BTLA could be an important hub within a large specific language network extending well beyond the VTC. We speculate that this area acts as a multimodal (visual and auditive) (Mandonnet et al., 2010) spread hub, connected with structures involved in semantic (ventral stream) and lexical (dorsal stream) functions. The discrepancies between ECS and inconstant post-resection naming deficit (defining dispensable eloquent cortex) (Abdallah et al., 2021), could be explained by the properties of the BTLA hub, i.e., ECS

would abruptly and transiently disturb large distant connected areas, while resection could determine early deficit by locally removing parts of the hub, but leaving the potential for functional resilience of the remaining network underlying the slow recovery over time.

Electrical cortical stimulations delivered via sEEG are useful and important in mapping dispensable eloquent language cortex like the BTLA. We believe that a particular attention must be payed to the individual variation in BTLA location along the VTC as individuals with the most anterior BTLA localization (within the usual limits of the so called "standard" anterior temporal lobectomy) are at high risk of early post-operative naming decline. Implantation of deep electrodes targeting the anterior and posterior ventral temporal cortex for the language mapping should be specifically designed when exploring with sEEG dominant temporal lobe epilepsies for subsequent surgery.

A particular advantage of sEEG is the ability to safely explore deep structures like hippocampus, insula (Salado et al., 2018), medial frontal cortex. Interestingly, several studies have reported an increased risk of naming decline after healthy hippocampal resection (Ives-Deliperi and Butler, 2012), after selective amygdalo-hippocampectomy based on open resection approach (Mansouri et al., 2014) but not after stereotactic laser amygdalohippocampotomy (Drane et al., 2015). Hamberger et al. (2010) found naming decline after hippocampal removal for visual but not auditory stimuli. While no consistent language impairment is obtained after hippocampal ECS, sEEG observations nevertheless suggest a role for this structure in naming. Hamamé et al. (2014) showed single-trial hippocampal dynamics between visual confrontation and naming using HFA responses. Moreover, hippocampal latency responses predict naming latency and efficiency (Llorens et al., 2016). In this last study, the authors showed a specific and reliable pattern of hippocampal activation in naming, modulated by repetition priming and semantic context, suggesting that hippocampus had a role in implicit learning and was an active component of naming network. As hippocampal ECS do not overtly produce naming impairments, hippocampus is not currently considered as an eloquent region for language and there is currently no consensus neither on the effect of dominant hippocampus resection on post-operative naming, nor on the ECS methods that could help to predict this outcome. We speculate hippocampus to be part of the naming larger multi-modal naming network but not acting as a critical hub and thus not directly impacted by ECS. Few authors reported insular positive language sites (Afif et al., 2010; Trébuchon and Chauvel, 2016) as well as insular HFA changes in response to naming (Cuisenier et al., 2020). As this structure is not included in the classical language network models, Ardila et al. (2016) speculated a role in language coordination while Afif et al. (2010) underlined the role of the insular middle short gyrus in speech production. A recent sEEG study reported speech arrest after medial frontal ECS sometimes associated with positive or negative motor phenomena of the mouth or tongue (Trevisi et al., 2018). These findings supports a phonological-articulatory network between supplementary motor area and ALA (Hertrich et al., 2016).

CONCLUSION AND PERSPECTIVES

Functional language mapping using ECS has a long history mainly supported by empirical clinical knowledge. Based on a whole body of available studies, there are strong evidences to consider sEEG as a valid, safe and reliable method for defining eloquent language cortices provided stimulation parameters, testing procedure and anatomical sampling have been rigorously designed. French guidelines on sEEG propose a common frame for stimulation parameters that globally parallels most of the reported parameters in studies across different countries. For language mapping high frequency protocols seems most appropriate with intensities ranging between 0.5 and 5 mA with longer phase duration (0.5–1 ms) compared to subdural grids that uses shorter phase duration but higher intensities. After discharge threshold should be carefully monitored to determine the maximal threshold of intensity used for language mapping.

In the cases of anterior and posterior language areas, sEEG ECS can be used for localizing eloquent cortex with a good negative predictive value in our experience that, however, needs further precise evaluation. This ESM should take into consideration inter-individual variability and functional reorganization resulting from an early onset and long lasting epilepsy. Discrete and limited patches of indispensable language eloquent cortex can thus be delineated, usually located in the posterior part of inferior frontal gyrus (pars opercularis) and posterior part of superior temporal gyrus (and angular gyrus), respectively. The eloquent sites would correspond to densely fold hubs with discrete borders. Surgery sparing those regions delineated by positive language ECS sites, would prevent post-operative important and permanent language deficit. Conversely, in the case of BTLA, language impairments can be obtained with ECS delivered to different VTC structures (fusiform gyrus, lateral occipital temporal gyrus, inferior temporal gyrus, and parahippocampal gyrus) with a great anatomical inter-individual variability. We hypothesize that in the VTC, eloquent sites correspond to strongly connected hubs within a large functional network including the BTLA but also medial temporal structures. Anomia evoked by local electrical stimulation of these hubs would result from the transient disorganization of the entire network. In contrast, surgical removal of these hubs could produce early but reversible post-operative deficits (defining dispensable language eloquent cortex) that could recover over time thanks to the resilience ability of the network.

Indispensable/dispensable cortex concept empirically prefigures the need of transition from mapping brain areas to mapping brain functions. Further research is needed in order to characterize the network properties of language eloquent cortex as network architecture could account for a rather local or more distant ECS effect. Low frequency ECS coupled with novel and powerful computational techniques allows news insights into effective connectivity through cortico-cortical evoked potentials. Comparing effective connectivity of the language positive (BTLA) versus negative sites in the VTC would allow testing this

hypothesis. Finally, ECS coupled with passive correlative sEEG methods like task related or electrically induced HFA responses could further contribute to the development of new biological markers of language network resilience in epilepsy surgery.

AUTHOR CONTRIBUTIONS

All authors listed have made a substantial, direct and intellectual contribution to the work, and approved it for publication.

REFERENCES

Abdallah, C., Brissart, H., Colnat-Coulbois, S., Pierson, L., Aron, O., Forthoffer, N., et al. (2021). Stereo-electro-encephalography language mapping of basal temporal cortex predicts postoperative naming outcome. *J. Neurosurg.* doi: 10.3171/2020.8.JNS202431

Afif, A., Minotti, L., Kahane, P., and Hoffmann, D. (2010). Middle short gyrus of the insula implicated in speech production: intracerebral electric stimulation of patients with epilepsy. *Epilepsia* 51, 206–213. doi: 10.1111/j.1528-1167.2009.02271.x

Alonso, F., Sweet, J., and Miller, J. (2016). Speech mapping using depth electrodes: the "electric Wada.". *Clin. Neurol. Neurosurg.* 144, 88–90. doi: 10.1016/j.clineuro.2016.03.017

Araki, K., Terada, K., Usui, K., Usui, N., Araki, Y., Baba, K., et al. (2015). Bidirectional neural connectivity between basal temporal and posterior language areas in humans. *Clin. Neurophysiol.* 126, 682–688. doi: 10.1016/j.clinph.2014.07.020

Ardila, A., Bernal, B., and Rosselli, M. (2016). How localized are language brain areas? A review of brodmann areas involvement in oral language. *Arch. Clin. Neuropsychol.* 31, 112–122. doi: 10.1093/arclin/acv081

Arya, R., Aungaroon, G., Zea Vera, A., Horn, P. S., Byars, A. W., Greiner, H. M., et al. (2018). Fosphenytoin pre-medication for pediatric extra-operative electrical stimulation brain mapping. *Epilepsy Res.* 140, 171–176. doi: 10.1016/j.eplepsyres.2018.01.017

Arya, R., Ervin, B., Dudley, J., Buroker, J., Rozhkov, L., Scholle, C., et al. (2019). Electrical stimulation mapping of language with stereo-EEG. *Epilepsy Behav.* 99:106395. doi: 10.1016/j.yebeh.2019.06.038

Aungaroon, G., Zea Vera, A., Horn, P. S., Byars, A. W., Greiner, H. M., Tenney, J. R., et al. (2017). After-discharges and seizures during pediatric extra-operative electrical cortical stimulation functional brain mapping: incidence, thresholds, and determinants. *Clin. Neurophysiol.* 128, 2078–2086. doi: 10.1016/j.clinph.2017.06.259

Balestrini, S., Francione, S., Mai, R., Castana, L., Casaceli, G., Marino, D., et al. (2015). Multimodal responses induced by cortical stimulation of the parietal lobe: a stereo-electroencephalography study. *Brain* 138, 2596–2607. doi: 10.1093/brain/awv187

Bank, A. M., Schevon, C. A., and Hamberger, M. J. (2014). Characteristics and clinical impact of stimulation-evoked seizures during extraoperative cortical mapping. *Epilepsy Behav.* 34, 6–8. doi: 10.1016/j.yebeh.2014.03.004

Bartolomei, F., Lagarde, S., Wendling, F., McGonigal, A., Jirsa, V., Guye, M., et al. (2017). Defining epileptogenic networks: contribution of SEEG and signal analysis. *Epilepsia* 58, 1131–1147. doi: 10.1111/epi.13791

Bédos Ulvin, L., Jonas, J., Brissart, H., Colnat-Coulbois, S., Thiriaux, A., Vignal, J.-P., et al. (2017). Intracerebral stimulation of left and right ventral temporal cortex during object naming. *Brain Lang.* 175, 71–76. doi: 10.1016/j.bandl.2017.09.003

Benzagmout, M., Gatignol, P., and Duffau, H. (2007). Resection of world health organization grade II gliomas involving Broca's areamethodological and functional considerations. *Neurosurgery* 61, 741–753. doi: 10.1227/01.NEU.0000298902.69473.77

Berger, H. (1929). Über das elektroenkephalogramm des menschen. *Arch. Für Psychiatr. Nervenkrankh.* 87, 527–570.

Blume, W. T., Jones, D. C., and Pathak, P. (2004). Properties of after-discharges from cortical electrical stimulation in focal epilepsies. *Clin. Neurophysiol.* 115, 982–989. doi: 10.1016/j.clinph.2003.11.023

Borchers, S., Himmelbach, M., Logothetis, N., and Karnath, H.-O. (2012). Direct electrical stimulation of human cortex – the gold standard for mapping brain functions? *Nat. Rev. Neurosci.* 13, 63–70. doi: 10.1038/nrn3140

Britton, J. W. (2018). Electrical stimulation mapping with stereo-EEG electrodes. *J. Clin. Neurophysiol.* 35, 110–114. doi: 10.1097/WNP.0000000000000443

Burnstine, T. H., Lesser, R. P., Hart, J., Uematsu, S., Zinreich, S. J., Krauss, G. L., et al. (1990). Characterization of the basal temporal language area in patients with left temporal lobe epilepsy. *Neurology* 40, 966–966. doi: 10.1212/WNL.40.6.966

Cauchoix, M., Crouzet, S. M., Fize, D., and Serre, T. (2016). Fast ventral stream neural activity enables rapid visual categorization. *NeuroImage* 125, 280–290. doi: 10.1016/j.neuroimage.2015.10.012

Chauvel, P., and McGonigal, A. (2014). Emergence of semiology in epileptic seizures. *Epilepsy Behav.* 38, 94–103. doi: 10.1016/j.yebeh.2013.12.003

Corina, D. P., Loudermilk, B. C., Detwiler, L., Martin, R. F., Brinkley, J. F., and Ojemann, G. (2010). Analysis of naming errors during cortical stimulation mapping: Implications for models of language representation. *Brain Lang.* 115, 101–112. doi: 10.1016/j.bandl.2010.04.001

Corley, J. A., Nazari, P., Rossi, V. J., Kim, N. C., Fogg, L. F., Hoeppner, T. J., et al. (2017). Cortical stimulation parameters for functional mapping. *Seizure* 45, 36–41. doi: 10.1016/j.seizure.2016.11.015

Cossu, M., Schiariti, M., Francione, S., Fuschillo, D., Gozzo, F., Nobili, L., et al. (2012). Stereoelectroencephalography in the presurgical evaluation of focal epilepsy in infancy and early childhood. *J. Neurosurg. Pediatr.* 9, 290–300. doi: 10.3171/2011.12.PEDS11216

Cuisenier, P., Testud, B., Minotti, L., Tiali, S. E. B., Martineau, L., Job, A.-S., et al. (2020). Relationship between direct cortical stimulation and induced high-frequency activity for language mapping during SEEG recording. *J. Neurosurg.* doi: 10.3171/2020.2.JNS192751 [Epub ahead of print].

de Ribaupierre, S., Fohlen, M., Bulteau, C., Dorfmüller, G., Delalande, O., Dulac, O., et al. (2012). Presurgical language mapping in children with epilepsy: clinical usefulness of functional magnetic resonance imaging for the planning of cortical stimulation. *Epilepsia* 53, 67–78. doi: 10.1111/j.1528-1167.2011.03329.x

Devinsky, O., Romanelli, P., Orbach, D., Pacia, S., and Doyle, W. (2003). Surgical treatment of multifocal epilepsy involving eloquent cortex. *Epilepsia* 44, 718–723. doi: 10.1046/j.1528-1157.2003.57102.x

Donos, C., Mîndruță, I., Ciurea, J., Mălîia, M. D., and Barborica, A. (2016). A comparative study of the effects of pulse parameters for intracranial direct electrical stimulation in epilepsy. *Clin. Neurophysiol.* 127, 91–101. doi: 10.1016/j.clinph.2015.02.013

Drane, D. L., Loring, D. W., Voets, N. L., Price, M., Ojemann, J. G., Willie, J. T., et al. (2015). Better object recognition and naming outcome with MRI-guided stereotactic laser amygdalohippocampotomy for temporal lobe epilepsy. *Epilepsia* 56, 101–113. doi: 10.1111/epi.12860

Duchowny, M., Jayakar, P., Harvey, A. S., Resnick, T., Alvarez, L., Dean, P., et al. (1996). Language cortex representation: effects of developmental versus acquired pathology. *Ann. Neurol.* 40, 31–38. doi: 10.1002/ana.410400108

Duffau, H., Moritz-Gasser, S., and Mandonnet, E. (2014). A re-examination of neural basis of language processing: proposal of a dynamic hodotopical model from data provided by brain stimulation mapping during picture naming. *Brain Lang.* 131, 1–10. doi: 10.1016/j.bandl.2013.05.011

Ebeling, U., Steinmetz, H., Huang, Y., and Kahn, T. (1989). Topography and identification of the inferior precentral sulcus in MR imaging. *Am. J. Neuroradiol.* 10, 937–942.

Enatsu, R., Kanno, A., Ookawa, S., Ochi, S., Ishiai, S., Nagamine, T., et al. (2017). Distribution and network of basal temporal language areas: a study of the combination of electric cortical stimulation and diffusion tensor imaging. *World Neurosurg.* 106, 1–8. doi: 10.1016/j.wneu.2017.06.116

Ervin, B., Buroker, J., Rozhkov, L., Holloway, T., Horn, P. S., Scholle, C., et al. (2020). High-gamma modulation language mapping with stereo-EEG: a novel analytic approach and diagnostic validation. *Clin. Neurophysiol.* 131, 2851–2860. doi: 10.1016/j.clinph.2020.09.023

Ferrier, D. (1873). Experimental researches in cerebral physiology and pathology. *J. Anat. Physiol.* 8(Pt 1), 152–155.

Flourens, P. (1824). *Recherches Expérimentales sur les Propriétés et les Fonctions du Système Nerveux, Dans Les Animaux Vertébrés*. Paris: Crevot.

Foerster, O. (1931). The cerebral cortex in man. *Lancet* 2, 309–312.
Foerster, O. (1936). The motor cortex in man in the light of Hughlings Jackson's doctrines. *Brain* 59, 135–159.
Foerster, O., and Altenburger, H. (1935). Elektrobiologische Vorgänge an der menschlichen Hirnrinde. *Dtsch Z Für Nervenheilkd.* 135, 277–288.
Fonseca, A. T.-D., Bénar, C.-G., Bartoloméi, F., Régis, J., Démonet, J.-F., Chauvel, P., et al. (2009). Electrophysiological study of the basal temporal language area: a convergence zone between language perception and production networks. *Clin. Neurophysiol.* 120, 539–550. doi: 10.1016/j.clinph.2008.12.042
Forseth, K. J., Kadipasaoglu, C. M., Conner, C. R., Hickok, G., Knight, R. T., and Tandon, N. (2018). A lexical semantic hub for heteromodal naming in middle fusiform gyrus. *Brain* 141, 2112–2126. doi: 10.1093/brain/awy120
Fritsch, G., and Hitzig, E. (1870). *Ueber die elektrische Erregbarkeit des Grosshirns*. Leipzig: Veit.
George, D. D., Ojemann, S. G., Drees, C., and Thompson, J. A. (2020). Stimulation mapping using stereoelectroencephalography: current and future directions. *Front. Neurol.* 11:320. doi: 10.3389/fneur.2020.00320
Gil Robles, S., Gelisse, P., Vergani, F., Moritz-Gasser, S., Rigau, V., Coubes, P., et al. (2008). Discrepancies between preoperative stereoencephalography language stimulation mapping and intraoperative awake mapping during resection of focal cortical dysplasia in eloquent areas. *Stereotact. Funct. Neurosurg.* 86, 382–390. doi: 10.1159/000175801
Hagoort, P. (2017). The core and beyond in the language-ready brain. *Neurosci. Biobehav. Rev.* 81, 194–204. doi: 10.1016/j.neubiorev.2017.01.048
Hamamé, C. M., Alario, F.-X., Llorens, A., Liégeois-Chauvel, C., and Trébuchon-Da Fonseca, A. (2014). High frequency gamma activity in the left hippocampus predicts visual object naming performance. *Brain Lang.* 135, 104–114. doi: 10.1016/j.bandl.2014.05.007
Hamberger, M. J. (2007). Cortical language mapping in epilepsy: a critical review. *Neuropsychol. Rev.* 17, 477–489. doi: 10.1007/s11065-007-9046-6
Hamberger, M. J., Seidel, W. T., Goodman, R. R., Perrine, K., and McKhann, G. M. (2003). Temporal lobe stimulation reveals anatomic distinction between auditory naming processes. *Neurology* 60, 1478–1483. doi: 10.1212/01.WNL.0000061489.25675.3E
Hamberger, M. J., Seidel, W. T., McKhann, G. M., and Goodman, R. R. (2010). Hippocampal removal affects visual but not auditory naming. *Neurology* 74, 1488–1493. doi: 10.1212/WNL.0b013e3181dd40f0
Hermann, B. P., Perrine, K., Chelune, G. J., Barr, W., Loring, D. W., Strauss, E., et al. (1999). Visual confrontation naming following left anterior temporal lobectomy: a comparison of surgical approaches. *Neuropsychology* 13, 3–9. doi: 10.1037/0894-4105.13.1.3
Hertrich, I., Dietrich, S., and Ackermann, H. (2016). The role of the supplementary motor area for speech and language processing. *Neurosci. Biobehav. Rev.* 68, 602–610. doi: 10.1016/j.neubiorev.2016.06.030
Horsley, V. (1887). Remarks on ten consecutive cases of operations upon the brain and cranial cavity to illustrate the details and safety of the method employed. *Br. Med. J.* 1, 863–865.
Horsley, V., and Schafer, E. A. (1888). A record of experiments upon the functions of the cerebral cortex. *Philos. Trans. R. Soc. Lond. B* 179, 1–45.
Isnard, J., Taussig, D., Bartolomei, F., Bourdillon, P., Catenoix, H., Chassoux, F., et al. (2018). French guidelines on stereoelectroencephalography (SEEG). *Neurophysiol. Clin.* 48, 5–13. doi: 10.1016/j.neucli.2017.11.005
Ius, T., Angelini, E., Schotten, M. T., Mandonnet, E., and Duffau, H. (2011). Evidence for potentials and limitations of brain plasticity using an atlas of functional resectability of WHO grade II gliomas: towards a "minimal common brain". *NeuroImage* 56, 992–1000. doi: 10.1016/j.neuroimage.2011.03.022
Ives-Deliperi, V. L., and Butler, J. T. (2012). Naming outcomes of anterior temporal lobectomy in epilepsy patients: a systematic review of the literature. *Epilepsy Behav.* 24, 194–198. doi: 10.1016/j.yebeh.2012.04.115
Jackson, J. H. (1863). Convulsive spasms of the right hand and arm preceding epileptic seizures. *Med. Times Gaz.* 1, 110–111.
Jayakar, P., Jayakar, A., Libenson, M., Arzimanoglou, A., Rydenhag, B., Cross, J. H., et al. (2018). Epilepsy surgery near or in eloquent cortex in children-Practice patterns and recommendations for minimizing and reporting deficits. *Epilepsia* 59, 1484–1491. doi: 10.1111/epi.14510
Kahane, P., Landré, E., Minotti, L., Francione, S., and Ryvlin, P. (2006). The Bancaud and Talairach view on the epileptogenic zone: a working hypothesis. *Epileptic Disord.* 8(Suppl. 2), S16–S26.
Kojima, K., Brown, E. C., Rothermel, R., Carlson, A., Fuerst, D., Matsuzaki, N., et al. (2013). Clinical significance and developmental changes of auditory-language-related gamma activity. *Clin. Neurophysiol.* 124, 857–869. doi: 10.1016/j.clinph.2012.09.031
Krauss, G. L., Fisher, R., Plate, C., Hart, J., Uematsu, S., Gordon, B., et al. (1996). Cognitive effects of resecting basal temporal language areas. *Epilepsia* 37, 476–483. doi: 10.1111/j.1528-1157.1996.tb00594.x
Lambon Ralph, M. A. (2013). Neurocognitive insights on conceptual knowledge and its breakdown. *Philos. Trans. R. Soc. B Biol. Sci.* 369:20120392. doi: 10.1098/rstb.2012.0392
Laplane, D., Talairach, J., Meininger, V., Bancaud, J., and Bouchareine, A. (1977). Motor consequences of motor area ablations in man. *J. Neurol. Sci.* 31, 29–49. doi: 10.1016/0022-510x(77)90004-1
Li, J., Grinenko, O., Mosher, J. C., Gonzalez−Martinez, J., Leahy, R. M., and Chauvel, P. (2020). Learning to define an electrical biomarker of the epileptogenic zone. *Hum. Brain Mapp.* 41, 429–441. doi: 10.1002/hbm.24813
Llorens, A., Dubarry, A.-S., Trébuchon, A., Chauvel, P., Alario, F.-X., and Liégeois-Chauvel, C. (2016). Contextual modulation of hippocampal activity during picture naming. *Brain Lang.* 159, 92–101. doi: 10.1016/j.bandl.2016.05.011
Llorens, A., Trébuchon, A., Liegeois-Chauvel, C., and Alario, F.-X. (2011). Intra-cranial recordings of brain activity during language production. *Front. Psychol.* 2:375. doi: 10.3389/fpsyg.2011.00375
Lochy, A., Jacques, C., Maillard, L., Colnat-Coulbois, S., Rossion, B., and Jonas, J. (2018). Selective visual representation of letters and words in the left ventral occipito-temporal cortex with intracerebral recordings. *Proc. Natl. Acad. Sci. U.S.A.* 115, E7595–E7604.
Lüders, H., Lesser, R., Hahn, J., Dinner, D., Morris, H., Resor, S., et al. (1986). Basal temporal language area demonstrated by electrical stimulation. *Neurology* 36, 505–510. doi: 10.1212/WNL.36.4.505
Lüders, H., Lesser, R. P., Hahn, J., Dinner, D. S., Morris, H. H., Wyllie, E., et al. (1991). Basal temporal language area. *Brain* 114, 743–754. doi: 10.1093/brain/114.2.743
Mălîia, M.-D., Donos, C., Barborica, A., Popa, I., Ciurea, J., Cinatti, S., et al. (2018). Functional mapping and effective connectivity of the human operculum. *Cortex* 109, 303–321. doi: 10.1016/j.cortex.2018.08.024
Mandonnet, E., Winkler, P. A., and Duffau, H. (2010). Direct electrical stimulation as an input gate into brain functional networks: principles, advantages and limitations. *Acta Neurochir. (Wien)* 152, 185–193. doi: 10.1007/s00701-009-0469-0
Mansouri, A., Fallah, A., McAndrews, M. P., Cohn, M., Mayor, D., Andrade, D., et al. (2014). Neurocognitive and seizure outcomes of selective amygdalohippocampectomy versus anterior temporal lobectomy for mesial temporal lobe epilepsy. *Epilepsy Res. Treat.* 2014:e306382. doi: 10.1155/2014/306382
Martin, S., Millán, J., del, R., Knight, R. T., and Pasley, B. N. (2019). The use of intracranial recordings to decode human language: challenges and opportunities. *Brain Lang.* 193, 73–83. doi: 10.1016/j.bandl.2016.06.003
Mullin, J. P., Shriver, M., Alomar, S., Najm, I., Bulacio, J., Chauvel, P., et al. (2016). Is SEEG safe? A systematic review and meta-analysis of stereo-electroencephalography–related complications. *Epilepsia* 57, 386–401. doi: 10.1111/epi.13298
Nakai, Y., Jeong, J., Brown, E. C., Rothermel, R., Kojima, K., Kambara, T., et al. (2017). Three- and four-dimensional mapping of speech and language in patients with epilepsy. *Brain* 140, 1351–1370. doi: 10.1093/brain/awx051
Nakai, Y., Sugiura, A., Brown, E. C., Sonoda, M., Jeong, J.-W., Rothermel, R., et al. (2019). Four-dimensional functional cortical maps of visual and auditory language: intracranial recording. *Epilepsia* 60, 255–267. doi: 10.1111/epi.14648
Ojemann, G. (1991). Cortical organization of language. *J. Neurosci.* 11, 2281–2287. doi: 10.1523/JNEUROSCI.11-08-02281.1991
Ojemann, G., Ojemann, J., Lettich, E., and Berger, M. (1989). Cortical language localization in left, dominant hemisphere. An electrical stimulation mapping investigation in 117 patients. *J. Neurosurg.* 71, 316–326. doi: 10.3171/jns.1989.71.3.0316
Ojemann, G. A. (1979). Individual variability in cortical localization of language. *J. Neurosurg.* 50, 164–169. doi: 10.3171/jns.1979.50.2.0164
Ojemann, G. A. (1983). Brain organization for language from the perspective of electrical stimulation mapping. *Behav. Brain Sci.* 6, 189–206. doi: 10.1017/S0140525X00015491

Penfield, W. (1954). *Epilepsy and the Functional Anatomy of the Human Brain by Wilder Penfield and Herbert Jasper*. Boston, MA: Little Brown.

Penfield, W., and Rasmussen, T. (1950). *The Cerebral Cortex of Man; A Clinical Study of Localization of Function*. Oxford: Macmillan.

Perrone-Bertolotti, M., Alexandre, S., Jobb, A. S., De Palma, L., Baciu, M., Mairesse, M. P., et al. (2020). Probabilistic mapping of language networks from high frequency activity induced by direct electrical stimulation. *Hum. Brain Mapp.* 41, 4113–4126. doi: 10.1002/hbm.25112

Pouratian, N., and Bookheimer, S. Y. (2010). The reliability of neuroanatomy as a predictor of eloquence: a review. *Neurosurg. Focus* 28:E3. doi: 10.3171/2009.11.FOCUS09239

Quiñones-Hinojosa, A., Ojemann, S. G., Sanai, N., Dillon, W. P., and Berger, M. S. (2003). Preoperative correlation of intraoperative cortical mapping with magnetic resonance imaging landmarks to predict localization of the Broca area. *J. Neurosurg.* 99, 311–318. doi: 10.3171/jns.2003.99.2.0311

Ritaccio, A. L., Brunner, P., and Schalk, G. (2018). Electrical stimulation mapping of the brain: basic principles and emerging alternatives. *J. Clin. Neurophysiol.* 35, 86–97. doi: 10.1097/WNP.0000000000000440

Salado, A. L., Koessler, L., De Mijolla, G., Schmitt, E., Vignal, J.-P., Civit, T., et al. (2018). sEEG is a safe procedure for a comprehensive anatomic exploration of the insula: a retrospective study of 108 procedures representing 254 transopercular insular electrodes. *Oper. Neurosurg.* 14, 1–8. doi: 10.1093/ons/opx106

Schaffler, L., Luders, H. O., and Beck, G. J. (1996). Quantitative comparison of language deficits produced by extraoperative electrical stimulation of Broca's, Wernicke's, and basal temporal language areas. *Epilepsia* 37, 463–475. doi: 10.1111/j.1528-1157.1996.tb00593.x

Schaffler, L., Luders, H. O., Morris, H. H., and Wyllie, E. (1994). Anatomic distribution of cortical language sites in the basal temporal language area in patients with left temporal lobe epilepsy. *Epilepsia* 35, 525–528. doi: 10.1111/j.1528-1157.1994.tb02472.x

Schwartz, T. H., Devinsky, O., Doyle, W., and Perrine, K. (1999). Function-specific high-probability "Nodes" identified in posterior language cortex. *Epilepsia* 40, 575–583. doi: 10.1111/j.1528-1157.1999.tb05559.x

Sherman, E. M. S., Wiebe, S., Fay-McClymont, T. B., Tellez-Zenteno, J., Metcalfe, A., Hernandez-Ronquillo, L., et al. (2011). Neuropsychological outcomes after epilepsy surgery: systematic review and pooled estimates: cognitive change after epilepsy surgery. *Epilepsia* 52, 857–869. doi: 10.1111/j.1528-1167.2011.03022.x

Shimotake, A., Matsumoto, R., Ueno, T., Kunieda, T., Saito, S., Hoffman, P., et al. (2015). Direct exploration of the role of the ventral anterior temporal lobe in semantic memory: cortical stimulation and local field potential evidence from subdural grid electrodes. *Cereb. Cortex* 25, 3802–3817. doi: 10.1093/cercor/bhu262

Skirboll, S. S., Ojemann, G. A., Berger, M. S., Lettich, E., and Winn, H. R. (1996). Functional cortex and subcortical white matter located within gliomas. *Neurosurgery* 38, 678–684; discussion684–685. doi: 10.1227/00006123-199604000-00008

Talairach, J., Bancaud, J., Bonis, A., Szikla, G., and Tournoux, P. (1962). Functional stereotaxic exploration of epilepsy. *Stereotact. Funct. Neurosurg.* 22, 328–331. doi: 10.1159/000104378

Tandon, N., Tong, B. A., Friedman, E. R., Johnson, J. A., Von Allmen, G., Thomas, M. S., et al. (2019). Analysis of morbidity and outcomes associated with use of Subdural Grids vs Stereoelectroencephalography in patients with intractable epilepsy. *JAMA Neurol.* 76, 672–681. doi: 10.1001/jamaneurol.2019.0098

Taussig, D., Chipaux, M., Lebas, A., Fohlen, M., Bulteau, C., Ternier, J., et al. (2014). Stereo-electroencephalography (SEEG) in 65 children: an effective and safe diagnostic method for pre-surgical diagnosis, independent of age. *Epileptic Disord. Int. Epilepsy J. Videotape* 16, 280–295. doi: 10.1684/epd.2014.0679

Trébuchon, A., and Chauvel, P. (2016). Electrical stimulation for seizure induction and functional mapping in stereoelectroencephalography. *J. Clin. Neurophysiol.* 33, 511–521. doi: 10.1097/WNP.0000000000000313

Trébuchon, A., Liegeois-Chauvel, C., and Martinez, J. G. (2020). Contributions of electrophysiology for identifying cortical language systems in patients with epilepsy. *Epilepsy Behav.* 112:107407.

Trevisi, G., Eickhoff, S. B., Chowdhury, F., Jha, A., Rodionov, R., Nowell, M., et al. (2018). Probabilistic electrical stimulation mapping of human medial frontal cortex. *Cortex* 109, 336–346. doi: 10.1016/j.cortex.2018.06.015

Wellmer, J., Weber, C., Mende, M., von der Groeben, F., Urbach, H., Clusmann, H., et al. (2009). Multitask electrical stimulation for cortical language mapping: hints for necessity and economic mode of application. *Epilepsia* 50, 2267–2275. doi: 10.1111/j.1528-1167.2009.02192.x

Wyler, A. R., Ojemann, G. A., Lettich, E., and Ward, A. A. (1984). Subdural strip electrodes for localizing epileptogenic foci. *J. Neurosurg.* 60, 1195–1200. doi: 10.3171/jns.1984.60.6.1195

Young, J. J., Coulehan, K., Fields, M. C., Yoo, J. Y., Marcuse, L. V., Jette, N., et al. (2018). Language mapping using electrocorticography versus stereoelectroencephalography: a case series. *Epilepsy Behav.* 84, 148–151. doi: 10.1016/j.yebeh.2018.04.032

Conflict of Interest: The authors declare that the research was conducted in the absence of any commercial or financial relationships that could be construed as a potential conflict of interest.

frontiers in Human Neuroscience

ORIGINAL RESEARCH
published: 15 March 2021
doi: 10.3389/fnhum.2021.616591

Multi-modal Mapping of the Face Selective Ventral Temporal Cortex–A Group Study With Clinical Implications for ECS, ECoG, and fMRI

Takahiro Sanada[1,2], Christoph Kapeller[3,4], Michael Jordan[3,4], Johannes Grünwald[3,4], Takumi Mitsuhashi[5,6], Hiroshi Ogawa[7], Ryogo Anei[2] and Christoph Guger[3,4]*

[1] Department of Neurosurgery, Nayoro City General Hospital, Nayoro, Japan, [2] Department of Neurosurgery, Asahikawa Medical University, Asahikawa, Japan, [3] g.tec Medical Engineering GmbH, Schiedlberg, Austria, [4] Guger Technologies OG, Graz, Austria, [5] Department of Neurosurgery, Juntendo University, Tokyo, Japan, [6] Department of Pediatrics, Children's Hospital of Michigan, Detroit Medical Center, Wayne State University, Detroit, MI, United States, [7] Division of Neurology, The Hospital for Sick Children, Toronto, ON, Canada

OPEN ACCESS

Edited by:
Riki Matsumoto, Kobe University, Japan

Reviewed by:
Adam Steel, Dartmouth College, United States
Masaki Iwasaki, National Center of Neurology and Psychiatry, Japan

***Correspondence:**
Takahiro Sanada
sanataka9103@gmail.com

Specialty section:
This article was submitted to Brain Imaging and Stimulation, a section of the journal Frontiers in Human Neuroscience

Received: *12 October 2020*
Accepted: *22 February 2021*
Published: *15 March 2021*

Citation:
Sanada T, Kapeller C, Jordan M, Grünwald J, Mitsuhashi T, Ogawa H, Anei R and Guger C (2021) Multi-modal Mapping of the Face Selective Ventral Temporal Cortex–A Group Study With Clinical Implications for ECS, ECoG, and fMRI. Front. Hum. Neurosci. 15:616591. doi: 10.3389/fnhum.2021.616591

Face recognition is impaired in patients with prosopagnosia, which may occur as a side effect of neurosurgical procedures. Face selective regions on the ventral temporal cortex have been localized with electrical cortical stimulation (ECS), electrocorticography (ECoG), and functional magnetic resonance imagining (fMRI). This is the first group study using within-patient comparisons to validate face selective regions mapping, utilizing the aforementioned modalities. Five patients underwent surgical treatment of intractable epilepsy and joined the study. Subdural grid electrodes were implanted on their ventral temporal cortices to localize seizure foci and face selective regions as part of the functional mapping protocol. Face selective regions were identified in all patients with fMRI, four patients with ECoG, and two patients with ECS. From 177 tested electrode locations in the region of interest (ROI), which is defined by the fusiform gyrus and the inferior temporal gyrus, 54 face locations were identified by at least one modality in all patients. fMRI mapping showed the highest detection rate, revealing 70.4% for face selective locations, whereas ECoG and ECS identified 64.8 and 31.5%, respectively. Thus, 28 face locations were co-localized by at least two modalities, with detection rates of 89.3% for fMRI, 85.7% for ECoG and 53.6 % for ECS. All five patients had no face recognition deficits after surgery, even though five of the face selective locations, one obtained by ECoG and the other four by fMRI, were within 10 mm to the resected volumes. Moreover, fMRI included a quite large volume artifact on the ventral temporal cortex in the ROI from the anatomical structures of the temporal base. In conclusion, ECS was not sensitive in several patients, whereas ECoG and fMRI even showed activation within 10 mm to the resected volumes. Considering the potential signal drop-out in fMRI makes ECoG the most reliable tool to identify face selective

locations in this study. A multimodal approach can improve the specificity of ECoG and fMRI, while simultaneously minimizing the number of required ECS sessions. Hence, all modalities should be considered in a clinical mapping protocol entailing combined results of co-localized face selective locations.

Keywords: functional brain mapping, face selective regions, prosopagnosia, ventral temporal cortex, electrical cortical stimulation, electrocorticography, functional magnetic resonance imagining, epilepsy surgery

INTRODUCTION

Recognizing faces seems to be a simple task, which most people perform often and unconsciously in daily life. Losing the ability to recognize unfamiliar or even familiar faces–even relatives–can tremendously decrease the quality of life. This disorder is called prosopagnosia and is characterized by impaired face recognition without other problems with visual acuity (Bodamer, 1947). It often occurs in cases with bilateral lesions in the occipital temporal cortex, especially the fusiform gyrus (Damasio et al., 1982), but also due to unilateral lesions in the right occipital temporal cortex (Benton, 1990; Takahashi et al., 1995; Wada and Yamamoto, 2001) and, in rare occasions, even on the left side (Mattson et al., 2000). Such lesions can be a side effect of neurosurgical operations of epilepsy or brain tumor (Mesad et al., 2003; Barton, 2008; Corrivetti et al., 2017). Generally, functional deficits are prevented, or at least reduced, by means of neuroimaging techniques. Most such testing has focused on brain regions responsible for language and motor functions (Penfield and Boldrey, 1937; Ojemann et al., 1989; Sagar et al., 2019). Face selective regions on the brain often remain unrevealed in clinical brain mapping protocols.

Initial hemodynamic neuroimaging studies, including positron emission tomography (PET) and functional magnetic resonance imagining (fMRI), localized the face area in ventral temporal occipital cortex (Sergent et al., 1992; Haxby et al., 1994; Puce et al., 1995). Later fMRI studies found a cluster specific to face recognition located at the lateral part of the middle/posterior fusiform gyrus, the fusiform face area (FFA) (Kanwisher et al., 1997), and also identified other face responsive regions in the inferior occipital gyrus, the occipital face area (OFA) (Puce et al., 1996; Gauthier et al., 2000), and superior temporal sulcus (STS) (Puce et al., 1998; Hoffman and Haxby, 2000). These three face selective regions are the core system for face perception that is processed by a distributed neural network (Haxby et al., 2000). While the STS processes changeable aspects, such as facial expressions and eye gaze, the FFA processes invariant face aspects, which is important for recognition. The OFA plays an important role in the perception of face parts and interacts with both FFA and STS (Haxby et al., 2000; Rossion et al., 2003; Ishai, 2008). Therefore, FFA and OFA play an important role for identification of faces, and, in case of a lesion, could cause prosopagnosia and related symptoms. Another hemodynamic imaging marker for visual perception can be obtained by PET, which requires the injection of radioactive markers for mapping (Haxby et al., 1994).

Electrophysiological signals, such as electrocorticography (ECoG), are a direct marker for neural activity. Subdural recordings from the human cortex showed face specific event related potentials (ERP) as an N200 potential in the fusiform gyrus (Allison et al., 1994a,b). Additional responses to presented faces include low frequency oscillations (Klopp et al., 1999), as well as broadband gamma activity (Lachaux et al., 2005; Schalk et al., 2017), which have been shown to be related to face N200 potentials (Engell and McCarthy, 2011; Ghuman et al., 2014). Analysis of temporal dynamics during visual perception have demonstrated that the FFA plays an important role in multiple face processing stages and that broadband gamma activity decay predicts the reaction time of percepts (Ghuman et al., 2014). Face selective broadband gamma activity also correlates with the hemodynamic response (Koch et al., 2009; Ojemann et al., 2010; Scheeringa et al., 2011; Hermes et al., 2012), and there is a good correspondence between ECoG potentials and fMRI face selective responses in posterior ventral temporal cortex (Puce et al., 1997; Jacques et al., 2016).

Electrical cortical stimulation (ECS) of face selective areas can induce inability to name familiar faces (Allison et al., 1994a,b), impairment of face discrimination (Mundel et al., 2003), or face categorization (Chong et al., 2013), illusory face responses (Parvizi et al., 2012; Rangarajan et al., 2014; Schalk et al., 2017), or transient prosopagnosia (Jonas et al., 2012, 2015). Like ECS, transcranial magnetic stimulation (TMS) has been demonstrated to disrupt face percepts (Pitcher et al., 2007). However, TMS mapping suffers from subject dependent protocols, especially for language mapping (Sollmann et al., 2018) and memory lateralization (Theodore, 2003), and requires a navigation system for localization (Romero et al., 2011).

All aforementioned imaging techniques have use cases in clinical practice. Especially, the non-invasive techniques can be relatively easily conducted for clinical investigations prior to brain surgeries. In case of epilepsy surgery, which this paper focuses on, invasive techniques can be considered as well as it often requires a two-stage surgery with intracranial electrodes for neuromonitoring. Hence, the most clinically relevant mapping techniques for epilepsy surgery are mainly ECS, fMRI, and ECoG.

Although ECS is the gold standard method for motor and language mapping (Ojemann et al., 1989), it is not necessarily the best method to localize sensory functions as visual perception or face recognition for two reasons. First, it is highly subjective and requires the ability of the patient to express symptoms. Second, it requires a time-consuming stimulation protocol (Wen et al., 2017). Hence, ECoG and fMRI mapping have been gaining attention as alternatives, especially to identify face selective areas. This raises the question which of the aforementioned modalities should be part of clinical mapping procedures to support surgical decision making. Mapping results obtained

in a single case study demonstrated spatial overlap of two distinct human fusiform face selective locations between fMRI and ECoG in a patient whose face perception was distorted while electrically stimulating those locations (Parvizi et al., 2012). Another case study showed that electrical stimulation of face selective ERP and gamma band locations on the anterior fusiform gyrus induced transient prosopagnosia. However, fMRI could not localize these regions because of a severe signal dropout by an artifact (Jonas et al., 2015).

For a clinically relevant mapping protocol, these findings should be explored in more patients. This study validates mapping of face selective locations in fMRI, ECoG, and ECS in a group study using within-patient comparisons, to better understand their clinical relevance and to reduce post-operative prosopagnosia. As for epilepsy surgery the occipital lobe is relatively uncommon in daily clinical situations (Taylor et al., 2003; Pfaender et al., 2004), the region of interest (ROI) focuses on the ventral temporal cortex, specifically the fusiform gyrus and the inferior temporal gyrus.

MATERIALS AND METHODS

Patients

Five consecutive patients at the Asahikawa Medical University Hospital underwent surgical treatment of intractable epilepsy between 2015 and 2018. All patients in this study required implantation of subdural electrodes followed by curative surgical treatment. They are four males and a female, whose age ranged from 17 to 37 years, and whose WAIS-III (Wechsler adult intelligence scale) full IQ was 58–105. Their pre-surgical assessment required the implantation of subdural grid electrodes on the ventral temporal cortex for diagnostic purposes, including video EEG monitoring to localize seizure onset zones and routine functional mapping. Additionally, the patients underwent an extensive ECS procedure to localize face selective locations and thus avoid post-operative deficits like prosopagnosia. The two additional functional mapping procedures in this study, ECoG and fMRI, provided supportive information. Wada test was performed in determining language lateralization. **Table 1** presents the patients' characteristics. All patients were defined as "unknown" etiology based on The International League Against Epilepsy Classification of the Epilepsies (Scheffer et al., 2017). The study was approved by the Institutional Review Board of the Asahikawa Medical University (Asahikawa Medical University Research Ethics Committee). Written informed consent, including detailed explanation, was obtained from each patient and their family.

Each patient had a pre-operative computerized tomography (CT) scan to identify electrode locations in conjunction with pre-operative magnetic resonance imaging (MRI) as part of the fMRI mapping. Each patient's brain was reconstructed in FreeSurfer (Martinos Center for Biomedical Imaging, Cambridge, MA, United States) using the T1-weighted MRI (Dale et al., 1999). Then, pre-operative MRI data were co-registered to post-operative CT scans using SPM12 (Wellcome Centre for Human Neuroimaging, London, United Kingdom) to localize electrode positions on the cortex (Penny et al., 2011). **Figure 1** shows the projected electrode locations of all patients on the MNI152 (Montreal Neurological Institute) brain.

Mapping Procedures

fMRI

The fMRI examinations were performed with a 3.0 T whole-body MR scanner with echo-planar capabilities and 32-channel surface coil (Discovery 750 W; General Electric, Milwaukee, WI, United States). All patients participated in the fMRI mapping, three of them pre-operatively (P3, P4, and P5) and two post-operatively (P1 and P2). Specifically, fMRI for P1 and P2 were obtained 3 and 1 year after surgery, respectively. During the scans, foam cushions stabilized their heads to prevent motion artifacts. First, a high-resolution T1-weighted 3D volumetric scan was obtained for co-registration of the functional maps, consisting of 1.2 mm thick axial slices with a resolution of 256 × 256 pixels in a field of view of 240 mm. As depicted in **Figure 2**, five task block conditions were acquired during fMRI to reveal functional brain regions specific to visual categorization. These conditions included photographs of faces and objects, either colored or grayscale, and black screens. Patients were asked to look at a 32′ monitor about 270 cm away, yielding a visual angle of 14.9° × 8.3°. They focused on the visual paradigm while they were shown visual stimuli (faces, objects or black screens) for 500 ms and subsequent 500 ms black screen over a period of 100 s in total. The relative luminance (Rec. ITU-R BT.709-6) of 0.058 for faces and 0.046 for objects was similar in both conditions, and the medium spatial frequency band of 5–15 cycles/face,

TABLE 1 | Demographic data for all five patients.

Patient	Age	WAIS-III Full IQ	Handedness	Language dominance	MRI findings	Seizure onset zone	OP	Symptoms	Etiology	ROI electrodes, n	Total electrodes, n	fMRI pre/post OP
1	26	96	R	L	None	R Temporal	R anterior temporal lobectomy	CPS	Unknown	R 22 L 27	R 56 L 132	Post
2	17	105	L	L	None	L Temporal	L lateral temporal lobectomy	CPS, GCS	Unknown	L 27	L 166	Post
3	22	63	R	L	None	R Temporal	R hippocampectomy	CPS, GCS	Unknown	R 37	L 160	Pre
4	23	78	R	L	None	R Temporal	R hippocampectomy	CPS, GCS	Unknown	R 40	R 160	Pre
5	37	58	R	L	None	R Temporal	R anterior temporal lobectomy	CPS, GCS	Unknown	R 25	R 102	Pre

R, right; L, left; OP, Operation; CPS, complex partial seizures; GCS, generalized convulsive status; ROI, region of interest; WAIS-III, Wechsler Adult Intelligence Scale-III.

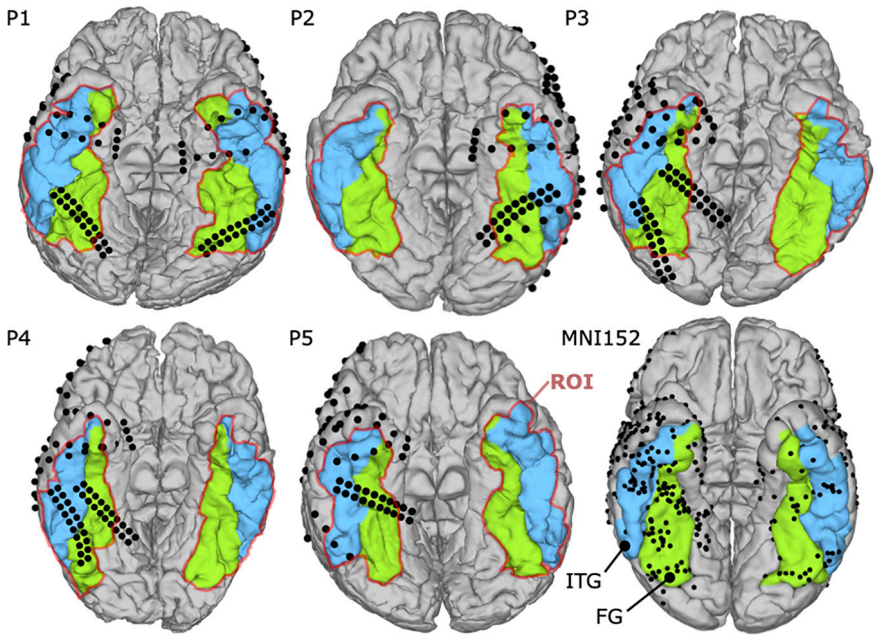

FIGURE 1 | Locations of the implanted electrodes (black balls) on the MNI152 brain and the individual coverage of each patient. The selected region of interest (ROI) is defined by colored cortex regions, including the fusiform gyrus (FG) (green colored) and the Inferior temporal gyrus (ITG) (blue colored).

which is most relevant for face processing (Collin et al., 2012), consisted of 13.2% or −8.79 dB of the whole signal energy for both, faces and objects.

The presenter in the g.HIsys online processing toolbox in Simulink (g.tec medical engineering GmbH, Austria) managed the paradigm and stimuli. Stimulus presentation was synchronized with the scanner using TTL trigger. During the presentation period, a T2-weighted echo-planar imaging sequence acquired dynamic volumes of the task block conditions (TE = 30 ms; TR = 4000 ms; flip angel: 80°; slice thickness: 3 mm; field of view: 240 mm; matrix: 64 × 64; number of 40 slices). Each block contained five echo-planar imaging volumes. The experiment was repeated four times in pseudo-randomized order, yielding 25 volumes per sequence and three additional preceding dummy scans. At the end of the fMRI mapping, 40 volumes per condition (face and object) were available for statistical analysis in SPM12 (Wellcome Centre for Human Neuroimaging, United Kingdom). Parameters were mainly selected based on the suggested analysis pipeline for the high-level visual cortex (Weiner and Grill-Spector, 2013) and previously used settings to obtain faces selective cortex regions on the ventral temporal cortex (Winston et al., 2004; Liu et al., 2008; Jonas et al., 2015; Schwarz et al., 2019; Farmer et al., 2020).

The fMRI scans were pre-processed including: (a) realignment of the fMRI time-series, (b) co-registration of the realigned functional images on the anatomical MRI volume by maximizing their normalized mutual information with the mean functional image, and (c) spatial smoothing with an isotropic Gaussian kernel (2 mm). For the analysis, a first-level model was specified and estimated, data were corrected for low frequency drifts (128 s high pass filter) and corrected for serial correlations with a first-order autoregressive model. A binary mask of gray matter was used to constrict the analysis. The mask was created by segmenting the structural MRI volume in SPM12. We concatenated all runs by replacing the usual mean column in the design matrix with regressors modeling each session and adjusting the high-pass filter and non-sphericity calculations as if sessions were separate. For each patient, a t-map volume was created using the contrast of interest (i.e., presentation times of gray and colored faces against those of gray and colored objects).

The SPM t-map volumes were mapped onto the surface of the corresponding reconstructed brains (triangulated meshes). The t-values were assigned to the surface vertices by averaging the voxel intensities along 6 mm of the vertex normal directions using Gaussian weights (FWHM = 10 mm) (Hermes et al., 2012; Gaglianese et al., 2017; Haufe et al., 2018). For each electrode location, a t-value was determined by averaging the highest 5% of the t-values within a radius of 6 mm (Hermes et al., 2012; Gaglianese et al., 2017; Haufe et al., 2018). Electrodes with a t-value > 3.3 were considered as fMRI positive, which corresponds to a statistically significant activation threshold of $p < 0.001$ (uncorrected, DOF = 87).

ECoG

Intracranial EEG was obtained from subdural grid electrodes (Unique Medical Co., Ltd., Japan) with 1.5–3.0 mm exposed diameter and 5–10 mm spacing, which were originally implanted for epilepsy monitoring. Data were recorded at the bedside by a DC coupled g.HIamp biosignal amplifier (g.tec medical engineering GmbH, Austria) and digitized with 24-bit resolution at a sampling rate of at least 1200 Hz. Dorsal parietal electrodes served as ground (GND) to ensure no overlap with the ROI.

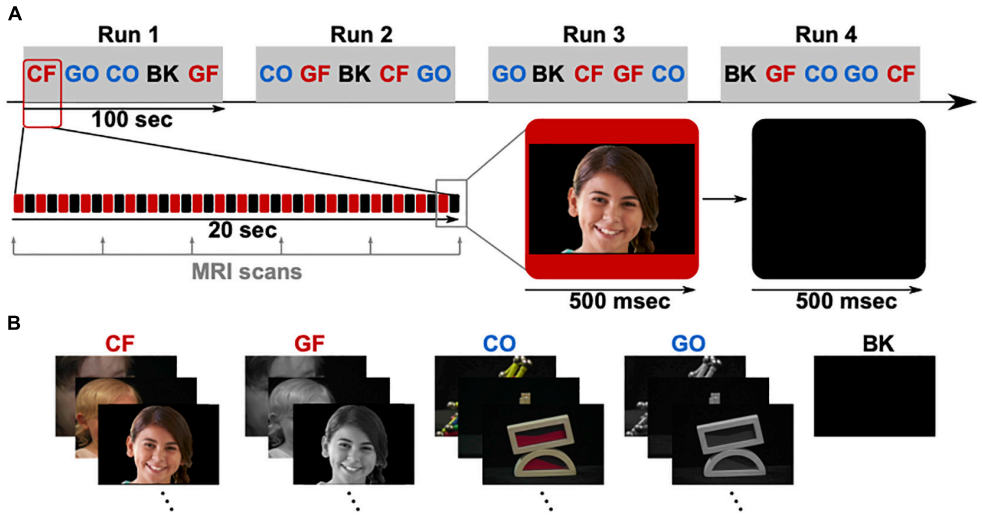

FIGURE 2 | (A) fMRI paradigm consisting of four runs (Run 1–4), each containing five blocks in pseudo-randomized order. The five blocks are colored faces (CF), grayscale faces (GF), colored objects (CO), grayscale objects (GO), and black screens (BK). Each block lasts 20 s, showing 20 stimuli (500 ms presentation time). **(B)** Example stimuli for each block. The visible face is representative for the original stimuli and used from a public database (copyright shutterstock).

A 14′ presentation monitor was placed at 80 cm in front of the patient's face, showing visual stimuli to the patients, who were instructed to look at the monitor and focus on the paradigm in **Figure 3**. The resultant visual angle was 22.0° × 12.5°. The visual stimulation paradigm contained seven different types in colored and grayscale variants. Among others, photographs of faces and objects were displayed for 200 ms and followed by black screen for 600–800 ms. Each type was presented 68 times, randomly chosen out of a pool of 20 different pictures. Presented images of faces and objects were identical with those during fMRI.

Electrocorticography data were acquired and processed by means of the g.HIsys real-time processing library (g.tec medical engineering, Austria), which also controlled the experimental paradigm and stimulus presentation. Initial processing steps included a remove drift filter (2 Hz high-pass, fourth order Butterworth) and a common average reference. Afterward, a combination of band-pass filter (110–140 Hz, Butterworth, low and high pass of fourth order each) and Hilbert transform resulted in broadband gamma signals, which were down-sampled (to 400 Hz) and square-root transformed to approximate Gaussianity. Finally, signals were standardized with respect to 300 ms periods immediately preceding stimulus presentation (−300 to 0 ms).

Changes in broadband high gamma activity of the active face phases (100–400 ms: post-stimulus period) compared with active object phases (100–400 ms: post-stimulus period) were calculated into coefficient of determination (r^2) for each individual electrode in each paradigm. The r^2 value can be translated to a t-value under consideration of the sample size (i.e., number of trials denoted by N_OBJ and N_FACE) as follows:

$$t = \sqrt{\frac{r^2(N_{\mathrm{OBJ}} + N_{\mathrm{FACE}} - 2)}{1 - r^2}}$$

Thus, an $r^2 > 0.02$ yields $t > 1.98$ ($p < 0.05$, two-tailed), and after Bonferroni correction for up to 188 electrode locations per patient, a critical $r^2 > 0.10$ ($t > 3.74$) reliably indicates significant difference of object and face related high gamma

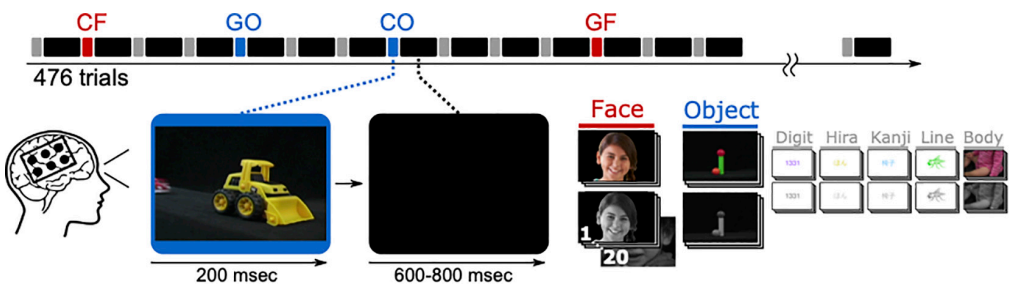

FIGURE 3 | One ECoG paradigm lasts 476 trials, each with 200 ms presentation time and 600–800 ms inter-stimulus-interval, resulting in 333 s on average. Trials showing faces (CF and GF) or objects (CO and GO) were considered in the analysis. The visible face is representative for the original stimuli and used from a public database (copyright shutterstock).

activity. Hence, ECoG locations were considered as face selective if they exceeded $r^2 > 0.1$.

ECS

Functional mapping through ECS was performed at the same locations as the ECoG mapping. Electrical stimulation trains of 3–10 s were injected into pairs of adjacent electrodes on the patient's brain surface using biphasic constant current pulses (50 Hz train rate; 0.2 ms pulse duration) using Neuromaster MEE-1232 (Nihon Kohden Co., Japan). Current amplitudes started from 3 mA and increased progressively until symptoms occurred, or up to 10 mA at maximum. In an initial motor mapping, the minimum current threshold necessary to elicit movement was determined in each patient. Then, stimulation was applied in the same way to map the temporal-occipital face recognition. During the stimulation, the patient sat and leaned back on the bed to relax. The patient was shown human face photographs and asked to report any change in perception. If a patient perceived any change or felt something while looking at the photographs, the patient was further asked to look at objects and the presenter's own faces to discriminate face related from object related responses. A region was defined as ECS positive (or face specific) if a patient reported consistent face illusions (or any consistent change in the face perception) that did not occur in objects while looking at faces and objects.

Surgical Outcome Evaluation

Post-operative T1-weighted MRI was obtained from each patient to extract the resected volumes. The electrode locations within 10 mm distance to the resected volume were defined as resected locations to comply with the 10 mm safety margin published in previous mapping studies (Haglund et al., 1994; Sanai et al., 2008; Swift et al., 2018).

RESULTS

ECS

Figure 4 shows the ECS results of patients P1 to P5. Two of five patients (P1, P2) reported face related symptoms in response to ECS in 17 locations within the ROI. On the other hand, 21 electrodes in ROI were not tested by ECS because of the electrode issues, time effort or burden for the patient, or the high risk of inducing a seizure near the seizure onset zone. Patient

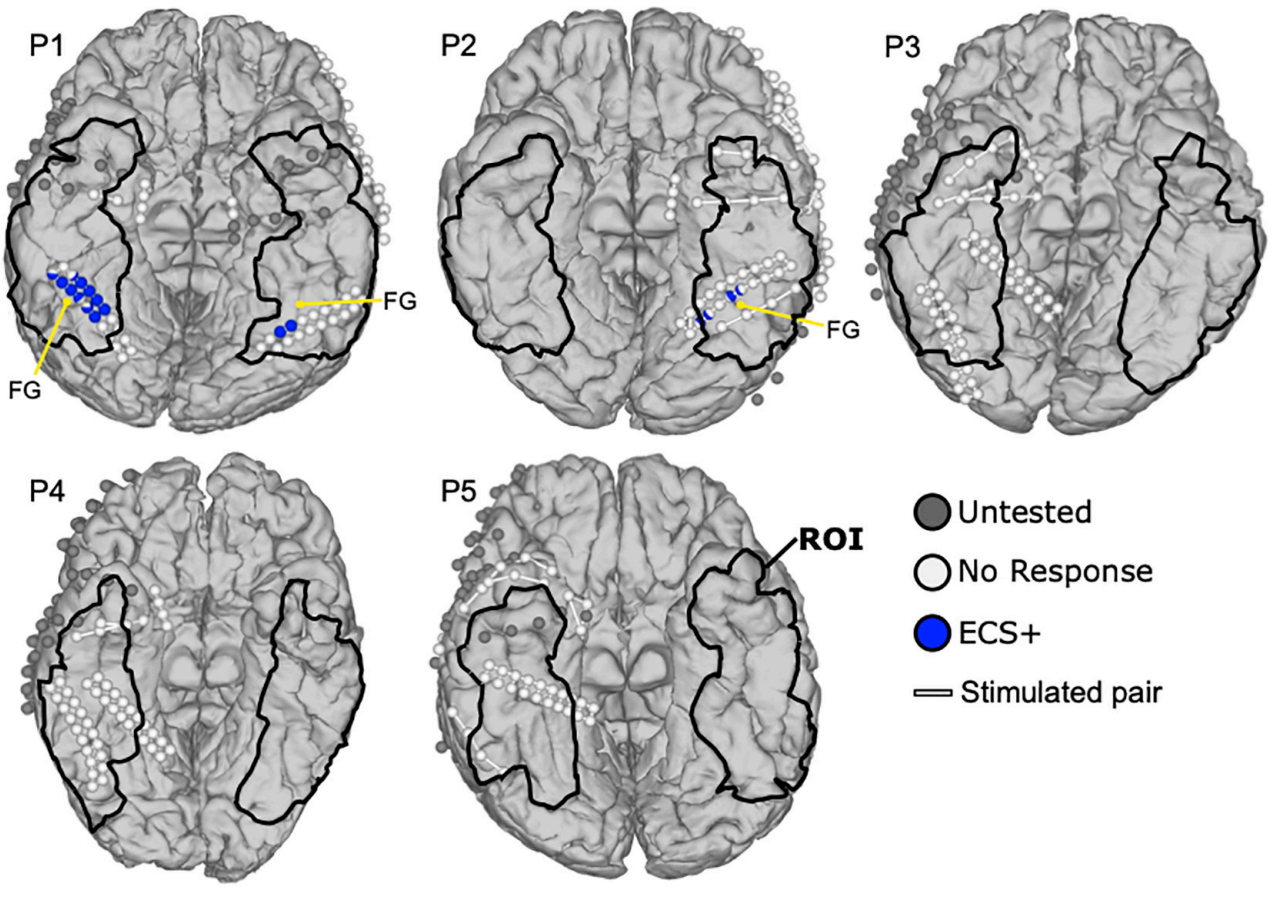

FIGURE 4 | Mapping results of ECS for face perception. Blue colored balls represent face selective locations during ECS that caused reported symptoms in the patients. White balls are silent locations without reported symptoms and gray ones were not stimulated because of limited mapping time. White lines connect the electrode pairs that were stimulated together. The region of interest (ROI) is marked with black lines. Anatomical landmarks show the fusiform gyrus (FG).

P1 reported that the face and eyes completely changed during stimulation while he observed a real face. He further mentioned seeing an eye and mouth on the box, the ball and the kanji and their shapes did not change. Thus, two functional clusters were revealed covering 13 ECS positive locations in blue, one on the right and the other one on the left lateral fusiform gyrus. Notably, the cluster on the right hemisphere (11 locations) was larger than the one on the left (two locations), but their locations were almost symmetric. Also, the four face specific locations in P2 could be clustered in two regions of the left fusiform gyrus, two at the medial side and the other two at the lateral side. During the stimulation, P2 experienced different sized right and left halves of the observed face, and reported that the right and left halves of the faces were from different people, which P2 described as "Picasso pictures." This ECS symptom occurred only while looking at faces, but not for objects. The remaining cases did not report any face specific symptoms elicited by ECS.

ECoG

Figure 5 shows the ECoG mapping results with face selective locations in the ROI. In total, 35 face locations were identified in four of five patients (P1–P4). Four electrodes in ROI were not tested by ECoG bad signal quality due to electrode attachment. In P1, two bilateral activation clusters of 8 (right) and 11 (left) locations were found at the middle lateral side of fusiform gyrus, with almost symmetric activation patterns. One location in the left inferior occipital gyrus was excluded as it was outside the ROI. P2 demonstrated three face selective locations in the ROI at the lateral side of fusiform gyrus. Another face selective location was in the parahippocampal gyrus, outside the ROI, and thus excluded. In P3, 11 face selective ECoG locations were assembled in a large cluster at the right lateral side of fusiform gyrus. Another two ECoG positive locations were at the occipital lobe and out of ROI. Finally, one face selective site was found in P4 and located on the right middle lateral side of fusiform gyrus, consistent with the expected face area. P5 had no ECoG positive locations, but showed high impedance in four ECoG locations, and hence these areas were not tested during the ECoG mapping.

fMRI

Figure 6 shows the fMRI mapping results from all cases. In all cases, the BOLD signals responded significantly higher to faces than objects in middle lateral regions of the fusiform gyrus in either one or both hemispheres. Those 38 face selective locations that were lying within 6 mm of ECoG locations were further denoted as fMRI positive locations and occurred in all patients. Artifacts in the fMRI caused a signal drop-out in 60 electrodes locations in the ROI. In P1, 21 fMRI positive (fMRI+) locations were detected in the ROI of both hemispheres. Thus, clusters of twelve in the right and nine in the left side were symmetrically located at the fusiform gyrus. Three locations in the right lingual gyrus, two in the right inferior occipital gyrus, and one in the left

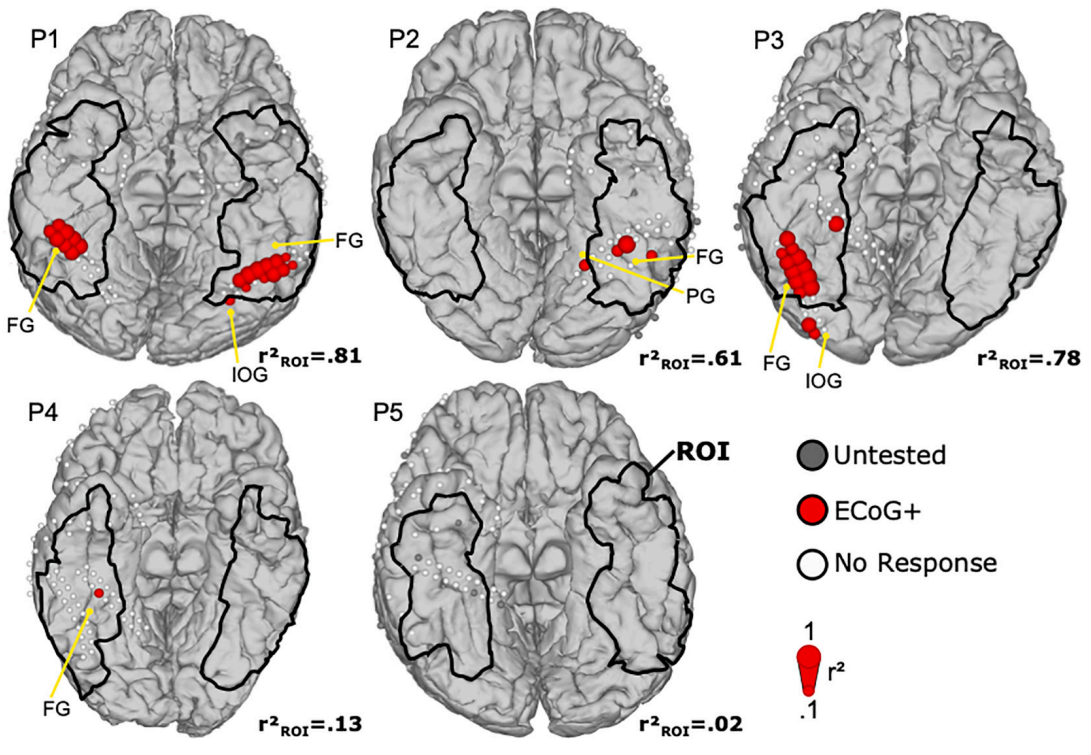

FIGURE 5 | Mapping results of ECoG for face perception. Face selective ECoG locations are denoted by filled red circles. The diameter of each circle corresponds to the face related r^2 value of that location. White ECoG locations did not exceed the significance threshold, and gray locations had to be excluded from further processing due to bad signal quality after visual inspection. The region of interest (ROI) is marked with black lines. Anatomical landmarks show the fusiform gyrus (FG), the inferior occipital gyrus (IOG), and the parahippocampal gyrus (PG).

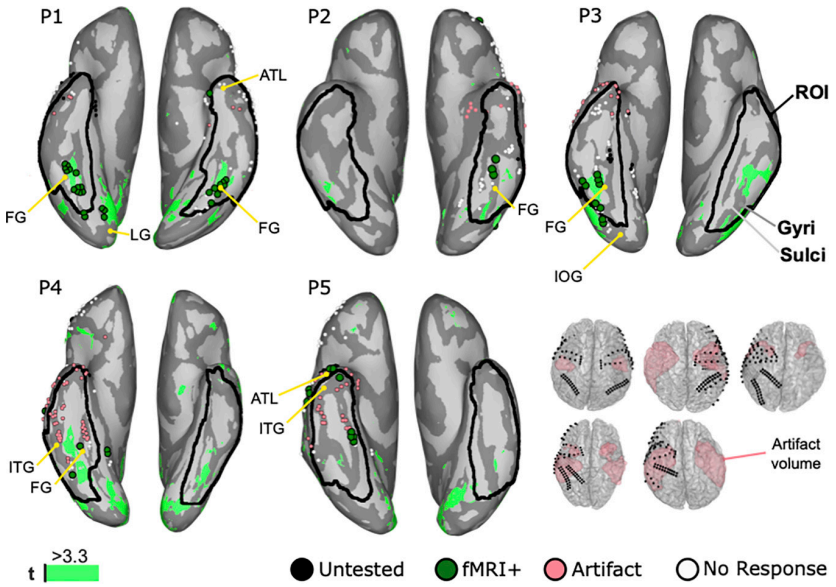

FIGURE 6 | Mapping results of fMRI for face perception on inflated brains of five patients with highlighted region of interest (ROI). Inflated brains illustrate gyri (dark gray) and sulci (light gray) to reveal hidden activation. Anatomical landmarks show the fusiform gyrus (FG), the inferior temporal gyrus (ITG), the lingual gyrus (LG), the inferior occipital gyrus (IOG), and the anterior temporal lobe (ATL). White dots represent electrodes' locations on the gyri. Significantly higher BOLD responses to faces compared to objects are colored in green (light green: $t \geq 3.3$). Black dots are untested locations due to post-surgical fMRI. Coral dots are locations contaminated by the MRI artifacts shown the volume plots.

anterior temporal lobe were outside the ROI and thus rejected. In P2, the cluster of three fMRI positive locations is in the left fusiform gyrus. P3 demonstrated seven fMRI positive locations in the lateral side of the right fusiform gyrus. Another two posterior locations were out of the ROI in the inferior occipital gyrus and thus excluded. In P4, two locations are in the right fusiform gyrus. On the other hand, two locations in the right lingual gyrus were excluded. In P5, one electrode was at the anterior rim of inferior temporal gyrus and four electrodes in the fusiform gyrus. Two locations in the anterior temporal lobe were out of the ROI. In addition to the aforementioned face selective fMRI locations, more regions were identified in the frontal lobe, the lateral temporal lobe, the parietal lobe, and the occipital lobe, but were rejected because those regions were outside the ROI.

Comparison Among Three Modalities

Figure 7 shows the combined results for ECoG, ECS, and fMRI. In total 178 locations were in the ROI and 54 face locations were identified by at least one modality in all patients. Detection rates were 70.4, 64.8, and 31.5% for fMRI, ECoG, and ECS, respectively. Thus, 28 of those areas were co-localized by at least two modalities, with detection rates of 89.3% for fMRI, 85.7% for ECoG, and 53.6% for ECS. Eight face locations were co-localized in all three modalities in P1 and P2. In P1, All of them covered the bilateral lateral fusiform gyrus in two small clusters, five adjacent locations on the right and two adjacent locations on the left hemisphere. The clusters were surrounded by face selective locations identified by two modalities (mixed paired combinations of ECoG, ECS, and fMRI). ECS biased toward the right one and both fMRI and ECoG equally distributed on both sides. Finally, four ECoG and four fMRI positive locations remained unconfirmed by another modality. P2 also reported face locations by all three modalities. One location in fusiform gyrus was co-localized in all three modalities and one location medial side to it was commonly activated in the lateral fusiform gyrus in both ECS and ECoG. On the other hand, two locations were identified by fMRI anterior to the co-localized face locations and one more lateral location was identified by ECoG only. Those face locations clustered in left fusiform gyrus.

Another two patients responded with face selective locations in at least two modalities. In P3, fMRI and ECoG mappings revealed 7 and 12 face selective locations, respectively. All seven fMRI positive locations were located in the right fusiform gyrus, co-activated in ECoG, and surrounded by the remaining five ECoG positive locations. In P4, ECoG mapping detected one positive location and fMRI found two positive locations, but no location was co-localized.

One patient, P5, showed activation in only a single modality. Thus, fMRI detected five positive locations, one at inferior temporal lobe and the other four at right medical fusiform gyrus within the ROI. P5 further had one "unknown electrode," because it was not tested by ECS and ECoG, and also affected by the fMRI artifact (closer than 6 mm).

Extent of Resection, Functional Outcome and Related Electrode Locations

Figure 8 shows the extent of resection together with 49 ECoG and ECS locations near the resected volumes. Five resected locations were identified as face selective, one by ECoG in P3 and the

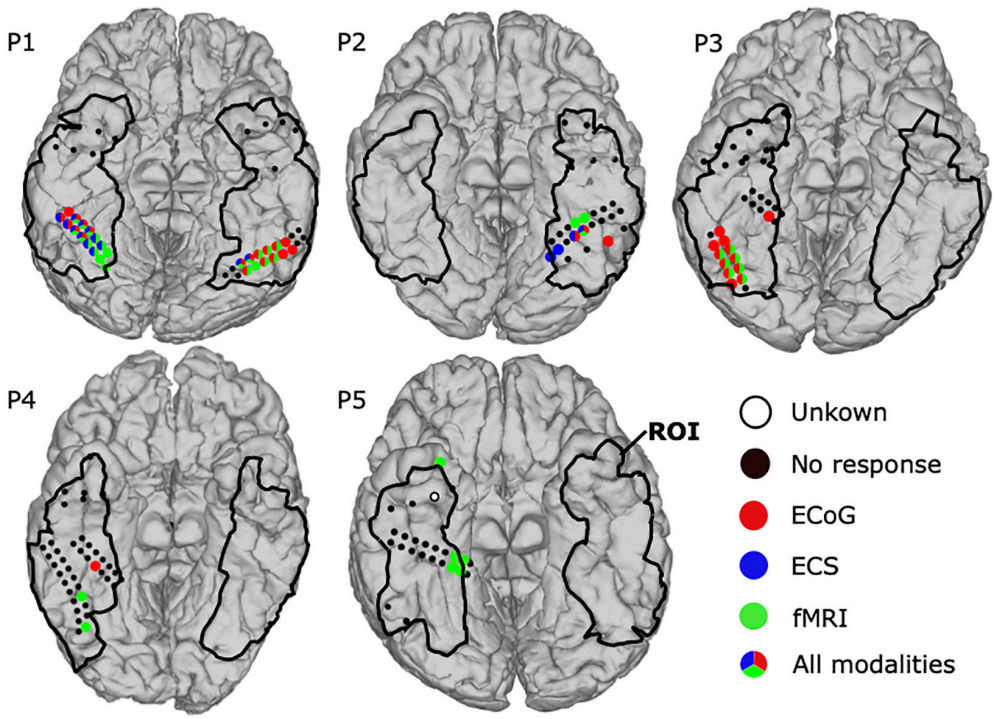

FIGURE 7 | Mapping results for comparison among three modalities: ECoG, ECS, and fMRI. Face selective locations in the ROI are shown as filled circles, detected by ECoG (red), ECS (blue), and fMRI (green). Locations identified by multiple modalities have circles with mixed colors. Black dots represent locations without any face related response. The region of interest (ROI) is marked with black lines. Untested locations are highlighted in white.

other four by fMRI in P5. None of the patients suffered from prosopagnosia, as each of them could recognize their doctors', nurses', and family faces after surgery. Hence, the five locations were considered as false positive. One location in P5 remained untested, yielding 43 locations which were tested by at least one modality near the resected area were considered as true negative.

Eleven ECS, three ECoG, and 33 fMRI locations could not be tested during the individual sessions, but got tested by at least another modality. Six electrodes inside the resection area in P1 were not stimulated because of after discharges and the high risk of inducing a seizure near the seizure onset zone. One resected location could not be stimulated in P3 due to bad electrode attachment. The last four not stimulated locations were located in P5, which included a broken electrode connection. During fMRI, two electrodes in P1 and one electrode in P2 inside the resection area were not tested by fMRI, as the scans were obtained post-operatively. Moreover, the number of locations in the resection area that were contaminated by an fMRI artifact was 3, 1, 2, 8, and 16 in P1 to P5, respectively. The four untested ECoG locations were excluded because of bad signal quality due to electrode attachment.

DISCUSSION

Face selective cortex regions have been revealed in numerous neuroimaging studies based on ECS, ECoG, or fMRI. Most of them either utilized only one modality or demonstrated findings in individual subjects. To the best of our knowledge, this is the first report on face functional mapping compared with surgical outcomes.

Although no face recognition deficits occurred after surgery, surprisingly, ECS elicited face processing symptoms in only 2/5 patients, revealing only 31.5% of all identified face selective locations. ECS did not elicit any face specific symptoms in P3, P4, and P5, while positive locations in P2 were similar to corresponding areas in the left sided cluster in P1. To date, ECS is still the gold standard method for functional brain mapping of motor and language areas (Penfield and Boldrey, 1937; Ojemann et al., 1989). However, the fact that only two out of five patients reported face selective symptoms raises doubts that ECS is robust enough to localize face perception in the brain. Previously, several studies have shown that electrocortical stimulation causes distortion of face perception or transient prosopagnosia, but the majority investigated single cases (Mundel et al., 2003; Parvizi et al., 2012; Schalk et al., 2017). In this group of five consecutive patients it seems that the inter-patient variability of the symptoms is quite high. As the ECS symptoms can be considered as transient apperceptive prosopagnosia it may be that the low sensitivity can be explained by the complex nature of the visual categorization network. The observed low sensitivity of ECS could be due to the inactivation of only parts of this network. This effect has been demonstrated in cases with prosopagnosia before, in whom it was more likely to occur in the right occipito-temporal areas,

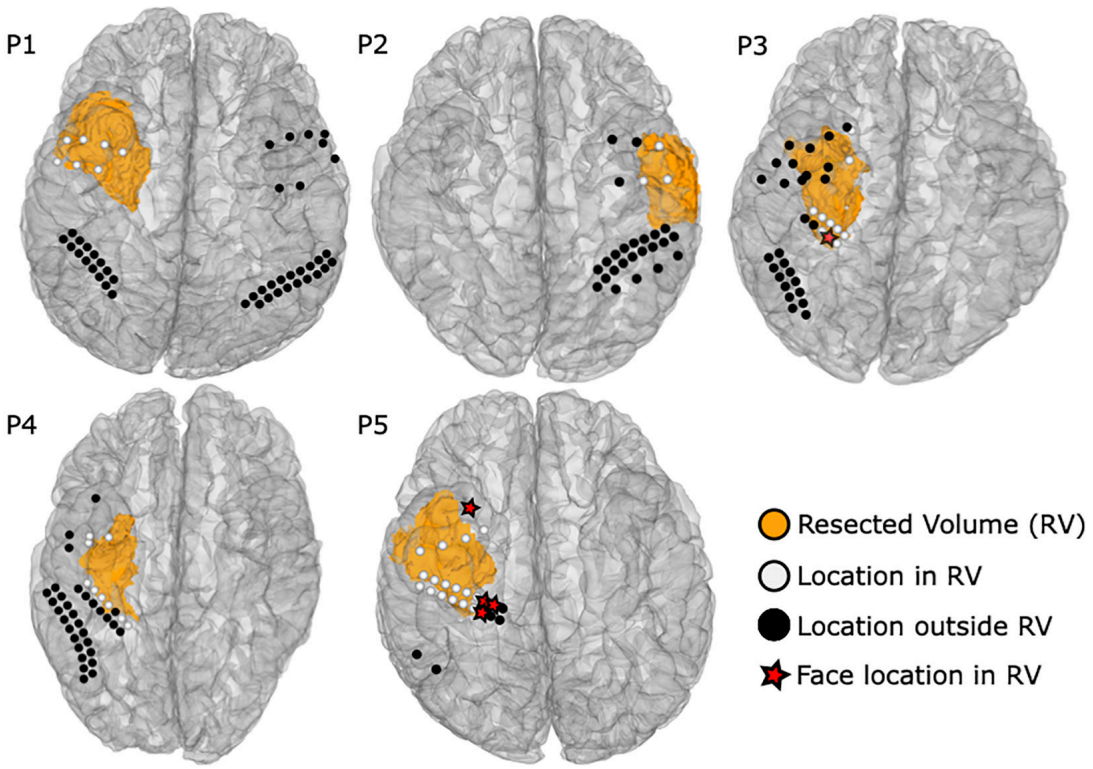

FIGURE 8 | Resected volumes from the post-operative MRI are shown as orange blobs. ECoG and ECS locations are colored white within 10 mm from the resected volume, whereas black labeled ROI locations were considered as distant and thus not relevant to the surgical outcome. Red stars highlight face selective locations in the resected volume.

often with combined multiple lesions, including the lingual, fusiform and anterior inferior temporal cortices (Meadows, 1974; Damasio et al., 1982; Barton et al., 2002; Bukach et al., 2006; Sorger et al., 2007). Therefore, ECS may struggle to inhibit the network, since it affects a small area of the brain surface through a stimulated electrode pair.

Broadband gamma ECoG activity seems to be a more robust marker to reveal face selective locations (Jonas et al., 2016), and significantly responded only to faces in four out of five cases in this study. ECoG mapping showed the second highest detection rate, revealing 64.8% or 35 of 54 face selective locations in 4/5 patients. Thus, 85.7% or 24 of 28 face selective locations were co-localized with ECoG. This indicates that broadband gamma activity in ECoG provides higher sensitivity compared to ECS. Interestingly, in P1, all three modalities successfully detected the face selective area at fusiform gyrus and also in P2 at left fusiform gyrus similar to a previous report (Schalk et al., 2017). Notably, ECoG revealed the locations that were ECS negative in P3 and P4, but located at the middle and posterior part of the fusiform gyrus, known as the FFA (Kanwisher et al., 1997). This could be due to the subjective reporting and evaluating or ECS symptoms. ECS has major problems when distinguishing face selective from visual processing locations, and a protocol that addresses any specific visual category would be time-consuming and demanding for the patient. ECoG clearly reveals face selective locations objectively that cannot be found by ECS, either because of insensitivity of the patient or difficulty classifying the reported symptoms. This suggests that ECoG could map the FFA more effectively than ECS, without long-lasting protocols and the burden to iteratively check only a few electrodes being stimulated at a time. Taking into account the broad and complex network that is involved in face perception, ECoG, as an observational technique, may be a more practical procedure to detect the face processing network.

Face selective BOLD responses during fMRI appeared on the ventral temporal cortex in all patients, exceeding the significance threshold $t > 3.3$. In P1, P2, and P3, the activated regions overlapped with electrode locations on the lateral fusiform gyrus and were co-identified in ECoG, containing 25 out of 28 locations found by at least these two modalities. Those results support the sustained and strong correlation between fMRI and ECoG signals in the high frequency broadband range of 30–160 Hz (Jacques et al., 2016). Furthermore, in P5, fMRI was only one modality that identified four face locations at fusiform gyrus and one positive face region at anterior tip of collateral sulcus (Nasr and Tootell, 2012; Tanji et al., 2012; Jonas et al., 2016). This area was not covered by subdural electrodes. Notably, P4 showed significant fMRI activation in the sulcus between fusiform and inferior temporal gyrus, which was not visible in ECoG or ECS locations on the gyrus above. Consequently, fMRI is useful for revealing functional regions that are not covered by electrodes, and may be considered for pre-surgical mapping. This is important for

surgical planning, because exact positioning of the electrodes at the temporal base can be difficult due to bridging veins, and the number of grids that can be implanted is limited. Furthermore, potential infections after implantation are a serious risk.

None of the brain surgeries required resecting ECS positive cortex locations. Notably, P1 had six locations inside the resected area, which were not stimulated because of frequent after-discharges near to the seizure onset zone and high risk of seizure. On the other hand, five face selective locations, one obtained by ECoG and another four by fMRI, were within 10 mm of the resected volumes. Thus, ECoG and, most of all, fMRI tend to be too sensitive, which is a known issue of observational mapping techniques (Tharin and Golby, 2007). Interestingly, the false positives remained unconfirmed by any other modality. All other face selective locations remained outside the resected volume, which of course cannot be validated with respect to functional outcome, since the resection area must be as small as possible. Meanwhile, 43 true negative and no false negative locations reliably predicted a safe operation without post-operative prosopagnosia. The lower specificity of ECoG and fMRI, caused by the false positive locations, could be overcome by combining mapping results of co-localized face selective locations.

Each modality comes with disadvantages that should be considered. ECS has side effects that include stimulation-induced pain and seizures. Stimulating the ventral temporal cortex caused facial pain in P2 and P5, facial numbness in P3, and uncomfortable face contraction in P4. Discomfort or pain during ECS may occur because of the limited space between dura mater and cortex. Thus, the current during ECS propagates to the dura mater or trigeminal nerve, which could obstruct the mapping or surgery. ECS also induced after discharges in P1, P3, P4, and P5, and caused a seizure in P5, and hence the mapping was stopped. fMRI could underestimate or fail to disclose face area because of other reasons, including susceptibility to artifact in the anterior half of ventral occipital temporal cortex arising from the ear canals (Weiner and Grill-Spector, 2010; Rossion et al., 2018) and in the inferior lateral temporal lobe due to the brain region adjacent to bone and air sinuses (Ojemann et al., 1997). Our study showed that 30 of 49 electrodes in resection volumes were contaminated by an fMRI artifact. This result suggests that fMRI is not sufficient for pre-surgical face mapping of the anterior ventral temporal cortex. On the other hand, based on the results in this study, face selective locations were found on the posterior parts of the ventral temporal cortex. Although the regions are quite close to those obtained with ECoG and ECS, the artifact volumes in **Figure 6** raise concerns about the feasibility of fMRI to reveal all relevant face regions. The observed artifacts were mainly visible in anterior regions of the temporal lobe, in which lesions could cause associative prosopagnosia (Evans et al., 1995; Gainotti et al., 2003). Nevertheless, significant activation of face selective locations was identified in the ROI in all patients, mainly in regions related to apperceptive prosopagnosia (Damasio et al., 1982; De Renzi, 1986; De Renzi et al., 1991; Bouvier and Engel, 2006; Gainotti, 2013).

On the other hand, although no adverse events occurred during the ECoG mapping, four locations were excluded due to their high impedance for recordings during the ECoG procedure because of the problem with the electrodes' attachment to brain surface. However, ECS faces this challenge too, because ECS also requires implanted electrodes. Thus, ECoG and fMRI have fewer disadvantages, which are basically conceptual limitations such as connection problems or artifacts. Therefore, ECoG and fMRI tend to be more practical procedures than ECS in terms of time effort (Wen et al., 2017), and–above all–they do not induce pain or seizures when mapping the ventral temporal cortex.

The current study extends existing literature using a multimodal approach with increased sensitivity and detection rate of face selective areas. Interestingly, this study showed that ECoG and fMRI could reveal face selective cortex regions that were not identified through ECS. Furthermore, fMRI negative results have to be handled with care, as not all tissue in the ROI can be mapped due to artifacts. It seems that ECoG results, although limited to the implanted locations, most reliably reveal face selective areas. In order to avoid prosopagnosia, it is also important to achieve a good predictor for the surgical outcome. Therefore, the high sensitivity of ECoG is not enough in clinical practice, considering the chance of false positive locations. To judge whether or not a resective surgery can be justified in terms of functional outcome it is important to co-localize face selective locations and thus, improve the specificity of the combined approach. In this study face selective locations were co-localized by more than two modalities in 3/5 patients at 28 locations. This also suggests that the multimodal approach is more sensitive for revealing face selective locations than ECS mapping alone. Mapping with ECS alone has a great specificity, as the symptoms caused by the stimulation mimic a potential prosopagnosia, but the low observed sensitivity for multiple patients may cause a lot of false negatives. A surgeon has to judge if the electrodes are truly negative, which can be achieved by adding multiple independent observations.

The present study has several limitations. First, the number of patients was limited to five. Hence, due to the high variability of the mapping results across the patients, it is possible that detection rates may change in a larger population. Nevertheless, this is the first study comparing face selective locations in multiple patients among ECS, ECoG and fMRI. Moreover, the 177 tested electrode locations in the ROI provide a large test population that justifies inferences based on the mapping results. Second, fMRI of P1 and P2 were taken after surgery. This still raises the concern of the remaining false negatives for fMRI. However, given the artifact effect, only two electrodes in P1 and one electrode in P2 were affected by post-surgical fMRI. Third, one electrode could not be tested by any modality, leaving a blind spot on that location. All other electrode locations were tested by at least one modality. However, the risk that locations may remain untested is high if only a single modality is used and the chance a location could not be tested was 11.80, 2.25, and 33.71% for ECS, ECoG, and fMRI, respectively. Testing all locations with each technique may not be possible given the aforementioned side effects, electrode issues, and patient condition. Therefore, combined results could at least ensure that the whole ROI is tested. Fourth, the anatomical T1 weighted image in P2 taken before surgery included severe artifacts which

caused missing parts of both sides of temporal lobes. It was not possible to repeat the MRI scans, because P2 suffered from mild claustrophobia during the fMRI, but merging the T1 weighted images taken before surgery and after surgery enabled us to visualize the anatomy of the ventral temporal cortex. Although there are still unclear parts on anterior fusiform gyrus, there are basically no problems to know the positional relationship between electrodes with the anatomy of the ventral temporal cortex. Fifth, the magnitude of *t*-values related to the BOLD responses in fMRI varied across patients. To make comparison easier, the threshold for fMRI positive locations was set to $t \geq 3.3$. Sixth, the fMRI acquisition protocol causes a signal drop-out on the anterior ventral temporal lobe due to the ear canal. Similar to other studies, a quite large volume artifact on the ventral temporal cortex in the ROI from the temporal bone, air sinuses, or ear canal, cannot be analyzed (Puce et al., 1995; Devlin et al., 2000; Ku et al., 2011; Golarai et al., 2017). The artifactual signal drop-out may be minimized by smaller voxel sizes to 1–2 mm, minimizing partial volume effects, but cannot be completely suppressed (Weiner and Grill-Spector, 2013). Seventh, the mapping protocols presented in this paper focus mainly on face perception areas of the brain, and thus, tend to avoid apperceptive prosopagnosia. Apperceptive prosopagnosia is more likely related to the damage of the fusiform gyrus (Meadows, 1974; Damasio et al., 1982; Bouvier and Engel, 2006), whereas a more associative variant is more likely related to anterior temporal damage (Evans et al., 1995; Gainotti et al., 2003). To avoid associative prosopagnosia an extension of the protocols testing for locations recognizing familiar faces could potentially improve the sensitivity of the mapping procedure. However, it could be difficult to establish such a protocol with ECS, which makes it less practicable in clinical practice. Finally, other fMRI studies revealed a cluster specific to face recognition located at the lateral part of inferior occipital gyrus, the OFA (Gauthier et al., 2000; Pitcher et al., 2011). This could be of interest for other brain surgeries like tumor resection. Since the current study focused on epilepsy surgery the inferior occipital gyrus was not included in the ROI (Taylor et al., 2003; Pfaender et al., 2004). Notably, in case of a one stage surgery under general anesthesia, like for occipital tumors, fMRI may be the most practical technique to prevent prosopagnosia.

To sum up, this is the first study for mapping of face selective locations among multimodalities, in ECS, ECoG, and fMRI, in a group study compared with surgical outcomes. Notably, ECS was least sensitive, whereas ECoG and fMRI tended to be too sensitive, as they had the face selective locations within 10 mm to the resected volumes even though the patients had no face recognition deficits. Each modality has its strengths and weaknesses. ECS is more invasive, time-consuming and subjective than ECoG and fMRI, and entails unique risks. Above all, fMRI had most false positive face selective locations within 10 mm to the resected volumes and was susceptible to artifact at ventral temporal cortex which varies from the individual anatomical structures at temporal base. Therefore, broadband gamma mapping with ECoG turned out to be the most useful and reliable markers to identify face selective locations. Moreover, a multimodal approach including these two modalities confirmed co-localized face locations along anatomical face area in 3/5 patients. This outcome suggests that combined mapping results of co-localized face selective locations can improve specificity by minimizing false positives. Combined mappings may also further reduce the risks of ECS by minimizing the required locations for stimulation. All modalities should be considered in a clinical mapping protocol, and combined mapping results of co-localized face selective locations improve the specificity of ECoG and fMRI, and at the same time improve the sensitivity of ECS.

DATA AVAILABILITY STATEMENT

The datasets presented in this article are not readily available because the datasets include hospital patient data. Requests to access the datasets should be directed to TS, sanataka9103@gmail.com.

ETHICS STATEMENT

The studies involving human participants were reviewed and approved by Asahikawa Medical University Research Ethics Committee. Written informed consent to participate in this study was provided by the participants' legal guardian/next of kin.

AUTHOR CONTRIBUTIONS

TS: drafting of manuscript, acquisition and analysis of data, interpreting and validation of the results, and operations. CK: study conception and design, acquisition and analysis of data, interpreting and validation of the results, and supervision. MJ: design of paradigms and data processing, analysis of data, and visualization. JG: design of paradigms and data processing. HO, TM, and RA: acquisition of data and operations. CG: software development, supervision, and project administration. All authors contributed to the article and approved the submitted version.

FUNDING

This work was supported in part by the Japanese government (Grant-in-Aid for Early-Career Scientists No. 19K18374 from 2019 to 2021). Furthermore, this study was in part funded by RAPIDMAPS 2020 (ID 9273).

REFERENCES

Allison, T., Ginter, H., Mccarthy, G., Nobre, A. C., Puce, A., Luby, M., et al. (1994a). Face recognition in human extrastriate cortex. *J. Neurophysiol.* 71, 821–825. doi: 10.1152/jn.1994.71.2.821

Allison, T., McCarthy, G., Nobre, A., Puce, A., and Belger, A. (1994b). Human extrastriate visual cortex and the perception of faces, words, numbers, and colors. *Cereb. Cortex* 4, 544–554. doi: 10.1093/cercor/4.5.544

Barton, J. J., Press, D. Z., Keenan, J. P., and O'connor, M. (2002). Lesions of the fusiform face area impair perception of facial configuration in prosopagnosia. *Neurology* 58, 71–78. doi: 10.1212/wnl.58.1.71

Barton, J. J. (2008). Structure and function in acquired prosopagnosia: lessons from a series of 10 patients with brain damage. *J. Neuropsychol.* 2, 197–225. doi: 10.1348/174866407x214172

Benton, A. (1990). Facial recognition 1990. *Cortex* 26, 491–499.

Bodamer, J. (1947). Die-Prosop-agnosie. Arch. Psychiatr. Nervenkrankh. 179, 6–54. English translation by Ellis, HD and Florence, M. (1990). *Cogn. Neuropsychol.* 7, 81-105. doi: 10.1080/02643299008253437

Bouvier, S. E., and Engel, S. A. (2006). Behavioral deficits and cortical damage loci in cerebral achromatopsia. *Cereb. Cortex* 16, 183–191. doi: 10.1093/cercor/bhi096

Bukach, C. M., Bub, D. N., Gauthier, I., and Tarr, M. J. (2006). Perceptual expertise effects are not all or none: spatially limited perceptual expertise for faces in a case of prosopagnosia. *J. Cogn. Neurosci.* 18, 48–63. doi: 10.1162/089892906775250094

Chong, S. C., Jo, S., Park, K. M., Joo, E. Y., Lee, M.-J., Hong, S. C., et al. (2013). Interaction between the electrical stimulation of a face-selective area and the perception of face stimuli. *NeuroImage* 77, 70–76. doi: 10.1016/j.neuroimage.2013.01.074

Collin, C. A., Therrien, M. E., Campbell, K. B., and Hamm, J. P. (2012). Effects of band-pass spatial frequency filtering of face and object images on the amplitude of N170. *Perception* 41, 717–732. doi: 10.1068/p7056

Corrivetti, F., Herbet, G., Moritz-Gasser, S., and Duffau, H. (2017). Prosopagnosia induced by a left anterior temporal lobectomy following a right temporo-occipital resection in a multicentric diffuse low-grade glioma. *World Neurosurg.* 97:756.e1–756.e5. doi: 10.1016/j.wneu.2016.10.025

Dale, A. M., Fischl, B., and Sereno, M. I. (1999). Cortical surface-based analysis: I. Segmentation and surface reconstruction. *NeuroImage* 9, 179–194. doi: 10.1006/nimg.1998.0395

Damasio, A. R., Damasio, H., and Van Hoesen, G. W. (1982). Prosopagnosia: anatomic basis and behavioral mechanisms. *Neurology* 32, 331–331. doi: 10.1212/wnl.32.4.331

De Renzi, E. (1986). "Current issues on prosopagnosia," in *Aspects of face Processing*, eds H. D. Ellis, M. A. Jeeves, F. Newcombe, and A. Young (Dordrecht: Springer), 243–252. doi: 10.1007/978-94-009-4420-6_26

De Renzi, E., Faglioni, P., Grossi, D., and Nichelli, P. (1991). Apperceptive and associative forms of prosopagnosia. *Cortex* 27, 213–221. doi: 10.1016/s0010-9452(13)80125-6

Devlin, J. T., Russell, R. P., Davis, M. H., Price, C. J., Wilson, J., Moss, H. E., et al. (2000). Susceptibility-induced loss of signal: comparing PET and fMRI on a semantic task. *NeuroImage* 11, 589–600. doi: 10.1006/nimg.2000.0595

Engell, A. D., and McCarthy, G. (2011). The relationship of gamma oscillations and face-specific ERPs recorded subdurally from occipitotemporal cortex. *Cereb. Cortex* 21, 1213–1221. doi: 10.1093/cercor/bhq206

Evans, J. J., Heggs, A., Antoun, N., and Hodges, J. R. (1995). Progressive prosopagnosia associated with selective right temporal lobe atrophy: a new syndrome? *Brain* 118(Pt 1), 1–13. doi: 10.1093/brain/118.1.1

Farmer, H., Hewstone, M., Spiegler, O., Morse, H., Saifullah, A., Pan, X., et al. (2020). Positive intergroup contact modulates fusiform gyrus activity to black and white faces. *Sci. Rep.* 10, 1–13. doi: 10.1038/s41598-020-59633-9

Gaglianese, A., Vansteensel, M. J., Harvey, B. M., Dumoulin, S. O., Petridou, N., and Ramsey, N. F. (2017). Correspondence between fMRI and electrophysiology during visual motion processing in human MT+. *NeuroImage* 155, 480–489. doi: 10.1016/j.neuroimage.2017.04.007

Gainotti, G. (2013). Is the right anterior temporal variant of prosopagnosia a form of 'associative prosopagnosia'or a form of 'multimodal person recognition disorder'? *Neuropsychol. Rev.* 23, 99–110. doi: 10.1007/s11065-013-9232-7

Gainotti, G., Barbier, A., and Marra, C. (2003). Slowly progressive defect in recognition of familiar people in a patient with right anterior temporal atrophy. *Brain* 126, 792–803. doi: 10.1093/brain/awg092

Gauthier, I., Tarr, M. J., Moylan, J., Skudlarski, P., Gore, J. C., and Anderson, A. W. (2000). The fusiform "face area" is part of a network that processes faces at the individual level. *J. Cogn. Neurosci.* 12, 495–504. doi: 10.1162/089892900562165

Ghuman, A. S., Brunet, N. M., Li, Y., Konecky, R. O., Pyles, J. A., Walls, S. A., et al. (2014). Dynamic encoding of face information in the human fusiform gyrus. *Nat. Commun.* 5:5672. doi: 10.1038/ncomms6672

Golarai, G., Liberman, A., and Grill-Spector, K. (2017). Experience shapes the development of neural substrates of face processing in human ventral temporal cortex. *Cereb. Cortex* 27, 1229–1244. doi: 10.1093/cercor/bhv314

Haglund, M. M., Berger, M. S., Shamseldin, M., Lettich, E., and Ojemann, G. A. (1994). Cortical localization of temporal lobe language sites in patients with gliomas. *Neurosurgery* 34, 567–576. doi: 10.1227/00006123-199404000-00001

Haufe, S., DeGuzman, P., Henin, S., Arcaro, M., Honey, C. J., Hasson, U., et al. (2018). Elucidating relations between fMRI, ECoG, and EEG through a common natural stimulus. *NeuroImage* 179, 79–91. doi: 10.1016/j.neuroimage.2018.06.016

Haxby, J. V., Horwitz, B., Ungerleider, L. G., Maisog, J. M., Pietrini, P., and Grady, C. L. (1994). The functional organization of human extrastriate cortex: a PET-rCBF study of selective attention to faces and locations. *J. Neurosci.* 14, 6336–6353. doi: 10.1523/jneurosci.14-11-06336.1994

Haxby, J. V., Hoffman, E. A., and Gobbini, M. I. (2000). The distributed human neural system for face perception. *Trends Cogn. Sci.* 4, 223–233. doi: 10.1016/s1364-6613(00)01482-0

Hermes, D., Miller, K. J., Vansteensel, M. J., Aarnoutse, E. J., Leijten, F. S., and Ramsey, N. F. (2012). Neurophysiologic correlates of fMRI in human motor cortex. *Hum. Brain Mapp.* 33, 1689–1699. doi: 10.1002/hbm.21314

Hoffman, E. A., and Haxby, J. V. (2000). Distinct representations of eye gaze and identity in the distributed human neural system for face perception. *Nat. Neurosci.* 3, 80–84. doi: 10.1038/71152

Ishai, A. (2008). Let's face it: it'sa cortical network. *NeuroImage* 40, 415–419. doi: 10.1016/j.neuroimage.2007.10.040

Jacques, C., Witthoft, N., Weiner, K. S., Foster, B. L., Rangarajan, V., Hermes, D., et al. (2016). Corresponding ECoG and fMRI category-selective signals in human ventral temporal cortex. *Neuropsychologia* 83, 14–28. doi: 10.1016/j.neuropsychologia.2015.07.024

Jonas, J., Descoins, M., Koessler, L., Colnat-Coulbois, S., Sauvée, M., Guye, M., et al. (2012). Focal electrical intracerebral stimulation of a face-sensitive area causes transient prosopagnosia. *Neuroscience* 222, 281–288. doi: 10.1016/j.neuroscience.2012.07.021

Jonas, J., Jacques, C., Liu-Shuang, J., Brissart, H., Colnat-Coulbois, S., Maillard, L., et al. (2016). A face-selective ventral occipito-temporal map of the human brain with intracerebral potentials. *Proc. Natl. Acad. Sci.U.S.A.* 113, E4088–E4097. doi: 10.1073/pnas.1522033113

Jonas, J., Rossion, B., Brissart, H., Frismand, S., Jacques, C., Hossu, G., et al. (2015). Beyond the core face-processing network: intracerebral stimulation of a face-selective area in the right anterior fusiform gyrus elicits transient prosopagnosia. *Cortex* 72, 140–155. doi: 10.1016/j.cortex.2015.05.026

Kanwisher, N., McDermott, J., and Chun, M. M. (1997). The fusiform face area: a module in human extrastriate cortex specialized for face perception. *J. Neurosci.* 17, 4302–4311. doi: 10.1523/jneurosci.17-11-04302.1997

Klopp, J., Halgren, E., Marinkovic, K., and Nenov, V. (1999). Face-selective spectral changes in the human fusiform gyrus. *Clin. Neurophysiol.* 110, 676–682. doi: 10.1016/s1388-2457(98)00039-x

Koch, S. P., Werner, P., Steinbrink, J., Fries, P., and Obrig, H. (2009). Stimulus-induced and state-dependent sustained gamma activity is tightly coupled to the hemodynamic response in humans. *J. Neurosci.* 29, 13962–13970.

Ku, S.-P., Tolias, A. S., Logothetis, N. K., and Goense, J. (2011). fMRI of the face-processing network in the ventral temporal lobe of awake and anesthetized macaques. *Neuron* 70, 352–362. doi: 10.1016/j.neuron.2011.02.048

Lachaux, J.-P., George, N., Tallon-Baudry, C., Martinerie, J., Hugueville, L., Minotti, L., et al. (2005). The many faces of the gamma band response to complex visual stimuli. *NeuroImage* 25, 491–501. doi: 10.1016/j.neuroimage.2004.11.052

Liu, J., Tian, J., Lee, K., and Li, J. (2008). A study on neural mechanism of face processing based on fMRI. *Prog. Nat. Sci.* 18, 201–207. doi: 10.1016/j.pnsc.2007.06.006

Mattson, A. J., Levin, H. S., and Grafman, J. (2000). A case of prosopagnosia following moderate closed head injury with left hemisphere focal lesion. *Cortex* 36, 125–137. doi: 10.1016/s0010-9452(08)70841-4

Meadows, J. (1974). The anatomical basis of prosopagnosia. *J. Neurol. Neurosurg. Psychiatry* 37, 489–501. doi: 10.1136/jnnp.37.5.489

Mesad, S., Laff, R., and Devinsky, O. (2003). Transient postoperative prosopagnosia. *Epilepsy Behav.* 4, 567–570. doi: 10.1016/j.yebeh.2003.07.012

Mundel, T., Milton, J. G., Dimitrov, A., Wilson, H. W., Pelizzari, C., Uftring, S., et al. (2003). Transient inability to distinguish between faces: electrophysiologic studies. *J. Clin. Neurophysiol.* 20, 102–110. doi: 10.1097/00004691-200304000-00003

Nasr, S., and Tootell, R. B. (2012). Role of fusiform and anterior temporal cortical areas in facial recognition. *NeuroImage* 63, 1743–1753. doi: 10.1016/j.neuroimage.2012.08.031

Ojemann, G., Ojemann, J., Lettich, E., and Berger, M. (1989). Cortical language localization in left, dominant hemisphere: an electrical stimulation mapping investigation in 117 patients. *J. Neurosurg.* 71, 316–326. doi: 10.3171/jns/2008/108/2/0411

Ojemann, J. G., Akbudak, E., Snyder, A. Z., McKinstry, R. C., Raichle, M. E., and Conturo, T. E. (1997). Anatomic localization and quantitative analysis of gradient refocused echo-planar fMRI susceptibility artifacts. *NeuroImage* 6, 156–167. doi: 10.1006/nimg.1997.0289

Ojemann, G. A., Corina, D. P., Corrigan, N., Schoenfield-Mcneill, J., Poliakov, A., Zamora, L., et al. (2010). Neuronal correlates of functional magnetic resonance imaging in human temporal cortex. *Brain* 133, 46–59. doi: 10.1093/brain/awp227

Parvizi, J., Jacques, C., Foster, B. L., Withoft, N., Rangarajan, V., Weiner, K. S., et al. (2012). Electrical stimulation of human fusiform face-selective regions distorts face perception. *J. Neurosci.* 32, 14915–14920. doi: 10.1523/jneurosci.2609-12.2012

Penfield, W., and Boldrey, E. (1937). Somatic motor and sensory representation in the cerebral cortex of man as studied by electrical stimulation. *Brain* 60, 389–443. doi: 10.1192/bjp.84.352.868-a

Penny, W. D., Friston, K. J., Ashburner, J. T., Kiebel, S. J., and Nichols, T. E. (2011). *Statistical Parametric Mapping: The Analysis of Functional Brain Images*. Burlington, MA: Elsevier.

Pfaender, M., D'Souza, W., Trost, N., Litewka, L., Paine, M., and Cook, M. (2004). Visual disturbances representing occipital lobe epilepsy in patients with cerebral calcifications and coeliac disease: a case series. *J. Neurol. Neurosurg. Psychiatry* 75, 1623–1625. doi: 10.1136/jnnp.2003.031229

Pitcher, D., Walsh, V., and Duchaine, B. (2011). The role of the occipital face area in the cortical face perception network. *Exp. Brain Res.* 209, 481–493. doi: 10.1007/s00221-011-2579-1

Pitcher, D., Walsh, V., Yovel, G., and Duchaine, B. (2007). TMS evidence for the involvement of the right occipital face area in early face processing. *Curr. Biol.* 17, 1568–1573. doi: 10.1016/j.cub.2007.07.063

Puce, A., Allison, T., Gore, J. C., and McCarthy, G. (1995). Face-sensitive regions in human extrastriate cortex studied by functional MRI. *J. Neurophysiol.* 74, 1192–1199. doi: 10.1152/jn.1995.74.3.1192

Puce, A., Allison, T., Asgari, M., Gore, J. C., and Mccarthy, G. (1996). Differential sensitivity of human visual cortex to faces, letterstrings, and textures: a functional magnetic resonance imaging study. *J. Neurosci.* 16, 5205–5215. doi: 10.1523/JNEUROSCI.16-16-05205.1996

Puce, A., Allison, T., Bentin, S., Gore, J. C., and Mccarthy, G. (1998). Temporal cortex activation in humans viewing eye and mouth movements. *J. Neurosci.* 18, 2188–2199. doi: 10.1523/JNEUROSCI.18-06-02188.1998

Puce, A., Allison, T., Spencer, S. S., Spencer, D. D., and Mccarthy, G. (1997). Comparison of cortical activation evoked by faces measured by intracranial field potentials and functional MRI: two case studies. *Hum. Brain Mapp.* 5, 298–305. doi: 10.1002/(SICI)1097-019319975:4<298::AID-HBM16<3.0.CO;2-A

Rangarajan, V., Hermes, D., Foster, B. L., Weiner, K. S., Jacques, C., Grill-Spector, K., et al. (2014). Electrical stimulation of the left and right human fusiform gyrus causes different effects in conscious face perception. *J. Neurosci.* 34, 12828–12836. doi: 10.1523/jneurosci.0527-14.2014

Romero, J. R., Ramirez, D. M., Aglio, L. S., and Gugino, L. D. (2011). Brain mapping using transcranial magnetic stimulation. *Neurosurg. Clin.* 22, 141–152. doi: 10.1016/j.nec.2010.11.002

Rossion, B., Caldara, R., Seghier, M., Schuller, A. M., Lazeyras, F., and Mayer, E. (2003). A network of occipito-temporal face-sensitive areas besides the right middle fusiform gyrus is necessary for normal face processing. *Brain* 126, 2381–2395. doi: 10.1093/brain/awg241

Rossion, B., Jacques, C., and Jonas, J. (2018). Mapping face categorization in the human ventral occipitotemporal cortex with direct neural intracranial recordings. *Ann. N. Y. Acad. Sci.* 1426, 5–24. doi: 10.1111/nyas.13596

Sagar, S., Rick, J., Chandra, A., Yagnik, G., and Aghi, M. K. (2019). Functional brain mapping: overview of techniques and their application to neurosurgery. *Neurosurg. Rev.* 42, 639–647. doi: 10.1007/s10143-018-1007-4

Sanai, N., Mirzadeh, Z., and Berger, M. S. (2008). Functional outcome after language mapping for glioma resection. *N. Engl. J. Med.* 358, 18–27. doi: 10.1056/nejmoa067819

Schalk, G., Kapeller, C., Guger, C., Ogawa, H., Hiroshima, S., Lafer-Sousa, R., et al. (2017). Facephenes and rainbows: causal evidence for functional and anatomical specificity of face and color processing in the human brain. *Proc. Natl. Acad. Sci.U.S.A.* 114, 12285–12290. doi: 10.1073/pnas.1713447114

Scheeringa, R., Fries, P., Petersson, K.-M., Oostenveld, R., Grothe, I., Norris, D. G., et al. (2011). Neuronal dynamics underlying high-and low-frequency EEG oscillations contribute independently to the human BOLD signal. *Neuron* 69, 572–583. doi: 10.1016/j.neuron.2010.11.044

Scheffer, I. E., Berkovic, S., Capovilla, G., Connolly, M. B., French, J., Guilhoto, L., et al. (2017). ILAE classification of the epilepsies: position paper of the ILAE commission for classification and terminology. *Epilepsia* 58, 512–521. doi: 10.1111/epi.13709

Schwarz, L., Kreifelts, B., Wildgruber, D., Erb, M., Scheffler, K., and Ethofer, T. (2019). Properties of face localizer activations and their application in functional magnetic resonance imaging (fMRI) fingerprinting. *PLoS One* 14:e0214997. doi: 10.1371/journal.pone.0214997

Sergent, J., Ohta, S., and Macdonald, B. (1992). Functional neuroanatomy of face and object processing: a positron emission tomography study. *Brain* 115, 15–36. doi: 10.1093/brain/115.1.15

Sollmann, N., Fuss-Ruppenthal, S., Zimmer, C., Meyer, B., and Krieg, S. M. (2018). Investigating stimulation protocols for language mapping by repetitive navigated transcranial magnetic stimulation. *Front. Behav. Neurosci.* 12:197. doi: 10.3389/fnbeh.2018.00197

Sorger, B., Goebel, R., Schiltz, C., and Rossion, B. (2007). Understanding the functional neuroanatomy of acquired prosopagnosia. *NeuroImage* 35, 836–852. doi: 10.1016/j.neuroimage.2006.09.051

Swift, J., Coon, W., Guger, C., Brunner, P., Bunch, M., Lynch, T., et al. (2018). Passive functional mapping of receptive language areas using electrocorticographic signals. *Clin. Neurophysiol.* 129, 2517–2524. doi: 10.1016/j.clinph.2018.09.007

Takahashi, N., Kawamura, M., Hirayama, K., Shiota, J.-I., and Isono, O. (1995). Prosopagnosia: a clinical and anatomical study of four patients. *Cortex* 31, 317–329. doi: 10.1016/s0010-9452(13)80365-6

Tanji, K., Iwasaki, M., Nakasato, N., and Suzuki, K. (2012). Face specific broadband electrocorticographic spectral power change in the rhinal cortex. *Neurosci. Lett.* 515, 66–70. doi: 10.1016/j.neulet.2012.03.020

Taylor, I., Scheffer, I. E., and Berkovic, S. F. (2003). Occipital epilepsies: identification of specific and newly recognized syndromes. *Brain* 126, 753–769. doi: 10.1093/brain/awg080

Tharin, S., and Golby, A. (2007). Functional brain mapping and its applications to neurosurgery. *Neurosurgery* 60(4 Suppl 2), 185–201; discussion 201–182.

Theodore, W. H. (2003). Transcranial magnetic stimulation in epilepsy. *Epilepsy Curr.* 3, 191–197. doi: 10.1046/j.1535-7597.2003.03607.x

Wada, Y., and Yamamoto, T. (2001). Selective impairment of facial recognition due to a haematoma restricted to the right fusiform and lateral occipital region. *J. Neurol. Neurosurg. Psychiatry* 71, 254–257. doi: 10.1136/jnnp.71.2.254

Weiner, K. S., and Grill-Spector, K. (2010). Sparsely-distributed organization of face and limb activations in human ventral temporal cortex. *NeuroImage* 52, 1559–1573. doi: 10.1016/j.neuroimage.2010.04.262

Weiner, K. S., and Grill-Spector, K. (2013). Neural representations of faces and limbs neighbor in human high-level visual cortex: evidence for a new

organization principle. *Psychol. Res.* 77, 74–97. doi: 10.1007/s00426-011-0392-x

Wen, J., Yu, T., Li, Y., and Li, X. (2017). Using electrocorticography for presurgical language mapping in epilepsy patients. *J. Clin. Neurosci.* 44, 320–322. doi: 10.1016/j.jocn.2017.06.015

Winston, J. S., Henson, R., Fine-Goulden, M. R., and Dolan, R. J. (2004). fMRI-adaptation reveals dissociable neural representations of identity and expression in face perception. *J. Neurophysiol.* 92, 1830–1839. doi: 10.1152/jn.00155.2004

Conflict of Interest: CK, MJ, and JG are employees of g.tec medical engineering GmbH. CG is the CEO of g.tec medical engineering GmbH.

The remaining authors declare that the research was conducted in the absence of any commercial or financial relationships that could be construed as a potential conflict of interest.

frontiers in Systems Neuroscience

ORIGINAL RESEARCH
published: 30 March 2021
doi: 10.3389/fnsys.2021.611507

Modulating Inhibitory Control Processes Using Individualized High Definition Theta Transcranial Alternating Current Stimulation (HD θ-tACS) of the Anterior Cingulate and Medial Prefrontal Cortex

Monika Klírová[1,2], Veronika Voráčková[1,2], Jiří Horáček[1,2], Pavel Mohr[1,2], Juraj Jonáš[1], Daniela Urbaczka Dudysová[1,2], Lenka Kostýlková[1,2], Dan Fayette[1,2], Lucie Krejčová[1], Silvie Baumann[1], Olga Laskov[1,2] and Tomáš Novák[1,2]*

[1] National Institute of Mental Health, Prague, Czechia, [2] Department of Psychiatry, Third Faculty of Medicine, Charles University, Prague, Czechia

OPEN ACCESS

Edited by:
Jorge Alvaro Gonzalez-Martinez, University of Pittsburgh, United States

Reviewed by:
Connie Lamm, University of Arkansas, United States
Gabriele Fusco, Sapienza University of Rome, Italy

***Correspondence:**
Monika Klírová
monika.klirova@nudz.cz

Received: 29 September 2020
Accepted: 04 March 2021
Published: 30 March 2021

Citation:
Klírová M, Voráčková V, Horáček J, Mohr P, Jonáš J, Dudysová DU, Kostýlková L, Fayette D, Krejčová L, Baumann S, Laskov O and Novák T (2021) Modulating Inhibitory Control Processes Using Individualized High Definition Theta Transcranial Alternating Current Stimulation (HD θ-tACS) of the Anterior Cingulate and Medial Prefrontal Cortex. Front. Syst. Neurosci. 15:611507. doi: 10.3389/fnsys.2021.611507

Increased frontal midline theta activity generated by the anterior cingulate cortex (ACC) is induced by conflict processing in the medial frontal cortex (MFC). There is evidence that theta band transcranial alternating current stimulation (θ-tACS) modulates ACC function and alters inhibitory control performance during neuromodulation. Multi-electric (256 electrodes) high definition θ-tACS (HD θ-tACS) using computational modeling based on individual MRI allows precise neuromodulation targeting of the ACC via the medial prefrontal cortex (mPFC), and optimizes the required current density with a minimum impact on the rest of the brain. We therefore tested whether the individualized electrode montage of HD θ-tACS with the current flow targeted to the mPFC-ACC compared with a fixed montage (non-individualized) induces a higher post-modulatory effect on inhibitory control. Twenty healthy subjects were randomly assigned to a sequence of three HD θ-tACS conditions (individualized mPFC-ACC targeting; non-individualized MFC targeting; and a sham) in a double-blind cross-over study. Changes in the Visual Simon Task, Stop Signal Task, CPT III, and Stroop test were assessed before and after each session. Compared with non-individualized θ-tACS, the individualized HD θ-tACS significantly increased the number of interference words and the interference score in the Stroop test. The changes in the non-verbal cognitive tests did not induce a parallel effect. This is the first study to examine the influence of individualized HD θ-tACS targeted to the ACC on inhibitory control performance. The proposed algorithm represents a well-tolerated method that helps to improve the specificity of neuromodulation targeting of the ACC.

Keywords: transcranial alternating current stimulation, tACS, ACC, theta frequency, inhibitory control, high definition

INTRODUCTION

The anterior cingulate cortex (ACC) plays an important role in the processing of cognition and emotions (Gasquoine, 2013; Onoda et al., 2017). While cognitive processes are attributed to the dorsal ACC (dACC), emotional processes are assigned to the rostral division of the ACC (Bush et al., 2000). According to recent comprehensive theory, the ACC is activated in response to a conflict between incompatible streams of information processing; it represents an essential structure for the inhibitory control process (van Veen and Carter, 2002). ACC disruptions in various neuropsychiatric disorders, such as schizophrenia and obsessive-compulsive disorder (OCD), have been documented by functional magnetic resonance imaging (fMRI) studies (Carter et al., 2001; Ursu et al., 2003; Fitzgerald et al., 2005). In schizophrenia, the reduction of ACC activity results in decreased activity in the processing of conflicting information and inhibition ability (Carter et al., 2001), while in OCD, higher ACC activity increases conflict-processing information and inhibitory activity (van Veen and Carter, 2002; Ursu et al., 2003; Fitzgerald et al., 2005; Gasquoine, 2013).

The medial prefrontal cortex (mPFC), also covering the dACC, generates theta oscillatory activity, so-called Frontal Midline Theta (FMT). FMT enhancement over the medial frontal cortex (MFC), recorded during conflict monitoring, error processing, and top-down behavior adjustments (Cohen et al., 2008; Cavanagh and Shackman, 2015; Van Noordt et al., 2016) has also been documented as having behaviorally relevant event-related potentials (ERPs) during resolution of conflict-related tasks (Nigbur et al., 2012; Cohen and Donner, 2013) associated with the procession of inhibitory control. The latter can be evaluated by verbal (Stroop Test) or non-verbal (Stop Signal, Visual Simon, or Flanker Task) tests (Kopp et al., 1996a,b; Gratton et al., 1988; Bush et al., 2000; Taylor et al., 2007; Cohen and Donner, 2013; Spielberg et al., 2015), measuring different parameters, such as commission of mistakes or those related to conflict and error.

Transcranial Alternating Current Stimulation (tACS) enables modulation of endogenous oscillations at the pacing rate (Paulus, 2011; Ali et al., 2013; Antal and Paulus, 2013; Herrmann et al., 2013; Antal and Herrmann, 2016), inducing frequency-specific activity changes (Vossen et al., 2015; Witkowski et al., 2016) and the subsequent induction of synaptic changes via neuronal plasticity, providing a post-modulation effect on brain oscillation activity (Antal et al., 2008; Zaehle et al., 2010; Vossen et al., 2015; Berger et al., 2018; Moliadze et al., 2019). The effect of various tACS frequencies on cognition was tested (Sela et al., 2012; Hoy et al., 2015; van Driel et al., 2015; Vosskuhl et al., 2015; Wischnewski et al., 2016; Fusco et al., 2018; Pahor and Jaušovec, 2018; Lehr et al., 2019; Moliadze et al., 2019). Specific cognitive abilities were significantly modified mostly by the theta frequency tACS (θ-tACS; Sela et al., 2012; van Driel et al., 2015; Vosskuhl et al., 2015; Wischnewski et al., 2016; Fusco et al., 2018, 2020; Pahor and Jaušovec, 2018; Lang et al., 2019; Lehr et al., 2019). Neuroimaging (MEG and fMRI) studies have also shown that FMT performance is influenced by θ-tACS, which modulates dACC network functions (Chander et al., 2016; Onoda et al., 2017). However, previous studies that documented the behavioral and electrophysiological effects of θ-tACS have mostly targeted various non-specific anatomic frontal cortex regions (van Driel et al., 2015; Vosskuhl et al., 2015; Chander et al., 2016; Onoda et al., 2017; Fusco et al., 2018; Pahor and Jaušovec, 2018), including the MFC (van Driel et al., 2015; Vosskuhl et al., 2015; Fusco et al., 2018).

So far, only a few studies have tested the impact of θ-tACS on inhibitory control performance (van Driel et al., 2015; Fusco et al., 2018, 2020; Lehr et al., 2019). For example, Lehr et al.'s (2019) study targeted the dorsolateral prefrontal cortex (DLPFC), which together with the ACC belongs to the inhibitory control circuit. Other studies (van Driel et al., 2015; Fusco et al., 2018, 2020) targeted the ACC indirectly via the MFC. With the exception of van Driel et al.'s (2015) study, these experiments monitored the effect of θ-tACS on inhibitory control performance only during the application of θ-tACS; the post-modulatory effect was not tested (Fusco et al., 2018, 2020; Lehr et al., 2019). The studies have yielded inconsistent results, ranging from enhancement (Fusco et al., 2018, 2020) to deterioration of inhibitory control performance (van Driel et al., 2015; Lehr et al., 2019).

It has been suggested that tACS may be used as a tool to investigate diseases with altered EEG activity (Antal et al., 2008; Ahn et al., 2019; Del Felice et al., 2019). Therefore, the effect of θ-tACS of the ACC on inhibitory control could be examined in neuropsychiatric disorders associated with disrupted dACC activity. We assume that θ-tACS targeted directly at the source of FMT via the mPFC-ACC may modify inhibitory control processes with a sustained effect.

However, standard transcranial Electrical Stimulation (tES; Nikolin et al., 2015) technologies (in terms of electrode assembly, number, shape, and size) are insufficient for more specific targeted tES (Lefaucheur et al., 2017); precise targeting of the deeper brain structures cannot therefore be documented. In addition, standard tES directly affects not only the selected area of interest but also the surrounding and interconnected structures.

High definition (HD) tES provides a solution to these methodological limitations. It is guided by structural neuroimaging, which allows a computer model of the electric field intensity distributions to be created. This model is essential for precise neuromodulation targeting with respect to the different conductivity of various brain tissues (Nikolin et al., 2015; Alam et al., 2016). Geodesic Transcranial Electrical Neuromodulation (GTEN) system with 256 electrodes enables Multielectrode Transcranial Electrical Stimulation (MTES), which optimizes the required current density in the targeted brain area. MTES analyses (Dmochowski et al., 2011; Alam et al., 2016; Fernández-Corazza et al., 2016) have shown that the use of a higher electrode density improves the focus, directionality, and stimulation intensity parameters by penetrating the deeper brain structures. MTES enables targeted neuromodulation of selected areas with greater specificity than the standard technologies; therefore, it is possible to modulate the ACC activity via mPFC-ACC stimulation more selectively.

Our study goal was to investigate the post-modulatory effects of θ-tACS in inhibitory control processing. For this purpose, we applied different θ-tACS neuromodulation protocols targeted

at the MFC in healthy subjects, and evaluated θ-tACS-induced post-modulatory changes in tasks specific to inhibitory control. We assumed that by strengthening an oscillating current at the theta frequency, θ-tACS would induce a persistent improvement of the inhibitory control performance in the post-modulation assessment. We hypothesized that the individualized HD θ-tACS, targeted according to the computational modeling for optimal electrode arrangement, would induce a post-modulatory effect of θ-tACS on inhibitory control. This effect would be significantly stronger than the effect of a non-individualized θ-tACS targeting the ACC indirectly via the MFC. Moreover, we also compared the effect of individualized HD θ-tACS with non-individualized θ-tACS and with a sham condition.

MATERIALS AND METHODS

Subjects

Twenty healthy volunteers (mean age 34.4 ± 7.2 years, 10 females) were included in the study. Exclusion criteria were a current diagnosis or history of a psychiatric disorder; substance use disorder (with the exception of nicotine); regular use of any medication that might affect cognitive functions (e.g., antihistamines and benzodiazepines); a history of serious head injury or a neurological disorder; a medical condition that could interfere with the tES administration (Poreisz et al., 2007); pregnancy; breastfeeding; or a sensory or motor impairment. All participants signed an informed consent form in accordance with the latest version of the Declaration of Helsinki; the study protocol was approved by the Independent Ethics Committee of the National Institute of Mental Health, Klecany.

Study Protocol

A double-blind, sham-controlled, three-condition, three-period cross-over study was carried out in random order, with a 1 week minimum wash-out period to avoid carryover effects. Following Williams' design (Williams, 1949) for the 3 × 3 cross-over trial, participants were randomly assigned to one of six different sequences of three θ-tACS conditions: (1) individualized targeting of the mPFC-ACC according to the individual head model; (2) non-individualized electrodes placed in the FCz and Pz areas according to the skull's anatomy (Vosskuhl et al., 2015; Fusco et al., 2018); and (3) the sham (**Figure 1A**). To assure a balanced number of subjects in each sequence, we used non-stratified blocked randomization with a block size of six (computer generated[1]). Every experimental session for each subject was carried out at the same time of day, on the same weekday. Participants were asked to abstain from caffeine and nicotine for at least 2 h prior to the cognitive assessment and the tACS session and to refrain from alcohol or any medication for 24 h prior to the tACS administration.

The study participants and the researchers evaluating the psychometric measurements remained blind to the stimulation conditions and parameters. Neuropsychological assessment of inhibitory control was performed before and after each tACS application (**Figure 1C**). To test for the integrity of the blinding procedure, all participants were asked the following question at the end of the study: "During which stimulation session was a placebo applied? Was it during the first, second, or third session?" There were three possible answers: a placebo was applied during the first (011), the second (101), or the third (110).

[1]http://www.randomization.com

Magnetic Resonance Imaging (MRI) and the Geodesic Photogrammetry System (GPS)

Individual magnetic resonance images obtained with a Siemens Magnetom Prisma 3T system (Siemens, Erlangen, Germany) were used to create an individual head model for each subject. The subjects were scanned using a T1 Sag MPR 1 mm ISO sequence (repetition time TR of 2,300 ms; echo time TE of 1.69 ms; field of view 288 mm; slice slab 256 mm; voxel size of 1 × 1 × 1 mm and total acquisition time 5 min 12 s).

Subsequently, to obtain accurate positions for the individual electrodes on the scalp, the head of the subject was targeted by a sensor-registration system determining the 3-dimensional position of each of 256 sensors (neuromodulation electrodes). Electrode sensor positions of the 256-channel HydroCel Geodesic Sensor Net (HCGSN) 100 (EGI, Eugene, OR, United States) were digitalized with a GPS (EGI, Eugene, OR, United States) (Luu et al., 2016).

Head Modeling

Figure 1B schematically illustrates the head modeling with tissue segmentation, co-registration of an individual head model with GPS electrode positioning, and the settings of a protocol to select the appropriate electrodes according to the individual cortical current density followed by the neuromodulation protocol settings.

The individual head models were processed by the Modal Image Pipeline, ver. 1.10 (EGI, Eugene, OR, United States). To calculate the accurate head model, the initial segmentation of the white matter, gray matter, and background ratio was processed. Particular attention was given to the manual correction of gray matter smoothing and cortical surface extraction, to avoid digital errors when calculating normal the cortical conductivity vectors (Fernández-Corazza et al., 2016). The MRI images were subsequently segmented into tissue types (scalp, skull, eyeballs, cerebrospinal fluid, gray matter, white matter, and air) and proportionalized to the right and left hemispheres. Following the scalp reconstruction necessary for co-registration with the GPS sensors, the landmarks corresponding to the exact positions of selected electrodes from the individual GPS images were marked on the head model. In the next step, a 3D cortical surface with a 4800 dipoles patch was created to describe the current flow from the scalp to the cortex (Fernández-Corazza et al., 2016; Luu et al., 2016). The head model of the cortical surface was subsequently co-registered in JavaScript with a GPS file containing the photographic images of the individual positions of each of the 256 sensors placed on the subject's head while images were taken by the GPS camera.

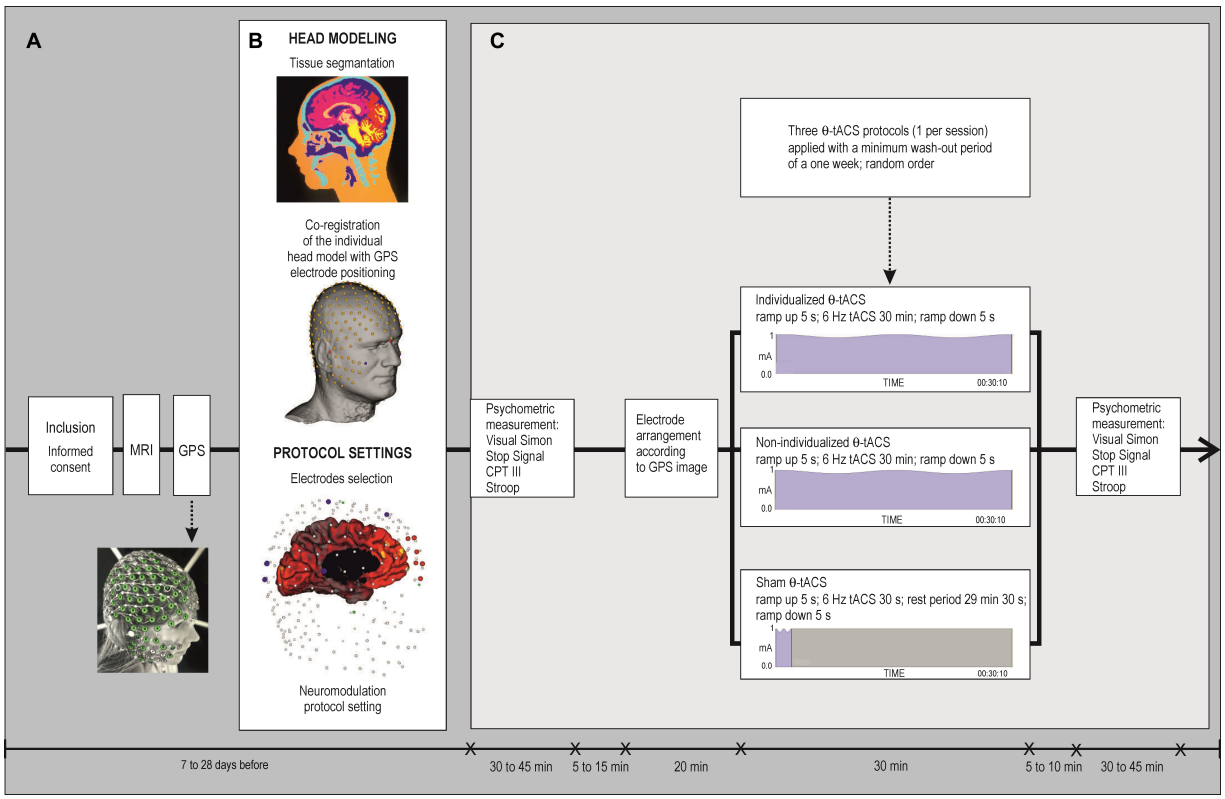

FIGURE 1 | Flow chart of the protocol. **(A)** Schematic overview of the study. **(B)** Illustration of head modeling with tissue segmentation, co-registration of an individual head model with GPS electrode positioning, and setting of a protocol to select the appropriate electrodes according to the individual cortical current density, followed by neuromodulation protocol settings. **(C)** Experimental procedure. A double-blind, cross-over study. Three neuromodulation sessions were carried out in random order with a minimum 1 week washout period. The psychometric measurement was tested immediately before and after the end of each neuromodulation session. Types of HD θ-tACS protocols: an individualized HD θ-tACS was targeted with the highest specificity to the mPFC-ACC; a non-individualized θ-tACS was targeted over the MFC with fixed electrode positions in the FCz and Pz areas; a sham tACS was administered with identical electrode montage (as used in the non-individualized protocol). Active θ-tACS sessions comprised a 5 s ramp up, 30 min of 6 Hz θ-tACS, and a 5 s ramp down. Sham condition comprised a 5 s ramp up and 30 s of 6 Hz θ-tACS followed by a 29 min 30 s rest period and a 5 s ramp down. Psychometric measurement was assessed by the Simon Task, Stop Signal Task, Conners' Continuous Performance Test 3rd edition (CPT III), and the Stroop Test.

The final head model with a neuromodulatory electrode selection and stimulation protocol setting was designed in the Reciprocity Visualization Environment, ver. 1.1 (EGI, Eugene, OR, United States), which allows the optimal electrode arrangement to be selected and the appropriate amount of current delivered by the current injection through each electrode (Luu et al., 2016) to be determined to achieve the maximum current density at a given target of the cortical surface model.

Neuromodulation Protocols

An optimal electrode arrangement based on computational modeling from individual MRI was used for the individualized protocol with the current flow targeted with the highest specificity at the mPFC-ACC, and to achieve maximum current density in the ACC. A mounting (up to 16 channels) with a maximum of six cathode-anodes and 10 anode-cathodes was employed, because the anatomical variations of the subjects would have a potentially significant impact on the field strength in a given area. The specification of the electrode layouts, including the number of electrodes, their position, and current intensity in each electrode for individualized tACS for each subject is shown in **Table 1**. The arrangement of the neuromodulatory electrodes for the individual head models was computed with respect to individual cortical geometry, the head shapes of the subjects, and the corresponding current densities of the cortical surface (**Figure 2**).

The non-individualized focusing of the electrode assembly (according to the skull anatomy) used MFC and medial parietal cortex electrode layouts (Vosskuhl et al., 2015; Fusco et al., 2018), specifically in the FCz and Pz areas (according to the international 10/20 EEG electrode system for "standard" anatomically guided positioning), and adapted for HCGSN 100 using the 10-channel mount with five anode-cathodes in the FCz area and five cathode-anodes in the Pz area (**Figure 2**).

The sham tACS was administered with an identical electrode montage, as used in the non-individualized protocol.

tACS Administration

Electrode positioning of the 256-channel HCGSN 100 was adjusted under the control of the GPS subordinate images prior

to each tACS application. An Elefix conductive paste (Nihon Kohden, Tokyo, Japan) was used as the conductive material between the scalp and selected neuromodulatory electrodes. The impedance of the electrodes was monitored immediately before tACS application; it was below 10 KΩ .

Subsequently, a pulsed alternating current was applied with Net Station Acquisition software, ver. 5.4.2 (EGI, Eugene, OR, United States), using a CE-certified Geodesic Transcranial Electrical Neuromodulation (GTEN) 100 system (EGI, Eugene, OR, United States) with the 256-channel HCGSN 100, which is an evenly spaced network of Ag-AgCl electrodes (Luu et al., 2016). The maximum current at any given electrode (1 cm^2) was 200 μA, with a total current of tACS 1 mA for each active session, under monitoring by a GTEN 100 Sentinel Circuit®.

The parameter settings for each active θ-tACS session were: a 5 s ramp up, 30 min of θ-tACS with 6 Hz, and a 5 s ramp down. For the sham condition, the application of θ-tACS after a 5 s ramp up was shortened to 30 s and was followed by a rest period of 29 min 30 s, terminated by a 5 s ramp down. A sham condition applied for a duration of 30 s has been previously described as a reliable blinding method for tACS (Zaghi et al., 2010; Pahor and Jaušovec, 2018). This reproduces somatic sensations similar to active stimulation. Tingling or heating up of the scalp occurs mostly at the beginning (ramp up and initial adaptation to θ-tACS) of the neuromodulation and at the end of the protocol (ramp down). During the θ-tACS application, the participants were in a resting condition (**Figure 1C**).

Psychometric Measurement

Psychometric measurements were performed immediately before and after each neuromodulation session by a rater blind to the treatment condition. The neuropsychological battery consisted of the following non-verbal tests: Visual Simon Task (Simon Task), Stop Signal Task, Conners' Continuous Performance Test 3rd edition (CPT III), and verbal tests: Stroop Color and Word Test (SCWT or Stroop; **Figure 3**). The tests focused primarily on specific parameters of the cognitive domains that are related to cognitive control and that have shown minimum practice effect. The Simon Task and the Stop Signal Task were administered using the program Inquisit 3 (Inquisit, 2007).

The Simon Task is used to measure the stimulus-response compatibility and the difference in reaction time (RT) between trials in which the prepotent association is congruent to the stimulus and the trials in which it is incongruent (Bialystok et al., 2004). Each trial of the task begins with a central fixation cross on the screen (800 ms), followed by a blank interval (250 ms). Then, a red or blue square appears on either the left or the

TABLE 1 | The specification of electrode layouts (256-channel HydroCel Geodesic Sensor Net), including the number of electrodes, their position, and current intensity in each electrode used for individualized HD θ-tACS in subjects.

No.	Sex	No. A/C	No. C/A	No. A/C + C/A	A/C Layout (200 μA)	A/C Layout (100 μA)	C/A Layout (200 μA)	C/A Layout (100 μA)	C/A Layout (50 μA)
1	2	6	10	16	20; 21 (Fz); 26; 27	14; 22	124; 125; 137	15	5; 6; 13; 23;28; 29
2	2	6	10	16	20; 21 (Fz); 26; 27	14; 22	124; 125; 137	15	5; 6; 13; 23;28; 29
3	2	6	10	16	20; 21 (Fz); 26; 27	14; 22	124; 125; 137	15	5; 6; 13; 23;28; 29
4	1	6	10	16	20; 21 (Fz); 26; 27	14; 22	124; 125; 137	15	5; 6; 13; 23;28; 29
5	2	6	10	16	20; 21 (Fz); 26; 27	14; 22	124; 125; 137	15	5; 6; 13; 23;28; 29
6	2	6	10	16	20; 21 (Fz); 26; 27	14; 22	124; 125; 137	15	5; 6; 13; 23;28; 29
7	1	6	10	16	20; 21 (Fz); 26; 27	14; 22	124; 125; 137	15	5; 6; 13; 23;28; 29
8	2	5	8	13	21; 26; 27; 28; 33		117; 125; 126 (Oz)	16; 70; 182	22; 32;
9	1	6	10	16	20; 21 (Fz); 26; 27	14; 22	124; 125; 137	15	5; 6; 13; 23;28; 29
10	1	5	6	11	20; 26; 27; 31 (NAS)	25; 32		15; 64; 81; 180	126 (Oz); 138; 139
11	2	5	10	15	20; 21 (Fz); 26; 27	14; 22	124; 125; 137	15	5; 6; 13; 23;28; 29
12	1	6	10	16	20; 21 (Fz); 26; 27	14; 22	124; 125; 137	15	5; 6; 13; 23;28; 29
13	2	6	10	16	20; 21 (Fz); 26; 27	14; 22	124; 125; 137	15	5; 6; 13; 23;28; 29
14	1	6	10	16	20; 21 (Fz); 26; 27	14; 22	124; 125; 137	15	5; 6; 13; 23;28; 29
15	2	5	7	12	20; 21 (Fz); 26; 27	14; 22	124; 125; 137	15	5; 6; 13; 23;28; 29
16	1	6	6	12	20; 26; 27; 31 (NAS)	25; 32		15; 64; 81; 180	126 (Oz); 138; 139
17	1	5	5	10	19; 20; 21; 25; 26		70; 125; 126 (Oz); 138; 179		
18	1	6	10	16	20; 21 (Fz); 26; 27	25; 32	137; 138; 148; 149		13; 14; 22; 28
19	2	5	6	11	20; 26; 27; 31 (NAS)	25; 32		15; 64; 81; 180	126 (Oz); 138; 139
20	1	5	7	12	20; 26; 27; 31 (NAS)	25; 32		15; 64; 81; 180	126 (Oz); 138; 139

Sex: 1 (male); 2 (female). Neuromodulatory electrode specification: A/C, cathode-anodes; C/A, anode-cathodes; μA defines the electric current used for each electrode. A total current 1 mA for each group of electrodes (A/C and C/A) was used for each subject. Fz, Midline Frontal; Oz, Midline Occipital; NAS, Nasion.

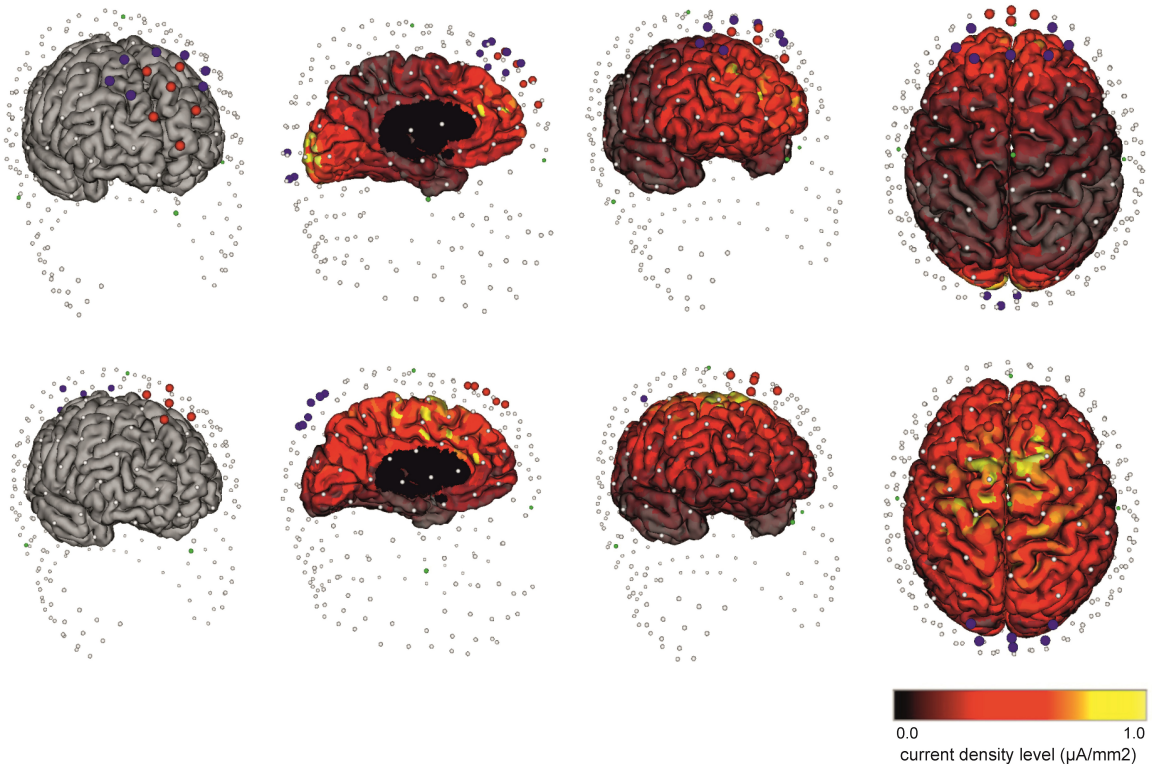

FIGURE 2 | The electrode placement used in the individualized and non-individualized HD θ-tACS protocols. **(Top)** The individualized placement of electrodes for HD θ-tACS of the ACC targeted through the mPFC-ACC was selected on the basis of a reciprocity-optimized selection of current injection electrodes. Six anode-cathodes (red electrodes) and 10 cathode-anodes (blue electrodes) are shown. Note that to select the optimal electrode arrangement and current injection electrode, the individualized flux pattern with the highest specificity of current flow for a given target region (mPFC-ACC) on the cortical surface model was used. This is an example montage. **(Bottom)** Non-individualized placement of electrodes in the FCz and Pz areas (Vosskuhl et al., 2015; Fusco et al., 2018) adapted for the HCGSN 100 using the 10-channel mount with five anode-cathodes (red electrodes) in the FCz area and five cathode-anodes (blue electrodes) in the Pz area for a MFC and medial parietal cortex electrode layout. **(Left)** anterior view without marking the current density; **(middle left)** sagittal view; **(middle right)** anterior view; and **(right)** view from above, with cortex coloring representing the calculated current density on the cortical surface from 0.0 $\mu A/mm^2$ (black) to 1.0 $\mu A/mm^2$ (yellow).

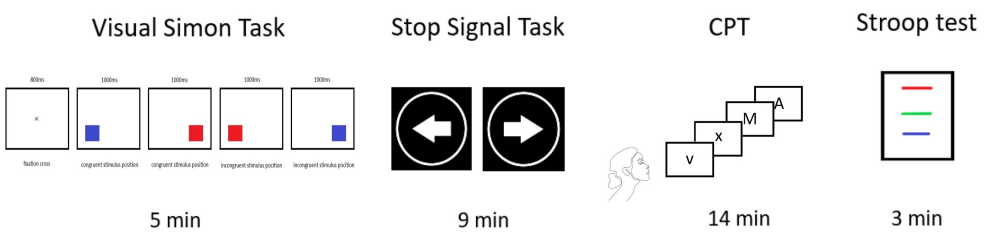

FIGURE 3 | Flow chart of the psychometric measurement. Flow chart of the psychometric measurement. Illustration of the individual assessments performed for the following periods: Visual Simon Task = 5 min, Stop Signal Task = 9 min, Conners' Continuous Performance Test 3rd edition (CPT III) = 14 min, Stroop test = 3 min.

right side of the screen and remains there if there is no response (1,000 ms). Participants are required to press the A key (left) when a blue square is presented or the L key (right) when a red square is presented. Response timing starts with the onset of the stimulus, and the participant's response terminates the stimulus. The task takes approximately 2 min to complete, and involves 5 min of instruction. Participants have to complete all eight practice trials without a mistake before the experimental trials begin. If participants fail to press the key within the available time, they receive additional practice trials until all eight attempts are completed correctly. The following experiment (28 trials) consists of 14 congruent trials (presenting the square on the same side as the related response key) and 14 incongruent trials (presenting the square on the opposite side), which are presented in random order (Inquisit, 2007).

The Stop Signal Task was selected to assess the ability to stop a planned or ongoing action (van Gaal et al., 2009). It is a go/nogo reaction time task that provides a means of estimating the time it

takes to stop executing a response that might already be underway but needs to be halted. This is called the stop signal reaction time. At the beginning of the task, a fixation circle is displayed in which an arrow points to the left or to the right. Participants are required to press the "←" key or "→" key, depending on the direction of the arrow, unless a beep sounds to stop the response before execution. Depending on performance, the delay between the appearance of the arrow and the beep sound is adjusted up or down. Previous successful trials make the delay longer in the new trial and previous unsuccessful trials make it shorter. Participants' responses are available until the end of the trial. Each task trial has a duration of 2,000 ms. The initial Stop Signal Delay (SSD) is set to 250 ms, and between 50 to 1,150 ms with adjustment steps of 50 ms thereafter. The task takes approximately 9 min to complete. Arrows with different directions (half to the right; half to the left) are presented in random order. The practice block includes 32 trials (8 signal trials and 24 no signal trials). The following three experimental blocks consist of 72 trials each (18 signal trials and 54 no signal trials; Inquisit, 2007).

CPT III, which is designed primarily to assess attention-related changes (Conners, 2014), was used to measure expected changes in commissions (incorrect response to non-targeted), perseverations (number of perseverative responses represented by responses with a reaction time of less than 100 ms); hit reaction time (average speed of correct responses), hit reaction time (HRT) block change (the slope of change in HRT across the six blocks of the administration), and detectability (the ability of a respondent to discriminate non-target from other targets) scores. During the task, participants are required to press the spacebar when any letter appears (with the exception of "X"). The interstimulus interval between each letter is 1, 2, or 4 s. The test takes 14 min to complete and consists of 18 blocks with 20 trials (360 in total).

The classic card version of the Stroop assesses the test parameters associated with inhibitory control, specifically the difficulty in warding off distractors (interference words) in the color-word (CW) condition (Lezak et al., 2004), where successful performance requires the ability to inhibit pre-potent verbal responses and conflict monitoring (Cipolotti et al., 2016), and the Stroop Interference Score (IG), a value obtained by subtracting the "predicted CW score" from the actual CW score; this reflects an ability to inhibit interference. The test consists of three subtests/charts: a word (W) chart, a color (C) chart, and a chart with colored words (CW). Each chart contains 100 items arranged in five columns of 20 items, printed on a white background. The individual charts are administered in the order W, C, and CW. The W chart consists of the words "red," "green," and "blue," printed in black. The words are arranged in random order so that two identical words do not follow each other within the column. C chart consists of the color items "XXX," which are printed in a corresponding color: red, green, or blue. The color of two consecutive items is always different. The CW chart contains colored words in the same order as the W cart, but no item is printed in a color corresponding to the meaning of the word. The time limit on each chart is 45 s. In total, even with the instruction, the test takes approximately 3 min.

In addition, a qualitative questionnaire of adverse effects, including bodily sensations and subjective mood changes induced by θ-tACS was administered during and after each neuromodulation session.

Statistical Analyses

All analyses were conducted using the software package Stata, ver. 15 (StataCorp, 2017; College Station, TX: StataCorp LLC). The tests were two-sided and $p < 0.05$ was regarded as being statistically significant. Differences in the effect of tACS conditions (individualized [A_1], non-individualized [A_2], and sham [S]) on cognitive performance (Visual Simon Task, Stop Signal Task, CPT III, and Stroop Test) were analyzed in a linear mixed-effect model fitted by a restricted maximum likelihood procedure and with a Kenward-Roger degrees of freedom approximation. In the model, sequence (six sequences: A_1A_2S, A_2SA_1, SA_1A_2, A_1SA_2, A_2A_1S, and SA_2A_1), period (three periods: sessions 1, 2, and 3), first-order carryover, and treatment (three tACS conditions: A_1, A_2, and S) were entered as fixed effects, baseline performance as a continuous covariate, subject within sequence as a random effect, and covariance structure as unstructured. Additionally, *post hoc* differences in least-square means (and 95% confidence intervals) between treatment conditions were obtained. Pairwise comparisons with Sidak's multiple testing adjustment were applied.

To assess blinding integrity we compared agreement/disagreement using Cohen's kappa with an expected chance agreement of 34.3%. To assess the side effects of θ-tACS, including bodily sensations or mood changes, the numbers of participants who experienced them were compared across treatment conditions using a Cochrane *Q*-test.

RESULTS

Twenty healthy volunteers randomized to treatment sequences completed three treatment conditions. The data obtained from cognitive testing were then analyzed.

The only significant treatment effect was found in the Stroop-CW subtest [$F_{(2,\ 27.2)} = 4.47$, $p = 0.021$] and Stroop-IG interference score [$F_{(2,\ 28.7)} = 4.05$, $p = 0.028$], whereas the effects of sequence [CW: $F_{(5,\ 19.6)} = 0.9$, $p = 0.5$; IG: $F_{(5,\ 16.4)} = 0.6$, $p = 0.7$], period [CW: $F_{(2,\ 27.5)} = 0.3$, $p = 0.7$; IG: $F_{(2,\ 27.7)} = 1.5$, $p = 0.2$], carryover [CW: $F_{(2,\ 26.2)} = 1.4$, $p = 0.3$; IG: $F_{(2,\ 27.2)} = 0.7$, $p = 0.5$], and treatment × period interaction [CW: $F_{(4,\ 27.1)} = 0.1$, $p = 1.00$; IG: $F_{(4,\ 27.9)} = 0.4$, $p = 0.8$] were non-significant. A significantly better performance was achieved after the individualized (rather than the non-individualized) tACS [CW: difference in least-square (LS) means = 3.89, 95%CI 0.30–7.46, $t = 2.72$, $p = 0.03$; IG: difference in LS means = 4.22, 95%CI 0.32–8.11, $t = 2.71$, $p = 0.03$], but when compared with the sham, neither the individualized nor the non-individualized tACS differed significantly (CW: individualized vs. sham: 0.47, 95%CI −3.19–4.12, $t = 0.32$, $p = 0.9$; non-individualized vs. sham: −3.40, 95%CI −0.16–6.98, $t = -2.40$, p = 0.07; IG: individualized

TABLE 2 | Post-modulatory effect of High Definition θ-tACS on cognitive performance.

High definition θ-tACS		Individualized		Non-individualized		Sham		Difference (*p*-value*)		
		Pre-	Post-	Pre-	Post-	Pre-	Post-	I – Non-I	I – Sham	Non-I – Sham
Visual Simon Task	Time k (ms)	402.7 (56.0)	392.5 (61.5)	416.9 (70.6)	397.9 (54.5)	393.9 (65.5)	389.7 (48.8)	0.93	0.94	0.65
	Time ink (ms)	443.6 (71.9)	423.9 (70.3)	430.2 (56.0)	415.9 (61.4)	424.6 (72.1)	418.3 (60.7)	0.94	0.66	0.92
Stop Signal Task	Time ns (ms)	603.1 (173.6)	578.9 (182.5)	602.5 (172.6)	579.3 (182.7)	550.8 (157.5)	567.3 (177.2)	0.99	0.82	0.66
	Time s (ms)	523.8 (139.5)	522.1 (173.8)	531.4 (161.9)	518.2 (160)	516.6 (162.8)	517.2 (163.9)	0.97	0.99	0.99
CPT III	Commissions	50.6 (9.9)	51.6 (10.3)	49.4 (9.9)	51.5 (11.5)	49.3 (9.4)	50.2 (10.0)	0.94	0.99	0.81
	Perseverations	46.3 (1.4)	47.7 (4.5)	46.6 (1.9)	47.5 (4.5)	46.2 (1.4)	48.4 (4.1)	0.86	0.59	0.32
	HRT (ms)	374.1 (31.6)	367.7 (28.0)	376.9 (32.7)	373.0 (33.9)	377.0 (29.8)	369.6 (29.0)	0.53	0.89	0.45
	HRT BC (ms)	1.5 (4.6)	1.9 (3.9)	0.01 (5.3)	2.1 (4.0)	−0.5 (4.5)	0.2 (3.7)	0.96	0.96	0.74
	Detectability	45.6 (6.8)	47.2 (8.4)	44.5 (6.9)	47.2 (8.8)	44.4 (7.1)	46.3 (8.0)	0.95	1.00	0.97
Stroop	C	84.8 (11.6)	86.2 (12.6)	83.8 (12.6)	86.2 (10.7)	83.1 (13.4)	86.0 (11.2)	0.52	0.41	0.36
	CW	55.6 (12.1)	59.7 (12.6)	587 (11.7)	59.4 (11.7)	59.1 (13.7)	62.8 (13.2)	0.02	0.50	0.13
	IG	8.5 (9.2)	13.0 (12.2)	12.2 (8.0)	12.3 (10.0)	13.1 (9.7)	14.9 (10.3)	0.01	0.26	0.39

*The data are presented as a mean (and SD) of pre-test or post-test values respective θ-tACS protocols; * linear mixed-effects model, post-hoc pairwise comparisons with Sidak's correction. I, Individualized θ-tACS montage of the mPFC-ACC. Non-I, Non-individualized (fixed) θ-tACS montage over the MFC. Visual Simon Task: Time k, mean reaction time for congruent stimuli; Time ink, mean reaction time for incongruent stimuli; Stop Signal Task: Time ns, mean reaction time for stimuli without noise; Time s, mean reaction time for stimuli with noise; CPT III, Continuous Performance Test III: Commissions = number of incorrect responses to non-targets "X"; Perseverations, number of perseverative responses; HRT, Hit Reaction Time; HRT BC, Hit Reaction Time Block Change; Detectability, ability to discriminate between targets "non-X" and non-targets "X"; Stroop Test: C, number of items properly named in 45 s in the color (C) congruous condition; CW, number of items properly named in 45 s in the color-word (CW) condition, where color-words are printed in an inconsistent color ink; IG, interference score. Data for Visual Simon Task and Stop Signal Task are presented as milliseconds (ms). Data for CPT III: Commissions, Perseverations and Detectability are presented as T-Scores; HRT and HRT BC are presented as milliseconds (ms).*

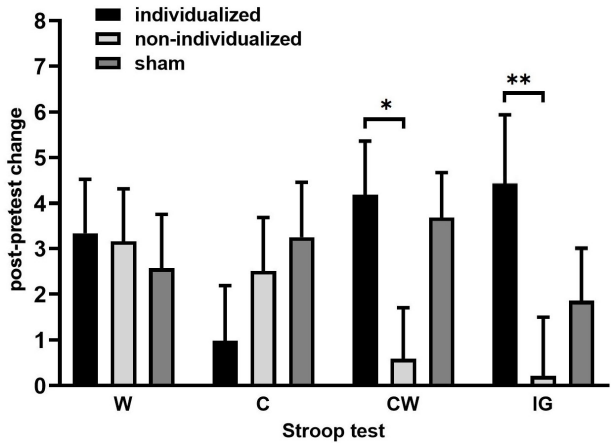

FIGURE 4 | Post-modulation changes in the Stroop task after HD θ-tACS. Post-pretest change in the Stroop task represented by the black (W) and colored ink (C) congruous conditions, by the incongruous color-word condition (CW), and by the interference score (IG). The data are presented as mean ± SE. *$p < 0.05$ and **$p < 0.01$ after Sidak's correction, linear mixed-effects model.

vs. sham: 2.39, 95%CI −1.60–6.47, $t = 1.18$, $p = 0.25$; non-individualized vs. sham: −1.82, 95%CI −5.66d–2.02, $t = -0.85$, $p = 0.4$ (**Table 2** and **Figure 4**).

Except for transient sensations of tingling or burning at the beginning of the tACS procedure, induction of phosphenes (visual sensations of a ring or spot) during the active protocols, and transient headache, HD θ-tACS was well-tolerated, with no serious adverse effects reported (**Table 3**). Interestingly, neuromodulatory conditions differed in emotional and mood effects at debriefing. Frequent irritation was reported after the non-individualized θ-tACS, while the individualized condition was associated more frequently with calm and harmonization (**Table 3**).

When evaluating blinding integrity, the observed agreement was 50%, with kappa 0.24, SE 0.15, $z = 1.58$, $p = 0.06$. The participants did not estimate the order of treatments (a position of placebo) significantly better than by chance (34%), so a major violation of blinding was not detected.

DISCUSSION

The present study is the first to examine the influence of individualized HD θ-tACS targeted at the ACC on inhibitory control performance. We used the optimal electrode arrangement based on computational modeling from individual MRIs to target the current flow with the highest specificity at the mPFC-ACC, with maximum current density in the ACC, to investigate the post-modulatory θ-tACS effect on inhibitory control. Based on the evidence from previous studies that confirmed the alteration of inhibitory control performance during θ-tACS neuromodulation (van Driel et al., 2015; Moliadze et al., 2019), we extended the experiment to include a θ-tACS condition that modulated the ACC indirectly through MFC.

The post-modulatory effects of different θ-tACS protocols on inhibitory control performance were investigated with a novel paradigm of individualized HD θ-tACS, non-individualized θ-tACS targeting the ACC indirectly via the MFC, and a sham condition.

The main finding of our study was the presence of a post-modulatory effect in the improvement of inhibitory control with individualized HD θ-tACS. In contrast with the non-individualized θ-tACS, it demonstrated a post-modulatory improvement of inhibitory control with a verbal component, as documented within 45 min post neuromodulation. Specifically, we found a significant improvement in Stroop-CW and Stroop-IG performances following individualized HD θ-tACS. Unlike the parameters in other selected tasks, these tasks reflect the inhibitory control function with a verbal component. The changes in the non-verbal cognitive tasks (Simon Task, Stop Signal Task, and CPT III) did not induce a parallel effect. Compared with the sham condition, neither of the active θ-tACS protocols (individualized or non-individualized) were able to alter inhibitory control performance.

In general, our findings are in keeping with previous studies that have reported θ-tACS modulation of ACC activity (Chander et al., 2016; Onoda et al., 2017) and inhibitory control performance (van Driel et al., 2015; Moliadze et al., 2019).

Our results confirm those of a previous study in which the effect of alpha band (α) tACS on phonological word decisions was monitored (Moliadze et al., 2019). Although the authors used a different frequency (10 Hz rather than 6 Hz), bilateral prefrontal electrode positioning, and a different task for inhibitory control performance monitoring, their results showed a similar post-modulatory effect of tACS on inhibitory control with a verbal component. Interestingly, Fusco et al.'s (2020) study, in which they monitor the effect of tACS over the MFC and the extrastriate body area (with an electrode arrangement in the FCz and P08 areas) in cognitive conflicts related to bodily stimuli, highlights the causal relationship between function-specific brain areas and category-specific conflict tasks. During θ-tACS, there was an improvement in the Hand-Flanker task (representing bodily stimuli), but not in the Letter-Flanker task.

However, our results did not correspond with the findings of a study that used a non-individualized θ-tACS over the MFC (Fusco et al., 2018), though the authors only tested the immediate effect of a short-lasting (240 s duration) θ-tACS during the activation of the ACC with a specific inhibitory control task. This may interfere directly with cognitive processes and boost the effect of neuromodulation, similar to the effect shown in tDCS studies involving additional on-line cognitive training (Dedoncker et al., 2016; Hill et al., 2016). In contrast, and in keeping with van Driel et al. (2015), we used long-lasting θ-tACS to evaluate changes in the post-session processing of inhibitory control.

The finding that the non-individualized protocol was not effective in altering inhibitory control may be attributed to more complex regulation of inhibitory control than simple dACC activation. It also supports the assumption that the effect of θ-tACS may be affected by the concurrent modulation of surrounding and interconnected structures, by parallel modulation of the DLPFC in the individualized protocol, and by simultaneous modulation of the frontal and parietal cortex, the inferior frontal gyrus (IFG) in particular. This would explain why van Lehr et al.'s (2019) study, in which the DLPFC was modulated, and Moliadze et al.'s (2019) study, in which the prefrontal cortex was targeted bilaterally, showed a tACS effect in altering the verbal component of inhibitory control (though the results were inconsistent).

Interestingly, the present study did not show any sustained changes in non-verbal performance. We speculate that the absence of the effect on inhibitory control in non-verbal tasks after θ-tACS may be related to the greater stability of simpler non-verbal inhibition processes that are possibly more difficult to affect. Inhibitory control of verbal performance, where the ACC is also responsible for the semantic coding process in verbal working memory and is considered to be the central neural base of the central executive processes (Kaneda and Osaka, 2008; Reverberi et al., 2015), is a more complex function that may be more sensitive to the changes induced by neuromodulation, including the post-modulatory effect. An alternative explanation may be the use of different cognitive control strategies in the Stroop and Simon Task. Each of these tests bias attention toward a different approach in resolving the conflict. While the Stroop enhances the processing of task-relevant cues (i.e., it enhances the processing of colors and does not inhibit processing of irrelevant cues—namely, the words), the Simon Task inhibits task-irrelevant cues (i.e., it suppresses the position of the button, but does not enhance processing of the relevant cue—namely, the color of the square (Egner and Hirsch, 2005; Egner et al., 2007; Egner, 2008; Soutschek et al., 2013). Although both control strategies employ the same network (Peterson et al., 2002), the first modulates the activity in the parietal cortex, while the response-based conflict resolution modifies premotor cortex activity (Egner et al., 2007). This difference is consistent with

TABLE 3 | Adverse or side effects, including bodily sensations and mood state changes induced by θ-tACS.

Bodily sensations and mood states changes		Individualized	Non-individualized	Sham	*p*-value*
Adverse or side post-modulation effects	Mild Headache	1	2	0	0.22
	Irritability	1	9	0	<0.001
	Harmonization or Calm	8	1	0	0.001
	Increase of Energy	0	3	0	0.05
	Fatigue	1	0	0	0.37
Tingling or burning during tACS		15	15	14	0.37
Phosphenes during tACS		3	2	0	0.25

*The data presents adverse or side effects, including bodily sensations and mood state changes in specific θ-tACS protocols during and after θ-tACS. The data show the number of participants who reported the symptoms. The cells "tingling" or "burning" refer to sensations on the skin in the area around the neuromodulatory electrodes at the beginning of θ-tACS application. *Cochrane Q-test.*

Pratte et al. (2010), who found that the Stroop interference effect is smallest in fast responses and increases with longer response times, while the Simon's effect is strongest in fast response time trials, and decreases as the response time increases. In the present study, the stimulation led to better performance in Stroop-CW (i.e., the Stroop effect was smaller), which meant a shorter RT per CW. This indicates a boost in the processing of task-relevant traits of the stimuli. On the other hand, no Simon effect modulation resulted in the improvement of response-selection processing. A possible explanation for this difference is the fact that partial (unintentional) stimulation of the premotor cortex may disrupt the overall effect in the Simon Task, but not in the Stroop.

A previous θ-tACS study that modulated PFC showed an altered processing in emotion evaluation/appraisal that corresponded to the integration function of the dACC (Onoda et al., 2017). Analogously, we observed unexpected mood changes induced by neuromodulation, where the volunteers reported irritation following the non-individualized protocol, and more often felt calm and harmonized after the individualized session (**Table 3**). We speculate that irritability after non-individualized θ-tACS may be mediated by the simultaneous modulation of the IFG and parietal region, which are not influenced by the individualized protocol. Therefore, non-individualized θ-tACS of the ACC may alter common brain activity (particularly motor and premotor) in other areas (Veniero et al., 2011; Alfonso et al., 2013), and this may impair the soothing effect of θ-tACS of the ACC. In contrast, a calm mood or mild fatigue induced by the individualized protocol may be attributed to simultaneous synchronization of the activity in the rostral ACC, which is associated with emotional processing (Bush et al., 2000).

For further exploration and verification of these observations, future protocols should include emotional tasks. For example, the emotional Stroop Test (Dresler et al., 2009), unlike the "standard" cognitive Stroop, is related to the rostral ACC activation, which was modulated simultaneously in both active protocols in the present study. It would also be beneficial to use specific scales to quantify emotional responses to neuromodulation.

To calculate individualized HD θ-tACS, we used high current density distribution to the mPFC-ACC along with low current density distribution in other cortical areas, including the parietal and temporal cortex. Electrode placement in the occipital area targeting the ACC via the mPFC also caused simultaneous neuromodulation of the visual cortex and may induce phosphenes, which could also be of a retinal origin (Kanai et al., 2010). Nevertheless, network analyses of inhibitory control-related network connections did not identify the occipital cortex as a region that is essential for inhibitory control (Spielberg et al., 2015). Moreover, the Stroop was measured before and after neuromodulation; therefore, visual performance during the cognitive tests could not be impaired.

In keeping with most previous studies testing the effect of θ-tACS on inhibitory control (van Driel et al., 2015; Lehr et al., 2019), our neuromodulation protocols used a total current of 1 mA. Fusco et al. (2018, 2020) administered a current of 1.5 and 2 mA, respectively. So far, the GTEN 100 used in our experiment has not allowed neuromodulation with a higher intensity of current. Previous findings have confirmed the dependence of tACS's efficacy on current strength (Vosskuhl et al., 2016). It may be presumed that the upgrading of GTEN technology to higher current intensities will enhance the effect of neuromodulation.

Fusco et al. (2018) protocol used two circular sponge-conductive-rubber electrodes (Sponstim, 25 cm^2, Neuroelectrics, Barcelona, Spain) placed over the MFC (in the FCz and Pz areas) for tACS. Our non-individualized protocol used MFC electrode layouts with 10 (five anode-cathodes; five cathode-anodes) circular electrodes (HCGSN 100, 1 cm^2, EGI, Eugene, OR, United States), where each group of electrodes (in the FCz and Pz areas) covered 16–25 cm^2, depending on the size of the subject's head. The contact area of 5 cm^2 was not changeable. The group of five electrodes was grouped in a square arrangement (four electrodes placed at the vertices of the square and the fifth central electrode in the FCz or Pz areas). Therefore, we cannot rule out the possibility that this methodological difference may lead to different results and outcomes.

The main shortcoming of the present study is the lack of neurophysiological evidence to confirm that the ACC was affected by tACS. Furthermore, individualized HD θ-tACS was applied via the mPFC, a cortical hub functionally connected with many associated brain areas, which might interfere with the effect. Therefore, we cannot rule out the possibility that the effect of individualized HD θ-tACS was influenced by concurrent modulation of the mPFC and its associated areas.

The study is limited by the lack of a control frequency condition. The testing could be enriched, in addition to the sham, by a control frequency condition to show that the detected behavioral changes are causally related to θ-tACS (6 Hz) and do not depend on other factors.

Future studies should also investigate the electrophysiological effects of θ-tACS (Bergmann et al., 2016; Cunillera et al., 2016; Neuling et al., 2017). In particular, it would be useful to monitor θ-tACS-induced changes in ERPs during performance tasks focused on cognitive functions. In the case of action monitoring, the suitable ERPs to study would be error-related negativity/error negativity (ERN; Gehring et al., 1995; Luu et al., 2000), or cognitive inhibition (N2; Yeung et al., 2004; Huster et al., 2013). Both, ERN and N2 are associated with the theta band (Luu et al., 2004; Cavanagh and Frank, 2014). In the latter, the nogo condition elicits a more negative response than the go condition (Lavric et al., 2004). Better performance in cognitive control tasks is associated with smaller N2 amplitudes (Lamm et al., 2006), while in ERN, the enhancement of negative amplitude is related to hyper-functioning error monitoring processes (Ruchsow et al., 2005).

CONCLUSION

In conclusion, we have demonstrated that, compared with non-individualized θ-tACS, individualized HD θ-tACS applied via the mPFC-ACC significantly improves the post-tACS verbal component of conflict-processing. The proposed algorithm of

the individualized HD θ-tACS confirmed better specificity in neuromodulation targeting. Our findings support the role of the ACC as the candidate region for inhibitory control processes and show that HD θ-tACS is a safe and well-tolerated method. Further studies examining the neuromodulation-induced changes in inhibitory control processes are warranted to verify the effect of the procedure and to optimize the neuromodulation parameters, including electrode assembly and current intensity. Future researchers should also investigate whether the individualized HD θ-tACS of the mPFC-ACC can modulate inhibitory control processes impaired by neuropsychiatric disorders associated with ACC disruption.

DATA AVAILABILITY STATEMENT

The raw data supporting the conclusions of this article will be made available by the authors, without undue reservation.

ETHICS STATEMENT

The studies involving human participants were reviewed and approved by the Independent Ethics Committee of the National Institute of Mental Health, Klecany, Czechia. The patients/participants provided their written informed consent to participate in this study. Written informed consent was obtained from the individual(s) for the publication of any potentially identifiable images or data included in this article.

AUTHOR CONTRIBUTIONS

MK: conceptualization, methodology, investigation, project administration, visualization, writing – original draft preparation, and supervision. VV: conceptualization, methodology, investigation, project administration, and writing Ű- reviewing and editing. JH: supervision and writing Ű- reviewing and editing. PM: conceptualization and writing Ű- reviewing and editing. JJ: investigation and writing – original draft preparation. DD: conceptualization, methodology, investigation, and writing Ű- reviewing and editing. LK, SB, and OL: investigation and writing Ű- reviewing and editing. DF: validation, data curation, and writing Ű- reviewing and editing. TN: conceptualization, formal analysis, writing – original draft preparation, and writing Ű- reviewing and editing. All authors contributed to the article and approved the submitted version.

FUNDING

The study was funded by the grants nos. 16-31380A, 17-30833A, NU20-04-00147, NV18-04-00260, and DRO (National Institute of Mental Health–NIMH, IN: 00023752) of the MH, CR, PharmaBrain No. CZ.02.1.01/0.0/0.0/16_0250007444, and grant no. 20-24782S by the Czech Science Foundation.

ACKNOWLEDGMENTS

We thank Dr. Martin Brunovsky for providing the excellent technical facilities that enabled us to carry out the project.

REFERENCES

Ahn, S., Mellin, J. M., Alagapan, S., Alexander, M. L., Gilmore, J. H., Jarskog, L. F., et al. (2019). Targeting reduced neural oscillations in patients with schizophrenia by transcranial alternating current stimulation. *Neuroimage* 186, 126–136. doi: 10.1016/j.neuroimage.2018.10.056

Alam, M., Truong, D. Q., Khadka, N., and Bikson, M. (2016). Spatial and polarity precision of concentric high-definition transcranial direct current stimulation (HD-tDCS). *Phys. Med. Biol.* 61, 4506–4521. doi: 10.1088/0031-9155/61/12/4506

Alfonso, M. R., Miquel, T. F., Xavier, B., and Blanca, A. S. (2013). Resting parietal electroencephalogram asymmetries and self-reported attentional control. *Clin. EEG Neurosci.* 44, 188–192. doi: 10.1177/1550059412465871

Ali, M. M., Sellers, K. K., and Fröhlich, F. (2013). Transcranial alternating current stimulation modulates large-scale cortical network activity by network resonance. *J. Neurosci.* 33, 11262–11275. doi: 10.1523/jneurosci.5867-12.2013

Antal, A., Boros, K., Poreisz, C., Chaieb, L., Terney, D., and Paulus, W. (2008). Comparatively weak after-effects of transcranial alternating current stimulation (tACS) on cortical excitability in humans. *Brain Stimul.* 1, 97–105. doi: 10.1016/j.brs.2007.10.001

Antal, A., and Herrmann, C. S. (2016). Transcranial alternating current and random noise stimulation: possible mechanisms. *Neural Plast.* 2016:3616807. doi: 10.1155/2016/3616807

Antal, A., and Paulus, W. (2013). Transcranial alternating current stimulation (tACS). *Front. Hum. Neurosci.* 7:317. doi: 10.3389/fnhum.2013.00317

Berger, A., Pixa, N. H., Steinberg, F., and Doppelmayr, M. (2018). Brain oscillatory and hemodynamic activity in a bimanual coordination task following transcranial alternating current stimulation (tACS): a combined EEG-fNIRS study. *Front. Behav. Neurosci.* 12:67. doi: 10.3389/fnbeh.2018.00067

Bergmann, T. O., Karabanov, A., Hartwigsen, G., Thielscher, A., and Siebner, H. R. (2016). Combining non-invasive transcranial brain stimulation with neuroimaging and electrophysiology: current approaches and future perspectives. *Neuroimage* 140, 4–19. doi: 10.1016/j.neuroimage.2016.02.012

Bialystok, E., Craik, F. I., Klein, R., and Viswanathan, M. (2004). Bilingualism, aging, and cognitive control: evidence from the Simon task. *Psychol. Aging* 19:290. doi: 10.1037/0882-7974.19.2.290

Bush, G., Luu, P., and Posner, M. I. (2000). Cognitive and emotional influences in anterior cingulate cortex. *Trends Cogn. Sci.* 4, 215–222. doi: 10.1016/S1364-6613(00)01483-2

Carter, C. S., MacDonald Iii, A. W., Ross, L. L., and Stenger, V. A. (2001). Anterior cingulate cortex activity and impaired self-monitoring of performance in patients with schizophrenia: an event-related fMRI study. *Am. J. Psychiatry* 158, 1423–1428. doi: 10.1176/appi.ajp.158.9.1423

Cavanagh, J. F., and Frank, M. J. (2014). Frontal theta as a mechanism for cognitive control. *Trends Cogn. Sci.* 18, 414–421. doi: 10.1016/j.tics.2014.04.012

Cavanagh, J. F., and Shackman, A. J. (2015). Frontal midline theta reflects anxiety and cognitive control: meta-analytic evidence. *J. Physiol. Paris* 109, 3–15. doi: 10.1016/j.jphysparis.2014.04.003

Chander, B. S., Witkowski, M., Braun, C., Robinson, S. E., Born, J., Cohen, L. G., et al. (2016). tACS phase locking of frontal midline theta oscillations disrupts working memory performance. *Front. Cell Neurosci.* 10:120. doi: 10.3389/fncel.2016.00120

Cipolotti, L., Spanò, B., Healy, C., Tudor-Sfetea, C., Chan, E., White, M., et al. (2016). Inhibition processes are dissociable and lateralized in human prefrontal cortex. *Neuropsychologia* 93, 1–12. doi: 10.1016/j.neuropsychologia.2016.09.018

Cohen, M. X., and Donner, T. H. (2013). Midfrontal conflict-related theta-band power reflects neural oscillations that predict behavior. *J. Neurophysiol.* 110, 2752–2763. doi: 10.1152/jn.00479.2013

Cohen, M. X., Ridderinkhof, K. R., Haupt, S., Elger, C. E., and Fell, J. (2008). Medial frontal cortex and response conflict: evidence from human intracranial EEG and medial frontal cortex lesion. *Brain Res.* 1238, 127–142. doi: 10.1016/j.brainres.2008.07.114

Conners, C. (2014). *Conners Continuous Performance Test*, 3rd Edn. North Tonawanda, NY: Multi-Health Systems Inc.

Cunillera, T., Brignani, D., Cucurell, D., Fuentemilla, L., and Miniussi, C. (2016). The right inferior frontal cortex in response inhibition: a tDCS–ERP co-registration study. *NeuroImage* 140, 66–75. doi: 10.1016/j.neuroimage.2015.11.044

Dedoncker, J., Brunoni, A. R., Baeken, C., and Vanderhasselt, M. A. (2016). A systematic review and meta-analysis of the effects of transcranial direct current stimulation (tDCS) over the dorsolateral prefrontal cortex in healthy and neuropsychiatric samples: influence of stimulation parameters. *Brain Stimul.* 9, 501–517. doi: 10.1016/j.brs.2016.04.006

Del Felice, A., Castiglia, L., Formaggio, E., Cattelan, M., Scarpa, B., Manganotti, P., et al. (2019). Personalized transcranial alternating current stimulation (tACS) and physical therapy to treat motor and cognitive symptoms in Parkinson's disease: a randomized cross-over trial. *NeuroImage Clin.* 22:101768. doi: 10.1016/j.nicl.2019.101768

Dmochowski, J. P., Datta, A., Bikson, M., Su, Y., and Parra, L. C. (2011). Optimized multi-electrode stimulation increases focality and intensity at target. *J. Neural Eng.* 8:046011. doi: 10.1088/1741-2560/8/4/046011

Dresler, T., Mériau, K., Heekeren, H. R., and van der Meer, E. (2009). Emotional Stroop task: effect of word arousal and subject anxiety on emotional interference. *Psychol. Res.* 73, 364–371. doi: 10.1007/s00426-008-0154-6

Egner, T. (2008). Multiple conflict-driven control mechanisms in the human brain. *Trends Cogn. Sci.* 12, 374–380. doi: 10.1016/j.tics.2008.07.001

Egner, T., Delano, M., and Hirsch, J. (2007). Separate conflict-specific cognitive control mechanisms in the human brain. *NeuroImage* 35, 940–948. doi: 10.1016/j.neuroimage.2006.11.061

Egner, T., and Hirsch, J. (2005). Cognitive control mechanisms resolve conflict through cortical amplification of task-relevant information. *Nat. Neurosci.* 8:1784. doi: 10.1038/nn1594

Fernández-Corazza, M., Turovets, S., Luu, P., Anderson, E., and Tucker, D. (2016). Transcranial electrical neuromodulation based on the reciprocity principle. *Front. Psychiatry* 7:87. doi: 10.3389/fpsyt.2016.00087

Fitzgerald, K. D., Welsh, R. C., Gehring, W. J., Abelson, J. L., Himle, J. A., Liberzon, I., et al. (2005). Error-related hyperactivity of the anterior cingulate cortex in obsessive-compulsive disorder. *Biol. Psychiatry* 57, 287–294. doi: 10.1016/j.biopsych.2004.10.038

Fusco, G., Fusaro, M., and Aglioti, S. (2020). Midfrontal-occipital θ-tACS modulates cognitive conflicts related to bodily stimuli. *Soc. Cogn. Affect. Neurosci.* nsaa125. doi: 10.1093/scan/nsaa125

Fusco, G., Scandola, M., Feurra, M., Pavone, E. F., Rossi, S., and Aglioti, S. M. (2018). Midfrontal theta transcranial alternating current stimulation modulates behavioural adjustment after error execution. *Eur. J. Neurosci.* 48, 3159–3170. doi: 10.1111/ejn.14174

Gasquoine, P. G. (2013). Localization of function in anterior cingulate cortex: from psychosurgery to functional neuroimaging. *Neurosci. Biobehav. Rev.* 37, 340–348. doi: 10.1016/j.neubiorev.2013.01.002

Gehring, W. J., Coles, M. G., Meyer, D. E., and Donchin, E. (1995). A brain potential manifestation of error-related processing. *Electroencephalogr. Clin. Neurophysiol.* Suppl. 44, 261–272.

Gratton, G., Coles, M. G. H., Sirevaag, E. J., Eriksen, C. W., and Donchin, E. (1988). Pre- and poststimulus activation of response channels: a psychophysiological analysis. *J. Exp. Psychol. Hum. Percept. Perform.* 14, 331–344. doi: 10.1037/0096-1523.14.3.331

Herrmann, C., Rach, S., Neuling, T., and Strüber, D. (2013). Transcranial alternating current stimulation: a review of the underlying mechanisms and modulation of cognitive processes. *Front. Hum. Neurosci.* 7:279. doi: 10.3389/fnhum.2013.00279

Hill, A. T., Fitzgerald, P. B., and Hoy, K. E. (2016). Effects of anodal transcranial direct current stimulation on working memory: a systematic review and meta-analysis of findings from healthy and neuropsychiatric populations. *Brain Stimul.* 9, 197–208. doi: 10.1016/j.brs.2015.10.006

Hoy, K. E., Bailey, N., Arnold, S., Windsor, K., John, J., Daskalakis, Z. J., et al. (2015). The effect of γ-tACS on working memory performance in healthy controls. *Brain Cogn.* 101, 51–56. doi: 10.1016/j.bandc.2015.11.002

Huster, R. J., Enriquez-Geppert, S., Lavallee, C. F., Falkenstein, M., and Herrmann, C. S. (2013). Electroencephalography of response inhibition tasks: functional networks and cognitive contributions. *Int. J. Psychophysiol.* 87, 217–233. doi: 10.1016/j.ijpsycho.2012.08.001

Inquisit, M. (2007). *3.0 [Computer Software]*. Seattle, WA: Millisecond Software.

Kanai, R., Paulus, W., and Walsh, V. (2010). Transcranial alternating current stimulation (tACS) modulates cortical excitability as assessed by TMS-induced phosphene thresholds. *Clin. Neurophysiol.* 121, 1551–1554. doi: 10.1016/j.clinph.2010.03.022

Kaneda, M., and Osaka, N. (2008). Role of anterior cingulate cortex during semantic coding in verbal working memory. *Neurosci. Lett.* 436, 57–61. doi: 10.1016/j.neulet.2008.02.069

Kopp, B., Mattler, U., Goertz, R., and Rist, F. (1996a). N2, P3 and the lateralized readiness potential in a nogo task involving selective response priming. *Electroencephalogr. Clin. Neurophysiol.* 99, 19–27. doi: 10.1016/0921-884X(96)95617-9

Kopp, B., Rist, F., and Mattler, U. (1996b). N200 in the flanker task as a neurobehavioral tool for investigating executive control. *Psychophysiology* 33, 282–294. doi: 10.1111/j.1469-8986.1996.tb00425.x

Lamm, C., Zelazo, P. D., and Lewis, M. D. (2006). Neural correlates of cognitive control in childhood and adolescence: disentangling the contributions of age and executive function. *Neuropsychologia* 44, 2139–2148. doi: 10.1016/j.neuropsychologia.2005.10.013

Lang, S., Gan, L., Alrazi, T., and Monchi, O. (2019). High definition transcranial alternating current stimulation of the right fusiform cortex improves visual associative memory. *Brain Stimul.* 12:429. doi: 10.1016/j.brs.2018.12.389

Lavric, A., Pizzagalli, D. A., and Forstmeier, S. (2004). When 'go'and 'nogo'are equally frequent: ERP components and cortical tomography. *Eur. J. Neurosci.* 20, 2483–2488. doi: 10.1111/j.1460-9568.2004.03683.x

Lefaucheur, J. P., Antal, A., Ayache, S. S., Benninger, D. H., Brunelin, J., Cogiamanian, F., et al. (2017). Evidence-based guidelines on the therapeutic use of transcranial direct current stimulation (tDCS). *Clin. Neurophysiol.* 128, 56–92. doi: 10.1016/j.clinph.2016.10.087

Lehr, A., Henneberg, N., Nigam, T., Paulus, W., and Antal, A. (2019). Modulation of conflict processing by theta-range tACS over the Dorsolateral prefrontal cortex. *Neural Plast.* 2019:6747049. doi: 10.1155/2019/6747049

Lezak, M. D., Howieson, D. B., Loring, D. W., and Fischer, J. S. (2004). *Neuropsychological Assessment*. New York, NY: Oxford University Press.

Luu, P., Essaki Arumugam, E. M., Anderson, E., Gunn, A., Rech, D., Turovets, S., et al. (2016). Slow-Frequency pulsed transcranial electrical stimulation for modulation of cortical plasticity based on reciprocity targeting with precision electrical head modeling. *Front. Hum. Neurosci.* 10:377. doi: 10.3389/fnhum.2016.00377

Luu, P., Flaisch, T., and Tucker, D. M. (2000). Medial frontal cortex in action monitoring. *J. Neurosci.* 20, 464–469. doi: 10.1523/JNEUROSCI.20-01-00464.2000

Luu, P., Tucker, D. M., and Makeig, S. (2004). Frontal midline theta and the error-related negativity: neurophysiological mechanisms of action regulation. *Clin. Neurophysiol.* 115, 1821–1835. doi: 10.1016/j.clinph.2004.03.031

Moliadze, V., Sierau, L., Lyzhko, E., Stenner, T., Werchowski, M., Siniatchkin, M., et al. (2019). After-effects of 10 Hz tACS over the prefrontal cortex on phonological word decisions. *Brain Stimul.* 12, 1464–1474. doi: 10.1016/j.brs.2019.06.021

Neuling, T., Ruhnau, P., Weisz, N., Herrmann, C. S., and Demarchi, G. (2017). Faith and oscillations recovered: on analyzing EEG/MEG signals during tACS. *NeuroImage* 147, 960–963. doi: 10.1016/j.neuroimage.2016.11.022

Nigbur, R., Cohen, M. X., Ridderinkhof, K. R., and Stürmer, B. (2012). Theta dynamics reveal domain-specific control over stimulus and response conflict. *J. Cogn. Neurosci.* 24, 1264–1274. doi: 10.1162/jocn_a_00128

Nikolin, S., Loo, C. K., Bai, S., Dokos, S., and Martin, D. M. (2015). Focalised stimulation using high definition transcranial direct current stimulation (HD-tDCS) to investigate declarative verbal learning and memory functioning. *NeuroImage* 117, 11–19. doi: 10.1016/j.neuroimage.2015.05.019

Onoda, K., Kawagoe, T., Zheng, H., and Yamaguchi, S. (2017). Theta band transcranial alternating current stimulations modulates network behavior of dorsal anterior cingulate cortex. *Sci. Rep.* 7:3607. doi: 10.1038/s41598-017-03859-7

Pahor, A., and Jaušovec, N. (2018). The effects of theta and gamma tACS on working memory and electrophysiology. *Front. Hum. Neurosci.* 11:651. doi: 10.3389/fnhum.2017.00651

Paulus, W. (2011). Transcranial electrical stimulation (tES – tDCS; tRNS, tACS) methods. *Neuropsychol. Rehabil.* 21, 602–617. doi: 10.1080/09602011.2011.557292

Peterson, B. S., Kane, M. J., Alexander, G. M., Lacadie, C., Skudlarski, P., Leung, H. C., et al. (2002). An event-related functional MRI study comparing interference effects in the Simon and Stroop tasks. *Cogn. Brain Res.* 13, 427–440. doi: 10.1016/S0926-6410(02)00054-X

Poreisz, C., Boros, K., Antal, A., and Paulus, W. (2007). Safety aspects of transcranial direct current stimulation concerning healthy subjects and patients. *Brain Res. Bull.* 72, 208–214. doi: 10.1016/j.brainresbull.2007.01.004

Pratte, M. S., Rouder, J. N., Morey, R. D., and Feng, C. (2010). Exploring the differences in distributional properties between Stroop and Simon effects using delta plots. *Atten. Percept. Psychophys.* 72, 2013–2025. doi: 10.3758/APP.72.7.2013

Reverberi, C., Kuhlen, A., Abutalebi, J., Greulich, R. S., Costa, A., Seyed-Allaei, S., et al. (2015). Language control in bilinguals: intention to speak vs. execution of speech. *Brain Lang.* 144, 1–9. doi: 10.1016/j.bandl.2015.03.004

Ruchsow, M., Grön, G., Reuter, K., Spitzer, M., Hermle, L., and Kiefer, M. (2005). Error-related brain activity in patients with obsessive-compulsive disorder and in healthy controls. *J. Psychophysiol.* 19, 298–304. doi: 10.1027/0269-8803.19.4.298

Sela, T., Kilim, A., and Lavidor, M. (2012). Transcranial alternating current stimulation increases risk-taking behavior in the balloon analog risk task. *Front. Neurosci.* 6:22. doi: 10.3389/fnins.2012.00022

Soutschek, A., Müller, H. J., and Schubert, T. (2013). Conflict-specific effects of accessory stimuli on cognitive control in the Stroop task and the Simon task. *Exp. Psychol.* 60, 140–148. doi: 10.1027/1618-3169/a000181

Spielberg, J. M., Miller, G. A., Heller, W., and Banich, M. T. (2015). Flexible brain network reconfiguration supporting inhibitory control. *Proc. Natl. Acad. Sci. U.S.A.* 112, 10020–10025. doi: 10.1073/pnas.1500048112

StataCorp (2017). *Stata Statistical Software: Release 15*. College Station, TX: StataCorp LLC.

Taylor, S. F., Stern, E. R., and Gehring, W. J. (2007). Neural systems for error monitoring: recent findings and theoretical perspectives. *Neuroscientist* 13, 160–172. doi: 10.1177/1073858406298184

Ursu, S., Stenger, V. A., Shear, M. K., Jones, M. R., and Carter, C. S. (2003). Overactive action monitoring in obsessive-compulsive disorder: evidence from functional magnetic resonance imaging. *Psychol. Sci.* 14, 347–353. doi: 10.1111/1467-9280.24411

van Driel, J., Sligte, I. G., Linders, J., Elport, D., and Cohen, M. X. (2015). Frequency band-specific electrical brain stimulation modulates cognitive control processes. *PLoS One* 10:e0138984. doi: 10.1371/journal.pone.0138984

van Gaal, S., Ridderinkhof, K. R., van den Wildenberg, W. P., and Lamme, V. A. (2009). Dissociating consciousness from inhibitory control: evidence for unconsciously triggered response inhibition in the stop-signal task. *J. Exp. Psychol. Hum. Percept. Perform.* 35:1129. doi: 10.1037/a0013551

Van Noordt, S. J. R., Campopiano, A., and Segalowitz, S. J. (2016). A functional classification of medial frontal negativity ERPs: theta oscillations and single subject effects. *Psychophysiology* 53, 1317–1334. doi: 10.1111/psyp.12689

van Veen, V., and Carter, C. S. (2002). The anterior cingulate as a conflict monitor: fMRI and ERP studies. *Physiol. Behav.* 77, 477–482. doi: 10.1016/S0031-9384(02)00930-7

Veniero, D., Brignani, D., Thut, G., and Miniussi, C. (2011). Alpha-generation as basic response-signature to transcranial magnetic stimulation (TMS) targeting the human resting motor cortex: a TMS/EEG co-registration study. *Psychophysiology* 48, 1381–1389. doi: 10.1111/j.1469-8986.2011.01218.x

Vossen, A., Gross, J., and Thut, G. (2015). Alpha power increase after transcranial alternating current stimulation at alpha frequency (α-tACS) reflects plastic changes rather than entrainment. *Brain Stimul.* 8, 499–508. doi: 10.1016/j.brs.2014.12.004

Vosskuhl, J., Huster, R. J., and Herrmann, C. S. (2015). Increase in short-term memory capacity induced by down-regulating individual theta frequency via transcranial alternating current stimulation. *Front. Hum. Neurosci.* 9:257. doi: 10.3389/fnhum.2015.00257

Vosskuhl, J., Huster, R. J., and Herrmann, C. S. (2016). BOLD signal effects of transcranial alternating current stimulation (tACS) in the alpha range: a concurrent tACS–fMRI study. *NeuroImage* 140, 118–125. doi: 10.1016/j.neuroimage.2015.10.003

Williams, E. J. (1949). Experimental designs balanced for the estimation of residual effects of treatments. *Aust. J. Chem.* 2, 149–168. doi: 10.1071/ch9490149

Wischnewski, M., Zerr, P., and Schutter, D. J. (2016). Effects of theta transcranial alternating current stimulation over the frontal cortex on reversal learning. *Brain Stimul.* 9, 705–711. doi: 10.1016/j.brs.2016.04.011

Witkowski, M., Garcia-Cossio, E., Chander, B. S., Braun, C., Birbaumer, N., Robinson, S. E., et al. (2016). Mapping entrained brain oscillations during transcranial alternating current stimulation (tACS). *NeuroImage* 140, 89–98. doi: 10.1016/j.neuroimage.2015.10.024

Yeung, N., Botvinick, M. M., and Cohen, J. D. (2004). The neural basis of error detection: conflict monitoring and the error-related negativity. *Psychol. Rev.* 111:931. doi: 10.1037/0033-295X.111.4.931

Zaehle, T., Rach, S., and Herrmann, C. S. (2010). Transcranial alternating current stimulation enhances individual alpha activity in human EEG. *PLoS One* 5:e13766. doi: 10.1371/journal.pone.0013766

Zaghi, S., de Freitas Rezende, L., de Oliveira, L. M., El-Nazer, R., Menning, S., Tadini, L., et al. (2010). Inhibition of motor cortex excitability with 15 Hz transcranial alternating current stimulation (tACS). *Neurosci. Lett.* 479, 211–214. doi: 10.1016/j.neulet.2010.05.060

Conflict of Interest: The authors declare that the research was conducted in the absence of any commercial or financial relationships that could be construed as a potential conflict of interest.

frontiers in Human Neuroscience

ORIGINAL RESEARCH
published: 14 April 2021
doi: 10.3389/fnhum.2021.661976

Spatial-Temporal Functional Mapping Combined With Cortico-Cortical Evoked Potentials in Predicting Cortical Stimulation Results

Yujing Wang[1], Mark A. Hays[2], Christopher Coogan[1], Joon Y. Kang[1], Adeen Flinker[3], Ravindra Arya[4,5], Anna Korzeniewska[1] and Nathan E. Crone[1]*

[1]Department of Neurology, Johns Hopkins University School of Medicine, Baltimore, MD, United States, [2]Department of Biomedical Engineering, Johns Hopkins University School of Medicine, Baltimore, MD, United States, [3]Department of Neurology, New York University School of Medicine, New York, NY, United States, [4]Comprehensive Epilepsy Center, Division of Neurology, Cincinnati Children's Hospital Medical Center, Cincinnati, OH, United States, [5]Department of Pediatrics, University of Cincinnati College of Medicine, Cincinnati, OH, United States

OPEN ACCESS

Edited by:
Shozo Tobimatsu, Kyushu University, Japan

Reviewed by:
Eishi Asano, Children's Hospital of Michigan, United States
Rei Enatsu, Sapporo Medical University, Japan
Naoto Kunii, The University of Tokyo, Japan

***Correspondence:**
Yujing Wang
ywang154@jhu.edu

Specialty section:
This article was submitted to Brain Imaging and Stimulation, a section of the journal Frontiers in Human Neuroscience

Received: *31 January 2021*
Accepted: *23 March 2021*
Published: *14 April 2021*

Citation:
Wang Y, Hays MA, Coogan C, Kang JY, Flinker A, Arya R, Korzeniewska A and Crone NE (2021) Spatial-Temporal Mapping Combined With Cortico-Cortical Evoked Potentials in Predicting Cortical Stimulation Results. Front. Hum. Neurosci. 15:661976. doi: 10.3389/fnhum.2021.661976

Functional human brain mapping is commonly performed during invasive monitoring with intracranial electroencephalographic (iEEG) electrodes prior to resective surgery for drug resistant epilepsy. The current gold standard, electrocortical stimulation mapping (ESM), is time consuming, sometimes elicits pain, and often induces after discharges or seizures. Moreover, there is a risk of overestimating eloquent areas due to propagation of the effects of stimulation to a broader network of language cortex. Passive iEEG spatial-temporal functional mapping (STFM) has recently emerged as a potential alternative to ESM. However, investigators have observed less correspondence between STFM and ESM maps of language than between their maps of motor function. We hypothesized that incongruities between ESM and STFM of language function may arise due to propagation of the effects of ESM to cortical areas having strong effective connectivity with the site of stimulation. We evaluated five patients who underwent invasive monitoring for seizure localization, whose language areas were identified using ESM. All patients performed a battery of language tasks during passive iEEG recordings. To estimate the effective connectivity of stimulation sites with a broader network of task-activated cortical sites, we measured cortico-cortical evoked potentials (CCEPs) elicited across all recording sites by single-pulse electrical stimulation at sites where ESM was performed at other times. With the combination of high gamma power as well as CCEPs results, we trained a logistic regression model to predict ESM results at individual electrode pairs. The average accuracy of the classifier using both STFM and CCEPs results combined was 87.7%, significantly higher than the one using STFM alone (71.8%), indicating that the correspondence between STFM and ESM results is greater when effective connectivity between ESM stimulation sites and task-activated sites is taken into consideration. These findings, though based on a small number of subjects to date, provide preliminary support for the hypothesis that incongruities between ESM and

STFM may arise in part from propagation of stimulation effects to a broader network of cortical language sites activated by language tasks, and suggest that more studies, with larger numbers of patients, are needed to understand the utility of both mapping techniques in clinical practice.

Keywords: language functional mapping, electrocortical stimulation, high gamma activation, effective connectivity, cortico-cortical evoked potentials

INTRODUCTION

Despite ongoing advances in non-invasive functional neuroimaging, electrocortical stimulation mapping (ESM) remains the gold standard for mapping cortical function in individual patients at a sufficiently fine spatial scale to guide the surgical resection of brain tissue for the treatment of drug-resistant epilepsy (Penfield and Jasper, 1954; Lesser et al., 1994) and brain tumors (Sanai et al., 2008). The major advantage of this technique is that it allows clinicians to simulate the neurological consequences of lesioning tissue before it is permanently resected (Ojemann et al., 1989). However, there are important practical limitations on its clinical application. Chief amongst these is the risk of triggering afterdischarges and clinical seizures (Lesser et al., 1984; Blume et al., 2004; Hamberger, 2007; Aungaroon et al., 2017) that can prevent comprehensive functional mapping. Additionally, ESM can elicit pain that prevents mapping at individual sites (Lesser et al., 1985). Last, because ESM is done sequentially at pairs of electrodes, each time finding the optimal stimulation current (Lesser et al., 1984; Pouratian et al., 2004) and then testing the effect of stimulation on different language tasks (Schäffler et al., 1993), it is time-consuming, which often forces clinicians to map only a subset of sites. This factor may ultimately pose a particularly acute limitation on ESM as the number and density of intracranial electroencephalographic (iEEG) electrodes used for long-term monitoring increases (Viventi et al., 2011; Bouchard and Chang, 2014).

In addition to the practical limitations on ESM's clinical application, there are concerns about its accuracy and predictive value. The neural populations and operations that are interrupted during stimulation are not well controlled, and it is difficult to rule out distant effects through diaschisis or the distant effects of action potentials evoked by stimulation (Ishitobi et al., 2000; Hamberger, 2007; Karakis et al., 2015). Furthermore, the simulated lesion of ESM cannot take into account the reorganization that occurs after real permanent lesions, and if it is done in only a subset of electrodes, it cannot identify other cortical sites that could potentially assume the function of the lesioned site (i.e., assess functional reserve). Finally, when ESM interrupts the performance of a cognitive task such as word production, the effect is usually all-or-none. The same observed effect can potentially result from interruption of different stages of processing or levels of representation that are necessary for successful task completion.

The limitations of ESM have long motivated the investigation of passive iEEG recordings as a tool for mapping cortical function prior to resective surgery (Crone et al., 1998a, 2001; Grossman and Gotman, 2001; Sinai et al., 2005; Cervenka et al., 2013). Intracranial EEG recordings, such as electrocorticography (ECoG) and stereo electroencephalographic (SEEG), cannot trigger seizures or pain, and they can be used to simultaneously survey task-related cortical activity in the entire set of implanted electrodes. Moreover, iEEG recordings yield a graded measure of task-related neural activity capable of resolving the activation of cortical sites at temporal scales comparable to the stages of processing that comprise language tasks (Edwards et al., 2010; Arya et al., 2019a). Thus, the relative degree and timing of activation at a given site can be used to estimate its contribution to these processing stages, providing clinicians with more detailed information as they weigh the benefits and risks of removing epileptogenic tissue vs. sparing eloquent cortex.

Despite the practical and theoretical advantages of iEEG spatial-temporal functional mapping (STFM) over ESM, STFM has not been widely used in clinical practice. One reason for this has been a lack of consensus on which signal components are most informative about task-related neural activity. In recent years, high gamma (60–200 Hz) power changes have been increasingly recognized as a robust and reliable index of task-related activation of cortical populations of neurons (Crone et al., 2006, 2011; Jerbi et al., 2009; Lachaux et al., 2012). This index is highly correlated with blood oxygen level-dependent (BOLD) responses in fMRI (Lachaux et al., 2007; Khursheed et al., 2011; Siero et al., 2014; Genetti et al., 2015) and with single unit activity recorded by microelectrodes (Ray et al., 2008; Manning et al., 2009). Accordingly, it is highly specific with respect to the location and timing of task-related cortical activation, and it has been observed in nearly every cortical functional-anatomical domain in which it has been studied, including sensorimotor, auditory, visual, and language areas (Jerbi et al., 2009; Crone et al., 2011; Lachaux et al., 2012). Moreover, recent technological developments have allowed STFM to be performed online, providing immediate feedback to clinicians (Wang et al., 2016; Milsap et al., 2019). STFM can also illuminate the temporal sequence of network activation (dynamics) with a time resolution that is far superior to fMRI, allowing greater insights into the functional role of individual sites.

These properties have made STFM an attractive tool for human research in cognitive and systems neuroscience. Indeed, recent studies have demonstrated extraordinary spatial and temporal selectivity in iEEG-recorded population responses (Flinker et al., 2010; Wang et al., 2021). In spite of these advances in research, the potential clinical application of STFM for pre-resective functional mapping has not yet been fully realized. To date, efforts to demonstrate the clinical utility of STFM have

used ESM for validation, and although several studies have found strong agreement between iEEG high gamma responses and ESM in motor and early sensory cortices (Crone et al., 1998b; Miller et al., 2007; Brunner et al., 2009; Sinai et al., 2009), there has been less agreement in language cortex (Sinai et al., 2005; Towle et al., 2008; Wu et al., 2010; Miller et al., 2011; Bauer et al., 2013; Arya et al., 2017, 2018; Babajani-Feremi et al., 2018). For example, in a study comparing STFM and ESM for localization of object naming in 13 patients (Sinai et al., 2005), the authors observed a tradeoff between sensitivity and specificity as the threshold for the magnitude of high gamma responses was varied, i.e., low thresholds yielded high sensitivity but low specificity and *vice versa*.

The reliance of spoken word production on the function of large-scale cortical networks in frontal, parietal, and temporal lobes has long been appreciated by behavioral neurologists and cognitive psychologists studying the effects of lesions on different brain regions. These effects can be exquisitely specific for different aspects of language function, including perceptual processing, semantic and phonological representations, and articulatory plans. Psychophysical investigations into the timing of these different cognitive operations have indicated that they occur in quasi-sequential stages that overlap in time (cascaded) (Indefrey and Levelt, 2004). EEG, MEG, and fMRI studies have provisionally localized these operations to different brain regions, but because of variations in functional anatomy, these insights cannot be clinically applied to individual patients (Ojemann, 1979; Rademacher et al., 1993). In contrast, iEEG high gamma power changes are sufficiently robust to yield statistically significant responses within individuals, revealing the location and timing of cortical processing at clinically useful resolutions. However, processing at a given site may not always be critical to task performance. Furthermore, processing at each stage likely occurs in sub-networks comprised of multiple cortical sites. The opportunity, and challenge, for iEEG STFM is thus to identify which sites in these sub-networks are most important for task performance so that impairments can be avoided.

Evidence from a variety of sources has called into question the assumption that the effects of ESM are restricted to tissue underneath each stimulating electrode (Ishitobi et al., 2000; Matsumoto et al., 2004; Karakis et al., 2015). Based on these findings, we hypothesize that at least some false negative STFM sites are due to propagation of ESM to distant nodes in a broader network of task-activated sites, resulting in task interference. We evaluated five patients who underwent invasive monitoring for seizure localization whose language and motor areas were identified using ESM. Additionally, all patients performed language tasks including picture naming, auditory naming, word reading and auditory word repetition during passive iEEG recordings. We also measured cortico-cortical evoked potentials (CCEPs) elicited by single-pulse electrical stimulation at distant cortical sites when the patients were awake and at rest. With the combination of high gamma power and CCEP results, we trained a logistic regression model to predict ESM results at individual electrode pairs. Our findings suggest that additional information about effective connectivity in the overall network of cortical regions activated by language tasks can enhance the ability of iEEG STFM to predict ESM results.

MATERIALS AND METHODS

Patient Information

Five English speaking patients (**Table 1**) with intractable epilepsy underwent placement of subdural electrodes in the left (dominant) hemisphere to localize their ictal onset zone and to identify language and motor areas using electrocortical stimulation mapping. In Patients 1–4, the implanted electrodes consisted of subdural arrays (grids and/or strips) of standard electrodes (2.3 mm exposed diameter, 1 cm center-to-center spacing, Adtech, Racine, WI, USA or PMT Crop, Chanhassen, MN, USA) as well as high-density electrodes (2 mm exposed diameter, 5 mm center-to-center spacing, PMT Crop, Chanhassen, MN, USA). In Patient 5, the implanted electrodes consisted of SEEG depth electrodes (0.86 mm diameter, 5–10 mm contact spacing, Adtech, Racine, WI, USA) implanted using a ROSA intraoperative robot (Zimmer Biomet Robotics, Montpellier, France). In all patients, the anatomical placement of electrodes was dictated solely by clinical considerations for recording seizures or mapping cortical function.

Standard Protocol Approvals, Registrations, and Patient Consents

Patients were admitted to the Johns Hopkins Epilepsy Monitoring Unit after electrode implantation for a period of 6–14 days. All patients gave informed consent to participate in research testing under a protocol approved by the Institutional Review Board of the Johns Hopkins Medical Institutions.

Experimental Paradigm

A battery of language tasks was performed under ESM and STFM (Shum et al., 2020). In the word reading task (STFM only), subjects were shown a word on a monitor directly in front of them and were instructed to read it out loud. In a paragraph reading task (ESM only), subjects read stories aloud as electrocortical stimulation was intermittently given. In the picture naming task (STFM and ESM), subjects were shown a picture of an object, as a stimulus on a monitor (STFM) or a piece of article (ESM) directly in front of them. Subjects were instructed to speak the name of the object in the picture or say "pass" if they could not recall the name (STFM only). In the auditory word repetition task (STFM only), subjects were played an audio recording of a spoken word through a speaker placed in front of them. Subjects were instructed to verbally repeat the cued word. In the auditory naming task (STFM and ESM), subjects were played an audio recording of a spoken sentence describing a certain object through a speaker placed in front of them. They were instructed to verbally name the object out loud. Trial numbers of each task for each patient were governed by the time constraints on patient testing and the set of stimuli used (50–100 trials for STFM, 15–30 trials for ESM).

TABLE 1 | Patient demographic and clinical information.

Patient	1	2	3	4	5
Age	25	32	26	49	42
Gender	M	M	F	M	F
Handedness	Right	Right	Both	Right	Right
Hemisphere Dominance	Left	Left	Left	Left	Left
Hemispheric coverage	Left	Left	Left	Left	Left
Seizure onset zone	Ventral left precentral gyrus + left inferior premotor area	Left superior parietal lobule	Left frontal lobe	Left fronto-central head regions	Bilateral neo-cortical temporal regions
Tasks performed	Word reading, Picture naming	Word reading, Word repetition	Word reading, Picture naming, Auditory naming	Word repetition, Picture naming, Auditory naming	Word reading, Word repetition, Picture naming

Electrode Localization

Electrode locations were identified in a high-resolution post-operative brain CT; they were then transformed onto a high-resolution pre-operative brain MRI by volumetrically co-registering the pre- and post-operative scans in Bioimage Suite (Duncan et al., 2004).

Data Acquisition and Analysis

Recordings of all standard and high-density electrodes were referenced to a single intracranial electrode to minimize extracranial sources of artifact. Raw iEEG signals were recorded with a 256-channel recording system (NeuroPort, BlackRock Microsystems, Salt Lake City, UT, USA; or Nihon Kohden America, Irvine, CA, USA), which amplified and sampled the data at a minimum of 1 kHz and a maximum of 30 kHz of sampling rate with an analog third-order Butterworth anti-aliasing filter. The anti-aliased recording was decimated to 1 kHz in all patients prior to any subsequent analysis. Channels with excessive amounts of noise were excluded from analysis. To remove spatial bias in the raw iEEG power, the remaining channels were grouped into blocks, and re-referenced using a common average reference (CAR) filter within each block:

$$X(t)_n^{\mathrm{CAR}} = X(t)_n - \frac{1}{N}\sum_{k=1}^{N} X(t)_k$$

where $X(t)_n$ represents the raw iEEG power on the nth channel, and $X(t)_n^{\mathrm{CAR}}$ represents the CAR-filtered iEEG power on the nth channel out of N recorded channels in a block after excluding bad channels. For Patients 1–4 (subdural grids/strips), separate CAR blocks were used for all the standard electrodes and all the high-density electrodes in each patient; for Patient 5 (SEEG depths), separate CAR blocks were used for each individual shank of depth electrodes.

ESM Analysis

All patients underwent functional mapping with electrocortical stimulation of motor and language cortex following routine clinical procedures (Lesser et al., 1987; Sinai et al., 2005). ESM was performed in 2- to 3-h blocks over 1–2 days. Electrode pairs were stimulated using either a GRASS S-12 Biphasic Stimulator (Grass-Telefactor/Astro-Med, Inc., West Warwick, RI, USA) or a Nihon Kohden MS-120BK Cortical Stimulator (Nihon Kohden America, Irvine, CA, USA). Intracranial EEG was continuously monitored for after discharges and seizures. Two- to five seconds trains of 50 Hz, 0.3-ms, alternating polarity square-wave pulses were delivered in 0.5-mA increments, titrated from 1-mA up to a maximum of 12-mA (typically between 7 and 12-mA), or the highest amperage that did not produce after discharges at a given electrode pair, maximizing currents at each cortical site regardless of adjacent after discharge thresholds (Lesser et al., 1984; Pouratian et al., 2004). If ESM interfered with voluntary movement or produced involuntary movement or unpleasant sensations in one or more body parts, ESM mapping of language function was not performed for that electrode pair. Language location was determined as follows: electrode pairs were considered ESM positive (ESM+) for language if stimulation resulted in absent or delayed responses, paraphasic errors, and/or incorrect responses not followed by after discharges during at least two trials at the same electrode pair, if these errors were also not present during baseline testing (Sinai et al., 2005). Otherwise, electrode pairs were defined as ESM negative (ESM−) for language, but not for hesitation, interruption or incorrect response.

High Gamma Response Analysis

The CAR-filtered iEEG signal was analyzed for the duration of the task in 128 ms epochs of data with 112 ms overlap. The Fast Fourier transform (FFT) was computed on each window, and the resulting coefficients were then multiplied by a modified flat-top Gaussian window with cutoff between 70 and 150 Hz, with notch filters applied to 60 Hz and 120 Hz for line noise elimination. The bandpass-filtered spectrum was converted to high gamma power by zeroing the negative frequency components, doubling the positive frequency components, computing the inverse FFT, and taking the magnitude of the result (i.e., the Hilbert transform) (Bruns, 2004; Canolty et al., 2007). The resulting high gamma power was then log transformed to approximate a normal distribution and decimated to a temporal resolution of 16 ms using a moving average filter. More details of spectral feature extraction methods can be found in Wang et al. (2016). A site was marked STFM positive (STFM+) if it exhibited a significant task-related high gamma power increase, and STFM

negative (STFM−) if there were no significant high gamma power increase.

Statistical Analysis

The baseline window used for each task was defined as a period from 1,000 ms before stimulus onset to 200 ms before stimulus onset, and a baseline distribution was formed per channel from the pooled high gamma power values during this period. A two-way *t*-test was performed between the distribution for each time-channel bin and that channel's baseline distribution. The resulting *p*-values were corrected for multiple comparisons using the Benjamini-Hochberg (BH) procedure, controlling the false discovery rate (FDR) at 0.05 (Benjamini and Hochberg, 1995; see Wang et al., 2016; Milsap et al., 2019 for more details).

Web-based Online Functional Brain Mapping (WebFM)

We used WebFM, an in-house designed software system, to perform online STFMs and CCEPs in a web-browser window, using local processing at the bedside, and to synchronize the results to a centrally hosted repository (Milsap et al., 2019). The system leverages the real-time experimental control and signal analysis capabilities of BCI2000 (Schalk et al., 2004), a standardized software platform for brain-computer interface (BCI) research used by over 400 labs over the past 15 years that can interface with a wide variety of commercial EEG amplifiers. WebFM integrates with BCI2000 in a browser-based user interface for immediately displaying spatial-temporal maps of functional activation (and now CCEPs) during the course of testing at the patient's bedside. This allows both researchers and clinicians to identify any technical problems during testing, ensure valid results, and to decide whether additional testing is needed.

Cortico-Cortical Evoked Potentials (CCEPs)

The methods used to elicit and analyze CCEPs is described in detail elsewhere (Matsumoto et al., 2004, 2007). Direct electrical stimulation was applied in a bipolar manner to a pair of adjacently placed subdural electrodes using a constant-current stimulator (Grass S12 stimulator, AstroMed, Inc., West Warwick, RI, USA; or Cerestim R96, Blackrock Microsystems, LLC, Salt Lake City, UT, USA). Single-pulse electrical stimuli (SPES, biphasic wave pulse: 0.3-ms duration) were delivered at jittered interstimulus intervals of 2–5 s (Patient 1: 2–2.5 s; Patient 2–4: 5 s; Patient 5: 2.5 s). The stimulation was monitored by physicians (NC and JK) experienced in iEEG interpretation and electrocortical stimulation mapping. One set of trials for each stimulation site comprised 50–167 stimuli (Patient 1: 51–167; Patient 2: 60; Patient 3–5: 50), depending on clinical circumstances and the time available for testing. During the recording, we asked the patients to recline comfortably awake on the bed and to continue their usual activities. We titrated stimulation intensity in increments of 0.5–1 mA, making sure that no afterdischarges were induced, up to a maximum of 5 mA for electrode arrays with 0.5 cm spacing or 10 mA for arrays with 1.0 cm spacing. More current was used for electrodes with larger surface area and interelectrode distances to achieve similar current densities. Because stimulation of sensorimotor or visual cortices can sometimes evoke symptoms at low intensities (i.e., movement or subjective sensory sensation of a part of the body, and phosphenes), we sometimes used 5 mA even for arrays with 1.0 cm spacing and confirmed that stimulation produced no symptom. At the maximum current for each stimulation, the N1 potential in the average CCEP response of each electrode was identified within 10–50 ms post-stimulus, thought to represent a direct excitatory connection from stimulation to response site (Matsumoto et al., 2004, 2007). Observed N1 latencies in our dataset had a mean of 9.63 ms and standard deviation of 8.94 ms. The magnitude of the N1 potential was normalized using the pre-stimulus baseline (−500 ms to −10 ms) to obtain a *z*-score that quantifies that electrode's effective connectivity.

Logistic Regression Model

We trained a logistic regression model to predict ESM results at individual electrode pairs using a linear combination of measures derived from STFM alone, or STFM and CCEPs (see Equations 1, 2 and 3 below). In order to validate the reliability of the model, we used a 5-fold cross-validation to protect against overfitting by partitioning the dataset into five folds and estimating accuracy in each fold.

Equation 1: $\mathrm{ESM} = \alpha_1 \frac{\sum_{\mathrm{Stim}}(\mathrm{HG}_{\mathrm{All\,time}})}{2} + \alpha_2$, where α_1 and α_2 are model coefficients.

Equation 2: $\mathrm{ESM} = \beta_1 \frac{\sum_{\mathrm{Stim}}(\mathrm{HG}_{\mathrm{PCA}})}{2} + \beta_2$, where β_1 and β_2 are model coefficients.

Equation 3: $\mathrm{ESM} = \gamma_1 \frac{\sum_{\mathrm{Stim}}(\mathrm{HG}_{\mathrm{PCA}})}{2} + \gamma_2 \frac{\sum_{\mathrm{Stim}}(\mathrm{Centrality}_{\mathrm{HG}})}{2} + \gamma_3 \frac{\sum_{\mathrm{grid}}(\mathrm{CCEPs} \times \mathrm{HG}_{\mathrm{PCA}})}{\#\mathrm{Electrodes}} + \gamma_4$, where γ_1, γ_2, γ_3 and γ_4 are model coefficients.

As a first approximation of the degree of activation (Equation 1) we integrated the magnitude of HG power increases over the duration of the task ($HG_{\mathrm{All\,time}}$). For a more temporally specific measure of activation (Equation 2), we integrated the magnitude of HG power increases within windows defined by principal component analysis of the HG time series (HG_{PCA}) (Collard et al., 2016). To estimate the importance of STFM+ sites to overall network activation (Equation 3), we computed Pearson's linear correlation coefficients between the temporal envelopes of high gamma power increases at all STFM+ sites (Collard et al., 2016), and then we computed the PageRank centrality of each STFM+ site ($Centrality_{\mathrm{HG}}$). To estimate the effective connectivity of ESM stimulation sites with the overall network of task-activated cortical sites, we computed the sum, across all sites with CCEPs, of the product of the (HG_{PCA}) at each site and the *z*-score of the CCEP elicited at that site by SPES at the ESM stimulation site. To account for potential ESM effects on an even broader network, including sites without significant (HG_{PCA}), we also computed the sum, across all sites with CCEPs, of the product of the (HG_{PCA}) at each site and the total number of significant CCEPs elicited by SPES at the ESM stimulation site.

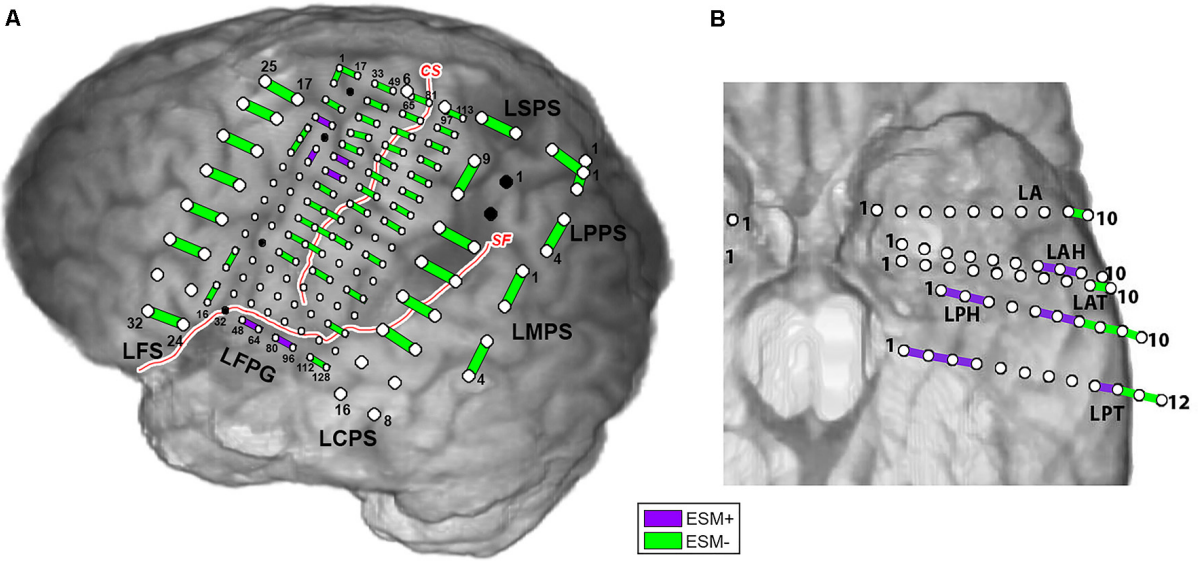

FIGURE 1 | Electrocortical stimulation mapping (ESM) results for Patient 2 **(A)** and Patient 5 **(B)**. Purple bars indicate electrode pairs that were positive during any language task (ESM+); green bars indicate those that were negative during all language tasks (ESM−). Red curves with white stroke represent anatomical landmarks—central sulcus (CS) and sylvian fissure (SF).

RESULTS

Examples of electrocortical stimulation mapping (ESM) results, for Patient 2 (subdural grids/strips) and Patient 5 (SEEG depth electrodes), are illustrated in **Figure 1**. Electrode pairs positive for language are shown in purple, and the ones negative for language are shown in green. ESM positive pairs are entered as value 1, and negative pairs entered as value 0 as the observed responses in the prediction model (for Equations 1, 2 and 3). For Patient 2, ESM+ pairs were located around left superior temporal gyrus (LFPG48-64, LFPG80-96) as well as left superior precentral gyrus (LFPG38-54, LFPG39-55) and premotor area (LFPG4-20, LFPG22-23). For Patient 5, ESM+ pairs were located along left hippocampus (LPH1-2, LPT1-2, 2-3), left fusiform gyrus (LPH2-3, LPT3-4), left superior temporal gyrus (LAH7-8, LAH8-9, LPH6-7), and left middle temporal gyrus (LPH5-6, LPT 9-10).

Figure 2 shows examples of spatial-temporal function mapping (STFM) results, for Patient 2 during a word reading task, and Patient 5 during a picture naming task. For each map, a raster plot on the left displays the magnitude of event-related changes in the high gamma analytic power at each time point after stimulus onset, as compared to the pre-stimulus baseline. The magnitudes are thresholded for significance ($p < 0.05$) using False Discovery Rate (FDR) correction for each channel in the channel raster. A brain map is displayed on the right to show the locations and relative magnitudes of activations either integrated over the entire post-stimulus interval or at any user-selectable time point in the channel raster ($t = 1.20$ s and $t = 0.51$ s post-stimulus onset shown in **Figure 2**, respectively). The magnitude of the high gamma power at a particular electrode and time is represented by the size and color of disks overlaid on iEEG electrode locations in a two-dimensional snapshot of the three-dimensional brain reconstruction. For Patient 2 during word reading, STFM+ electrodes were located around superior temporal gyrus, as well as pre- and post-central gyri. For Patient 5 during picture naming, STFM+ electrodes were located along left hippocampus, left fusiform gyrus, left superior temporal gyrus, and left middle temporal gyrus. STFM results for all patients in this article are available at http://webfm.io.

Note that ESM+ and STFM+ were sometimes observed outside of classical language areas. In some cases, these sites were in sensorimotor cortex and likely corresponded to preparation and execution of spoken responses. In other cases, they may have been due to reorganization in response to a prior surgical resection in the parietal cortex.

Examples of cortico-cortical evoked potential (CCEPs) results for one stimulation pair (LFPG21-LFPG22) in Patient 2, and one pair (LPT1–LPT2) in Patient 5, are shown in **Figure 3**. The normalized response amplitudes of the average CCEPs observed at each electrode, defined as that electrode's z-score relative to the pre-stimulus baseline, was used to quantify the effective connectivity between the stimulation and response site. Responses with a z-score greater than 6 were considered significant, as a previous study has shown this threshold to optimize sensitivity and specificity in identification of CCEP responses (Keller et al., 2011). Significant responses are represented here as lines from the stimulation site to the sites with significant CCEPs.

Based on Equations 1, 2 and 3 from "Materials and Methods" section: Logistic Regression Model, we trained our classifier using generalized linear model. The model accuracy for Patients 2 and 5 is listed on **Table 2** as examples.

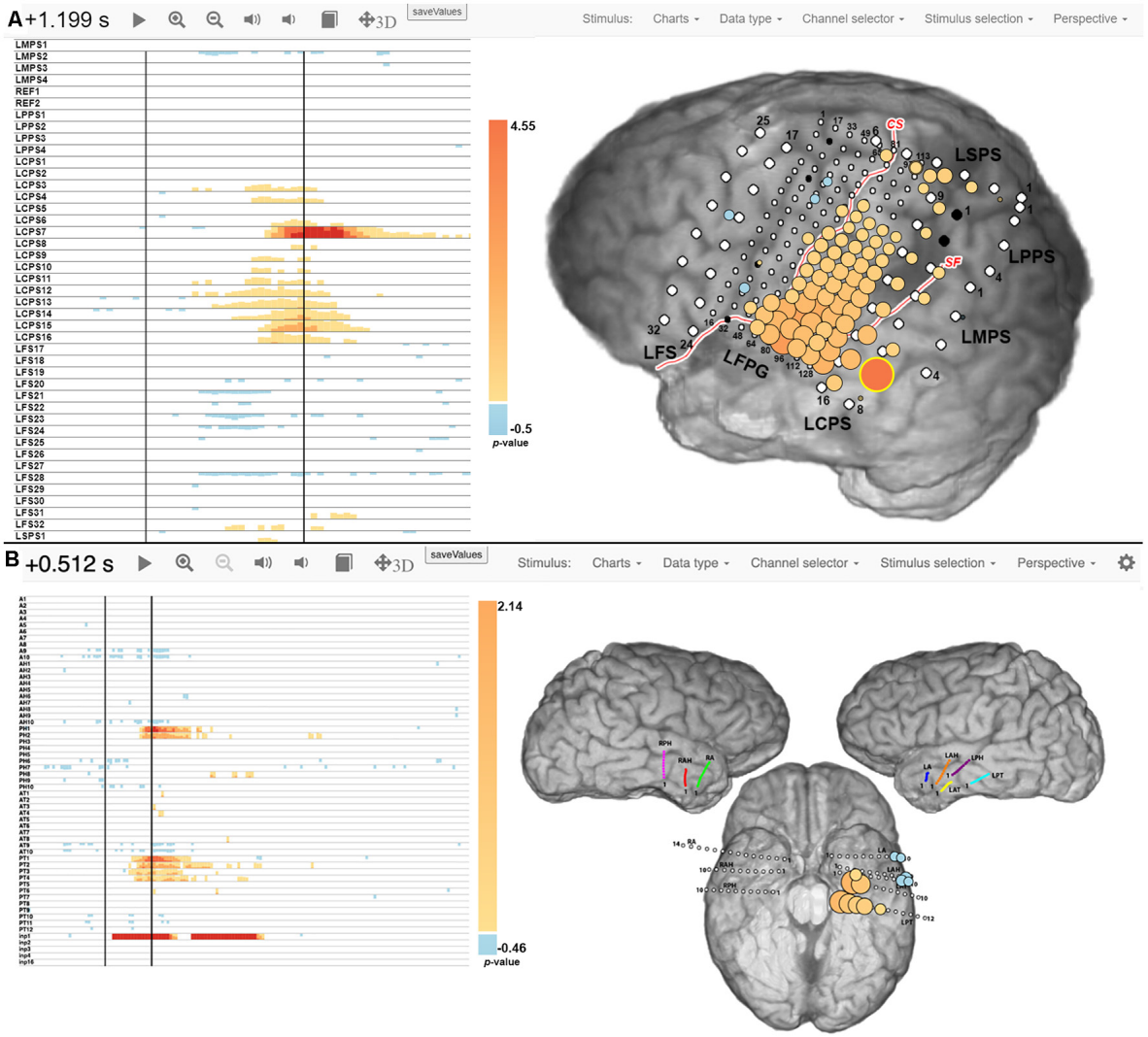

FIGURE 2 | Spatial-temporal functional mapping (STFM) results for Patient 2 during a word reading task **(A)** and Patient 5 during a picture naming task **(B)**. The raster plot on the left shows trial-averaged STFM results in a time by channels manner, and the brain map on the right shows STFM results on an anatomical illustration at a specific time stamp. More details can be found at Wang et al. (2016) and Milsap et al. (2019).

The average accuracy of the classifier was 76.5% and 52.9% for patients 2 and 5, respectively, using high gamma power integrated over the duration of the task (Equation 1), 76.5% and 58.8% using high gamma power within windows defined by PCA (Equation 2), and 82.4% and 88.2% using high gamma power and centrality/CCEP results combined, respectively (Equation 3).

Figure 4 illustrates how ESM compares to its prediction by two different models: one in which only STFM is used (left) and one in which both STFM and CCEPs results are used (right). These illustrate how the correspondence between passive iEEG maps and ESM results is greater when the effective connectivity of ESM stimulation sites with a larger network of task- activated sites is taken into consideration.

As shown in **Table 3**, the average accuracy and area under the receiver operating characteristic curve (AUC) of the classifier was 71.8% and 0.43 respectively, using high gamma power integrated over the duration of the task (Equation 1), 74.4% and 0.55 respectively, using high gamma power within windows defined by PCA (Equation 2), and 87.7% and 0.83 using high gamma power and centrality/CCEP results combined (Equation 3). We then performed a two-sample t-test between results using Equations 2 and 3, and the p-values for differences between accuracy and AUC under the two models were 0.022 and 0.046 respectively, meaning that both accuracy and AUC using Equation 3 were statistically larger than those using Equation 2 ($p < 0.05$).

DISCUSSION

Results from the five patients performing a variety of language tasks demonstrated that combining the results of iEEG STFM

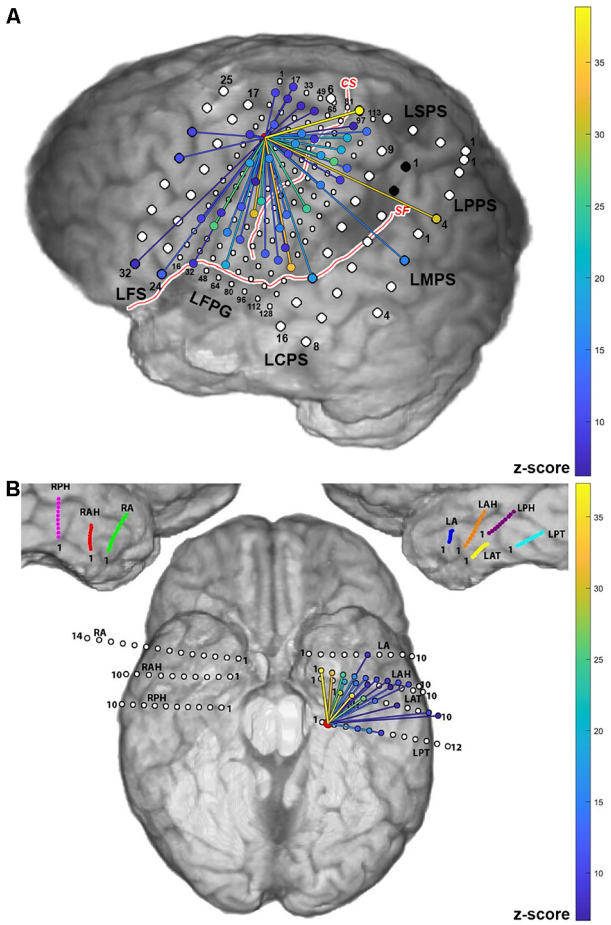

FIGURE 3 | Cortico-cortical evoked potential (CCEP) results for Patients 2 **(A)** and 5 **(B)** when stimulating individual electrode pairs (red circle between stimulated electrodes. The normalized response amplitude of the average CCEP observed at each electrode, defined as that electrode's *z*-score, is used to quantify the effective connectivity between the stimulation and response site. Responses with a *z*-score greater than 6 were considered significant and are represented here as lines from the stimulation site (denoted in red) to the sites with significant CCEPs, colored according to the magnitude of the *z*-score observed at that electrode (color scale shown on right).

and CCEPs improved the accuracy of predicting ESM results for language functional mapping during intracranial monitoring for epilepsy surgery.

ESM is still the gold-standard for localizing eloquent cortex, but when compared to ground-truth patient outcomes, unpredicted resective deficits can and do still occur (Sinai et al., 2005; Hamberger, 2007; Asano et al., 2009; Cervenka et al., 2011, 2013; Kojima et al., 2012; Sakpichaisakul et al., 2020). Passive iEEG mapping has been investigated as a replacement for ESM, but to date, its combined sensitivity and specificity relative to ESM have been suboptimal, especially for language mapping (Bauer et al., 2013). Both methods have potential strengths and limitations. ESM reversibly simulates the behavioral effect of a lesion at the site of stimulation, but its effects, particularly for long trains, may not be confined to the stimulation site, potentially eliciting action potentials in fibers of passage and interfering with function at distant sites.

Indeed, evidence from a variety of sources has called into question the assumption that the effects of ESM are restricted to tissue underneath each stimulating electrode. First, a large number of studies have shown that brief single pulses of cortical stimulation at intensities comparable to ESM can elicit evoked cortical potentials (Matsumoto et al., 2004), as well as changes in high gamma power (and thus population firing rates) (Usami et al., 2015, 2019). Cortico-cortical evoked potentials (CCEPs) have been increasingly used to map the effective connectivity between the cortical components of language networks and motor networks (Matsumoto et al., 2007, 2017; Tamura et al., 2016). Although single-pulse electrical stimulation (SPES) is too brief to disrupt cortical function locally or at distant sites, the CCEPs elicited by SPES provide direct evidence for distant electrophysiological effects from ESM. ESM typically employs 50 Hz trains of stimuli at the same or greater intensity as SPES for several seconds, and can thus recruit a far greater neuronal population than SPES, both locally and distantly. However, the massive stimulus artifact created by ESM usually obscures any potentials elicited either locally or at distant sites. Yet, investigators have observed trains of intra-stimulation potentials locked to ESM stimulation trains at cortical sites several centimeters away from the site of ESM (Karakis et al., 2015). In one such report, stimulation in sub-temporal cortex elicited discharges in left posterior superior temporal gyrus that were associated with language impairment (Ishitobi et al., 2000). Based on these findings we hypothesize that at least some false negative STFM sites are due to the effects of ESM on a broader network of STFM+ sites (see left panel of **Figure 5** for illustration).

A longstanding concern for mapping techniques that depend on functional activation (e.g., PET, fMRI) is that sites may be recruited without being critical to task performance. Likewise, STFM+ sites may sometimes be ESM−. We hypothesize that some of these STFM false positives occur because the site plays a relatively minor role in task performance. This could be because there are other sites with equal or greater activation and/or because the site's centrality to network dynamics is low (see right panel of **Figure 5** for illustration).

Previously, our team had taken an admittedly coarse approach to validation of STFM by testing its ability to independently identify functional cortex defined by regions of interest (ROIs) drawn from the literature. Using this approach, we made a preliminary case for arguing that iEEG STFM outperforms ESM (Wang et al., 2016). In this article, we provide evidence that the correspondence between STFM and ESM results is significantly greater when the effective connectivity between ESM stimulation sites and a larger network of task-activated sites is taken into consideration. Ultimately, however, STFM will need to show superior performance in predicting post-operative deficits to truly replace ESM (Arya et al., 2019b). In addition to being an independent standard, predicting post-operative deficits is the ultimate goal of epilepsy surgery planning.

TABLE 2 | Model accuracy for Patients 2 (word reading) and 5 (picture naming).

	Accuracy (%)	STFM+/ESM+	STFM−/ESM+	STFM−/ESM−	STFM+/ESM−	Sensitivity (%)	Specificity (%)	AUC	*p*-value	Equation
Patient 2										
HG all duration	76.5%	8	3	5	1	72.7%	83.3%	0.79	0.0465	(1)
HG PCA selected duartion	76.5%	8	3	5	1	72.7%	83.3%	0.7	0.0439	(2)
HG scaled by centrality	82.4%	10	1	4	2	90.9%	66.7%	0.83	0.134	(3) $\gamma_3 = 0$
HG + CCEPs *z*-score	82.4%	9	2	5	1	81.8%	83.3%	0.83	0.103	(3) CCEPs = *z*-score
HG + CCEPs edges	82.4%	9	2	5	1	81.8%	83.3%	0.86	0.0747	(3) CCEPs = Edges
Patient 5										
HG all duration	52.9%	9	1	0	7	90.0%	0.0%	0.31	0.881	(1)
HG PCA selected duartion	58.8%	8	2	2	5	80.0%	28.6%	0.39	0.952	(2)
HG scaled by centrality	82.4%	8	2	6	1	80.0%	85.7%	0.73	0.947	(3) $\gamma_3 = 0$
HG scaled by CCEPs *z*-score	82.4%	8	2	6	1	80.0%	85.7%	0.8	0.0673	(3) CCEPs = *z*-score
HG scaled by CCEPs edges	88.2%	9	1	6	1	90.0%	85.7%	0.81	0.0462	(3) CCEPs = Edges

Accuracy (%), areas under ROC curve (AUC), and p-values were calculated using Classification Learner from Matlab. Sensitivity was calculated using STFM+ESM+ and STFM−ESM+ electrode numbers, and specificity using STFM−ESM− and STFM+ESM− electrodes. Results for Equation 1 are listed on the first row of each subtable; results for Equation 2 are listed on the second row; results for Equation 3 are listed in several steps on the rest of the rows.

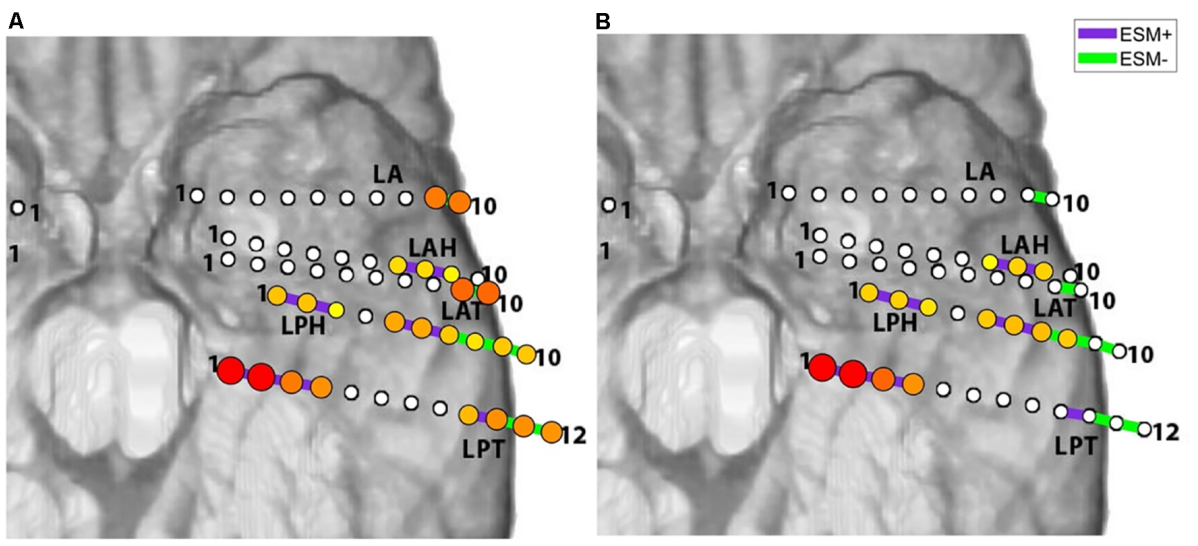

FIGURE 4 | ESM vs. its predictions by different models, for picture naming for Patient 5. Model in **(A)** is based on task-related STFM alone. Model in **(B)** uses STFM and CCEPs to estimate importance of sites to overall network dynamics and connectivity of ESM+ sites (purple bars) to other sites of importance to network dynamics. Note that ESM− sites have fewer HGM+ sites under the model on the right.

The use of post-operative deficits as a gold standard for validation of ESM and STFM is certainly not without its own challenges. Aggregating databases of post-operative deficits and their relationships with functional mapping results is difficult since putative eloquent cortex identified by either technique is usually spared. This can lead to an

TABLE 3 | Summary of classification accuracy and area under curve using different classification models.

Patient	Accuracy (%) Model 1	AUC Model 1	Accuracy (%) Model 2	AUC Model 2	Accuracy (%) Model 3	AUC Model 3
1	76.5	0.70	76.5	0.83	82.4	0.86
2	75.0	0.19	75.0	0.31	83.3	0.56
3	71.4	0.25	78.6	0.48	92.9	0.92
4	83.3	0.72	83.3	0.72	91.7	1.00
5	52.9	0.31	58.8	0.39	88.2	0.81
Averaged	71.8	0.43	74.4*	0.55**	87.7*	0.83**

*The two numbers with * (accuracy) and two numbers with ** (AUC) indicates that the two-sample t-test rejects the null hypothesis that the two numbers are equal at the 5% significance level.*

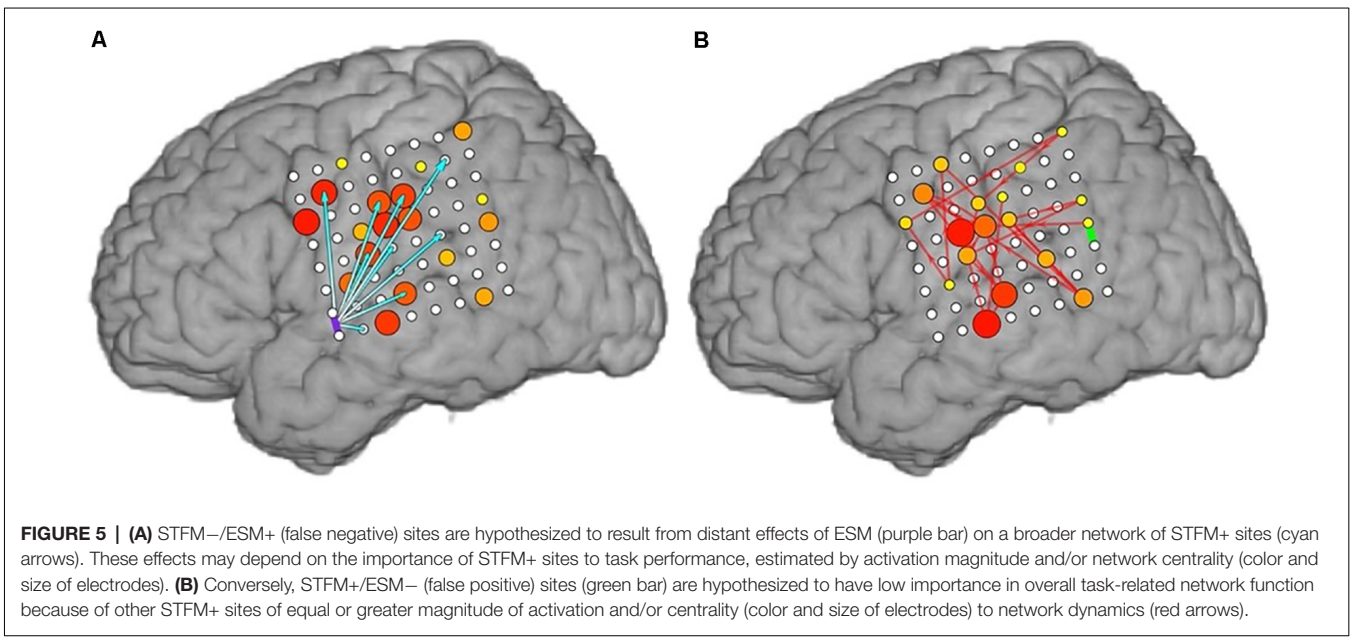

FIGURE 5 | (A) STFM−/ESM+ (false negative) sites are hypothesized to result from distant effects of ESM (purple bar) on a broader network of STFM+ sites (cyan arrows). These effects may depend on the importance of STFM+ sites to task performance, estimated by activation magnitude and/or network centrality (color and size of electrodes). **(B)** Conversely, STFM+/ESM− (false positive) sites (green bar) are hypothesized to have low importance in overall task-related network function because of other STFM+ sites of equal or greater magnitude of activation and/or centrality (color and size of electrodes) to network dynamics (red arrows).

underrepresentation of resected ESM+ sites. The net effect this sampling bias can potentially overestimate STFM's relative sensitivity and ESM's relative specificity. This could potentially be overcome by including enough patients in the database such that these factors are balanced appropriately. Beyond the issue of sampling bias, however, is the complication that deficits are not truly binary: they may be incomplete or vary in duration (e.g., deficits may be chronic or resolve several months after surgery). Segmenting the database into sub-categories could potentially highlight a role for STFM but would further increase the size requirements of the cohort.

CONCLUSIONS

Our study represents a preliminary attempt to reconcile inconsistencies between the results of STFM and ESM that we and other groups have observed. Agreement between these methods has not been as good for language mapping as it has been for motor mapping. Here, we hypothesized that incongruities between ESM and STFM of language function may arise due to propagation of the effects of ESM to cortical areas with strong effective connectivity with the site of stimulation. To estimate the effective connectivity of stimulation sites with a broader network of task-activated cortical sites, we measured CCEPs elicited across all recording sites by single-pulse electrical stimulation at sites where ESM was performed at other times. With the combination of STFM as well as CCEP results, we were able to train a logistic regression model to significantly better predict ESM results at individual electrode pairs. Our findings suggest that the correspondence between STFM and ESM results is greater when the effective connectivity of ESM stimulation sites with a larger network of task-activated sites is taken into consideration. This provides preliminary support for the hypothesis that ESM can have distant effects on a wider network of cortical language sites and suggests that cortical network mapping with CCEPs may help resolve the observed discrepancies between ESM and STFM results. Because these findings are based on a relatively small number of subjects to date, we believe that studies with more patients are needed, including studies of post-operative outcomes, to understand the relative strengths and weaknesses of STFM and ESM, and their comparative utilities for mapping language cortex in advance of surgical resections.

DATA AVAILABILITY STATEMENT

The raw data supporting the conclusions of this article will be made available by the authors, without undue reservation.

ETHICS STATEMENT

The studies involving human participants were reviewed and approved by the Johns Hopkins Medicine Institutional Review Boards. The patients/participants provided their written informed consent to participate in this study.

AUTHOR CONTRIBUTIONS

YW and NC designed the study. YW, MH, CC and JK conducted the experiments. YW and MH analyzed the data. YW, CC and MH generated figures in the article. YW wrote the article with input from all authors. AK and NC supervised the project. All authors contributed to the article and approved the submitted version.

FUNDING

This research was supported by National Institute of Neurological Disorders and Stroke (1R01NS115929 and 1R01NS091139 to NC).

ACKNOWLEDGMENTS

We thank Kiyohide Usami for help with CCEPs data collection as well as data analysis, and Raphael Bechtold for help on 3D brain reconstruction. We would like to thank the nurses and EEG technicians for help on collecting ESM data. We also want to thank all patients for participating in the task.

REFERENCES

Arya, R., Babajani-Feremi, A., Byars, A. W., Vannest, J., Greiner, H. M., Wheless, J. W., et al. (2019a). A model for visual naming based on spatiotemporal dynamics of ECoG high-gamma modulation. *Epilepsy Behav.* 99:106455. doi: 10.1016/j.yebeh.2019.106455

Arya, R., Roth, C., Leach, J. L., Middeler, D., Wilson, J. A., Vannest, J., et al. (2019b). Neuropsychological outcomes after resection of cortical sites with visual naming associated electrocorticographic high-gamma modulation. *Epilepsy Res.* 151, 17–23. doi: 10.1016/j.eplepsyres.2019.01.011

Arya, R., Horn, P. S., and Crone, N. E. (2018). ECoG high-gamma modulation versus electrical stimulation for presurgical language mapping. *Epilepsy Behav.* 79, 26–33. doi: 10.1016/j.yebeh.2017.10.044

Arya, R., Wilson, J. A., Fujiwara, H., Rozhkov, L., Leach, J. L., Byars, A. W., et al. (2017). Presurgical language localization with visual naming associated ECoG high- gamma modulation in pediatric drug-resistant epilepsy. *Epilepsia* 58, 663–673. doi: 10.1111/epi.13708

Asano, E., Juhasz, C., Shah, A., Sood, S., and Chugani, H. T. (2009). Role of subdural electrocorticography in prediction of long-term seizure outcome in epilepsy surgery. *Brain* 132, 1038–1047. doi: 10.1093/brain/awp025

Aungaroon, G., Zea Vera, A., Horn, P. S., Byars, A. W., Greiner, H. M., Tenney, J. R., et al. (2017). After-discharges and seizures during pediatric extra-operative electrical cortical stimulation functional brain mapping: incidence, thresholds, and determinants. *Clin. Neurophysiol.* 128, 2078–2086. doi: 10.1016/j.clinph.2017.06.259

Babajani-Feremi, A., Holder, C. M., Narayana, S., Fulton, S. P., Choudhri, A. F., Boop, F. A., et al. (2018). Predicting postoperative language outcome using presurgical fMRI, MEG, TMS, and high gamma ECoG. *Clin. Neurophysiol.* 129, 560–571. doi: 10.1016/j.clinph.2017.12.031

Bauer, P. R., Vansteensel, M. J., Bleichner, M. G., Hermes, D., Ferrier, C. H., Aarnoutse, E. J., et al. (2013). Mismatch between electrocortical stimulation and electrocorticography frequency mapping of language. *Brain Stimul.* 6, 524–531. doi: 10.1016/j.brs.2013.01.001

Benjamini, Y., and Hochberg, Y. (1995). Controlling the false discovery rate: a practical and powerful approach to multiple testing. *J. R. Stat. Soc. Ser. B Methodol.* 57, 289–300. doi: 10.1111/j.2517-6161.1995.tb02031.x

Blume, W. T., Jones, D. C., and Pathak, P. (2004). Properties of after-discharges from cortical electrical stimulation in focal epilepsies. *Clin. Neurophysiol.* 115, 982–989. doi: 10.1016/j.clinph.2003.11.023

Bouchard, K. E., and Chang, E. F. (2014). Neural decoding of spoken vowels from human sensory-motor cortex with high-density electrocorticography. *Annu. Int. Conf. IEEE Eng. Med. Biol. Soc.* 2014, 6782–6785. doi: 10.1109/EMBC.2014.6945185

Brunner, P., Ritaccio, A. L., Lynch, T. M., Emrich, J. F., Wilson, J. A., Williams, J. C., et al. (2009). A practical procedure for real-time functional mapping of eloquent cortex using electrocorticographic signals in humans. *Epilepsy Behav.* 15, 278–286. doi: 10.1016/j.yebeh.2009.04.001

Bruns, A. (2004). Fourier-, Hilbert- and wavelet-based signal analysis: are they really different approaches? *J. Neurosci. Methods* 137, 321–332. doi: 10.1016/j.jneumeth.2004.03.002

Canolty, R. T., Soltani, M., Dalal, S. S., Edwards, E., Dronkers, N. F., Nagarajan, S. S., et al. (2007). Spatiotemporal dynamics of word processing in the human brain. *Front. Neurosci.* 1, 185–196. doi: 10.3389/neuro.01.1.1.014.2007

Cervenka, M. C., Boatman-Reich, D. F., Ward, J., Franaszczuk, P. J., and Crone, N. E. (2011). Language mapping in multilingual patients: electrocorticography and cortical stimulation during naming. *Front. Hum. Neurosci.* 5:13. doi: 10.3389/fnhum.2011.00013

Cervenka, M. C., Corines, J., Boatman-Reich, D. F., Eloyan, A., Sheng, X., Franaszczuk, P. J., et al. (2013). Electrocorticographic functional mapping identifies human cortex critical for auditory and visual naming. *NeuroImage* 69, 267–276. doi: 10.1016/j.neuroimage.2012.12.037

Collard, M. J., Fifer, M. S., Benz, H. L., McMullen, D. P., Wang, Y., Milsap, G. W., et al. (2016). Cortical subnetwork dynamics during human language tasks. *NeuroImage* 135, 261–272. doi: 10.1016/j.neuroimage.2016.03.072

Crone, N. E., Hao, L., Hart, J. Jr., Boatman, D., Lesser, R. P., Irizarry, R., et al. (2001). Electrocorticographic gamma activity during word production in spoken and sign language. *Neurology* 57, 2045–2053. doi: 10.1212/wnl.57.11.2045

Crone, N. E., Korzeniewska, A., and Franaszczuk, P. J. (2011). Cortical gamma responses: searching high and low. *Int. J. Psychophysiol.* 79, 9–15. doi: 10.1016/j.ijpsycho.2010.10.013

Crone, N. E., Miglioretti, D. L., Gordon, B., and Lesser, R. P. (1998a). Functional mapping of human sensorimotor cortex with electrocorticographic spectral analysis. II. Event-related synchronization in the gamma band. *Brain* 121, 2301–2315. doi: 10.1093/brain/121.12.2301

Crone, N. E., Miglioretti, D. L., Gordon, B., Sieracki, J. M., Wilson, M. T., Uematsu, S., et al. (1998b). Functional mapping of human sensorimotor cortex with electrocorticographic spectral analysis. I. Alpha and beta event-related desynchronization. *Brain* 121, 2271–2299. doi: 10.1093/brain/121.12.2271

Crone, N. E., Sinai, A. S., and Korzeniewska, A. (2006). High-frequency gamma oscillations and human brain mapping with electrocorticography. *Prog. Brain Res.* 159, 279–302. doi: 10.1016/S0079-6123(06)59019-3

Duncan, J. S., Papademetris, X., Yang, J., Jackowski, M., Zeng, X., and Staib, L. H. (2004). Geometric strategies for neuroanatomic analysis from MRI. *NeuroImage* 23, S34–S45. doi: 10.1016/j.neuroimage.2004.07.027

Edwards, E., Nagarajan, S. S., Dalal, S. S., Canolty, R. T., Kirsch, H. E., Barbaro, N. M., et al. (2010). Spatiotemporal imaging of cortical activation

during verb generation and picture naming. *NeuroImage* 50, 291–301. doi: 10.1016/j.neuroimage.2009.12.035

Flinker, A., Chang, E. F., Kirsch, H. E., Barbaro, N. M., Crone, N. E., and Knight, R. T. (2010). Single-trial speech suppression of auditory cortex activity in humans. *J. Neurosci.* 30, 16643–16650. doi: 10.1523/JNEUROSCI.1809-10.2010

Genetti, M., Tyrand, R., Grouiller, F., Lascano, A. M., Vulliemoz, S., Spinelli, L., et al. (2015). Comparison of high gamma electrocorticography and fMRI with electrocortical stimulation for localization of somatosensory and language cortex. *Clin. Neurophysiol.* 126, 121–130. doi: 10.1016/j.clinph.2014.04.007

Grossman, M., and Gotman, J. (2001). As time goes by: high temporal and spatial resolution in cognitively related cortical function. *Neurology* 57, 1947–1948. doi: 10.1212/wnl.57.11.1947

Hamberger, M. J. (2007). Cortical language mapping in epilepsy: a critical review. *Neuropsychol. Rev.* 17, 477–489. doi: 10.1007/s11065-007-9046-6

Indefrey, P., and Levelt, W. J. (2004). The spatial and temporal signatures of word production components. *Cognition* 92, 101–144. doi: 10.1016/j.cognition.2002.06.001

Ishitobi, M., Nakasato, N., Suzuki, K., Nagamatsu, K., Shamoto, H., and Yoshimoto, T. (2000). Remote discharges in the posterior language area during basal temporal stimulation. *Neuroreport* 11, 2997–3000. doi: 10.1097/00001756-200009110-00034

Jerbi, K., Ossandón, T., Hamamé, C. M., Senova, S., Dalal, S. S., Jung, J., et al. (2009). Task-related gamma-band dynamics from an intracerebral perspective: review and implications for surface EEG and MEG. *Hum. Brain Mapp.* 30, 1758–1771. doi: 10.1002/hbm.20750

Karakis, I., Leeman-Markowski, B. A., Leveroni, C. L., Kilbride, R. D., Cash, S. S., Eskandar, E. N., et al. (2015). Intra-stimulation discharges: An overlooked cortical electrographic entity triggered by direct electrical stimulation. *Clin. Neurophysiol.* 126, 882–888. doi: 10.1016/j.clinph.2014.08.011

Keller, C. J., Bickel, S., Entz, L., Ulbert, I., Milham, M. P., Kelly, C., et al. (2011). Intrinsic functional architecture predicts electrically evoked responses in the human brain. *Proc. Natl. Acad. Sci. U S A* 108, 10308–10313. doi: 10.1073/pnas.1019750108

Khursheed, F., Tandon, N., Tertel, K., Pieters, T. A., Disano, M. A., and Ellmore, T. M. (2011). Frequency-specific electrocorticographic correlates of working memory delay period fMRI activity. *NeuroImage* 56, 1773–1782. doi: 10.1016/j.neuroimage.2011.02.062

Kojima, K., Brown, E. C., Rothermel, R., Carlson, A., Matsuzaki, N., Shah, A., et al. (2012). Multimodality language mapping in patients with left-hemispheric language dominance on Wada test. *Clin. Neurophysiol.* 123, 1917–1924. doi: 10.1016/j.clinph.2012.01.027

Lachaux, J.-P., Axmacher, N., Mormann, F., Halgren, E., and Crone, N. E. (2012). High-frequency neural activity and human cognition: past, present and possible future of intracranial EEG research. *Prog. Neurobiol.* 98, 279–301. doi: 10.1016/j.pneurobio.2012.06.008

Lachaux, J. P., Fonlupt, P., Kahane, P., Minotti, L., Hoffmann, D., Bertrand, O., et al. (2007). Relationship between task-related gamma oscillations and BOLD signal: new insights from combined fMRI and intracranial EEG. *Hum. Brain Mapp.* 28, 1368–1375.doi: 10.1002/hbm.20352

Lesser, R. P., Lüders, H., Klem, G., Dinner, D. S., Morris, H. H., and Hahn, J. (1984). Cortical afterdischarge and functional response thresholds: results of extraoperative testing. *Epilepsia* 25, 615–621. doi: 10.1111/j.1528-1157.1984.tb03471.x

Lesser, R. P., Lüders, H., Klem, G., Dinner, D. S., Morris, H. H. III., and Hahn, J. (1985). Ipsilateral trigeminal sensory responses to cortical stimulation by subdural electrodes. *Neurology* 35, 1760–1763. doi: 10.1212/wnl.35.12.1760

Lesser, R. P., Lüders, H., Klem, G., Dinner, D. S., Morris, H. H., Hahn, J. F., et al. (1987). Extraoperative cortical functional localization in patients with epilepsy. *J. Clin. Neurophysiol.* 4, 27–53. doi: 10.1097/00004691-198701000-00003

Lesser, R., Gordon, B., and Uematsu, S. (1994). Electrical stimulation and language. *J. Clin. Neurophysiol.* 11, 191–204. doi: 10.1097/00004691-199403000-00004

Manning, J. R., Jacobs, J., Fried, I., and Kahana, M. J. (2009). Broadband shifts in local field potential power spectra are correlated with single-neuron spiking in humans. *J. Neurosci.* 29, 13613–13620. doi: 10.1523/JNEUROSCI.2041-09.2009

Matsumoto, R., Kunieda, T., and Nair, D. (2017). Single pulse electrical stimulation to probe functional and pathological connectivity in epilepsy. *Seizure* 44, 27–36. doi: 10.1016/j.seizure.2016.11.003

Matsumoto, R., Nair, D. R., LaPresto, E., Bingaman, W., Shibasaki, H., and Luders, H. O. (2007). Functional connectivity in human cortical motor system: a cortico-cortical evoked potential study. *Brain* 130, 181–197. doi: 10.1093/brain/awl257

Matsumoto, R., Nair, D. R., LaPresto, E., Najm, I., Bingaman, W., Shibasaki, H., et al. (2004). Functional connectivity in the human language system: a cortico-cortical evoked potential study. *Brain* 127, 2316–2330. doi: 10.1093/brain/awh246

Miller, K. J., Abel, T. J., Hebb, A. O., and Ojemann, J. G. (2011). Rapid online language mapping with electrocorticography. *J. Neurosurg. Pediatr.* 7, 482–490. doi: 10.3171/2011.2.PEDS1156

Miller, K. J., Leuthardt, E. C., Schalk, G., Rao, R. P., Anderson, N. R., Moran, D. W., et al. (2007). Spectral changes in cortical surface potentials during motor movement. *J. Neurosci.* 27, 2424–2432. doi: 10.1523/JNEUROSCI.3886-06.2007

Milsap, G., Collard, M., Coogan, C., and Crone, N. E. (2019). BCI2000Web and WebFM: browser-based tools for brain computer interfaces and functional brain mapping. *Front. Neurosci.* 12:1030. doi: 10.3389/fnins.2018.01030

Ojemann, G. A. (1979). Individual variability in cortical localization of language. *J. Neurosurg.* 50, 164–169. doi: 10.3171/jns.1979.50.2.0164

Ojemann, G., Ojemann, J., Lettich, E., and Berger, M. (1989). Cortical language localization in left, dominant hemisphere. An electrical stimulation mapping investigation in 117 patients. *J. Neurosurg.* 71, 316–326. doi: 10.3171/jns.1989.71.3.0316

Penfield, W., and Jasper, H. (1954). *Epilepsy and the Functional Anatomy of the Human Brain.* 1st Edn. Boston, MA: Little, Brown and Company.

Pouratian, N., Cannestra, A. F., Bookheimer, S. Y., Martin, N. A., and Toga, A. W. (2004). Variability of intraoperative electrocortical stimulation mapping parameters across and within individuals. *J. Neurosurg.* 101, 458–466. doi: 10.3171/jns.2004.101.3.0458

Rademacher, J., Caviness, V. S. Jr., Steinmetz, H., and Galaburda, A. M. (1993). Topographical variation of the human primary cortices: implications for neuroimaging, brain mapping, and neurobiology. *Cereb. Cortex* 3, 313–329. doi: 10.1093/cercor/3.4.313

Ray, S., Crone, N. E., Niebur, E., Franaszczuk, P. J., and Hsiao, S. S. (2008). Neural correlates of high-gamma oscillations (60–200 Hz) in macaque local field potentials and their potential implications in electrocorticography. *J. Neurosci.* 28, 11526–11536. doi: 10.1523/JNEUROSCI.2848-08.2008

Sakpichaisakul, K., Byars, A. W., Horn, P. S., Aungaroon, G., Greiner, H. M., Mangano, F. T., et al. (2020). Neuropsychological outcomes after pediatric epilepsy surgery: role of electrical stimulation language mapping. *Seizure* 80, 183–191. doi: 10.1016/j.seizure.2020.06.029

Sanai, N., Mirzadeh, Z., and Berger, M. S. (2008). Functional outcome after language mapping for glioma resection. *N. Engl. J. Med.* 358, 18–27. doi: 10.1056/NEJMoa067819

Schäffler, L., Lüders, H. O., Dinner, D. S., Lesser, R. P., and Chelune, G. J. (1993). Comprehension deficits elicited by electrical stimulation of Broca's area. *Brain J. Neurol.* 116, 695–715. doi: 10.1093/brain/116.3.695

Schalk, G., McFarland, D. J., Hinterberger, T., Birbaumer, N., and Wolpaw, J. R. (2004). BCI2000: a general-purpose brain-computer interface (BCI) system. *IEEE Trans. Biomed. Eng.* 51, 1034–1043. doi: 10.1109/TBME.2004.827072

Shum, J., Fanda, L., Dugan, P., Doyle, W. K., Devinsky, O., and Flinker, A. (2020). Neural correlates of sign language production revealed by electrocorticography. *Neurology* 95, e2880–e2889. doi: 10.1212/WNL.0000000000010639

Siero, J. C. W., Hermes, D., Hoogduin, H., Luijten, P. R., Ramsey, N. F., and Petridou, N. (2014). BOLD matches neuronal activity at the mm scale: a combined 7 T fMRI and ECoG study in human sensorimotor cortex. *NeuroImage* 101, 177–184. doi: 10.1016/j.neuroimage.2014.07.002

Sinai, A., Bowers, C. W., Crainiceanu, C. M., Boatman, D., Gordon, B., Lesser, R. P., et al. (2005). Electrocorticographic high gamma activity versus electrical cortical stimulation mapping of naming. *Brain* 128, 1556–1570. doi: 10.1093/brain/awh491

Sinai, A., Crone, N. E., Wied, H. M., Franaszczuk, P. J., Miglioretti, D., and Boatman-Reich, D. (2009). Intracranial mapping of auditory perception: event-related responses and electrocortical stimulation. *Clin. Neurophysiol.* 120, 140–149. doi: 10.1016/j.clinph.2008.10.152

Tamura, Y., Ogawa, H., Kapeller, C., Prueckl, R., Takeuchi, F., Anei, R., et al. (2016). Passive language mapping combining real-time oscillation analysis with cortico-cortical evoked potentials for awake craniotomy. *J. Neurosurg.* 125, 1580–1588. doi: 10.3171/2015.4.JNS15193

Towle, V. L., Yoon, H.-A., Castelle, M., Edgar, J. C., Biassou, N. M., Frim, D. M., et al. (2008). ECoG gamma activity during a language task: differentiating expressive and receptive speech areas. *Brain* 131, 2013–2027. doi: 10.1093/brain/awn147

Usami, K., Korzeniewska, A., Matsumoto, R., Kobayashi, K., Hitomi, T., Matsuhashi, M., et al. (2019). The neural tides of sleep and consciousness revealed by single-pulse electrical brain stimulation. *Sleep* 42:zsz050. doi: 10.1093/sleep/zsz050

Usami, K., Matsumoto, R., Kobayashi, K., Hitomi, T., Shimotake, A., Kikuchi, T., et al. (2015). Sleep modulates cortical connectivity and excitability in humans: direct evidence from neural activity induced by single-pulse electrical stimulation. *Hum. Brain Mapp.* 36, 4714–4729. doi: 10.1002/hbm.22948

Viventi, J., Kim, D. H., Vigeland, L., Frechette, E. S., Blanco, J. A., Kim, Y. S., et al. (2011). Flexible, foldable, actively multiplexed, high-density electrode array for mapping brain activity *in vivo*. *Nat. Neurosci.* 14, 1599–1605. doi: 10.1038/nn.2973

Wang, Y., Fifer, M. S., Flinker, A., Korzeniewska, A., Cervenka, M. C., Anderson, W. S., et al. (2016). Spatial-temporal functional mapping of language at the bedside with electrocorticography. *Neurology* 86, 1181–1189. doi: 10.1212/WNL.0000000000002525

Wang, Y., Korzeniewska, A., Usami, K., Valenzuela, A., and Crone, N. E. (2021). The dynamics of language network interactions in lexical selection: an intracranial EEG study. *Cereb. Cortex* 31, 2058–2070. doi: 10.1093/cercor/bhaa344

Wu, M., Wisneski, K., Schalk, G., Sharma, M., Roland, J., Breshears, J., et al. (2010). Electrocorticographic frequency alteration mapping for extraoperative localization of speech cortex. *Neurosurgery* 66, E407–E409. doi: 10.1227/01.NEU.0000345352.13696.6F

Conflict of Interest: The authors declare that the research was conducted in the absence of any commercial or financial relationships that could be construed as a potential conflict of interest.

frontiers in Human Neuroscience

PERSPECTIVE
published: 17 August 2021
doi: 10.3389/fnhum.2021.702773

Functional Topography of Auditory Areas Derived From the Combination of Electrophysiological Recordings and Cortical Electrical Stimulation

*Agnès Trébuchon[1], F.-Xavier Alario[2,3] and Catherine Liégeois-Chauvel[1,3]**

[1] INSERM, Institute of Systems Neuroscience, Aix-Marseille University, Marseille, France, [2] CNRS, LPC, Aix-Marseille University, Marseille, France, [3] Department of Neurological Surgery, School of Medicine, University of Pittsburgh, Pittsburgh, PA, United States

The posterior part of the superior temporal gyrus (STG) has long been known to be a crucial hub for auditory and language processing, at the crossroad of the functionally defined ventral and dorsal pathways. Anatomical studies have shown that this "auditory cortex" is composed of several cytoarchitectonic areas whose limits do not consistently match macro-anatomic landmarks like gyral and sulcal borders. The only method to record and accurately distinguish neuronal activity from the different auditory sub-fields of primary auditory cortex, located in the tip of Heschl and deeply buried in the Sylvian fissure, is to use stereotaxically implanted depth electrodes (Stereo-EEG) for pre-surgical evaluation of patients with epilepsy. In this prospective, we focused on how anatomo-functional delineation in Heschl's gyrus (HG), Planum Temporale (PT), the posterior part of the STG anterior to HG, the posterior superior temporal sulcus (STS), and the region at the parietal-temporal boundary commonly labeled "SPT" can be achieved using data from electrical cortical stimulation combined with electrophysiological recordings during listening to pure tones and syllables. We show the differences in functional roles between the primary and non-primary auditory areas, in the left and the right hemispheres. We discuss how these findings help understanding the auditory semiology of certain epileptic seizures and, more generally, the neural substrate of hemispheric specialization for language.

Keywords: cortical stimulation, auditory areas, functional mapping, intracerebral recordings, language

OPEN ACCESS

Edited by:
Riki Matsumoto,
Kobe University, Japan

Reviewed by:
Naoto Kunii,
The University of Tokyo, Japan
Kiyohide Usami,
Kyoto University, Japan

***Correspondence:**
Catherine Liégeois-Chauvel
CAL207@pitt.edu

Specialty section:
This article was submitted to Brain Imaging and Stimulation, a section of the journal Frontiers in Human Neuroscience

Received: *29 April 2021*
Accepted: *27 July 2021*
Published: *17 August 2021*

Citation:
Trébuchon A, Alario F-X and Liégeois-Chauvel C (2021) Functional Topography of Auditory Areas Derived From the Combination of Electrophysiological Recordings and Cortical Electrical Stimulation. Front. Hum. Neurosci. 15:702773. doi: 10.3389/fnhum.2021.702773

INTRODUCTION

Mapping cortical auditory functions in humans has provided valuable insights about inter-areal anatomo-physiological distinctions, or about left-right functional asymmetries. This approach has updated our vision of auditory cortex and of the hemispheric dominance for language. Here, we describe how electrical cortical stimulation can be combined with anatomy and electrophysiology to decipher the sensory and cognitive aspects of the auditory functions.

ANATOMICAL DESCRIPTION OF THE AUDITORY CORTEX

The auditory cortex in humans is largely confined in the posterior part of the superior temporal gyrus (STG), including Heschl's gyrus (HG) and Planum Temporale (PT) (**Figure 1A**). The precise posterior and anterior boundaries of these structures within STG have not been clearly defined (Berman et al., 2013), but it is clearly established that this territory is composed of several anatomically and physiologically distinct sub areas (Brodmann, 1909; Braak, 1980; Rivier and Clarke, 1997; Morosan et al., 2001). Once these multiple subdivisions are identified, a consistent pattern can be discerned as follows.

The core region labeled primary cortex (BA 41) is easily identified on the basis of its cytoarchitectonic structure (Braak, 1980). Macroscopically, it appears to be deeply buried in the sylvian fissure, confined to the postero-medial two thirds of HG, with substantial inter-hemispheric and inter-individual anatomical variations (Rademacher et al., 1993; Hackett, 2015). The primary auditory cortex is flanked by bands of secondary areas (BA 42) that extend in the lateral part of HG and, posteriorly, toward the PT. Anteriorly, on to the Planum Polare, lie associative areas (BA 22). Posteriorly, the ascendant segment of the PT has been distinguished from its horizontal segment based on where the Sylvian sulcus splits into ascending ramus and descending ramus, labeled as Sylvian-Parieto-temporal region (Spt) (Witelson and Kigar, 1992; Sweet et al., 2005). This simplified description provides a standard working hypothesis that disregards more elaborate accounts where up to 30 anatomical sub-areas may be distinguished (Galaburda and Sanides, 1980; Wallace et al., 2002; Hackett, 2015).

ANATOMO-FUNCTIONAL DELINEATION OF AUDITORY AREAS

In vivo electrophysiological recordings and direct electrical stimulation are invasive experimental methods that can be used to advance our understanding of the human auditory cortex. This type of research is performed in patients with intractable epilepsy undergoing pre-surgical diagnostic investigations with a stereotactic method [stereo-electroencephalography (SEEG)] involving depth electrodes (Chauvel et al., 2019), or with electrocorticographic (ECoG) electrodes apposed on the surface of the brain (Hamberger et al., 2005). The goal of the pre-surgical evaluation protocol is to define the organization of the epileptogenic zone as well as the functionally "eloquent" cortical regions. While ECoG recordings provide surface cortical maps of gyral activity, SEEG electrodes record activity from both gyri and sulci; importantly, SEEG access deep cortical structures, allowing to disentangle activity from sub-regions within auditory cortex (**Figure 1B**).

Auditory Evoked Potentials

The latencies of auditory evoked potentials (AEPs) elicited by clicks or pure tones reflect an anatomical segregation (**Figure 1C**). The sources of the different components lie in HG along the medio-lateral axis. Primary components (latencies below 30 ms) are generated in the tip of HG allowing a physiological delineation of primary auditory cortex (BA 41) (Liégeois-Chauvel et al., 1991). Sources with intermediate latency components (50–80 ms) are distributed from the lateral part of BA 41 to BA 42. Late components (above 80 ms) are generated in BA 42, the lateral parts of HG and PT, and at the posterior part of STG (BA 22) (Celesia and Puletti, 1969; Celesia, 1976; Liégeois-Chauvel et al., 1994, 2003, 2004; Howard et al., 2000; Brugge et al., 2008, 2009).

Spectro-Temporal Analysis

Time frequency analysis (TFA) has been important for revealing non-phase locked cortical activity and allowed for distinguishing single-trial spatio-temporal response patterns elicited across the auditory cortex by verbal and non-verbal stimulations (Chang et al., 2010). These patterns provide evidence for the tuning properties of cortical sites (Nourski et al., 2014) and they are modulated by the repetition rate of the stimulation (Nourski and Brugge, 2011). All these patterns reveal the representation of stimulus features which can be used to predict responses to novel stimuli or reconstruct the presented stimuli from pattern of cortical activity (Pasley et al., 2012).

Electrical Stimulation of Auditory Areas

The functional properties of the human auditory cortex were first described by W. Penfield using electrical stimulation to perform functional mapping during awake craniotomy procedures. The primary goal was to generate seizures to localize their origin. The clinical effects of the stimulation of each site were documented, along with intraoperative photographs of the anatomic locations of the stimulated sites. In 1938, Penfield reported hallucinations of sounds previously heard or experienced, provoked by electrical stimulation of the temporal cortex. In subsequent seminal publications, Penfield and collaborators showed that the primary auditory area lied on the anterior part of HG within the sylvian fissure (Penfield and Rasmussen, 1950; Penfield and Jasper, 1954; Mullan and Penfield, 1959). The stimulation of those locations resulted in an auditory sensation like a tone, a buzzing, or knocking sounds. This research thread is summarized in Penfield and Perot (1963).

An anatomo-functional dissociation was proposed between the sites from which electrical stimulation triggered elementary auditory hallucinations (i.e., crude auditory sensations) versus auditory illusions (i.e., altered interpretations of heard sounds: "sounds heard seemed louder or clearer, fainter or more distinct, nearer or farther"). The auditory hallucinations were triggered by the stimulation of the deep part of HG while the illusions were linked to the lateral part of HG, extending forward and back along the STG. More complex auditory "psychical responses" (e.g., relatives' voices, music, and meaningful sounds) have been reported mostly after stimulation of the Planum Polare. They probably result from a complex and widely distributed activation, involving brain regions beyond the auditory cortex.

In De Graaf et al.'s (2000) study, most of stimulation (62% of 180 stimulations) provoked auditory subjective symptoms. Among them, 32% consisted in simple hallucinations, mainly

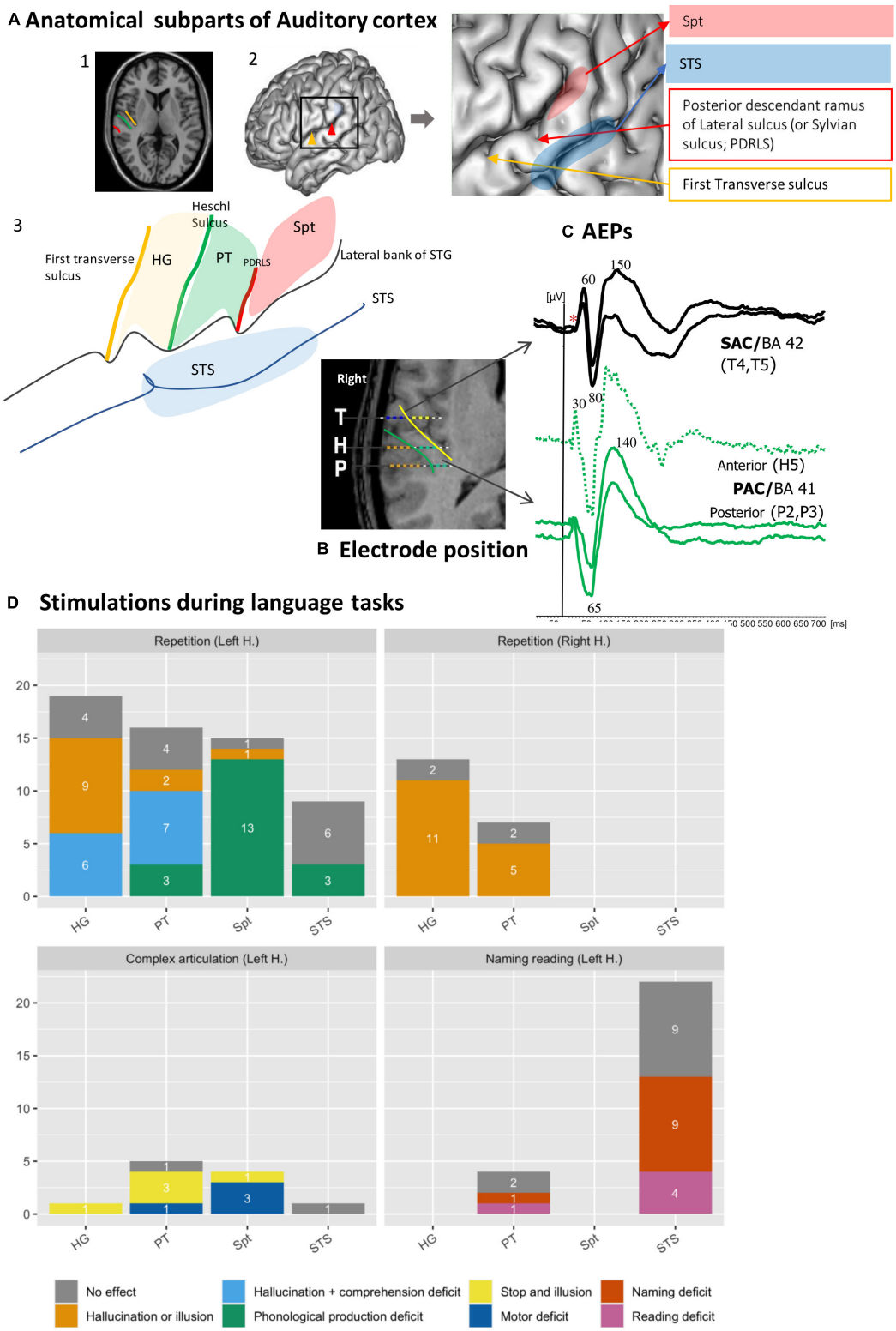

FIGURE 1 | Functional heterogeneity of auditory cortices. **(A)** Anatomical subpart of Auditory Cortices. The subparts of auditory cortices are delimited according to the different sulcus of the posterior part of the temporal Gyrus. Heschl's Gyrus (HG) by the transverse sulcus (yellow line) and posteriorly by Heschl sulcus (HS, green line). The Planum Temporale (PT) is limited anteriorly by the HS and posteriorly the horizontal PT is limited where the Sylvian sulcus splits into ascending ramus and descending ramus (red line). The Sylvian-Parieto-temporal region (Spt in red) lies between PDRLS and the posterior ascendant ramus of the sylvian sulcus.

(Continued)

FIGURE 1 | Continued
The several subparts according to the anatomical landmark are showed on (1) MRI axial view of auditory cortex; (2) 3D lateral brain representation and (3) on a schematic representation of auditory regions described above. **(B)** Example of electrode position along the auditory cortex. The 3 electrodes cross the two main sulci. The medial contacts of T electrode (yellow dots), explore the planum polare and the lateral contacts (blue dots) after crossing the transverse sulcus (yellow line) record the anterior part of HG (BA 42). H explore the medial part of HG (green dots, BA 41), then after crossing HS (green line) explore PT. The electrode contacts of P explore the medial part of HG (green dots, BA 41), then after crossing HS (green) explore PT. **(C)** Example of AEPS in the several sub-part of the auditory cortices in response of tone burst sound. Note the difference of the latency of the first component, around 30 ms for primary auditory cortex (BA 41) and 60 ms for secondary auditory cortex. **(D)** Stimulation of auditory cortex according to the subpart of the auditory cortices during language task (original data). The *Y*-axis corresponds to the number of stimulations performed, and the color codes for the different type of errors. Each bars graph corresponds to a sub-region (HG, PT, STS, and Spt). Each panel corresponds to repetition on left or right hemisphere (1 and 2), motor (3) and reading and naming (4) tasks. Solely hallucinations or illusions are predominantly induced in HG and PT and, specifically in the left hemisphere, sometimes accompanied by comprehension deficit. Stimulation of Spt induced phonological errors. The deficit in Naming and reading task is mainly observed in the posterior part of the STS. *Absence of early primary components.

recorded in the postero-medial part of HG (BA 41). On the contrary, stimulation of the lateral part of HG provoked more illusions than hallucinations. More generally, there was a gradient in the subjective responses from area 41 to 42 in HG, changing from high frequency sounds to broadband noise, to illusions. In the PT, auditory illusions and hallucinations were observed with equal frequency. Anteriorly to HG (BA 22), illusions were most often reported. They could be perceived contralateral to the stimulation or bilaterally. In summary, stimulation data consistently reveal two types of positive responses, with a clear-cut difference in the subjective auditory symptoms between the stimulation of BA 41 (primary cortex) eliciting mostly hallucinations and BA 42's (secondary cortex) provoking illusions. This is in line with the functional differences in electrophysiological responses (early vs. mid latency evoked components, respectively) recorded from these areas. The stimulation of the posterior lateral superior temporal area at the site of maximal potentials evoked by clicks elicited either hallucinations or illusions (Howard et al., 2000).

More rarely, hearing suppression was observed, for example following the stimulation of the "posterolateral aspect of the STG" or the "anterior part of HG" (Mullan and Penfield, 1959) see also (Sinha et al., 2005) and (Fenoy et al., 2006). Those hearing suppressions were not lateralized and they outlasted the duration of the stimulation. They could be accompanied by an altered perception of the timing in series of acoustic stimuli, or by a temporal dissociation between the experimenter's lips movements and the speech sounds they uttered.

Effects on Language Processing

Besides inducing auditory sensations, electrical cortical stimulations can impair language perception and production when they are delivered during behavioral tasks (Trébuchon and Chauvel, 2016). **Figure 1D** shows the outcome of 117 stimulations of 39 electrodes from 26 patients, sorted according to the different sub-regions of posterior STG. During a word repetition task, left HG and PT stimulation produced hallucinations or illusions sometimes along with comprehension deficit. Articulatory or phonological errors are elicited by the stimulation of Spt during word or pseudo word repetition, presumably due to a difficulty to maintain task-relevant representations in a phonological loop [in keeping with (Buchsbaum et al., 2011; Hickok, 2012)]. Lastly, the posterior part of left STS seems involved in more high-level language processes required in naming and reading tasks, because its stimulation did not induce positive auditory symptoms but naming or reading deficits (e.g., delayed responses, phonological errors, or semantics errors). The reading deficit included grapheme decoding, comprehension deficit and grapheme to phoneme deficit.

The contrastive consequences HG and PT electrical stimulations have been replicated in a recent study where stimulations were applied at the onset or the offset of a sentence the patient was asked to repeat (Forseth et al., 2020). Speech comprehension was disrupted by the stimulation of HG at the onset of the sentence while the disruption of speech production was observed when the stimulation of PT was applied at the end of the sentence, about the time when the patient must start to repeat. Performance impairments were observed specifically in the left hemisphere in cases of typical language organization. When we compared left/right HG and PT stimulations during a repetition task we did not observe comprehension deficits on the right side (**Figure 1D**, bottom panel). The fact that comprehension deficits are selectively observed in the language specialized hemisphere is consistent with the hypothesis that the hemispheric dominance would result from the asymmetry of auditory cortical tuning (Liégeois-Chauvel et al., 1999; Kell et al., 2011).

FUNCTIONAL ASYMMETRY BETWEEN THE RIGHT AND LEFT AUDITORY CORTICES

There is suggestive neuroanatomical evidence for structural differences between the left and right auditory cortices in humans. The primary auditory cortex (BA 41) is larger in the left hemisphere, with a higher density of gray and white matter, irrespective of handedness (Penhune et al., 1996; Dorsaint-Pierre et al., 2006). The left auditory cortex (HG and PT) contains larger cortical columns than its right counterpart, with a higher number of large pyramidal cells in cortical layer III (Hutsler and Galuske, 2003). The PT, or secondary auditory cortex, is also larger in the left hemisphere in the majority of individuals, and this structural asymmetry is related with the hemispheric dominance for language (Shapleske et al., 1999). Such differences in

cytoarchitectonic organization coincide with electrophysiological and functional differences between auditory regions.

Building on these observations, Poeppel (2003) hypothesized that two endogenous oscillations, in the low-gamma (25–45 Hz) and in the theta (4–8 Hz) bands, underlie asymmetric sampling in time (AST) of auditory signals. These two rhythms are asymmetric at rest in HG, with theta dominating in right and gamma in left auditory cortex (Sinha et al., 2005; Fenoy et al., 2006). This observation is compatible with distinct integration properties in right and left auditory cortices underlying the chunking of continuous speech into phonemic and syllabic segments, respectively, (Poeppel, 2003; Giraud and Poeppel, 2012). This functional asymmetry is a plausible neurophysiological substrate of the greater sensitivity of the left auditory cortex to short sound segments and brief speech features (Jamison et al., 2006; Obleser et al., 2008) and of the greater sensitivity of the right auditory cortex to slower acoustic fluctuations and longer steady speech signals such as vowels and syllables (Boemio et al., 2005; Abrams et al., 2008).

As a paradigmatic example, consider Voice Onset Time (VOT), which is the primary phonetic cue for the phonological distinction between voiced and voiceless stop consonants in a large variety of languages (Serniclaes, 1987; Cho and Ladefoged, 1999). VOT is the time lag between the release of the oral constriction for the consonant and the onset of the vibration of the vocal folds [i.e., the voicing: (Lisker and Abramson, 1964)].

Several studies have reported VOT discrimination deficits in patients with damage to the left hemisphere (Blumstein et al., 1977). Liégeois-Chauvel et al. (1999) showed lateralized processing of acoustic elements of the French voiced stops (e.g., /ba/) by time locking neural signals in the left dominant auditory cortex to the consonant onset or the release burst. These findings have been replicated and used as an electrophysiological marker of the hemispheric dominance for language (Trébuchon et al., 2005). **Figures 2A–C** illustrates the asymmetry between left and right auditory cortices in the case of a typical left organization for language. Conversely, **Figure 2D** (bottom frame) shows one patient with an atypical language organization. These temporal processing patterns are a function of the specific features of the syllables, with different electrophysiological patterns across languages (e.g., English vs. French). However, regardless the native language of the patients, the enhanced sensitivity to the temporal acoustic characteristics of sounds that is only present in BA 41 and BA 42 reflects information processes needed for tagging further phonetic processing which likely take place in BA 22 (Morillon et al., 2012; Giroud et al., 2020).

Following spectro-temporal analysis of the acoustic signal in the auditory cortex which is the first stage of the speech processing, the phonetic and phonological processes take place in posterior part of STG (Hickok and Poeppel, 2007; Morillon et al., 2012). High gamma frequency band has been correlated with phonetic and categorical features (Chang et al., 2010). More recently, decoding algorithms have been developed, synthetizing acoustic features from parameters predicted from the brain activity. These studies showed successful decoding of spectro-temporal features of speech in the STG [for review see, (Martin, 2019)].

Ictal Auditory Symptomatology

Auditory auras reported by patients during spontaneous seizures include a spectrum of phenomena ranging from simple auditory hallucinations to complex hallucinations or illusions. Simple auditory hallucinations, when they occur as a first ictal sign, are reliable signs to localize the epileptogenic zone (EZ) in the lateral posterior temporal regions (Maillard et al., 2004; Barba et al., 2007). Auditory hallucinations are most often heard contra-laterally to the EZ, which is largely consistent with what is observed during electrical cortical stimulations. Retrospective studies including a large number of patients show that the prevalence is weak (∼2% of the temporal lobe patients) (Florindo et al., 2006; Balgetir et al., 2018). The localization value of illusion is less consistent and suggest a more large and complex organization of the EZ, for instance in case of temporal lobe plus epilepsy (Barba et al., 2007). Auditory auras has been also report in context of autosomal dominant partial epilepsy characterized by auditory features (Ottman et al., 1995) for which the responsible gene LGI1 has been defined (Morante-Redolat, 2002).

There are only a few case reports of ictal verbal and musical hallucinations. Verbal hallucinations appear to be linked to EZs in the dominant hemisphere (Florindo et al., 2006) while musical hallucinations are linked to the right temporal lobe regardless of dominance (Wieser, 1980; Fénelon et al., 1993; Griffiths et al., 1997) [reviewed in Wieser et al. (1997), Kaplan (2003)]. As was argued for stimulation-induced hallucinations of similar content, hallucinatory perceptions may be construed as re-experiencing stored perceptual experiences, presumably involving a broad network.

Finally, ictal illusions or post-ictal palinacousis (i.e., auditory illusions consisting of the perseveration or echoing of an external auditory stimulus after it has ceased) are rarely reported in patients with temporo-parietal seizures [for a review, (Di Dio et al., 2007)].

APPLICATIONS TO TINNITUS

Auditory hallucinations evoked by electrical cortical stimulation share features with tinnitus, commonly defined as the perception of sound in the absence of an external auditory source. The rare observations of hearing suppression after cortical stimulation have opened new perspectives to treat tinnitus. It has been postulated in tinnitus patients that networks connecting the primary sensory cortices to other cortical areas and the periphery exhibit hyperexcitability leading to hallucinations (De Ridder et al., 2014).

In this context, a treatment strategy which seems to generate long and robust tinnitus suppression is to stimulate the auditory cortex using epidural electrodes (De Ridder et al., 2006, 2011).

The seemingly contradictory behavioral effects of suppression in tinnitus vs. hallucinations-illusions in epileptic patients could depend on the stimulation parameters and on the individual state of the cortical sites. In tinnitus, the peripheral deafferentation (hair cell deterioration) changes the spontaneous rate, synchrony

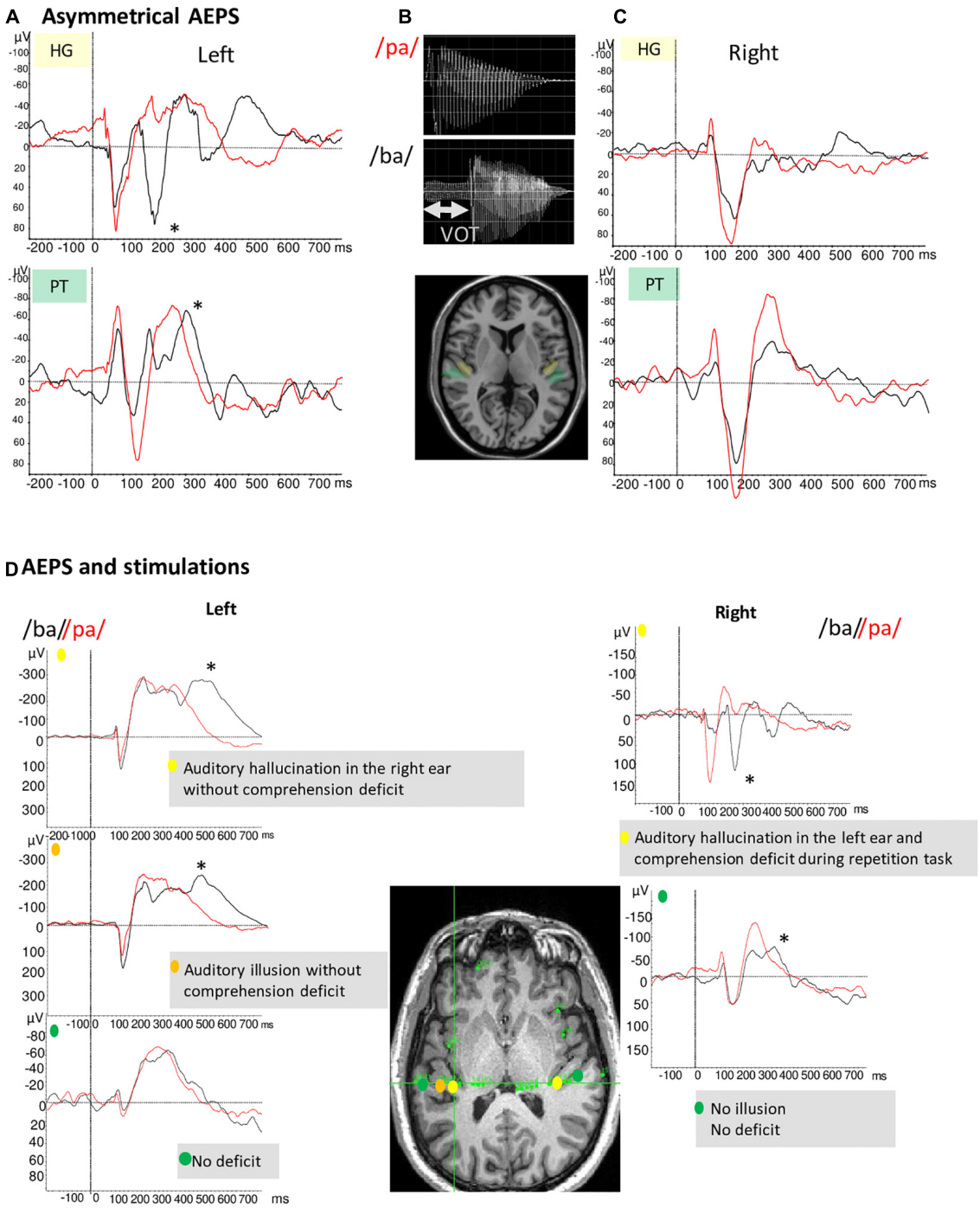

FIGURE 2 | (A,C) Illustration of example of AEP in response to voice /ba/ and /pa/ of two patients with typical language organization (according to handedness: RH, fMRI-activation in the left hemisphere during language task, stimulation, and ictal speech disturbance in the left hemisphere). **(A)** The temporal auditory coding of VOT took place specifically in the left HG and PT **(A)**. The /ba/ (black curve) elicited a first complex N1/P2 at the onset of voicing and a second component (marked by *) time-locked to release whereas the /pa/(red curve) elicited only one complex N1/P2. **(C)** On the right PT and HG no difference between /pa/ and /ba/ is observed. **(B)** Voiced stop consonants /ba/ and voiceless stop consonants /pa/. The VOT refers to the time between a phonetically relevant supra-laryngeal event, such as release, and glottal paulsing. In French, VOT it is a long negative value (~ −110 ms) for voiced stop consonants (/ba/) and a short positive value (~ +20 ms) for voiceless syllable (/pa/). **(D)** AEP in response to voice /ba/ and /pa/ and stimulations results of one patient with atypical language organization (left handed; no language deficit during seizure and stimulation of the left temporal regions whereas stimulation of the right temporal region induced language deficit). AEP and stimulations results are presented together to underline their complementarity. Left hemisphere/AEP, the temporal auditory coding of VOT took place in the left HG; Left hemisphere/Stimulation, typical hallucination and illusion are elicited in two parts of HG; Right hemisphere/AEP, the temporal auditory coding of VOT has been recorded on the HG and the PT; Right hemisphere/Stimulation, the stimulation of the right HG induced auditory hallucinations associated to a comprehension deficit.

and entails a cortical reorganization; the electrical stimulation might induce a decorrelation of the spontaneous activity. On the healthy auditory cortex, stimulations excite all neurons and elicit hallucinations (as noted above, only in rare cases does it result in temporary deafness).

DISCUSSION: INTERPRETING THE SYMPTOMATOLOGY ELICITED BY ELECTRICAL STIMULATION FOR CLINICAL AND RESEARCH PURPOSES

It is important to remember that electrical stimulation during SEEG explorations is performed primarily for eliciting seizures. The electrophysiological mapping of sensory and associative areas involved in cognitive networks should be conducted alongside, to answer the fundamental question of whether there is a spatio-temporal overlap between the epileptogenic and the functional networks. The identification of cortical structures that are essential to cognitive or perceptual functions is challenging because the human brain is a complex system in which a vast range of function arises from coordinated neural activity across diverse spatial and temporal scales (Sporns and Betzel, 2016; Bassett and Bullmore, 2017).

Effects arising from the stimulation of the primary sensory cortices are more localizing than that of associative cortices which involves the activation of a network or networks that underpins the functional emergence of language impairments.

Trebuchon (Trébuchon, 2021) described the procedure to follow, including stimulation parameters such as duration and timing, to avoid pitfalls such as "false negative stimulation." They also described how to interpret the symptoms in relation with collateral electrophysiological changes such as after-discharges. It is especially important to interpret the role of the PT and the posterior part of the superior temporal sulcus in language perception and production. Choosing the task according to the stimulated sub-region is particularly crucial (**Figure 1A**). HG and PT should be tested with a repetition or repetition and designation task; Spt should be tested with repetition and repetitive motor tasks, STS should be preferentially tested with naming and reading tasks.

The relationship between phenomena induced by cortical electrical stimulation and normal brain physiology is also a fair question to ask, given that the epilepsy condition may result in the functional alterations of the networks it affects. The auditory manifestations following the stimulation of auditory cortex could result from a perturbation of the efferent pathway between the cortex and the periphery (cochlea), that would lead to abnormal auditory processing.

A stimulation induced deficit could result from an inhibitory effect of the stimulation due to the temporary inactivation of a local population of neurons, either pyramidal cells or interneurons. However, we are far from a perfect understanding of the functional or physiological effects of pulse or train stimulations. It is very common that the stimulation of the same region with the same parameters leads to various effects. One explanation could be that the "inhibitory effect" of the stimulation induces a rapid plasticity of the system that lasts for at least a few minutes following the trial (Trébuchon, 2021).

Overall, the available data favor the view that a positive response is evidence of an activation of the stimulated cortical neurons while a negative response could be interpreted as an inhibition of behavior attributed to neuronal inactivation (Borchers et al., 2012). The stimulation of auditory cortex at the base of the cortical hierarchy of networks involved in auditory perception elicited frequent and simple effects and allows a reliable assessment of sensory function. But these effects become increasingly rare, heterogeneous and complex in heteromodal networks making the evaluation of speech perception and production functions more uncertain (Fox et al., 2020).

The use of single pulse electrical stimulation could help to resolve how adjacent and remote areas are inter-connected by measuring the cortico-cortical evoked potentials and identify the role of the auditory cortex in the language network [(Matsumoto et al., 2004, 2017), for review see David et al. (2010)].

In our view, solid physiological foundations underlying the effect of electrical stimulation need to be established, and the labeling of direct electrical stimulation as the "gold standard for mapping brain function" remains the matter of an interesting debate (Grande et al., 2020).

DATA AVAILABILITY STATEMENT

The original contributions presented in the study are included in the article/supplementary material, further inquiries can be directed to the corresponding author.

ETHICS STATEMENT

The studies involving human participants were reviewed and approved by the Comite de Protection des Personnes. The patients/participants provided their written informed consent to participate in this study.

AUTHOR CONTRIBUTIONS

All authors listed have made a substantial, direct and intellectual contribution to the work, and approved it for publication.

FUNDING

Research supported by grant ANR-16-CONV-0002 (ILCB) and the Excellence Initiative of Aix-Marseille University (A*MIDEX).

ACKNOWLEDGMENTS

We would like to thank Manuel Mercier for his contribution to the figures and providing valuable feedback on this manuscript.

REFERENCES

Abrams, D. A., Nicol, T., Zecker, S., and Kraus, N. (2008). Right-hemisphere auditory cortex is dominant for coding syllable patterns in speech. *J. Neurosci.* 28, 3958–3965. doi: 10.1523/JNEUROSCI.0187-08.2008

Balgetir, F., Müngen, B., Gönen, M., Müngen, E., and Taşcı, Ý (2018). Epileptic auditory illusions as reliable findings in the determination of the lateralization and localization of epileptogenic zone. *Epilepsy Behav.* 88, 21–24. doi: 10.1016/j.yebeh.2018.08.017

Barba, C., Barbati, G., Minotti, L., Hoffmann, D., and Kahane, P. (2007). Ictal clinical and scalp-EEG findings differentiating temporal lobe epilepsies from temporal "plus" epilepsies. *Brain* 130, 1957–1967. doi: 10.1093/brain/awm108

Bassett, D. S., and Bullmore, E. T. (2017). Small-world brain networks revisited. *Neuroscientist* 23, 499–516. doi: 10.1177/1073858416667720

Berman, J. I., Lanza, M. R., Blaskey, L., Edgar, J. C., and Roberts, T. P. L. (2013). High angular resolution diffusion imaging probabilistic tractography of the auditory radiation. *AJNR Am. J. Neuroradiol.* 34, 1573–1578. doi: 10.3174/ajnr.A3471

Blumstein, S. E., Cooper, W. E., Zurif, E. B., and Caramazza, A. (1977). The perception and production of voice-onset time in aphasia. *Neuropsychologia* 15, 371–383. doi: 10.1016/0028-3932(77)90089-6

Boemio, A., Fromm, S., Braun, A., and Poeppel, D. (2005). Hierarchical and asymmetric temporal sensitivity in human auditory cortices. *Nat. Neurosci.* 8, 389–395. doi: 10.1038/nn1409

Borchers, S., Himmelbach, M., Logothetis, N., and Karnath, H.-O. (2012). Direct electrical stimulation of human cortex — the gold standard for mapping brain functions? *Nat. Rev. Neurosci.* 13, 63–70. doi: 10.1038/nrn3140

Braak, H. (1980). *Architectonics of the Human Telencephalic Cortex: With 43 fig.* Berlin: Springer.

Brodmann, K. (1909). *Vergleichende Lokalisationslehre der Grosshirnrinde in ihren Prinzipien Dargestellt auf Grund des Zellenbaues [Comparative Localization Theory of the Cerebral Cortex Presented in Its Principles Based on the Cell Structure]*. Leipzig: Barth.

Brugge, J. F., Nourski, K. V., Oya, H., Reale, R. A., Kawasaki, H., Steinschneider, M., et al. (2009). Coding of repetitive transients by auditory cortex on Heschl's gyrus. *J. Neurophysiol.* 102, 2358–2374. doi: 10.1152/jn.91346.2008

Brugge, J. F., Volkov, I. O., Oya, H., Kawasaki, H., Reale, R. A., Fenoy, A., et al. (2008). Functional localization of auditory cortical fields of human: click-train stimulation. *Hear. Res.* 238, 12–24. doi: 10.1016/j.heares.2007.11.012

Buchsbaum, B. R., Baldo, J., Okada, K., Berman, K. F., Dronkers, N., D'Esposito, M., et al. (2011). Conduction aphasia, sensory-motor integration, and phonological short-term memory – an aggregate analysis of lesion and fMRI data. *Brain Lang.* 119, 119–128. doi: 10.1016/j.bandl.2010.12.001

Celesia, G. G. (1976). Organization of auditory cortical areas in man. *Brain* 99, 403–414. doi: 10.1093/brain/99.3.403

Celesia, G. G., and Puletti, F. (1969). Auditory cortical areas of man. *Neurology* 19, 211–211. doi: 10.1212/WNL.19.3.211

Chang, E. F., Rieger, J. W., Johnson, K., Berger, M. S., Barbaro, N. M., and Knight, R. T. (2010). Categorical speech representation in human superior temporal gyrus. *Nat. Neurosci.* 13, 1428–1432. doi: 10.1038/nn.2641

Chauvel, P., Gonzalez-Martinez, J., and Bulacio, J. (2019). "Presurgical intracranial investigations in epilepsy surgery," in *Handbook of Clinical Neurology Clinical Neurophysiology: Diseases and Disorders*, eds K. H. Levin and P. Chauvel (Amsterdam: Elsevier), 45–71. doi: 10.1016/B978-0-444-64142-7.00040-0

Cho, T., and Ladefoged, P. (1999). Variation and universals in VOT: evidence from 18 languages. *J. Phonet.* 27, 207–229. doi: 10.1006/jpho.1999.0094

David, O., Bastin, J., Chabardès, S., Minotti, L., and Kahane, P. (2010). Studying network mechanisms using intracranial stimulation in epileptic patients. *Front. Syst. Neurosci.* 4:148. doi: 10.3389/fnsys.2010.00148

De Graaf, J. B., Liégeois-Chauvel, C., Vignal, J. P., and Chauvel, P. (2000). "Electrical stimulation of the auditory cortex," in *Epileptic Seizures: Pathophysiology and Clinical Semiology*, eds H. O. Luders and S. Noachtar (New York, NY: Churchill Livingston), 228–236.

De Ridder, D., De Mulder, G., Verstraeten, E., van der Kelen, K., Sunaert, S., Smits, M., et al. (2006). Primary and secondary auditory cortex stimulation for intractable tinnitus. *ORL* 68, 48–55. doi: 10.1159/000090491

De Ridder, D., Vanneste, S., and Freeman, W. (2014). The Bayesian brain: phantom percepts resolve sensory uncertainty. *Neurosci. Biobehav. Rev.* 44, 4–15. doi: 10.1016/j.neubiorev.2012.04.001

De Ridder, D., Vanneste, S., Kovacs, S., Sunaert, S., Menovsky, T., van de Heyning, P., et al. (2011). Transcranial magnetic stimulation and extradural electrodes implanted on secondary auditory cortex for tinnitus suppression: clinical article. *J. Neurosurg.* 114, 903–911. doi: 10.3171/2010.11.JNS10197

Di Dio, A. S., Fields, M. C., and Rowan, A. J. (2007). Palinacousis-auditory perseveration: two cases and a review of the literature: *PALINACOUSIS-AUDITORY PERSEVERATION*. *Epilepsia* 48, 1801–1806. doi: 10.1111/j.1528-1167.2007.01179.x

Dorsaint-Pierre, R., Penhune, V. B., Watkins, K. E., Neelin, P., Lerch, J. P., Bouffard, M., et al. (2006). Asymmetries of the planum temporale and Heschl's gyrus: relationship to language lateralization. *Brain* 129, 1164–1176.

Fénelon, G., Marie, S., Ferroir, J. P., and Guillard, A. (1993). Hallucinose musicale: 7 cases. *Rev. Neurol.* 149, 7.

Fenoy, A. J., Severson, M. A., Volkov, I. O., Brugge, J. F., and Howard, M. A. (2006). Hearing suppression induced by electrical stimulation of human auditory cortex. *Brain Res.* 1118, 75–83. doi: 10.1016/j.brainres.2006.08.013

Florindo, I., Bisulli, F., Pittau, F., Naldi, I., Striano, P., Striano, S., et al. (2006). Lateralizing value of the auditory aura in partial seizures. *Epilepsia* 47(Suppl. 5), 68–72. doi: 10.1111/j.1528-1167.2006.00881.x

Forseth, K. J., Hickok, G., Rollo, P. S., and Tandon, N. (2020). Language prediction mechanisms in human auditory cortex. *Nat. Commun.* 11:5240. doi: 10.1038/s41467-020-19010-6

Fox, K. C. R., Shi, L., Baek, S., Raccah, O., Foster, B. L., Saha, S., et al. (2020). Intrinsic network architecture predicts the effects elicited by intracranial electrical stimulation of the human brain. *Nat. Hum. Behav.* 4, 1039–1052. doi: 10.1038/s41562-020-0910-1

Galaburda, A., and Sanides, F. (1980). Cytoarchitectonic organization of the human auditory cortex. *J. Comp. Neurol.* 190, 597–610. doi: 10.1002/cne.901900312

Giraud, A.-L., and Poeppel, D. (2012). Cortical oscillations and speech processing: emerging computational principles and operations. *Nat. Neurosci.* 15, 511–517. doi: 10.1038/nn.3063

Giroud, J., Trébuchon, A., Schön, D., Marquis, P., Liegeois-Chauvel, C., Poeppel, D., et al. (2020). Asymmetric sampling in human auditory cortex reveals spectral processing hierarchy. *PLoS Biol.* 18:e3000207. doi: 10.1371/journal.pbio.3000207

Grande, K. M., Ihnen, S. K. Z., and Arya, R. (2020). Electrical stimulation mapping of brain function: a comparison of subdural electrodes and stereo-EEG. *Front. Hum. Neurosci.* 14:611291. doi: 10.3389/fnhum.2020.611291

Griffiths, T. D., Jackson, M. C., Spillane, J. A., Friston, K. J., and Frackowiak, R. S. J. A. (1997). neural substrate for musical hallucinosis. *Neurocase* 3:72.

Hackett, T. A. (2015). "Chapter 2 - Anatomic organization of the auditory cortex," in *Handbook of Clinical Neurology The Human Auditory System*, eds M. J. Aminoff, F. Boller, and D. F. Swaab (Amsterdam: Elsevier), 27–53. doi: 10.1016/B978-0-444-62630-1.00002-0

Hamberger, M. J., Seidel, W. T., Mckhann, G. M. I. I., Perrine, K., and Goodman, R. R. (2005). Brain stimulation reveals critical auditory naming cortex. *Brain* 128, 2742–2749. doi: 10.1093/brain/awh621

Hickok, G. (2012). Computational neuroanatomy of speech production. *Nat. Rev. Neurosci.* 13, 135–145. doi: 10.1038/nrn3158

Hickok, G., and Poeppel, D. (2007). The cortical organization of speech processing. *Nat. Rev. Neurosci.* 8, 393–402. doi: 10.1038/nrn2113

Howard, M. A., Volkov, I. O., Mirsky, R., Garell, P. C., Noh, M. D., Granner, M., et al. (2000). Auditory cortex on the human posterior superior temporal gyrus. *J. Comp. Neurol.* 416, 79–92. doi: 10.1002/(SICI)1096-9861(20000103)416:1<79::AID-CNE6<3.0.CO;2-2

Hutsler, J., and Galuske, R. A. (2003). Hemispheric asymmetries in cerebral cortical networks. *Trends Neurosci.* 26, 429–435. doi: 10.1016/S0166-2236(03)00198-X

Jamison, H. L., Watkins, K. E., Bishop, D. V. M., and Matthews, P. M. (2006). Hemispheric specialization for processing auditory nonspeech stimuli. *Cereb. Cort.* 16, 1266–1275. doi: 10.1093/cercor/bhj068

Kaplan, P. W. (2003). Musicogenic epilepsy and epileptic music: a seizure's song. *Epilepsy Behav.* 4, 464–473. doi: 10.1016/s1525-5050(03)00172-0

Kell, C. A., Morillon, B., Kouneiher, F., and Giraud, A.-L. (2011). Lateralization of speech production starts in sensory cortices—a possible sensory origin of

cerebral left dominance for speech. *Cereb. Cortex* 21, 932–937. doi: 10.1093/cercor/bhq167

Liégeois-Chauvel, C., Trebuchon-Da Fonseca, A., Regis, J., Marquis, P., and Chauvel, P. (2003). Auditory evoked potentials in the definition of eloquent cortical areas. *Handbook Clin. Neurophysiol.* 3, 305–316.

Liégeois-Chauvel, C., de Graaf, J. B., Laguitton, V., and Chauvel, P. (1999). Specialization of left auditory cortex for speech perception in man depends on temporal coding. *Cereb. Cortex* 9, 484–496. doi: 10.1093/cercor/9.5.484

Liégeois-Chauvel, C., Lorenzi, C., Trébuchon, A., Régis, J., and Chauvel, P. (2004). Temporal envelope processing in the human left and right auditory cortices. *Cereb. Cortex* 14, 731–740. doi: 10.1093/cercor/bhh033

Liégeois-Chauvel, C., Musolino, A., Badier, J. M., Marquis, P., and Chauvel, P. (1994). Evoked potentials recorded from the auditory cortex in man: evaluation and topography of the middle latency com- ponents. *Electroencephalogr. Clin. Neurophysiol.* 92, 204–214.

Liégeois-Chauvel, C., Musolino, A., and Chauvel, P. (1991). Localization of the primary auditory area in man. *Brain* 114(Pt 1A), 139–151.

Lisker, L., and Abramson, A. S. A. (1964). Cross-language study of voicing in initial stops: acoustical measurements. *Word* 20, 384–422. doi: 10.1080/00437956.1964.11659830

Maillard, L., Vignal, J.-P., Gavaret, M., Guye, M., Biraben, A., McGonigal, A., et al. (2004). Semiologic and electrophysiologic correlations in temporal lobe seizure subtypes. *Epilepsia* 45, 1590–1599. doi: 10.1111/j.0013-9580.2004.09704.x

Martin, S. (2019). The use of intracranial recordings to decode human language: challenges and opportunities. *Brain Lang.* 193, 73–83. doi: 10.1016/j.bandl.2016.006.003

Matsumoto, R., Kunieda, T., and Nair, D. (2017). Single pulse electrical stimulation to probe functional and pathological connectivity in epilepsy. *Seizure* 44, 27–36. doi: 10.1016/j.seizure.2016.11.003

Matsumoto, R., Nair, D. R., LaPresto, E., Najm, I., Bingaman, W., Shibasaki, H., et al. (2004). Functional connectivity in the human language system: a cortico-cortical evoked potential study. *Brain* 127, 2316–2330. doi: 10.1093/brain/awh246

Morante-Redolat, J. M. (2002). Mutations in the LGI1/Epitempin gene on 10q24 cause autosomal dominant lateral temporal epilepsy. *Hum. Mol. Genet.* 11, 1119–1128. doi: 10.1093/hmg/11.9.1119

Morillon, B., Liégeois-Chauvel, C., Arnal, L. H., Bénar, C. G., and Giraud, A.-L. (2012). Asymmetric function of theta and gamma activity in syllable processing: an intra-cortical study. *Front. Psychol.* 3:248. doi: 10.3389/fpsyg.2012.00248

Morosan, P., Rademacher, J., Schleicher, A., Amunts, K., Schormann, T., and Zilles, K. (2001). Human primary auditory cortex: cytoarchitectonic subdivisions and mapping into a spatial reference system. *NeuroImage* 13, 684–701. doi: 10.1006/nimg.2000.0715

Mullan, S., and Penfield, W. (1959). Illusions of comparative interpretation and emotion: production by epileptic discharge and by electrical stimulation in the temporal cortex. *AMA Arch. Neurol. Psychiatry* 81, 269–284. doi: 10.1001/archneurpsyc.1959.02340150001001

Nourski, K. V., and Brugge, J. F. (2011). Representation of temporal sound features in the human auditory cortex. *Rev. Neurosci.* 22, 187–203. doi: 10.1515/rns.2011.016

Nourski, K. V., Steinschneider, M., Oya, H., Kawasaki, H., Jones, R. D., and Howard, M. A. (2014). Spectral organization of the human lateral superior temporal gyrus revealed by intracranial recordings. *Cereb. Cortex* 24, 340–352. doi: 10.1093/cercor/bhs314

Obleser, J., Eisner, F., and Kotz, S. A. (2008). Bilateral speech comprehension reflects differential sensitivity to spectral and temporal features. *J. Neurosci.* 28, 8116–8123. doi: 10.1523/JNEUROSCI.1290-08.2008

Ottman, R., Risch, N., Hauser, W. A., Pedley, T. A., Lee, J. H., Barker-Cummings, C., et al. (1995). Localization of a gene for partial epilepsy to chromosome 10q. *Nat. Genet.* 10, 56–60. doi: 10.1038/ng0595-56

Pasley, B. N., David, S. V., Mesgarani, N., Flinker, A., Shamma, S. A., Knight, R. T., et al. (2012). Reconstructing speech from human auditory cortex. *PLoS Biol.* 10:13. doi: 10.1371/journal.pbio.1001251

Penfield, W., and Jasper, H. H. (1954). *Epilepsy and the Functional Anatomy of the Human Brain*. Boston, MA: Little Brown & Co.

Penfield, W., and Perot, P. (1963). The brain's record of auditory and visual experience: a final summary and discussion. *Brain* 86, 595–696. doi: 10.1093/brain/86.4.595

Penfield, W., and Rasmussen, T. (1950). *The Cerebral Cortex of Man. A Clinical Study of Localization of Function*. New York, N.Y: Macmillan Company.

Penhune, V. B., Zatorre, R. J., MacDonald, J. D., and Evans, A. C. (1996). Interhemispheric anatomical differences in human primary auditory cortex: probabilistic mapping and volume measurement from magnetic resonance scans. *Cereb. Cortex* 6, 661–672. doi: 10.1093/cercor/6.5.661

Poeppel, D. (2003). The analysis of speech in different temporal integration windows: cerebral lateralization as 'asymmetric sampling in time.'. *Speech Commun.* 41, 245–255. doi: 10.1016/S0167-6393(02)00107-3

Rademacher, J., Caviness, V. S. Jr., Steinmetz, H., and Galaburda, A. M. (1993). Topographical variation of the human primary cortices: implications for neuroimaging, brain mapping, and neurobiology. *Cereb. Cortex* 3, 313–329. doi: 10.1093/cercor/3.4.313

Rivier, F., and Clarke, S. (1997). Cytochrome oxidase, acetylcholinesterase, and NADPH-diaphorase staining in human supratemporal and insular cortex: evidence for multiple auditory areas. *NeuroImage* 6, 288–304. doi: 10.1006/nimg.1997.0304

Serniclaes, W. (1987). *Etude Expérimentale de la Perception du Trait de Voisement des Occlusives du Français*. Ph.D. Dissertation. Bruxelles: Université Libre de Bruxelles.

Shapleske, J., Rossell, S. L., Woodruff, P. W. R., and David, A. S. (1999). The planum temporale: a systematic, quantitative review of its structural, functional and clinical significance. *Brain Res. Rev.* 29, 26–49. doi: 10.1016/S0165-0173(98)00047-2

Sinha, S. R., Crone, N. E., Fotta, R., Lenz, F., and Boatman, D. F. (2005). Transient unilateral hearing loss induced by electrocortical stimulation. *Neurology* 64, 383–385. doi: 10.1212/01.WNL.0000149524.11371.B1

Sporns, O., and Betzel, R. F. (2016). Modular brain networks. *Annu. Rev. Psychol.* 67, 613–640. doi: 10.1146/annurev-psych-122414-033634

Sweet, R. A., Dorph-Petersen, K.-A., and Lewis, D. A. (2005). Mapping auditory core, lateral belt, and parabelt cortices in the human superior temporal gyrus. *J. Comp. Neurol.* 491, 270–289. doi: 10.1002/cne.20702

Trébuchon, A., and Chauvel, P. (2016). Electrical stimulation for seizure induction and functional mapping in stereoelectroencephalography. *J. Clin. Neurophysiol.* 33, 511–521. doi: 10.1097/WNP.0000000000000313

Trébuchon, A., Giraud, K., Badier, J. M., Chauvel, P., and Liégeois-Chauvel, C. (2005). Hemispheric lateralization of voice onset time (VOT) comparison between depth and scalp EEG recording. *NeuroImage* 27, 1–14.

Trébuchon, A. (2021). "Electrical stimulation for functional mapping during stereo EEG exploration," in *A Practical approach to Stereo EEG,* ed. S. U. Schuele (Springer Publishing Company), 361–382.

Wallace, M. N., Johnston, P. W., and Palmer, A. R. (2002). Histochemical identification of cortical areas in the auditory region of the human brain. *Exp. Brain Res.* 143, 499–508. doi: 10.1007/s00221-002-1014-z

Wieser, H. G. (1980). Temporal lobe or psychomotor status epilepticus. A case report. *Electroencephalogr. Clin. Neurophysiol.* 48, 558–572. doi: 10.1016/0013-4694(80)90291-6

Wieser, H. G., Hungerbuhler, H., Siegel, A. M., and Buck, A. (1997). Musicogenic epilepsy: review of the literature and case report with ictal single photon emission computed tomography. *Epilepsia* 38, 200–207. doi: 10.1111/j.1528-1157.1997.tb01098.x

Witelson, S. F., and Kigar, D. L. (1992). Sylvian fissure morphology and asymmetry in men and women: bilateral differences in relation to handedness in men. *J. Comp. Neurol.* 323, 326–340. doi: 10.1002/cne.903230303

Conflict of Interest: The authors declare that the research was conducted in the absence of any commercial or financial relationships that could be construed as a potential conflict of interest.

Publisher's Note: All claims expressed in this article are solely those of the authors and do not necessarily represent those of their affiliated organizations, or those of the publisher, the editors and the reviewers. Any product that may be evaluated in this article, or claim that may be made by its manufacturer, is not guaranteed or endorsed by the publisher.

Advantages of publishing in Frontiers

OPEN ACCESS
Articles are free to read for greatest visibility and readership

FAST PUBLICATION
Around 90 days from submission to decision

HIGH QUALITY PEER-REVIEW
Rigorous, collaborative, and constructive peer-review

TRANSPARENT PEER-REVIEW
Editors and reviewers acknowledged by name on published articles

Frontiers
Avenue du Tribunal-Fédéral 34
1005 Lausanne | Switzerland

Visit us: www.frontiersin.org
Contact us: frontiersin.org/about/contact

REPRODUCIBILITY OF RESEARCH
Support open data and methods to enhance research reproducibility

DIGITAL PUBLISHING
Articles designed for optimal readership across devices

FOLLOW US
@frontiersin

IMPACT METRICS
Advanced article metrics track visibility across digital media

EXTENSIVE PROMOTION
Marketing and promotion of impactful research

LOOP RESEARCH NETWORK
Our network increases your article's readership